SEPTEMBER 1971

ANALYTICAL CHEMISTRY

High-Speed
Current
Measurements 91 A

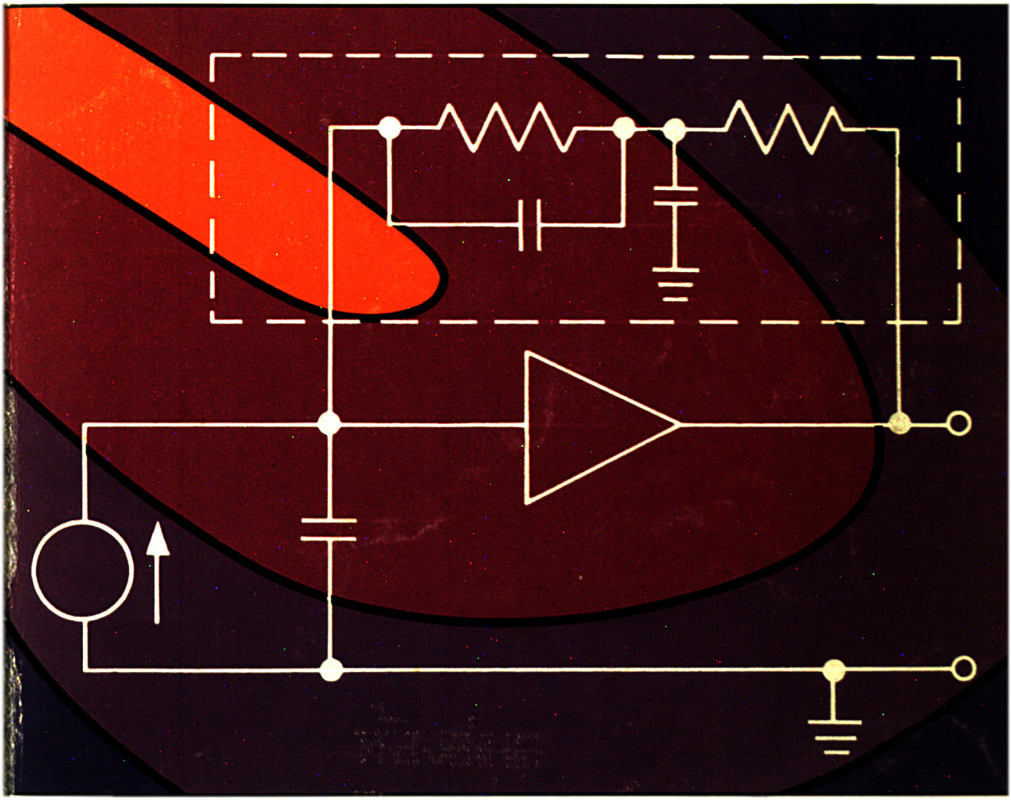

Matchless AA

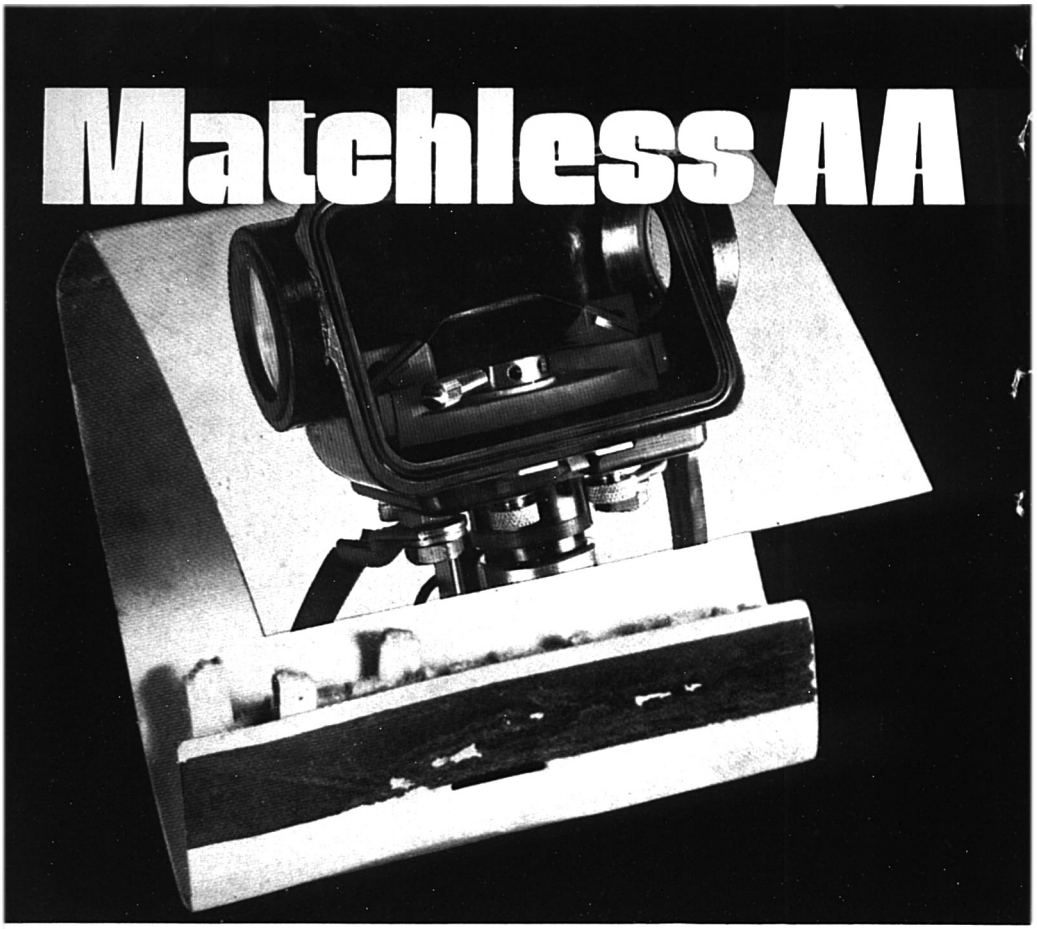

Matchless AA . . . . the IL355 Flameless Sampler.

A complete, simple to operate system for trace element determinations in atomic absorption spectroscopy. The enclosed volume of the chamber permits atomization in a controlled, inert or reducing atmosphere to intensify absorption and to minimize side reactions and interferences. The constant current power supply and a unique tantalum ribbon furnace enhance analytical precision.

Matchless AA . . . . in trace element detection.

One nanogram of cadmium will provide a sample peak of 0.5 absorbance! This a typical example of the vastly improved sensitivities made possible by the IL355's innovative design features. Direct sampling on many matrices is readily achieved. A thousand fold gain in sensitivity is a common occurrence.

Matchless AA . . . . in simplicity of operation.

The IL355 is a simple, uncomplicated system. It is easily and quickly set up. Because of the tantalum furnace, neither an elaborate source of power nor a cumbersome water cooling system is required. Determinations are rapidly made with push button operation.

Matchless AA . . . . in laboratory economy.

The IL355 costs less to purchase, costs less to operate, costs less to maintain. The IL355's chamber and control module are independently operated, and can be used with contemporary AA instrumentation.

Matchless AA . . . . the IL355 Flameless Sampler.

With sensitivities equal to or better than any current technique, the IL355 is truly matchless — whatever the consideration. Call or send today for completely detailed information.

Instrumentation Laboratory Inc. 113 Hartwell Avenue/Lexington, Mass. 02173/Tel 617-861-0710/Telex 92-3440

CIRCLE 91 ON READER SERVICE CARD

FLUORESCENCE FAMILY PLANNING

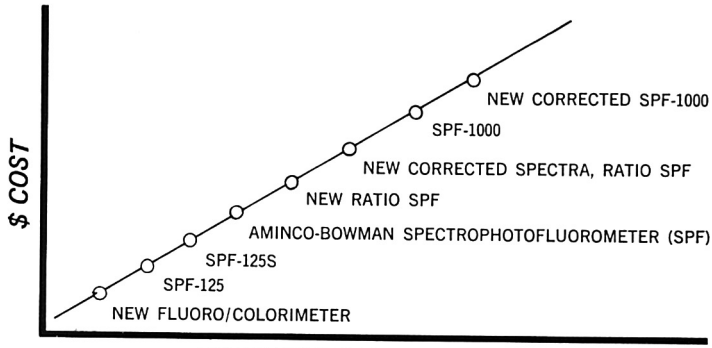

Only AMINCO offers the wide selection of fluorescence instrumentation shown above. There is an instrument designed for every fluorescence measurement in every application from routine processing in a clinical lab to esoteric research. Every instrument is designed to deliver optimum performance within its operating parameters, at economical cost to you. If your interest is in quantitative and/or qualitative measurement via fluorescence, choose the instrument best suited to your application from the list below and contact us for more information.

NEW FLUORO/COLORIMETER A direct-reading filter fluorometer which serves as a colorimeter, turbidimeter and nephelometer. Permits rapid (15 to 20 samples per minute), quantitative, sequential analysis of samples whose luminescence or photometric characteristics are known. Two solid-state models with blank subtraction in three ranges, allowing ten decade blank suppression, so that even small changes in signal can be measured with increased precision. Seven fixed steps of sensitivity. Optional recorder. Circle No. 13 on Reader Service Card.

AMINCO SPF-125 A direct reading spectrofluorometer ideally suited to standard procedures, clinical tests and teaching. Two monochromators for independent setting of excitation and emission wavelengths eliminate the guesswork and bother of filter combinations. Resolution adjustable from 1.5 to 44nm; 85w high-pressure mercury lamp provides high intensity; parts-per-trillion sensitivity for quinine sulfate; wavelength range of 200 to 800nm, each monochromator; utilizes an S4 PMT with response beyond 600nm. Circle No. 14 on Reader Service Card.

AMINCO SPF-125S A scanning version of the SPF-125 described above. Provides some of the versatility of the Aminco-Bowman Spectrophotofluorometer at a lower cost. Ideal for those applications where prime utilization of the instrument is routine analysis but some research experimentation is done. In this model scanning monochromators are utilized and a high energy xenon lamp provides a continuum light source. Circle No. 14 on Reader Service Card.

AMINCO-BOWMAN SPECTROPHOTOFLUOROMETER (SPF) This famous research "workhorse" performs quantitative and/or qualitative measurements. Either fluorescence or phosphorescence studies are possible by a simple interchanging of cell compartments. Sensitivity: one part per trillion, quinine sulfate, when excited at 250 or 350nm. Resolution: better than 1nm. Cell compartment and lamp housing provide means to maintain optimum temperature for sample and lamp. Less noise: low ripple power supply reduces arc wander. Applications include: fluorescence probes, enzyme assays, phosphorescence studies, thin-layer chromatography, physical chemistry measurements. Circle No. 15 on Reader Service Card.

NEW RATIO SPF The simple addition of a Ratio Attachment, at the factory or in the field (for instruments already in operation) provides superior stability, brings excitation and emission spectra closer to known spectral characteristics, corrects for low intensity peak shift in far UV and increases the signal-to-noise ratio and the useful life of the lamp. Circle No. 15 on Reader Service Card.

NEW CORRECTED SPECTRA, RATIO SPF The addition of a Corrected Spectra Attachment to a Ratio SPF provides both excitation and emission correction over the entire 200-800nm wavelength range. Circle No. 15 on Reader Service Card.

AMINCO SPF-1000 HIGH PERFORMANCE SPECTROPHOTOFLUOROMETER Features: High Resolution: 0.2nm with digital readout; Bandpass of .2, .5, 1, 2, 5, 10, 20 and 40nm. Monochromator wavelength range: 200-1000nm; Spectrum: starting wavelength of 200, 300, 400, 500, 600, 700, 800 or 900nm and spectral width of 100, 200 or 400nm may be selected by front panel switches. Spectra may also be displayed as a function of wavenumber. Large up-front sample compartment. Ellipsoidal Condensing System included. Solid-state blank-subtract Photomultiplier Microphotometer allows use of any side-on or end-on photomultiplier tubes. Photometer responds to phenomena having lifetimes as short as 5 microseconds, allowing the SPF-1000 to be used as a precise phosphorescence lifetime instrument. Circle No. 16 on Reader Service Card.

CORRECTED SPF-1000 The most sophisticated fluorescence instrument available. Provides all the qualities of the SPF-1000 and, in addition, operates in a corrected excitation and emission mode; as a ratio spectrophotofluorometer; and as a double beam spectrophotometer. Excitation spectra can be plotted as quantum intensity versus wavelength or wavenumber; or as watts versus wavelength. Emission spectra may be plotted in any of three modes: 1) quantum intensity per unit wavenumber versus wavenumber; 2) quantum intensity per unit wavelength versus wavelength; or 3) watts per unit wavelength versus wavelength. 500w lamp permits highest light throughput of any commercial instrument. Accessories permit corrected phosphorescence and polarization studies. Circle No. 16 on Reader Service Card.

VOLUME 43, NO. 11 SEPTEMBER 1971

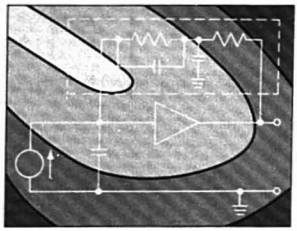

Our cover design is based on the Instrumentation feature, "High-Speed Current Measurements," page 00 A, by Pieter G. Cath and Alan M. Peabody of Keithley Instruments, Inc. Since the measurement of small electrical currents by electrometers furnishes the basis for a number of instrumental methods used by the modern analyst, the design techniques and optimization considerations discussed in this article should be of wide interest. Several approaches to rapid, sensitive current measurements are presented, and a discussion of amplifier-response tailoring is included.

This month's Report for Analytical Chemists, "Selection of an Optimum Analytical Technique for Process Control," page 00 A, by Frank A. Leemans of Dutch State Mines, reminds us that analytical chemists today are constantly confronted with the problem of making the right selection from a great variety of analytical techniques in solving problems. Dr. Leemans discusses some of the methodological and cost parameters to be considered in finding the optimum solution to a given analytical problem.

The Seventh International Symposium on Advances in Chromatography will be held November 29–December 3, 1971 at Caesar's Palace in Las Vegas, Nev. Details, including the technical program, are given on pages 00 A–00 A. Publication of the papers is planned for the December 1971 issue of ANALYTICAL CHEMISTRY.

ANCHAM

ANALYTICAL CHEMISTRY

Contents

Contributed Articles

Notes

Correspondence

Aids for Analytical Chemists

MANUSCRIPT REQUIREMENTS published in December 1970 issue, page 1879, outlines scope and copy requirements to be observed in preparing manuscripts for consideration. Manuscript (4 copies) should be submitted to ANALYTICAL CHEMISTRY, 1155 Sixteenth St., N.W., Washington, D. C. 20036.

The American Chemical Society assumes no responsibility for the statements and opinions advanced by contributors to its publications. Views expressed in the editorials are those of the editors and do not necessarily represent the official position of the American Chemical Society.

1971 Subscription Rates

	1 yr.	2 yr.	3 yr.
Members, domestic and foreign	$ 5.00	$ 9.00	$12.00
Nonmembers, domestic and Canada	7.00	12.00	16.00
Nonmembers, foreign except Canada	15.00	27.50	40.00

Postage: Canada and Pan-American Union, $2.50; foreign, $3.50. Single copies: current, $2.00 except Annual Reviews, $3.00 each. Rates for back issues and volumes are available from Special Issues Sales Dept., 1155 Sixteenth St., N.W., Washington, D. C. Claims for missing numbers will not be allowed if received more than 60 days from date of mailing plus time normally required for postal delivery of journal and claim. No claims allowed because of failure to notify the Subscription Service Department of a change of address or because copy is "missing from files."

Those interested in joining the American Chemical Society should write to Admissions Department at the Washington Office.

Published monthly with Review issue added in April and a Laboratory Guide in July by the American Chemical Society, from 20th and Northampton Sts., Easton, Pa. 18042; Executive Offices, Editorial Headquarters, and Subscription Service Department, 1155 Sixteenth St., N.W., Washington, D. C. 20036; Advertising Office, 142 East Ave., Norwalk, Conn. 06851. ANALYTICAL CHEMISTRY and other ACS periodicals are available on microfilm. For information write to: MICROFILM, Special Issues Sales, American Chemical Society, 1155 Sixteenth St., N.W., Washington, D. C. 20036. Second class postage paid at Easton, Pa.

CHANGE OF ADDRESS: Notify Subscription Service Department, American Chemical Society, 1155 Sixteenth St., N.W., Washington, D. C. 20036. Such notification should include both old and new addresses, with ZIP code numbers, and be accompanied by mailing label from a recent issue. Allow four weeks for change to become effective.

If you're not a statistician or a market researcher, don't read this page.

Model 1766. The Statistician. Available everywhere in the USA and Canada. Call (800) 631-1971 free for the Monroe office nearest you. In New Jersey call (800) 962-2804.

Single key summation of x, x^2 and n.

Σ_n^2

Two-key automatic summation of grouped data.

$\Sigma_n^2 \frac{0}{n}$ =

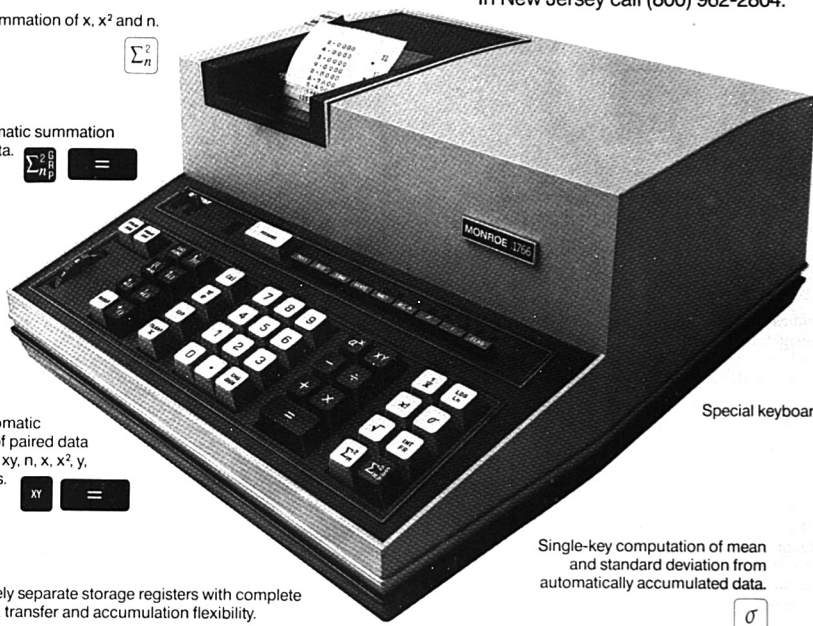

Two-key automatic summation of paired data accumulates xy, n, x, x^2, y, and y^2 factors.

XY =

Special keyboard functions for:

LOG Ln | $\frac{1}{x}$

$\sqrt{}$ | π e

a^x | x!

INT FR | EXP

Single-key computation of mean and standard deviation from automatically accumulated data.

σ

10 completely separate storage registers with complete entry, recall, transfer and accumulation flexibility.

Selective printout of entries and answers.

PRINT ENT | PRINT ANS

Up to 256 steps of decision-making learn-mode programming. Accessory card reader available for automatic entry of programs.

Litton **Monroe. The Calculator Company.**

550 Central Avenue, Orange, New Jersey 07051
81 Advance Road, Toronto 18, Ontario, Canada

CIRCLE 126 ON READER SERVICE CARD

Author Index

If you're not an engineer, scientist or technician, don't read this page.

Model 1666. Available everywhere in the USA and Canada.
Call (800) 631-1971 free for the Monroe office nearest you.
In New Jersey call (800) 962-2804.

Programming: Choose either 128 or 256-step models.

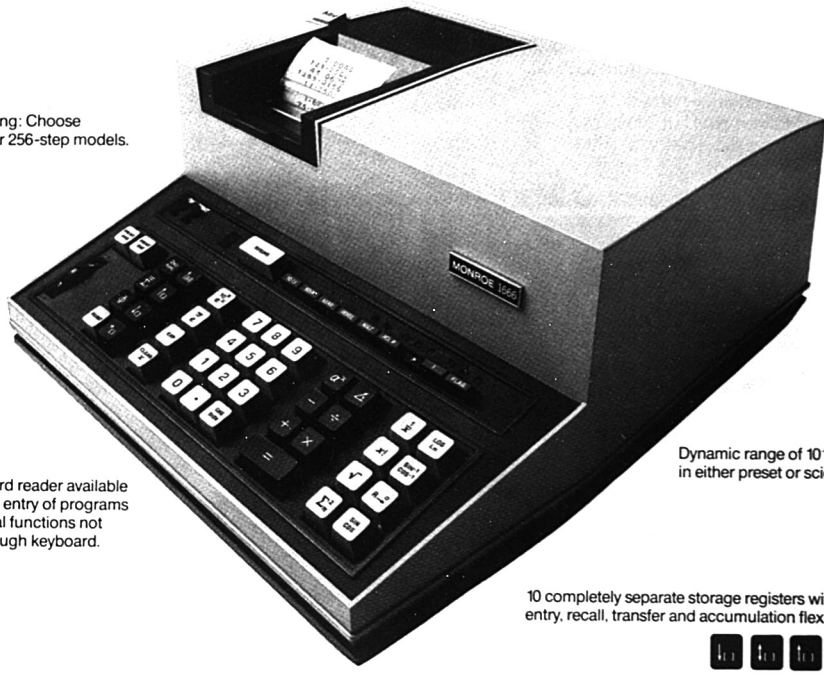

Dynamic range of 10^{+99} to 10^{-98} in either preset or scientific notation.

Accessory card reader available for automatic entry of programs and additional functions not available through keyboard.

10 completely separate storage registers with complete entry, recall, transfer and accumulation flexibility.

Automatic special functions for:

$\frac{1}{x}$ $\sqrt{\ }$

SIN COS LOG Ln

Σ_n^2 SIN^{-1} COS^{-1}

$R \rightarrow P$ π e

a^x $x!$

Complete program library covering every scientific and engineering discipline available to Monroe users.

Litton **Monroe. The Calculator Company.**

550 Central Avenue, Orange, New Jersey 07051
81 Advance Road, Toronto 18, Ontario, Canada

CIRCLE 127 ON READER SERVICE CARD

If you haven't read pages, please

Programmable models with accessory card reader for automatic program entry.

Printing models from under $300.00.
Non-printing models from $395.00.

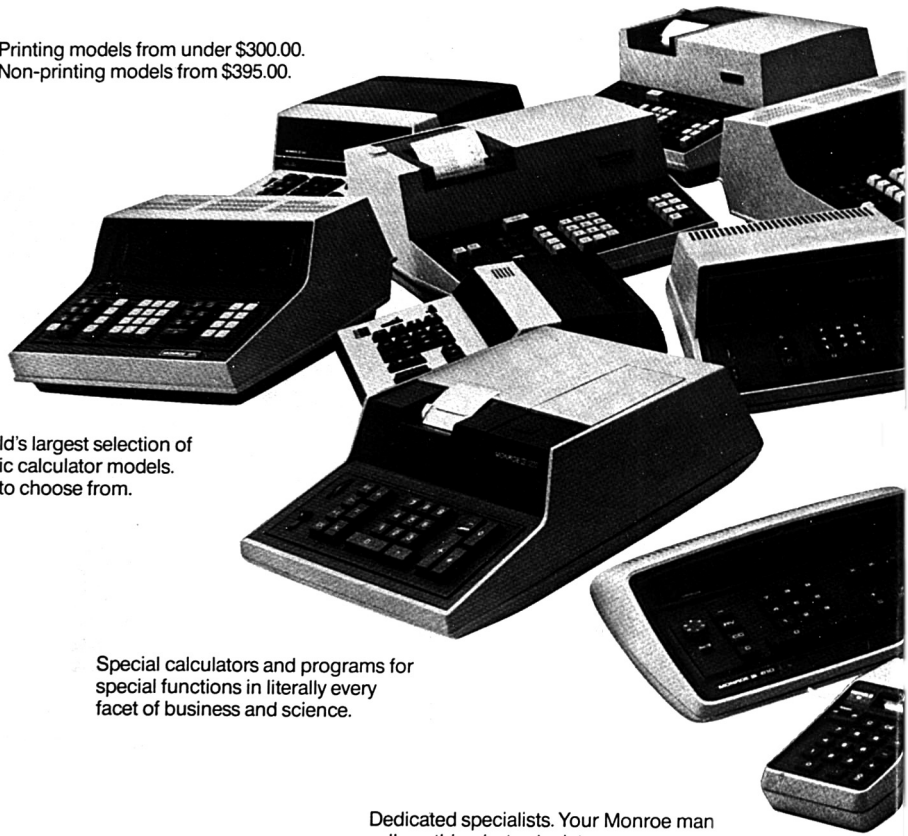

The world's largest selection of electronic calculator models. Over 30 to choose from.

Special calculators and programs for special functions in literally every facet of business and science.

Dedicated specialists. Your Monroe man sells nothing but calculators.
He knows them and your needs best.

any of the preceding read these two.

Service where you need it. From over 350 company-owned branches coast-to-coast.

Service when you need it. Over 2000 full time servicemen offer same-day service in every branch office.

Extra services: Your Monroe man stays with you long after the sale, training your staff and putting your calculators to work for you.

Litton Monroe.

The Calculator Company.

550 Central Avenue, Orange, New Jersey 07051
81 Advance Road, Toronto 18, Ontario, Canada

CIRCLE 128 ON READER SERVICE CARD

Titration

When you think Titration... think Radiometer!

Radiometer, a world leader in modular systems for potentiometric titrations, offers you a broad selection of titration control units, autoburettes, reaction vessels and recorders to form the capabilities that match your requirements and also meet your budget.

The modular system shown below provides pH stat and titration curve recording with unusual expanded scale capabilities, digital titrant volume readout, constant pH monitoring, quick change titrant burette assembly, BCD output for printer or data processor . . . and many additional features. In addition, its fine recorder may be used in many other laboratory activities.

Exclusive plug-in modules provide additional independent capabilities including: two channel operation, dual end-point titration and two way pH stat.

Whatever your potentiometric requirement, there is a Radiometer modular system for you . . . call your London Company representative or contact us directly.

THE LONDON COMPANY / 811 SHARON DRIVE / CLEVELAND, OHIO 44145
In Canada: Bach-Simpson Ltd. **Telephone:** (216) 871-8900

See us at Booth 231, ACS meeting, Washington, D.C.

CIRCLE 115 ON READER SERVICE CARD

What's NEW from BRUKER?

NEW INSTRUMENTS:

MINISPEC P20
Automated mini pulsed NMR spectrometer for quality control, routine laboratory tests and teaching purposes.

WIDELINE SPECTROMETER B-KR22-S
Variable frequency range: 3–31 MHz, based on crystal locked frequency synthesizer.

NEW SPECIFICATIONS for our HX90:

Our High Resolution Spectrometer HX90 is guaranteed for these additional specifications:

a. **LINE SHAPE:** line width of chloroform signal at average half height of the ^{13}C satellite:

	with 15" magnet	with 18" magnet
for 5 mm sample	15 Hz	12 Hz
for 10 mm sample	25 Hz	25 Hz
for 13 mm sample	–	30 Hz

at one fifth of the height of the ^{13}C satellite:

	with 15" magnet	with 18" magnet
for 5 mm sample	35 Hz	30 Hz
for 10 mm sample	50 Hz	50 Hz
for 13 mm sample	–	70 Hz

b. **SPINNING SIDEBANDS** for chloroform sample

	with 15" magnet	with 18" magnet
for 5 mm sample	1.0%	1.0%
for 10 mm sample	2.5%	2.5%
for 13 mm sample	–	4.0%

For excellence in design, engineering and service...

GO FOR BRUKER

For details, call or write:

IN U.S.A.
Bruker Scientific Inc.
1 Westchester Plaza, Elmsford, N.Y. 10523
(914) 592-5470

Bruker Magnetics Inc
1 Vinebrook Park, Burlington, Mass. 01802
(617) 272-9250

IN CANADA
Bruker Spectrospin Canada Ltd.
797 Don Mills Road, Don Mills, Ontario
(416) 429-2263

ENGLAND
Bruker Spectrospin Ltd.
19, Nordic Drift
Coventry CV 2 2 DE
Tel. (0203) 32 69 45

FRANCE
Bruker Spectrospin SA
7, rue de la Paix
(67) Wissembourg
Tel. (088) 94.02.42

ITALY
Bruker Spectrospin srl.
Via Pasquale Miglioretti, 2
20161 Milano
Tel. (02) 64 64 261

SWITZERLAND
Spectrospin AG
8117 Zurich-Fallanden
Industriestrasse 26
Tel. (051) 85 48 55

W. GERMANY
Bruker-Physik AG
7501 Forcheim
Tel. (0721) 5 80 70
Tx. (07) 826 836

CIRCLE 40 ON READER SERVICE CARD

This analytical balance weighs almost nothing

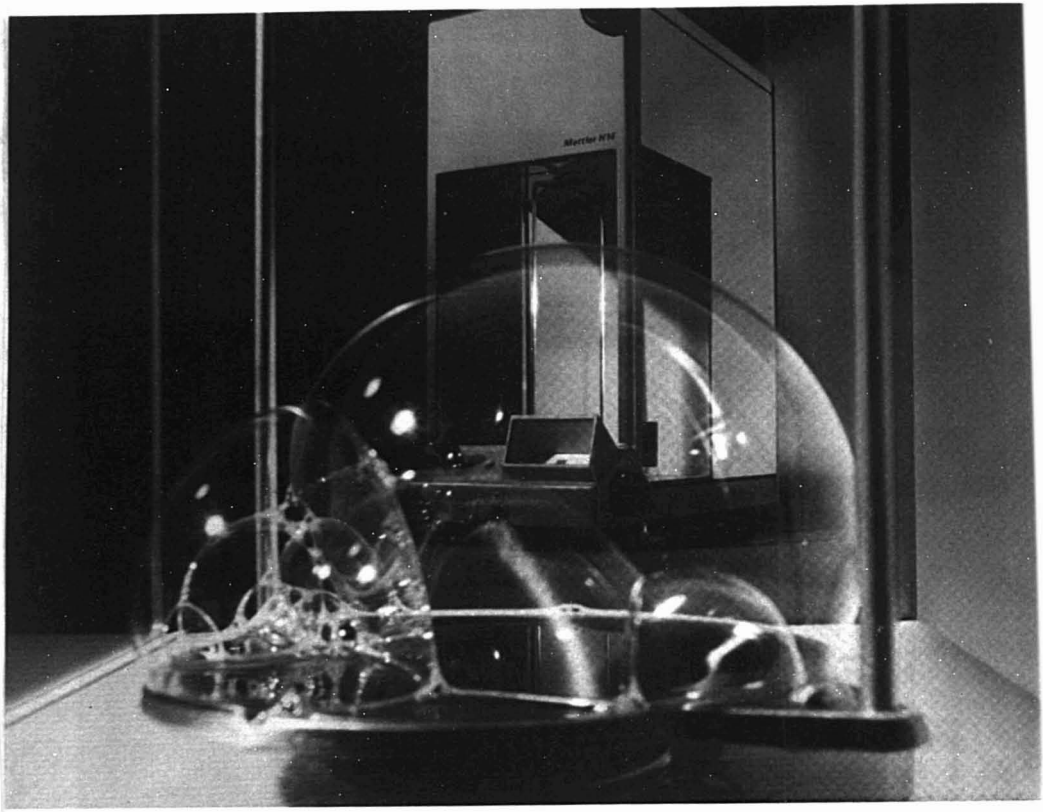

...even elusive bubbles to one part in 3,220,000

All 17 Mettler analytical balances, model for model, have the highest precision/capacity ratios obtainable. From the macro balance H8 with a capacity of 160 g and a precision of ±0.3 mg to the ultra micro UM7 with a capacity of 3 mg and a precision of ±0.1 ug. And all Mettler analyticals offer unparalleled speed.

Other Mettler features make the whole weighing task easier, more convenient while minimizing risk of error. Rapid taring lets you dial off container weights, up to the full capacity of the balance, in seconds. Thus there are no arithmetic computations. And automatic preweighing shows approximate weight on the pan instantly. A filling guide reduces weighing-in time. Weight locking prevents operation of the weight knob for heavier weights when the beam is released ...extending the life of the instrument. Weight knob direction indicator on the optical readout shows the way to dial mechanical weights.

Various readouts of weighing results are available... digital, analog, vernier, micrometer... depending on the instrument model.

The newest Mettler analyticals have the ability to convert results into electrical signals to be fed to recorders, digital printers, calculators, tape and card punchers, computers and electronic data storage systems.

Ask us for our analytical balance catalog. We are Mettler Instrument Corporation, Box 3000, Princeton, N. J. 08540. Phone: 609-448-3000.

Mettler

CIRCLE 122 ON READER SERVICE CARD

A C BRIEFS

Highlights of Articles in This Issue

Electrophoretic Separation of Alkylsulfate, Alkylbenzenesulfonate, and Alkylethoxysulfate Homologs, Using Aqueous Dioxane Agarose Gels

The necessity for using media with micelle denaturizing properties, for the separation of these homologs, is demonstrated.

JOHN R. BODENMILLER and HOWARD W. LATZ, Department of Chemistry, Ohio University, Athens, Ohio 45701

Anal. Chem., 43, 1354 (1971)

Computer Techniques for Identifying Low Resolution Mass Spectra

Several search algorithms were implemented as computer programs and tested using 125 "unknown" mass spectra. Very high search speeds and excellent recognition performance were achieved with even the simplest algorithm.

STANLEY L. GROTCH, Jet Propulsion Laboratory, California Institute of Technology, Pasadena, Calif. 91103

Anal. Chem., 43, 1362 (1971)

Effect of pH and Ionic Strength on Ion Exchange and Chelating Properties of an Iminodiacetate Ion Exchange Resin with Alkaline Earth Ions

Competition between chelation and ion exchange occurs at intermediate pH. Average coefficient of multiple correlation is 0.9765 for log V_{max} equations. Apparent pK_1 value agrees with values by other methods.

GEORGE H. LUTTRELL, Jr., CARL MORE, and CHARLES T. KENNER, Department of Chemistry, Southern Methodist University, Dallas, Texas 75222

Anal. Chem., 43, 1370 (1971)

Spectrophotometric Determination of Niobium with 4-(2-Pyridylazo)Resorcinol and Colored Complexes Separated from Oxalic and Tartaric Acid Systems

Extractable niobium complexes containing mixed-ligand spheres are involved in spectrophotometric determination with PAR in oxalato media, and oxo-tartrato-PAR niobium complexes are present in aqueous tartrato systems, as shown by solutions and solid state study.

MARIJA ŠIROKI, Laboratory of Analytical Chemistry, Faculty of Science, Institute for Inorganic and Analytical Chemistry, The University, Zagreb, Yugoslavia, and CIRILA DJORDJEVIC, Department of Chemistry, College of William and Mary, Williamsburg, Va. 23185

Anal. Chem., 43, 1375 (1971)

Gas Chromatographic Determination of Rafoxanide [3'-Chloro-4'-(4-Chlorophenoxy)-3,5-Diiodosalicylanilide] in Plasma by Electron Capture Detection of Its Trimethylsilyl Derivative

Rafoxanide has been determined in plasma by gas chromatography on a four-inch column with electron capture detection. The method is quantitative down to 0.01 μg rafoxanide per ml of plasma.

CHARLES P. TALLEY, NELSON R. TRENNER, GEORGE V. DOWNING, Jr., and W. J. A. VANDENHEUVEL, Merck Sharp & Dohme Research Laboratories, Rahway, N. J. 07065

Anal. Chem., 43, 1379 (1971)

Method for Calculating Cross-Contamination in Column Chromatographic Separation of Radioactive Parent–Daughter Pairs

A general method has been devised for analyzing distorted chromatograms resulting from column separations of genetically coupled radioactive species, P and D, where transformation from P to D occurs at a rate comparable to the duration of the elution process.

P. J. KAROL, Department of Chemistry, Carnegie-Mellon University, Pittsburgh, Pa. 15213

Anal. Chem., 43, 1383 (1971)

Separation of Uranium from Seawater by Adsorbing Colloid Flotation

A rapid absorbing colloid flotation technique based on a ferric hydroxide–sodium dodecyl sulfate–air system has been developed for the separation of uranium from seawater.

YOUNG S. KIM and HARRY ZEITLIN, Department of Chemistry and Hawaii Institute of Geophysics, University of Hawaii, Honolulu, Hawaii 96822

Anal. Chem., 43, 1390 (1971)

Analysis of Binary Mixtures by Thermometric Titration Calorimetry

A mixture of two reactants having equal or nearly equal equilibrium constants for reaction with a common titrant can be analyzed with a relative error of 5% by a single calorimetric titration.

LEE D. HANSEN and EDWIN A. LEWIS, Chemistry Department, University of New Mexico, Albuquerque, N. M. 87106

Anal. Chem., 43, 1393 (1971)

Rotated Mercury Cell for Controlled Potential Coulometry. Elimination of Background Current by Digital Normalization

A rotated mercury cell for controlled potential coulometry has been developed and evaluated with several chemical systems. Electrolytic rate constants that are relatively large, rapid sparging, and low cell noise are some of the advantages of this cell.

RAY G. CLEM, FREDI JAKOB, DANE H. ANDERBERG, and LAWRENCE D. ORNELAS, Nuclear Chemistry Division and Lawrence Radiation Laboratory, University of California, Berkeley, Calif. 94720

Anal. Chem., 43, 1398 (1971)

Analytical Applications of X-Ray Excited Optical Fluorescence. Direct Determinations of Rare Earth Nuclear Poisons in Uranium at the Part per Giga (1 in 10^9) Level

The nuclear poisons Gd, Sm, Eu, and Dy can be directly determined at the ppg level (1 in 10^9) in nuclear grade uranium by the optical fluorescence emitted under X-ray excitation.

ARTHUR P. D'SILVA and VELMER A. FASSEL, Institute for Atomic Research and Department of Chemistry, Iowa State University, Ames, Iowa

Anal. Chem., 43, 1406 (1971)

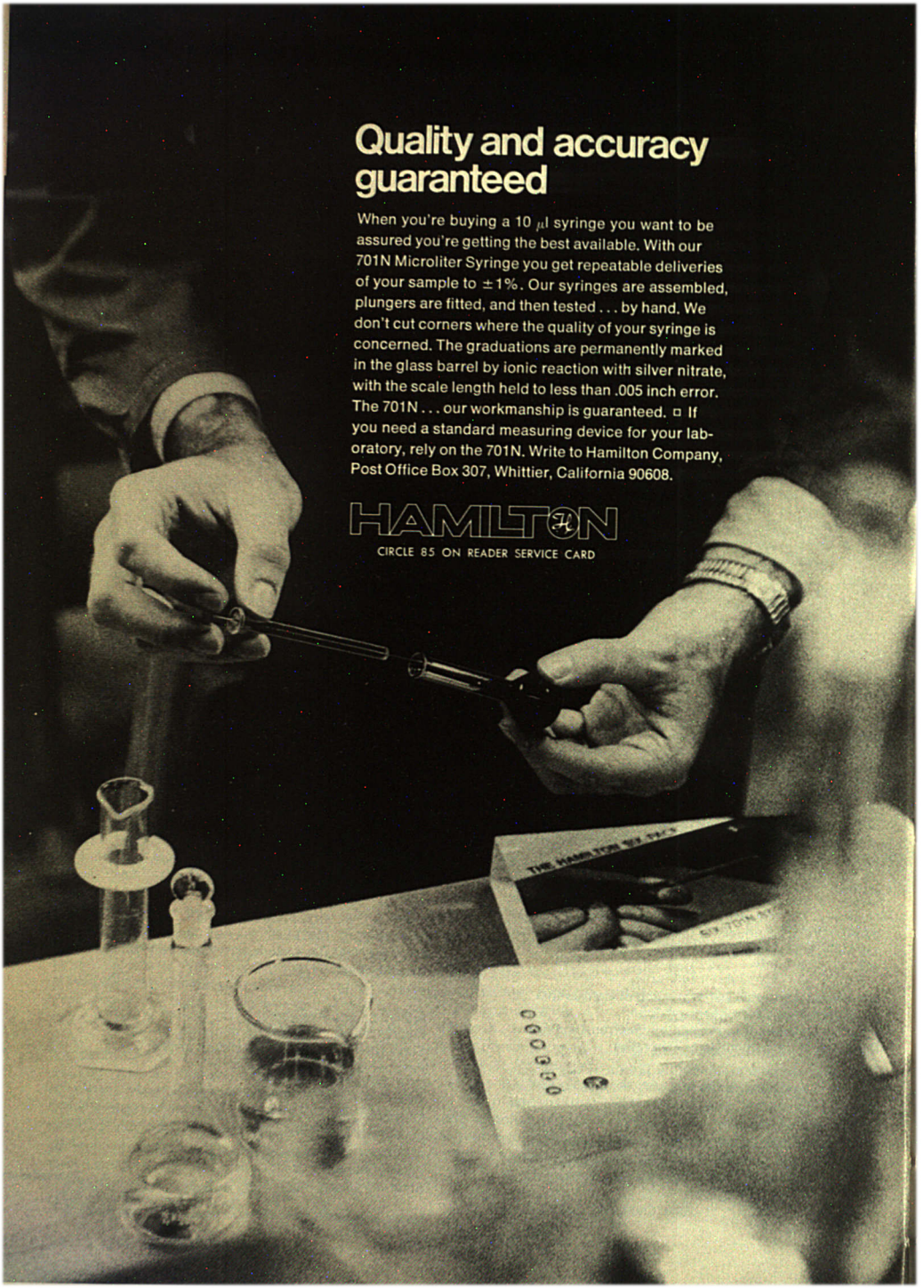
Quality and accuracy guaranteed
When you're buying a 10 μl syringe you want to be assured you're getting the best available. With our 701N Microliter Syringe you get repeatable deliveries of your sample to ±1%. Our syringes are assembled, plungers are fitted, and then tested . . . by hand. We don't cut corners where the quality of your syringe is concerned. The graduations are permanently marked in the glass barrel by ionic reaction with silver nitrate, with the scale length held to less than .005 inch error. The 701N . . . our workmanship is guaranteed. ▫ If you need a standard measuring device for your laboratory, rely on the 701N. Write to Hamilton Company, Post Office Box 307, Whittier, California 90608.
HAMILTON
CIRCLE 85 ON READER SERVICE CARD

Analysis of Mixtures of Isomeric Polynuclear Hydrocarbons by Nuclear Magnetic Resonance Spectrometry. Methylated Derivatives of Anthracene, Benz[a]anthracene, Benzo[c]phenanthrene, and Pyrene

An NMR method suitable for the qualitative and quantitative determination of methylaromatic compounds in environmental mixtures is described.

LARRY K. KEEFER, LAWRENCE WALLCAVE, JAMES LOO, and RUTH S. PETERSON, The Eppley Institute for Research in Cancer, University of Nebraska Medical Center, Omaha, Neb. 68105

Anal. Chem., 43, 1411 (1971)

Gas Chromatographic Determination of Aqueous Trace Hydrazine and Methylhydrazine as Corresponding Pyrazoles

The quantitative reaction of 2,4-pentanedione with selected hydrazines to form substituted pyrazoles is followed by the gas chromatographic determination of 0.1 to 50 ppm hydrazine and methylhydrazine in aqueous solution.

L. A. DEE, Air Force Rocket Propulsion Laboratory, Air Force Systems Command, United States Air Force, Edwards, Calif.

Anal. Chem., 43, 1416 (1971)

Determination of Mercury in Biological and Environmental Samples by Neutron Activation Analysis

Mercury is determined in various samples from aquatic environment and biological tissues using a neutron activation analysis procedure. Concentrations of several ppb are measurable by this method.

K. K. SIVASANKARA PILLAY, CHARLES C. THOMAS, Jr., JAMES A. SONDEL, and CAROLYN M. HYCHE, Western New York Nuclear Research Center, State University of New York at Buffalo, Buffalo, N. Y. 14214

Anal. Chem., 43, 1419 (1971)

Low-Resolution Mass Spectrometric Determination of Aromatics and Saturates in Petroleum Fractions

A new low-resolution mass spectrometric procedure determines up to 25 saturated and aromatic compound types in petroleum fractions boiling in the 200–1100 °F range without need for physical separations.

C. J. ROBINSON, Research and Development Department, American Oil Company, Whiting, Ind. 46394

Anal. Chem., 43, 1425 (1971)

Spectrofluorimetric Determination of Orthophosphate as Rhodamine B Molybdophosphate

0.04 to 0.6 μg of orthophosphate is determined spectrofluorimetrically as Rhodamine B molybdophosphate after extraction into chloroform:butanol. Of 37 ions examined, only arsenic and vanadium interfere, but these can be tolerated at 25- and 50-fold excesses, respectively.

G. F. KIRKBRIGHT, R. NARAYANASWAMY, and T. S. WEST, Chemistry Department, Imperial College, London, S.W. 7, U.K.

Anal. Chem., 43, 1434 (1971)

Application of an Iodide-Specific Resin to the Determination of Iodine in Biological Fluids by Activation Analysis

Selective and quantitative retention of iodide is achieved with an "iodinated" resin. A simple and rapid method based on the isolation of ^{128}I with this resin has been applied to the activation analysis of biological fluids.

MICHEL HEURTEBISE and W. J. ROSS, Sección Química, Instituto Venezolano de Investigaciones Científicas, Apartado 1827, Caracas, Venezuela

Anal. Chem., 43, 1438 (1971)

Qualitative Studies of Trace Constituents by Plasma Chromatography

Qualitative plasmagram patterns characteristic of benzoic acid, salicylaldehyde, phenethyl alcohol, acetophenone, and naphthalene are interpreted for sub-ppb concentrations in a gas.

FRANCIS W. KARASEK, University of Waterloo, Waterloo, Ontario, and WALLACE D. KILPATRICK and MARTIN J. COHEN, Franklin GNO Corporation, P.O. Box 3250, West Palm Beach, Fla. 33402

Anal. Chem., 43, 1441 (1971)

An Instrument for Measuring the Hydrogen Content of Metals

The instrument described in this article was designed to measure the hydrogen content of a metal in the range from 0.01 wppm to 100 wppm using a specimen size ranging from 0.1 gram to 5.0 grams.

J. B. CONDON, R. A. STREHLOW, and G. L. POWELL, Union Carbide Corporation, Nuclear Division, Oak Ridge, Tenn. 37830

Anal. Chem., 43, 1448 (1971)

Effect of Atmosphere on Spectral Emission from Plasmas Generated by the Laser Microprobe

Signal-to-background ratios from iron and magnesium samples in argon, air, oxygen, nitrogen, helium, and vacuum were investigated at 1.2, 3.6, and 8.0 mJ laser energy levels.

WILLIAM J. TREYTL, KENNETH W. MARICH, JAMES B. ORENBERG, PETER W. CARR, D. CRAIG MILLER, and DAVID GLICK, Division of Histochemistry, Department of Pathology, Stanford University School of Medicine, Stanford, Calif. 94305

Anal. Chem., 43, 1452 (1971)

Improved Enzyme Electrode for Amygdalin

An enzyme electrode responsive to amygdalin is constructed by immobilizing the enzyme β-glucosidase in a polyacrylamide gel layer on the surface of a crystal membrane cyanide electrode.

R. A. LLENADO and G. A. RECHNITZ, Department of Chemistry, State University of New York, Buffalo, N. Y. 14214

Anal. Chem., 43, 1457 (1971)

THE COLUMN YOU ARE LOOKING FOR

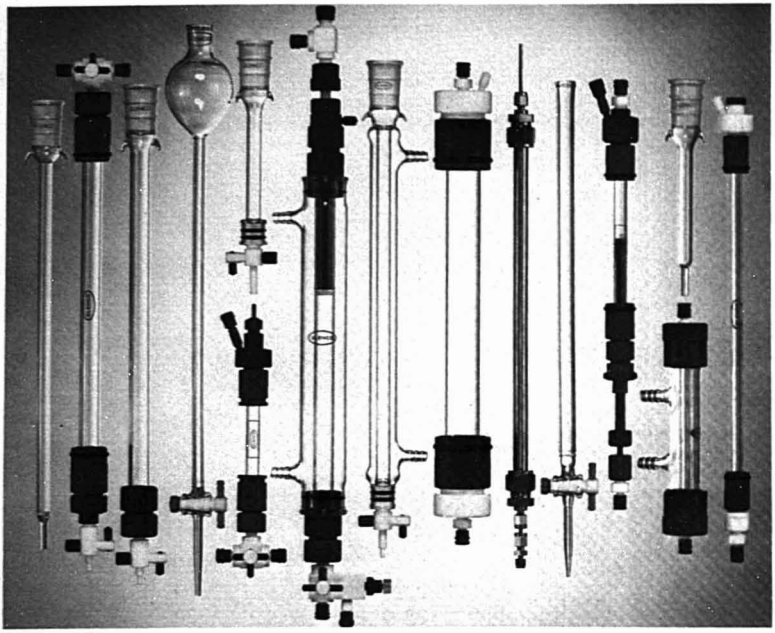

HAS A GLENCO STOCK NUMBER

Membrane Probe–Spectral Emission Type Detection System for Mercury in Water

Mercury compounds are reduced to Hg^0 and diffused through a rubber membrane into a helium gas stream. Using a dc discharge and the 2537-Å line, 4 ppt or 0.4 ng Hg is detected.

ROBERT S. BRAMAN, Department of Chemistry, University of South Florida, Tampa, Fla. 33620

Anal. Chem., 43, 1462 (1971)

Direct Enthalpimetric Determination of Olefins

Direct injection enthalpimetry, taking advantage of the heat of hydrogenation of olefins on Pd, permits their rapid determination in quantities of 1–100 μmoles with an error of 1–2%.

DONALD W. ROGERS, Chemistry Department, The Brooklyn Center, Long Island University, Brooklyn, N. Y. 11201

Anal. Chem., 43, 1468 (1971)

Automated Data Acquisition System and Computer Analysis for Sedimentation Equilibrium Experiments

An automated data acquisition system and computer analysis, which can be used with a wide variety of sedimenting systems at sedimentation equilibrium, are described.

A. C. BECKWITH, H. C. NIELSEN, and R. O. BUTTERFIELD, Northern Regional Research Laboratory, Northern Marketing and Nutrition Research Division, Agricultural Research Service, U. S. Department of Agriculture, Peoria, Ill. 61604

Anal. Chem., 43, 1471 (1971)

Simplified Rapid Procedure for Determination of Agmatine and Other Guanidino-Containing Compounds

Described is a colorimetric procedure applicable for routine laboratory determinations of agmatine in the presence of arginine and quantitation of agmatine and other guanidino-containing compounds by this method.

MILLICENT C. GOLDSCHMIDT and BETTY M. LOCKHART, Department of Clinical Pathology, The University of Texas M. D. Anderson Hospital and Tumor Institute at Houston, and The University of Texas Graduate School of Biomedical Sciences, Houston, Texas 77025

Anal. Chem., 43, 1475 (1971)

On-Line Interactive Data Processing. I. As Applied to Mass Spectrometry and Gas Chromatography

An on-line interactive computer system with an oscilloscopic display terminal is described. The approach taken allows the chemist to impose his experienced judgment on the net data processing procedure.

J. W. FRAZER, L. R. CARLSON, A. M. KRAY, and M. R. BERTOGLIO, Lawrence Radiation Laboratory, University of California, Livermore, Calif. 94550, and S. P. PERONE, Chemistry Department, Purdue University, Lafayette, Ind. 47907

Anal. Chem., 43, 1479 (1971)

On-Line Interactive Data Processing. II. Processing Voltammetric Electrochemical Data

This work illustrates the application of a computerized interactive processing system to single-sweep and cyclic-sweep voltammetric data.

S. P. PERONE, Chemistry Department, Purdue University, Lafayette, Ind. 47907, and J. W. FRAZER and ARTHUR KRAY, Lawrence Radiation Laboratory, University of California, Livermore, Calif. 94550

Anal. Chem., 43, 1485 (1971)

Molecular Interactions of Asphalt. Tentative Identification of 2-Quinolones in Asphalt and Their Interaction with Carboxylic Acids Present

Hydrogen-bonding association between 2-quinolones and carboxylic acids in asphalt was studied by infrared spectrometry using a silylation reaction. Solvent effects on hydrogen-bonding complexes and carbonyl compounds are demonstrated.

J. C. PETERSEN, R. V. BARBOUR, S. M. DORRENCE, F. A. BARBOUR, and R. V. HELM, Laramie Energy Research Center, Bureau of Mines, U. S. Department of Interior, P.O. Box 3395, University Station, Laramie, Wyo. 82070

Anal. Chem., 43, 1491 (1971)

Notes

Application of Rapid Infrared Spectrometry to Air Pollution Research

Composition of a gas stream was continuously monitored, in-line, upstream, and downstream from a reaction vessel by infrared spectrometry. Sulfur dioxide concentrations were determined as low as 200 ppm.

JOSEPH R. COMBERIATI, Morgantown Energy Research Center, Bureau of Mines, United States Department of the Interior, Morgantown, W. Va.

Anal. Chem., 43, 1497 (1971)

Analysis of Deuteriobenzonitriles by Carbon-13 Nuclear Magnetic Resonance Spectrometry

The use of ^{13}C magnetic resonance to determine the qualitative and quantitative composition of deuterium-substituted benzonitriles is described; compared to ordinary proton magnetic resonance techniques, the method is simpler and more accurate.

G. L. LEBEL, J. D. LAPOSA, B. G. SAYER, and R. A. BELL, Department of Chemistry, McMaster University, Hamilton, Ontario, Canada

Anal. Chem., 43, 1500 (1971)

Differential Reduction and Atomic Absorption Determination of Selenium

This paper presents a technique for the quantitative separation of selenium from impure materials, and its differential determination by hydrazine sulfate reduction and atomic absorption measurement.

WLADISLAW REICHEL, Canadian Copper Refiners Limited, Montreal East, Quebec, Canada

Anal. Chem., 43, 1501 (1971)

DETERMINE LEAD AT THE PART-PER-BILLION LEVEL

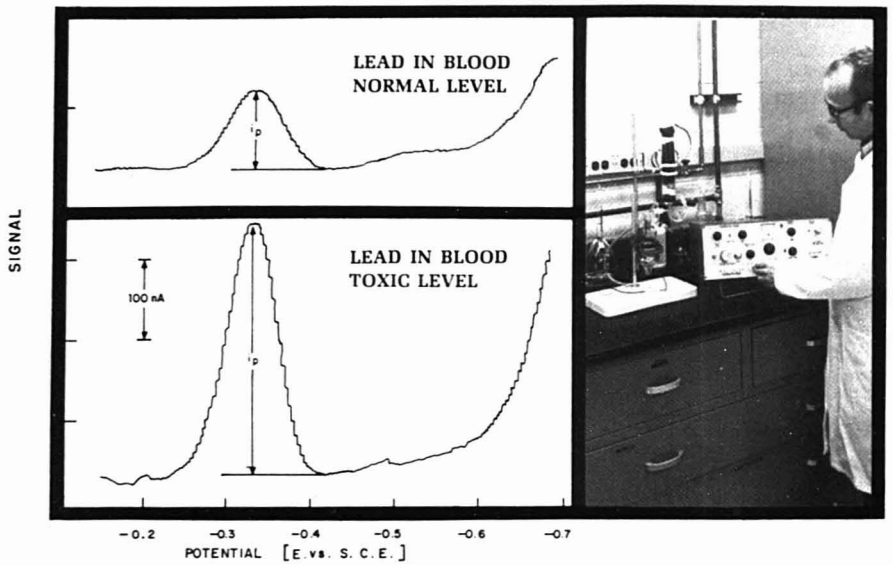

For example, the above curves show the ability of the PAR™ Model 174 Polarographic Analyzer to accurately determine **lead in blood.** Blood samples of 50 μl can be employed and lead concentrations well below toxic levels can be easily determined.

But if you're not interested in detecting lead, it's important to note that the 174 can analyze hundreds of different materials as well, including organics, inorganics and other trace metals.

The PAR™ Model 174 Polarographic Analyzer is the only instrument in its price range to provide this capability. Its part-per-billion sensitivity permits accurate simultaneous qualitative and quantitative analyses to be performed. Low initial and operating costs and ease of operation make this the instrument of choice where measurements must be performed quickly and easily. These features have been important factors in application of the 174 in the analysis of pharmaceuticals, pollutants, metallurgical samples and a broad variety of analytes.

Techniques possible include dc, pulse and differential pulse polarography, stripping analyses, differential pulse stripping analysis and linear sweep voltammetry. Accessories permit dual cell differential operation, ac polarography and other useful techniques. A complete line of cells and electrodes is also available. Price of the 174 is $2250 including mechanical drop timer. Contact P.A.R. for the latest information about how this versatile instrument can improve your analytical results. Phone (609) 452-2111 or write Princeton Applied Research Corporation, Dept. A , P.O. Box 2565, Princeton, New Jersey 08540.

PAR PRINCETON APPLIED RESEARCH CORPORATION

CIRCLE 166 ON READER SERVICE CARD

Filters for X-Ray Spectrometry Prepared by Thin-Layer Electrodeposition

The preparation of X-ray filters by electrodeposition of metals onto pyrolytic graphite is described. Such filters have high uniformity and stability, and can be produced in precisely controlled thicknesses.

BASIL H. VASSOS, ROLAND F. HIRSCH, and DONALD G. PACHUTA, Chemistry Department, Seton Hall University, South Orange, N. J. 07079

Anal. Chem., 43, 1503 (1971)

Hydrated Porosity Macroreticular Cation Exchange Resins *via* Nuclear Magnetic Resonance

The hydrated porosity of a macroreticular cation exchange resin has been obtained via NMR. The dry porosity has been obtained via conventional techniques. The effect of resin swelling on the hydrated porosity is considered.

L. S. FRANKEL, Rohm and Haas Company, 5000 Richmond Street, Philadelphia, Pa. 19137

Anal. Chem., 43, 1506 (1971)

Ultraviolet Refractive Indices of Aqueous Solutions of Urea and Guanidine Hydrochloride

Refractive index data down to 1950 Å are reported for aqueous solutions of urea and guanidine hydrochloride. Comparison with N_{D} values and with values reported at 2655 Å give an expected error of 0.6 to 0.8%.

J. R. KRIVACIC and D. W. URRY, Division of Molecular Biophysics Laboratory of Molecular Biology, University of Alabama Medical Center, 1919 Seventh Avenue South, Birmingham, Ala. 35233

Anal. Chem., 43, 1508 (1971)

Determination of Mercury by a Combustion Technique Using Gold as a Collector

Thermal decomposition of mercury-containing substances allows mercury to be collected on a gold-coated substrate for subsequence analysis. The results are compared with those obtained by neutron activation and atomic absorption methods.

D. H. ANDERSON, J. H. EVANS, J. J. MURPHY, and W. W. WHITE, Industrial Laboratory, Kodak Park Division, Eastman Kodak Company, Rochester, N. Y. 14650

Anal. Chem., 43, 1511 (1971)

High-Speed Ion Exchange Chromatography of Several Monosubstituted Pyridine Isomers

Results are presented for the separation of several monosubstituted pyridine isomers and the quantitation of the three isomeric cyanopyridines. Relative standard deviation is about 1%.

CHARLES P. TALLEY, Merck Sharp & Dohme Research Laboratories, Rahway, N. J. 07065

Anal. Chem., 43, 1512 (1971)

Determination of Water Associated with Metal Chelates by Gas Chromatography

Either a direct method, in which the chelate solution and the blank water-saturated solvent solution are injected separately, or a differential method, in which the chelate and blank are injected simultaneously through two identical columns of a dual channel instrument, can be used.

DENNIS GAEDE and CLIFTON E. MELOAN, Department of Chemistry, Kansas State University, Manhattan, Kan. 66502

Anal. Chem., 43, 1515 (1971)

Gas Chromatographic Separation and Determination of Isomeric Methylbenzene Tricarbonylchromium Complexes

The GC separation and determination of isomeric di-, tri-, and tetra-methylbenzene tricarbonylchromium complexes is reported. All of the complexes were determined pyrolytically on a SCOT column. The trimethylbenzene complexes were determined without decomposition on a packed column.

JANET S. KELLER, HANS VEENING, and BENNETT R. WILLEFORD, Department of Chemistry, Bucknell University, Lewisburg, Pa. 17837

Anal. Chem., 43, 1516 (1971)

Polarimetric Studies of Alkali Metal Ion Complexes of *l-trans*-1,2-Diaminocyclohexane-*N,N,N′,N′*-Tetraacetic Acid

The interactions of the alkali metal ions, lithium, sodium, potassium and cesium, with *l-trans*-1,2-diaminocyclohexane-*N,N,N′,N′*-tetraacetic acid are investigated over the pH range 1.5–13.5.

JAMES D. CARR and D. G. SWARTZFAGER, Department of Chemistry, University of Nebraska, Lincoln, Neb. 68508

Anal. Chem., 43, 1520 (1971)

Titration Errors in Chelometric Titrations Employing Ion-Selective Indicator Electrodes

The error in chelometric titrations using ion-selective indicator electrodes is less than 1% when sample ion concentration $\geq 10^{-2}$, metal-complex dissociation constant $\leq 10^{-8}$, and potentiometric interference level $\leq 10^{-3}$.

FRANKLIN A. SCHULTZ, Department of Chemistry, Florida Atlantic University, Boca Raton, Fla. 33432

Anal. Chem., 43, 1523 (1971)

Automated Method for Determination of Mercury

An automated version of the cold vapor atomic absorption technique for mercury analysis is described. The method allows 22 samples to be analyzed per hour with good accuracy and precision.

B. W. BAILEY and F. C. LO, Division of Laboratories and Research, New York State Department of Health, Albany, N. Y. 12201

Anal. Chem., 43, 1525 (1971)

The Precision Performer in the Thermal Analysis Field
—from CSI-Stone

Unequaled system sensitivity—5microvolts full scale

FULL SCALE RANGE:
.01 millical/sec/inch at 0° C system temperature.
Pressure operation 10^{-2} torr to 3000 psig.
Temperature ranging from -160° to 1800° C.

COMPLETE RANGE OF SAMPLE HOLDERS:
Ring or post type T/C.
Pressure from 3000 psig to 10^{-6} torr.
Temperature from -160° to 1600° C.
Single and dual sample capacity.

COLUMBIA SCIENTIFIC INDUSTRIES, INC.
ANALYTICAL & INDUSTRIAL DIVISION
P. O. Box 6190, Austin, Texas 78702 Telephone 512/926-1530
CIRCLE 41 ON READER SERVICE CARD

A C BRIEFS

Countercurrent Distribution as a Tool for Purification of Hypothalamic Hormones on a Preparative Scale

The technique of countercurrent distribution by the single withdrawal method was successfully used for the purification of LH-releasing hormone (LH-RH) on a preparative scale. The advantages and suitability of the CCD method for this type of separation were discussed.

A. V. SCHALLY, R. M. G. NAIR, and W. H. CARTER, Endocrine and Polypeptide Laboratories, Veterans Administration Hospital and Department of Medicine, Tulane University School of Medicine, New Orleans, La. 70140

Anal. Chem., 43, 1527 (1971)

Solvent Isotope Effects on Decomposition of N,N-Dialkyldithiocarbamic Acids

Solvent isotope effects on the decomposition of several *N,N*-dialkyldithiocarbamic acids are reported. It is concluded that depending on the size of substituent, the rate-determining step is either proton transfer or cleavage of the dithiocarbamic acid molecule.

K. I. ASPILA, S. J. JORIS, and C. L. CHAKRABARTI, Department of Chemistry, Carleton University, Ottawa, Ontario, K1S 5B6, Canada

Anal. Chem., 43, 1529 (1971)

Gas Chromatographic Determination of Penicillins

The quantitative determination of several penicillins by a gas–liquid chromatographic method is described. Silyl esters of penicillin G, penicillin V, phenethicillin, methicillin, oxacillin, cloxacillin, and dicloxacillin have been chromatographed isothermally at 245° or 275° C on a column packed with 2% OV-17 on a diatomaceous earth.

CHARLES HISHTA, DAVID L. MAYS, and MICHAEL GAROFALO, Bristol Laboratories, Division of Bristol-Myers Company, Syracuse, N. Y.

Anal. Chem., 43, 1530 (1971)

Correspondence

The Internal Reflection Probe

N. J. HARRICK, Harrick Scientific Corporation, Ossining, N. Y. 10562

Anal. Chem., 43, 1533 (1971)

Changes of Drop-Shapes on Freezing

R. A. STAIRS, Department of Chemistry, Trent University, Peterborough, Ontario, Canada

Anal. Chem., 43, 1535 (1971)

Aids for Analytical Chemists

New Use for a 0.5-Nanometer Molecular Sieve Gas Chromatography Column

W. A. McALLISTER and W. V. SOUTHERLAND, Department of Chemistry, East Carolina University, Greenville, N. C. 27834

Anal. Chem., 43, 1536 (1971)

Our helium does nothing 0.0004% better.

We guarantee it to be 99.9999% pure. Better than any current government specification.
You can use it for chromatographic separations, even without further purification. And when the analysis comes out 2 parts per million Nitrogen you can be sure it's in the sample. Not in the carrier gas.
So if you'd like to find out more about how our helium does less, just call Hank Grieco at (201) 464-8100. Or write to him at Airco Industrial Gases, 575 Mountain Avenue, Murray Hill, New Jersey 07974. Where we do a lot to make sure our helium doesn't.

CIRCLE 2 ON READER SERVICE CARD

AIRCO
Industrial Gases

KEITHLEY WIDEBAND LOCK-IN AMPLIFIERS

...Price, Performance and now, *Guaranteed User Satisfaction**

NEW LINE/BATTERY POWERED MODEL 850 AUTOLOC™ AMPLIFIER ranks as Keithley's premier wideband lock-in amplifier. A complete, compact, state-of-the-art instrument, the 850 easily recovers signals over 100 dB below noise, with full scale sensitivities from 1 microvolt to 100 millivolts. Convenient push-button selected line frequency notch and low pass filters improve signal recovery capability. Non-coherent inputs 1000 times full scale up to 1.0 volt provide no difficulty for the 850. Set-up problems are virtually eliminated, allowing users to get on with the business of making measurements. The 850's powerful reference channel does all the work. Just put in your reference and let the 850 take over with automatic frequency tracking and 3 second acquisition time. It will handle almost any waveform and still give you 370° calibrated phase adjustment, built-in second harmonic and quadrature switching with unsurpassed accuracy. There's no better signal recovery system at $1,995. Line power only version — $1,895.

MODEL 88 BOXCAR DETECTOR offers user versatility and low price. Sensitive to 100 microvolts, the 88 has 3 nanosecond gate opening time with scan rates to 5 microseconds. Linearity is better than 0.1%, providing for excellent waveform analysis. Up to 1 volt input noise can be handled without loss in linearity. Only $2,500.

NEW LOW COST MODEL 840 AUTOLOC™ AMPLIFIER takes the work out of using lock-in amplifiers. Affording high-performance and economy, the 840 measures from 25 nanovolts to 1 volt with convenient differential input. Selectable AC and DC gain optimize stability and noise rejection. Signals up to 90 dB below noise are easily recovered and extension to 140 dB is possible with filter cards. Versatile wideband operation to 15 kHz and convenient signal and reference monitoring points make the 840 a pleasure to use. The powerful reference channel offers automatic frequency tracking, 370° calibrated phase adjustment, switched quadrature, and built-in second harmonic. Virtually any reference may be used. The 840 is a lot of lock-in for only $1,395.

MODEL 103A NANOVOLT AMPLIFIER is an ideal companion for Keithley Lock-in Amplifiers. Single ended or differential input permits measurements to 1 nanovolt and input noise figures to 0.02 dB. Power is furnished by the Model 840 or accessory Model 1031A Power Source. Model 103A...$495.

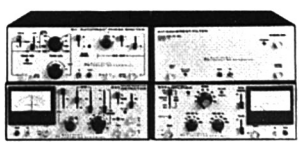

SYSTEM 80 AUTOTRAC™ is a lock-in system for measuring 3 nV to 0.3 V. Stability is better than 0.005%/°C. Usable center frequencies span 1 Hz to 1 MHz. The system features a signal extraction ratio of 100 dB, automatic frequency tracking, 370° calibrated phase adjustment, built-in second harmonic and quadrature operation, accommodation of practically any waveform. Like other Keithley lock-in amplifiers, the System 80 provides the wideband freedom from tuning, tweaking or adjusting. Complete price is $3,455.

***WHAT GUARANTEED USER SATISFACTION MEANS**

If a Keithley lock-in amplifier, or lock-in system, fails to perform to your satisfaction, you may return it for a full refund, including return shipping. We require only that your purchase order carry a reference to our user satisfaction guarantee and that the instrument(s) be returned within 30 days. (This offer good in the U.S.A. only.)

SEND FOR FREE LOCK-IN AMPLIFIER GUIDE

Whether you prefer a complete Keithley lock-in amplifier or a modular system, you'll want this handy "Guide to Evaluating and Selecting Lock-in Amplifiers". Write or call for it today.

KEITHLEY INSTRUMENTS

U.S.A.: 28775 AURORA ROAD, CLEVELAND, OHIO 44139
EUROPE: 14, AVENUE VILLARDIN, 1009 PULLY, SUISSE

CIRCLE 100 ON READER SERVICE CARD

How good can a $5,985* NMR system be?

Take a close look at the crotonaldehyde spectrum on this page and you'll see that the low-cost EM-300 Spectrometer is more than capable of producing high resolution results.

There are, of course, many reasons why more than 60 industrial and academic users have already selected the EM-300.

One reason is that with our built-in integrator you can perform quantitative analysis. Another is the fact that you can have calibrated spectra as a result of the EM-300's calibrated sweeps and linear readout which can be referenced to any particular peak.

For more information on the EM-300, including more than 20 representative spectra from our EM-300 reference book which covers 150 compounds, call (415) 326-4000. Or write Varian Anaspect, 611 Hansen Way, Palo Alto, California 94303.

$5,270 without recorder

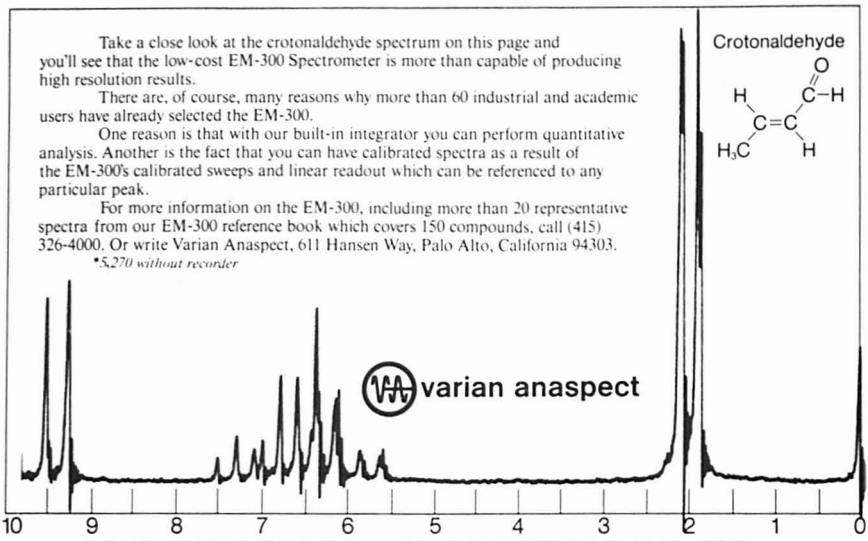

"See all 3 Anaspect Instruments at the National ACS Meeting in Washington D. C. September 14-16."

CIRCLE 193 ON READER SERVICE CARD

The following spectrum is brought to you by the new EM-600, a medium resolution mass spectrometer system that costs a mere $6925:*

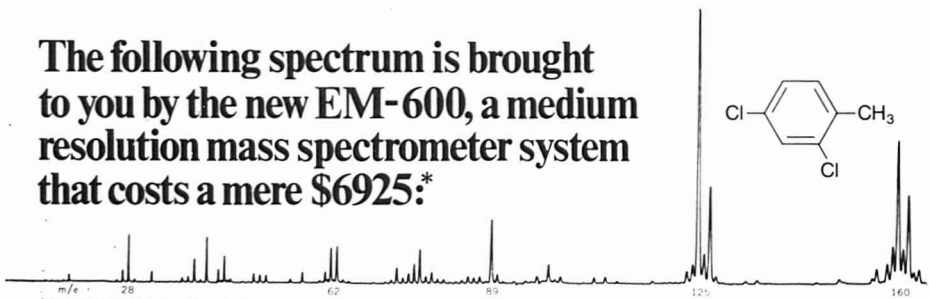

(2, 4-Dichlorotoluene Spectrum)

Before leaving, we might mention that the 60° sector, magnetically scanned EM-600 is a complete, easy-to-use system which also features a heated inlet for volatile organic compounds up to mass 330 or higher and linear mass readout.

For complete details or a demonstration, call (415) 326-4000 Ext. 2207. Or write Varian Anaspect, 611 Hansen Way, Palo Alto, California 94303.

*$6210 without recorder

varian anaspect

CIRCLE 194 ON READER SERVICE CARD

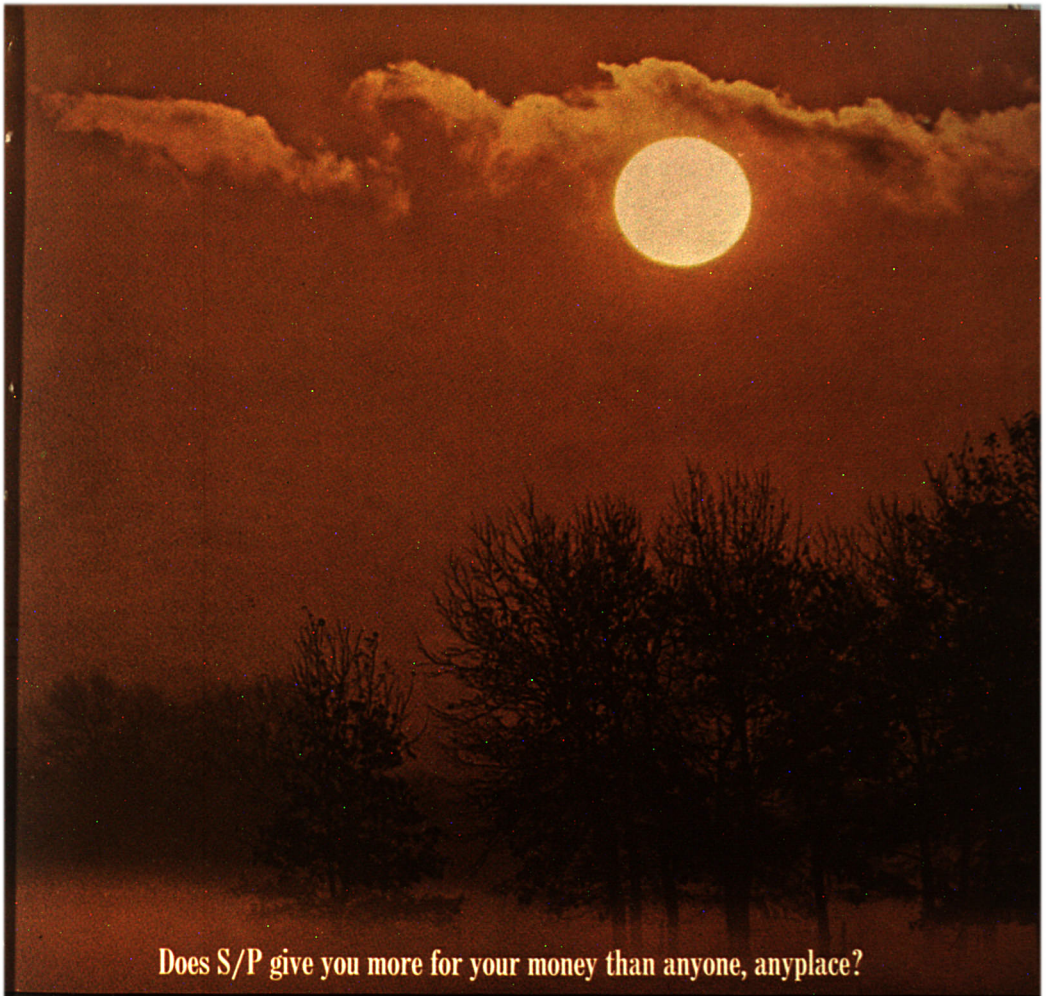

Does S/P give you more for your money than anyone, anyplace?

Does the sun rise?

You might spend days, weeks or even months determining which manufacturer's product to buy. So maybe you should spend a few minutes to determine which laboratory equipment and supply distributor you should buy it from. The product might be the same, but the service isn't. For example, S/P has more laboratory-trained representatives than anyone. (Over 300 in 17 coast-to-coast distribution centers.) More servicemen than anyone (150), including manufacturer-trained technical specialists for complex systems. More warehouse space than anyone (13,553,000 cubic feet). More in-stock items than anyone (129,000). More inventory than anyone ($28,000,000 worth)—with every item of national stock available to any customer through our computer program. More delivery capabilities than anyone (every major carrier plus our 43 S/P truck fleet). More backup people than anyone (1,580). Our prices are competitive. But if anyone offers you a better price, ask what they offer in service. You'll find S/P gives you more for your money than anyone. As sure as the sun rises.

To take advantage of our More-For-Your-Money Service, call your S/P Representative or write Scientific Products, Division of American Hospital Supply Corporation, 1430 Waukegan Road, McGaw Park, Illinois 60085. S/P...a single source for laboratory equipment, supplies and scientific instruments.

S/P

CIRCLE 170 ON READER SERVICE CARD

new high-efficiency GC automates drug, pesticide, biomedical analyses

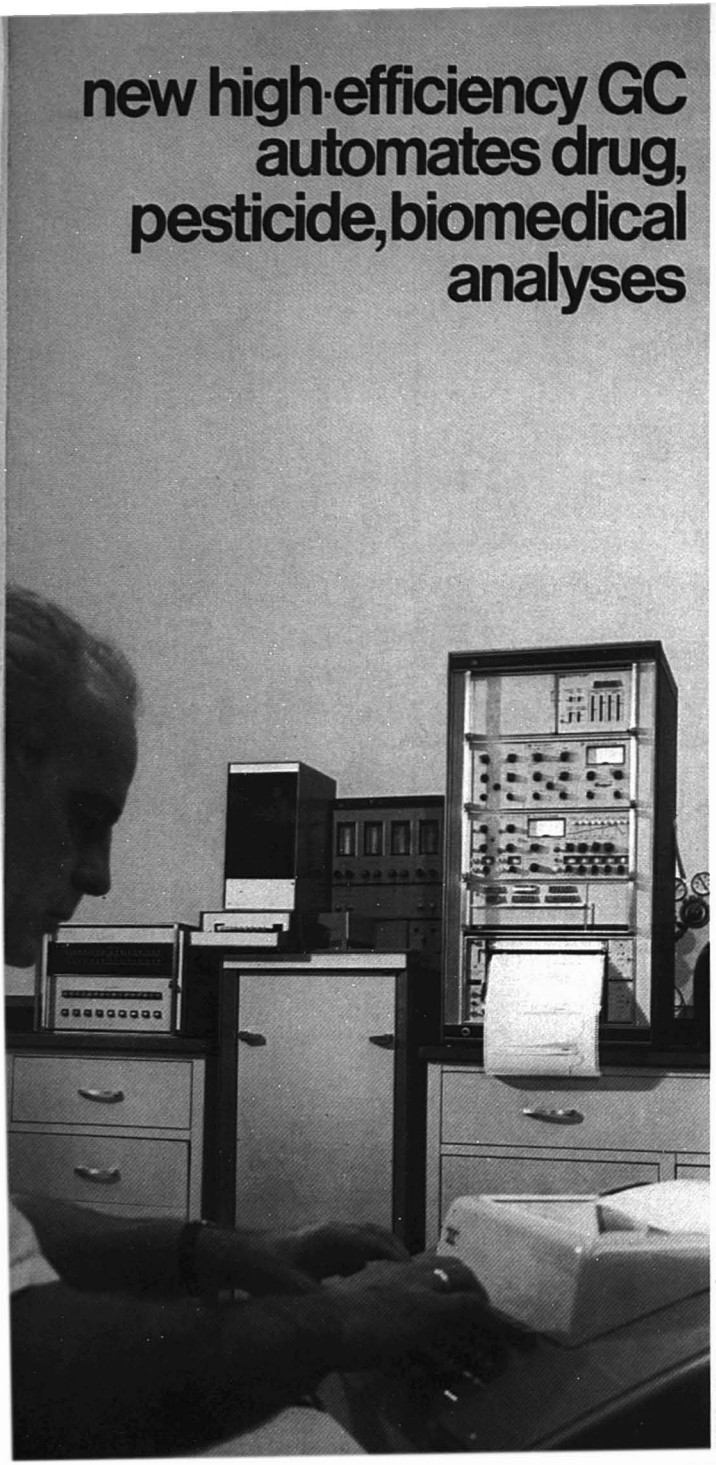

The new 7610A GC brings the benefits of automation to high-efficiency gas chromatography . . . for the repetitive analysis of drugs and pesticide residues where the economic payoff is large and immediate . . . for unique biomedical research where automation can improve analytical precision by an order of magnitude.

Because the 7610A is a completely modular instrument, you can order it initially with a bare minimum of equipment and build it up, one step at a time, as the need for automation arises and your expense budget permits. You use standard HP accessories that are completely compatible: all you do is plug them in.

Automatic oven cooling. All 7610A's have this built-in feature which is essential for fully automatic operation. At the end of any programmed run, the programmer turns on a blower, forcing cool air into the oven and exhausting hot air through a rear vent, until the oven has cooled and re-equilibrated at the starting temperature.

Automatic sample injection. The new 7671A Automatic Sampler installs directly on the 7610A and makes its unattended use possible around the clock. It completely automates sample measurement and injection for as many as 36 consecutive samples and synchronizes oven cooling and the operation of integrator and recorder.

Automatic data handling. The 7610A is completely compatible with HP Series 3370 Integrators and the 3360A GC Data Processing System which automatically prepares a full analytical report for each sample, including component name, retention time and % concentration. The 3360A System is completely programmed for GC and handles as many as eight instruments simultaneously in real time.

A state-of-the-art instrument, the 7610A performs difficult analyses as no other GC can. The many reasons include: all-glass system, on-column injection, low dead volume design, four-column five-detector capability, flow control for up to 16 gases, feedback temperature control for all detectors and heated zones. Get the full story from the nearest HP sales office or write for Bulletin 7610. Prices start at $6405. Hewlett-Packard, Route 41, Avondale, Pa. 19311. In Europe: 1217 Meyrin-Geneva, Switzerland.

HEWLETT hp PACKARD

ANALYTICAL INSTRUMENTS

43109

CIRCLE 87 ON READER SERVICE CARD

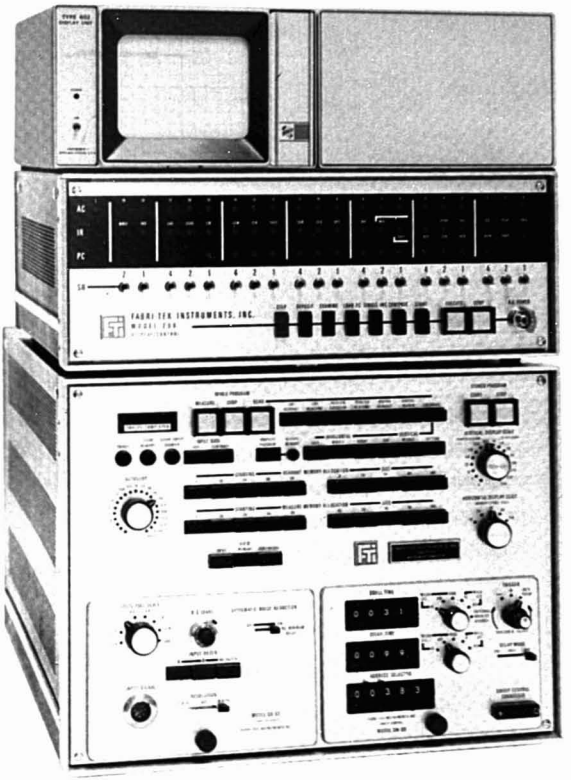

a dedicated, turnkey data system for your NMR spectrometer

the 1080 system...

■ **20-bit word length** eliminates memory- and time-consuming double precision data storage.

■ **Data memory is expandable** to 32K in 4K increments. Buy memory as you need it—software does not change.

■ **Combination of stored program and wired program** techniques yields computational flexibility with speed and accuracy.

■ **Plug-in modules** for analog-to-digital conversion and for sweep and time base control provide versatility to meet today's and future requirements.

■ **Hardware multiply/divide and bit-inversion accessory** increases 1080 FFT processing speed by a factor of 6.

■ **Software package** includes automatic baseline correction, exponential filtering for sensitivity or resolution enhancement, apodization to minimize distortion due to truncation effects, fast Fourier transformation of free induction decay data, rotation of real and imaginary axes for phase correction, integration or background subtraction of spectra, and expansion of displays for detailed observation.

■ **Data readout** is via oscilloscope, X-Y plotter, ASR-33 Teletype, or computer-compatible magnetic tape.

■ **Signal conditioning** includes differential amplifier input, d.c. level adjustment, and adjustable (24 position) 4-pole Butterworth filtering.

■ **Pre- and post-sweep delays** are front panel selectable for optimal data collection efficiency and spin-spin relaxation studies.

■ **Systematic noise reduction** technique makes practical experiments requiring 500,000 or more sweeps.

Complete 1080 Systems with 8K of memory start at $26,800. For full details write or call collect to discuss your specific NMR data problems.

In April 1971, Fabri-Tek Instruments, Inc., changed its name to Nicolet Instrument Corporation. Personnel, products, service, contractual obligations, and the address and telephone number remain the same. We appreciate your past interest in Fabri-Tek Instruments, Inc., and assure you that Nicolet Instrument Corporation stands ready to help solve your signal averaging/data processing problems.

NICOLET INSTRUMENT CORPORATION

5225 Verona Road, Madison, Wisconsin 53711
Phone: 608/271-3333 TWX: 910-286-2713
(formerly Fabri-Tek Instruments, Inc.)

CIRCLE 136 ON READER SERVICE CARD

Smooth Spinners

The clinical "g" machines from MSE

Smooth, quiet operation . . . the culmination of years of experience, thoughtful design, superb craftsmanship. You get it all with our General Purpose centrifuges. There are two for the table-top, two for the floor—to cover every clinical centrifuging requirement. And our exclusive use of universal heads and unique multi-tube carrier system eliminates the cost of a multitude of accessories.

Turn them on in *your* lab. They'll cast a long shadow for years of efficient service. Ask for our Catalog GPC-6-71. (If you're interested in refrigerated or high speed models ask your VWR Scientific dealer or write us.) VWR Scientific, Box 981, Rochester, New York 14603.

*The GT-2—one of the most widely used centrifuges in the world. Has stepless speed control, automatic timer, and cast aluminum bowl.
Maximum tube size—50ml.
Maximum capacity—400ml.
Max. RPM—3800.
Max. RCF—2100 x g.

*The GT-4—combines unusually high speed and "g" with large capacity. Has electric brake, timer and speed indicator.
Max. tube size—100ml.
Max. total cap.—800ml.
Max. RPM—6750.
Max. RCF—6990 x g.

*The GF-6—has speed indicator, automatic timer, electric brake. Max. bottle size—380ml.
Max. total cap.—1520ml.
Max. RPM—5600.
Max. RCF—5230 x g.

*The GF-8—extra large, 6-liter capacity; accepts 4 and 6 place angle heads in addition to an optional super speed attachment permitting speeds to 20,000 RPM and developing 31,000 x g.
Max. bottle size—1000ml.
Max. total cap.—6 liters.
Max. RPM—6000.
Max. RCF—6200 x g.

VWR Scientific (VWR UNITED)

CIRCLE 191 ON READER SERVICE CARD

NEUTRON ACTIVATION

New generation compact tube ideal for industry and the smaller laboratory.

The advantages of the nuclear activation analysis technique are considerable. They include fast element detection down to microgram levels - a whole order of magnitude greater than that of conventional methods.

The only problem, up to now, has been the source. Pumped accelerators which produce adequate outputs have pumping, target decay and consequent health hazard problems. And sealed tubes are limited by their fundamentally low output and the problem of target decay. This has meant that practical applications were limited to large research laboratories having reactor facilities.

Constant 3×10^{10} neutrons/sec output for over 1,000 hrs.

The figure of 1,000 hours applies to the full output i.e. no target decay. This is an improvement of about x10 over previous sealed generators, which, moreover, defined life time as that in which the output decreases to 50%.

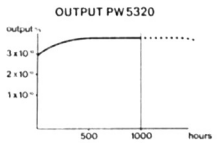

Not only does the Philips compact neutron generator have a high output, but when combined with the specially-designed irradiation station this is converted into the very high flux of 3×10^9 neutrons/sec/cm^2.

NOW A PRACTICAL ANALYTICAL TECHNIQUE

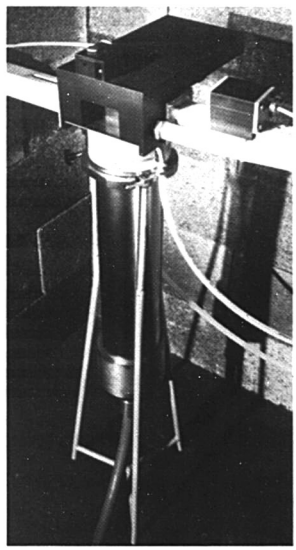

This density is sufficiently high to overcome the low reaction cross sections of many materials and the generator is thus ideal for a wide variety of industrial and laboratory analytical applications.

Easy installation.

The generator is extremely compact and needs either a well 3 meters deep and 1 meter in diameter, or an area of 4 x 5 meters with a shielding of 1.5 meters at full output. Cooling is by ordinary tap water.

Complete systems supplied.

Philips can also supply complete high-speed transfer systems and all the associated control and analysis equipment.

The transfer system is the more or less conventional "rabbit" type sample holder, but with a unique application of the monitor foil technique. This allows the foil activity to be matched to the sample activity, instead of the standard matching the sample. Thus a single standard is all that is needed to calibrate a wide range of sample percentages, and the second major barrier to widespread use of activation technique thereby eliminated.

Send for the brochure.

Full details on the new generation tube and the monitor foil technique, plus all the transfer, control, measurement and analysis equipment are given in a 12-page brochure.

If you're interested in high-speed, highly economic analysis you should send for it. Contact your local Philips sales organisation or write to:

N.V. Philips' Gloeilampenfabrieken
Analytical Equipment Department
Eindhoven, the Netherlands

PHILIPS ANALYTICAL EQUIPMENT

PHILIPS

CIRCLE 155 ON READER SERVICE CARD

The ADVANCES IN CHEMISTRY Series...

Excellent Reviews in Book Form of Specialized Chemical Topics

For comprehensive reviews of all the important aspects of a chemical subject... read the books in the ADVANCES IN CHEMISTRY Series.

Ranging up to 750 pages in length, ADVANCES volumes include...

- Authoritative, thought-provoking articles by as many as several dozen scientists per volume.
- Carefully compiled collections of data.
- Groups of related papers presented at important national and international symposia.
- Invited reviews of current work written by researchers eminent in the field discussed.

With the ADVANCES you learn about brand-new chemical subjects... and bring yourself up to date on familiar chemical topics. The numerous scientists contributing to each volume provide you with stimulating reading enriched by a variety of viewpoints. And the ADVANCES bring material together under one cover which would otherwise be scattered among many journals... *or not available at all.*

... Put chemical topics of interest to you in proper perspective. Read the ADVANCES IN CHEMISTRY Series.

The order form lists the 20 most recent titles in the ADVANCES IN CHEMISTRY Series. Use it to order your ADVANCES *now.*

No.	Title	Price	Number of copies ordered	Cost
96	Engineering Plastics and Their Commercial Development 128 pp (1969)	$7.50	___	_____
95	Cellulases and Their Applications 460 pp (1969)	$14.50	___	_____
93	Radionuclides in the Environment 522 pp (1970)	$15.00	___	_____
92	Epoxy Resins 224 pp (1970)	$10.50	___	_____
91	Addition and Condensation Polymerization Processes 767 pp (1969)	$19.50	___	_____
90	Fuel Cell Systems—II 446 pp (1969)	$17.50	___	_____
89	Isotopes Effects in Chemical Processes 278 pp (1969)	$13.00	___	_____
88	Propellants Manufacture, Hazards, and Testing 395 pp (1969)	$12.00	___	_____
87	Interaction of Liquids at Solid Substrates 212 pp (1968)	$9.50	___	_____
86	Pesticidal Formulations Research. Physical and Colloidal Chemical Aspects 212 pp (1969)	$9.50	___	_____
85	Stabilization of Polymers and Stabilizer Processes 332 pp (1968)	$12.00	___	_____
84	Molecular Association in Biological and Related Systems 308 pp (1968)	$10.50	___	_____
83	Chemical Marketing: The Challenges of the Seventies 199 pp (1968)	$9.50	___	_____
82	Radiation Chemistry—II 558 pp (1968)	$16.00	___	_____
81	Radiation Chemistry—I 616 pp (1968)	$16.00	___	_____
81	and 82 ordered together	$30.00	___	_____
80	Chemical Reactions in Electrical Discharges 514 pp (1969)	$15.00	___	_____
79	Adsorption from Aqueous Solution 212 pp (1968)	$10.00	___	_____

TOTAL COST _____

Postpaid U.S. and Canada; all others please add $0.20 for each volume ordered.

Payment must be in U.S. funds, by international money order, UNESCO coupon, or U.S. bank draft; or order through your book dealer.

Please ship my ADVANCES to:

Name _____

Address _____

City _____ State/Country _____ Zip _____

☐ Bill me. ☐ Payment enclosed.

Return this order form to AMERICAN CHEMICAL SOCIETY, Special Issues Sales, Dept. LG-68, 1155 16th Street, N.W., Washington, D.C. 20036.

... There are over 50 other volumes in the ADVANCES Series. To receive your pricelist for all the ADVANCES, just send us your request... or note it on your order. You'll receive the list by return mail.

THERE ARE OVER 100 GOOD REASONS WHY YOU SHOULD HAVE THE NEW WHATMAN PRODUCTS CATALOG... THESE ARE 4 OF THE NEWEST...

WHATMAN GAMMA-12 HIGH PERFORMANCE IN-LINE FILTER UNIT

WHATMAN 1PS PHASE SEPARATING PAPER THE WORLD'S FIRST DISPOSABLE SEPARATORY FUNNEL

WHATMAN BENCHKOTE PROTECTS BENCHTOPS AGAINST STAINS, CORROSION, DIRT

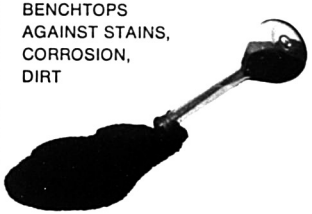

WHATMAN GLASS FIBER FILTER PAPERS OFFER EFFICIENT RETENTION OF MICRON (μm) SIZE PARTICLES AND VERY HIGH FLOW RATE

Whatman®

THE OTHER 96 GOOD REASONS CAN BE FOUND IN THE NEW 24-PAGE WHATMAN PRODUCTS CATALOG. USE THE COUPON BELOW TO GET YOUR FREE COPY.

Please send me the new Whatman Products Catalog

Name_____

Institution_____

_____

Address_____

City_____

State_____ Zip_____

®Registered trademark of W. & R. Balston, Ltd., Springfield Mill, Maidstone (Kent), England

SOLE DISTRIBUTORS IN NORTH AMERICA

reeve angel 9 BRIDEWELL PLACE, CLIFTON, NEW JERSEY 07014

CIRCLE 167 ON READER SERVICE CARD

Coleman AUTOFILL™ CELL ASSEMBLY

for the Coleman Junior® II, Junior IIA, 6A, 6C, 6D and 44 Spectrophotometers

If you are using any type of Coleman Junior Spectrophotometer . . . or the new Coleman Model 44, and especially if you are performing multiple analyses, then you will save the cost of this new accessory many times over.

The Autofill Cell Assembly provides a new breakthrough in sample handling. Not only does it reduce substantially the time required for inserting samples and making tests, but it simplifies and speeds procedures . . . eliminates the need for handling cuvettes . . . and permits you to perform a series of tests with a minimum of sample — as little as 1.5 ml! It also provides a convenient system for direct linear absorbance readout and/or recording with fast, automatic sampling.

In short, with the Autofill, you can increase the work output of your spectrophotometer.

Cell volume of the Autofill is 0.25 ml.

The Autofill Control Unit is 5½" wide x 8¾" high x 14" deep. It is made of steel and aluminum, finished in baked enamel and epoxy.

S-4700-20X Autofill Cell Assembly, as described, complete with flow cell and cell holder, power supply unit, pump, tubing, and reservoir, but without standard cuvettes. For 110/220 volts, 60 Hz. Price $395.00

Illustration shows the new Coleman Junior IIA . . . a linear absorbance spectrophotometer with unique, snap-in scales for direct concentration readout. Model 44 is similar, except that it has a 7" wide, linear absorbance meter scale in place of the 8" snap-in scale panel. Ask us for a descriptive brochure.

SCIENTIFIC GLASS APPARATUS CO. INC.
BLOOMFIELD, NEW JERSEY

LABORATORY...
♦ APPARATUS
♦ INSTRUMENTS
♦ CHEMICALS
♦ GLASSWARE

Branches: Boston Mass. • Danbury Conn. • Elk Grove Village Ill. • Fullerton Calif. • Philadelphia Penna. • Silver Spring Md. • Syracuse N. Y.

CIRCLE 171 ON READER SERVICE CARD

USE THIS CHECK LIST WHEN YOU NEED A LOW COST LOCK-IN AMPLIFIER

☐ **CHOICE OF WIDEBAND OR SELECTIVE FRONT END**
The simplicity of wideband design will prove helpful in some applications. However, when noise or harmonics of the signal must be suppressed, the ability to switch in high and/or low pass filtering can be extremely important.

☐ **INTERNAL OSCILLATOR**
Having a built-in voltage-controlled oscillator enables you to simultaneously modulate your experiment and drive the reference channel of the lock-in. The VCO is also useful for general laboratory work.

☐ **PLUG-IN, LOW-NOISE PREAMPLIFIERS**
Plug-in preamplifiers provide a low-cost method of matching the lock-in to the experiment and optimizing noise performance and sensitivity. With an extender kit, preamps may be located away from the main frame of the lock-in close to the signal pickup, to minimize noise, hum and stray capacitance.

☐ **BROAD FREQUENCY RANGE**
A lock-in with an extremely wide operating range is suited to both low frequency applications (such as those using thermopiles) and high frequency experiments (such as EPR)—an important consideration for present and future requirements.

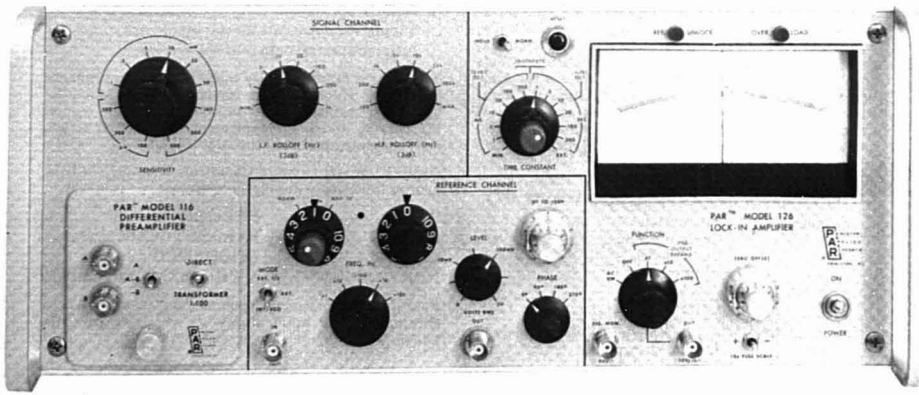

If you're investigating lock-in amplifiers, you're probably weary of the old price/performance compromise. Consider our Model 126 which costs less than $2,000, including differential preamplifier. It's the one lock-in that provides real versatility for people locked into a tight budget. Features include wideband or selective front end, a choice of four plug-in preamps to provide sensitivities down to 10 nV *full scale*, a special preamp for measuring currents to 10^{-13} A full scale in photometric applications and capacitance studies, automatic frequency tracking of the reference signal, 0.2 Hz to 210 kHz range, VCO output to 10 V rms and many others borrowed from our top of the line Model 124 Lock-in.

You'll find that the Model 126's signal processing capabilities surpass those of any competitively-priced instrument. For complete information, write or call "The Lock-in People" at Princeton Applied Research Corporation, Box 565, Princeton, New Jersey 08540; telephone (609) 452-2111.

PAR **PRINCETON APPLIED RESEARCH CORPORATION**

126

CIRCLE 157 ON READER SERVICE CARD

SciChemCo

PHILLIPS-DRUCKER CENTRIFUGES

Model 807 A **Floor model centrifuge:** Size 1 centrifuge — general purpose. Direct drive shaft with operating speeds from 3,300 with 8 place trunnion head to over 5,000 rpm with some fixed angle heads. Complete with automatic timer, electronic tachometer, automatic accelerator and many more important features. Only **$895.00**

Model 803 Size 1½ — general purpose. Larger than size 1, the 803 will accommodate swingout and fixed angle heads for size 1 and most fixed angle heads for size 2. The guard bowl is 20½ inches in diameter. The motor is a powerful ¾ h.p. series wound, high torque (115v., 60 cycle) for extended brush wear. Rpm from 3,600 to over 5,000. Sale price — **$995.00**

Model 7020 C Size 2 — Floor model — non-refrigerated, general purpose. Direct drive, self balancing, safety shut down, electric tachometer. Operating speeds from 2,700 rpm. **$1165.00**

Model UML-A Special heavy duty refrigerated floor model. Designed for commercial and industrial uses as well as research laboratories and blood banks. Operating speeds from 3,200 rpm with sixteen 500 ML blood bags or 288 12mm x 75mm tubes. Up to 6,000 rpm with fixed angle heads. Temperature range from −10° to +30° C. Optional features include built-in vacuum, stroboscopic tracking device. Price on request.

Model 806 C5 Size 2 — refrigerated — economy centrifuge. Operating speeds from 2,500 rpm. Temperature range from +5° to +30° C. with fixed heads and 25° C. ambient temperature. +15° to +30° C. with trunnion heads. Specify whether 208v or 230v if desired. **$1995.00**

Model 806 C1 Size 2 — refrigerated, floor model centrifuge capable of accommodating swing out and fixed heads for sizes 1 and 2. Full 23½ inch bowl, heavy gauge steel with refrigeration coils on exterior surfaces. Operating speeds from 2,700 rpm with 16-place trunnion head (50 ml shields) to 5,000 rpm with most fixed angle heads. Temperature range from −5° to +30° C. Optional features include built-in vacuum; stroboscopic tracking device, and others (available on request). **$2750.00** **Model 806 C2** Same as 806 C1 but designed for procedures requiring higher speeds. **$2880.00**

SciChemCo is proud of our new affiliation with Phillips-Drucker, a division of Bio-Consultants, Inc. For surgical and laboratory apparatus remember SciChemCo.

SciChemCo guarantees these Centrifuges to conform to published standards or we will replace with any comparable equipment of your choice. Bench top models available as well. For further information, or to order, call or write . . .

SciChemCo **P. O. Box 23616, Los Angeles, CA. 90023 • Ph. (213) 263-1181**

SciChemCo.
Frese Division
Los Angeles, Calif.

SciChemCo.
Howe & French Division
Boston, Massachusetts

SciChemCo.
Durham Division
Durham, North Carolina

CIRCLE 176 ON READER SERVICE CARD

Mobile Air Pollution Monitoring Station

Safely generate hydrogen wherever you need it.

All Elhygen® R needs for operation is electrical power and a liter of distilled water, so this portable electrolytic generator is used in air pollution monitoring stations, conventional laboratories, aboard ships, and just about anywhere else a safe supply of dry, ultrapure hydrogen under pressure is needed for accurate flame ionization detector analysis and critical carrier gas applications in chromatography.

Elhygen R continuously generates on demand up to 150 milliliters/minute hydrogen (STP) by dissociating distilled water and separating the hydrogen in a patented process. One liter of distilled water results in 1000 liters of dry hydrogen with fewer than ten parts per billion impurities and far less costly than commercial grade gas. Output pressure is dual regulated and adjustable from 0 to 60 psig, ±0.025 psi.

Two units can be manifolded for greater output, and a special model is available for output pressures to 400 psig. Safety is inherent in the Elhygen R because the unit never contains more than a few milliliters of hydrogen at any one time — eliminating the explosion hazard of stored H_2.

For full details, write to Milton Roy Company, 5000 Park Street, N., St. Petersburg, Florida 33733. Telephone (813) 544-2581. In Canada, Milton Roy Industries, Ltd., Ontario.

MILTON ROY COMPANY
ST. PETERSBURG, FLORIDA

CIRCLE 168 ON READER SERVICE CARD

Our SENSITIVITY goes back 150.000.000 years

When you consider the advantages of the AEI MS30 mass spectrometer, assess it as a single beam instrument that offers the unique facility of a double beam.

As a single beam instrument the MS30 is outstandingly advanced. The double beam eliminates reference-sample doublets.

The extra sensitivity of the MS30 was recently invoked to identify a stearate in fossil bones 150 m. years old – those of a plesiosaurus. From a few nanograms of sample, elemental lists can be obtained at resolutions of only 1000.

Other features are: *Low and high resolution spectra can be recorded simultaneously . . . samples can be examined at low and high electron voltages . . . chemical mass marking allowing unambiguous calibration of spectra . . . scan start and sensitivity control are automatic with gas chromatograph . . . direct sample introduction; sample and chamber temperatures independently controlled.*

The brochure is fully descriptive. Ask for a copy.

MS30 DOUBLE BEAM MASS SPECTROMETER

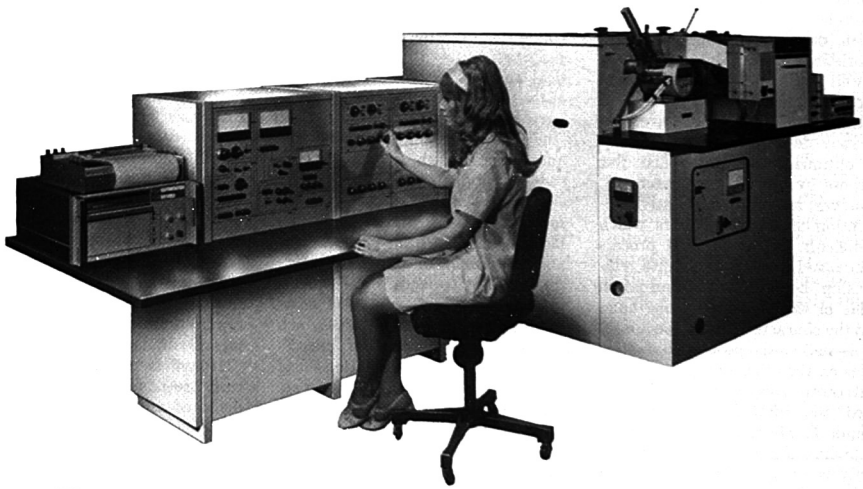

The world's most advanced mass spectrometer

AEI scientific apparatus

AEI SCIENTIFIC APPARATUS LTD.
Barton Dock Road, Urmston, Manchester M31 2LD
Telephone: 061-865 4466 Telex 668482 Telegrams: Sciapp Manchester, England
In the U.S.A.
AEI Scientific Apparatus Inc., 500 Executive Boulevard,
Cross Westchester Executive Park, Elmsford, New York 10523.

A14064

CIRCLE 8 ON READER SERVICE CARD

Selection of an Optimum Analytical Technique for Process Control

ANALYTICAL CHEMISTS TODAY are constantly confronted with the problem of making the right selection from a great variety of analytical techniques in solving problems. R. Müller has called it the *N*-Dimensional Nature of Analytical Chemistry (*1*). The selection is governed by a set of parameters which describe the specific characteristics of the analytical problem as well as the analytical technique. Once parameters for an analytical method and a process are accurately described, they can easily be optimized for any particular purpose by use of a computer (*2*). However, it is the quantitative description of the parameters which is difficult. If a chemical process is involved, there is a definite relationship between the information value of the analysis on one hand and the characteristics of the analysis as well as the process characteristics on the other hand.

Recently some authors have applied the information theory of Claude E. Shannon to the problem of quantitating the value of an analysis (*2–4*). With the work of Van der Grinten (*5*), we can describe one dimension of the selection problem, that is, the quality of the control loop. A second dimension is formed by the costs, which arise from damage to process equipment, costs due to poor product quality, wages, and control costs.

As process control improves, production costs decrease; however, analysis costs rise. The selection of an optimum analytical method depends on minimizing the sum total of these costs (*6*).

Procedure

The selection procedure we have been using for the last few years involves the following steps:

Statistical Analysis. A statistical analysis is made of that part of the process in which disturbances have been noted. This statistical study identifies the source, the frequency bandwidth, and the magnitude of the disturbances.

Process Costs vs. Analytical Information. A calculation of the relationship between the process costs and the amount of analytical information used to control the process is then made. The process costs are caused by fluctuations which are too large in certain process quantities. These fluctuations lead to catastrophic events resulting in, for example, a plant shut-down; nonoptimal operating conditions resulting in losses and low yield; poor product quality resulting in a need for recycling or lower selling prices; and higher product quality than is required to meet specifications. Process costs will, in general, diminish with increased use of analytical information in controlling the process.

Analysis Criteria and Techniques. A search is instigated for measuring criteria and related analytical techniques which can be used in the control loop. It also involves calculation of the information content of these techniques.

Analysis Costs vs. Analytical Information. It is then necessary to calculate the relationship between the cost of analyses and the amount of information produced by the analyses. The information can be produced in many different ways, resulting in different costs. These costs are wages, depreciation of equipment, maintenance, and research and development.

Optimization. The process costs will, in general, diminish when more information is extracted and fed back into the process. However, at the same time, the analysis costs will increase. At some point the total costs will be minimal, resulting in an optimum analytical technique.

It will be clear that parallel to this procedure a study could be made of alternative methods suitable for elimination of process disturbances. Such methods may consist of eliminating the source of the fluctuations by a different plant design, or by compensation in some way. However, it is beyond the scope of this paper to go into these methods.

Meaning of Analytical Information

To quantify the value of an analysis, we have to think about its

As process control improves, production costs decrease; however, analysis costs rise. The selection of an optimum analytical method depends on minimizing the sum total of these costs.

FRANK A. LEEMANS
Dutch State Mines
Heerlen, The Netherlands

purpose. The analysis should always be part of a control loop and never stand by itself. With the aid of an analysis, we want to extract information from some proceeding event and feed this information back so that we can control the direction in which the event proceeds. This event can be a chemical process, a research study, or the curing of a patient.

Figure 1 shows the fluctuation of a certain process quantity as a function of time. The fluctuation pattern is the result of a great number of external and internal disturbances. In a chemical process these disturbances can be changes in raw material composition, fouling of process equipment, adjustments made by operators, changes in the activity of catalysts, or nonreproducible material delivery and transport systems. These disturbances occur mostly in a completely random manner, having different frequencies and amplitudes. However, in most cases actually studied, the total path along which the disturbances enter the process and travel with the process is dominated by one time constant. This time constant, for example, can be the average residence time in a mixer, a buffertank, or a reactor. It can also be the time required to use a shipload of raw material.

The existence of one dominating time constant means that the differential equation, which describes the response of the process output quantity to a certain change of the process input quantity, is a linear one, analogous to the equation for an ideal mixer,

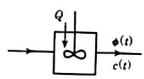

If we inject an amount, Q, of a certain material into an ideal mixer, at a moment $t = 0$, then the concentration of this material in the outgoing stream follows from:

$$\phi(t) \cdot c(t) = -\frac{d[c(t) \cdot V]}{dt}$$

(provided that the time taken for injection is short in comparison to the time constant of the mixer), where $\phi(t)$ = volume flow, $c(t)$ = concentration, and V = volume of mixer.

The above differential equation is linear, and its solution, in the case that $\phi(t)$ and V are both constant, is given by:

$$c(t) = c(0) \cdot e^{-t/t_1}$$

with $t_1 = V/\phi$ = time constant of the mixer.

In the chemical process, because of the existence of one dominating time constant in the travel path of the disturbances, an analogy can be made with the system of an ideal mixer. All different disturbances acting upon the chemical process can be considered as a single disturbance $Y(t)$ which has passed through a time constant T_p.

So if we look at the process deviation, $Y(t)$, it is very likely, that at

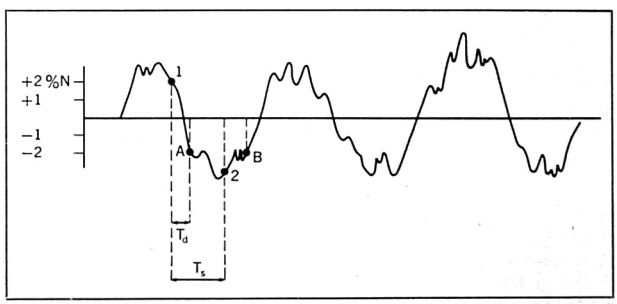

Figure 1. Fluctuation of a process quantity as a function of time

a certain moment, $(t + \tau)$, the deviation will equal

$$Y(t + \tau) = Y(t) \cdot e^{-\tau/T_p} \qquad (1)$$

where T_p is the dominating time constant.

Even in systems which are not linear for large changes of the input quantity, Equation 1 can often be applied. Because most processes in industry are not completely chaotic, the changes are very often small enough to transform a differential equation of higher order into a linear one.

When there are a great number of random disturbances acting on a linear process, the resulting fluctuation pattern (Figure 1), can be described by two parameters, σ_p and T_p. σ_p is the standard deviation of the Gaussian-distributed difference between the actual value of the process quantity and its average value. The value of σ_p is a measure of the average amplitude of the process fluctuation. The value of $1/T_p$ is a measure of the frequency bandwidth of the process fluctuation.

If $ij(t)$ describes the value of the process quantity as a function of time, then it follows:

$$Y(t) = ij(t) - \overline{ij(t)}$$

$$\overline{Y(t)} = 0$$

$$\sigma_p^2 = \overline{[Y(t) - \overline{Y(t)}]^2} = \overline{[Y(t)]^2} \qquad (2)$$

The value of T_p follows from a calculation of the autocorrelation function, $\phi(\tau)$, which is given by definition in Equation 3:

$$\phi(\tau) = \overline{Y(t) \cdot Y(t + \tau)} \qquad (3)$$

$\phi(\tau)$ is called the autocorrelation function because it correlates the value of a signal at a certain time with the value of the same signal at a time τ earlier.

For $\tau = 0$, it follows from Equation 3 that:

$$\phi(0) = \overline{[Y(t)]^2} = \sigma_p^2$$

For small values of τ, it sometimes happens that $Y(t)$ and $Y(t + \tau)$ have opposite signs (where the signal crosses the zero axis). Mostly, however, $Y(t)$ and $Y(t + \tau)$ have the same sign, so that for small values of τ, the value of $\phi(\tau)$ will be a little less than σ_p^2. For larger values of τ, chances are in-

creasing that $Y(t)$ and $Y(t + \tau)$ have opposite signs. Thus, with increasing values of τ, the corresponding values of $\phi(\tau)$ rapidly diminish to zero.

It can be proved (5) that with one dominating time constant, the process autocorrelation function will equal

$$\phi(\tau) = \sigma_p^2 \cdot e^{-\tau/T_p} \qquad (4)$$

Equations 1, 2, 3, and 4 enable us to characterize the fluctuation pattern of a process quantity. It is very important to realize that despite the complete randomness of the disturbances acting on the process, the final fluctuation pattern of the process quantity (Figure 1) has a distinct correlation function with respect to time. This does not mean that the pattern will have the shape of a nice waveform. It means that we are able to make a statistical prediction of what the process quantity is likely to be at a time t after the actual analysis. In other words, we can describe the effect of time delays, such as sampling time and analysis time, in the control loop.

The purpose of control is to make the fluctuation of a process quantity around its average value (desired value) as small as possible. To do so, the fluctuation is measured. The result of the measurement is translated into an action upon the process. The action is such that the process deviation caused by the action compensates exactly for the process fluctuation at the moment of the action. The quality of the control loop is, by definition, given by the controllability factor r according to

$$r^2 = \frac{\sigma_p^2 - \sigma_r^2}{\sigma_p^2} \qquad (5)$$

σ_r is the average amplitude of the process fluctuation which is still left after control. Therefore, the numerator in Equation 5 represents that part of the fluctuation which has been reduced to zero by means of effective control. A maximum reduction of the fluctuation will correspond to r equal to 1, while absence of any control will correspond to r equal to zero.

The value of r is determined by a number of separate parameters such as:

Dead time of sampling, $(T_d)_p$—i.e., the process time between the point where the sample is taken and the point where the correction is made.

Dead time of sampling, $(T_d)_s$—i.e., the time between the moment that the sample is taken and the starting point of the analysis.

Dead time of analysis, $(T_d)_a$—i.e., the time between the starting point of the analysis and the moment that the result is produced.

Sample frequency

Reproducibility of the analysis

The effect of dead time is illustrated in Figure 1. At time 1 a sample is taken from the process stream. The sample is sent to the control laboratory and analyzed; the result is calculated and sent back to the operator in the plant. At time A the operator acts upon the process. However, in the time T_d, the total dead time between the moments 1 and A, the deviation of the process quantity from its average value has been changed. This change can be predicted using Equation 1. This equation says that if one measures at a certain moment, t, a deviation, $Y(t)$, the most probable value for the deviation after a time, T_d, will be

$$Y(t) \cdot e^{-T_d/T_p}$$

This is the amount of the original deviation $Y(t)$, that can be completely reduced to zero.

From Equations 2 and 5, it follows:

$$r^2 = \frac{\overline{[Y(t + T_d)]^2}}{[Y(t)]^2}$$

And using Equation 1:

$$r^2 = e^{-2 T_d/T_p}$$

$$r = e^{-T_d/T_p} \qquad (6)$$

The dead time, T_d, is the sum of the separate time delays in the control loop according to:

$$T_d = (T_d)_p + (T_d)_s + (T_d)_a + \ldots$$

Substituting this into Equation 6 will give:

$$r = e^{-(T_d)_p/T_p} \cdot e^{-(T_d)_s/T_p} \cdot e^{-(T_d)_a/T}$$

$$r = r_p \cdot (m_d)_s \cdot (m_d)_a \qquad (7)$$

with

$$r_p = e^{-(T_d)_p/T_p} \qquad (8)$$

$$(m_d)_s = e^{-(T_d)_s/T_p} \qquad (9)$$

$$(m_d)_a = e^{-(T_d)_a/T_p} \qquad (10)$$

The relationship between the controllability factor and the sampling frequency can be approximated as follows: Suppose we sample at a constant time interval, T_s, and there is no other dead time in the control loop. Now if we want to correct for the process deviation just before sampling we have to predict over a time, T_s, while if we want to correct just after sampling we need make no prediction. On the average we have to predict over a time, $T_s/2$, so that a sampling time T_s is analogous to a dead time of $T_s/2$. So by approximation, the controllability factor will equal

$$r = m_s \cong e^{-T_s/2T_p} \qquad (11)$$

Because intermittent sampling has the character of dead time, it is clear that when there are also dead times $(T_d)_p$, $(T_d)_s$, and $(T_d)_a$ present in the control loop, the total controllability factor will be given by

$$r = r_p \cdot (m_d)_s \cdot (m_d)_a \cdot m_s \qquad (12)$$

In his original paper, Van der Grinten (*5*) also derived a relationship between the controllability factor and the reproducibility of analysis. This relationship is given by Equation 13:

$$m_n \cong 1 - \frac{\sigma_n}{\sigma_p}\sqrt{\frac{T_s}{T_p}} \qquad (13)$$

The value of m_n is a function of the signal-to-noise ratio, which averages σ_p/σ_n. However, m_n is also a function of the ratio between the frequency of the noise and the frequency of the signal. If the ratio of frequencies is large, it is possible to construct a simple electronic filter which blocks the noise of the analytical apparatus and lets the signal through. Then even with a high noise-to-signal ratio, a reproducible measurement can be executed. With intermittent sampling, the frequency of the noise equals $1/T_s$. When all effects, such as dead time, intermittent sampling, and limited reproducibility are present, the total controllability factor will be given by

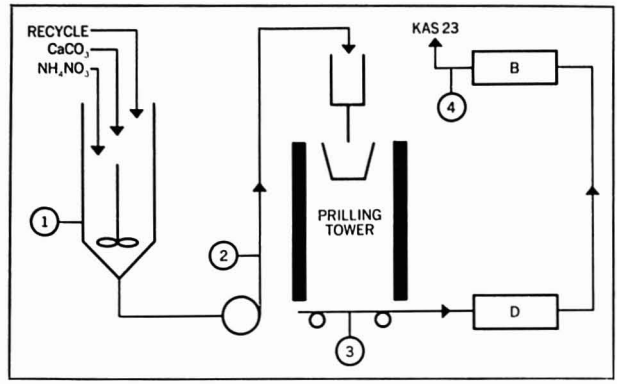

Figure 2. Part of a process for the production of a fertilizer

$$r = r_p \cdot (m_d)_s \cdot (m_d)_a \cdot m_s \cdot m_n \quad (14)$$

That part of the controllability factor which is determined by the applied analytical technique is given by

$$m_{tot} = (m_d)_s \cdot (m_d)_a \cdot m_s \cdot m_n \quad (15)$$

We have already seen that the controllability factor is related to the reduction of the average amplitude of the process fluctuation. If there is no dead time in the process, it follows from Equation 5:

$$\sigma_e = \sigma_p \cdot \sqrt{1 - m_{tot}^2} \quad (16)$$

So the reduction of the amplitude amounts to 100%, 56%, 13%, and 0% for m_{tot} values of 1, 0.9, 0.5, and 0.0, respectively. The reduction apparently decreases rapidly with decreasing values of m_{tot}. From Equation 15 it follows that the maximum value of $m_{tot} = 1$, corresponding to a maximum reduction of the amplitude.

There is some analogy to sending a cable message. If you just send enough words so that the receiver can completely understand your message, you have sent the maximum amount of information and attained a 100% reduction of the uncertainty of the receiver. You cannot send more information by sending more words because the receiver already knows everything he needs to know. If you send fewer words, the reduction of the uncertainty of the receiver rapidly decreases. We could, therefore, define m_{tot} also as the amount of information transmitted by the applied analytical technique.

Summarizing, we see that with Equation 15 we can quantify the amount of information produced by the analytical technique. With Equations 2, 3, and 4 we can quantify the process, which is the receiver of the analytical information. This theory can be applied to any linear process in which the fluctuation is Gaussian in nature.

In the following paragraphs, the procedure for selecting an optimum analytical technique is applied to a problem that we had in our plant and that we could solve successfully. The reason for showing a special application is twofold:

It demonstrates clearly the proposed procedure.

One cannot quantify information without connecting the source and the receiver. In other words, to quantify the information of the analytical technique, we have to connect the parameters of the analytical technique with the parameters of the process.

Analysis of a Process

Figure 2 shows the last part of a process for making KAS-23, one of our nitrogen fertilizers. (KAS-23 is a mixture of NH_4NO_3 and $CaCO_3$; the NH_4NO_3 is produced in the first part of the process, which is not shown in the figure.)

At point 1, mixing takes place between a melt of ammonium nitrate and solid particles of calcium carbonate. The product, a viscous melt with a temperature of 135°C, contains some gas bubbles. The melt is pumped to a prilling tower, where grains of a uniform size are made. The grains are refined in places D and B.

At point 4, the final product has to contain a nitrogen content of 23.0%, with 22.3% as the lowest permissible limit.

Analysis at point 4 shows a strong fluctuation of the nitrogen percentage. A statistical study of the periodically sampled data shows a Gaussian distribution with a standard deviation of 1.2% nitrogen. A correlation study with respect to time, executed on the same data, shows a process correlation time of 66 min. This follows from Equations 3 and 4, by plotting $\phi(\tau)$ graphically as a function of τ.

A similar study on samples taken at point 3 in the process, produces approximately the same results. It turns out that the deviations are caused by discontinuities in the amount of recycle and by a nonreproducible delivery of the humid calcium carbonate.

When we apply a feedback control, the analysis can be done at points 1, 2, 3, and 4. The point where the operator corrects for the process deviations will be the ammonium nitrate delivery to tank 1. Because point 4 is located 90 min away from the correction point, it will introduce too large a dead time in the control loop. From Equation 8 it follows that r_p would equal 0.26. In this case, any reasonable reduction of the process fluctuations cannot be achieved even with the best analysis ($m_{tot} = 1$).

At point 1, it is not practical to take a representative sample. The mixture of melt and solid is not yet homogeneous, and side reactions are still producing gas bubbles. At point 2, the pressure amounts to 10 atm, so that possibly an on-line measurement of the specific gravity can be executed. At point 3, grains can be sampled from a conveyor belt. Thus, suitable points for analysis are points 2 and 3, which are located about 22 min from the correction point. The correspond-

Table I. Average Value of Process Quantity (Set Point) as Function of Analytical Information (m_{tot})

$\sigma_p = 1.2\%$ N, $T_p = 66$ min, $r_p = 0.7$, $T_a = 120$ min

m_{tot}	σ_ϵ, % N	T_ϵ, min	σ_a, % N	Set point, % N
0	1.2	66	0.9	24.1
0.5	1.1	22	0.6	23.5
0.8	1.0	12	0.4	23.1
1.0	0.85	8	0.3	22.9

ing value of r_p follows from Equation 8 and equals 0.70.

Process Costs vs. Analytical Information

What we want to know is the effect of increased analytical information on the standard deviation of the average nitrogen content of a lot of final product. A standard deviation of σ_a forces us to hold the average value of the process quantity on a level of $22.3\% + 2\,\sigma_a$, the value of 22.3% being the lowest permissible nitrogen content. In other words, the larger the standard deviation, the higher the set point. However, everything we produce above 23.0% nitrogen is not paid for, so the process costs are proportional to the set point value minus 23.0%. The standard deviation of a lot of final product follows from Equation 17 (*5*):

$$\sigma_a^2 = \frac{2\,\sigma_\epsilon^2 T_\epsilon (T_a - T_\epsilon + T_\epsilon e^{-T_a/T_\epsilon})}{T_a^2} \quad (17)$$

T_a is the time period during which the lot has been produced; in this case, $T_a = 120$ min. σ_ϵ follows by solving Equation 5:

$$\sigma_\epsilon = \sigma_p \sqrt{1 - r^2} \quad (18)$$

The value of r follows from Equation 14:

$$r = r_p \cdot (m_d)_s \cdot (m_d)_a \cdot m_s \cdot m_n$$

$$r = r_p \cdot m_{tot} \quad (19)$$

The value of r_p is fixed by the dead time of 22 min in the process. In the previous paragraph we found for r_p a value of 0.70.

We can now vary m_{tot} arbitrarily from zero to one, in spite of the fact that we don't know yet how we will get this analytical information. For every chosen value of m_{tot}, there is, according to Equations 18 and 19, a corresponding value of σ_ϵ. In this way we have composed Table I. The value of T_ϵ follows from Equation 20 (*3*):

$$T_\epsilon = -\frac{T_p \ln r}{\pi} \quad (20)$$

The set points presented in Table I equal $22.3\% + 2\,\sigma_a$.

The process costs due to fluctuations only follow from Equation 21:

$$\text{costs} = (\text{set point} - 23\%) \times P \times \text{price} \quad (21)$$

P = KAS-23 production, tons/day and Price = price of KAS-23 in guilders/ton. These process costs are graphically shown with a dotted line in Figure 3.

Analysis Criteria and Techniques

We want to control the percentage of total nitrogen in a product which contains ammonium nitrate as the only nitrogen source. Therefore, we can use the following criteria: total nitrogen, ammonia nitrogen, and nitrate nitrogen. Another point is the fact that the rest of the product contains calcium carbonate. Calcium carbonate has a specific gravity of 2.7 vs. 1.4 for the ammonium nitrate melt. Therefore, we have two other criteria: the ratio of ammonium nitrate to calcium carbonate and the specific gravity. Some of the analytical techniques, which can be used to measure these criteria, are summarized in Table II. The dead time of analysis is the time between the start of sample preparation and the moment that the final result has been produced.

The factor $(m_d)_a$ follows from Equation 10, substituting for T_p a

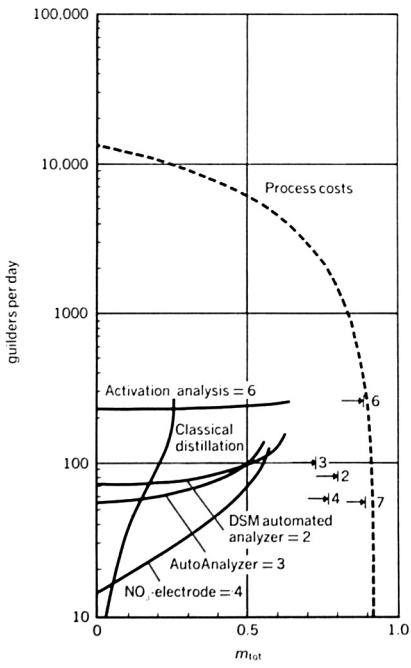

Figure 3. Process costs due to process fluctuations (dotted line) and analysis costs (full line) as a function of analytical information. The horizontal lines (with arrows) refer to the fully automated techniques

Now, Automatic Quantitative Microscopic Image Analysis—from Zeiss!

We've added a unique precision scanning stage to our great optics, and the result is the most sophisticated system ever made for microphotometry. It's the Zeiss Scanning Microscope Photometer 05 for **all** types of photometric measurements in transmittance, absorbance, reflectance and fluorescence . . . and either on-line or off-line computer analysis. Cancer cytologists have already found it an invaluable tool . . . and other applications are developing daily in both the life sciences and industry.

Here's what this unusual system consists of:

A Zeiss Universal or Photomicroscope. Any analytical system that utilizes a microscope, no matter how sophisticated the electronics, cannot be any better than its optics allow. Information that's lost in the optical channels will not be retrieved in the electronic channels. That's why it's important to start with world-famous Zeiss optics.

A unique Zeiss precision scanning stage. The two available scanning stages allow, respectively, minimum increments of 0.5 and 10 microns, perform up to 200 steps per second, and travel 75mm and 25mm in the X and Y directions in several different scanning patterns, including meander, comb or line.

Much more. A modular electronic system that permits you to select components as you need them and as your budget permits. All the famous Zeiss accessories and photographic and analytical attachments—everything you might ever need for qualitative and quantitative microscopy—are, of course, available. We can even supply a PDP-12 computer with a number of programs prepared by well-known scientists. For the full story, write Carl Zeiss, Inc., 444 5th Ave., New York, N.Y. 10018. Or phone (212) 736-6070.

CIRCLE 197 ON READER SERVICE CARD

Nationwide Service.

ATLANTA, BOSTON, CHICAGO, COLUMBUS, DALLAS, DENVER, FORT LAUDERDALE, HOUSTON, KANSAS CITY, LOS ANGELES, PHILADELPHIA, PHOENIX, SAN FRANCISCO, SEATTLE, WASHINGTON, D.C.

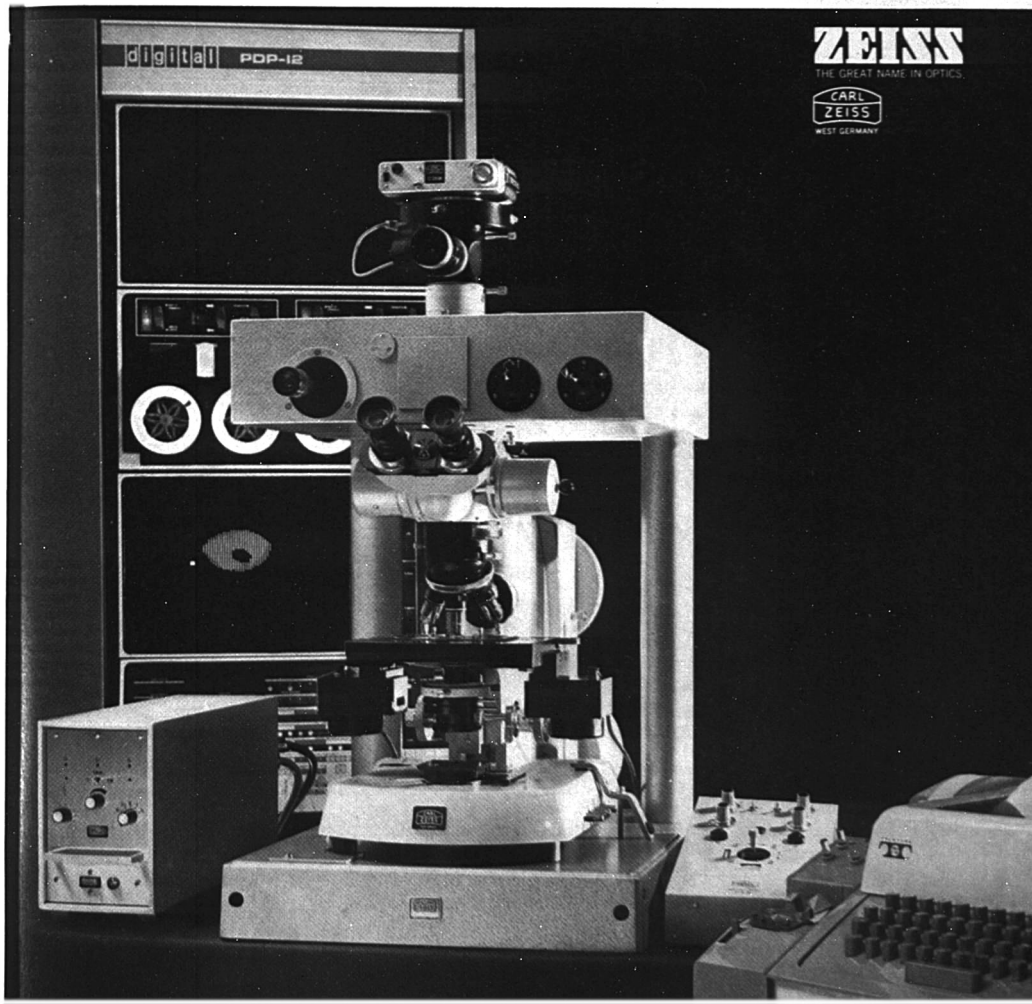

Table II. Information Factors of Some Analytical Techniques for Analysis of Nitrogen

(Assumed is a sampling frequency of 2 samples/hr, which means that $m_s = 0.80$. The related process characteristics are mentioned in text.)

Criterion and analytical technique	Dead time of analysis, min	Std. dev. of analysis, % N	$(m_d)_a$	m_s	m
Total N, classical distillation	75	0.17	0.32	0.99	0.24
Total N, DSM automated analyzer	12	0.25	0.84	0.97	0.65
NO_3-N, Technicon AutoAnalyzer	15½	0.51	0.79	0.92	0.58
NO_3-N, specific electrode	10	0.76	0.86	0.85	0.58
$NH_4NO_3/CaCO_3$ ratio, X-ray diffraction	8	0.8	0.89	0.83	0.59
Total N, fast neutron activation analysis	5	0.17	0.93	0.99	0.74
Specific gravity γ-Ray absorption	1	0.64	0.98	0.88	0.69

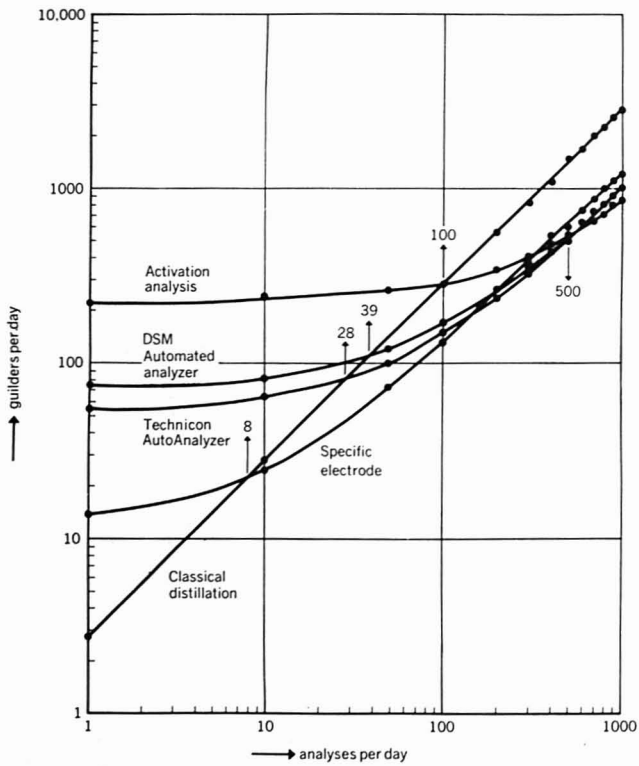

Figure 4. Costs of some off-line analytical techniques for the analysis of inorganic nitrogen (1968)

value of 66 min. The factor m_n follows from Equation 13, substituting for σ_p a value of 1.2% nitrogen. We have already seen that m_n depends upon the sample frequency $1/T_s$. The m_n factors of Table II are calculated for a sampling frequency of 2 samples/hr. This means that $T_s = 30$ min. From Equation 11 it follows that in this case $m_s = 0.80$. The total information produced by the analytical technique, excluding dead time of sampling, is $m = (m_d)_a \cdot m_s \cdot m_n$ and is indicated in the last column of Table II.

The following remarks can be made about the techniques:

(1) The classical distillation produces the least amount of information in spite of its high reproducibility. This is caused by the large dead time of analysis.

(2) In the DSM automated distillation we have sacrificed some reproducibility to speed up the analysis. The total information has been increased dramatically in comparison to the manual distillation.

(3) The Technicon AutoAnalyzer has a cost advantage over technique 2 because it can analyze more different components.

(4) The nitrate-specific electrode is not quite reproducible, but fast and inexpensive.

(5) For the measurement of a ratio with X-ray diffraction, no weighing is required and the adding of a standard is not necessary. This saves time.

(6) Fast neutron activation analysis is a powerful technique —no sample preparation, and practically no matrix effect. The technique is fast and at the same time reproducible. Unfortunately, however, it is expensive.

(7) A nonspecific technique, such as the measurement of the specific gravity with X-ray absorption is, in general, simple and fast. Although the reproducibility is not very good, the method is ideal for on-line control.

Analysis Costs vs. Analytical Information

The total costs for some off-line analytical techniques are represented in Figure 4. The costs were derived from depreciation on in-

Now, Zeiss lets you count and measure the previously uncounted and immeasurable.

You do it with the Zeiss Micro-Videomat, a unique TV microscope for quantitative stereometric analysis. With it you can determine areas, particle counts, chord lengths, mean diameters, numerous gray values, particle size distributions, shape factors, interior or exterior surface areas, volumes, weights . . . of cells, alloys, ores, plastics, ceramics . . . wherever you can use a microscope.

Here's what this unusual system consists of:

A Zeiss Universal or Photomicroscope with the world's greatest optics. Any analytical system that utilizes a microscope, no matter how sophisticated the electronics, cannot be any better than its optics allow. That's why it's important to start with a world-famous Zeiss microscope that permits you to use all methods of enhancing image quality.

A unique Zeiss precision scanning stage. The two available scanning stages allow, respectively, minimum increments of 0.5 and 10 microns, perform up to 200 steps per second, and travel 75mm and 25mm in the X and Y directions in several different scanning patterns, including meander, comb or line.

Much more. A TV camera with a high-performance Plumbicon tube. A TV monitor with control panel that lets you manipulate images for convenient and speedy determinations. An electronic console with an analog computer displaying values on a multi-scale meter or a digital indicator. Provision for off-line or on-line use with a digital computer such as the Wang model shown below. All the famous Zeiss accessories and photographic and analytical attachments—everything you might ever need for qualitative and quantitative microscopy—can, of course, be used. For the full story, write Carl Zeiss, Inc., 444 5th Avenue, New York, N.Y. 10018. Or phone (212) 736-6070.

Nationwide Service. CIRCLE 196 ON READER SERVICE CARD

ATLANTA, BOSTON, CHICAGO, COLUMBUS, DALLAS, DENVER, FORT LAUDERDALE, HOUSTON, KANSAS CITY, LOS ANGELES, PHILADELPHIA, PHOENIX, SAN FRANCISCO, SEATTLE, WASHINGTON, D.C.

vestments, labor, and maintenance. Classical distillation requires manual labor, and its total costs go up linearly with the number of analyses. Its cost line is at the same time an iso-cost line, because every point on it renders the same price for one analysis. The points of inflection of the iso-cost line with the other cost curves indicate the number of manual distillation analyses necessary to pay off the investment of the indicated techniques.

If the samples are taken at constant intervals, each number of analyses/day corresponds to a definite value of T_s and therefore to a definite value of m_s and m_n, according to Equations 11 and 13. The horizontal axis of Figure 4 can, therefore, be readily transformed into an information axis. For the off-line techniques the dead time of sampling is 9 min. According to Equation 9, the corresponding $(m_d)_s$ value equals 0.87. The $(m_d)_a$ value was already calculated (Table II), so that m_{tot} follows from Equation 15. The results are shown in Figure 3. The analysis costs are represented by fully drawn lines.

Optimization

From Figure 3 it is apparent that the costs for off-line techniques increase very rapidly with increased information. It is clear that the classical distillation method is of no value in diminishing process costs. Because of the limiting manual sampling time of 9 min, the off-line techniques cannot render more information than a value of about 0.65 for m_{tot}. This amount of information is not yet sufficient for a satisfactory level of process costs.

The completely automated on-line techniques have virtually no variable costs, so their cost curves run horizontally. However, their investment level is naturally higher than that of their corresponding off-line techniques. The arrow points indicate the maximum attainable information. The γ-ray absorption technique (indicated by 7) produces the largest amount of information for the least amount of money. This is clearly the technique to be selected. The apparatus has been installed in a transport pipe at the pressure side of a

pump (point 2 of Figure 2). Because this point is located closer to the correction point than has been assumed for the calculations, the controllability factor is slightly better as indicated. In fact, the process costs due to fluctuations have been completely reduced to zero.

Acknowledgment

The author thanks W. T. Buyk for his contribution to calculations and discussions. He is also grateful to F. Steffin for preparation of drawings and tables.

Nomenclature

$ij(t)$ = process quantity
$Y(t)$ = $Y(t) = ij(t) - \overline{ij(t)}$
$\phi(\tau)$ = process autocorrelation function
r = controllability factor
σ_p = standard deviation of the uncontrolled process quantity
σ_c = standard deviation of the controlled process quantity
r_p = factor describing the effect of dead time in the process
$(m_d)_s$ = factor for dead time in sampling
$(m_d)_a$ = factor for dead time in the analysis
m_s = factor for sample frequency
m_a = factor for the reproducibility of the analysis
m_{tot} = factor describing the information produced by the applied analytical technique, including dead time of sampling
m = factor describing the information produced by the applied analytical technique, excluding dead time of sampling
T_d = dead time
T_p = correlation time of the uncontrolled process quantity
T_s = time between two samples
σ_a = reproducibility of analysis
σ_d = standard deviation of the averaged, controlled process quantity
T_a = averaging time
T_c = correlation time of the controlled process quantity

References

(1) R. H. Müller, ANAL. CHEM., 40, 109A–110A (1968).
(2) H. Kaiser, *ibid.*, 42, 24A–41A (1970).
(3) H. Zettler, *Fresenius Z. Anal. Chem.*, 245, 1–11 (1969).
(4) A. Dijkstra, *Chem. Weekbl.*, 40, p 19 (1968).
(5) P. M. van der Grinten, *ISA J.*, 12 (1) p 48 (1965); *ibid.*, 1 (2), p 58 (1966).
(6) F. A. Leemans, *Chem. Weekbl.*, 20, p 17–22 (1969).

Frank A. Leemans *is assistant to the purchasing manager of the DSM Co. working in the field of planning and strategy of raw materials supply. He studied at Eindhoven Technological University, The Netherlands, where he did his thesis in 1964 under Dr. J. F. K. Huber and Prof. A. I. M. Keulemans. He has been an instructor in analytical chemistry at Eindhoven Technological University, research associate in engineering at the Lipid Research Institute of Baylor University College of Medicine, Houston, Tex., and manager of the Automation and Efficiency Department of the Control Laboratories, DSM Co., Heerlen, The Netherlands.*

Doing two jobs well is its job.

The Model PAX Digital-Indicating pH/Activity Meter. $995.

Job No. 1 — the measurement of pH.

Which the Model PAX accomplishes as both a full-range (0 to 14 pH) instrument *and* as an expanded-scale meter (span: 1.999 pH).

How well does the Model PAX do here? Its accuracy over the 0-14 pH range is 0.01 pH. When used as an expanded-scale meter, the Model PAX reads to 0.001 pH (especially useful where changes of a few thousandths of a pH unit are of critical interest).

Further, the Model PAX functions as a high-impedance millivoltmeter, giving direct indication of electrode potentials to 1 mv in the 0 to ± 1999 mv range.

Job No. 2 — the measurement of activity.

With proper reference and ion-selective electrodes, the Model PAX derives and displays ionic activity over a range of three decades (1:1000).

In this switch-selectable operating mode, the Model PAX exhibits an accuracy of ± 0.25% (reference conditions). And perhaps most importantly, activity readout is digital and direct, requiring no subsequent calculations.

And more.

The Model PAX also gives you all this: a true-tracking, four-place, luminescent display free from lag and jitter; wide-range, locking slope and intercept controls; manual temperature compensation with ATC optional for the 0 to 14 pH range; single-cycle, two-point calibration in all modes without repetitive "successive approximation"; both analog and digital (B. C. D., 8-4-2-1 code) outputs; and push-button operation of the more frequently used controls.

CIRCLE 173 ON READER SERVICE CARD

The Model PAX, the all-purpose digital meter for pH and specific ion potentiometry, costs only $995, about half of what you would expect to pay for a meter doing the same job(s). Investigate—ask your Sargent-Welch representative. Or write. 1-211

SARGENT-WELCH

Scientific instruments, apparatus, chemicals.
Sargent-Welch Scientific Company
7300 N. Linder Ave.; Skokie, Illinois 60076

Chicago/Anaheim/Birmingham/Cincinnati
Cleveland/Dallas/Denver/Detroit
Springfield, N.J./Toronto/Montreal/Vancouver

Our new GC/MS Data System has only one limitation.

Your head.

Free your mind to do what it does best. Interpretive thinking. Let Du Pont's new system supply you with answers —not just piles of data. The Data System converts masses of GC/MS data to chemical answers. You can then be what you are. A chemist. Applying your creative energy to interpretive thought.

It's easy to operate. You or your assistant can run it. It's simple, highly reliable. It opens up the whole world of GC/MS analysis to scientists who aren't instrument specialists.

The system urges you to explore. You can automatically profile selected masses in each chromatogram. You can list the most abundant masses from all mass spectra. And call for normalized mass spectra easily selected from all GC peaks in a chromatogram. All of it in charts, tables, and graphs produced in moments.

So you save weeks of manual computation.

The data system consists of a computer, digital tape unit, interface, and readout. Plus a full library of software based on thirty years of mass spectrometer problem solving.

You get more capability than in any other system. New economy. Single-source responsibility for all products and software. The only open-ended mass spectrometer and data system. You can do more when you add more, according to future needs. You also get our reputation.

Write or call Urie McCleary, Jr. for full information. 1500 South Shamrock Avenue, Monrovia, California 91016 • Phone: 213-357-2111

DU PONT Instruments

Tomorrow's Mass Spectrometers for Tomorrow's Needs.

CIRCLE 46 ON READER SERVICE CARD

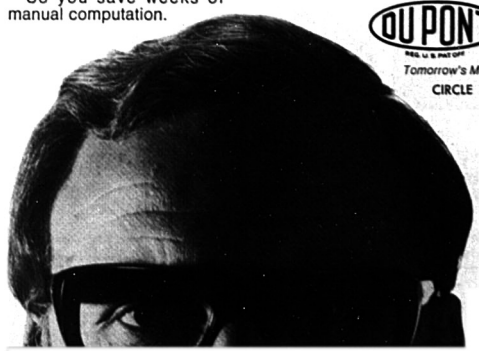

Perkin-Elmer GC/Mass Spectrometer. When you want a trace analysis capability approaching 10^{-9} grams.

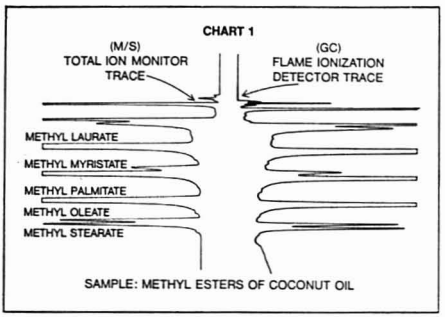

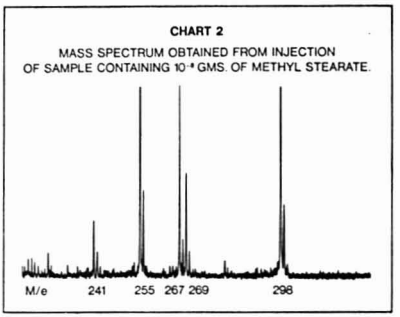

The finest GC/MS system ever designed for trace analysis, it combines a true mass spectrometer with the famed Perkin-Elmer Model 990—the standard for gas chromatographs.

It is particularly ideal for applications such as air and water pollution, toxicology, forensics and pharmaceuticals.

As an example of how this instrument operates, we have reproduced here an analysis of methyl stearate.

Note how accurate identification is assured by the chart from the double pen recorder. It gives an instant side-by-side qualitative comparison of each compound as it passes through the flame ionization detector of the gas chromatograph and the total ion monitor of the mass spectrometer. (Visible proof that what has gone through the GC is going through the mass spectrometer.) For complete and accurate identification, the mass spectrum of each component can be run as shown in chart 2.

Be positive about your trace analyses with a Perkin-Elmer Gas Chromatograph/Mass Spectrometer System. Write for full particulars to: Instrument Division, Perkin-Elmer Corporation, 702 Main Ave., Norwalk, Conn. 06852.

PERKIN-ELMER

CIRCLE 164 ON READER SERVICE CARD

162nd National American Chemical Society Meeting Washington, D.C., September 12–17, 1971

The 162nd National Meeting of the American Chemical Society will take place September 12–17, 1971, in Washington, D.C. The Analytical Chemistry Division has scheduled sessions from Monday, September 13 through Friday morning, September 17. In addition to general papers, there will be several special symposia: Critical Analytical Problems Facing Government Laboratories; Recent Trends in the Determination of Molecular Weight (Joint with the Division of Polymer Chemistry); Evaluated Reference Data: The Key to Research Productivity; and Chromatography and Computers—An Economical Approach for Every Laboratory. The complete technical program of the Division is given below.

The Division banquet will be held on Wednesday evening and will feature Dr. Thomas Cairns of the Los Angeles County Museum of Art who will speak on "Everything You Have Always Wanted to Know about Art but Were Afraid to Ask."

Registration facilities at the meeting will be located at the ACS Headquarters Building Lobby; Sheraton-Park Concourse of States; and Washington Hilton Exhibit Hall. Analytical Division technical sessions will be held at the Statler Hilton. An exposition of laboratory equipment and books will take place at the Sheraton-Park Hotel. There will be three short courses just before the meeting, one on interfacing the minicomputer. This will be held September 11 and 12 with R. E. Dessy and D. G. Larsen as instructors. Registration for this course during the two-week period prior to the meeting should be made by telephone: 202-737-3337, ext. 258.

Complete details of the National Meeting appear in *C&EN*, August 9 issue.

DIVISION OF ANALYTICAL CHEMISTRY

J. C. White, *Chairman*

R. S. Juvet, Jr., *Secretary*

Monday Morning — Section A

CRITICAL ANALYTICAL PROBLEMS FACING GOVERNMENT LABORATORIES

W. W. Meinke, *Presiding*

9:05 Critical Analytical Problems Encountered by Customs Laboratories. R. E. Lang, U.S. Customs Laboratory, 201 Varick St., New York, N.Y. 10014

9:35 FDA Analytical Problems Related to Food Contamination. E. O. Haenni, Div. of Chemistry and Physics, Food and Drug Administration, Washington, D.C. 20204

10:05 Some Recent USDA Problems in Identification of Pesticide Residues and Contaminants. J. R. Plimmer, Plant Science Research Div., U.S. Dept. of Agriculture, Beltsville, Md. 20705

10:35 Problems of Quantitative Analysis in Study of Health and Disease at NIH. H. R. Sloan, National Heart and Lung Institute, National Institutes of Health, Bethesda, Md. 20014

11:05 Analytical Problems within Walter Reed Army Institute of Research, an Interdisciplinary Institute. C. R. Angel, D. J. Beach, Div. of Biochemistry, Walter Reed Army Institute of Research, Washington, D.C. 20012

11:35 U.S. Geological Survey Problems in Trace Element Geochemistry. Irving May, U.S. Geological Survey, Washington, D.C. 20242

Section B

GENERAL

G. D. Christian, *Presiding*

9:05 Colorimetric Determination of Water in Acetone. C. E. Matkovich, G. D. Christian, Univ. of Kent., Lexington, Ky. 40506

9:15 Electrometric Titration Procedure for Determination of Aqueous Solubility of Organic Acids and Bases. W. W. Davis, C. J. Kreutler, Eli Lilly & Co., Indianapolis, Ind. 46206

9:30 Electrometric Titration Procedure for Determination of Oil-to-Water Partition of Organic Acids and Bases. W. W. Davis, C. J. Kreutler, Eli Lilly & Co., Indianapolis, Ind. 46206

9:45 Simple Control and Data Logging System for Base Hydrolysis of Esters. K. M. Wellman, R. Lorusso, S. Zapico, R. W. Dively, T. Manning, Univ. of Miami, Coral Gables, Fla. 33124

10:05 Reaction Curve: Generalization of Buffer Capacity Curve and Its Applicability to Analysis. K. W. Loach, State Univ. of N.Y. College of Arts & Science, Plattsburgh, N.Y. 12901

10:20 Selective Chelometric Determination of Calcium with EGTA at Silver Billet Electrode. I. E. Lichtenstein, Corning Glass Works, Chemical Analysis Res. Dept., Corning, N.Y. 14830

10:50 Pressurized Differential Thermal and Autoignition Analysis of Ammonium Perchlorate Filled Propellant. R. C. Raisor, Thiokol Chem. Corp., Wasatch Div., P.O. Box 524, Brigham City, Utah 84302

11:20 Self-Balancing Bridge for Differential Capacitance Measurements. D. H. Chidester, R. R. Schroeder, Wayne State Univ., 175 Chemistry Bldg., Detroit, Mich. 48202

Monday Afternoon — Section A

CRITICAL ANALYTICAL PROBLEMS FACING GOVERNMENT LABORATORIES

B. F. Scribner, *Presiding*

2:05 Analytical Chemistry at NBS: Improving Accuracy Through Standard Reference Materials. W. W. Meinke, Analytical Chemistry Div., National Bureau of Standards, Washington, D.C. 20234

2:35 New Research Areas in the Bureau of Mines Challenge the Analytical Chemist. T. H. Henrie, U.S. Dept. of the Interior, Bureau of Mines, Washington, D.C. 20240

3:05 NRL's Approach to Analytical Chemistry Problems at Sea. F. E. Saalfeld, Naval Research Lab., Washington, D.C. 20390

3:35 Analytical Problems in NASA's Aeronautics and Space Programs. F. C. Gross, Materials Engineering Branch, En-

gineering Physics Div., NASA, Goddard Space Flight Center, Greenbelt, Md. 20771

4:05 Role of Analytical Chemistry in Scientific Crime Detection. M. J. Pro, Rm. 7575, Alcohol, Tobacco & Firearms Div., IRS Bldg., 1111 Constitution Ave., N.W., Washington, D.C. 20224

Section B

GENERAL

J. Knoeck, *Presiding*

2:05 Structure, Bonding, and Fluorescence of Divalent Metal Chelates of o,o'-Dihydroxyazobenzene. J. Knoeck, J. A. Buchholz, North Dakota State Univ., Fargo, N.D. 58102

2:20 Fluorometric Determination of Submicrogram Quantities of Tin. T. D. Filer, U.S. Atomic Energy Commission, Analytical Chemistry Branch, Health Services Lab., P.O. Box 2108, Idaho Falls, Idaho 83401

2:40 Synergic Extraction of Iron(III) as Method of Preparing Volatile Complexes. J. W. O'Laughlin, B. B. Tomazic, 329 Metallurgy Bldg., Ames, Lab. USAEC, Iowa State Univ., Ames, Iowa 50010

3:00 Analysis of Gold in Serum and Urine by Atomic Absorption. P. A. Ullucci, J. Y. Hwang, Instrumentation Lab. Inc., 113 Hartwell Ave., Lexington, Mass. 02173

3:20 Detection and Colorimetric Determination of Amines with Trinitrobenzene in Dimethyl Sulfoxide. J. A. Vinson, D. M. Kozak, H. E. Holets, Washington & Jefferson College, Washington, Pa. 15301

3:40 Computer Enhancement of Weak Porphyrin Fluorescence Spectra. E. A. Cohen, J. H. Rho, Space Sciences Div., Jet Propulsion Lab., Calif. Inst. of Tech., 4800 Oak Grove Dr., Pasadena, Calif. 91103

4:00 Use of Nondispersive X-Ray Spectrometer in Scanning Electron Microscopy. H. Prakash, Pratt Inst., Brooklyn, N.Y. 11205; K. G. Mayhan, Materials Research Center, Univ. of Missouri, Rolla, Mo. 65401

4:20 Iterative Least Squares Development of Discriminant Functions for Spectroscopic Data Analysis by Pattern Recognition. L. Pietrantonio, P. C. Jurs, Pennsylvania State Univ., University Park, Pa. 16802

4:40 Signal-to-Noise Ratio Considerations in Quantitative Molecular Absorption Spectrometry. J. D. Ingle, Jr., S. R. Crouch, Michigan State Univ., East Lansing, Mich. 48823

Tuesday Morning — Section A

RECENT TRENDS IN DETERMINATION OF MOLECULAR WEIGHT

(Joint with Division of Polymer Chemistry)

M. Ezrin, *Presiding*

9:10 Light-Scattering Photometry for Molecular Weight Measurements: Current State-of-the-Art. J. P. Kratohvil, Clarkson College of Technology, Potsdam, N.Y. 13676

9:55 Characterization of Extremely High Molecular Weight Polymers. E. Slagowski, L. J. Fetters, D. McIntyre, Institute of Polymer Science, Univ. of Akron, Akron, Ohio 44304

10:20 Graphical Treatment of Calibration Data in Vapor Pressure Osmometry. B. E. Hudson, Jr., Esso Research & Engineering Co., P.O. Box 121, Linden, N.J. 07036

10:45 Determination of Number-Average Molecular Weights by Ebulliometry. C. A. Glover, Research Lab., Tennessee Eastman Co., Div. of Eastman Kodak Co., Kingsport, Tenn. 37662

11:15 Application of the Summative Fractionation Method to Determination of $\bar{M}_w/\bar{M}_n$ for Narrow Distribution Polymers. F. W. Billmeyer, Jr., L. R. Siebert, Rensselaer Polytechnic Institute, Troy, N.Y. 12181

11:35 Polymer Standard Reference Material Program at National Bureau of Standards. H. L. Wagner, National Bureau of Standards, Washington, D.C. 20234

Section B

EVALUATED REFERENCE DATA: KEY TO RESEARCH PRODUCTIVITY

A. L. Smith, *Presiding*

9:10 National Standard Reference Data System. D. R. Lide, Jr., Office of Standard Reference Data, National Bureau of Standards, Washington, D.C. 20234

9:30 Need for Evaluated Data. S. W. Fenton, Chem. Bldg., Univ. of Minnesota, Minneapolis, Minn. 55455

10:00 Technical Considerations and Practical Limitations in Program for Publishing Evaluated Infrared Spectra. C. D. Craver, 761 W. Kirkham, Glendale, Mo. 63122

10:30 Precision in Infrared Data for Computer Retrieval. D. S. Erley, Computations Research Lab., 1707 Bldg., Dow Chemical Co., Midland, Mich. 48640

11:00 Evaluation and Uses of Gas Chromatographic Reference Data. O. E. Schupp, III, Eastman Kodak Co., Rochester, N.Y. 14650

Tuesday Afternoon — Section A

RECENT TRENDS IN DETERMINATION OF MOLECULAR WEIGHT

(Joint with Division of Polymer Chemistry)

M. Ezrin, *Presiding*

2:05 Homodyne Spectroscopy and Molecular Weight. R. Gabler, N. C. Ford, Jr., Dept. of Physics & Astronomy, Univ. of Massachusetts, Amherst, Mass. 01002; F. E. Karasz, Polymer Science & Engineering Program, Univ. of Massachusetts, Amherst, Mass. 01002

2:40 Thin-Layer Methods of Determining Molecular Weight Distribution. E. P. Otocka, Bell Labs., Murray Hill, N.J. 07974

3:10 The Use of Mass Chromatography to Measure Molecular Weights and to Identify Compounds Related to the Polymer Field. C. E. Bennett, D. G. Paul, Chromalytics Corp., Unionville, Pa. 19375

3:40 Molecular Weight Determination by Plasma Chromatography. F. W. Karasek, Univ. of Waterloo, Waterloo, Ont., Canada; M. J. Cohen, Franklin GNO Corp., P.O. Box 3250, West Palm Beach, Fla. 33402

4:05 Electrospray Mass Spectroscopy. M. Dole, H. L. Cox, J. Gieniec, Baylor Univ., Waco, Tex. 76703

4:30 Determination of Number-Average Molecular Weights by Pulsed Nmr. B. Crist, Research Triangle Inst., Camille Dreyfus Lab., P.O. Box 12194, Research Triangle Park, N.C. 27709

Section B

EVALUATED REFERENCE DATA: KEY TO RESEARCH PRODUCTIVITY

A. L. Smith, *Presiding*

2:00 Proton Nmr Spectra: Information Content and Assessment Strategy. B. L. Shapiro, Texas A&M Univ., College Station, Tex. 77843; M. R. Willcott, Univ. of Houston, Houston, Tex. 77004

2:30 Proton Nmr Spectral Quality Assessment: Preliminary Results and Conclusions. M. R. Willcott, Univ. of Houston, Houston, Tex. 77004; B. L. Shapiro, Texas A & M Univ., College Station, Tex. 77843

3:00 Evaluated Mass Spectral Reference Data Program. J. G. Dillard, Virginia Polytechnic Institute & State Univ., Blacksburg, Va. 24061

3:30 Future Trends in Raman Spectroscopy. E. R. Lippincott, J. W. Brasch, Center of Materials Res., Univ. of Maryland, College Park, Md. 20742

4:00 Applied Microwave (Nrr) Spectroscopy—Problems and Progress. W. F. White, NASA-Langley Research Center, Hampton, Va. 23365

Wednesday Morning — Section A

RECENT TRENDS IN DETERMINATION OF MOLECULAR WEIGHT

(Joint with Division of Polymer Chemistry)

E. E. Drott, *Presiding*

9:05 Simultaneous Determination of Molecular Weight and Partial Specific Volume from Measurements of (R_θ/C) and (dn/dc). W. Heller, Wayne State Univ., Detroit, Mich. 48202

9:30 Recent Trends in the Determination of Molecular Weights and Molecular Sizes of Elastomers. W. S. Bahary, Fairleigh Dickinson Univ., Teaneck, N.J. 07666

10:00 A Supplement to the Equilibrium Theory for Gpc. W. W. Yau, C. P. Malone, Engineering Physics Lab., E. I. du Pont de Nemours & Co., Wilmington, Del. 19898

Now... Determine Magnetic Susceptibility Over a 1.5 K to 1050 K Temperature Range

Three new accessories plus important design advancements provide the PAR™ Vibrating Sample Magnetometer with expanded capabilities in investigations of magnetic susceptibility.

Samples are easily changed and can be maintained at any temperature in the range of 1.5 K to 1050 K. Changes in magnetic moment can be measured to a maximum sensitivity of $5x10^{-5}$ emu. A bidirectional output simplifies the measurement of hysteresis loops by going smoothly through zero with either an increasing or decreasing magnetic field. Data is digitally displayed and is suitable for interface with a computer or teleprinter.

The system will analyze ferromagnetic, paramagnetic, diamagnetic, ferrimagnetic, antiferromagnetic, metamagnetic and superconducting materials.

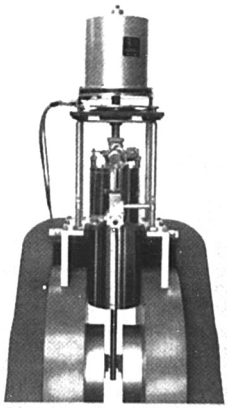

For the investigation of Curie points—or other high temperature magnetic phenomena—the Model 151 High Temperature Chamber allows the sample zone to be maintained at any temperature from ambient to 1050 K. Bifilar-wound heating element minimizes magnetic interference. Power required is 25 watts max. to reach 1050 K. Price: $1,050.

For research into the magnetic properties of materials under cryogenic conditions, or other low temperature investigations, the Model 153 Cryostat permits rapid variation of sample temperature from 1.5 K to 300 K. It uses a helium vapor shield, liquid helium cooling and has a hold time in the order of eight hours with LHe loss as low as 150 cm³/hr. Price: $4,425.

The Model 152 Cryogenic Temperature Controller employs a gallium arsenide diode sensor to provide continuous temperature control in the region of 1.5 K to 300K. Day-to-day repeatability is better than ±0.1 K; stability better than ±0.02 K per hour. Price: $1,095 less Sensor. Gallium Arsenide sensors suitable for use with the Model 153 Cryostat are priced at $180 (when ordered with the Temperature Controller).

Price of the Model 155 Vibrating Sample Magnetometer, successor to Model FM-1, is $13,500. For more information about its operation, application and accessories, write Princeton Applied Research Corporation, Box 565, Princeton, New Jersey 08540. Telephone: (609) 924-6835.

PAR

PRINCETON APPLIED RESEARCH CORPORATION

CIRCLE 159 ON READER SERVICE CARD

10:25 Fractionation of Linear Polyethylene with Gel Permeation Chromatography, Part V—IUPAC Samples. N. Nakajima, Allied Chemical Corp., Plastics Div., Morristown, N.J. 07960

10:55 Reproducibility of Molecular Weight Measurements by Gpc with Infrared Detectors. J. H. Ross, Jr., R. L. Shank, Union Carbide Corp., Chemicals & Plastics, P.O. Box 8361, South Charleston, W.Va. 25303

11:20 Gel Permeation Chromatography of Semipolar Materials. M. Ezrin, M. Brown, DeBell & Richardson, Inc., Enfield, Conn. 06082

Section B

CHROMATOGRAPHY AND COMPUTERS—ECONOMICAL APPROACH FOR EVERY LABORATORY

J. M. Gill, *Presiding*

9:00 State of Chromatography Automation. J. M. Gill, VIDAR AutoLab, 77 Ortega Ave., Mountain View, Calif. 94040

9:25 Computer Programming in Chemistry—Past, Present, and Future. R. E. Anderson, Lawrence Radiation Lab., P.O. Box 808 L-404, Livermore, Calif. 94550

9:50 Time-Shared Computer and Chemical Laboratory Applications. D. L. Schroeder, On-Line Systems, Inc., 4721 McKnight Rd., Pittsburgh, Pa., 15237

10:30 Gas Chromatography Automation by Integrator and Time Share. H. W. Jackson, Kraftco Corp., 801 Waukegan Rd., Glenview, Ill., 60025

11:00 Closing Loop with a Laboratory Gc/Computer System. L. Mikkelsen, Hewlett-Packard Co., Avondale, Pa. 19311

11:25 New Computing Integrator for Chromatography. J. R. Hubbard, J. M. Gill, L. Miller, VIDAR AutoLab, 77 Ortega Ave., Mountain View, Calif. 94040.

Wednesday Afternoon Section A

RECENT TRENDS IN DETERMINATION OF MOLECULAR WEIGHT

(Joint with Division of Polymer Chemistry)

J. F. Johnson, *Presiding*

2:05 Gel Permeation Chromatography Calibration. II Preparative Gpc Fractionation and Characterization of Poly-(Methyl Methacrylate) for Calibration in 2,2,2-Trifluoroethanol. T. Provder, SCM Corp., Glidden-Durkee Div., 16651 Sprague Rd., Strongsville, Ohio 44136; J. H. Clark, Monsanto Co., 800 N. Lindbergh Blvd., St. Louis, Mo. 63166; E. E. Drott, Monsanto Co., Texas City, Tex. 77590

2:30 Gel Permeation Chromatography—Data Acquisition and Processing System Using a Minicomputer. G. Walther, A. E. Hamielec, J. D. Wright, Dept. of Chem. Engineering, McMaster Univ., Hamilton, Ont., Canada

2:55 Molecular Weight Averages from Gel Permeation Chromatography Employing the Universal Calibration Method. E. Nichols, Gulf Oil of Canada Ltd., Ste. Anne de Bellevue, P.Q., Canada

3:30 Gpc Analysis of Block Copolymer. F. S. C. Chang, Borg-Warner Corp., Roy C. Ingersoll Res. Center, Wolf and Algonquin Rds., Des Plaines, Ill. 60018

3:55 Preparative Separations by Gpc. J. N. Little, J. L. Waters, W. A. Dark, Waters Assoc. Inc., 61 Fountain St., Framingham, Mass. 01701

4:20 Treating Gpc as Summation of Narrow Fraction Chromatograms to Obtain MWD. B. S. Ehrlich, W. V. Smith, Uniroyal, Inc., Res. Center, Wayne, N.J. 07470

6:30 Divisional Social Hour and Banquet at Blackie's Restaurant. Speaker: Dr. Thomas Cairns, Los Angeles County Museum of Art. "Everything You Have Always Wanted to Know About Art but Were Afraid to Ask"

Section B

CHROMATOGRAPHY AND COMPUTERS—ECONOMICAL APPROACH FOR EVERY LABORATORY

D. R. Deans, *Presiding*

2:10 Use of Magnetic Tape Cassette Recorder with On-Line Gas Chromatography Data System. J. T. Frazer, B. T. Guran, Eastman Kodak Co., Kodak Park Div., Industrial Lab., Rochester, N.Y. 14650

2:40 New Applications of Expanded Gas Chromatography/Computer System. J. G. W. Price, J. C. Scott, L. O. Wheeler, Celanese Chem. Co., P.O. Box 9077, Corpus Christi, Texas 78408

3:10 Gc Automation—Operator Problems and System Reliability. D. R. Deans, Imperial Chem. Ind. Ltd., HOC Div., Billington, Teesside, UK

3:40 Chromatography On-Line to Mulheim Computer System. G. Schomburg, E. Ziegler, Max-Planck-Institut, fur Kohlenforschung, D-433 Mulheim a.d. Ruhr, Kaiser-Wilhelm-Platz 1, West Germany

4:20 Laboratory Automation via Hierarchical Computers. C. E. Klopfenstein, Univ. of Ore., Eugene, Ore. 97403

4:50 Computer Analysis of Asymmetrical Gc Peaks. H. M. McNair, M. Cooke, Virginia Polytechnic Institute, Blacksburg, Va. 24060

Thursday Morning Section A

RECENT TRENDS IN DETERMINATION OF MOLECULAR WEIGHT

(Joint with Division of Polymer Chemistry)

K. A. Bori, *Presiding*

9:05 Average Degree of Polymerization of Cellulose by Gpc without Viscosity Measurements. J. I. Wadsworth, L. Segal, J. D. Timpa, Southern Regional Res. Lab., USDA, ARS, P.O. Box 19687, New Orleans, La. 70119

9:35 Gel Permeation Chromatography: Molecular Weight Averages and Molecular Weight Distribution of Cellulose Nitrate. A. C. Ouano, IBM Res. Lab., Monterey & Cottle Rds., San Jose, Calif. 95114; A. Broido, Pacific Southwest Forest & Range Experiment Station Forest Service, U.S. Dept. of Agriculture, Berkeley, Calif. 94701; E. M. Barrall II, IBM Res. Lab., Monterey & Cottle Rds., San Jose, Calif. 95114; A. C. Javier-Son, Univ. of Calif., Statewide Air Pollution Res. Ctr., Riverside, Calif. 92502

10:00 Molecular Weight Characterization of Resole Phenol-Formaldehyde Resins. F. L. Tobiason, C. Chandler, P. Negstad, Pacific Lutheran Univ., Tacoma, Wash. 98447; F. E. Schwarz, Reichhold Chemicals, Inc., 2340 Taylor Way, Tacoma, Wash. 98401

10:25 Approximate Solution to Transport Equations Involving Weak Diffusion Effects. G. H. Weiss, Physical Sciences Lab., Div. of Computer Research & Technology, National Institutes of Health, Bethesda, Md. 20014

10:50 New Way of Determining Molecular Weight Distribution Including Low Molecular Weight, from Equilibrium Sedimentation. M. Gehatia, U.S. Air Force, AFML/LNP, Wright-Patterson AFB, Ohio 45433

11:15 Molecular-Weight Distributions from Sedimentation Equilibrium Experiments. E. T. Adams, Jr., P. J. Wan, Texas A&M Univ., College Station, Tex. 77843; D. A. Soucek, Illinois Institute of Technology, Chicago, Ill. 60616; G. H. Barlow, Molecular Biology Dept., Abbott Labs., Inc., N. Chicago, Ill. 60064

Section B

GENERAL

D. H. Freeman, *Presiding*

9:05 Pyrographic Analysis and Differentiation between Various Industrial Waste Effluents. P. R. Newton, Rocketdyne Field Lab., P.O. Box 5220, Athens, Ga. 30604

9:20 Analysis of Vapor-Phase Pyrolysis Products of Four Trimethylpentane Isomers. J. Q. Walker, McDonnell Res. Labs., P.O. Box 516, St. Louis, Mo. 63166; J. B. Maynard, Res. Lab., Shell Oil Co., Wood River, Ill. 62095

9:40 Problems of Standardization and Interlaboratory Reproducibility in Pyrolysis Gas Chromatography (Pgc). R. L. Levy, C. J. Wolf, McDonnell Douglas Res. Labs., McDonnell Douglas Corp., P.O. Box 516, St. Louis, Mo. 63166

10:00 Vapor Phase Pyrolysis Combined with High-Resolution Gas Chromatography for Analysis of Organic Mixtures. J. Q. Walker, C. J. Wolf, McDonnell Douglas Res. Labs., McDonnell Douglas Corp., P.O. Box 516, St. Louis, Mo. 63166

10:15 Gas Chromatographic Analysis of Hydrophobic Groups of Surface Active Ethylene Oxide Adducts Using Specific Reagent for Ether Cleavage. K. Konishi, K. Tsuji, Industrial Res. Labs., Kao Soap Co., Wakayamashi, Japan

10:30 Gas-Solid Chromatography on Macroreticular Cation-Exchange Resins. R. F. Hirch, Seton Hall Univ., South Orange, N.J. 07079; H. C. Stober, A. W. O'Connell, Ciba-Geigy Corp., Summit, N.J. 07901; M. Kowblansky, Warner Lambert Co., Morris Plains, N.J. 07950

10:50 Interactive Gel Networks for Organic Separations. D. H. Freeman, D. P. Enagonio, A105 Chemistry, National Bureau of Standards, Washington, D.C. 20234

11:15 Separation and Determination of Alpha Olefin Sulfonates by Salting-Out Chromatography. K. Konishi, S. Fudano, Industrial Res. Labs., Kao Soap Co., Ltd., Wakayama-shi, Japan

11:30 Instrument for Measuring Hydrogen Content in Metals. G. L. Powell, J. B. Condon, R. A. Strehlow, Oak Ridge National Lab., Nuclear Div., Oak Ridge, Tenn. 37830

Thursday Afternoon — Section A

RECENT TRENDS IN DETERMINATION OF MOLECULAR WEIGHT

(Joint with Division of Polymer Chemistry)

D. Yphantis, *Presiding*

2:05 Use of Stepping Motor with Photoelectric Scanner of Analytical Ultracentrifuge. D. E. Wampler, Dept. of Biochemistry, Univ. of Connecticut Health Center, Farmington, Conn. 06032

2:25 Study of Mixed Associations by Sedimentation Equilibrium and Light Scattering. A. H. Pekar, The Lilly Res. Labs, Eli Lilly & Co., Indianapolis, Ind. 46206; P. J. Wan, E. T. Adams, Jr., Texas A&M Univ., College Station, Tex. 77843

3:00 Determination of Molecular Weights of Interacting Biological Macromolecules by Light-Scattering and Small-Angle X-Ray Scattering. S. N. Timasheff, Pioneering Res. Lab., U.S. Dept. of Agriculture, Brandeis Univ., Grad. Dept. of Biochemistry, Waltham, Mass. 02154

3:25 Use of Thin-Film Dialysis and High-Resolution Nmr in Study of Conformation and Association Phenomena. L. C. Craig, H. C. Chen, W. A. Gibbons, The Rockefeller Univ., York Ave. & 66th St., New York, N.Y. 10021

3:55 Theoretical Aspects of Study of Aggregation Stoichiometry by Equilibrium Gel Filtration. B. F. Cameron, Papanicolaou Cancer Research Institute, 1155 N.W. 14th St., Miami, Fla. 33136; A. D. Adler, New England Institute, Ridgefield, Conn. 06877

4:15 Polypeptide Chain Molecular Weights by Gel Filtration in 6*M* Guanidinium Chloride. K. G. Mann, D. N. Fass, Dept. of Biochemistry, Univ. of Minn., St. Paul, Minn. 55101; W. W. Fish, Dept. of Biochemistry, Medical Univ. of South Carolina, Charleston, S.C. 29401

Section B

GENERAL

R. Rowan, Jr., *Presiding*

2:05 Calculations in Programmed Temperature Gas Chromatography When Void Volume Is Not Negligible—New Approach. R. Rowan, Jr., E. W. Leach, New Mexico State Univ., P.O. Box 3C, Las Cruces, N.M. 88001

2:20 Time Normalization Chromatography. E. Grushka, M.Yepes-Baraya, State Univ. of New York at Buffalo, Buffalo, N.Y. 14214; W. D. Cooke, Cornell Univ., Ithaca, N.Y. 14850

2:40 Effect of Dead Volume on Efficiency of Gas Chromatographic System. V. Maynard, E. Grushka, State Univ. of New York at Buffalo, Buffalo, N.Y. 14214

3:00 Quantitative Sampling of Vertical Tube Reactor. F. W. Williams, Naval Res. Lab., Code 6180, Washington, D.C. 20390; W. L. Stumpf, Jr., Ohio State Univ., Columbus, Ohio

3:15 Ohm's Law Analogy to Depulsed Mobile Phase Flow in Liquid Chromatography. W. L. Zielinski, Jr., H. D. Dixon, P. J. Byrne, D. H. Freeman, A105, Chemistry, National Bureau of Standards, Washington, D.C. 20234

3:35 Porous Layer Open Tubular Columns Made by Dynamic Method. J. G. Nikelly, Philadelphia College of Pharmacy & Science, Philadelphia, Pa. 19104

3:50 Carbon Molecular Sieve. D. M. Ottenstein, W. R. Supina, Supelco, Inc., Supelco Park, Bellefonte, Pa. 16823

4:05 Spectral Response of Alkali Flame Detector. R. F. Moseman, W. A. Aue, Rm. 4, Agriculture Bldg., Univ. of Missouri, Columbia, Mo. 65201

4:20 Solvent Extraction and Gas Chromatography of Volatile Mixed-Ligand Complexes of Lanthanides. R. F. Sieck, Eli Lilly & Co., Greenfield Lab., Box 708, Greenfield, Ind. 46140; C. V. Banks, Institute for Atomic Res. & Dept. of Chem., Iowa State Univ., Ames, Iowa 50010

Friday Morning — Section A

GENERAL

O. Menis, *Presiding*

9:05 Potentiostat and Cell Design for Study of Rapid Electrochemical Systems. S. P. Perone, Purdue Univ., Lafayette, Ind. 47907; J. E. Mumby, E. I. du Pont Co., Experimental Station, Plastics Dept., Wilmington, Del.

9:25 Electroanalytical Measurements of Flash Photolyzed Ferrioxalate. S. P. Perone, Purdue Univ., Lafayette, Ind. 47907; R. A. Jamieson, Procter & Gamble Co., Winton Hill Tech. Center, 6071 Center Hill Rd., Cincinnati, Ohio 45224

9:45 Mercury-Platinum Optically Transparent Electrode. W. R. Heineman, T. Kuwana, Case Western Reserve Univ., Cleveland, Ohio 44106

10:05 Electrochemistry of Triphenylgermanium Halides. R. S. Bottei, Univ. of Notre Dame, Notre Dame, Ind. 46556; R. J. Boczkowski, Univ. of Cincinnati, Cincinnati, Ohio 45221

10:25 Polarographic Determination of Stability Constants in Acetonitrile. J. D. Miller, I. D. Eubanks, F. J. Abbott, Oklahoma State Univ., Stillwater, Okla. 74074

10:40 Analysis of Botanical Standard Reference Materials by Cathode Ray Polarography. E. J. Maienthal, Rm. A227 Chem., National Bureau of Standards, Washington, D.C. 20234

10:55 Electrochemical Investigation of Tris(1,10-phenanthroline) Chromium Complexes. D. M. Soignet, Southern Regional Res. Lab., U.S. Dept. of Agriculture, P.O. Box 19687, New Orleans, La. 70119; L. G. Hargis, Louisiana State Univ. in New Orleans, Lakefront, New Orleans, La. 70122

11:15 Electrochemical Investigation of Dichlorobis (2,2'-Bipyridine) Chromium(III) Chloride. D. M. Soignet, Southern Regional Res. Lab., U.S. Dept. of Agriculture, P.O. Box 19687, New Orleans, La. 70119; L. G. Hargis, Louisiana State Univ. in New Orleans, Lakefront, New Orleans, La. 70122

11:30 Coulometric Titration of Weak Acids in Tetrahydrofuran. C. E. Champion, D. G. Bush, Res. Labs., Bldg. 82, Eastman Kodak Co., Rochester, N.Y. 14650

Section B

GENERAL

G. G. Guilbault, *Presiding*

9:05 Application of Substrate-Gradient Automated Assay to Enzyme Kinetic Studies. W. E. Kurtin, Trinity Univ., San Antonio, Tex. 78212; A. Himoe, Dept. of Biochemistry, Baylor College of Medicine, Houston, Tex. 77025

9:20 Fluorescence Monitoring of Reaction Rates on Solid Surfaces. G. G. Guilbault, R. L. Zimmerman, Louisiana State Univ. in New Orleans, New Orleans, La. 70122

9:40 Determination of Sulfate by Atomic Absorption Inhibition Titration. R. W. Looyenga, C. O. Huber, Univ. of Wisconsin-Milwaukee, Milwaukee, Wis. 53201

10:00 Major, Minor, and Trace Elements in Minerals from Bruderheim Meteorite by Atomic Absorption and Instrumental Neutron Activation Analysis. D. Nava, Planetology Branch, Goddard Space Flight Center, NASA, Greenbelt, Md. 20771; P. Buhl, J. Barker, Univ. of Maryland, College Park, Md. 20742

10:15 Determination of Methyl Mercury Compounds by Membrane-Spectral Emission Technique. R. S. Braman, S. M. Kincaid, B. S. Kincaid, Univ. of South Florida, Tampa, Fla. 33620; D. K. Young, Dept. of Biology, Univ. of South Florida, Tampa, Fla. 33620

10:35 Coulometric Microdetermination of Some Aminopolycarboxylic Acids Using Mercury(II). J. L. Vanderbalck, C. A. Ducarmois, G. J. Patriarche, Free Univ. of Brussels, 50, Av. F. D. Roosevelt, 1050 Brussels, Belgium

10:50 Highly Accurate Calibration Instrument for Sensitive Specific Air Pollution Monitors. J. G. Green, W. D. Llewelyn, W. D. Reynolds, Electro/Mass Lab., P.O. Box 112, Danville, Calif. 94526

11:10 Development of a Computer Based Real Time Data Acquisition and Reduction System for Mass Spectrometry. M. B. Fallgatter, Carroll College, Waukesha, Wis. 53186; R. J. Hanrahan, 406 Nuclear Sciences Bldg., Univ. of Florida, Gainesville, Fla. 32601

11:30 Design of a High-Precision Fluorometer for Biochemical Measurements. J. I. Peterson, W. S. Friauf, S. B. Leighton, Biomedical Engineering & Instrumentation Branch, DRS National Inst. of Health, Bethesda, Md. 20014

15th Conference on Analytical Chemistry in Nuclear Technology

The 15th Conference on Analytical Chemistry in Nuclear Technology will take place at the Oak Ridge Playhouse, Jackson Square, Oak Ridge, Tenn. 37830, October 12–14, 1971. All interested persons are invited to attend; registration is $15 and includes tickets to the social hour and buffet on October 12 and the picnic dinner at Carbide Park on October 13. Extra tickets for these events are available for $6.00 and $4.50, respectively. For preregistration, send the fee to L. J. Brady, Oak Ridge National Laboratory, P.O. Box X, Oak Ridge, Tenn. 37830.

The complete technical program of this meeting appears below.

Tuesday Morning, October 12

CHROMATOGRAPHIC METHODS OF ANALYSIS

Gerald Goldstein, Oak Ridge National Laboratory, Oak Ridge, Tenn. 37830, Presiding

9:00 **Welcoming Remarks.** Myron Kelley, Director, Analytical Chemistry Division, Oak Ridge National Laboratory, Oak Ridge, Tenn. 37830

9:10 **High-Speed Separation of Rare Earths by Ion Exchange.** D. H. Sisson, Allan Mode, University of California, Lawrence Radiation Laboratory, Livermore, Calif. 94550; David Campbell, Oak Ridge National Laboratory, Oak Ridge, Tenn. 37830

9:30 **In-Line Radiochemical Analysis for Controlling Rapid Ion Exchange Recovery of Transplutonium Elements.** M. A. Laket, S. F. Peterson, E. I. du Pont de Nemours and Co., Savannah River Laboratory, Aiken, S.C. 29801

9:50 **Ion Exchange Methods in Trace Analysis.** John Faris, Argonne National Laboratory, Argonne, Ill. 60439

10:30 **Biochemical Analysis of Human Genetic Defects.** J. L. Epler, J. X. Khym, J. D. Regan, W. E. Barnett, Oak Ridge National Laboratory, Oak Ridge, Tenn. 37830

11:00 **The Application of Coupled Cation and Anion Exchange Columns to Solve a Practical Analytical Problem in the Analysis of Physiologic Body Fluids.** John Mrochek, Oak Ridge National Laboratory, Oak Ridge, Tenn. 37830

11:20 **The Separation of Indole Compounds of Physiologic Interest by Liquid Chromatography.** D. D. Chilcote, J. E. Mrochek, Oak Ridge National Laboratory, Oak Ridge, Tenn. 37830

Tuesday Afternoon, October 12

M. R. Guerin, Oak Ridge National Laboratory, Oak Ridge, Tenn. 37830, Presiding

2:05 **Process Gas Chromatography for Monitoring a Noble Gas Separation System.** J. G. Million, Oak Ridge Gaseous Diffusion Plant, Oak Ridge, Tenn. 37830

2:40 **The Extraction-Derivatization-Gc Determination of Trace Phosphate in Aqueous Media.** D. R. Matthews, W. D. Shults, M. R. Guerin, Oak Ridge National Laboratory, Oak Ridge, Tenn. 37830; J. A. Dean, University of Tennessee, Knoxville, Tenn. 37916

3:00 **Determination of Nitrogen, Sulfur, Phosphorus, and Carbon in Solid Ecological Materials via Hydrogenation and Element-Sensitive Detectors.** A. D. Horton, W. D. Shults, A. S. Meyer, Oak Ridge National Laboratory, Oak Ridge, Tenn. 37830

3:35 **Quantitative Application of Pyrography.** Ihor Lysyj, Rocketdyne, North American Rockwell Corp., Athens, Ga. 30604

3:55 **Combined Gc-Mass Spectrometry for the Identification of Compounds of Biological Interest.** W. T. Rainey, W. C. Butts, Oak Ridge National Laboratory, Oak Ridge, Tenn. 37830; F. Snyder, Oak Ridge Associated Universities, Oak Ridge, Tenn. 37830

4:15 **Separation and Detection of Barium Using Electrochromatography.** Robert Morse, George Welford, Health and Safety Laboratory, U.S. Atomic Energy Commission, New York, N.Y. 10014

Wednesday Morning, October 13

APPLICATIONS OF PHOTOELECTRON SPECTROSCOPY IN ANALYTICAL CHEMISTRY

L. D. Hulett, Oak Ridge National Laboratory, Oak Ridge, Tenn. 37830, Presiding

9:05 **Chemical Applications of Electron Spectroscopy."** David Hercules, University of Georgia, Athens, Ga. 30601

10:15 **Chemical Shifts Observed in Photoelectron Spectroscopy as a Function of Periodic Table.** Thomas Carlson, Oak Ridge National Laboratory; Nils Fernelius, Research Consultants, Inc., Oak Ridge, Tenn. 37830

11:00 **High Performance and Versatile Photoelectron Spectrometer for ESCA.** Paul Larson, John Rendina, McPherson Instrument Corp., Acton, Mass. 01720

Wednesday Afternoon, October 13

APPLICATIONS OF PHOTOELECTRON SPECTROSCOPY IN ANALYTICAL CHEMISTRY

Thomas Carlson, Oak Ridge National Laboratory, Oak Ridge, Tenn. 37830, Presiding

1:30 **Photoelectron Spectroscopy of Transition Metal Compounds.** J. C. Carver, T. A. Carlson, Oak Ridge National Laboratory, Oak Ridge, Tenn. 37830; G. K. Schweitzer, F. A. Grimm, University of Tennessee, Knoxville, Tenn. 37916

2:15 **Case Studies in Soft X-Ray Spectrometry Using an Electron Energy Analyzer of Well-Defined Characteristics.** M. O. Krause, Oak Ridge National Laboratory, Oak Ridge, Tenn. 37830

3:15 **Analysis of the Surfaces of Solids by Photoelectron Spectroscopy.** L. D. Hulett, A. L. Bacarella, Oak Ridge National Laboratory, Oak Ridge, Tenn. 37830

3:45 **X-Ray and Uv-Induced Electron Emission Studies of IIB-VIA Compounds.** C. J. Vesely, D. W. Langer, Aerospace Research Laboratories (AFSC), Wright-Patterson Air Force Base, Ohio 45433

Thursday Morning, October 14

APPLICATIONS OF PHOTOELECTRON SPECTROSCOPY IN ANALYTICAL CHEMISTRY

M. O. Krause, Oak Ridge National Laboratory, Oak Ridge, Tenn. 37830, Presiding

9:05 **Photoelectron Spectroscopy of Coordination Compounds.** J. R. Blackburn, G. Kumar, W. E. Moddeman, R. G. Albridge, M. M. Jones, Vanderbilt University, Nashville, Tenn. 37203

9:45 **Studies of the Oxidation States of Transition Metals.** Louis Wilson, John Helmer, Varian Assoc., Palo Alto, Calif. 94304

10:45 **Application of the HP 5950A ESCA Spectrometer to the Analysis of Metallic Surfaces.** A. Melera, H. E. Weaver, Hewlett-Packard Co., Palo Alto, Calif. 94304

11:15 **Electron Impact Spectroscopy.** John Rendina, Paul Larson, McPherson Instrument Corp., Acton, Mass. 01720

Thursday Afternoon, October 14

GENERAL PAPERS

L. J. Brady, Oak Ridge National Laboratory, Oak Ridge, Tenn. 37830, Presiding

1:30 **Liquid Scintillation Assay of Strontium-89 in Plant and Soil Samples.** J. E. Hardcastle, W. H. Fuller, R. J. Hannapel, Dept. of Agricultural Chemistry and Soils, University of Arizona, Tucson, Ariz.

1:55 **The Determination of Uranium by Flame Emission Spectroscopy.** Orlando Vita, Roger Fischer, Technical Div., Goodyear Atomic Corp., Piketon, Ohio 45661

2:20 **Direct Determination of Volatile Metal Fluorides in UF_6 by Atomic Absorption Spectrometry.** Roger Fischer, O. A. Vita, Technical Div., Goodyear Atomic Corp., Piketon, Ohio 45661

2:45 **Spectrographic Determination of Refractory Elements in Uranium —Direct Spark Excitation of a BPHA-Acetone Extract Using a Solution Transport System.** C. R. Walker, H. R. Boggs, Technical Div., Goodyear Atomic Corp., Piketon, Ohio 45661

Andrew A. Husovsky Joins ANALYTICAL CHEMISTRY'S Editorial Staff

Dr. Andrew A. Husovsky has joined the editorial staff of ANALYTICAL CHEMISTRY as an Editorial Assistant. Dr. Husovsky was born in Wilkes-Barre, Pa. in 1943. He received a BS degree in chemistry from King's College in Wilkes-Barre in 1965 and earned a PhD degree at Georgetown University in 1971. Under Robert deLevie, he worked on a study of the negative faradaic admittance in the region of the polarographic minimum of In(III) in aqueous NaSCN solutions. His major professional interests are in electrochemistry, chemical instrumentation, electronics, and chemical literature. Dr. Husovsky will be involved in all editorial phases in the publication of ANALYTICAL CHEMISTRY.

7th International Symposium— Advances in Chromatography

The Seventh International Symposium on Advances in Chromatography will be held November 29–December 3, 1971, at Caesar's Palace, Las Vegas, Nev. A special feature of the meeting will be an exhibit of the latest instrumentation and books. Registration must be made in advance of the meeting. Preregistration forms and programs may be obtained from Dr. A. Zlatkis, Chemistry Department, University of Houston, Houston, Texas 77004. The detailed technical program is given below.

Monday Morning, November 29

NEW HORIZONS

L. S. Ettre, Presiding

9:00 Welcome to the Symposium

9:15 **Electron Capture Detector: New Model of Operation.** R. J. Maggs, J. E. Lovelock, University of Reading, Berkshire, England; P. E. Joynes, Tye Unicam, Ltd., Cambridge, England; A. J. Davis, Shell Research, Ltd., Cheshire, England

9:55 **Gas-Liquid Chromatography with Concentration Gradient in Liquid Phase.** B. A. Rudenko, W. E. Harris, University of Alberta, Edmonton, Alberta, Canada; H. W. Habgood, Research Council of Alberta, Edmonton, Alta., Canada

10:20 **The Sample as Its Own Stationary Phase in Gas Chromatography.** D. R. Deans, ICI Ltd., Billingham, Teesside, England

11:00 **Systematic Study of Quantitative Effects of Instrument Control on Analytical Precision in Flame Ionization Gas Chromatography.** D. W. Grant, A. Clarke, The Coal Tar Research Association, Gomersal, Yorkshire, England

11:25 **Precision and Accuracy of Statistical Moment Analyses in Chromatography from Digital Data.** S. N. Chester, S. P. Cram, University of Florida, Gainesville, Fla.

11:50 **Effects of the Solute Mass-Transfer on Gas Chromatographic Retention Data.** S. Wicar, J. Novak, J. Janak, Czechoslovak Academy of Sciences, Brno, Czechoslovakia

Monday Afternoon, November 29

GAS CHROMATOGRAPHY DETECTORS

C. Horvath, Presiding

2:00 **Combination of Gas Chromatography with Nuclear Magnetic Resonance.** E. Bayer, University of Tuebingen, Tuebingen, Germany

2:30 **Detection of Fluorine by Flame Ionization.** Arthur Karmen, Eileen L. Kelly, New York University Medical Center, New York, N.Y.

2:55 **High-Temperature Tritium Source for Electron Capture Detectors: Application to Low-Volume Detector.** D. C. Fenimore, P. R. Loy, Texas Research Institute of Mental Sciences, Houston, Tex; A. Zlatkis, University of Houston, Houston, Tex.

3:15 **Helium Photoionization Detector Utilizing a Microwave Discharge Source.** R. R. Freeman, W. E. Wentworth, University of Houston, Houston, Tex.

3:40 **Fluorescence Detector for Analysis of Polynuclear Arenes by Gas Chromatography.** H. P. Burchfield, R. J. Wheeler, J. B. Bernos, Gulf South Research Institute, New Iberia, La.

4:15 **Plasma Chromatography of Polychlorinated Biphenyls.** F. W. Karasek, University of Waterloo, Waterloo, Ontario, Canada

4:40 **Highly Precise Quantitative Gas-Chromatographic Method and Its Application to Determination of Copolymerization Kinetics.** A. L. German, D. Heikens, Eindhoven University of Technology, The Netherlands

5:00 **Interpretation of Asymmetric Curves in Chromatography.** O. Grubner, Harvard School of Public Health, Boston, Mass.

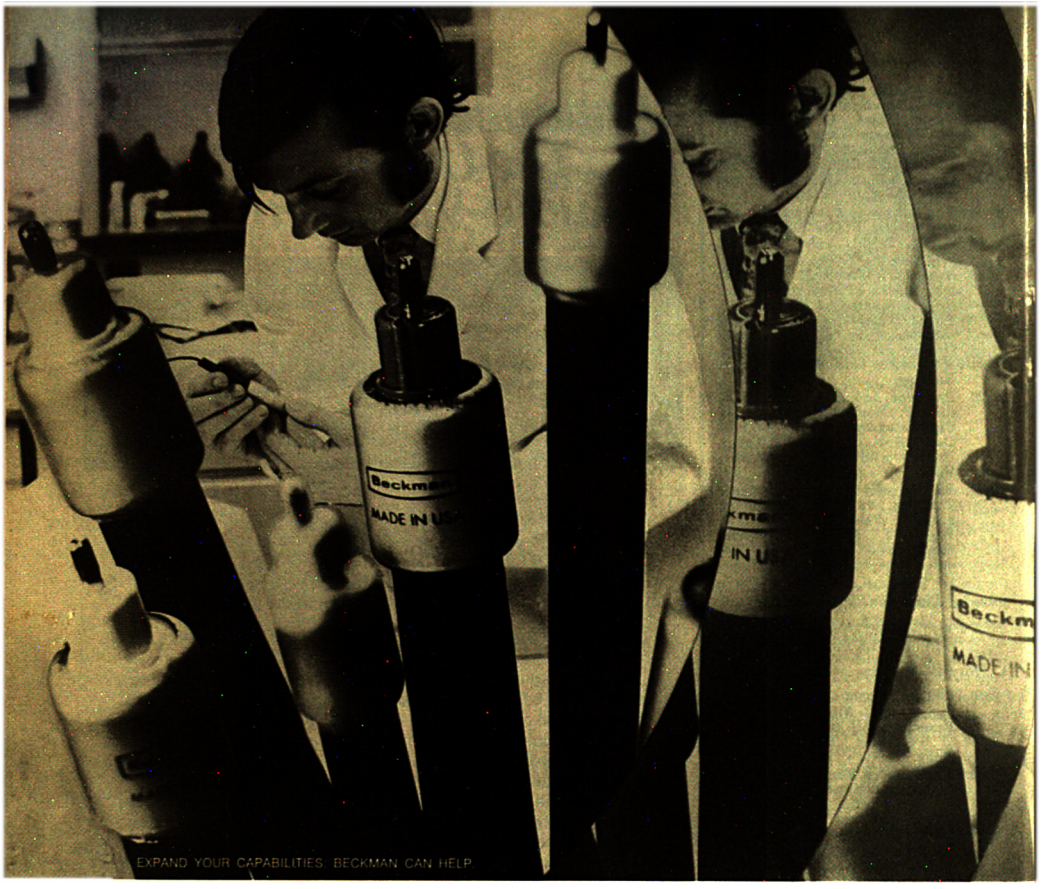

There are two ways to learn when, why and how to use selective ion electrodes: 1. Hard work 2. Ask Beckman

Beckman has spent years perfecting selective ion technology so you won't have to. The result: a broad line of Selectlon® Electrodes, each backed by Beckman's superior quality, performance and reliability. And each backed by complete technical and applications support.

Whatever you need to know about selective ion electrodes, Beckman is ready to help. Our selective ion experts will examine your specific situation (even duplicate your application in our own lab, if necessary). Then we'll submit your personal Selectlon Electrode Profile directly to you, with recommended electrodes *and procedures* for best results.

You can rely on Beckman's broad product capability and technical know-how. We offer Selectlon Electrodes for ammonium, bromide, calcium, chloride, copper, fluoride, fluoroborate, iodide, nitrate, perchlorate, potassium, sulfide/silver and water hardness, plus both laboratory and clinical style sodium and cation electrodes and a combination fluoride electrode. Each is backed by complete technical data and performance specifications, plus specific product data sheets for chloride, fluoride, sulfide, sodium, potassium and ammonium.

To obtain *your* Selectlon Electrode Profile covering specific requirements, just complete our convenient Selectlon Electrode Profile Questionnaire and we'll do the rest. For your questionnaire – and complete information on Beckman pH meters and Selectlon Electrodes – write for Data File 23, Beckman Instruments, Inc., Scientific Instruments Division, 2500 Harbor Boulevard, Fullerton, California 92634.

Beckman® INSTRUMENTS, INC.

HELPING SCIENCE AND INDUSTRY IMPROVE THE QUALITY OF LIFE.

INTERNATIONAL SUBSIDIARIES: AMSTERDAM, CAPE TOWN, GENEVA, GLENROTHES, SCOTLAND, LONDON, MEXICO CITY, MUNICH, PARIS, STOCKHOLM, TOKYO, VIENNA

CIRCLE 25 ON READER SERVICE CARD

Tuesday Morning, November 30

LIQUID CHROMATOGRAPHY

J. J. Kirkland, Presiding

9:00 **Influence of Column Parameters on Peak Broadening in High-Pressure Liquid Chromatography.** I. Halasz, M. Naefe, Institut fur Angewandte Physikalische Chemie der Universitat Saarbrucken, West Germany

9:30 **Some Aspects of Liquid-Solid Vacancy Chromatography.** R. P. W. Scott, C. G. Scott, P. Kucera, Hoffmann-LaRoche, Nutley, N.J.

10:00 **New Method for the Prediction of Partition Coefficients in Liquid-Liquid Systems and Its Experimental Verification for Steroids by Static and Chromatographic Measurements.** J. F. K. Huber, C. A. M. Meijers, J. A. R. J. Hulsman, University of Amsterdam, The Netherlands, and St. Anna Hospital, Geldrop, The Netherlands

10:45 **Interactive Gel Networks. Treatment of Simple Complexation and Masking Phenomena.** D. H. Freeman, National Bureau of Standards, Washington, D.C.

11:15 **Coupled Anion and Cation Exchange Chromatography of Complex Biochemical Mixtures.** C. D. Scott, D. D. Chilcote, N. E. Lee, Oak Ridge National Laboratory, Oak Ridge, Tenn.

11:45 **Rapid Separation of Nonionic Detergents of Polyethyleneglycol Monoalkylphenyl Ether Type by Column Liquid Chromatography.** J. F. K. Huber, F. F. Kolder, J. M. Miller, University of Amsterdam, The Netherlands

Tuesday Afternoon, November 30

LIQUID CHROMATOGRAPHY

L. R. Snyder, Presiding

2:00 **Optimization of Parameters for Fast Separations by Liquid Chromatography.** T. W. Smuts, Victor Pretorius, University of Pretoria, South Africa

2:30 **Bonded Stationary Phases for Chromatography.** D. C. Locke, J. E. Schmermund, B. Banner, Queens College, Flushing, N.Y.

2:55 **Rational Solvent System for Graded Elution in Liquid-Solid Chromatography.** R. P. W. Scott, B. Buglio, Hoffmann-La Roche, Nutley, N.J.

3:25 **VPO Detector for Liquid Chromatography.** W. Simon, E.T.H., Zurich, Switzerland

4:00 **Separation and Identification of Carbon-14 Diphenamid Metabolites Using Chromatographic Techniques.** L. F. Krzeminski, B. L. Cox, A. W. Neff, The Upjohn Co., Kalamazoo, Mich.

4:25 **Novel Inexpensive Gas Displacement Pump for Continuous Operation at Low Noise Levels with High Sensitivity Detectors in Liquid Chromatography.** B. L. Karger, L. V. Berry, Northeastern University, Boston, Mass.

4:50 **Analysis of Blends of Mixtures Using Multivariate Statistics.** S. C. Elliott, N. A. Hartmann, S. J. Hawkes, Oregon State University, Corvallis, Ore.

Wednesday Morning, December 1

Informal panels for small discussion groups. Topics to be considered will include Liquid Chromatography Columns, Quantitative Analysis, Gas Chromatographic Detection Systems, Theory and Instrumentation.

Wednesday Afternoon, December 1

R. S. Juvet, Presiding

2:00 **Identification and Column Selection. A Gas Chromatographic Method of Volatile Substances Characterization.** L. Rohrschneider, Chemische Werke Huls AG, Marl, Germany

2:30 **Gas-Solid Chromatographic Analysis of Aromatic Amines, Pyridine, Picolines, and Lutidines on Cobalt Phthalocyanine with Porous Layer Open Tube Columns.** J. J. Franken, C. Vidal-Madjar, G. Guiochon, Ecole Polytechnique, Paris, France

2:55 **Spherosil in Modified Gas-Solid Chromatography.** C. L. Guillemin, M. Deleuil, S. Cirendini, J. Vermont, Pechiney-Saint-Gobain, Aubervilliers, France

3:20 **Gas Chromatography of Monoolefins with Stationary Phases Containing Rhodium Coordination Compounds.** E. Gil-Av, V. Schurig, The Weizmann Institute of Science, Rehovot, Israel

4:00 **Evaluation of Dendritic Salt as Support for Gas-Liquid Chromatography.** R. D. Schwartz, R. G. Mathews, J. E. Rountree, D. M. Irvine, Pennzoil United, Inc., Shreveport, La.

4:20 **Ultratrace Analysis for Beryllium in Terrestrial, Meteoritic, and Apollo 11 and 12 Lunar Samples Using Electron Capture Gas Chromatography.** K. J. Eisentraut, D. J. Griest, R. E. Sievers, Wright-Patterson AFB, Ohio

4:45 **Use of Sample Loops with Micropacked Columns.** D. E. Durbin, Honeywell, Inc., Houston, Tex.

Thursday Morning, December 2

BIOMEDICAL APPLICATIONS

A. Karmen, Presiding

9:00 **Analysis of Steroids by Gas and Liquid Chromatography.** A. I. M. Keulemans, Eindhoven University of Technology, Eindhoven, The Netherlands

9:25 **Design Studies for Biomedical Gas Chromatograph.** E. C. Horning, C. D. Pfaffenberger, A. Moffat, Baylor College of Medicine, Houston, Tex.

9:50 **Off-Line Computerized Gas Chromatography–Mass Spectrometry in Analysis of Steroids.** R. Reimendal, J. Sjovall, Karolinska Institute, Stockholm, Sweden

The new Gilson Micro-fractionator is only so big*

Model FC-80
$495.00
FOB Middleton, Wisconsin

It's an ideal combination of low cost, small size and rugged construction!

THE MODEL FC-80 — drop counting or time-actuated Fraction Collector. Single-unit collector with base, drop detector, timer and digital counter; includes 2 test tube racks. Holds 80 glass test tubes 13 x 100 mm (9 ml).
* Size: 29 x 15 cm (11½ x 6 in.)

Ask about the Gilson Master-Slave System for multiple column collection.

Gilson Medical Electronics, Inc.
3000 West Beltline Highway
Middleton, Wisconsin 53562
Telephone 608/836-1551

GILSON

European Manufacturing Plant:
GILSON MEDICAL ELECTRONICS, FRANCE
69, rue Gambetta
95-Villiers-le-Bel, FRANCE
Telephone 990-10-38

CIRCLE 72 ON READER SERVICE CARD

10:15 **Comparison of Corticosteroid Derivatives by Gas Chromatography–Mass Spectrometry.** T. A. Baillie, C. J. W. Brooks, B. S. Middleditch, University of Glasgow, Glasgow, Scotland

10:55 **High-Temperature Gas Chromatographic Separations Using Glass Capillary Columns and Carborane Stationary Phases.** M. Novotny, R. Segura, A. Zlatkis, University of Houston, Houston, Tex.

11:25 **Gas Chromatography of Volatiles from Breath and Urine.** R. Teranishi, P. Cary, T. R. Mon, A. Robinson, L. Pauling, Stanford University, Palo Alto, Calif.

11:50 **Combined Gas-Liquid Chromatography–Mass Spectrometry Study of Cambendazole and Related Compounds.** W. J. A. VandenHeuvel, R. P. Buhs, J. R. Carlin, T. A. Jacob, F. R. Koniuszy, J. L. Smith, N. R. Trenner, R. W. Walker, D. E. Wolf, F. J. Wolf, Merck Sharp & Dohme Research Laboratories, Rahway, N.J.

Thursday Afternoon, December 2

Informal panels for small discussion groups. Topics to be considered will include Liquid Chromatography Detectors, Auxiliary Techniques, Biomedical Applications, Data Handling Systems, Lunar and Meteorite Analyses.

Friday Morning, December 3

PYROLYSIS, ENVIRONMENTAL PROBLEMS

E. Gil-Av, Presiding

9:00 **Curie Point Pyrolysis.** W. Simon, E.T.H., Zurich, Switzerland

9:20 **Temperature Rise Time and True Pyrolysis Temperature in Pulse Mode Pyrolysis Gas Chromatography.** R. L. Levy, D. L. Fanter, and C. J. Wolf, McDonnell Douglas Corp., St. Louis, Mo.

9:40 **Laser Pyrolysis of Polymers.** D. L. Fanter, R. L. Levy, and C. J. Wolf, McDonnell Douglas Corp., St. Louis, Mo.

10:00 **Qualitative Analysis of Gas Chromatographic Eluates by Vapor Phase Pyrolysis.** C. Merritt, Jr., U. S. Army Natick Laboratories, Natick, Mass.

10:25 **Polymer Identification and Quantitative Determination of Additives by Photolysis-Gas Chromatography.** R. S. Juvet, J. L. Smith, K. P. Li, University of Illinois, Urbana, Ill., and Arizona State University, Tempe, Ariz.

10:50 **Identification of Hydrocarbon Pollutants on Seas and Beaches by Gas Chromatography.** E. R. Adlard, L. F. Creaser, P. H. D. Matthews, Shell Research Ltd., Chester, England

11:15 **Continuous Determination of Carbon Monoxide by Frontal Analysis.** L. Monkman, L. Dubois, Air Pollution Control Division, Environmental Health Centre, Ottawa, Canada

11:35 **Rare Gases of Atmosphere: Gas Chromatography Using Thermal Conductivity Detector and Palladium Transmodulator.** J. E. Lovelock, P. G. Simmonds, G. R. Shoemake, Jet Propulsion Laboratories, Pasadena, Calif.

19th Anachem Conference

The 19th Anachem Conference and Instrument Exhibit sponsored by the Association of Analytical Chemists, Inc., affiliated with the Detroit Section of the American Chemical Society, will be held October 11–13, 1971, at the Dearborn Inn, Dearborn, Mich. The Conference will consist of six symposia and a session of general papers. The following is a summary of the technical program:

Monday Morning, October 11. Symposium on Pharmaceutical Analysis

Monday Afternoon. Symposium on Instrumentation and Automated Analysis (Applications to Kinetic Studies and Analyses)

Tuesday Morning, October 12. Anachem Award Symposium (Honoring Velmer A. Fassel, 1971 Anachem Award Recipient, page 42 A, Aug.)

Tuesday Afternoon. Anachem Award Symposium (contd.)

Wednesday Morning, October 13. Symposium on Air Pollution and Industrial Hygiene
General Papers

Wednesday Afternoon. Symposium on Analysis of Contaminants in Foods and Water

The Anachem Award Address by Dr. Fassel is titled "Electrical Plasmas as Free-Atom Generators and Reservoirs for Analytical Atomic Absorption, Emission, and Fluorescence Spectroscopy."

Additional information regarding the Conference is available by writing to Peter Warner, Wayne County Department of Health, Air Pollution Control, 1311 East Jefferson, Detroit, Mich. 48226

AAMI Meeting

issued a call for its annual meeting and exhibit program. The seventh annual meeting will be held April 24 to 26, 1972, at Caeser's Palace, Las Vegas, Nev. The scientific program will include papers by physicians, engineers, other scientists, and administrators concerned with increasing the efficiency and

The Association for the Advancement of Medical Instrumentation has effectiveness of medical care and research through the development and use of medical instruments, devices, and systems. The deadline for submission of abstracts is October 1, 1971. Further information is available from Michael J. Miller, Executive Director, AAMI, 9650 Rockville Pike, Bethesda, Md. 20014. 301-530-2800

The Ace-Burlitch Inert Atmosphere System
Convenient bench top unit for handling air sensitive compounds!

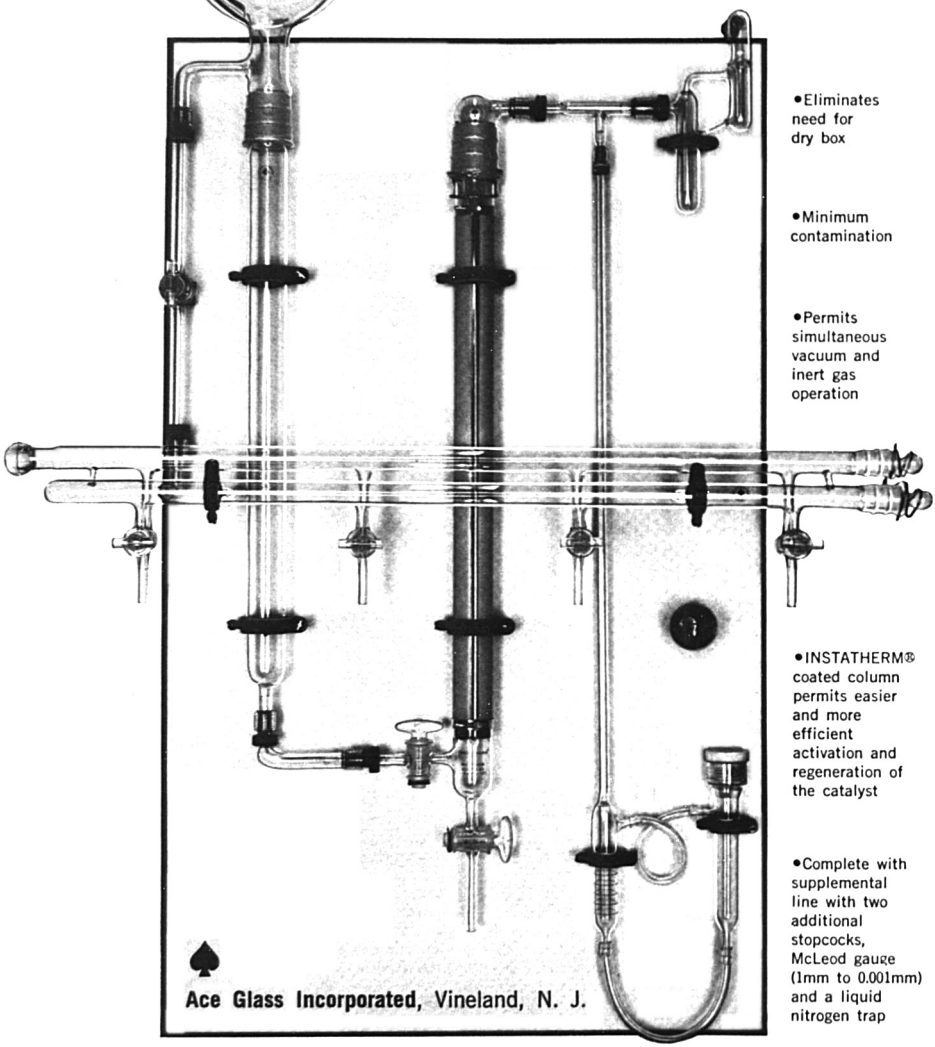

- Eliminates need for dry box
- Minimum contamination
- Permits simultaneous vacuum and inert gas operation
- INSTATHERM® coated column permits easier and more efficient activation and regeneration of the catalyst
- Complete with supplemental line with two additional stopcocks, McLeod gauge (1mm to 0.001mm) and a liquid nitrogen trap

Developed in collaboration with Dr. James M. Burlitch of the Chemistry Department of Cornell University. Send for our new brochure describing the Ace-Burlitch Inert Atmosphere System and Ace No-Air Labware.

Ace Glass Incorporated, Vineland, N. J. 08360 • Louisville, Ky. 40201 • Ludlow, Mass. 01056

CIRCLE 6 ON READER SERVICE CARD

1972 Pittsburgh Conference

The 23rd Pittsburgh Conference on Analytical Chemistry and Applied Spectroscopy will be held at the Cleveland Convention Center, Cleveland, Ohio, March 6–10, 1972. Symposia on the following subjects are being arranged:

Analytical Applications of ESCA

Analysis of Surfaces—What Can the New Techniques Tell Us?

Dedicated Computers—State of the Art in Their Use in Analytical Chemistry

Biochemical Applications of Mass Spectrometry

Standard Methods for Ambient Air Analysis

Analytical Applications of X-Ray Diffraction

Teaching Analytical Chemistry—Industrial and Academic Views

Scientists—The "Out" Group

The Role of the Analytical Chemist in Process Control

Thermal Methods of Analysis—Applications

Coblentz Award Symposium

Spectroscopy Society of Pittsburgh Award Symposium

Papers are not restricted to these topics, and papers on all phases of analytical chemistry and spectroscopy are invited. Authors wishing to contribute should submit three copies of a 150-word abstract to Oswald E. Wilkinson, program chairman, Alcoa Technical Center, P.O. Box 2970, Pittsburgh, Pa. 15230. Final date for receipt of abstracts is Oct. 1, 1971.

In addition to the technical program, more than 250 companies will be represented at the exposition of modern laboratory equipment. Information concerning the exhibits should be directed to A. J. Kavoulakis, exposition chairman, Shenago, Inc., 200 Neville Rd., Pittsburgh, Pa. 15225

Coming Events

Oct. 3 to 6—45th Annual Fall Meeting of American Oil Chemists' Society. Atlantic City, N. J. Includes sessions on environmental science and industrial processing and analytical and biochemical techniques. *Contact:* C. H. Hauber, American Oil Chemists' Society, 35 E. Wacker Dr., Chicago, Ill. 60601. 312-782-2455

Oct. 3 to 7—Tenth Annual Meeting of ASTM Committee on Chromatography. Jung Hotel, New Orleans, La. *Contact:* F. H. Fager, Union Carbide Corp., Box 65, Tarrytown, N. Y. 10592

Scheduled Courses in Analytical Techniques

Information is given in the following order: date, name of course, location of course, professional person(s) in charge of course, and/or sponsoring organizations, and Contact (numbers in parentheses refer to addresses and telephone numbers given at the bottom of the list of scheduled courses).

Sept. 20 to 24—Two Separate Courses: Nuclear Magnetic Resonance; Electron Absorption Spectroscopy. Philadelphia, Pa. Sadtler Research. *Contact (1)*

Sept. 27 to 29—Fourier Transform Spectroscopy. Philadelphia, Pa. Sadtler Research. *Contact (1)*

Sept. 27 to Oct. 1—Infrared, Part I. Philadelphia, Pa. Sadtler Research. *Contact (1)*

Sept. 27 to Oct. 1—Color and the Behavior of Colorants. Attleboro, Mass. *Contact:* Miss Elaine Keller, Kollmorgen Corp., 67 Mechanic St., Attleboro, Mass. 02703

Oct. 4 to 6—Instrumental Methods. Philadelphia, Pa. Sadtler Research. *Contact (1)*

Oct. 4 to 8—Thin Layer Chromatography. Philadelphia, Pa. Sadtler Research. *Contact (1)*

Oct. 4 to 8—Photomicrography. Chicago, Ill. McCrone Research Institute. *Contact (2)*

Oct. 9 to 10—Modern Liquid Chromatography. Buffalo, N. Y. L. R. Snyder, J. J. Kirkland. ACS. *Contact (3)*

Oct. 11 to 13—Liquid Chromatography. San Francisco Area. Varian Aerograph. *Contact (4)*

Oct. 11 to 14—Electronics for Chemists. Philadelphia, Pa. Sadtler Research. *Contact (1)*

Oct. 11 to 15—Laboratory Management. Philadelphia, Pa. Sadtler Research. *Contact (1)*

Oct. 11 to 15—Industrial Use of the Polarizing Microscope. Chicago, Ill. McCrone Research Institute. *Contact (2)*

Oct. 11 to 15—Three Courses: Vacuum Technology; Vacuum Processes; and Vacuum System Technology. Sheraton-Boston Hotel, Boston, Mass. *Contact:* American Vacuum Society Short Course, P.O. Box 655, Livermore, Calif. 94550. 415-447-1000, ext 7144

Oct. 14 to 16—Liquid Chromatography. San Francisco Area. Varian Aerograph. *Contact (4)*

Oct. 16—Column Selection in Gas Chromatography. Boston, Mass. H. M. McNair, W. R. Supina. ACS. *Contact (3)*

Oct. 18 to 19—Thermoanalysis. Philadelphia, Pa. Sadtler Research. *Contact (1)*

Oct. 18 to 22—Infrared, Part II. Philadelphia, Pa. Sadtler Research. *Contact (1)*

Oct. 18 to 22—Identification of Small Particles. Chicago, Ill. McCrone Research Institute. *Contact (2)*

Oct. 20—Applied Spectroscopy. St. Louis, Mo. SAS. Merlyn L. Salmon. *Contact:* Joan E. Westermeyer, Titanium Pigment Div., N L Industries, Inc., Carondelet Station, St. Louis, Mo. 63111. 314-638-3200, ext. 216

Oct. 20 to 22—Basic Gas Chromatography. Chicago, Ill., Area. Varian Aerograph. *Contact (5)*

Oct. 21 to 22—ACS-SAS Short Course on Water Analysis. Disneyland Hotel, Calif. Two-day lecture-workshop being held in conjunction with the Pacific Conference on Chemistry and Spectroscopy. *Contact:* W. W. Ulrich, Beckman Instruments, Inc., 2500 Harbor Blvd., Fullerton, Calif. 92634

Oct. 22 to 23—Interfacing the Minicomputer. New York City area. R. E. Dessy, D. G. Larsen. ACS. *Contact (3)*

Oct. 25 to 27—Dispersion Staining in Optical Crystallography. Chicago, Ill. McCrone Research Institute. *Contact (2)*

Nov. 1 to 3—Techniques of Infrared Spectroscopy. Philadelphia, Pa. Sadtler Research. *Contact (1)*

Nov. 1 to 5—Gas Chromatography. Philadelphia, Pa. Sadtler Research. *Contact (1)*

Nov. 1 to 5—X-Ray Techniques in the Industrial Laboratory. Chicago, Ill. McCrone Research Institute. *Contact (2)*

Nov. 8 to 12—Industrial Use of the Polarizing Microscopy. Chicago, Ill. McCrone Research Institute. *Contact (2)*

Nov. 10 to 12—Basic Gas Chromatography. Houston, Tex., Area. *Contact:* Don Brasseaux, Varian Aerograph, Suite 180, 3939 Hillcroft Ave., Houston, Tex. 77027

Nov. 13 to 14—Modern Liquid Chromatography. New York City. L. R. Snyder, J. J. Kirkland. ACS. *Contact (3)*

Nov. 13 to 14—X-Ray Diffraction for Industrial Chemists. New York City. R. J. Fredericks. ACS. *Contact (3)*

(1) Sadtler Educational Div., Sadtler Research Laboratories, Inc., 3316 Spring Garden St., Philadelphia, Pa. 19104. 215-382-7800
(2) Mrs. Miriam Fallert, Registrar, McCrone Research Institute, 451 E. 31st St., Chicago, Ill. 60616. 312-842-7105
(3) Education Dept., American Chemical Society, 1155 Sixteenth St., N.W., Washington, D.C. 20036. 202-737-3337, ext. 258
(4) Willard Wilson, Varian Aerograph, 1025A Shary Circle, Concord, Calif. 94520
(5) Ed Klein, Varian Aerograph, 205 W. Touhy Ave., Park Ridge, Ill. 60068
(6) Ed Gelb, Varian Aerograph, #25 Route 22, Springfield, N.J. 07081

Oct. 3 to 8—44th Annual Conference Water Pollution Control Federation. Civic Auditorium, San Francisco, Calif. *Contact:* R. A. Canham, WPCF, 3900 Wisconsin Ave., N. W., Washington, D. C. 20016

Oct. 3 to 8—Electrochemical Society National Meeting. Sheraton-Cleveland, Cleveland, Ohio. *Contact:* Electrochemical Society, 30 E. 42nd St., New York, N. Y. 10017. 212-867-4430

Oct. 4 to 7—26th Annual ISA Conference. McCormick Place, Chicago, Ill. *Contact:* G. I. Doering, Instrument Society of America, 400 Stanwix St., Pittsburgh, Pa. 15222. 412-281-3171

Oct. 4 to 9—16th International Spectroscopy Colloquium. Heidelberg, Germany. *Contact:* Herrn Dr. W. Fritsche, p.A. Gesellschaft Deutscher Chemiker, 6 Frankfurt/Main 8, Postfach 119075, Germany. Page 72 A, Nov.

Oct. 5 to 8—International Symposium on Nuclear Research Materials. Gatlinburg, Tenn. Sponsor: AEC-ORNL. *Contact:* E. H. Kobisk, Oak Ridge National Laboratory, P. O. Box X, Oak Ridge, Tenn. 37830. Page 86 A, Feb.

Oct. 5 to 8—IMEKO: Symposium on Moisture Measurement. Budapest, Hungary. *Contact:* MM Symposium, IMEKO Secretariat, Budapest 5, P. O. B. 457, Hungary

Oct. 11 to 13—Anachem Conference. Detroit, Mich. *Contact:* Peter Warner, Wayne County Dept. of Health, Air Pollution Control, 1311 E. Jefferson St., Detroit, Mich. 48226 Page 65 A, Sept.

Oct. 11 to 13—ACS Northeast Regional Meeting. Statler Hilton, Buffalo, N. Y. *Contact:* Roland Gladieux, 1500 Colvin Blvd., Kenmore, Buffalo, N. Y. 14223

Oct. 11 to 14—85th Annual Meeting of the Association of Official Analytical Chemists. Marriott Motor Hotel, Twin Bridges, Washington, D. C. *Contact:* L. G. Ensminger, AOAC, Box 540, Benjamin Franklin Station, Washington, D. C. 20044. Page 40 A, Aug.

Oct. 11 to 15—International Vacuum Congress and Conference on Solid Surfaces. Boston, Mass. *Contact:* American Vacuum Society, 335 E. 45th St., New York, N. Y. 10017. 212-685-1940

Oct. 12 to 14—Fifteenth Conference on Analytical Chemistry in Nuclear Technology. Oak Ridge, Tenn. *Contact:* L. J. Brady, Oak Ridge National Laboratory, P. O. Box X, Oak Ridge, Tenn. 37830. Page 58 A, Sept.

Oct. 14 to 20—Interkama '71. Dusseldorf, Germany. *Contact:* Intergama '71, Düsseldorfer, Messegesellschaft mbH, 4 Düsseldorf 10, Postfach 10203, Germany. Page 68 A, Apr.

Oct. 14 to 20—International Exhibition of Chemical Equipment—MAC 71. Milan, Italy. Includes laboratory equipment. *Contact:* Gennaro Dini, XI Mostra Internazionale Delle Apparecchiature Chimiche, Via Tiziano 19, 20145 Milano, Italy

Oct. 18 to 20—Pacific Conference on Chemistry and Spectroscopy. Disneyland Hotel, Anaheim, Calif. *Contact:* Lee Kalbus, California State College, San Bernardino, Calif. 92407. 714-887-6311. Page 40 A, Aug.

Oct. 18 to 20—Trends in Polymer Characterization. Sarnia, Ontario. *Contact:* A. J. Stephenson, Imperial Oil Enterprises, Ltd., Sarnia, Ontario, Canada. Page 43 A, Aug.

Oct. 18 to 20—18th Spectroscopy Symposium and Exhibition. Toronto, Ontario. Sponsor: Spectroscopy Society of Canada. *Contact:* G. D. Hoffmann, Gulf Oil Canada, Ltd., Sheridan Park, Ontario, Canada. 416-822-6770

Oct. 18 to 21—1971 Metal Show and Materials Engineering Congress. Cobo Hall, Detroit, Mich. Includes

CALENDAR OF EVENTS

Sept. 7 to 10	**International Conference on Electron Spectroscopy.** Asilomar Conference Grounds, Pacific Grove, Calif. *Contact:* David A. Shirley, Dept. of Chemistry, University of California, Berkeley, Calif. 94720
Sept. 12 to 17	**162nd National ACS Meeting.** Washington, D. C. Includes Analytical Chemistry Division sessions. *Contact:* J. C. White, Analytical Chemistry Div., Oak Ridge National Laboratory, Oak Ridge, Tenn. 37830. 615-483-8611, ext. 3-1472. Page 53 A, Sept.
Sept. 13 to 16	**International Symposium on Liquid Scintillation Counting.** Hotel Metropole, Brighton, England. *Contact:* M. A. Crook, The Society for Analytical Chemistry, 9/10 Saville Row, London W1X 1AF, England
Sept. 13 to 18	**General Assembly Gesellschaft Deutscher Chemiker.** Karlsruhe, Germany. *Contact:* Gesellschaft Deutscher Chemiker, D-6000 Frankfurt (M), Germany, Postfach 119075
Sept. 20 to 22	**Nondestructive Measurement and Identification Techniques in Nuclear Safeguards.** Ispra (Varese), Italy. *Contact:* M. Cuypers, CCR Euratom, 21020, Ispra (Va), Italy
Sept. 20 to 24	**Inter/Micro-71.** Imperial College, London, England. *Contact:* McCrone Research Institute, 2 McCrone Mews, Belsize Lane, London, N.W.3 5BG, England. Page 44 A, July
Sept. 20 to 24	**5th Conference on Molecular Spectroscopy.** Brighton, England. *Contact:* C. H. Maynard, The Institute of Petroleum, 61 New Cavendish St., London W.1, England
Sept. 21 to 23	**Labware '71.** London, England. *Contact:* British Information Services, 845 Third Ave., New York, N. Y. 10022. 212-752-8400
Sept. 22 to 23	**High Voltage Electron Microscopy Conference.** Teddington, England. *Contact:* Meetings Officer, The Institute of Physics, 47 Belgrave Square, London S.W.1, England. Page 43 A, Aug.
Sept. 22 to 26	**National Conference on Analytical Chemistry.** Brasov, Romania. *Contact:* Dr. Constantin Luca, Consiliul National al Ingineriilor si Tehnicienilor, Conferinta de Chimie Analitica, Calea Victoriei 118, Bururesti, Romania. Page 71 A, Nov.
Sept. 23 to 24	**Conference on Data Processing and Display for Inspection Purposes.** University of Lancaster. *Contact:* The Institute of Physics and The Physical Society, 47 Belgrave Square, London, S.W.1, England. Page 44 A, July
Sept. 27 to Oct. 1	**Interlab '71.** 2nd International Exhibition of Laboratory and Measuring Techniques and International Symposium on Modern Analytical Methods and Laboratory Apparatus. Ostrava, Czechoslovakia. *Contact:* Jan Marsik, RAPID, Ostrava-Cerna Louka, Pavilion K/Czechoslovakia
Sept. 27 to Oct. 1	**Third International Congress on Absorption Spectrometry and Atomic Fluorescence.** Paris. *Contact:* Secretariat du 3e CISAFA, GAMS, 1, rue Gaston Boissier, Paris XVe, France. Page 73 A, Nov.
Sept. 28 to 29	**Symposium on Analysis of Organic Traces in Water.** Essen, Germany. *Contact:* Gesellschaft Deutscher Chemiker, D-6000 Frankfurt (M), Germany, Postfach 119075

Progress Report... We're expanding in the East. Already there are four new facilities in the East bringing the total to over 300,000 square feet. We're modifying, modernizing, improving, enhancing . . . to bring you peak service. Our Eastern sales force has been increased by over 40%. And soon there'll be the unsurpassed computer facilities now serving our Western customers. Video displays that interlink all offices and warehouses—providing instantaneous readouts of inventories and total customer sales histories. And we are installing the latest automated materials-handling systems that reduce costs, expedite deliveries.

East or West, VWR Scientific offers the broadest line of highly-regarded instruments and supplies. The lines we sell come from proven-quality manufacturers and are accepted only if they meet our standards of excellence. In addition, a unique group of top-quality products under our VAN-LAB® label, designed and packaged for user convenience, is available.

We're dedicated to providing you with the finest selection of superior products, optimum service and unexcelled value. That's why we're growing. Look for us . . . if we're not there already . . . we'll be there soon. We're still growing.

Formerly—VW&R/Will Scientific • Albuquerque • Anchorage • Atlanta • Baltimore • Boston • Buffalo • Columbus • Denver • Detroit El Paso • Honolulu • Kansas City • Los Angeles • New York City • Phoenix • Portland • Rochester • Salt Lake City San Diego • San Francisco • Seattle • Tucson • West Sacramento

CIRCLE 190 ON READER SERVICE CARD

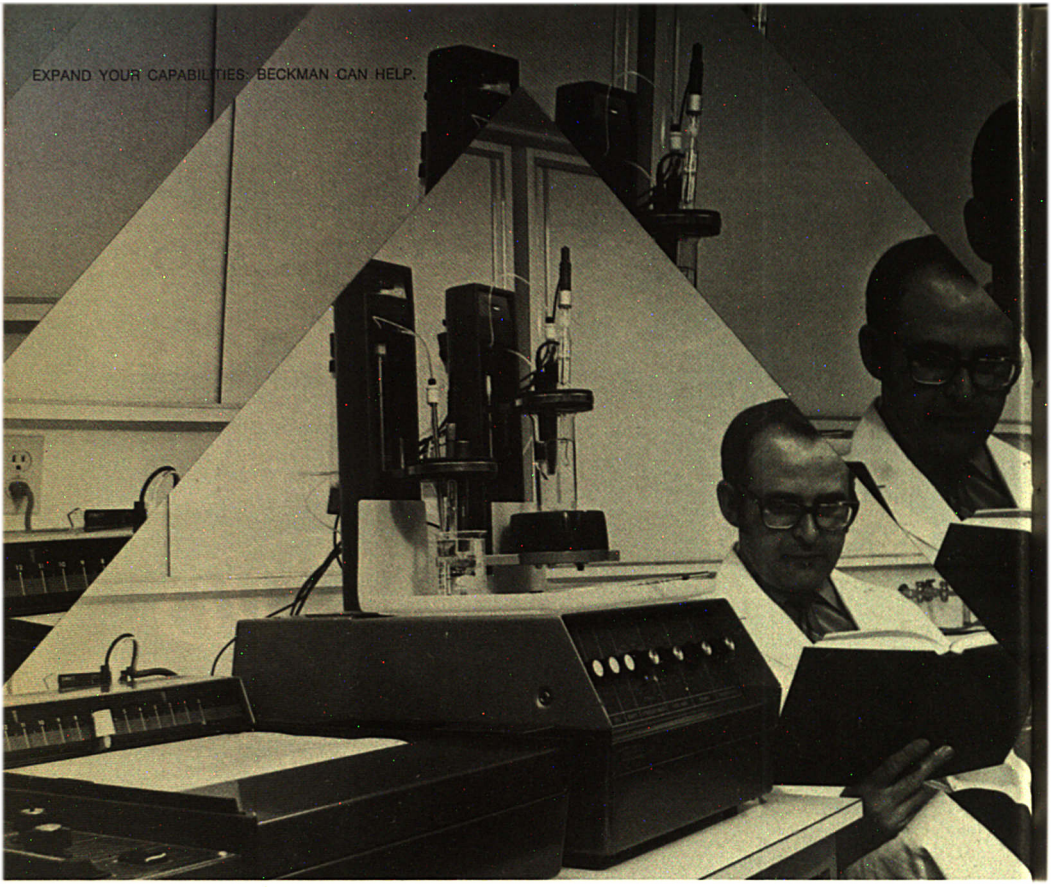

Most automatic recording titrators aren't. Beckman's is.

The Beckman Automatic Recording Titrator is *truly* automatic... designed to give you maximum ease of operation, precision, repeatability, versatility. Consider these exclusive Beckman features:

All-electronic automatic mode. You can run completely unknown titration curves without adjustment and without overshoot. Slows automatically as the endpoint nears.

Combination mode. The titrator races to a preset critical point and slows to a preset speed while passing through the endpoint. Extremely precise titrations in only 40 to 60 seconds.

Automatic refill. Completely eliminates mechanical buret stopcocks.

Digital display of titrant added. Fast, simplified reading eliminates operator error.

Widest range. Full, calibrated, 0-14 pH range with expansion scales of 1.4, 2.8, 7 and 14 pH (140, 280, 700 and 1400 mv).

Maximum economy. Buy only what you need, single or double column models. Second column can be added when required. Price: $3200, single column model; $3460, double column model.

Write for Data File 25, Scientific Instruments Division, Beckman Instruments, Inc., 2500 Harbor Boulevard, Fullerton, California 92634.

Now Beckman offers a low-cost Endpoint Titrator System for industrial quality control applications. Ask about it.

Beckman® INSTRUMENTS, INC.

HELPING SCIENCE AND INDUSTRY IMPROVE THE QUALITY OF LIFE

INTERNATIONAL SUBSIDIARIES: AMSTERDAM; CAPE TOWN; GENEVA; GLENROTHES, SCOTLAND; LONDON; MEXICO CITY; MUNICH; PARIS; STOCKHOLM; TOKYO; VIENNA

CIRCLE 24 ON READER SERVICE CARD

participation by the American Society for Nondestructive Testing and The Metallurgical Society of AIME, NYC, with other societies and associations. *Contact:* American Society for Metals, Metals Park, Ohio 44073. 216-338-5151

Oct. 18 to 21—American Society for Nondestructive Testing 31st National Fall Conference. Detroit, Mich. *Contact:* Philip D. Johnson, ASNT, 914 Chicago Ave., Evanston, Ill. 60202

Oct. 18 to 21—5th Materials Research Symposium, Solid State Chemistry. NBS, Gaithersburg, Md. *Contact:* R. S. Roth, B214, National Bureau of Standards, Washington, D. C. 20234. Page 43 A, July

Oct. 18 to 22—10th National Meeting of the Society for Applied Spectroscopy. St. Louis, Mo. *Contact:* E. F. Kaelble, Monsanto Co., Inorganic Research Dept., 800 N. Lindbergh Blvd., St. Louis, Mo. 63166. Page 74 A, Nov.

Oct. 28 to 29—ACS Midwest Regional Meeting. Jefferson Hotel, St. Louis, Mo. *Contact:* Charles O. Gerfen, Mallinckrodt Chemical Works, 3600 N. Second St., P. O. Box 5439, St. Louis, Mo. 63100

Oct. 31 to Nov. 4—24th Annual Conference on Engineering in Medicine and Biology. International Hotel, Las Vegas, Nev. *Contact:* A. W. Stewart, Beckman Instruments, 2500 Harbor Blvd., Fullerton, Calif. 92632. 714-871-4848

Industry Items

MC/B Manufacturing Chemists of Milwaukee, Wis., has opened a new Chemical Center in Raleigh, N.C., near the rapidly growing research and chemical industry center in the Triangle Research Park area. The Raleigh Chemical Center will service N.C., S.C., Md., Va., Ga., Fla., and Washington, D.C.

Varian of 611 Hansen Way, Palo Alto, Calif. 94303, 415-326-4000, announces that its Vacuum Division will provide an analysis service on a fee basis to determine the elemental composition of surfaces with an Auger spectrometer. Prepurchase feasibility studies of the applicability of the Auger technique are also available.

Perkin-Elmer Corp. has produced a 20-min. film, in color and sound, on the theory and practice of absorption spectrophotometry. Prints in 16-mm format with optical sound track may be borrowed in the U.S. free of charge by qualified organizations, from any of the six offices of **Modern Talking Pictures, Inc.:** 1145 N. McCadden Pl., Los Angeles, Calif. 90038; 16 Spear St., San Francisco, Calif. 94105; 160 East Grand Ave., Chicago, Ill. 60611; 714 Spring St., N.W., Atlanta, Ga. 30308; 1212 Ave. of the Americas, New York, N.Y. 10020; and 1411 Slocum St., Dallas, Tex.

Harris Laboratories, Inc., P.O. Box 80837, 624 Peach St., Lincoln, Neb. 68501, 402-432-2811, a large independent research, development, and testing laboratory, has a complete series of new stream pollution test packages designed to meet water and waste water analysis requirements of EPA and the Army Corps of Engineers. The company will provide complete consultation and testing services. A testing program and complete schedule for the suggested program can be supplied by Harris.

Calbiochem, producer of pharmaceuticals, diagnostic reagents, and biochemicals for research, has relocated from Los Angeles to its newly constructed world headquarters at 10933 N. Torrey Pines Rd., La Jolla, Calif. 92037. 714-453-7331

Trapelo/West, 2030 Wright Ave., Richmond, Calif. 94804, 415-235-2633, offers an integrated environmental pollution service that includes consulting, program design, sample collection, sample analysis, and data evaluation. Included are air analysis, water and waste water analysis, stack emission, and ambient air analysis, particle analysis, and toxicological studies of marine organisms.

Scientific and industrial photography in the macro (1–30×), micro (30–2000×), and ultramicro (2000–2 million×) range is now available through the photomicrography group at **Walter C. McCrone Assoc., Inc.,** Chicago, Ill. For more information write to Michael Donner, Walter C. McCrone Assoc., Inc., 493 E. 31st St., Chicago, Ill. 60616

A commercial testing service for pollution detection and control of water and waste water is available from **Alpha Metals, Inc.,** Analytical Division, 56 Water St., Jersey City, N.J. 07304. The testing service is geared to serve municipal governments and industry.

Daylin Laboratories, Inc., has acquired **Griffin-Hasson Laboratories,** a Los Angeles commercial testing laboratory. Operations of the two labs will be merged into Daylin Laboratory facilities at 2800 Jewel Ave., Los Angeles, Calif. Griffin-Hasson is involved in bacteriology, chemical analysis, sanitation processing and processing control, product development, general plant layout, and operational efficiency. It is USDA approved for water and waste water analysis. Daylin Laboratories was formed two years ago when Daylin, Inc., acquired 17-year-old **Terminal Testing Laboratories, Inc.**

Be selective

Not just pH but also pI, pBr, pCl, pCN, pNa, pNH_4, pS, pAg and pK.

Philips are currently the only European manufacturer of ion-selective electrodes. Which means that our prices are European prices.

We're also the only manufacturer to offer easy replenishment of the electrolyte and easy replacement of the membrane in our solid-state models. Which means that maintenance is no longer a problem - whatever the task.

Philips also have one of the widest ranges of laboratory pH and conductivity measuring equipment. Digital pH meter (as shown),flat-bed recorders, analogue conductivity and pH meters, standard pH electrodes, conductivity cells. You'll find them all in our latest brochure.

And of course when you do put the ion-sensitive technique to work you'll find it backed up by Philips industrial pH and conductivity equipment.

For full details on our current ion-selective range, and to be put on the mailing list for new developments, contact your local Philips organisation or write to:

N.V. Philips Gloeilampenfabrieken,
Analytical Equipment Department,
Eindhoven, the Netherlands

PHILIPS ANALYTICAL EQUIPMENT

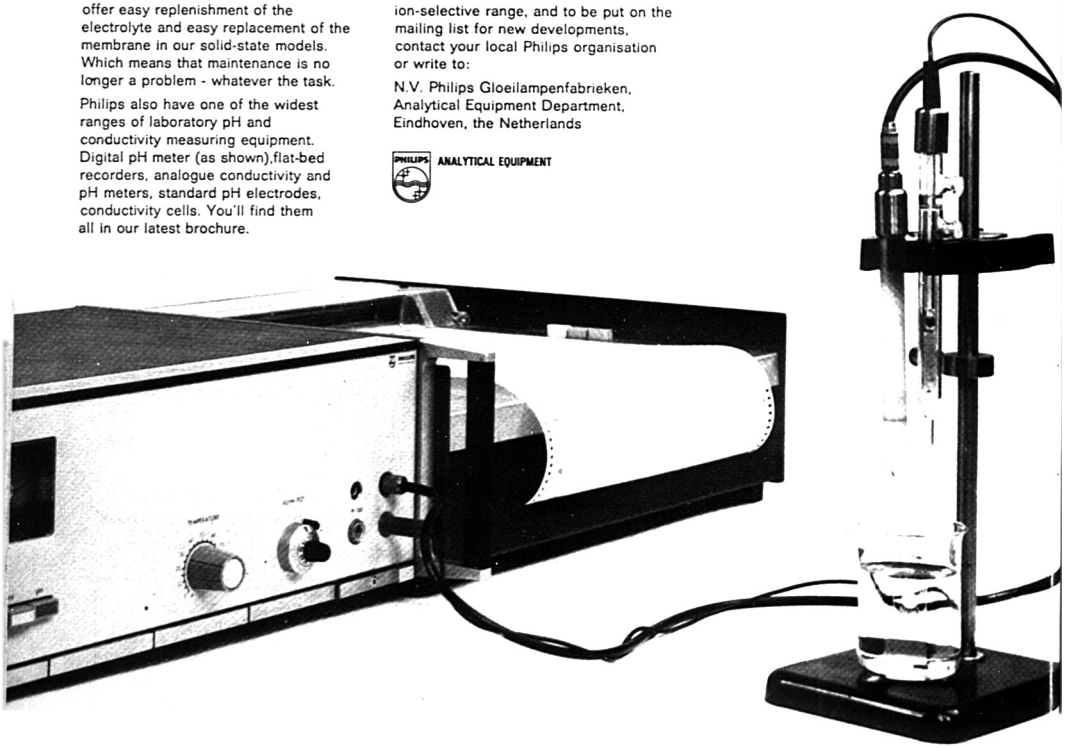

PHILIPS

CIRCLE 152 ON READER SERVICE CARD

HARSHAW'S 30 INCH INORGANIC SCINTILLATORS

NaI(Tl)
CsI(Tl)
CsI(Na)

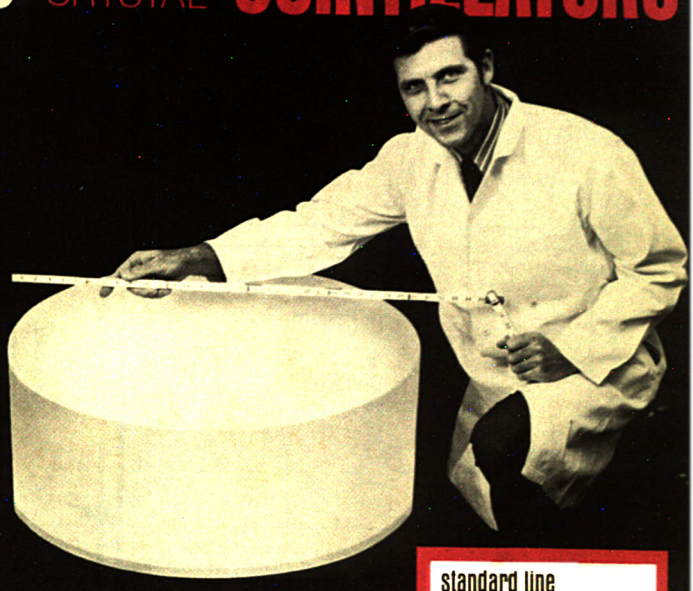

The world's largest NaI(Tl) scintillation crystal—30 inches in diameter by 10 inches thick. It weighs in at over one-half ton.

Scintillation phosphors and detectors for every nuclear event

Need some help in determining detector size, shape or material? We offer an endless combination of scintillation phosphor materials, sizes, geometries and packaging for gamma-ray, x-ray, alpha, beta, neutron and proton detection. Let Harshaw's staff of scientists help solve your detector problem. Our Physicists design many different nuclear detection systems for today's most advanced disciplines including: Nuclear Spectroscopy, X-Ray Spectroscopy, High Energy Physics Research, Nuclear Life Science and the Environmental Sciences. Put their experience to work for you.

Our design engineering staff are experts in hardware and functional design work. And, Harshaw's long standing and time tested guarantee stands behind all our work.

Chemists, Chemical Engineers and Crystal Growers exercise complete control and impose exacting specifications on the crystal growing procedure—starting with the raw material. We synthesize our own starting materials. It's a lot of work but there are rewards—for example, we guarantee the amount of Potassium in a NaI(Tl) scintillation crystal to be less than .5ppm. Now that's low background.

The scintillation phosphors listed above are our most popular materials. We have others—ask about $Li^6I(Eu)$ as a neutron detector and $CaF_2(Eu)$ as an x-ray and charged particle detector. Plus our two new high Z scintillators: BaF_2 and $TlCl(Be,I_2)$

Harshaw scintillators detect nuclear events and pass the information along to downstream electronics. We offer NIM modular electronics completely compatible with all scintillation detectors. The electronic line includes: preamplifier, amplifiers, counting and timing modules and interfaces to a large variety of readouts. And Harshaw will check-out and guarantee total system specifications.

Write or call for complete information.

standard line

integral line

matched window assemblies

THE HARSHAW CHEMICAL COMPANY
DIVISION OF KEWANEE OIL COMPANY
Crystal & Electronic Products Department
6801 Cochran Road • Solon, Ohio 44139 • (216) 248-7400

CIRCLE 84 ON READER SERVICE CARD

Save $700*on your water bill

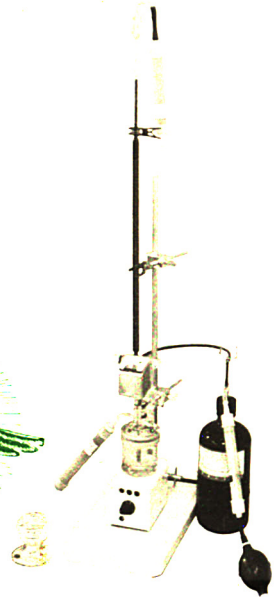

(Karl Fischer determinations at a budget price.)

Labindustries offers the least expensive Karl Fischer apparatus you can buy. It also happens to be **at least** as precise, rapid, and convenient as anybody else's.

Sensitivity. 1 ppm to 100% water with one buret.

Precision. 1% accuracy, 0.5% reproducibility. Color-coded positive indication of end point.

Rapid. 2-minute determinations. Uses 4 oz. disposable jars for reaction vessels; avoids delays between runs. Detect 3 nanoliters of water with L/I's 2 ml micro vessel, interchangeable with 4 oz. jar.

Applications. Unlimited. Includes petroleum products, pharmaceuticals, freeze-dried products, waxes, dehydrated materials, cosmetics, detergents, plastics, foods, wood products, paint, explosives, and many more.

Price. $355 complete. Meter electrode alone, $132.25. Many accessories available, including Grunbaum pipet for standardizing with pure water.

Contact L/I for free brochure and price list.

LABINDUSTRIES

1802A Second Street, Berkeley, CA 94710.
Phone (415) 843-0220

CIRCLE 113 ON READER SERVICE CARD

New from Perkin-Elmer: a blood lead method without sweat or tears.

And practically without blood.

Now you can determine lead in blood samples as small as 10 microliters taken from finger punctures.

Speed of analysis is at least 10 times faster than the dithizone method, 30-50 samples per hour; operator skill requirements are incomparably lower; and precision and accuracy are equal to the "wet" methods.

Anyone who can run an atomic absorption spectrophotometer can learn this new method in a half hour.

How It Works: The method utilizes a Perkin-Elmer atomic absorption unit, a laboratory recorder, and something new—the Delves Microsampling Cup™ analytical system (patent pending).

You simply pipette your 10 microliter blood sample into the cup. Dry on a hot plate at 140°C for about 30 seconds. Add 20 microliters of H_2O_2. Dry again for about two minutes. Twenty samples can be prepared at the same time. Then pick up each cup with tweezers, insert it in the sample holder and push it into the flame of the atomic absorption unit. The sample is atomized and absorbs light from the sample beam of the instrument.

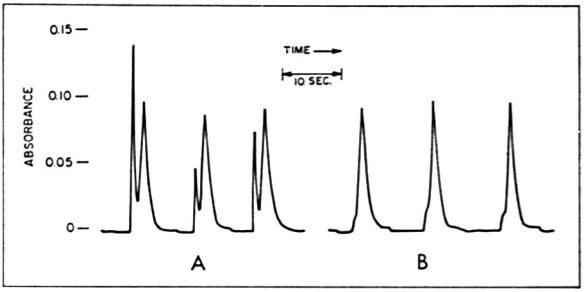

How The Data Look: The laboratory recorder will give you tracings like those in figure A, which shows three analyses of the same sample. The first peak of each analysis is smoke, the second is lead. Peak height is proportional to concentration, in this case, 22μg/100 ml (0.22 ppm) lead.

Figure B shows the tracing from an instrument with a Deuterium Background Corrector. The smoke peak disappears, and only the lead peak is left, simplifying the analysis even more.

To learn more about this new Perkin-Elmer blood lead method—and also about very sensitive analyses for arsenic, cadmium, thallium and other metals—write to Instrument Division, Perkin-Elmer Corporation, 702 Main Avenue, Norwalk, Conn. 06852.

PERKIN-ELMER

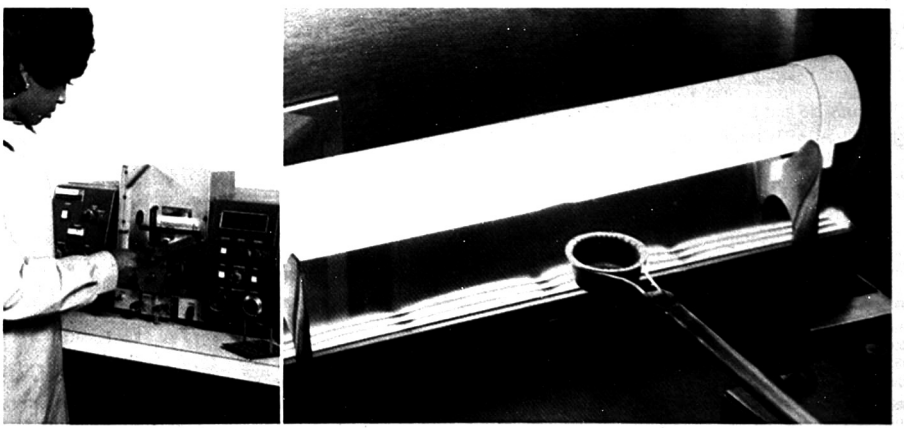

CIRCLE 165 ON READER SERVICE CARD

SYSTEMATICS

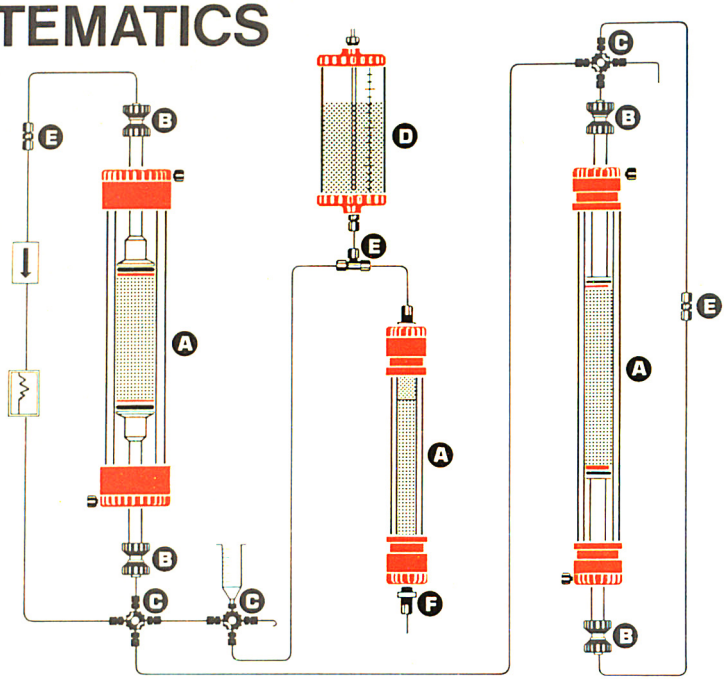

A Systematic approach to chromatography
All components for complete systems

Pharmacia Fine Chemicals offers a wide range of compatible components for a variety of gel filtration and ion exchange chromatographic systems.

A COLUMNS. A comprehensive range of jacketed and unjacketed columns available in diameters from 0.9 to 21.5 cm. Lengths from 15 to 100 cm. Special solvent resistant columns also available in diameter 2.5 cm. Lengths 45 and 100 cm.

B FLOW ADAPTORS. Permit upward flow elution, sample application, recycling, flow reversal, etc.

C VALVES. 3- and 4-way valves allow easy operation and flexibility for sample application, recycling, flow reversal, by-pass, etc.

D RESERVOIRS. Bi-functional gel and eluant reservoirs for column packing and elution at constant pressure.

E CONNECTORS. 2- and 3-port connectors for capillary tubing allow easy interconnection of chromatographic components without flanging or flaring.

F FLOW CONTROL VALVE. Designed for shut-off as well as flow control.

NEW

Jacketed columns with new design. Diameters 1.6 and 2.6 cm (K16 and K26).
Lengths 40, 70 and 100 cm. Special 1.6x20 cm column for ion exchange chromatography.
Flow adaptors for 1.6 and 2.6 cm columns (A16 and A26).
Flow control valve (FCV-1). Standard on 1.6 and 2.6 cm columns.

Pharmacia Fine Chemicals Inc.
800 Centennial Avenue
PISCATAWAY
New Jersey 08854

Pharmacia Fine Chemicals

Pharmacia (Canada) Ltd. 110 Place Crémazie, Suite 412, Montreal 11, P. Q.
(Inquiries outside U.S.A. and Canada should be directed to PHARMACIA FINE CHEMICALS Uppsala Sweden.)

CIRCLE 156 ON READER SERVICE CARD

BOOK REVIEWS

Principles of Mass Spectrometry and Negative Ions. Charles E. Melton. xii + 313 pages. Marcel Dekker, Inc., 95 Madison Ave., New York, N. Y. 10016. 1970. $17.75

Reviewed by G. P. Arsenault, Department of Chemistry, Massachusetts Institute of Technology, Cambridge, Mass. 02139

The title of this book should have been "Physical Principles of Mass Spectrometry—A Mathematical Treatment." Admittedly, more space is devoted to negative ions in this book than in other texts on mass spectrometry; nevertheless, the strength of the book lies in its mathematical treatment. This should have been emphasized in the title.

Melton's manuscript has no equivalent among the many books written about mass spectrometry in the last decade. It is a textbook written for a "course in the principles of mass spectrometry" (Preface, p vi) and it "is not intended to teach an immediately useful art" (Preface, p v). It is intended for students in chemistry or physics and for professionals engaged in research. A complete understanding of the material covered requires a knowledge of calculus and differential equations, considerably more knowledge, in fact, than the average graduate student in chemistry would have.

The overall organization of the book is faultless, but the detailed presentation of the subject matter within each chapter lacks in organizational clarity. Take, for example, Chapter 3 entitled "Ion Sources" which has 10 subheadings of equal weight. A reorganization of this chapter into A. Types of Ion Sources (1. Electron Impact; 2. Surface Ionization; 3. Field Emission; 4. Gas Discharge; and 5. Photon Impact) and B. Characteristics of Ion Sources (1. Ion Source Optics; and 2. Mass Discrimination) would greatly improve the clarity of presentation. The remaining material discussed in Chapter 3 (the author's subheadings 6. Monoenergetic Electron Sources; 8. Multiple Electron Beam Ion Sources; and 10. Source Magnets) could be included under 1. Electron Impact. The detailed organization of the book leads, at times, to bizarre results. For example, the quadrupole mass filter (p 125–6) is, in effect, discussed under Time of Flight in the chapter devoted to mass analysis.

The book has few typographical errors but some rather confusing ones involving equations. Two examples follow: (1) σ_0 in Equations 3–8 is erroneously labelled σ on the following line when it is defined; and (2) reference is made on p 244, 1.2, to Equations 8–30, but it should have been made to Equations 8–28 instead. To confuse matters more in a manuscript with so many mathematical formulas, a symbol is sometimes given several meanings. Thus, Q is the total cross section (p 203), the amount of energy converted to kinetic energy from internal energy (p 207) and the flow (p 247).

Reading Melton's book has left me with ambivalent feelings. Its lack of overall perspective, its poor readability, and its awkward detailed organization prevent it from being a first-rate textbook. Its bibliography is too sparse—this is indeed intended by the author—and too selective to make it a good secondary reference. Yet the book has redeeming features which should be noted. Sample calculations are interspersed throughout the text. Problems are also available—and sometime their answers are given—at the end of all chapters. And the book is unique in that it presents the physical principles of mass spectrometry and gives a mathematical treatment as well. Whether a potential reader should place this book on his reading list depends on his interest in mass spectrometry. If, like most scientists, he is not interested in mass spectrometry for its own sake but only for its applications, the book is unlikely to have much appeal to him. For all others, the book is likely to be of some value.

Modern Analytical Chemistry. W. F. Pickering. xii + 622 pages. Marcel Dekker, Inc., 95 Madison Ave., New York, N. Y. 10016. 1971. $13.75

Reviewed by James J. Lingane, Department of Chemistry, Harvard University, Cambridge, Mass. 02138

That this is an unorthodox book is indicated by the very first sentence of the Preface, "The advent of the nuclear age has created a need for reappraisal of all past ideas and preconceived notions." The author then goes on to express his opinion that most textbooks of analytical chemistry and courses in the subject have not responded effectively enough to this challenge either to meet modern requirements or to rebut current adverse criticism of the way analytical chemistry continues to be taught. In concluding his prefatory argument for writing this book, the author states that "Its aim is to create a new image of analytical chemistry, to provide thought and discussion, and to challenge tradition." Wilhelm Ostwald's "Wissenschaftlichen Grundlagen der Analytischen Chemie" succeeded in this aim three generations ago, and Isaac Kolthoff has held this same torch aloft for nearly 60 years. The time has come to pass it on, and it is fortunate that there are so many outstretched hands, including those of Prof. Pickering.

This is intended to be a textbook for a lecture course, emphasizing basic principles rather than actual procedures. Presumably, the student already has acquired laboratory experience elsewhere. All of the analytical methods commonly thought of as physicochemical, which is to say methods based on optical, electrical, thermal, magnetic, and nuclear disintegration phenomena, are included. Furthermore, most of the more purely chemical methods, such as titrimetry, chromatography, ion exchange, solvent extraction, and kinetic techniques, also are discussed. In addition, there are chapters on the rationale of selecting the most appropriate method for a particular problem, on the statistical treatment of analytical data, on the elucidation of structure, and on the "Challenge of Automation." All this in only about 600 pages!

The cardinal principles underlying each method are presented, with brief indication of the measuring techniques, scope of application, and limitations. Each chapter concludes with a list of references (mostly specialized monographs) and with a set of problems. These problems are challenging, and many of them evidently have been designed to supplement the text by asking the student to write an essay on a particular topic after consulting re-

view articles and specialized monographs.

In general, the treatment is sophisticated and reflects the author's mastery of the essential principles of the very wide range of topics covered. Because practically the whole of analytical chemistry has been touched on in one way or another (text or problems) in a book of only average size, the discussions of each topic necessarily are brief and specialists in each subject may feel that their subject has been slighted. However, considering the purpose of the book, it seems to me that the author has avoided the pitfall of superficiality as successfully as can be reasonably expected, and this has been no easy task.

To assimilate a lecture course based on this book, the student will need to have had some background in the basic principles and techniques of quantitative analysis, as well as elementary physical chemistry. It would seem to be appropriate as an advanced course for third and fourth year chemistry majors, and for first year graduate students.

So much has happened so fast and so recently in physical science and in the technology resulting from it that science teaching is, to say the least, in a revolutionary state. Academic analytical chemists have been caught up in this maelstrom and are currently engaged in a great deal of soul-searching which is resulting in a variety of changes in analytical chemistry curricula.

Whether the approach taken by Prof. Pickering will be successful will, of course, only be decided ultimately by the test of usage in courses other than his own. My impression, after spending only a few hours examining this book, is that I would enjoy sitting in on Prof. Pickering's course.

Chemical Reaction Mechanisms. George M. Fleck. xi + 235 pages. Holt, Rinehart, & Winston, Inc. 383 Madison Ave., New York, N. Y. 10017. 1971. $10.95

Reviewed by R. G. Pearson, Northwestern University, Evanston, Ill. 60201

This is a short monograph (some 200 pages) which contains some useful material, while omitting most of what one might expect to find. The title is misleading as the subject of chemical reaction mechanisms, as ordinarily understood, is hardly dealt with. A much

(Continued on page 80 A)

GAS CHROMATOGRAPHY

2nd Edition

by A. B. LITTLEWOOD, School of Chemistry, The University Newcastle upon Tyne, England

This wholly rewritten version of the author's well-received first edition presents an integrated, up-to-date treatment of all the fundamental aspects of gas chromatography, both practical and theoretical. Strong emphasis is placed upon the way in which the principles can be used in practice to apply the technique to its best advantage.

CONTENTS: Definitions and Technical Terms. Retention Volume and Column Variables. Retention Volume and Thermodynamic Variables. Adsorbent Stationary Phases. Column Performance-Fundamentals. Column Performance-Mechanisms. The Preparation and Use of Columns. The Use of Detectors for Quantitative Analysis. Ionisation Detectors. Thermal Conductivity Detectors. Ancillary Apparatus and Techniques. Applications of Gas Chromatography. List of Symbols-Author Index-Subject Index.

1970, 521 pp., $22.50

A STATISTICAL MANUAL FOR CHEMISTS

Second Edition

by EDWARD L. BAUER, Winthrop Laboratories, Rensselaer, N. Y.

This book is for chemists who perform experiments, make measurements, and interpret data. It shows how to apply statistics to their greatest advantage in all areas of analytic and research chemistry through the use of addition subtraction and the slide rule.

CONTENTS: Fundamentals. The Average. Experimental Design and the Analysis of Variance. The Comparison of Two Averages. Analysis of Variance by Range. Control Charts. Correlated Variables. Sampling. Control of Routine Analysis.

1971, 208 pp., $9.50

SPECTROSCOPY IN INORGANIC CHEMISTRY

Volume 2

edited by C. N. R. RAO, Department of Chemistry, Indian Institute of Technology, Kanpur, India, **and J. R. FERRARO,** Chemistry Div., Argonne National Laboratory, Argonne, Ill.

CONTENTS: JACK M. WILLIAMS and S. W. PETERSON, Molecular Structure Determination by Neutron and X-Ray Diffraction. J. R. FERRARO, High Pressure Vibrational Spectroscopy. J. A. KONINGSTEIN, Electronic Raman Transitions of Rare Earth Ions and Crystal Field Effects. K. D. J. ROOT and MAX T. ROGERS, Electron Spin Resonance Spectra of Inorganic Radicals and Radical Ions. H. A. KUSKA and MAX T. ROGERS, Electron Spin Resonance of Coordination Compounds. BRIAN G. RAMSEY, Electronic Spectra of Organometalloids. A. P. B. SINHA, Fluorescence and Laser Action in Rare Earth Chelates. Author Index-Subject Index.

1971, 320 pp., $18.00

THE NUCLEAR OVERHAUSER EFFECT

Chemical Applications

by JOSEPH H. NOGGLE, Department of Chemistry, Univ. of Wisconsin, Madison, Wisc., **and ROGER E. SCHIRMER,** Eli Lilly and Co., Indianapolis, Ind.

CONTENTS: Introduction. Nuclear Spin Lattice Relaxation. Mechanisms of Spin-Lattice Relaxation. The Nuclear Overhauser Effect in Rigid Molecules. The Effect of Internal Motions. Experimental Methods. Transient Methods. The Effects of Chemical Exchange. Applications of the Nuclear Overhauser Effect: A Review of the Literature. Appendix I: Tightly Coupled Spins. Appendix II: Mathematical Methods. Author Index-Subject Index.

October 1971, about 240 pp., $14.50

IONIC INTERACTIONS

From Dilute Solutions to Fused Salts

Volume 2: **Structure and Kinetics**

edited by SERGIO PETRUCCI, Department of Chemistry, Polytechnic Inst. of Brooklyn, Brooklyn, N. Y.

This book is a comprehensive survey of ionic interactions in the entire range of concentrations from dilute solutions to fused salts. The chapters, which deal with the subject both theoretically and experimentally, are written by specialists in the fields of statistical mechanics, inorganic stereochemistry, chemical kinetics, and chemical structure. Volume 2 contains two chapters on chemical kinetics and mechanism, one of which emphasizes the recently developed relaxation tools for the study of ionic association, and two chapters on the spectra and structure of electrolytes.

CONTENTS: C. H. LANGFORD, Complex Formation and Solvent-Exchange Kinetics: A Dynamic Approach to Electrolyte Solutions. S. PETRUCCI, Kinetic Approach to the Study of Ionic Association and Complexation: Relaxation Kinetics. S. L. HOLT, Ultraviolet and Visible Spectra of Electrolyte Solutions and Fused Salts. D. E. IRISH, Vibrational Spectral Studies of Electrolyte Solutions and Fused Salts. Author Index-Subject Index.

1971, 292 pp., $16.50

HANDBOOK OF FLUORESCENCE SPECTRA OF AROMATIC MOLECULES

Second Edition

by ISADORE B. BERLMAN, Radiological Physics Div., Argonne National Laboratory, Argonne, Ill.

This handbook is a major collection of fluorescence and absorption data of over 200 aromatic compounds, more than twice the number in the previous edition. Beginning with benzene, the list continues through larger and more complicated systems. The text has been revised and new data is included in the appendices.

CONTENTS: Introduction. The Free Electron Model. General Information. Compounds. Uses of Fluorescent Compounds. Graphs. Appendix. Name Index of Spectra. Formula Index of Spectra.

1971, 490 pp., $19.00

PAPER CHROMATOGRAPHY AND ELECTROPHORESIS

by GUNTER ZWEIG, Director, Life Sciences Division, Syracuse Univ. Research Corp., Syracuse, N. Y., **and JOHN R. WHITAKER,** Department of Food Science and Technology, College of Agriculture, Univ. of California, Davis, Calif.

Volume 2/**Paper Chromatography**

by JOSEPH SHERMA, Lafayette College, Easton, Pa. **and GUNTER ZWEIG**

With contributions by ARTHUR BEVENUE, Univ. of Hawaii, Honolulu, Hawaii

This volume is an up-to-date treatise devoted to the techniques of paper chromatography. It deals briefly with the history and theory of paper chromatography and covers in detail selected techniques and quantitative methods.

CONTENTS: History and Introduction. Theory, Mechanism, and Fundamentals of Paper Chromatography. Techniques of Paper Chromatography. Quantitative Paper Chromatography. Amines, Amino Acids, Peptides, and Proteins. Carbohydrates. Aliphatic Acids. Steroids, Bile Acids, and Cardiac Glycosides. Purines, Pyrimidines, and Related Compounds. Indoles, Phenols, and Aromatic Acids. Naturally Occurring Pigments. Pesticides. Antibiotics and Vitamins. Micellaneous Organic Compounds. Inorganic Analysis. Author Index-Subject Index.

1971, 604 pp., $27.50

ACADEMIC PRESS NEW YORK AND LONDON
111 FIFTH AVENUE, NEW YORK, N.Y. 10003

CIRCLE 3 ON READER SERVICE CARD

better title might have been "The Handling of Kinetic Data."

Essentially there are three kinds of material in the book. Several kinetic experiments are described in detail, as they would be in a laboratory manual. These sections are well done and provide useful information for the beginner as to the meaning of the measurements.

The greater part of the book consists of mathematical methods for solving rate equations, with a minimal use of calculus. It is mostly the algebra of linear equations, including the use of determinants. The methods are necessarily restricted largely to coupled first-order systems. The mathematics of chemical relaxation methods are treated in some detail.

The third kind of topic consists of short chapters on kinetic paradoxes, or philosophical difficulties, solved by the principle of microscopic reversibility.

In spite of the peculiar choice of material, the book can be useful. It was presumably written for selected freshman students, but anyone doing kinetics at any level may find material in the mathematics sections which can be of help.

New Books

Vacuum Microbalance Techniques, Vol. 7. C. H. Massen and H. J. Van Beckum, Editors. xv + 238 pages. Plenum Publishing Corp., 114 Fifth Ave., New York, N. Y. 10011. 1970. $22.50

This book contains 21 of the 23 papers which were presented at the Eindhoven Conference in the Netherlands, June 17–18, 1968. Some of the topics discussed in this volume are: New designs in micro-mass-determination techniques, numerous applications of vacuum microbalances under widely divergent experimental conditions, and mass determination by quartz resonators.

Vacuum Microbalance Techniques, Vol. 8. A. W. Czanderna, Editor. xiii + 251 pages. Plenum Publishing Corp., 114 Fifth Ave., New York, N. Y. 10011. 1971. $22.50

Included in this volume are the proceedings of the Eighth Conference on Vacuum Microbalance Techniques held at Wakefield, Mass., June 12–13, 1969. Specific topics included are mass defect produced by thermal gradients, interpretation of oxidation data obtained during high-temperature oxidation of materials, and applications of the crystal oscillator microbalance.

Standards Methods of Clinical Chemistry, Vol. 6. Roderick P. MacDonald, Editor. xiv + 281 pages. Academic Press, Inc., 111 Fifth Ave., New York, N. Y. 10003. 1970. $14.50

This volume describes, in detail, tested and confirmed methods for clinical laboratory determinations. The methods presented are appropriate for general use in the average clinical laboratory, and each has been standardized to maximize its usefulness and highlight any pitfalls to the user. Two or more laboratories have checked each method, and any classifications, modifications, or improvements made by these laboratories have been incorporated into the discussion. The book will be of interest to biochemists, clinical chemists, and all those associated with academic, hospital, or private laboratories.

Heat Transfer, 2nd ed. Benjamin Gebhart. xi + 596 pages. McGraw-Hill Book Co., 330 West 42nd St., New York, N. Y. 10036. 1970. $18.50

This is a revision of a book which appeared in 1961. The main intent of the text is to present a description of the more important physical processes, theories, and methods of analysis grouped in the area conventionally referred to as heat transfer. In this edition, greater emphasis has been placed on detailed presentations of conduction mechanism, the nature of radiation processes, basic mechanisms of transport of fluids, and particularly, the nature of flows and transports in fluids. Other sections of this edition have been extensively reworked.

Dipole Moments in Organic Chemistry. V. I. Minkin et al. xi + 288 pages. Plenum Publishing Corp., 227 West 17th St., New York, N. Y. 10011. 1970. $19.50

As the first publication on this subject in 15 years, this book presents the most complete treatment of the topic to date. The Russian version of this text was published in 1968. This volume can serve as a supplementary text in advanced work in organic chemistry because it is a systematic combination of method and application of dipole moment studies applied to various structural problems in the field. This text also offers a wealth of up-to-date references to both Western and Soviet chemical literature.

Analytical Flame Spectroscopy. R. Mavrodineanu, Editor. xxii + 772 pages. Springer-Verlag New York, Inc., 175 Fifth Ave., New York, N. Y. 10010. 1970. $36.00

This collection of papers gathers together reference material and discussions on almost every aspect of analytical flame spectroscopy. It includes discussions of the basic principles of flame photometry and of emission and absorption spectroscopy and includes papers dealing with optical design of spectroscopic systems, the theory and use of hollow cathodes, and the basic principles of analog circuits. Another useful feature of this book is the bibliography which contains more than 2000 references to published materials on all branches of flame spectroscopy.

Annual Survey of Photochemistry, 1968. Nicholas J. Turro et al. xiv + 412 pages. John Wiley & Sons, Inc., 605 Third Ave., New York, N. Y. 10016. 1970. $19.95

The authors of this volume have presented a summary of the progress in certain areas of photochemistry published during 1968. The book is divided into four specific areas: (1) Organic photochemistry, (2) physical processes in organic photochemistry, (3) photochemistry of gases, 1968, and (4) progress in the study of inorganic and organometallic spectroscopy and photochemistry.

Proceedings of the Conference on the Application of the Mössbauer Effect. I. Dézsi, Editor. 803 pages. Akadémiai Kiadó, Budapest, P.O.B. 149, Hungary. 1971. $26.40

A conference was held in Tihany, Hungary, from June 17–21, 1969, on the application of the Mössbauer effect. The main sections of this book are: General Problems, Relaxation Effects, The Goldanskii-Karyagin Effect, Surface Phenomena, Alloys,

Oxides, Frozen Solutions, Biology, Chemistry, and Miscellany. This text contains a comprehensive picture of the application of the Mössbauer effect in the different branches of science. Chemists, physicists, and other research workers engaged in pertinent fields of science will find the text to be of value, as it will serve as a useful source of reference and will stimulate further studies connected with the Mössbauer effect.

Mössbauer Effect Methodology, Vol. 6. Irwin J. Gruverman, Editor. viii + 237 pages. Plenum Publishing Corp., 227 West 17th St., New York, N. Y. 10011. 1971. $19.50

This monograph presents the proceedings of the Sixth Symposium on Mössbauer Effect Methodology, which was held in Chicago, Ill., Jan. 25, 1970. It is the sixth volume of a series which provides a continuing forum for the publication of developments in Mössbauer effect techniques, spectroscopy, and applications. The highlight of the symposium was a session on lunar samples. Many other papers were presented including recent work in the area of frozen aqueous solutions and others on methodological developments including a report on polarized sources, on a coincidence technique, and on the use of radio frequency to perturb hyperfine levels.

Electron Spin Resonance of Metal Complexes. Teh Fu Yen, Editor. ix + 204 pages. Plenum Press Corp., 227 West 17th St., New York, N. Y. 10011. 1969. $15.00

This monograph contains the Symposium on ESR of Metal Chelates at the Pittsburgh Conference on Analytical Chemistry and Applied Spectroscopy, which was held in Cleveland, Ohio, March 4–8, 1968. It was designed to bridge the gap between chemical theory and application, and to acquaint the chemist with the potentially immense amount of information that can be obtained from ESR data. It presents a wide scope of the main problems in ESR of metal complexes—e.g., the structure and bonding of the transition metals and their ions; the charge transfer, symmetry reduction, and ligand type of their chelates; computer synthesis of spectra; and high-resolution techniques. Other topics discussed also involve organometallic chemistry, solid state physics, biomedical science, instrumentation, geoscience, and computer programming.

Our all-glass U-column GC may well be the established standard in the life sciences.

HERE ARE SOME OF THE REASONS WHY NUCLEAR-CHICAGO'S SERIES 5000 HAS ACHIEVED SUCH WIDE ACCEPTANCE:

Reason No. 1.

The Series 5000 makes great separations. Fatty acids. Drugs. Pesticides. Bile acids. Steroids. Sugars. Vitamins. Even amino acids. And it makes them with minimum sample decomposition. Even the tough ones.

The inlet system is all glass to keep metal away from your samples in this high-temperature zone. (And we've just improved the port for more efficient injection and easier septum replacement.) In fact, sample degradation is minimized throughout the *entire* system.

The system has intake and exhaust dampers for efficient cool-down after each temperature-programmed separation.

The column is re-equilibrated at the *initial* temperature before the next run can start. Peak retention times are routinely reproducible. The electronic temperature programmer gives you oven-temperature reproducibility on a day-to-day basis. The gas flow controllers are insulated *and* isolated for the best stability available today.

Reason No. 2.

The Series 5000 can perform a greater variety of analyses than any other U-column GC. Accessory options such as Radioactivity Monitoring (RAM), Automatic Sample Injection (see below), Automatic Temperature Programming and Cool-Down, Pyrolysis (with better reproducibility than any other pyrolyzer), and Cryogenic Programming are all easily incorporated in this completely modular system.

Reason No. 3.

The Series 5000's low noise levels and excellent reproducibility permit smooth interface with all of the popular computers in laboratory use.

All system modules, including our new solid-state electrometer, are designed to help achieve this interface. The Series 5000 electrometer has unique temperature-controlled FET's, single-point grounds on individual PCB's, and independent outputs for recorder, integrator, and computer. That means exceptional baseline stability, very low noise level, short warmup time, and outstanding computer compatibility.

Our detectors have extremely low S/N ratios and unexcelled sensitivity. Our dual-zone detector oven has independent temperature controls for the successful use of multiple detectors. And it permits servicing of one zone while operating a detector at full sensitivity in the other.

Reason No. 4.

Our Model 5141 Automatic Sample Injection System multiplies your productivity. Permits 24-hour unattended operation for either isothermal or temperature-programmed analyses. Utilizes metal gauzes (to eliminate solvent peak) or "Hot Pop" PTFE capsules (to prevent sample evaporation prior to injection). Up to 72 solid samples, 35 liquid samples.

Reasons No. 5, 6, 7, 8 . . . . .

We maintain a complete inventory of chromatography supplies: Columns, phases, supports, syringes, recorders, detectors, hydrogen generator, et al.

We also maintain more than 30 sales and service offices in major cities from coast to coast.

But we can't tell it *all* here. The *proven* accuracy, the *proven* reliability, the *proven* productivity. All about all Series 5000 features and what they can mean to you.

Our new Series 5000 U-column brochure tells and *shows* it all. Send for it. Then you'll have *all* the facts. 0-228

The Series 5000.
From Nuclear-Chicago.
The Up-and-Coming Chromatography People.

NUCLEAR-CHICAGO
A SUBSIDIARY OF G. D. SEARLE & CO.

2000 Nuclear Drive, Des Plaines, Illinois 60018, U.S.A.
Donker Curtiusstraat 7, Amsterdam W. The Netherlands ACS-13

CIRCLE 135 ON READER SERVICE CARD

EDITORS' COLUMN

WHERE WORKLOADS can justify it, the trend toward computer networks seems likely to gain headway in large laboratory installations. In a network, two or more processors are linked together; each functions not only as an individual computer, but also can share network resources to give added capabilities. Advantages include specialization of tasks to optimize individual processor capabilities; shared system resources to minimize hardware and software redundancies; increased reliability of operations with system component backup; and the establishment of a common data base. These advantages mean that the capabilities in a network system are demonstrably larger than the sum of the individual computer capabilities. A hierarchical structure can be designed with a network executive computer to monitor the entire system and dispatch tasks appropriate to specific processors.

For less demanding needs in a smaller laboratory operation, a computer, such as the Digital Equipment Corp. PDP-12/LDP, can be used. This computer can operate up to 16 different slow instruments in an asynchronous mode simultaneously—instruments such as nmr, gc, ir, or X-ray spectrometer. It can also operate with a pulsed nmr to perform Fourier analysis. In addition, with a mass spec interface, it can be used in a dedicated fashion to acquire, display, report, and encode data from a low (single-focusing) resolution sector or quadrupole mass spectrometer.

The MASH (mass spectrometry handler) program is designed to be versatile and allow operator intervention, yet easy to set up. The operating functions include calibration (manual or automatic), acquisition, data manipulation, and library. Acquisition requires several parameters to be established, such as the numbers of scans to be made (maximum 250); repetitive or

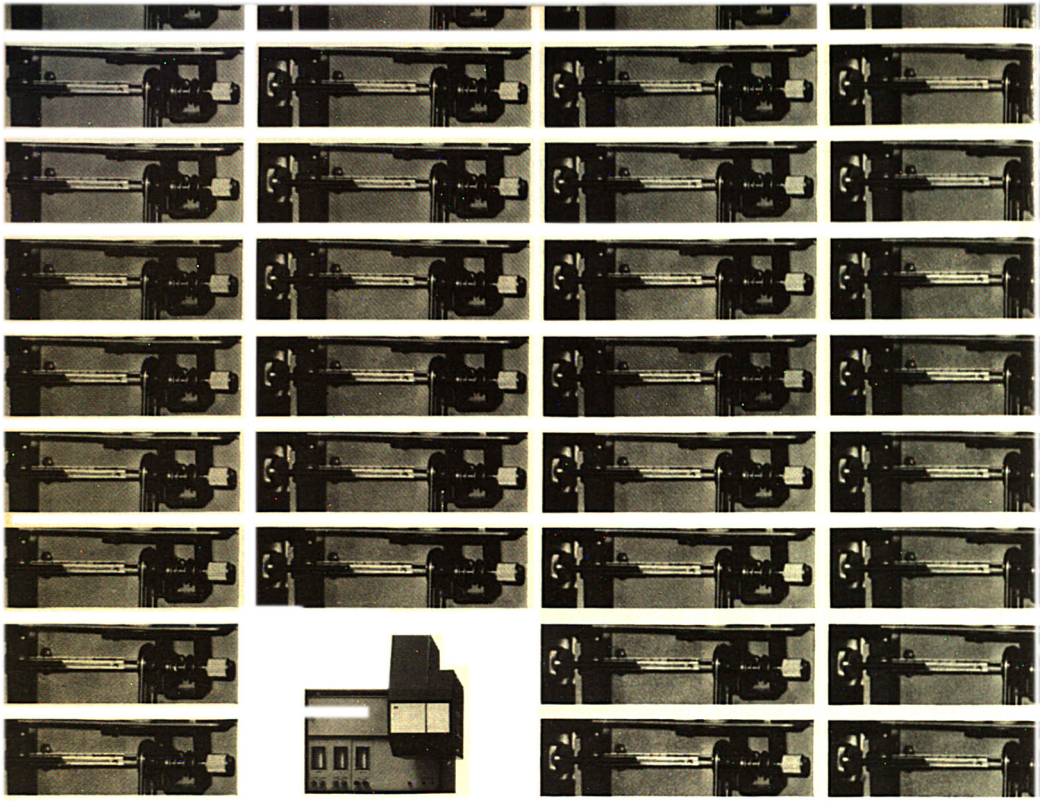

We operated the 7670A automatic sampler 24,000 times to prove its reliability

In our own laboratories, we have repeatedly performed 24,000 continuous injections—equal to two years of continuous use—without a major failure and with amazingly little wear.

Hundreds of GC labs are taking a dramatic yet inexpensive first step toward automation by installing the 7670A Automatic Sampler on their GC's. There's a good reason: each GC equipped with a 7670A can operate unattended overnight and on weekends, more than tripling its output.

If you're contemplating the purchase of an automatic sampler, you should know something about its reliability. Now that a year has passed since its introduction, we can tell you quite a lot about the reliability of the 7670A:

1—Hundreds of customer laboratories around the world have found the 7670A to be completely reliable, even when used around the clock. We know because all service calls during the first year are at our expense, and warranty service has been virtually nonexistent.

2—Our designers have a hard-nosed theory for automatic samplers: automation is required, reliability is demanded, precision is essential. To test their theory, we measured the analytical performance of the 7670A before and after 1000 continuous cycles. In all cases, we found that component concentrations agreed within ±0.2% and absolute retention times within ±0.01 min. (We used a C_{12} to C_{18} methyl ester sample and measured the results with a 3370 GC Integrator.)

Call the nearest HP sales office to learn how an investment of $3250 for the 7670A can improve the precision as well as productivity of your GC lab. Or write for our new 4-page data sheet. Hewlett-Packard, Route 41, Avondale, Pa. 19311. In Europe: 1217 Meyrin-Geneva, Switzerland.

HEWLETT hp PACKARD

ANALYTICAL INSTRUMENTS

CIRCLE 88 ON READER SERVICE CARD

43103

single scans; scan time and delay between scans; and threshold limits above which scans are saved. Data manipulation allows advantages such as flexibility in viewing all scans, selecting scans, normalizing data, and providing lists and plots. Data can be acquired from two channels up to 10 kHz each, and hard copy of the scopes display can be obtained from the teletype or plotter. The program has been designed to have general applicability and yet greater flexibility for adaptation to specific needs. The usefulness of this program has been demonstrated at Dow's Eastern Research Laboratory at Wayland, Mass.

Air Pollutant Measurements

C. Kumar, N. Patel, and Lloyd B. Kreuzer of Bell Laboratories have devised a system for measuring several kinds of oxides of nitrogen to levels as low as 10 ppb in air. The new technique uses tunable infrared radiation from a spin-flip Raman laser to measure the absorption spectrum of a gas sample by optoacoustic spectroscopy. In optoacoustic spectroscopy [*J. Appl. Phys.*, **42**, 2934, (June 1971)], a calorimetric method is used. In detecting pollutants by infrared radiation, a problem has been that at small concentrations the ir absorption is too small to be measured by direct determination of transmission through a reasonable pathlength. In the new technique, a cell containing the gaseous pollutant is periodically subjected to infrared radiation from a CO laser. If the wavelength of the ir radiation coincides with the wavelength of an absorption line, a periodic heating of the gas takes place. The resulting pressure fluctuations are detected by a capacitor microphone placed in the cell. The sensitivity of the method is limited by the Brownian motion of the microphone diaphragm. The details of the use of optoacoustic spectroscopy in this application are described in *Science*, 173, No. 3991, 45 (1971).

J. P.

How much should you pay for x-ray spectroscopy?

There is no easy answer.

If you check the systems on the market, you'll find an enormous spread in prices. From over $100,000 for a fully automated system to less than $20,000 for a simple manually operated instrument. What you spend should be determined by the work that must be performed.

Will a stripped down model meet your requirements?

Since there isn't a lot of money around these days, you may want to start at the bottom with a simple manually operated unit. The problem is to decide which of the extras you can afford to do without.

To make selection easier, Siemens has just introduced the Compak-3, a low-cost model that will give you some significant state-of-the-art extras. Its $28,000 price tag includes generator, x-ray tube spectrometer and detecting equipment for the analysis of solids, powders and liquids in a vacuum, air or helium atmosphere. It will handle elements down to Fluorine (9). And it has such innovations as x-ray tubes with asymetrically positioned targets, close sample coupling, and an optional pulse spectroscope.

Should you move up to an automated system?

If your company plans to use x-ray spectroscopy for production control, your requirements are different. Here, your choice is between speed of operation and versatility in handling different types of samples.

Siemens has completely automated systems from about $70,000, which for this type of set up is an unusually good price. For about $40,000 we can

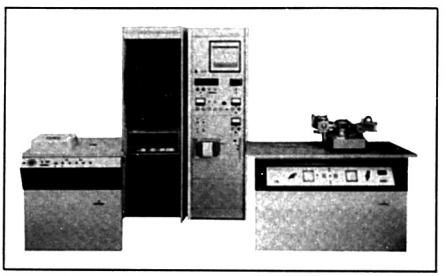

provide you with a manual sequential spectrometer system that can later be expanded to a fully-automated system.

Have you considered all of the hidden costs?

Extensive planning and programming is also necessary for the proper application of your equipment. Without early and thorough consideration of the day-to-day application of a system, it could take you six months or more to work out all evaluation techniques to determine the true concentration of analyzed elements. That will add considerably to your costs. And you may still end up with a system that doesn't do the job.

At Siemens, we're prepared to help you both in selecting the proper system and in providing the planning and software needed to put you into operation in the fastest possible time. And we'll see to it that you don't pay more than you should.

Write or call Dieter Meusel, Siemens Corporation, 186 Wood Avenue South, Iselin, New Jersey 08830 (201) 494-1000.

Siemens. A four billion dollar name in quality products.

SIEMENS

CIRCLE 177 ON READER SERVICE CARD

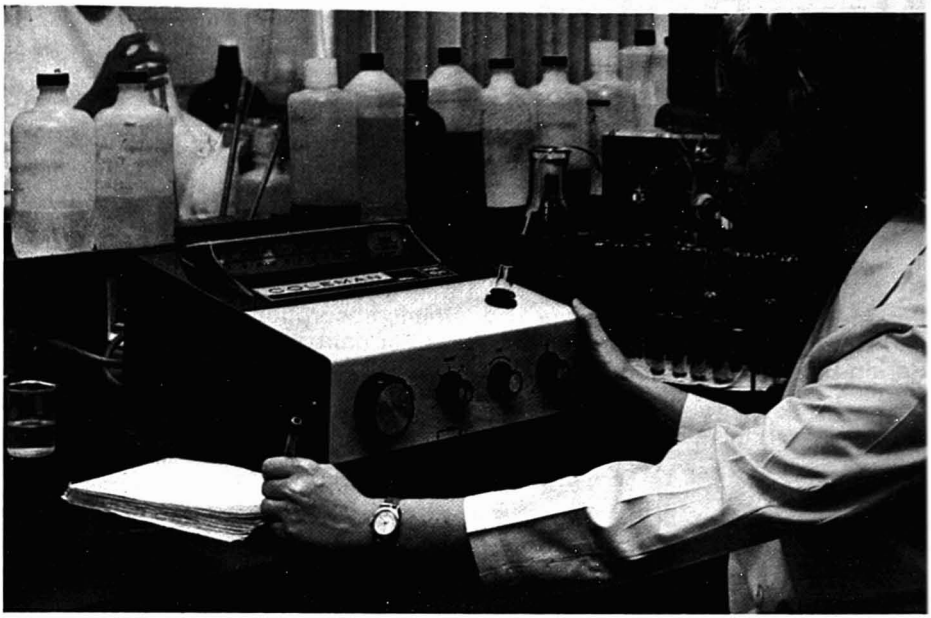

New Coleman Junior II Spectrophotometer

Easier reading, faster response, new UV-Visible-NIR range —all at low cost!

Here is the new spectrophotometer that gives you the fast, simple operation you need for control work and provides the wavelength range and versatility found in slower, more expensive instruments.

Wide range. A turn of a knob selects any wavelength—from 325 to 825 mμ—for rapid, routine determinations. No detector switching. No slit adjustments. Fixed 20 mμ bandpass.

Easier reading. Big, shielded, 8-inch absorbance/transmittance scale panel has readout so bright you can read it at a glance.

Faster response. Unique, highly sensitive galvanometer movement "locks in" on its reading in two seconds, without vibration or overshoot.

Solid-state detector. No phototubes, no vacuum tubes. Built-in power supply is fully transistorized. You have just one compact case on your lab bench.

Industrial applications. Include water quality control, wastewater treatment, ferrous and nonferrous metals, agricultural test labs and pharmaceutical labs.

The Coleman Junior II has output for a recorder, printer or digital readout. There's a Flame Photometer attachment for Na, K, Ca, Mg and Li . . . And wide range of cuvette sizes, up to 25 mm, including automatic emptying Vacuvettes for rapid sample handling.

Send today for details on the new Coleman Junior II. Request Bulletin A-310

Write to Coleman Instruments Division, The Perkin-Elmer Corporation, 42 Madison St., Maywood, Illinois 60153

PERKIN-ELMER

"SEE COLEMAN MODELS—ISLAND 2, ACS MEETING"
CIRCLE 36 ON READER SERVICE CARD

New. Perkin-Elmer goes atomic absorption 6 better.

Perkin-Elmer is introducing four new atomic absorption spectrophotometers and two high-sensitivity sampling systems. For data, write Instrument Division, Perkin-Elmer Corporation, XXX Main Avenue, Norwalk, Conn. 06852.

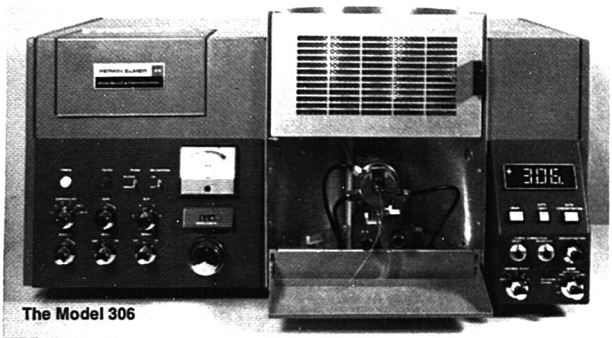

The Model 306

1. New: The Model 103
A compact, low-cost instrument which does absorption and emission analyses with equal ease. To light the flame, push a lever and actuate an "electric match." To set zero on the 12-cm meter, push the AUTO-ZERO button. To go from absorption to emission, flip a switch. To read out results, select between three damping times and two INTEGRATION modes. With meter integration, the needle rises to a stable reading; it doesn't quiver. The same stable signals can be read on a laboratory recorder.

2. New: The Model 107
To many, it's worth a little extra to read concentration on electronic digits. In the 107, the meter of the 103 is replaced by a four-digit read-out with adjustable decimal point. To set concentration, use the integration mode, then "unlock" the digits and set them to any value you want. Both instruments have a 0-1 absorbance range, and 50X scale expansion; 0.02 absorbance unit can be set to read full-scale on the digits. Both instruments have all-mirror optics to cover all the wavelengths from arsenic to cesium (1900-9000 A).

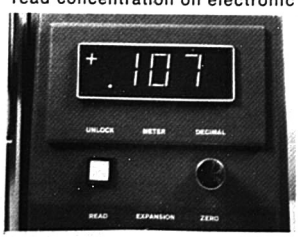

3. New: The Model 306
A double-beam instrument which reads concentration, in absorption or emission, on four electronic digits. An electric match is standard; fully automatic ignition is a little extra. To set zero, push the button. Then, use AUTO-CONCENTRATION. Just dial the concentration of the standard, aspirate the standard solution, and push the button. Calibration is now completed. Is the working curve non-linear? Straighten it with two controls, each used only once. The 306, too, has integration on both digits and recorder; the recorder traces appear noise free, and are easy to read. Conventional damping can also be used.

4. New: The Model 305A
The 305A has built-in flame emission, a new burner, a phase switch to improve the effectiveness of the Deuterium Background Corrector, and a metal instrument cover which gives easy access to optics and electronics. Result: proved reliability, improved performance.

5. New: The HGA-70 Graphite Furnace
A flameless system which gives far better detection limits than the burner-nebulizer. A small amount of sample is pipetted into a hollow graphite cylinder. The cylinder is then electrically heated as high as 2700° C in an inert atmosphere. Many metals are detected in amounts down to 10^{-12} grams.

6. New: The Delves Microsampling Cup™ System

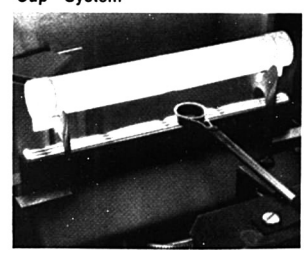

A modification of the Sampling Boat™ system, developed to determine lead in 10 μl of blood. The Delves system can also determine other volatile metals including cadmium, arsenic, selenium, and mercury.

PERKIN-ELMER

CIRCLE 163 ON READER SERVICE CARD

High-Speed Current Measurements

PIETER G. CATH
ALAN M. PEABODY
Keithley Instruments, Inc., 28775 Aurora Rd., Cleveland, Ohio 44139

Electrometers provide the means of detection and measurement of small electrical currents in many important instrumental methods utilized in chromatography, electrochemistry, and spectroscopy. A consideration of several approaches to high-speed current measurements can prove helpful in designing or selecting an optimum detector for a particular instrumental application.

THE MEASUREMENT of small electrical currents has been the basis for a number of instrumental methods used by the analyst. Ion chambers, high-impedance electrodes, many forms of chromatographic detectors, phototubes, and multipliers are commonly used transducers which require the measurement of small currents. Devices used for this measurement are often called electrometers. It is the purpose of this article to point out the trade offs that one makes to obtain desired characteristics and to present in some detail the design techniques for a new type of electrometer which is optimized for measurements in the 1 Hz to 5 kHz region (10^{-14} to 10^{-11} A resolution).

Current-Detection Limitations. In any measurement, if source noise greatly exceeds that added by the instrumentation, optimization of instrumentation is unimportant. When source noise approaches the theoretical minimum, optimization of instrumentation characteristics becomes imperative. To determine the category into which his measurement falls, the researcher needs to be familiar with the characteristics which impose theoretical and practical limitations on his measurement.

Most researchers are familiar with the theoretical limitations present in voltage measurements. The noise increases with source resistance, and the familiar equation for the mean-square noise voltage is

$$\overline{e_n^2} = 4\,kTR\Delta f \qquad (1)$$

where k is the Boltzmann constant, T is the absolute temperature of the source resistance, R, and Δf is the noise bandwidth ($\pi/2$ times the 3 dB bandwidth for a single RC roll-off).

In the case of current measurements, it is more appropriate to consider the noise current generated by the source and load resistances. The mean-square noise current generated by a resistor is given by Equation 2.

$$\overline{i_n^2} = \frac{4\,kT\Delta f}{R} \qquad (2)$$

From this equation, it is immediately apparent that the measurement of a small current requires large values of R—i.e., high impedance levels.

However, this presents difficulties for measurements requiring wide bandwidths because of the RC time constant associated with a high-megohm resistor and even a few picofarads of circuit capacitance. Figure 1 shows a current source generating a voltage across a parallel RC. The frequency response of this current measurement is limited by the RC time constant. Figure 2 shows this response and the —3 dB point occurs at a frequency

$$F_0 = \frac{1}{2\,\pi RC} \qquad (3)$$

Low noise and high speed, therefore, are contradictory require-

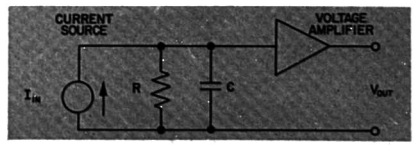

Figure 1. In the shunt method, current is measured by the voltage drop across a resistor

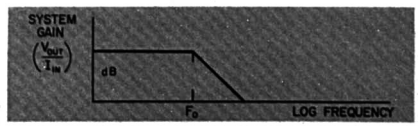

Figure 2. The frequency response of the shunt method is limited by omnipresent shunt capacitance

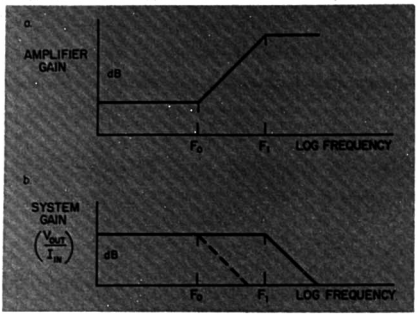

Figure 3. By tailoring the frequency response of the amplifier (3a), the frequency response of the shunt method can be extended (3b)

ments. To optimize a current-measuring system, techniques must be used which obtain high speed using high-impedance devices.

High-Speed Methods

High speed can, of course, be obtained in a shunt-type measurement by using a low value for the shunt resistor. As pointed out above, such a small resistor value introduces excessive noise into the measurement.

A second method to achieve bandwidth is to keep R large, to accept the frequency roll-off starting at F_0, and to change the frequency response of the voltage amplifier as shown in Figure 3*a*. The combined effects of the RC time constant followed by this amplifier are shown in Figure 3*b*, and it is seen that the frequency response of the current measurement has been extended to F_1. The frequency at which the amplifier gain starts to increase must be exactly equal to the frequency F_0 determined by the RC time constant in order for this approach to result in a flat frequency response. Therefore, this method is useful only for applications where the shunt capacitance, C, is constant. Aside from this drawback, this is a legitimate approach being used in low-noise, high-speed current-measuring applications.

In addition to current noise in the shunt and in the amplifier input stage, a major source of noise in this system arises from the voltage-noise generator associated with the input stage (reflected as current noise in the shunt resistor) caused by the high-frequency peaking in the following stages of amplification. More will be said about this in the discussion on noise behavior.

A third method used for speeding up a current measurement employs guarding techniques to eliminate the effects of capacitances. Unfortunately, only certain types of capacitances, such as cable capacitance, can be conveniently eliminated in this manner. Eliminating the effect of parasitic capacitances associated with the source itself becomes very cumbersome and may not be feasible in many instances. The major sources of noise in this system are identical to those mentioned in the second system.

A fourth circuit configuration combines the capability of low-noise and high-speed performance with tolerance for varying input C and eliminates the need for a separate guard by making the ground plane an effective guard. This is the current-feedback technique. This technique gives a typical improvement of a factor of three over shunt techniques. Again, the major sources of noise are identical to those mentioned in the second system.

Current-Feedback Technique

The basic circuit configuration used in the current-feedback technique is shown in Figure 4. In this configuration, the current-measuring resistor, R, is placed in the feedback loop of an inverting amplifier with a gain of A_0. The frequency response obtained with this circuit is identical to that shown in Figure 3*b*. F_0 again is the frequency associated with the RC time constant

$$F_0 = \frac{1}{2\pi RC} \tag{4}$$

The frequency response of the system is extended to a frequency F_1 where

$$F_1 = A_0 F_0 \tag{5}$$

Note that the frequency response is automatically flat without having to match break points. However, the total bandwidth of the system, F_1, is still limited by the value of the shunt capacitance, C, across the input.

This improved frequency response of the feedback technique avoids the use of low values for R which could generate excessive current noise.

Refinements of the Feedback System. A major difficulty of the feedback system arises from shunt capacitance associated with the high-megohm resistor, R, in the feedback path. If the shunt capacitance across this resistor is C_F, then the bandwith, F_F, of the system is determined by the time constant, RC_F

$$F_F = \frac{1}{2\pi RC_F} \tag{6}$$

A slight modification of the feedback loop can correct this problem, as shown in Figure 5. If the time constant, R_1C_1, is made equal to the time constant, RC_F, it can be shown

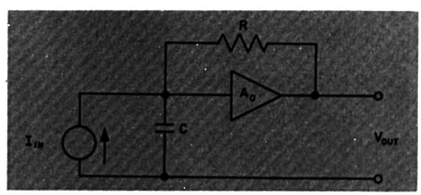

Figure 4. Basic circuit configuration for the feedback method

that the circuit within the dotted line behaves exactly as a resistance R. The matching of time constants in this case does not become a drawback because the capacitances involved are all constant and not affected by input capacitance.

Noise in Current Measurements

Noise forms a basic limitation in any high-speed current-measuring system. The shunt system gives the simplest current measurement but does not give low-noise performance. A properly designed feedback system gives superior noise-bandwidth performance.

Noise Behavior of the Shunt System. High speed and low noise are contradictory requirements in any current measurement because some capacitance is always present. The theoretical performance limitation of the shunt system can be calculated as follows:

The rms thermal noise current, i_n, generated by a resistance R is given by

$$i_n = \sqrt{\frac{4\,kT}{R}\Delta f} \qquad (7)$$

The equivalent noise bandwidth, Δf, of a parallel RC combination is $\Delta f = 1/(4\,RC)$ and the signal bandwidth (3 dB bandwidth) is $F_0 = 1/(2\,\pi RC)$. For practical purposes, peak-to-peak noise is taken as five times the rms value.

The peak-to-peak noise current can now be written as

$$i_{npp} = 2 \times 10^{-9} F_0 \sqrt{C} \qquad (8)$$

In practice, a typical value for shunt capacitance is 100 pF. With this value, the following rule of thumb is obtained:

> The lowest ratio of detectable current divided by signal bandwidth using shunt techniques is 2×10^{-14} A/Hz for a peak-to-peak signal-to-noise ratio equal to 1.

A corollary for this rule of thumb expresses the noise current in terms of obtainable rise time (10–90% rise time $t_r = 2.2\,RC$).

> The lowest product of detectable current and rise time using shunt techniques is 7×10^{-15} Asec.

In this derivation it has been assumed that the voltage amplifier does not contribute noise to the measurement.

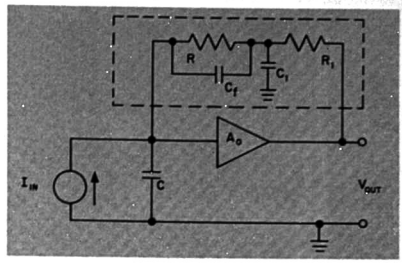

Figure 5. Frequency compensation in the feedback method removes the effect of shunt capacitance across the high-impedance measuring resistor

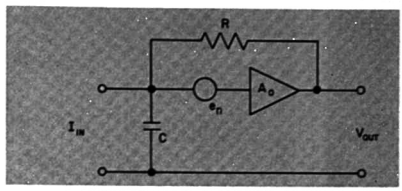

Figure 6. The voltage noise associated with the amplifier input device is an important source of noise in the high-speed feedback system

Noise Behavior of the Feedback System. There are three sources of noise in the feedback system that have to be looked at closely. The first two, input-stage shot noise and current noise from the measuring resistor, are rather straightforward. The third, voltage noise from the input device of the amplifier, causes some peculiar difficulties in the measurement.

Any resistor connected to the input injects white current noise (Equation 7). In the circuit of Figure 4, the only resistor that is connected to the input is the feedback resistor, R. As in the shunt system, R must be made large for lowest noise. Because this noise is white, the total contribution can be calculated by equating Δf to the equivalent noise bandwidth of the system.

The second source of noise is the current noise from the amplifier input. This component is essentially the shot noise associated with the gate leakage current, i_g, of the input device. Its rms value equals

$$\overline{i_n} = \sqrt{2\,ei_g\Delta f} \qquad (9)$$

where e is the electronic charge. The contribution of this noise generator is also white. Not only do these two noise sources generate white current noise, the noise in a given bandwidth is also independent of the input capacitance, C.

The major source of noise in a feedback current measurement is the noise contribution associated with the voltage noise of the input amplifier. The voltage noise can be represented by a voltage noise generator, e_n, at the amplifier input as shown in Figure 6. This noise generator itself is assumed to be white. However, its total noise contribution to the current-measuring system is not white.

Inspection of Figure 6 will reveal that at low frequencies a large amount of feedback is applied around the voltage noise source, e_n. However, the RC combination attenuates the high-frequency components of V_{out} so that no feedback is present at high frequencies. Thus, the noise contribution to the output voltage, V_{out}, from the voltage noise source, e_n, is no longer independent of frequency. The noise is "colored" and increases in intensity for all frequencies higher than F_0. The resulting noise spectrum is shown in Figure 7*b*. The total system noise is related to the area under this curve. Because the logarithm of frequency is plotted on the horizontal axis, the area under the curve at higher frequencies represents a significantly larger amount of noise than a similar area at low frequencies.

For comparison, Figure 7*a* shows

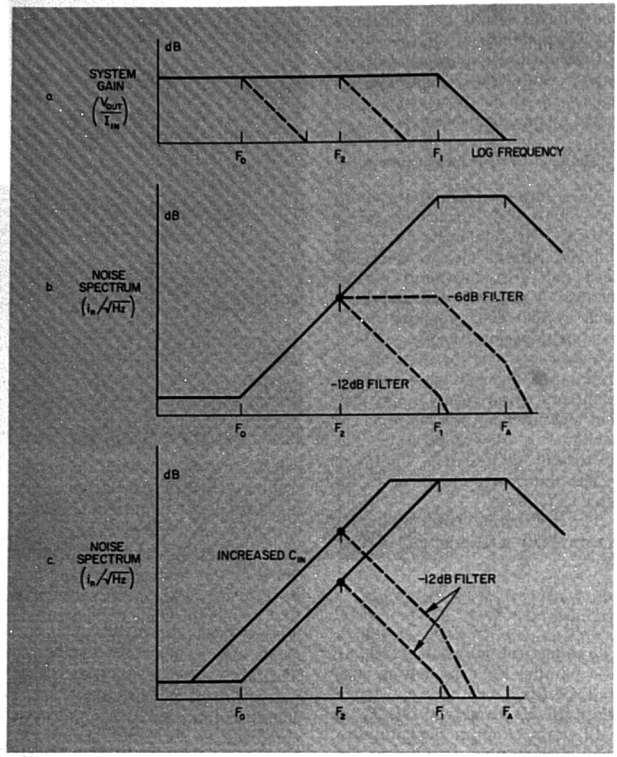

Figure 7. The bandwidth of the high-speed feedback system (*a*) can be limited by using a filter with either a −6 dB/octave or a −12 dB/octave roll-off. The effect of the filter on the noise spectrum is shown in *b*. Effect of input capacitance on noise is shown in *c*

the frequency response of the current-measuring system. Figure 7*a* is identical to Figure 3*b*.

It is interesting at this point to compare this noise spectrum with the frequency response of the voltage amplifier in Figure 1 as shown in Figure 3*a*. A voltage noise source at the input of the amplifier would generate a noise spectrum according to the amplifier frequency response as shown in Figure 3*a*. The noise spectrum of such a system, then, is identical to the noise spectrum of the feedback system as given in Figure 7*b*. This illustrates the well-known fact that signal-to-noise performance of a measurement cannot be improved by feedback techniques.

At the high-frequency end, the voltage noise is limited by the frequency, F_A, which is the high-frequency roll-off point of the operational amplifier. It should be noted that even though the useful bandwidth of the system extends only to F_1, there are noise components of higher frequency present. To obtain best wideband noise performance, these high-frequency noise components have to be removed. This can be achieved by adding a low-pass filter section following the feedback input stage. If the bandpass of this low-pass filter is made adjustable, this filter can serve the dual purpose of removing high-frequency noise and of limiting the signal bandwidth of the system.

To obtain optimum wideband noise performance under these conditions, a filter with a single high-frequency roll-off—i.e., —6 dB/octave—is not sufficient and —12 dB/octave is required. The effect of a —6 dB-filter is shown in Figure 7*a*, *b*. The filter is used to limit the system bandwidth to a frequency F_2, smaller than F_1. The effect of this filter on the noise spectrum is shown in Figure 7*b*. It can be seen that there are again high-frequency noise components above F_2, the useable bandwidth of the system. These can be eliminated by using a filter with a —12 dB/octave roll-off. The result of such a filter on noise performance is also shown in Figure 7*b*.

The reason that a —12 dB-filter gives superior performance over a —6 dB-filter in this application arises from the unusual manner in which the noise is colored. In most other cases, the noise is reasonably white across the bandwidth of interest and a —12 dB-filter then gives only marginal improvement.

One parameter affecting the noise behavior remains to be discussed. This is the effect of the input capacitance, C, on the voltage noise. An increase in the input capacitance will lower the frequency, F_0, and also F_1 since $F_1 = A_0F_0$. Figure 7*c* shows how an increase in input capacitance changes the noise spectrum. Because total-system wideband noise is related to the area under the noise-spectrum curve, this increase in input capacitance results in more wideband noise.

For the same reason, increased noise also results from adding capacitance across the feedback resistor, R, which is often done to limit the signal bandwidth and is referred to as damping. For low-noise wideband performance, signal bandwidth should be limited by use of a filter amplifier.

Narrowband signal-noise performance, as when using the amplifier in a lock-in system, is dependent only on the net system noise at the chosen operating frequency and is independent of any bandwidth limiting in the input amplifier. As can be seen in Figure 7*c*, increased input capacitance increases narrowband noise if F_0 falls below the operating frequency.

Event-Counting Techniques

An entirely different approach to the measurement of small currents is possible with event-counting techniques. In these techniques, individual electrons are counted in a fashion similar to the counting of radiation quanta in photon counting. These techniques are limited to measuring small currents in a vacuum.

To be detectable, electrons must be detected with an electron multiplier or photo-multiplier. Very small currents can be measured, but circuit speed limits the maximum detectable current to the range of 10^{-12} to 10^{-13} A. Resolution in this technique is determined by statistical considerations, and the product of resolution and rise time for this method is 4×10^{-18} Asec.

High Performance Current Amplifier

As an example of what can be achieved with the feedback technique, the performance of a commercially available current amplifier will be described. This amplifier (Keithley Model 427) is designed to incorporate the principles described above. Figure 8 shows a block diagram of this high-speed current-measuring system. The input amplifier is a wideband, high-gain feedback system using a field-effect transistor input.

The choice of input device is determined by the trade-offs involving the desired sensitivity, stability, and frequency response. Figure 9 shows the frequency and sensitivity areas for which different input devices have proved optimum, taking into account that most of the devices are limited by the practical rule of thumb of 10^{-14} A/Hz. Electron counting is the exception with a practical limit of 10^{-17} A/Hz.

The input amplifier is followed by an adjustable low-pass filter having a −12 dB/octave roll-off and a voltage gain of 10×. The voltage gain in the low-pass filter avoids

(Continued on page 99A)

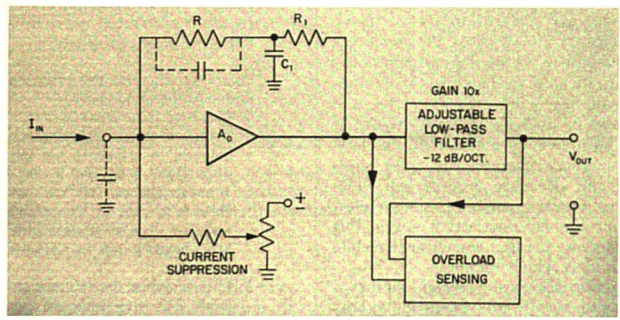

Figure 8. Block diagram of a high-speed current amplifier (Keithley Model 427)

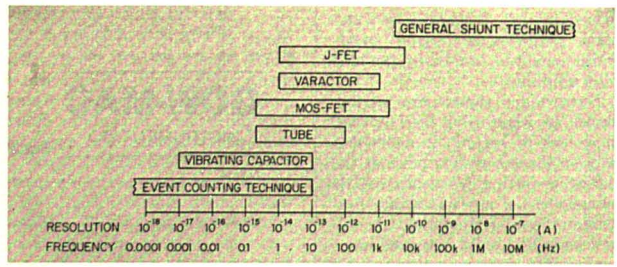

Figure 9. Optimum performance area for different input devices depends on desired frequency response and sensitivity

The Cary 401 Vibrating Reed Electrometer. (We should have called it the Cary 0.0000000000000001)

The Cary 401 vibrating reed electrometer detects currents on the order of 10^{-17} ampere, charges as small as 5×10^{-16} coulomb and potentials down to 2×10^{-5} volt from high impedance sources. Its list of standard features includes solid state circuitry, multiple resistor input switching, remote input shorting, critical damping, measurement of potentials from grounded sources, and master-slave operation. And it can be rack or bench mounted.

So, if your application is in mass spectrometry, radioactivity, physical measurement or biomedical research, the Cary 401 can tackle just about any problem you've got to solve. For example:

MASS SPECTROMETRY

The 401 provides sensitive, stable ion current measurements in any mass spectrometer system with an optional remote ranging modification available for computer-controlled systems. And, in isotope ratio studies such as uranium 238/235, a pair of our electrometers can determine ion ratios with an accuracy of about 0.02%.

RADIOACTIVITY

Combine a Cary 401 with one of our 100 ml to 14.8 liter flow-type ionization chambers and you'll have a radioactivity analysis system without equal. One capable of detecting as little as 10^{-6} microcurie of carbon-14 or 10^{-5} microcurie of tritium per cc of air, or measuring trace quantities of sulfur-35, iodine-131 and phosphorous-32 in gases.

Other radioactivity applications include the determination of tagged compounds from the effluent of gas chromatographs, in-vivo metabolism studies, and the monitoring of radioactive compounds in reactor stack gases and nuclear power plant atmospheres.

PHYSICAL MEASUREMENTS

With the 401, you can investigate resistance, charging, hysteresis, polarization, absorption and dielectric phenomena. Or study the photoelectric, thermoelectric and electrochemical properties of matter. Semiconductor studies include conductivity, resistivity, impurity and Hall effect measurements. And, because input resistance is greater than 10^{16} ohms, the 401 is ideal for measuring transistor leakage currents, diode reverse currents and MOS FET gate resistances.

BIOMEDICAL RESEARCH

When measuring ion transfer, potentials, and resistances across membranes, the 401 gives unmatched performance. Other biomedical applications include in-vivo respiratory analyses of $C^{14}O_2$, intermediary metabolism investigations, polysaccharide synthesis and degradation analyses and gas chromatographic studies of steroid and fatty acid molecular systems.

Twenty-four years of experience stand behind the Cary 401, the world's finest commercially available vibrating reed electrometer. By far. For complete details, write Cary Instruments, a Varian subsidiary, 2724 S. Peck Road, Monrovia, California 91016. Ask for data file P103-91.

cary instruments

CIRCLE 192 ON READER SERVICE CARD

AMERICAN CHEMICAL SOCIETY

ACS Short Courses

FALL SESSIONS

The following ACS Short Courses are newly scheduled for October and November 1971. The premier session of "X-Ray Diffraction for Industrial Chemists" is being offered in conjunction with the Eastern Analytical Symposium in November. Additional fall sessions are planned and will be announced shortly.

ACS members who are unemployed may request deferment of payment of the course fee. An unemployed member should add his request for deferment to the registration form for the course and state that he is an ACS member.

To register or obtain complete information on the courses, convenient lodging, student discounts, and fee deferments for unemployed ACS members, please write to Education Department, American Chemical Society, 1155—16th St., N.W., Washington, D.C. 20036. During the two-week period prior to a course, registration should be made by telephone: area code 202, 737-3337 ext. 258.

MODERN LIQUID CHROMATOGRAPHY

Oct. 9–10—Buffalo, N.Y. Dr. Lloyd R. Snyder and Dr. J. J. Kirkland; fee $95; required text, J. J. Kirkland, ed., "The Modern Practice of Liquid Chromatography," Wiley-Interscience, New York, 1971, $15; sponsor, Western New York Section in conjunction with 3rd ACS Northeast Regional Meeting.

For description of course content, see below.

COMMUNICATION SKILLS FOR CHEMISTS AND CHEMICAL ENGINEERS

Oct. 15–16—Chicago, Ill. Sponsor, Chicago Section.

Nov. 19–20—Philadelphia, Pa. Sponsor, Philadelphia Section.

Dr. Frederick G. Sawyer; fee $100, including lunches.

This course introduces the principles and techniques of effective communication via the written and spoken word. It is designed primarily for industrial chemists and chemical engineers, especially recent graduates and those who want to improve their skill in communicating the results of research, development, production, and marketing. Individual participation will be by workshop sessions and discussion of specific problems.

POLYMER ENGINEERING

Oct. 15–17—Cleveland, Ohio. Dr. Frank E. Karasz and Dr. Thomas W. Huseby; fee $115; in conjunction with ACS Rubber Division fall meeting.

This course is designed to introduce the graduate chemist or engineer to the basic engineering practices associated with polymer use. Topics include processing and fabrication, current commercial polymers, engineering and processing requirements, polymer testing, and specific applications. Equipment demonstrations are included. Some background in polymer science is desirable but not a requirement, since pertinent fundamentals are first reviewed.

COLUMN SELECTION IN GAS CHROMATOGRAPHY

Oct. 16—Boston, Mass. Dr. Harold M. McNair and Dr. Walter R. Supina; fee $70, including lunch; sponsor, Northeastern Section.

This course explores the critical step in gas chromatography, the selection of the proper column, from both the theoretical and practical point of view. Column material, length, diameter, solid support, and per cent liquid phase are discussed. The results obtained with different columns and different operating parameters are shown in chromatograms. Rules are developed to aid in choosing proper conditions. It is assumed that the registrant has been working with a gas chromatograph. No background in higher mathematics is required.

INTERFACING THE MINICOMPUTER

Oct. 22–23—New York City area. Dr. Raymond E. Dessy and David G. Larsen; fee $120, including lunches.

This course demonstrates in detail how to interface analytical equipment and other instruments to a minicomputer. The goal is to enable the registrant to build his own multipurpose interface. The basic building blocks of an interface are displayed in actual operation. Then various interface packages are assembled, with closed circuit TV being used to allow viewing of all steps. Multiplexing, device-code addressing, computer timing cycles, and ADC/DAC elements are emphasized. Registrants should have some background in instrumentation.

AT THE EASTERN ANALYTICAL SYMPOSIUM IN NYC

MODERN LIQUID CHROMATOGRAPHY

Nov. 13–14—Dr. Lloyd R. Snyder and Dr. J. J. Kirkland; fee $95; required text, J. J. Kirkland, ed., "The Modern Practice of Liquid Chromatography," Wiley-Interscience, New York, 1971, $15.

This course provides a basic introduction to the principles and practice of modern—high speed, high efficiency—liquid chromatography. No background in chromatography is assumed. Theory, applications, equipment, and techniques are covered for each of the important areas of modern LC: liquid-liquid (partition), liquid-solid (adsorption), ion exchange, gel permeation, gel filtration. Emphasis throughout is on practical aspects. A B.S. in chemistry, biochemistry, or chemical engineering is sufficient background. Technicians with some experience in chromatography will also benefit.

X-RAY DIFFRACTION FOR INDUSTRIAL CHEMISTS

Nov. 13–14—Dr. Robert J. Fredericks; fee $95; required text, B. D. Cullity, "Elements of X-ray Diffraction," Addison-Wesley Publishing Co., Inc., Reading, Mass., 1956, $15.

This course is intended for those who are newly entering the field of x-ray diffraction. It deals with those areas of x-ray diffraction most often practiced in industrial laboratories. These include the characterization of polymers and powder diffraction and its applications, such as qualitative and quantitative analysis, the determination of crystallite size, and polymorphism and isomorphism. Mathematics is kept to a minimum, and a B.S. in chemistry or other natural science is sufficient background.

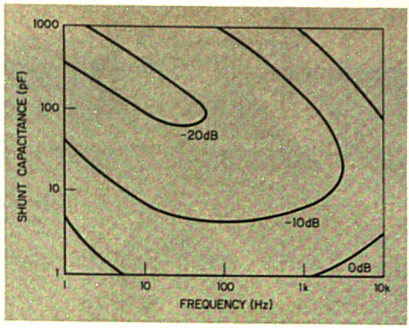

Figure 10. Plot of noise-improvement contours illustrating the improvement that can be obtained with the feedback method over the best that can be achieved with the shunt method at different operating frequencies

premature overloading in the input amplifier which can be seen as follows. The maximum output voltage V_{out} is ± 10 V. The maximum signal level at the input of the low-pass filter is, therefore, ± 1 V. At this point in the circuit, wideband noise could still be present and exceed the 1-V signal level. The voltage gain of 10 in the filter allows the total pre-filter wideband noise to exceed the full-scale signal by a factor of 10 (20 dB). The frequency response of this filter is adjustable for variable damping control.

To complete the 427 Current Amplifier a current-suppression circuit is added and overload-sensing circuits monitor pre- and post-filter overloads.

Noise performance must be examined for two methods of measurement. First, dc techniques for real-time measurements with bandwidth equal to the current-amplifier frequency response must be considered. Second, we must examine ac techniques (lock-in, Boxcar) where the current-amplifier frequency response must extend to the operating or center frequency while bandwidth is limited to a much lower value by the demodulator time constant.

It should be noted that use of ac techniques is to be avoided if the prime noise contributors are white, that is, if they have a constant noise per unit bandwidth. First, by definition, white noise increases with bandwidth regardless of center frequency, even if that frequency is dc. Second, a current-amplifier—shunt or feedback—requires lower shunt resistors as operating frequency is raised and noise per unit bandwidth increases with operating frequency. Thus, translating the operating frequency from dc provides no reduction in noise and may actually increase it.

The sensitivity and speed of the 427 Current Amplifier for either dc or ac measurements can be compared to the best performance obtainable with the shunt method. The best noise–rise time product that can be achieved for dc measurements with a 100-pF shunt capacitance in a shunt system is equal to 7×10^{-15} Asec. The feedback amplifier achieves 2×10^{-15} Asec with a 100-pF input shunt capacitance, which is approximately a 10-dB improvement. This 10-dB improvement over a theoretically perfect shunt system typically covers the span of bandwidths from 1 Hz to 3 kHz, with input shunt capacitance between 10 and 1000 pF.

When used in ac narrowband systems, the degree of improvement depends on the amount of input capacitance and the operating frequency. The achievable improvement over the shunt method can be plotted in a graph similar to a set of noise contours. Figure 10 shows the measured improvement (negative dB) that can be obtained with the 427 amplifier at any given frequency and input capacitance compared to a shunt method using an ideal (noiseless) voltage amplifier.

Acknowledgment

The contributions of G. Angeline, J. Maisel, and R. Babinec are gratefully acknowledged.

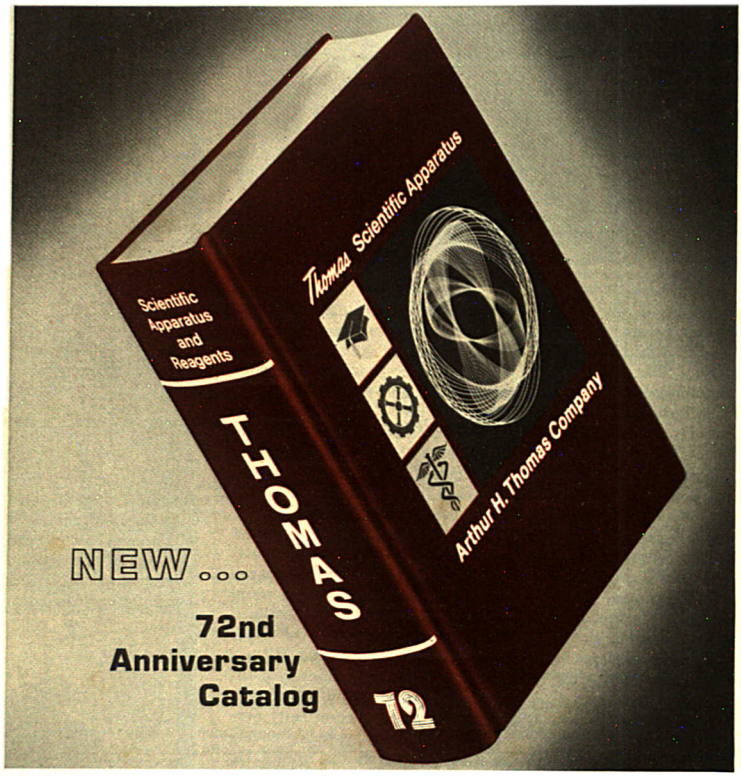

A new 1424-page edition of our general catalog, SCIENTIFIC APPARATUS AND REAGENTS selected especially for Academic, Industrial and Medico-Biological Laboratories, is now being distributed.

More than 2,400 new items are listed, with detailed factual descriptions, carefully indexed and cross-referenced. Included are recent developments both of our company and of the makers of standard brands.

All items are carefully selected and continually inspected for quality and performance. *Stocks of all items listed are regularly maintained for immediate shipment.*

Shipments are made directly from our Philadelphia headquarters, which offers unexcelled national transport networks, an international airport, and a major seaport.

Copy sent upon request to laboratory and purchasing personnel.

Thomas **ARTHUR H. THOMAS COMPANY**

Scientific Apparatus and Reagents

VINE STREET AT 3RD • P.O. BOX 779 • PHILADELPHIA, PA. 19105, U.S.A.

CIRCLE 182 ON READER SERVICE CARD

FIRST CLASS
Permit No. 1411-R
Washington, D. C.

BUSINESS REPLY MAIL
No postage stamp necessary if mailed in the United States

Postage will be paid by

AMERICAN CHEMICAL SOCIETY
1155 Sixteenth Street, N.W.
Washington, D. C. 20036

Attn: H. C. Spencer

ANALYTICAL CHEMISTRY

September 1971, Vol. 43, No. 11

EDITORIAL

For submission of manuscripts, see page 4 A.

Analytical Chemistry in Environmental Science

III. The Importance of Sampling

IN ENVIRONMENTAL SCIENCE, even more than in analysis generally, the truth of the old homily, "no analysis is better than the sample on which it is based," should be emphasized. There are two basic considerations involved.

First, the samples may be extremely diverse in character, and the materials of interest are often present at great dilution in situations of chemical, physical, or biological instability. The operation of procuring a representative sample from a dynamic, heterogenous system can present quite a challenge. The storage of the sample, to prevent loss of trace constituents or contamination by interaction of the sample with the walls of the container or with the atmosphere, needs consideration. Segregation of the sample prior to analysis may occur. Of course, all of these problems are inherent to analysis in general and are by no means unique to environmental science. It is just that they tend to be exacerbated by the nature of the problem.

The second consideration is the use to be made of analytical data, often by nonscientists. Improper inferences can be drawn, not necessarily through conscious efforts to distort data to strengthen an argument, but also through ignorance or lack of information about the sampling procedure. Proper experimental design involves drawing a representative sample from a population appropriate to the problem, and recognizing the nature of that population in applying the data. For example, it is clear that entirely different sampling procedures would be involved in the two problems: (a) What is the total mercury content of the fish in Lake Michigan, or (b) What is the mercury content of the edible portions of Coho salmon from the same lake? Data obtained to answer one of these questions would give no valid information about the other; yet, improper interpretations can be innocently made in the absence of sampling information. Another common error of interpretation is an improper averaging of analytical data without proper attention being paid to weighting. Indeed, in environmental science, the individual peak readings are often of more significance than average data.

The analytical chemist should play his role from the beginning of the measurement problem in collaborating in the experimental design, to the end, in helping with the interpretation of the data. In this way, he can make his full professional contribution and help avoid the pitfalls of drawing erroneous conclusions from experimental data.

Electrophoretic Separation of Alkylsulfate, Alkylbenzenesulfonate, and Alkylethoxysulfate Homologs, Using Aqueous Dioxane Agarose Gels

John R. Bodenmiller and Howard W. Latz
Department of Chemistry, Ohio University, Athens, Ohio 45701

Electrophoresis is used for the separation of members of homologous series which are common to anionic surfactants. The separation of members of homologous series could not be obtained in aqueous agarose gels. This is due to the monomer–micelle equilibrium which exists in these solutions. The effects of the surrounding media on the monomer/micelle ratio are demonstrated. Separations of homologous members of synthetic and commercial mixtures of alkylbenzenesulfonates and alkylsulfates, as well as commercial alkylethoxysulfates and alkylarylethoxysulfates are obtained in media which are not conducive to the existence of micelles. These electrophoretic separations are carried out using aqueous agarose gels containing up to 50% dioxane. Migration distances of 25 to 30 cm and time periods of 2.00 to 2.75 hours are required to obtain complete resolution of adjacent members, with ionic weights not greater than 325, of these homologous series. Greater migration distances are needed to obtain complete resolution of heavier adjacent homologs. After separation, the components of the mixture are detected with pinacryptol yellow and are identified by comparing their migration distances with standards run at the same time. Separation profiles are obtained by direct photometric scanning of the fluorescent pinacryptol yellow–surfactant adducts.

QUALITATIVE AND QUANTITATIVE analysis, of the hydrophobic portion of members of the homologous series which are common to anionic surfactants, is a problem which still lacks a satisfactory solution. Early work on the separation of homologs of anionic surfactants was done by Holness and Stone (*1*), Franks (*2*), and Borecky (*3*), using paper chromatographic methods. Puschel and Prescher (*4*) published a more recent paper using paper chromatographic methods for the separation of alkylsulfates, alkylsulfonates, and various other homologous series of aliphatic sulfonates. The running times for such paper chromatographic methods are generally eight to sixteen hours. Another popular approach to this problem has been by gas chromatography (*5–10*). This method requires a chemical or pyrolytic conversion of the nonvolatile salts to more volatile compounds that can be separated in the gas chromatograph. The separation and identification of cationic surfactants by paper electrophoresis was attempted by Fumasoni, Mariani, and Torraca (*11*), and by Noshiro, Izawa, and Kimura (*12*) but the migration rate varied with the sample concentration. Latz and coworkers investigated the electrophoretic properties of anionic surface active agents in aqueous agar and acrylamide gels (*13*). Their results indicated that the relative mobilities of surfactant types were dependent on pH and buffer type.

This paper presents an electrophoretic method for the separation and identification of members of homologous series which are common to anionic surfactants. Explanations are offered for the electrophoretic behavior of surfactants under various conditions. The present authors are aware of no other successful attempts to apply electrophoresis to the separation and identification of the members of various homologous series which are common to anionic surfactants. Specifically, the method was applied to alkylbenzenesulfonates (ABS), alkylsulfates (AS), alkylethoxysulfates (AES), and alkylarylethoxysulfates (AAES), but it can be applied to similar anionic series and also to cationic surfactants. The electrophoresis was carried out using aqueous dioxane agarose gels.

EXPERIMENTAL

Apparatus. A Desaga/Brinkmann Apparatus for Thin-Layer Electrophoresis (Brinkmann Instruments Inc., Westbury, N. Y.) was used for preliminary studies. Other investigations, where indicated, were done using an electrophoresis cell of similar design except the length was such that a 14-inch (35.6-cm) × 8-inch (20.3-cm) glass plate was used instead of the 20-cm × 20-cm plate used in the former. Power for electrophoresis was supplied by a Savant constant voltage source (Savant Instruments Inc., Hicksville, N. Y.).

The wicks can be divided into three components, paper, gauze, and cellophane. A paper wick (Brinkmann Instruments Inc.) extends from the bottom of the upper buffer chamber to the lower buffer chamber. A paper wick also extends from the front bottom edge of the upper buffer chamber and overlaps the gel layer 1.5 cm. A paper carton wick (Brinkmann Instruments Inc.) was placed in the buffer chamber. The paper wicks and paper carton were then covered by a post-op sponge, SR-8254 (The Seamless Rubber Co., New Haven, Conn.). A second carton wick was placed in the upper buffer chamber on top of the gauze sponge. A strip of cellophane, obtained by splitting 1 1/8-inch dialyzing tubing (10886 Will Scientific Inc., New York, N. Y.) was placed on the under side of the wick so that contact between the wick and gel was made by the cellophane strip.

The spectrophotofluorometer with thin layer scanner attachment was the same as that used by Madsen and Latz (*14*).

Materials. The agarose, Catalog No. J-2404-S, was purchased from the Fisher Scientific Co., New York, N. Y.

(1) H. Holness and W. R. Stone, *Nature*, **176**, 604 (1955).
(2) F. Franks, *ibid.*, p 693.
(3) J. Borecky, *Collect. Czech. Chem. Commun.*, **28**, 229 (1963).
(4) F. Puschel and D. Prescher, *J. Chromatogr.*, **32**, 337 (1968).
(5) J. J. Kirkland, ANAL. CHEM., **32**, 1388 (1960).
(6) T. H. Liddicoet and L. H. Smithson, *J. Amer. Oil Chem. Soc.*, **42**, 1097 (1964).
(7) L. L. Lew, *ibid.*, **44**, 359 (1967).
(8) C. B. Puchalsky, ANAL. CHEM., **42**, 803 (1970).
(9) S. Siggia and L. R. Whitlock, *ibid.*, p 1719.
(10) P. Bore and F. Degremont, *Rev. Fr. Corps Gras*, **17**, 315 (1970).
(11) S. Fumasoni, E. Mariani, and G. Torraca, *Chem. Ind. (London)*, **75**, 69 (1956).
(12) T. Noshiro, Y. Izawa, and W. Kimura, *Kogyo Kagaku Zasshi*, **68**, 1587 (1965).
(13) H. W. Latz and Coworkers, Union Carbide Corp., Tarrytown, N. Y., unpublished work, 1965.
(14) B. C. Madsen and H. W. Latz, *J. Chromatogr.*, **50**, 288 (1970).

and was manufactured by L'Industries Biologie Francaise S.A.

The 1-ABS and *p*-(1-ethyldecyl)benzenesulfonate (*p*-3-12-S) were synthesized with H_2SO_4, using standard methods from alkylbenzenes purchased from Eastman Organic chemicals, Rochester, N. Y. The 1-AS were prepared by the method of Dreger, Keim, Miles, Shedlovsky, and Ross (*15*) from alcohols purchased from Eastman Organic Chemicals. The ABS mixtures, 215, 225, and 230, were synthesized with H_2SO_4, using standard methods, from linear alkylbenzenes supplied by Monsanto Co., St. Louis, Mo. The numbers refer to the alkylate numbers assigned to the alkylbenzene mixtures by Monsanto Co. The homolog distribution of these alkylbenzenes are given in Table I. The sources of other commercial surfactants are given in Table II.

Procedure. PREPARATION OF THE GEL. The procedure for the preparation of a 50% dioxane gel is presented. All other preparations were similar with the appropriate substitutions.

The gel was prepared by adding 1.08 grams of agarose to 45 ml of 0.020*M*, pH 6 phosphate buffer in a 250-ml beaker. The beaker was covered with a watch glass and suspended in a water bath which was heated to boiling temperature. After the agarose was completely dissolved, the gel solution was removed from the water bath and 45 ml of dioxane was quickly added by pipet to the partially covered beaker. The contents of the beaker were mixed by a slight circular motion while the dioxane was added. The hot solution was then either heated or cooled to 60–70 °C and then poured on a 35-cm × 20-cm × 2.5-mm glass plate.

Prior to pouring the gel, the glass plate was placed on a level surface and other 6-mm thick glass plates were arranged so as to build a form for the gel. The seams were sealed with paraffin, which was accomplished by quickly moving a medicine dropper of hot paraffin down the seam.

One to two minutes after the gel was poured, the glass forms were removed by carefully lifting up the side opposite the gel and then pulling it away from the gel. In this manner, the paraffin wax remained on the form and not on the gel plate. A strip of gel was then cut away from the two sides of the plate so that there was about 1.5 cm between the gel and the edge of the glass plate. A template containing eight holes, 2.0 cm apart was placed over the plate and a melting point capillary (1.5-mm diameter) was used to cut the gel. The gel cylinders were then removed by applying a vacuum with a second capillary connected to an aspirator. The holes were usually made about 4 cm from one end of the plate. This gives a gel which is 0.010*M* in pH 6 phosphate, 1.2% agarose, 50% dioxane and 50% water, and is about 1.3 mm thick.

ELECTROPHORESIS OF THE SAMPLE. A light petroleum grease was applied to the aluminum cooling block in order to get better contact between the glass and aluminum surfaces. The prepared plate was placed on the cooling block and the wicks, which were already in the buffer vessels, were placed about 1.5 cm on the ends of the gel layer. The buffer vessels contained pH 6, 0.010*M* phosphate in pure aqueous solution. The circulation of the cooling water was then started. Sample, 1.6 μl, was deposited in the prepared holes by the use of a blunt needle microsyringe. The cover of the cell was closed and the appropriate potential was applied to the electrodes. The anode and cathode ends were altered after each run and the buffer was replaced after every fourth run.

DETECTION. After completion of the run, the plate was removed from the cell and was placed on a flat surface. A saturated solution of pinacryptol yellow was applied slowly until it completely covered the second half of the plate. This was allowed to stand for 15 minutes and then removed by tilting the plate. The pinacryptol yellow solution remaining on the surface was rinsed off by water from a wash bottle. A solution of 3*M* NaCl was poured on the plate and allowed to stand for 5 minutes. The purpose of the chloride was to quench the background fluorescence of the pinacryptol yellow. The fluorescent sample spots were detected under ultraviolet light.

If the separation profile was to be recorded, the following preparations were made. The gel was cut across the center midway between the two ends. The plate was submerged in water and the gel half containing the samples was floated onto a 20-cm × 20-cm × 1-mm glass plate. This transference was necessary because only 20-cm × 20-cm plates will fit into the thin-layer scanner. This was accomplished by carefully sliding the 20-cm plate between the gel and the 35-cm plate and presented no problems. After the 20-cm plate was carefully removed from the water tank, it was tilted at a slight angle against an absorbing substance to remove surface water. The gel was positioned with a straight edge, by sliding, so that the near edge was 2.54 cm from the end of the plate. A 1-cm strip was then trimmed off the other three sides and the plate was allowed to stand for 30 minutes. After this time was completed, the gel plate was submerged in water for approximately 30 minutes to remove excess pincryptol yellow from the gel. Free water was removed and the gel was repositioned in the same manner as before.

RECORDING OF SEPARATION PROFILES. The yellow and orange-yellow fluorescence, of the pinacryptol yellow–anionic surfactant adduct, made possible the recording of emission profiles for the separation. The technique used to record the separation profiles was that of Madsen and Latz (*14*) for their direct qualitative thin-layer chromatogram analysis. The 356-nm emission of a mercury–xenon lamp was employed for excitation and the emission monochromator was set at 532 nm. The slit program was 5-4-0.5-5-5 and the meter multiplier dial on the photomultiplier microphotometer was set at 0.01.

Table I. Homolog Distribution of Monsanto Phenylalkanes, Per Cent[a]

Alkyl chain	215	225	230
C_{10}	7	4	...
C_{11}	56	42	4
C_{12}	33	38	24
C_{13}	4	15	49
C_{14}	...	1	23
Av mol wt	237	242	259

[a] Technical Data Sheet I-269 Monsanto Company.

Table II. Names and Sources of Commercial Surfactants

Sample	Manufacturer	Source
Ucane-11	Union Carbide Corp.	Union Carbide Corp., Tarrytown, N. Y.
Ucane-12	Union Carbide Corp.	Union Carbide Corp., Tarrytown, N. Y.
Ucane-13	Union Carbide Corp.	Union Carbide Corp., Tarrytown, N. Y,
Tergitol 15-s-4.6A	Union Carbide Corp.	Union Carbide Corp., Tarrytown, N. Y.
Tergitol 45-s-3A	Union Carbide Corp.	Union Carbide Corp., Tarrytown, N. Y.
Tergitol 15-s-3S	Union Carbide Corp.	Union Carbide Corp., Tarrytown, N. Y.
Tergitol Anionic 4	Union Carbide Corp.	Union Carbide Corp., Tarrytown, N. Y.
Neodol 25-s-3A	Shell Corporation	Intermediary
Alipal CO 436	G. A. F.	Intermediary
P.D. L.S.-1	Alcolac Chem. Corp.	Intermediary
L.S.-2		Sigma Chemicals, St. Louis, Mo.

(15) E. E. Dreger, G. I. Keim, G. D. Miles, L. Shedlovsky, and J. Ross, *Ind. Eng. Chem.*, **36**, 610 (1944).

Table III. Number of Fractions Obtained for the Separation of Commercial ABS, under Various Buffer Conditions in Aqueous Agarose

pH	Concn, *M*	Buffer type	Number of fractions 215	225	230
	0.025	Triethylamine			
10	0.020	Acetic acid	3	3	3
8	0.050	Phosphate	1	1	2
8	0.025	Phosphate	1	1	2
7	0.050	Phosphate	2	2	2
7	0.025	Phosphate	1	1	2
7	0.050	Tris-HCl	1	1	1
6	0.050	Phosphate	2	2	2
6	0.025	Phosphate	1	1	2–3
5	0.025	Acetate	1	1	2
5	0.025	Phthalate	1	1–2	2
5	0.025	Phosphate	1	1	2
5	0.020	Citrate	1	1	1
5	0.025	Butanoate	2	2	2
	0.025	Acetate			
5	0.012	Trimethylamine HCl	3	3	3
	0.012	Acetate			
5	0.010	$N(CH_3CH_2)_4Br$	2	2	2
	0.025	Triethylamine			
5	0.050	Acetic acid	3	3	3
	0.025	Triethylamine			
5	0.050	Butanoic acid	3	3	3
5	0.012	Acetate	1	1	1
	0.025	Tris			
·4–5	0.050	Acetic acid	1	1	1
4	0.050	Acetate	1	1	3
4	0.050	Phosphate	2	2	2

RESULTS AND DISCUSSION

Aqueous Agarose Gels. PRELIMINARY STUDIES. Early results indicated that the relative electrophoretic mobilities of surfactant types were dependent on the buffer used in the media. Under some conditions, certain surfactants had similar mobilities while under other conditions their mobilities were quite different. Higher ionic weight 1-AS had, under certain experimental conditions, a greater mobility than lighter homologs. Commercial ABS and AES mixtures had mobilities greater than *p*-methylbenzenesulfonate (*p*-1-1-S), *p*-butylbenzenesulfonate (*p*-1-4-S), and *p*-heptylbenzenesulfonate (*p*-1-7-S) under most conditions. The order of relative migration rates of various surfactants tended to approach the order expected, on the basis of relative ionic weight, when they were run in lower pH media.

All of this erratic behavior is due to the monomer–micelle equilibrium that exists in these surfactant solutions. The tendency to approach normal behavior in lower pH media is thought to be due to an increase in the monomer/micelle ratio. AS, ABS, and AES are salts of strong acids and any acid–base equilibrium effects would be negligible in weakly acidic (pH 3) media. This increase in the monomer/micelle ratio is probably due to the greater amount of diffusion that occurs in the less structured gels formed at this pH. These results indicate that the relative mobilities of monomers and micelles as well as the monomer/micelle ratio are affected by the media.

1-ALKYLBENZENESULFONATES. The electrophoretic properties of the 1-ABS in aqueous agarose were investigated using the 20-cm cell. Initial runs were made using 0.50 mm thick, 1.0% agarose gels at cooling temperatures 17 to 20 °C. The applied potential was usually 500 volts and the time was varied from 60 to 20 minutes. Malachite green or $BaCl_2$ was used to detect the samples after migration. Runs were made using pH 7, 0.025*M* phosphate, pH 6, 0.0125*M* phosphate, and pH 9, 0.05*M* H_3BO_3-NaOH-KCl buffers, with the complete series of 1-ABS. The migration distances for *p*-1-1-S to *p*-1-6-S were always in the correct order and if the concentration of the samples was reduced from 50 mg/ml to 25 mg/ml, the order of migration was correct for *p*-1-1-S to *p*-1-8-S. The low solubility of 1-ABS homologs heavier than *p*-1-8-S, necessitated the use of saturated solutions, at 20–40 °C, of these samples. The electrophoresis of the heavier homologs resulted in precipitation at the starting point or narrow streaks from the starting point to various distances. Also *p*-1-8-S gave an elongated spot, whereas the spots were round for the smaller members of the series.

In an effort to solubilize and avoid precipitation of the higher molecular weight 1-ABS, they were dissolved in solutions of lauryl sulfate or commercial ABS. The electrophoresis of these samples gave one major fraction and sometimes a minor secondary fraction. The secondary fraction was u shaped and usually appeared at the same distance for all of the higher members of the 1-ABS series. The secondary compact u shaped fraction in both the lauryl sulfate and commercial ABS solutions, was suspected of being precipitated during the run. This probably results from a decrease in the local concentration by diffusion, of the solubilizing lauryl sulfate or commercial ABS. When the concentration is decreased below the critical micelle concentration, the lauryl sulfate or ABS can no longer solubilize the 1-ABS in their micelles, thus the 1-ABS are precipitated.

COMMERCIAL ABS MIXTURES. The commercial ABS mixtures, 215, 225, and 230, were investigated using the 20-cm cell. Several runs were made under various experimental conditions in 1.0-mm, 1.0% aqueous agarose gels at cooling temperatures of 25 to 27 °C. The ABS mixtures were 50 mg/ml in aqueous solution. The results of some of these runs are listed in Table III.

The number of fractions obtained from each sample and the relative migration rates of fractions from a particular sample were both dependent on the buffer used. The relative amounts of material found in these fractions were dependent on the buffer used. Also *p*-3-12-S usually separated into two fractions and the relative migration rate of *p*-3-12-S/laurylsulfate was dependent on the buffer used. Laurylsulfate which was later found to contain 1-dodecylsulfate, 1-tetradecylsulfate, and 1-hexadecylsulfate always gave one spot under these conditions.

Thus, separations obtained from surfactant mixtures containing micelles cannot be interpreted on the basis of ionic weight distribution. To gain more information about the monomer-micelle behavior, solutions of individual 1-alkylsulfates were investigated.

1-ALKYLSULFATES. Electrophoresis was applied in the same manner as in the preceding study of the ABS. The electrophoresis of dodecylsulfate (1-10-s), undecylsulfate (1-11-s), and dodecylsulfate (1-12-s) at 50 mg/ml in pH 5, 0.025*M* acetate and pH 5, 0.0125*M* citrate buffers produced two fractions, one more dense than the other. The smaller the alkylsulfate, the more material it had in the less dense fraction. In pH 5, 0.050*M* acetic acid–0.025*M* triethylamine

buffer, the order of migration was 12 > 14 > 11 > 10. The same results were obtained using a pH 10, 0.020*M* acetic acid–0.030*M* triethylamine buffer.

A series of runs were made using pH 3.5 and pH 4.5 acetate buffers ranging in concentration from 0.025*M* to 0.125*M* with a triethylamine concentration of 0.01*M*. The triethylamine was added in order to keep 1-14-s in solution. As the ionic strength was increased, the proportion of material in the dense fraction also increased.

In general, the members of the 1-AS, depending upon concentration, ionic weight, and experimental conditions, appeared as a single compact spot, a diffuse spot, a leading compact spot with either diffuse tailing or a diffuse spot with a slower migration rate, and a spot with a compact center and diffuse outer ring. Diffuse areas are attributed to the presence of monomers whereas the compact spots result from high micelle concentration. These results clearly indicated the necessity for the elimination of micelles from all surfactant samples if a meaningful separation of surfactant mixtures was to be attained. It was thought that the presence of micelles could be eliminated by the addition of organic solvents to the gel composition and this prospect was investigated.

Aqueous Organic Agarose Gels. PRELIMINARY STUDIES. The first organic solvent selected for study was dimethylformamide (DMF). Aqueous solutions of DMF, as high as 50%, form rigid transparent gels with agarose. The first results using DMF were an increase in diffusion, a decrease in mobility, and a decrease in detectability with the dye malachite green. However, these early results also showed that the relative migration rates of the 1-alkylsulfate series were, for the first time, in correct order. The undesirable effects caused by the addition of DMF were diminished by the use of pinacryptol yellow as the detecting agent, decreasing the concentration of the samples in order to decrease the rate of diffusion, and by increasing the electric field strength. A search of the literature produced the names of other organic compounds that had micelle-denaturizing effects on aqueous solutions of ionic surfactants (*16–18*).

A study was made on the effects of several of these organic additives on the electrophoretic properties of a homologous series of 1-AS and 1-ABS. These studies were carried out using pH 4–5, 0.025–0.0125*M* acetate buffered, 1.2%, 1.0-mm thick agarose gels. The concentration of organic additives varied from 10 to 50%. The initial studies were made using the 20-mm cell, with cooling temperatures 17 to 20 °C and an applied potential of 500 volts.

The 1-ABS were soluble in aqueous 1-propanol which has micelle-denaturizing properties at high concentrations and micelle-stabilizing properties at low concentrations in aqueous solutions (*17*, *18*). In an experiment using a 35% propanol gel, the effects of surfactant concentration on its monomer–micelle composition can be clearly seen. *p*-1-12-S was run at concentrations of 10, 5, 2.5, 1.25, 0.62, and 0.31 mg/ml for a duration of 0.5 hour. The shape of the spot progressed from an elongated elliptical form (micelles present) at 10 mg/ml to a circular form (monomer) at 1.25 mg/ml and below. The near end of all the spots was the same distance from the origin, while the distance from the front of the spot to the origin decreased with decreasing concentration.

If the results of running the 1-ABS series, *p*-1-10-S to *p*-1-14-S at 20 mg/ml in 20% propanol gel are compared to the results obtained from a 35% propanol gel, the order of migration is completely reversed. The effectiveness of the elimination of micelles in various aqueous organic additive gels was thus evaluated by the spot shape and order of migration rate for the 1-ABS or 1-AS homologous series.

The various organic additives used and found to form gels containing 1.2% agarose were DMF, 1-propanol, *p*-dioxane, acetamide, cellosolve, ethyleneglycol, glycerol, 1,2-propanediol, and urea. From this study, it was concluded that the DMF and dioxane systems gave the best results. However, these results also indicated that a longer migration distance was needed for resolution of adjacent members of the ABS series. A cell with the same design as the Desaga-Brinkmann cell, except with a cooling block that would accept a 35-cm plate, was built and put into service.

When the run time was increased from 1.5 to 2.75 hours to obtain the maximum migration distance in the 35-cm cell, an undersirable characteristic, under the previous conditions, became a major problem. There had been some surface solvent transport in both the DMF–acetate and dioxane–acetate systems when using the 20-cm cell, but it did not interfere, to any extent, with the separation. However, the longer time period allowed the solvent, which travels from the anode toward the cathode, to intercept and pass the samples which are migrating toward the anode. A loss in definition of the sample spots was caused directly by diffusion of the sample into the free surface solvent, and indirectly by electric field disturbances. There was also a high resistance line, which moved from the anode toward the cathode, though not necessarily originating at the anode. The visible effects, caused by the encounter of a sample with a high resistance line, was to cause the spot to become elliptical with its major axis perpendicular to the direction of migration. This sometimes caused better resolution to be obtained for mixtures, but more often than not it also caused gel deterioration and its effects were not constant throughout the width of the gel. Dioxane gels were then run in pH 6 and 7, 0.010*M* phosphate buffer, which eliminated all surface solvent transport. However, the high resistance line still occurred but with less frequency. Another problem was that the gel between the cathode wick and starting holes became quite thin. This problem of apparent solvent loss was solved by placing a cellulose strip between the gel and the paper-gauze wicks so that all transport between the gel and wick passed through the cellulose strip.

1-ALKYLSULFATES. The separation of C_{10-14} 1-alkylsulfates had been attained using 10–15% DMF, 1.0% agarose gels buffered at pH 4–5 with 0.0125*M* acetate in the 20-cm cell. The concentration of each alkylsulfate in the mixture was 1.25 mg/ml.

In order to attain better resolution for mixtures of greater concentration, the 1-AS were run in the 35-cm cell using dioxane, 1.2% agarose gels, buffered at pH 6 with 0.01*M* phosphate. The results of two typical runs under these conditions are listed in Table IV and Table V.

The results of this study indicate that 1-14-s, at a concentration of 5.0 mg/ml, usually tails in a gel of dioxane concentration less than or equal to 30%. If the concentration of 1-14-s is lowered to 2.5 mg/ml, tailing does not usually occur in a 20% dioxane gel. This tailing by 1-14-s is due to its insolubility in the lower per cent dioxane gels at the indicated temperature. All 1-AS lower than 1-14-s are quite soluble in aqueous or aqueous dioxane solutions and do not tail

(16) K. Shirahama and R. Matuura, *Bull. Chem. Soc. Japan*, **38**, 373 (1965).
(17) M. F. Emerson and A. Holtzer, *J. Phys. Chem.*, **71**, 3320 (1967).
(18) K. Shirahama, M. Hayashi, and R. Matuura, *Bull. Chem. Soc. Japan*, **42**, 1206 (1969).

Table IV. Typical Migration Distances for 1-Alkylsulfates in 20% Dioxane/Agarose Gels

Run Time Was 2.25 Hours at a Potential of 1120 Volts and a Cooling Temperature of 18 °C with a Current of 55 mA

Individual standards	Concn, mg/ml in 50% DMF	Migration, cm	
		Front	Back
1-10-s	5.0	28.8	27.7
1-11-s	5.0	27.7	26.3
1-12-s	5.0	26.5	25.1
1-14-s	5.0	23.3	21.8
Mixture			
1-10-s	1.25	29.0	28.1
1-11-s	1.25	27.5	26.5
1-12-s	1.25	25.9	24.9
1-14-s	1.25	24.0	22.9

Table V. Typical Migration Distances for 1-Alkylsulfates in 50% Dioxane/Agarose Gels

Run Time Was 2.0 Hours at a Potential of 1540 Volts and a Cooling Temperature of 18 °C with a Current of 46 mA

Individual standards	Concn, mg/ml in 50% DMF	Migration, cm.	
		Front	Back
1-10-s	2.5	...	
1-11-s	2.5	24.3	23.5
1-12-s	2.5	23.2	22.2
1-14-s	2.5	21.1	19.6
Mixture			
1-10-s	1.25	...	...
1-11-s	1.25	24.2	23.8
1-12-s	1.25	22.9	22.3
1-14-s	1.25	20.9	20.1

Table VI. Typical Migration Distances for 1-Alkylbenzenesulfonate Mixtures in 50% Dioxane/Agarose Gels

Run Time Was (a) 2.67 Hours (b) 2.83 Hours at a Potential of 1540 Volts and a Cooling Temperature of 18 °C with a Current of 46 mA

Sample	Concn, mg/ml in 40% 1-propanol	Migration, cm	
		Front	Back
Mixture (a)			
p-1-10-S	0.50	29.4	29.8
p-1-11-S	0.50	28.5	27.9
p-1-12-S	0.50	27.6	26.9
Mixture			
p-1-12-S	0.50	27.6	26.9
p-1-13-S	0.50	26.9	26.0
p-1-14-S	0.50	26.0	25.2
Mixture (b)			
p-1-10-S	0.50	28.5	27.7
p-1-12-S	0.50	26.3	25.3
p-1-14-S	0.50	24.6	23.7

even at much higher concentrations. All evidence indicates that 1-14-s, at a concentration of 5.0 mg/ml was completely in monomer form during its migration in a 30% dioxane gel. The results also indicate that 1-12-s and lower members of the series, at 5.0 mg/ml concentration, are in monomer form in gels containing only 10% dioxane.

There was no problem in visualizing the spot given by a 1.25 mg/ml sample of 1-10-s in a 20% dioxane gel. However, for dioxane concentration between 25 and 50%, 1-10-s, at 1.25 mg/ml was not usually detected. The solubility of the 1-10-s pinacryptol yellow adduct was also a problem in the DMF systems. The only solution so far is to vary the dioxane concentration for the particular needs of the sample. However, this does not detract from the good separations obtained by this system. A gel of 40–50% dioxane concentration should probably be used when working with samples

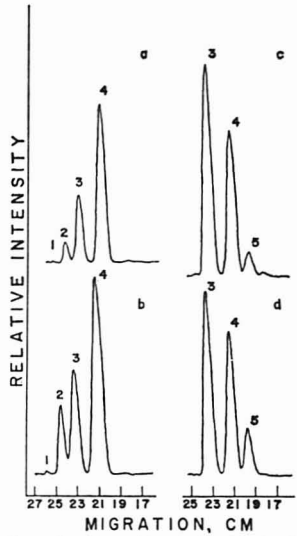

Figure 1. Separation profiles of standard and commercial AS mixtures: (*a*) standard, 3 mg/ml/component; (*b*) standard, 5 mg/ml/component; (*c*) LS-1, 10 mg/ml; (*d*) LS-2, 10 mg/ml

1. Decylsulfate
2. Undecylsulfate
3. Dodecylsulfate
4. Tetradecylsulfate
5. Hexadecylsulfate

between 5–10 mg/ml, especially ones containing a large percentage of the higher 1-AS.

1-Alkylbenzenesulfonates. Table VI lists some typical results for the separation of 1-ABS mixtures obtained in pH 6, 0.01*M* phosphate, 50% dioxane, 1.2%, 1.25-mm thick agarose gels.

The resolution obtained for the mixtures was quite adequate for qualitative comparisons between mixture and standards. However, for any intended quantitative use, better resolution would be required for mixtures containing *p*-1-13-S, *p*-1-14-S, and *p*-1-15-S. The absolute differences in migration distances for members of both the ABS and AS series are dependent only on the distance of migration. Their relative migration rates have not changed under the various running conditions, for which it was assumed all species were in monomer form. Therefore, considering a set distance of migration, resolution can best be improved by reduction in spot size. Spot size is dependent on diffusion and on the original size of sample application. Diffusion is dependent, among other factors, on concentration and time, and so the effects of a reduction in both of these were studied.

While the higher 1-ABS can be detected at concentrations lower than 0.50 mg/ml, the goal of this study is to separate and detect the more soluble ABS isomers. A distinction should be made between real separations and apparent separations. Because of the solubilities of the pinacryptol yellow adducts, the precipitated zones may not necessarily correspond to the total sample zone. Therefore, reducing the concentrations of the 1-ABS below the detection limit

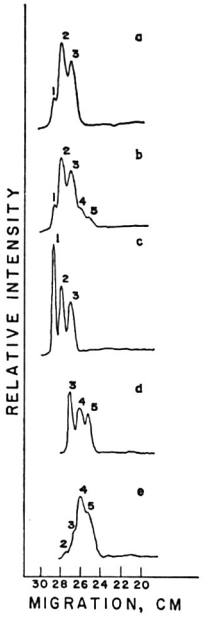

Figure 2. Separation profiles of standard 1-ABS and commercial ABS mixtures: (*a*) 215, 5 mg/ml; (*b*) 225, 5 mg/ml; (*c*) S_1, 0.5 mg/ml component; (*d*) S_2, 0.5 mg/ml/component; (*e*) 230, 5 mg/ml

1. *p*-*-10-S
2. *p*-*-11-S
3. *p*-*-12-S
4. *p*-*-13-S
5. *p*-*-14-S

* All isomers of a specific alkyl chain length are identified by a single number

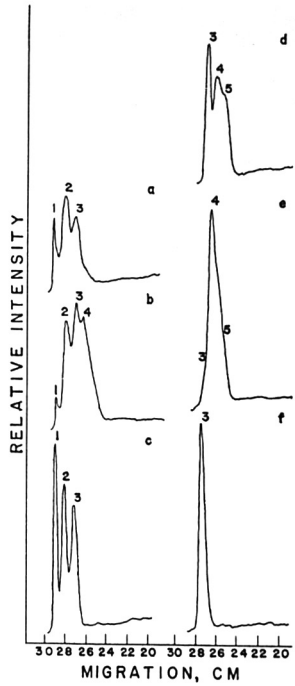

Figure 3. Separation profiles of standard 1-ABS and commercial ABS mixtures: (*a*) Ucane 11, 5 mg/ml; (*b*) Ucane 12, 5 mg/ml; (c) S_1, 0.5 mg/ml/component; (*d*) S_2, 0.5 mg/ml/component; (*e*) Ucane 13, 5 mg/ml; (*f*) *p*-3-12-S, 2.5 mg/ml

1. *p*-*-10-S
2. *p*-*-11-S
3. *p*-*-12-S
4. *p*-*-13-S
5. *p*-*-14-S

* See caption to Figure 2

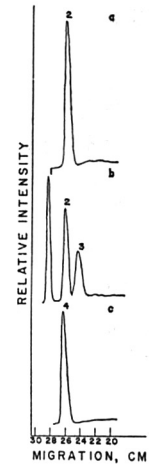

Figure 4. Separation profiles of standard ABS: (*a*) *p*-1-12-S, 0.5 mg/ml; (*b*) *p*-1-10-S, *p*-1-12-S, and *p*-1-14-S, 0.5 mg/ml/component; (*c*) *p*-3-12-S, 2.5 mg/ml

1. *p*-1-10-S
2. *p*-1-12-S
3. *p*-1-14-S
4. *p*-3-12-S

of the more soluble ABS isomers would not contribute to this final goal.

By decreasing the buffer concentration to 0.005*M* phosphate and increasing the voltage while keeping joule heat output near constant, the time for a 28-cm migration for *p*-1-10-S was reduced to 2.0 hours. This reduction in time did not result in a significant decrease in diffusion and thus no improvement in resolution. In fact, the spots for the higher 1-ABS homologs tended to be slightly elongated, thus resolution for mixtures of the higher homologs was decreased under these conditions.

Another approach to gain better resolution was to reduce the size of the starting holes from 1.5-mm to 1.0-mm diameter, but this led to no significant reduction in spot size or resolution. The gel thickness was increased slightly while using the same amount of sample. This study was inconclusive because just a few runs indicated that the cooling process was not sufficient for these systems.

Separation Profiles of Commercial and Standard Mixtures. All the following separations were obtained using the 50% dioxane gel described under Procedure. The use of this particular gel, cooling temperature of 18 °C, and applied potential of 1540 volts will henceforth be referred to in this paper as standard conditions.

ALKYLSULFATES. Mixtures of 1-10-s, 1-11-s, 1-12-s, and 1-14-s have been separated in 2.0 hours under standard conditions. The migration distance of 1-12-s in 2.0 hours under these conditions is approximately 24 cm. The separation profiles, Figure 1, indicate good resolution for this standard mixture when each component is at a concentration of 5.0 mg/ml. However, the indication of resolution at this concentration is misleading due to the solubility of the pinacryptol yellow adduct of the lower members of the series. As previously mentioned, a distinction must be made between apparent and real separations. A more critical evaluation would probably indicate that a 2.0 mg/ml concentration for each component is the maximum concentration for this particular mixture to obtain complete resolution of all its components. The separation profiles of lauryl sulfate samples (LS), when compared to the profile of the standard mixture, Figure 1, show the presence of dodecyl-, tetradecyl-, and hexadecylsulfates. No fraction corresponding to decylsulfate has ever been detected even under conditions that were more favorable for its detection. However, it may be present as a minor component. These profiles of lauryl sulfate show the high degree of resolution that may be attained for derivatives of natural products.

The sodium sulfate derivative of 7-ethyl-2-methyl-4-undecanol was also examined under these conditions and migrated the same distance as 1-14-s as expected. The branched four-substituted isomer is, of course, more soluble than the straight chain primary isomer. It cannot be detected

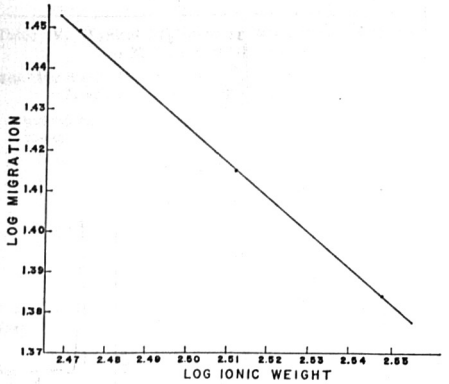

Figure 5. Log migration distance *vs.* log ionic weight for the 1-ABS separation profile shown in Figure 4

below the 5-μg level whereas 1-14-s can be easily detected at the 1.0-μg level using present techniques.

ALKYLBENZENESULFONATES. Six commercial mixtures of ABS have been investigated using this method. They were run under standard conditions for 2.75 hours in which time (*p*-1-12-S) migrated a distance of 27 cm. The components of these mixtures are identified by comparing their separation profiles with those of standard mixtures, Figures 2 and 3. The standard mixture, S_1, contains (*p*-1-10-S), (*p*-1-11-S), and (*p*-1-12-S), each at a concentration of 0.50 mg/ml in 40% 1-propanol. The standard mixture, S_2, contains (*p*-1-12-S), (*p*-1-13-2), and (*p*-1-14-S), each at a concentration of 0.50 mg/ml in 40% 1-propanol. A sample of (*p*-3-12-S) was also run as an additional standard. The commercial mixtures were run at concentrations of 5.0 mg/ml as the best compromise between resolution of major components and the detection of minor components.

The separation profiles, Figures 2 and 3, indicate the resolution that was attained for both the synthetic standards and commercial mixtures. The leading spots in these separations were very close to the anode wick and thus the profiles do not give the natural separation distance between the first and second spots. Figure 4 is the separation profile of a mixture of *p*-1-10-S, *p*-1-12-S, and *p*-1-14-S obtained under standard conditions, but for a shorter time period (2 hr, 35 min). If it is assumed that the migration distance (*d*), for a given run, is inversely proportional to the ionic weight (*w*), then a plot of log *d vs.* log *w* should yield a straight time. Figure 5 is such a plot for the separation profile of Figure 4. These results show that while *p*-1-13-S and *p*-1-14-S can be distinguished from one another, a greater distance of migration is needed for complete resolution.

All experimental results indicate that there is no difference in mobility between isomers of the same ionic weight. However, there is a large difference in solubility between the 1-ABS and other isomers. The 1-ABS–pinacryptol yellow adduct fluoresces yellow while *p*-3-12-S and the commercial ABS adducts fluoresce orange-yellow. Thus the detection limit for the 1-ABS isomer is lower than for the other isomers, Figure 4,*a* and *c*.

ALKYLETHOXYSULFATES AND ALKYLARYLETHOXYSULFATES. The commercial AES mixtures of 25-s-3A, 45-s-3A, 15-s-3S, and 15-s-5A were examined using this method under standard conditions. The samples were at a concentration of 20

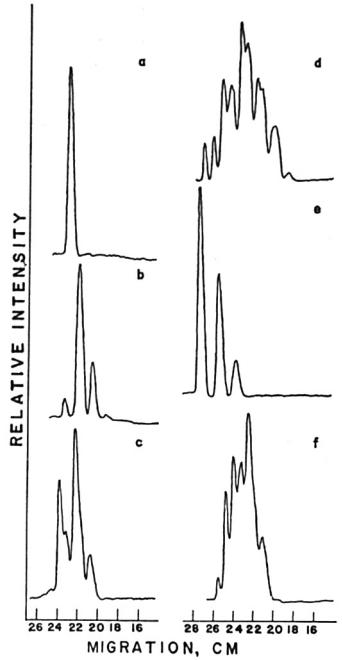

Figure 6. Separation profiles of commercial AES and AAES mixtures, AS and ABS standards: (*a*) *p*-3-12-S, 2.5 mg/ml; (*b*) Alipal CO 436, 20 mg/ml; (*c*) 45-s-3A, 20 mg/ml; (*d*) 25-s-3A, 20 mg/ml; (*e*) LS-2, 10 mg/ml; (*f*) 15-s-3S, 20 mg/ml

mg/ml and run times were 2.0 to 2.5 hours. Electrophoresis of these mixtures gave eight to twelve fractions for 25-s-3A, seven fractions for 15-s-3S, and six fractions for 45-2-3A. Although a few very light spots could be seen for 15-s-5A, they were of such poor definition that no data could be recorded for them. This is due to the solubility of their pinacryptol yellow adduct. The products, 25-s-3A, 45-s-3A, and 15-s-3S are all similar in that they are derived from primary linear alcohols and are suppose to contain three moles of ethylene oxide adduct. 15-s-5A is derived from linear secondary alcohols and is suppose to contain five molecules of ethylene oxide adduct. The nature of the mixture is described by the code name of the sample. The first number of the code name 25-s-3A denotes that the product was derived from C_{12-15} alcohols, s denotes sulfate, 3 denotes number of ethylene oxide molecules added to the alkyl chain, and A denotes the ammonium salt while an S in this position denotes the sodium salt.

The separation profiles of these products, shown in Figures 6, 7, and 8 are difficult to interpret without standard mixtures of these compounds and/or knowledge of the distribution of the starting materials. A standard alkylsulfate mixture and a standard 1-ABS mixture were run along with these compounds to identify them by an ionic weight/mobility comparison. However, there are a number of combinations of ethylene oxide groups and starting alcohols which give products of ionic weight within three atomic units of each

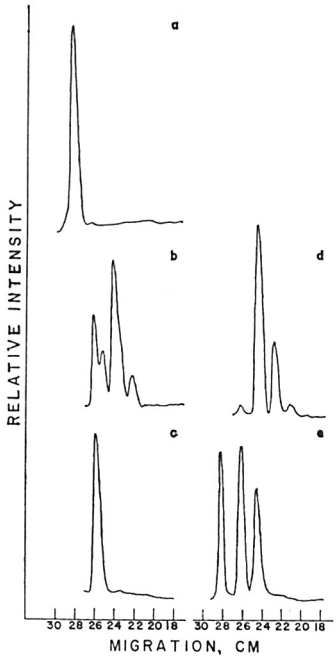

Figure 7. Separation profiles of commercial AES and AAES mixtures, AS and ABS standards: (*a*) tetradecylsulfate, 2.5 mg/ml; (*b*) 45-s-3A, 20 mg/ml; (*c*) *p*-3-12-S, 2.5 mg/ml; (*d*) Alipal CO 436, 20 mg/ml; (*e*) *p*-1-10-S, *p*-1-12-S, and *p*-1-14-S, 0.50 mg/ml/component

other. This, along with the fact that an alkylethoxysulfate may not have the same mobility as an alkylsulfate or alkylbenzenesulfonate ion with the same weight, would indicate that this method of comparison by itself is unsatisfactory. However, the separations obtained from these mixtures are quite reproducible in respect to the separation itself and in comparison to the mobilities of other compounds. Thus it is believed that positive identification can be made by the use of proper standards.

CONCLUSION

A great number of runs were made in the development of the present system using several different buffers at various pH, several organic additives, and many variations in experimental conditions. An improvement in resolution without a radical change in cell design is not expected. In theory, resolution could be improved by extending the length of the migration path. This could be accomplished by building a cell of the same design but slightly longer. However, there are indications that many of the factors in the present system are already beyond their maximum efficiency.

The main problems in the present system are the occasional occurrence of the high resistance line, which can cause minor to total disruption of the separation, and the difficulty of detection of the lighter surfactants at low concentrations with pinacryptol yellow.

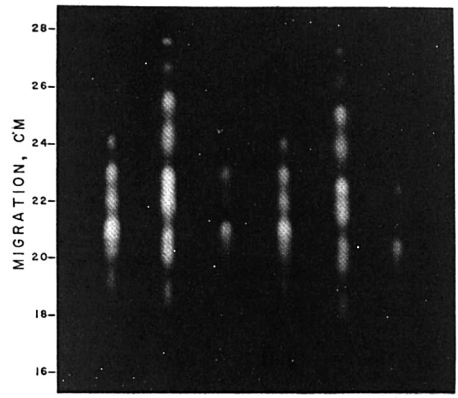

Figure 8. Separation of commercial alkylethoxysulfate mixtures in a 50% dioxane/agarose gel. Run time was 2.33 hours at a potential of 1540 volts and a cooling temperature of 18 °C with a current of 45 mA

The high resistance line is caused by the precipitation of buffer salts or association of buffer ions. The cause for the progressive movement of this region toward the cathode has not been thoroughly investigated. However, the following observation has been made. An acidic front develops from the anode, due to the low buffer capacity, which, as it moves toward the cathode, redissolves the precipitated salts. It is thought that the initial build up of salts takes place in the region where the anode wick makes contact with the gel. However, it is not certain whether the movement toward the cathode is caused by the development of new regions or by the travel of a single region. It is felt that this problem can be eliminated with the proper cell design.

The analysis of a homologous series of ionic surface active agents by electrophoresis in aqueous-organic solvent agarose gels has advantages over paper and thin-layer chromatographic methods. Run times are considerably shorter and mobility is strictly dependent on ionic weight. The sample can also be extracted from the gel, as in the former methods, for quantitative work. The advantage of an electrophoretic method over pyrolytic-gas chromatography methods is that the molecules remain unchanged, which leads to a simple separation profile, based on ionic weight, as opposed to the very complicated distributions obtained from the latter method when isomers are present.

The authors believe that the method presented in this paper can be used to advantage in the qualitative analysis of ionic surface active agents and other ionic substances. This is particularly true in the instances where electrophoretic methods fail because of micelle formation in aqueous solutions. With proper calibration, the area under the separation profiles can be used for quantitative estimates of the components and more accurate quantitative results can be obtained by applying established methods to the separated components.

Future studies will be concerned with the quantitative aspects of the present system and the design of a new cell, which hopefully will eliminate the undesirable characteristics of the present system and extend the migration path.

RECEIVED for review February 17, 1971. Accepted May 25, 1971.

Computer Techniques for Identifying Low Resolution Mass Spectra

Stanley L. Grotch

Jet Propulsion Laboratory, California Institute of Technology, Pasadena, Calif. 91103

A number of computer programs have been developed for identifying low resolution mass spectra through search of an extensive library file. One set of programs used as a disagreement criterion the sum of the absolute values of the differences in peak height levels when peak height was encoded to 2, 8, or 10^4 levels at each nominal mass. Another program employed the maximum coincidence of the top *N* peaks. The programs were tested using 125 unknowns and the recognition performances were compared. The maximum coincidence criterion was significantly poorer in recognition performance than the other techniques which increased in reliability as the number of levels increased. However, even the two-level system attained very high reliability. Since computer requirements and economic costs are likely to be minimal for this case, it might suffice for many applications.

In the past few years, a number of computer techniques for the identification of low resolution mass spectra have been described (*1–7*). This continued interest is spurred by instruments such as the gas chromatograph/mass spectrometer (GC/MS) which produce large numbers of spectra for interpretation. Since computers are already serving data handling (*8*) and control functions (*9*), spectral data are already in computer-readable format, greatly facilitating further detailed computer interpretation.

Generally, the two most desirable features of any computer identification scheme are high reliability of identification and low economic cost. In most situations, reliability of identification can be improved by increasing the complexity of the criterion used which generally increases computer costs. For example, Knock *et al.* (*7*) found improved identification when considering not only agreements in the *N* most intense peaks irrespective of order, but also considering the *ranking* order in the agreement criterion. Since it has been found in many studies that even very simple criteria can produce excellent results, it is important for any potential user of these techniques to be aware of the simplest of these, as they may very well satisfy his reliability needs at minimum cost.

Workers in this field have found that very high reliability of identification (>90–95%) can be achieved through a file search with low resolution mass spectra. Much still remains to be done in optimizing search procedures for specific applications. For example, computer-related factors such as available memory size, peripherals (disk, magnetic tape), batch processing *vs.* time sharing, will exert a profound influence on the optimal scheme for a particular application. For this reason, it is important to have available alternative techniques which can be tailored to specific applications. It is also important to compare various schemes in detail to delineate more clearly their respective advantages and disadvantages.

In the present work several identification algorithms have been implemented into computer programs which have been tested using low resolution mass spectral data obtained from five different sources (*10–14*). These spectra have been compared against a library of 6880 known spectra. This library is substantially the same as the one used by Knock *et al.* (*7*). Statistics regarding the library are presented in Table I. The results of these tests as well as the assets and liabilities of the matching techniques will be discussed.

Principles of Library Search. In the technique of library searching, an unknown spectrum vector X is compared in turn against the jth individual library member L_j, generally over a specified number of channels M. Let x_i and l_{ij} represent the individual elements of the vectors X and L. A criterion of agreement or disagreement C_j, is usually calculated as the linear function:

$$C_j = \sum_{i=1}^{i=M} F(x_i, l_{ij}) \qquad (1)$$

The functions F represent the desired criterion for the individual vector elements i. The "best" spectral match is that library number yielding the minimum value of C for a disagreement criterion (or the maximum value of C for agreement).

If, for example, a least-square criterion is used with respect to peak height over channels M_1 to M_2:

$$C_j = \sum_{i=M_1}^{i=M_2} (x_i - l_{ij})^2 \qquad (2)$$

Here x_i and l_{ij} are the peak heights in channel i (*i.e.*, nominal mass i). In this case the "best" spectral fit yields the mini-

(1) S. Abrahamsson, G. Haggstrom, and E. Stenhagen, 14th Annual Conference on Mass Spectrometry and Allied Topics, Dallas, Texas, May 1966 [see also S. Abrahamsson, *Sci. Tools*, **14**, 29 (1967)].
(2) C. Cone, P. Fennessey, R. Hites, N. Mancuso, and K. Biemann, 15th Annual Conference on Mass Spectrometry and Allied Topics, Denver, Colo., May 1967.
(3) R. A. Hites and K. Biemann, "Advances in Mass Spectrometry," Vol. 4, E. Kendrich, Ed., Institute of Petroleum, London, 1968, p 37.
(4) L. R. Crawford and J. D. Morrison, Anal. Chem., **40**, 1464 (1968).
(5) B. Pettersson and R. Ryhage, *Ark. Kemi*, **26**, 293 (1967).
(6) S. L. Grotch, 18th Annual Conference on Mass Spectrometry and Allied Topics, San Francisco, Calif., June 1970.
(7) B. A. Knock, I. C. Smith, D. E. Wright, and R. G. Ridley, Anal. Chem. **42**, 1516 (1970).
(8) C. C. Sweeley, B. D. Ray, W. I. Wood, J. F. Holland, and M. I. Krichevsky, *ibid.*, p 1505.
(9) W. E. Reynolds, V. A. Bacon, J. C. Bridges, T. C. Coburn, B. Halpern, J. Lederberg, E. C. Levinthal, E. Steed, and R. B. Tucker, *ibid.*, p 1122.
(10) R. M. Silverstein and G. C. Bassler, "Spectrometric Identification of Organic Compounds," 2nd ed., Wiley, New York, N. Y., 1967.
(11) A. J. Baker, G. Eglinton, F. J. Preston, and T. Cairns, "More Spectroscopic Problems in Organic Chemistry," Heyden & Son, Ltd., London, 1967.
(12) K. Biemann, Massachusetts Institute of Technology, Cambridge, Mass., personal communication, June 1970.
(13) H. Boettger, Jet Propulsion Laboratory, Pasadena, Calif., personal communication, Oct. 1970.
(14) Mass Spectrometry Data Centre, Aldermaston, England.

mum value of C. It is not necessary that the range M_1 to M_2 be contiguous, although this is generally the case.

With Equation 1, it is also possible to consider a criterion such as the maximum number of agreements of the N most intense peaks in the spectrum. This criterion forms the basis of the manual table-lookup methods used with spectral tabulations (*15*, *16*). Several computer versions of this technique have been reported by Knock *et al.* (*7*). This approach was also investigated in the present study. To recast Equation 1 for this criterion, let

$$x_i = 1 \quad \text{if channel } i \text{ is among the } N \text{ most intense peaks in the unknown} \tag{3}$$

$$x_i = 0 \quad \text{otherwise} \tag{4}$$

Similar conditions hold for the channels l_{ij} in each library member L_j. The criterion of agreement in this case is simply:

$$C_j = \sum_{i=1}^{i=M} x_i l_{ij} \tag{5}$$

Since an agreement criterion is used here, the "best" spectra are those maximizing C_j. It should be noted that the product criterion in Equation 5 is equivalent to the logical "AND" process. This fact is exploited in the computer program described later.

Algorithms Investigated. In the present study two simple criteria have been investigated. The first of these is that mentioned earlier (Equation 5): given the masses corresponding to the N_1 most intense peaks in an unknown spectrum, and the masses corresponding to the N_2 most intense peaks in the library, (N_1 not necessarily equal to N_2), find those library members which maximize the number of coincidences in mass. By utilizing the techniques described below, extremely rapid search speeds can be achieved with this criterion.

The second criterion is the minimization of the sum of the absolute differences in levels between the unknown and the library.

$$C_j = \sum_{i=1}^{i=M} |x_i - l_{ij}| \tag{6}$$

In this case, both the unknown and library peak heights are assumed known to only K levels; *i.e.*, in each of the M channels considered, $x_i, l_{ij} = 0, 1, 2, 3, 4, \ldots, K-1$. Equivalently, the peak height at each mass is represented by $\log_2 K$ bits. In the present study, peak height was encoded to either 2, 8, or 10^4 levels. [The last condition retains peak height to the maximum reported range in the library (0.01–100), 10^4 levels.]

The choice of the absolute difference criterion coupled with peak height encoded to a small number of bits results in several beneficial effects: very high search speeds can be achieved by packing many channels into each computer word and utilizing essentially parallel processing; computer memory requirements are reduced; the quantity of data to be entered into the computer for both unknown and library is substantially reduced, significantly reducing data input/output time.

Computer Program Design. In all of the computer techniques described here, an unknown spectrum is compared against a library of known spectra stored on magnetic tape. As the search proceeds, a record is maintained of the ten compounds in the library yielding the *minimum* value of the selected criterion. These "top 10" spectra are summarized at the conclusion of the search. All of the programs can accommodate up to 30 unknowns on each pass through the library.

Table I. Spectral Library Characteristics (6880 Spectra)

Molecular weight	
Minimum	2
Maximum	1318
Average	169
Average number of peaks reported	
≥0.01% base	92.6
≥1% base	40.4
No. of compounds containing only	
C, H	1795
C, H, O	2461
C, H, N	433

The search programs have been written almost exclusively in Fortran IV and tested on an IBM 360/44 computer. (Only a few essential subroutines are coded in assembly laungauge.) Each complete search package consists of approximately 500 Fortran statements.

Since all programs follow the same search strategies, a common subroutine structure has been found to be highly valuable. With this structure it is a relatively simple matter to modify programs to investigate various search algorithms or other parameters. Each program is divided into the following five subprograms.

1. A main control program performing initialization of variables and the calling of the other required subroutines.
2. A subroutine for reading unknown spectral data (from either cards or tape) and encoding these data in a format compatible with the search algorithm and the spectral library.
3. A subroutine in which the actual library search is performed. For each unknown, after suitable prefiltering (see below), the criterion of disagreement is calculated by a comparison with each library member.
4. A subroutine which maintains a detailed record of relevant library information for the 10 compounds with the minimum value of the criterion or disagreement.
5. A subroutine summarizing at the end of the search the spectral characteristics of the "top 10" library members for each unknown (see Figure 1 for a typical example and the Appendix for further details).

Although all programs utilized the above gross structure, in an attempt to optimize performance and to better investigate various parameters, each of the algorithms resulted in rather different spectral packing arrangements. This, in turn, necessitated different calculation schemes in the comparison subroutine. Some of the more important details of these procedures are discussed in the Appendix.

Unknown Data. In order to test and compare reliability of identification and program performance (speed, computer requirements), 125 low resolution mass spectra were considered as unknowns. These spectra were collected from five different sources (*10–14*) and were known to be different measurements from those in the library. Some characteristics of these unknowns are summarized in Table II.

(15) A. Cornu and R. Massot, "Compilation of Mass Spectral Data," Heyden and Son, Ltd., London, 1966.
(16) "Index of Mass Spectral Data, AMD II," American Society for Testing and Materials, Philadelphia, Pa., 1969.

SEQ = 21 UNKNOWN ID = 630 ISO-AMYL ACETATE (B630) C7.H14.02. MOLWT = 130 MOLWT RANGE SEARCHED = 69 TO 1000 PEAKS = 11
0/1 TRANSITION = 1.250 PCT TOTAL ION CURRENT

HI MASS PK = 87 FIVE HIGHEST INTENSITY PKS = 43 55 41 70 39

RESTRICTIONS ON SEARCH
BASE PEAK OF UNKNOWN IN TOP FIVE OF LIBRARY
BASE PEAK OF LIBRARY IN TOP FIVE PEAKS OF UNKNOWN
MIN MOLWT LIB.GE. 0.8 * HIGHEST MASS PEAK UNKNOWN

INPUT MASSES.GT. TRANSITION =
39 41 42 43 55 57 61 69 70 73 87

NO.	NDIS	SEQ	CMPD NAME	MOLWT	MOLION	BASE	SECD	THRD	FOURTH	FIFTH	SIXTH
1	7	550	ISOAMYL-ACETATE	130	130.	43.	70.	55.	42.	61.	41.
2	9	3034	N-AMYL ACETATE 4CE	130	131.	43.	70.	42.	55.	27.	15.
3	9	2049	N AMYL ACETATE	130	131.	43.	70.	42.	55.	27.	15.
4	10	2088	N HEPTYL ACETATE	158	117.	43.	56.	70.	41.	55.	61.
5	10	3700	N-HEPTYL ACETATE	158	117.	43.	56.	70.	41.	55.	61.
6	12	551	N-AMYL-ACETATE	130	117.	43.	70.	61.	42.	55.	73.
7	15	5726	NOR-TETRADECANE	198	205.	43.	57.	41.	71.	85.	55.
8	15	5789	NOR-PENTADECANE	212	215.	43.	57.	41.	71.	85.	55.
9	15	5790	NOR-HEXADECANE	226	229.	43.	57.	41.	71.	85.	55.
10	16	5499	NOR-DODECANE	170	172.	43.	57.	41.	71.	85.	55.

SPECIFIC CMPDS DESIRED = 3
3035 ISOAMYL ACETATE 16
2046 ISOAMYL ACETATE 16
550 ISOAMYL-ACETATE 7

HISTOGRAM OF DISAGREEMENTS =

0	1	2	3	4	5	6	7	8	9	10	11	12	13	14	15	16	17	18	19	20	21	22	23	24	25
0	0	0	0	0	0	0	1	0	2	2	0	1	0	0	3	11	19	14	19	30	38	45	30	27	36

26	27	28	29	30	31	32	33	34	35	36	37	38	39	40	41	42	43	44	45	46	47	48	49	50
37	36	32	34	47	27	35	23	33	28	14	18	24	15	8	9	7	7	19	10	5	7	3	3	0

MU USED IN SEARCH = 3

Figure 1. Typical printout from search program

Table II. Characteristics of the 125 Compounds Used as Unknowns

	Source reference				
	(*10*)	(*11*)	(*12*)	(*13*)	(*14*)
Total spectra used	28	25	20	34	18
Minimum molecular weight	73	58	112	57	68
Average molecular weight	117	125	158	104	111
Maximum molecular weight	176	210	256	197	234

Two preconditions were imposed on these data before selection. Only spectra of compounds (or close isomers) known to be in the library were included; the library spectrum corresponding to a given unknown had to have a significant peak (>20% base) at the mass of the unknown's base peak. This condition provides some assurance that obviously incorrect spectra are not considered.

Matching Results—General Procedure. For each type of encoding, each of the 125 unknowns was compared against the library of 6880 spectra. For each criterion of disagreement, two modes of searching were employed: Unrestricted search—*all* members of the library were compared; and filtered search—only library members satisfying certain spectral preconditions were considered.

The filtering preconditions used in this study were:

1. The mass corresponding to the maximum intensity peak (base peak) of the unknown must be among the 5 highest peaks of the library member.
2. The mass of the base peak of the library member must be among the 5 highest peaks of the unknown.
3. The molecular weight of the library member must be greater than an arbitrary specified fraction (generally, 0.7) of the mass of the highest unknown peak with an intensity greater than 0.5% of the total ion current.

Conditions 1 and 2 require that both the library and unknown spectra have significant peaks at the mass of the base peak. Knock *et al.* (*7*) used similar prefiltering conditions with the top 6 peaks. Hites and Biemann (*3*) required that the base peak in the unknown correspond to a peak of at least 25% intensity in the library, and vice versa. For the library used here, the distribution of the average % base peak corresponding to the *N*th most intense peak is presented in Figure 2. The average height of the 5th highest peak is 26.6% base peak and the 6th is 22.1% base. On the average, for the library used here a threshold of 20% of the base peak would require about 6.3 masses to be stored for each library member.

Condition 3 removes lower molecular weight compounds from consideration. One potential danger of imposing this condition is that if significant higher molecular weight impurities are present, the prefiltering might restrict the search to too high a minimum molecular weight. However, it is not as stringent a requirement as that imposed by Knock *et al.* (*7*) who generally assumed that the molecular weight was known and searched in a narrow range ($<\pm 3$ amu) about the molecular weight.

The filtered search served two important functions. Search speeds were generally increased by about a factor of 2–3 by employing prefiltering, and many compounds which would

otherwise fall in the ten best list were removed, making spectral identification much less ambiguous. The consequences of the second factor will be particularly evident from later discussions.

The major disadvantage of prefiltering is that the true compound may be excluded from consideration if the preconditions imposed are too stringent. The advantages cited above must be clearly weighed against this liability in any particular application. For example, filtering conditions 1 and 2 were responsible for about three quarters of the recognition improvement found using filtering. Therefore, in cases where higher molecular weight impurities are likely, the additional slight improvement obtained by imposing condition 3 may not be worth the risk of missing the true compound.

In the search programs used here, the choice of unrestricted or restricted search is governed by data input. A simple parameter modification is required to select any combination of the above prefiltering conditions.

The recognition performance of a particular matching procedure is measured here in terms of compound "confusion." For a given unknown, the "confusion" is defined as the number of different library compounds found (after prefiltering, if required) which yield a value of the disagreement criterion which is less than or equal to that of the correct answer. In essence, the confusion is the number of different incorrect compounds which would have to be considered to also include the correct answer. One practical difficulty occurs in the determination of this quantity: namely, the multiplicity of isomers in the library. The convention adopted here is the close isomers (for example, *o*, *m*, *p*, di-substituted benzenes), are considered as one compound in determining spectral confusion.

One-Bit Encoding. In one-bit encoding of peak height, it is assumed that at a given nominal mass, one knows only whether or not a peak is present with an intensity above a specified threshold. One-bit encoding was investigated in an earlier study (*17*) in terms of special pattern uniqueness. It was found that spectra encoded to one bit were highly specific chemical signatures. Similar results were observed in a study using the "learning machine" approach (*18*). These results imply that this minimal encoding might prove sufficient for identification purposes.

There are several advantages which make one-bit encoding worthy of study:

1. Since one-bit encoding permits highly efficient packing: (a) Computer memory requirements are minimized; (b) the amount of data required to represent the library is minimized. (Reading the library into core may be the time determining factor for the search); (c) parallel processing (see below) is possible and search speeds are much higher than conventional channel by channel serial comparisons.
2. In a more theoretical sense, a better understanding of the simplest one-bit case may shed valuable insights on the more complex multi-bit situation.

One important question is: "Where should the transition between level '0' and '1' be set in channel *i*?" For simplicity, in the present study it was assumed that all transitions between levels (for both the one-bit and multi-bit cases) were constant, independent of mass. As was pointed out earlier (*17*), this may not be the optimal setting for identification purposes. Additionally, in all work reported here only contiguous mass ranges were considered, generally from mass 12 to about mass 200–300. Again, significant degrees of data compression might be achieved by considering only particular channels in a given application.

A second question arises, "Should the transition levels be determined in terms of the total ion current (*i.e.*, the sum of all of the peak heights) or in terms of the base peak alone?"

To facilitate examining the second question for the one-bit case, two library tapes were prepared, one with the transition set as a function of the total ion current, the other as a function of the base peak. On each tape, five different libraries were prepared corresponding to transitions of 0.0025, 0.25, 0.50, 1.25, 2.5% of the total ion current and 0.01, 1, 2, 5, 10% of the base peak. By the use of the appropriate tape and input data, any one of the 10 different transition conditions could be examined.

To greatly increase comparison speeds, all one-bit spectra were packed into computer words. Since the word size of the IBM-360 system is 32 bits, 32 masses could be accommodated in each word. In all cases of one-bit encoding, each spectrum was stored in 10 computer words, covering a mass range of 12–331.

Matching Criteria for the One-Bit Case. For a linear criterion such as Equation 1, it is useful to consider the individual channel functions, $F(x_i, l_{ij})$, in terms of a Boolean "truth table" (See Table III). If, for example, the unknown spectrum has $x_i = 1$ in channel i and the jth library member has $l_{ij} = 0$, for this truth table, the incremental value of the criterion for the channel is = 1.

In previous work (*6*) a truth table corresponding to the logical "exclusive or" function (XOR) was utilized (Table III). In this table, the incremental value of the criterion is

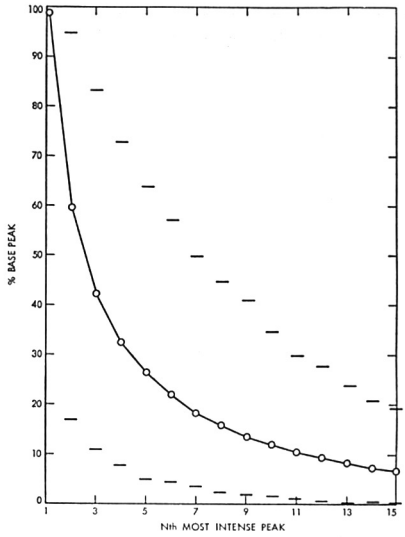

Figure 2. Distribution of the average % base peak corresponding to the *N*th most intense peak

○ Average value
— Bar denotes range which includes 90% of library

(17) S. L. Grotch, ANAL. CHEM., **42**, 1214 (1970).
(18) P. Jurs, B. R. Kowalski, T. L. Isenhour, and C. N. Reilley, *ibid.*, **41**, 690 (1969).

Table III. Logical XOR Truth Table

x_i \ l_{ij}	0	1
0	0	1
1	1	0

Table IV. Logical AND Truth Table

x_i \ l_{ij}	0	1
0	0	0
1	0	1

Table V. Logical Truth Table for Function XOR $-$ μ(AND)

x_i \ l_{ij}	0	1
0	0	1
1	1	$-\mu$

unity when the two spectra disagree in a channel and zero otherwise. Since this is a disagreement criterion, the "best" spectral matches are those minimizing the value of this criterion.

A closer inspection of the XOR truth table reveals a potential deficiency of this function, namely, that the condition $x_i = l_{ij} = 0$ is equivalent to the condition $x_i = l_{ij} = 1$. That is, in terms of this matching criterion, the condition when both spectra have a peak in the same channel is considered no more significant than when neither has a peak at a given channel.

From an intuitive knowledge of the matching process, it seems obvious that some additional weighting should be given to the situation where both spectra have a peak in contrast to that where neither does. This can conveniently be done by also considering the logical AND process (see Table IV). Here the incremental value of the criterion is unity only when both spectra have a peak in a given channel.

If the AND process is weighted relative to the XOR by a value of $-\mu$, the two criteria may be combined linearly as: (XOR) $-$ μ(AND). A negative weight is used since in a single minimization criterion we want to minimize disagreements *minus* agreements. From the truth table for the process (Table V) it can be seen that wherever the spectra disagree in a channel a liability of $+1$ accrues, where they both have a peak, the liability is reduced by μ, and where neither has a peak there is no effect on the criterion. For convenience, to ensure that the minimum value of the criterion is zero, an offset of μN is added. [N is the number of peaks (ones) in the unknown.] The criterion which is minimized becomes:

$$C = \mu N + \sum_{i=1}^{i=M} [(\mathrm{XOR})_i - \mu(\mathrm{AND})_i] \qquad (7)$$

Note that $C = 0$ only if a perfect match occurs, since in this case ΣXOR $= 0$ and ΣAND $= N$. Also, if $\mu = 0$ the criterion is solely the XOR, and as $\mu \to \infty$ the criterion tends to the AND function.

What value of μ should be used to "optimize" the one-bit matching process? "Optimize" is used here to mean the maximum separation of the value of the criterion for the correct answer from the remainder of the library. It has been found experimentally, that the optimum value of μ is close to that value which yields, on the average, for a given unknown, equal contributions to the criterion from XOR and (N-AND). That is, the optimum $\mu = \mu^*$ occurs when:

$$\overline{X} = \frac{1}{L}\sum_{j=1}^{L}\sum_{i=1}^{M}(\mathrm{XOR})_i \qquad (8)$$

$$\overline{A} = \frac{1}{L}\sum_{j=1}^{L}\sum_{i=1}^{M}(\mathrm{AND})_i \qquad (9)$$

$$\mu^* = \overline{X}/(N - \overline{A}) \qquad (10)$$

For a given unknown, $\overline{X}$ and $\overline{A}$ are the summed values of the XOR and AND criteria, respectively averaged over the entire library. In the double sums, the j index runs over the L library members, the i index over the range of M channels investigated.

It is a simple matter to calculate $\overline{X}$ and $\overline{A}$, a priori, knowing the probabilities of occurrence of a "1" in a given channel for the library. (These probabilities are, of course, a function of the 0/1 transition chosen.) If for the library, p_i is the probability that channel i contains a "1," and x_i is the value ($=0$ or 1) in the ith channel of the unknown

$$\overline{X} = \sum_i (x_i + p_i - 2p_ix_i) \qquad (11)$$

$$\overline{A} = \sum p_ix_i \qquad (12)$$

If Equation 10 holds, the optimum μ is calculated as:

$$\mu^* = 1 + \frac{\sum p_i(1 - x_i)}{\sum x_i(1 - p_i)} \qquad (13)$$

Since both numerator and denominator in Equation 13 are positive, $\mu^* \geq 1$.

For the 6880 compound library, the average value of μ^* for the entire library compared against itself is approximately 2.1–2.4 depending on the 0/1 transition chosen. In essence $\mu^* = 2$ implies that the condition $l_{ij} = x_i = 1$ should be weighted twice as heavily as the condition $l_{ij} \neq x_i$.

In the one bit case with the IBM-360 computer, 32 channels are packed into each computer word. By employing the XOR and AND operations on a word basis, it is possible to achieve parallel processing (*i.e. simultaneous* channel by channel comparisons) on the essentially serial digital computer. (See Ref. *17*, p 1217.) Because of this factor, extremely rapid search speeds can be achieved.

One-Bit Matching Results. In the one-bit case, the unknowns were compared against the library while varying the following factors:

1. The transition between level "0" and level "1." The normalization is either in terms of the % base peak (0.01, 1, 2, 5, 10) or the % total ion current (0.0025, 0.25, 0.5, 1.25, 2.5)
2. Weighting factor μ in the generalized criterion of disagreement (Equation 7)
3. Prefiltering (conditions 1–3 described above)

In all cases a maximum of 320 channels (10 computer words) was considered, covering a nominal mass range of 12–331. (To further speed calculations, the actual XOR and AND calculations need only be carried out for computer word pairs which are non-zero. Thus, the actual mass range calculated in a given match will frequently be less than this maximum.)

Typically, using the IBM-360/44, a complete search of the library (with prefiltering) required about 15–20 sec for one unknown per pass and about 2 minutes for 30 unknowns. For one unknown per pass, the rate limiting process is the tape reading speed entering the library into core.

The effects of factors 2 and 3 above are shown in Table VI for a constant 0/1 transition set at 1.25% of the total ion current. The results are expressed as the percentage of unknowns which were identified with a "confusion" less than or equal to a specific value. ["Confusion" is defined as the number of library compounds (excluding the unknown) which had a criterion of disagreement as good as or better than the correct answer.] In the last column the results are given for the "optimum" μ^* calculated for each unknown using Equation 13.

In the unrestricted search (no prefiltering at all), it can be seen that if, for each unknown, the "optimum" μ^* is used in Equation 7, approximately two thirds of the unknowns are identified as the *unique best answer*. If a confusion of up to 5 compounds is permitted, about 83% of the unknowns are identified. With prefiltering, about 70% of the compounds are identified uniquely, and about 94% have a confusion of less than 5 compounds.

Knock *et al.* (*7*) frequently imposed a much more stringent prefiltering condition than 3 above—namely, that the molecular weight of the unknown is known and that the search considers only library members within ±3 masses of this value. If this prefiltering condition is imposed here (as well as prefiltering conditions 1 and 2) *all* compounds are identified within a confusion of 3. It is felt, however, that in many cases the molecular weight will not be known and that this prefiltering is too restrictive. Obviously, if the unknown molecular weight is known, the search job is far simpler.

It can be seen that the effect of μ is significant, but that the maximum reliability of identification occurs over a rather broad range of μ. Values of μ from 2 to 3 were found to generally yield the best results. This agrees well with the average value found from Equation 13 for the entire library ($\mu^* = 2.1$). Similar results were obtained at other transitions. For simplicity, therefore, it may be unnecessary to optimize μ for each unknown, but use an average value of about 2 to 3. It may be seen that the AND process alone ($\mu = \infty$) results in significantly poorer recognition performance than even the XOR alone ($\mu = 0$).

The effect of the 0/1 transition level on these results was less significant than had been anticipated. Comparable performance to that presented in Table VI was observed for transitions from 0.25–2.5% of the total ion current.

The results obtained using very low transitions (0.01% of the base peak or 0.0025% of the total ion current) were significantly poorer than those presented in Table VI. This is due to several factors. Some of the unknown spectral data were transcribed from small plots, and the intensity of peaks below about 5% of the base peak is very uncertain. The library itself contains much variability in the reporting of low intensity peaks. The influence of noise is, of course, much more significant as the transition level is lowered.

It was observed that, for the same average number of peaks in the library, normalization in terms of the per cent total ion current gave slightly better results than normalization in terms of the base peak. The sample size used in this work was too small to draw a definite conclusion on this point. It does, however, seem reasonable that % ion current is likely to be more reproducible, since normalization here is in terms of the sum of many peaks, rather than the single highest intensity peak as for base peak normalization.

Table VI. Effects of μ and Prefiltering

Unrestricted search	% of Compound with Confusion $\leq C_o$				
Confusion = C_o	$\mu = 0$	$\mu = 3$	$\mu = 6$	$\mu = \infty$	$\mu = \mu^*$
0	53.6	64.8	59.8	30.4	65.6
1	68.0	76.0	73.6	47.2	76.0
5	79.2	82.4	84.0	65.6	83.2
10	82.4	86.4	86.4	70.4	86.4
Restricted search Confusion = C_o					
0	67.2	70.4	69.6	45.6	68.8
1	81.6	79.2	80.0	63.2	81.6
5	93.6	95.2	91.2	76.0	94.4
10	96.8	99.2	95.2	85.6	97.6

It is interesting to examine in more detail those cases in which the restricted search did *not* yield the correct answer with a confusion of 5 compounds or less. For a 0/1 transition of 1.25% of the total ion current and $\mu = 3$, of the 125 unknowns only 6 compounds (4.8%) had a confusion greater than 5. (Only one compound was not in the top 10.)

These 6 unknowns are shown in Figure 3 with the top 5 library compounds identified as the best choices. In many cases the incorrect answers would yield a mass spectrum close to that of the true unknown and the confusion observed is not surprising. The point to be made is that even in the rare cases when the correct answer is not obtained in the one-bit search, a close structural match is likely to be found. This result also indicates that one-bit encoding would not be sufficient to distinguish close structures by their mass spectra alone. This, too, is not surprising considering that one-bit encoding throws away virtually all intensity information in the spectrum.

Three-Bit Encoding. In 3-bit encoding, peak height is assumed known to one of 8 levels (0–7). To achieve high comparison rates, the packing scheme employed here utilized an extra bit for each channel, or 4 bits for each mass. (See Appendix for details.) In the IBM-360 system, 8 channels could be packed into each computer word (instead of the 32 for one-bit encoding).

The criterion used was that of Equation 6: the sum of the absolute differences in levels over the mass range desired. Twenty-nine computer words, covering a maximum mass range of 12–243, were used to encode each spectrum in this work.

The transitions between levels were set logarithmically at 0.5, 1, 2, 4, 8, 16, and 32% of the total ion current. The logarithmic scale followed the results of earlier work (*19*) which indicated that the peak heights of mass spectra were distributed log-normally. By choosing a logarithmic scale, roughly equal numbers of peaks will fall in each level and hence the independent channel information entropy (*17*) will be maximized. Jurs (*20*) also observed in his work with learning machines that the logarithmic transformation optimized his separations. In any case, comparisons with other transition settings (for example, linear in % total ion current) indicated that the selected scale gave significantly better results.

(19) S. L. Grotch, 17th Annual Conference on Mass Spectrometry and Allied Topics, Dallas, Texas, May 1969.
(20) P. Jurs, ANAL. CHEM., **43**, 22 (1971).

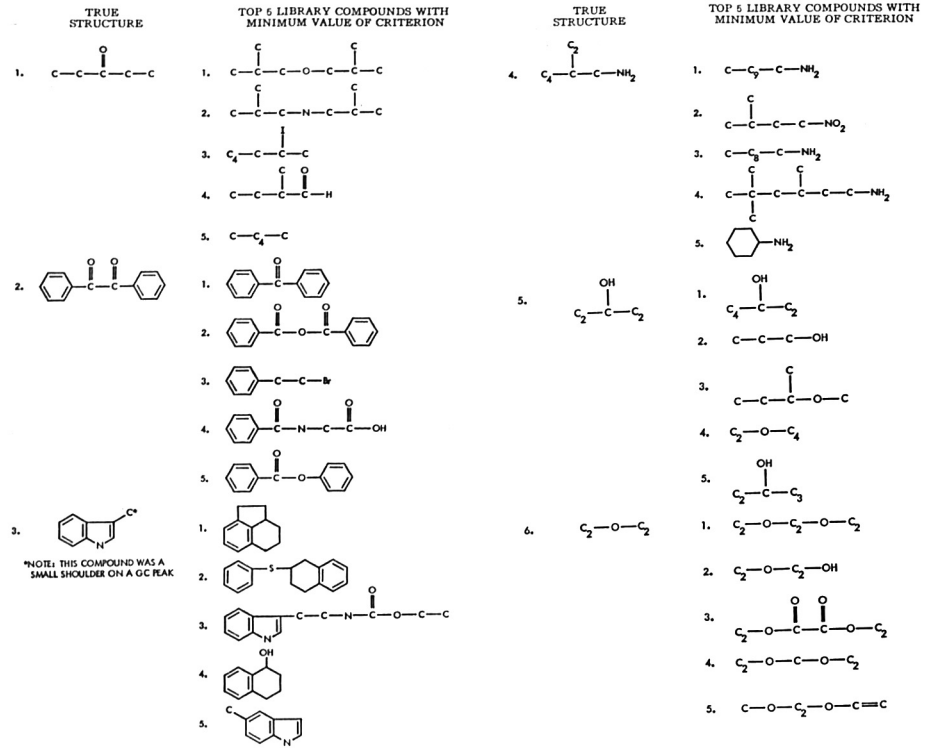

Figure 3. Compounds not in the top 5 for the restricted one-bit search
(Transition = 1.25% total ion current, $\mu = 3$)

Table VII. Comparison of One-Bit, Three-Bit, 32-Bit, and Top 20 Results

Unrestricted search Confusion = C_o	% of Compounds with Confusion $\leq C_o$			
	1 Bit ($\mu = 3$)	3 Bits	32 Bits	Top 20 *vs.* Top 20
0	64.8	73.6	80.8	48.0
1	76.0	84.0	88.0	54.2
5	82.4	91.2	96.0	71.2
10	86.4	93.6	97.6	77.6
Restricted search Confusion = C_o				
0	70.4	80.8	84.0	60.0
1	79.2	88.0	94.4	71.2
5	95.2	97.6	98.4	85.6
10	99.2	100.0	99.2	92.0

The results of three-bit encoding for unrestricted and restricted searches are presented in Table VII where they are compared with the results for the other techniques. In the restricted three-bit search, 81% of the compounds are identified uniquely and *all* 125 compounds are found in the top 10 list.

As would be expected, three-bit encoding yields improved recognition performance when compared with the one-bit case. However, this improvement is achieved at the expense of increased storage requirements and slower search speeds (about a factor of 3 with the system used here).

This is a typical example of the tradeoffs which will occur in any application of these techniques. If, for example, the data input for the library is rate determining (as is likely if only one unknown is searched at a time), the three-bit search will take approximately 4 times as long as one bit. Whether this increased time is intolerable will depend on the application and the absolute values of the search times.

Encoding to 10^4 Levels. The spectra in the library have peak heights reported from a minimum of 0.01% base peak to a maximum of 100% in increments of 0.01%. Thus, a maximum of 10^4 levels ($\sim$13 bits) exists. To compare the previous results with the spectra in which peak height is not reduced in information content, a program was developed using the full intensity range stored in 32 bits (1 amu/computer word).

The level transitions were set linear in either % base peak or % total ion current. The recognition performance found for normalization in terms of the % total ion current was only slightly better than that using % base peak. The same maximum mass range as the one bit case was used (amu = 12–231).

The results of these calculations are presented in Table VII. It can be seen that, particularly for the unique best answer,

full encoding generally gives better results than any of the other techniques. Interestingly, however, in the restricted search, three-bit encoding correctly identified all compounds, in the top 10, whereas the full encoding missed one.

Once again this improved accuracy is achieved at a price—much slower search speeds and greatly increased data input. For the programs developed here, the search rates in this case were about an order of magnitude slower than for the one-bit case.

Coincidences in the Top N Peaks. Using the same program structure as described above, the algorithm of Equation 5 was developed into a computer program. In this case, the search is for those library members which yield the maximum number of coincidences in the N most intense peaks. Five different libraries (corresponding to the top 4, 8, 12, 16, 20 peaks) were stored on a single magnetic tape.

Each spectrum was encoded in the same manner as in the one-bit case (*e.g.*, 10 computer words covering a mass range of 12–331). Here, however, each member of the top N peak library had N "ones" scattered through the 320 bits representing each spectrum. (In the one-bit encoding scheme, a variable number of ones was found in any spectrum.)

By means of data input it was possible to compare the top N_1 peaks of the unknown with the top N_2 peaks of the library. Although it was not necessary that $N_1 = N_2$, it was generally found that this made little difference in performance and so only cases where $N_1 = N_2$ were extensively examined. Investigations were made for $N_1 = N_2 = 4$, 8, and 20.

The results of this technique are compared with the other methods in Table VII for $N_1 = N_2 = 20$. The performance here is significantly poorer than any of the other techniques. Results for $N_1 = N_2 = 8$ were comparable to that of $N = 20$, whereas those for $N = 4$ were decidedly poorer. Since the computer requirements and search speeds using this method are comparable to one-bit encoding, there seems little reason to utilize this technique in preference to the one-bit case.

It should be noted that here all top N peaks are assumed equivalent and no distinction is made of their relative ranking. Knock *et al.* (7) found that introducing relative ranking improved the recognition performance. However, it does not appear that the parallel processing advantages (and attendant high search speeds) can be easily implemented if relative ranking is included.

CONCLUSIONS

The criterion of the sum of the absolute differences in levels proved to be remarkably effective for identifying low resolution mass spectra even when peak height was encoded to 1 or 3 bits. These algorithms could be implemented as computer programs yielding extremely rapid search speeds because of parallel processing devices employed. Results using the maximum coincidence of the top N peaks were significantly poorer than the other techniques. Prefiltering of the library before comparison had significantly beneficial effects on both search speeds and recognition performance.

Because of minimal computer requirements, rapid search speeds, and high reliability of identification, one-bit encoding may prove economically attractive in certain applications.

Further details regarding these computer programs may be obtained by contacting the author.

APPENDIX

Computer Program Details. Packing for 3-Bit Encoding. The 3-bit spectra were packed as shown symbolically in Figure 4. Note that an extra bit is inserted in front of each 3-bit peak height. This bit is always "1" for the library and always "0" for the unknown. The three bits of the library channel are placed in positions L_1, L_2, L_3 and the corresponding 3 bits of the unknown are stored in X_1, X_2, X_3.

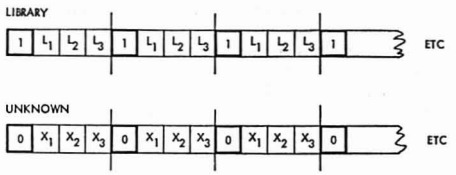

Figure 4. Packing for 3-bit encoding

The function of this leading bit is to ensure that if the unknown coded word is subtracted (in binary) from the library coded word, each 4-bit grouping will always have a positive value—*i.e.*, there will be no interactions (carry over) between groups. By this artifice it is possible to subtract 8 channels with one instruction. The resultant absolute difference is determined by a table lookup of each grouping of 8 bits.

The procedure can be readily implemented at extremely rapid speeds. For the IBM 360/44 computer, the summed absolute differences covering the full mass range 12–243 (29 words) can be calculated in about 1 millisecond. Since the actual mass range examined is generally less than the maximum the actual attainable speeds are even higher than this.

Factors for Increasing Calculation Speed. The majority of the time in the search is spent in the calculation of the disagreement criterion. These calculations may be made significantly faster by employing the following two devices: (1) In the calculation of AND, contributions to the criterion will only arise when *both* the library member and the unknown have non-zero codes in a given word. For XOR, if both words are zero, there is no point in even comparing the words since no contribution is added. If, in the library data the value of the maximum non-zero word is stored, it is possible to determine what upper range should be examined for any unknown. (2) As the search through the library proceeds, a record is maintained of the ten compounds with the least number of disagreements. If, as a given comparison is being made, the value of the disagreement criterion exceeds the 10th best member in the list for that unknown, the particular comparison is terminated since it is obvious that this library member cannot be in the top 10 list.

Information in Final Printout. A typical printout of the list of the top ten compounds is given in Figure 1. In addition to information supplied by the user regarding the unknown (identifying name, masses at which peaks are present, etc.) the printout consists of three major sections.

(1) The top 10 list sorted in increasing order of the value of the criterion (NDIS) and containing for each library member: name, identifying accession number, molecular weight, masses of the five highest peaks, highest mass ion. This information is contained on the library tape and is added to the list as the search proceeds. The information is of great value in further narrowing the choice of a correct answer.

(2) The user may enter with the unknown data up to five identifying accession numbers for compounds in the library. The calculated value of the disagreement criterion will be displayed for these library members even if they do not satisfy the prefiltering condition or fall in the top ten list. This feature is

useful if the user wishes to have the unknown compared to specific library compounds.

(3) A histogram is also presented for each unknown of the number of library compounds which yielded a given value of the disagreement criterion. These compounds satisfy any prefiltering conditions and have been calculated over the requisite mass range. (Compounds which have been rejected because the disagreement criterion exceeded the 10th best member are not included in the histogram.) This feature is particularly useful in determining the distribution of the disagreement criterion beyond the top ten list.

RECEIVED for review March 15, 1971. Accepted June 2, 1971. The work regarding one-bit encoding was presented at the 18th Annual Conference on Mass Spectrometry and Allied Topics, San Francisco, Calif, June 1970. The remainder of the work was presented at the 19th Annual Conference on Mass Spectrometry and Allied Topics, Atlanta, Ga., May 1971. This paper presents the results of one phase of research carried out at the Jet Propulsion Laboratory, California Institute of Technology, under Contract No. NAS 7-100, sponsored by the National Aeronautics and Space Administration.

Effect of pH and Ionic Strength on Ion Exchange and Chelating Properties of an Iminodiacetate Ion Exchange Resin with Alkaline Earth Ions

George H. Luttrell, Jr.,[1] Carl More,[2] and Charles T. Kenner

Department of Chemistry, Southern Methodist University, Dallas, Texas 75222

By using a column procedure, the iminodiacetate resin is shown to react with the alkaline earth ions primarily by simple ion exchange at pH values below 4 and by chelation at pH values above 6. Between these values, both mechanisms take place. The volume to the elution peak maxima (V_{max}), which is a function of the distribution coefficient, is affected by both pH and ionic strength. At ionic strengths above 0.1, log V_{max} passes through a maximum in the pH range of 4.2 to 4.8 and a minima in the range of pH 5.6 to 6.0. The maxima and minima are shifted to lower pH values by increasing ionic strength. Empirical equations are derived from the data by multiple regression techniques on a high-speed digital computer which relate log V_{max} to pH at constant ionic strength and to ionic strength at constant pH.

THE IMINODIACETATE ION EXCHANGE RESIN Dowex A-1 (Chelex 100) has been used for the separation of various metal ions from high ionic strength solutions (*1–4*) and for the concentration of trace constituents (*5*). Leyden and Underwood (*6*) and Sides and Kenner (*7*) studied the effects of pH, ionic strength, and temperature upon the distribution coefficients of alkaline earths and transition metal ions using a batch process. Leyden and Underwood (*6*) noted that the distribution coefficients for alkaline earth ions were not affected greatly by temperature and that the coefficients increased with pH up to pH 4 or 5 at which the distribution coefficients became essentially constant at constant ionic strength. Sides and Kenner (*7*) confirmed this result but found that the distribution coefficients for these ions again increased in the region of pH 7 and above. They also showed that an increase in ionic strength caused a decrease in the coefficients. With transition metal ions, the distribution coefficients increase rapidly to a maximum in the range of pH 4 to 5 and are not further affected by rise in pH or ionic strength (*6, 7*).

Leyden and Underwood (*6*) estimated that the apparent pK values of the resin lie between 2.37 and 3.45 for pK_1 and between 8.15 and 8.58 for pK_2. Krasner and Marinsky (*8*) determined the thermodynamic value of pK_1 to be 2.77. In general, all the reported literature values are in agreement with the reported values for benzyliminodiacetic acid (the monomeric analog of the resin) (*6*) and for iminodiacetic acid (*9*). Lowenschuss and Schmuckler (*10*) have shown the structure of chelated complexes with the resin to be two five-membered rings with a 1:1 molar ratio of metal ion to diacetate group.

The distribution coefficients of metal ions with ion exchange resins are usually determined by the batch method and defined as (*11*)

$$D = \frac{\text{mmoles metal/g resin}}{\text{mmoles metal/ml solution}} \quad (1)$$

However, distribution coefficients can be obtained by a column method and Szidon and Fritz (*12*) define the column distribution coefficient D_v as

$$D_v = (V/Ad) - i \quad (2)$$

in which V is the volume of eluant in milliliters needed to advance the metal band a distance of d (in cm) down a column

[1] Present address, Alcon Laboratories, Ft. Worth, Texas 76134

[2] Present address, Dallas District, Food and Drug Administration, 3032 Bryan, Dallas, Texas 75204

(1) W. I. Childs, Abstracts, 135th National Meeting, American Chemical Society, Boston, Mass., April 1959, p 11L.
(2) L. A. Mattano, *ibid.*, p 11L.
(3) R. L. Olsen *et al.*, *Talanta*, **7**, 187 (1961).
(4) A. J. van der Reyden and R. L. M. van Linger, *Z. Anal. Chem.*, **187**, 241 (1962).
(5) R. Turse and W. Rieman III, *Anal. Chim. Act*, **24**, 202 (1961).
(6) Donald Leyden and A. L. Underwood, *J. Phys. Chem.*, **68**, 2093 (1964).
(7) Jerry Sides and C. T. Kenner, ANAL. CHEM., **38**, 707 (1966).
(8) J. K. Krasner and J. A. Marinsky, *J. Phys. Chem.*, **67**, 2529 (1963).
(9) S. Chaberek, Jr., and A. E. Martell, *J. Amer. Chem. Soc.*, **74**, 5052 (1952).
(10) H. Loewnschuss and G. Schmuckler, *Talanta*, **11**, 1399 (1964).
(11) Robert Kunin, "Ion Exchange Resins," Wiley, New York, N. Y., 1950, p 30.
(12) R. E. Szidon and J. S. Fritz, *U. S. At. Energy Comm. Rept.*, **IS-340**, May 1961.

with cross section area A (in cm²) and interstitial volume i. The column distribution coefficient is a function of the eluant volume (V_{max}) utilized to drive the maximum concentration from the bottom of the column and is related to the batch method coefficient D by

$$D_v = D\rho \quad (3)$$

where ρ is the density of the resin bed. V_{max} is related to D and D_v by the expression

$$D = D_v/\rho = [(V_{max}/Ad) - i]/\rho \quad (4)$$

The present study reports an investigation of the variation of maximum elution volumes for alkaline earth metals with pH and ionic strength. The results indicate that simple ion exchange occurs at low pH values, that chelation probably occurs at high pH values, and that both ion exchange and chelation probably occur in competition with each other at intermediate pH values. The results also substantiate previously reported apparent pK_1 values and the two five-membered ring structure.

EXPERIMENTAL

Reagents. Primary standard $CaCO_3$ and ACS reagent grade $MgSO_4 \cdot 7H_2O$ were used to prepare the Ca^{2+} and Mg^{2+} standard solutions. The Dowex A-1 resin (Chelex 100, 50–100 mesh) was supplied by Bio-Rad Laboratories as reagent quality in the sodium form. All other chemicals used were ACS reagent grade quality. Lanthanum oxide, Code 529 (American Potash and Chemical Co.) was used to prepare 5% (w/v) $LaCl_3$ in 25% (v/v) HCl. Deionized water was used in all procedures.

Buffers and Stock Solutions. The Clarke and Lubs buffers (*13*) were used for solutions for which the pH value was less than 5.9. For higher pH values, a buffer utilizing tris-(hydroxymethyl)aminomethane was used (*14*). In all cases the desired ionic strengths were maintained by addition of the proper amount of sodium chloride. The standard cation solutions for introduction onto the column and for the standard atomic absorption calibration curve were prepared in each case with the same pH and ionic strength as the eluent buffer.

Apparatus. The data for ionic strengths of one and below which were used to derive the mathematical relationships were obtained using an automatic fraction collector (Micro Chemical Specialty Co., No. 651) to collect various volumes of effluent from a 1.5-cm i.d. Labcrest column (Sargent No. S18825-30-B). The data for ionic strengths 2 and 3 (and some for ionic strength 1) were obtained using an Ace Glass Co. filter tube, porosity A [No. 7195-02 (1)] with manual collection of 25-ml aliquots. The concentrations of calcium and magnesium in each fraction were determined with a Perkin-Elmer 303 atomic absorption spectrophotometer using the instrumental conditions specified in the Perkin-Elmer Analytical Methods for Atomic Absorption Spectrophotometry (1968) with lanthanum added to suppress the interference due to sodium.

Procedure. The wet sodium form resin was placed in the column to a depth of 2.5 cm (6.3 cm of air-dried resin for ionic strengths 2 and 3) and equilibrated by flow of a buffer solution of the specific pH and ionic strength desired until the pH of the effluent was the same as the buffer. The liquid in the column was adjusted to the height of the resin, and 1.00 ml of solution containing 500 μg of the metal cation was pipetted onto the equilibrated resin (10.00 ml of 0.0500M for ionic strengths 2 and 3). The metal ion was eluted with buffer at a drop rate of one drop per two seconds; volumetric fractions of between 5.0 and 500 ml were collected and, after addition of lanthanum chloride, diluted to a volume satisfactory for analysis by atomic absorption methods.

Regeneration of Resin. The resin was regenerated by passing successively two bed volumes of 2N HCl, four bed volumes of water, two bed volumes of 3M NaOH, and five 10-ml portions of water through the column. After regeneration, the resin was removed from the column for storage in the wet sodium form.

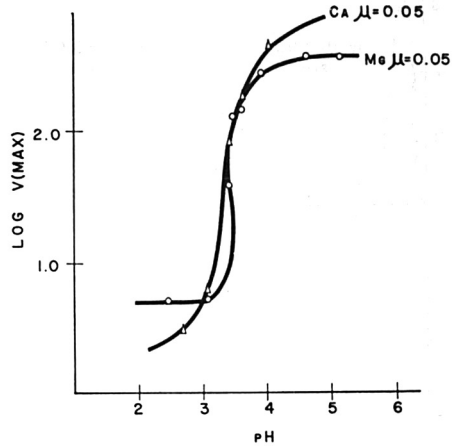

Figure 1. Variation of log V_{max} with pH at low ionic strength

RESULTS AND DISCUSSION

Variation of V_{max} with pH and Ionic Strength. The variation of log V_{max} values with pH at an ionic strength (μ) of 0.05 for calcium and magnesium is shown in Figure 1. The value of log V_{max} increases sharply between a pH of 3 and 4 and becomes constant at approximately 4. These curves are of the same general shape as those showing the variation

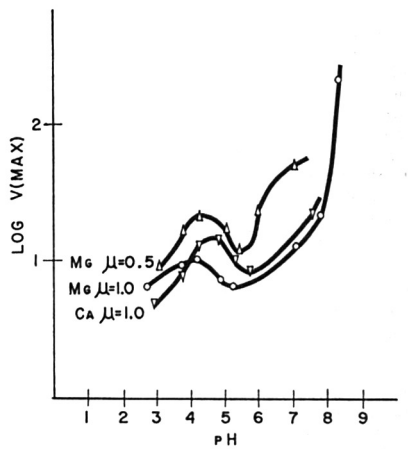

Figure 2. Variation of log V_{max} with pH at high ionic strengths

(13) W. M. Clark and H. Lubs, *J. Biol. Chem.*, **25**, 479 (1916).
(14) R. G. Bates and V. E. Bower, ANAL. CHEM., **28**, 1322 (1956).

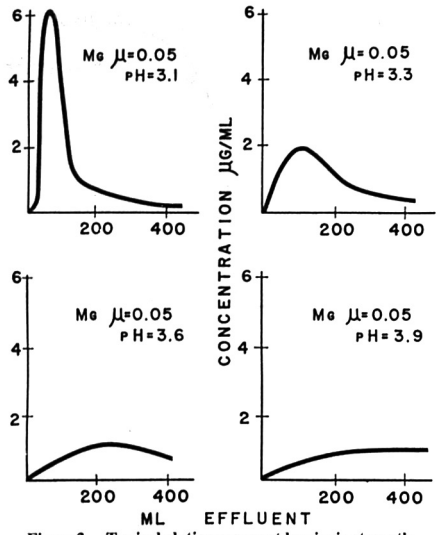

Figure 3. Typical elution curves at low ionic strength

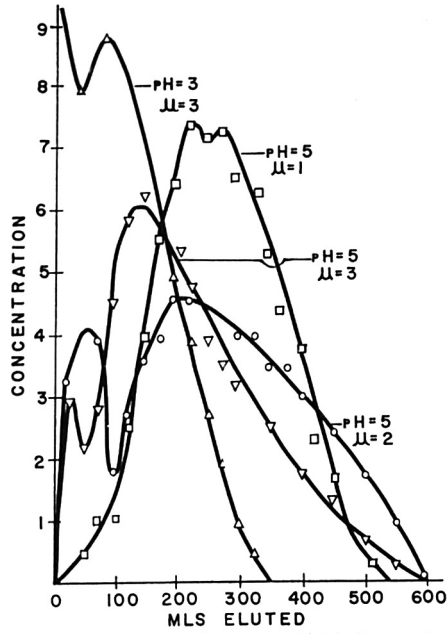

Figure 4. Typical elution curves at high ionic strength

of the distribution coefficients of calcium and magnesium with pH as determined by Leyden and Underwood (*6*) and Sides and Kenner (*7*) by batch methods.

The results of the present investigation differ from the previous results (*7*) at higher ionic strengths in that the variations of the distribution coefficients with pH shown in Figure 2 indicate maximum and minimum values are obtained at approximately pH 4 and 5.8, respectively, rather than an essentially constant value in this pH range.

Elution curves for magnesium at low ionic strength in the ion exchange region below pH 4 are shown in Figure 3. They are generally unsymmetrical and show an increase in the tailing effect and a decrease in the concentration of the metal ion at the elution curve maximum with increasing pH. The tailing effect is more pronounced in the elution curves for calcium than for magnesium since calcium chelates more readily than magnesium. Similar tailing was noted by Turse and Rieman (*5*) who attributed it to slow exchange kinetics within the resin.

The calcium elution curves at higher ionic strength and pH shown in Figure 4 are typical of those obtained with either calcium or magnesium. These curves show two peaks rather than a single peak and the peaks occur at lower eluant volumes as the ionic strength is increased at a given pH or as the pH is decreased at a given ionic strength.

Empirical equations of the form

$$\log V_{max} = A(\mathrm{pH})^3 + B(\mathrm{pH})^2 + C(\mathrm{pH}) + D \qquad (5)$$

derived from the data of Figures 1 and 2 by multiple regression techniques on a high speed digital computer allow calculation of log V_{max} as a function of pH or of molar hydrogen ion concentration at a specified ionic strength. Equation 5 indicates that the total distribution process seems to approximate the algebraic sum of two independent reactions—ion exchange and chelation. Detailed information of the parameters and statistics for the equation derived are given in Table I. The coefficient of multiple correlation (R^2) between the variables for all these equations is above 0.95 and, for all except one, the standard error of the estimate for log V_{max} is less than 0.1. A comparison of the calculated and experimental results is given in Table II.

At constant pH, the values of log V_{max} for calcium and magnesium decrease with increasing ionic strength as shown in Figure 5. The effect of ionic strength on the distribution

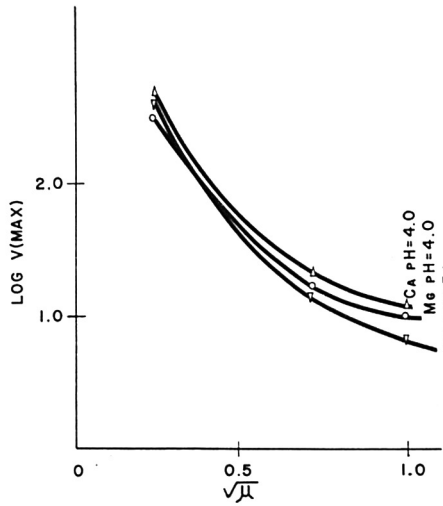

Figure 5. Variation of log V_{max} with ionic strength

Table I. Constants for Predicting Log V_{max} at a Given pH at a Specific μ

A. $\log V_{max} = A(pH)^3 + B(pH)^2 + C(pH) + D$

Metal	A	B	C	D	Coef. of multiple correlation, R^2
Mg, μ = 1.0	0.0443	−0.650	3.06	−3.69	0.9755
Mg, μ = 0.5	0.0667	−1.01	4.92	−6.58	0.9575
Ca, μ = 1.0	−0.110	1.20	−3.98	4.82	0.9851
Ca, μ = 0.5	−0.121	1.25	−3.72	4.01	0.9547

B. $\log V_{max} = A(H^+)^3 + B(H^+)^2 + C(H^+) + D$

Mg, μ = 0.05	6.09×10^8	-1.62×10^6	-1.62×10^3	2.67	0.9868
Ca, μ = 0.05	1.25×10^9	-2.27×10^6	-1.64×10^3	2.82	0.9996

Table II. Calculated and Experimental Values of Log V_{max} as a Function of pH at a Definite μ

Magnesium				Calcium			
	Log V_{max}				Log V_{max}		
pH	Obsd	Calcd	Difference	pH	Obsd	Calcd	Difference
	μ = 1.0				μ = 1.0		
2.85	0.778	0.772	0.006	2.90	0.653	0.651	0.002
3.70	0.954	0.969	−0.015	3.70	0.875	0.888	0.013
4.10	1.00	0.972	0.028	4.10	1.02	1.01	0.010
4.80	0.875	0.908	−0.033	4.80	1.12	1.09	0.030
5.20	0.813	0.859	−0.046	5.20	0.929	0.973	−0.044
5.60	0.875	0.824	0.051	5.70	0.602	0.589	0.013
7.05	1.18	1.07	0.11				
7.68	1.35	1.51	−0.16		μ = 0.50		
8.30	2.28	2.22	0.06	2.50	0.644	0.604	0.039
	μ = 0.50			3.00	0.699	0.793	−0.094
3.00	0.903	0.908	−0.004	3.80	1.30	1.22	0.08
3.80	1.22	1.22	0.00	4.20	1.40	1.39	0.01
4.20	1.26	1.24	0.01	4.95	1.43	1.43	0.00
4.95	1.18	1.16	0.02	5.30	1.18	1.26	−0.08
5.30	1.04	1.11	−0.07	5.55	1.10	1.04	0.06
5.90	1.10	1.05	0.05				
7.10	1.40	1.40	0.00		μ = 0.05		
	μ = 0.05			2.70	0.398	0.398	0.00
2.50	0.653	0.653	0.00	3.10	0.699	0.703	0.004
3.10	0.699	0.671	0.028	3.40	1.90	1.88	0.02
3.40	1.60	1.81	−0.21	3.64	2.31	2.34	−0.03
3.50	2.15	2.02	0.13	4.07	2.68	2.67	0.01
3.60	2.22	2.17	0.05				
3.90	2.51	2.44	0.07				
4.60	2.63	2.63	0.00				
5.10	2.63	2.66	−0.03				
6.00	2.63	2.67	−0.04				

Table III. Log V_{max} as a Function of Ionic Strength (μ): Coefficients of Equation

$\log V_{max} = a\mu + b\sqrt{\mu} + c$

Metal	pH	a	b	c
Mg	4.00	2.59	−5.14	3.55
Mg	5.10	2.54	−5.43	3.70
Mg	6.00	3.35	−6.26	3.85
Ca	4.00	2.47	−5.14	3.69
Ca	5.00	1.62	−4.15	3.55

coefficients is different at very low ionic strengths than at moderate ionic strengths as is shown by a comparison of the curves in Figures 1 and 2.

Empirical equations of the form

$$\log V_{max} = a\mu + b\sqrt{\mu} + c \qquad (6)$$

where μ is the ionic strength may be derived from the data of Figure 5. Equation 6 is similar to the equation derived by Sides and Kenner (7) for the effect of ionic strength on the distribution coefficients of the alkaline earth metals. The various parameters for the equations representing the data are given in Table III and the experimental and calculated values for log V_{max} are shown in Table IV.

The double peaks shown in Figure 4 and the decrease in the value of log V_{max} (and thus in D and D_e) from the maximum in the region of pH 4.2 to 4.8 to the minimum in the range of pH 5.6 to 6.0 shown in Figure 2 may be explained by the decrease of ionic sites within the resin which takes place as chelation occurs. Chelation of the alkaline earths evidently cannot occur unless both hydrogens have been removed from a diacetate group by neutralization or ionic displacement. The favorable energy relationship caused by the increased stability due to chelation will force the ionization of the second hydrogen before it would be ionized normally at the pH involved. The temporary increase in hydrogen ions due to chelation upsets the equilibrium between ionic sites and hydrogen ions so that a few of the liberated hydrogen ions migrate out of the resin but the majority react with other

Table IV. Log V_{max} as a Function of Ionic Strength

Metal	pH	Ionic strength	Log V_{max} Obsd	Log V_{max} Calcd	Difference
Mg	4.00	0.05	2.51	2.53	−0.02
Mg	4.00	0.50	1.22	1.21	0.01
Mg	4.00	1.00	1.00	1.00	0.00
Mg	5.10	0.05	2.63	2.62	0.01
Mg	5.10	0.50	1.18	1.13	0.05
Mg	5.10	1.00	0.81	0.81	0.00
Mg	6.00	0.05	2.63	2.63	0.00
Mg	6.00	0.50	1.10	1.13	−0.03
Mg	6.00	1.00	0.94	0.94	0.00
Ca	4.00	0.05	2.68	2.66	0.02
Ca	4.00	0.50	1.30	1.31	−0.01
Ca	4.00	1.00	1.02	1.02	0.00
Ca	5.00	0.05	2.68	2.50	0.18
Ca	5.00	0.50	1.43	1.42	0.01
Ca	5.00	1.00	1.02	1.02	0.00

Table V. Apparent pK_1 Values of Dowex A-1

	For Mg μ = 1.0	Leyden and Underwood neutralization titration at μ = 1.0 (6)
α = 0.25	pK_1 = 2.46	pK_1 = 2.42
α = 0.50	pK_1 = 2.94	pK_1 = 2.96
α = 0.75	pK_1 = 3.06	pK_1 = 3.04
	For Mg μ = 0.05	Krasner and Marinsky "Intrinsic" pK_1 (8)
α = 0.5	pK_1 = 2.77	pK_1 = 2.77

ionic sites to form nonionized carboxyl groups. As a consequence, each metal ion which is chelated causes an average decrease of a little less than two in the number of fixed ionic sites. This decrease in ionic sites has two effects. One, the decrease caused a decrease in the fixed site ionic strength inside the resin which causes an increase in the activity coefficients of the metal ions inside the resin. Two, the ratio of alkaline earth ions to ionic sites changes because of the decrease of one in metal ions and two in ionic sites. Also, since some of the ionic sites are occupied by sodium or other ions, the number of ionic sites is greater than twice the number of alkaline earth ions. These two effects combine to create a migration of alkaline earth ions from the resin and thus decrease the distribution coefficient and V_{max}. As the pH is increased in the external solution, more hydrogens ionize and migrate from the resin until the effect of chelation is offset by the increase in pH. This occurs in the pH range of 5.6 to 6.0, above which chelation increases rapidly and alkaline earth metal ions migrate into the resin to maintain equivalent activities inside and outside the resin.

The divalent metal ions experience both ion exchange and chelation as retarding effects during elution down the column. Both these retarding effects are pH dependent because they depend upon the number of available ionic sites inside the resin particle. At lower pH, the main effect is ion exchange with each divalent ion neutralizing the charge on two ionic sites, each of which is furnished by a different diacetate group. Ion exchange increases with pH as more ionic sites become available by migration of hydrogen ions out of the resin until a pH of approximately 4 is reached at which chelation can start. The half neutralization point (50% dissociation) inside the resin has been shown to occur at a pH of approximately 5.6 ± 0.2 by Leyden and Underwood (6), which helps to explain the rapid increase in chelation above this pH range.

The decrease in the value of log V_{max} with increase in ionic strength shown in Figure 5, together with the fact that the maxima and minima of the curves in Figure 2 are shifted to lower pH values as the ionic strength increases, further substantiates the decreased effect of ion exchange and the increased effect of chelation as the pH is increased. The imbibition of neutral sodium chloride ion pairs caused by the increase in ionic strength (7) increases the sodium ion concentration inside the resin. The sodium ions which entered by imbibition compete with hydrogen ions and alkaline earth ions for the ionic sites, and chelation becomes effective at a lower pH since there is increased ionization due to the effect of the sodium ions. At very low ionic strengths, chelation of the alkaline earth metals probably does not occur until after the ionization of both hydrogens of a diacetate group at pH 5.8 and above as is indicated by the magnesium curve in Figure 1 for an ionic strength of 0.05.

The fact that double peaks occur in the elution curves also indicates that there are two retardation effects occurring inside the resin. Since the first peak is probably related to the ion exchange phenomenon and the second to chelation, the fact that the two peaks become more pronounced and are shifted to lower effluent volumes with increase in ionic strength or decrease in pH further substantiates that chelation occurs at lower pH values as the ionic strength increases and the number of doubly ionized diacetate groups inside the resin is correspondingly increased.

Apparent pK_1 Values of the Resin. The equation

$$pK = pH + \log\left(\frac{1-\alpha}{\alpha}\right) + \log [X] - \log [Na^+] \quad (7)$$

as given by Helfferich (15) was used to determine apparent pK_1 values utilizing the data from the curves in Figure 2 and the derivatives of Equation 5 together with the pH and sodium ion concentrations in the external solution. The term α is the degree of dissociation, $[X]$ is the total concentration of dissociated and undissociated ionogenic groups in the resin, and $[Na^+]$ is the sodium ion concentration in the external solution. The pH values corresponding to the various degrees of dissociation were obtained from the maximum and minimum points on the magnesium (μ = 1.0) curve of Figure 2, with the maximum assumed to correspond to 25% dissociation and the minimum of 50% dissociation. Also one value of pK_1 was obtained from the magnesium (μ = 0.05) curve by relating pH to V_{max}/V'_{max} where V'_{max} is the largest value of V_{max} obtained. The results are tabulated in Table V along with some reported values from the literature.

The theoretical justification for this method of determining the pK_1 of the resin can be attributed to the dependence of the distribution coefficient on the number of available ionized sites within the resin. In turn the number of available ionized sites reflects the dependence of the pK on the external factors of pH and total ionic strength. A similar proposal relating pK and D was put forth by Leyden and Underwood (6) which assumes that the pH and ionic strength in the equilibrated resin and the pH of the external solution at a particular ionic strength are related through the apparent pK of the resin. Therefore, as the relatively small amount of magnesium is eluted down the column, it becomes dis-

(15) Friedrich Helfferich, "Ion Exchange," McGraw-Hill, New York, N. Y., 1962, p 85.

tributed between the resin and the external solution, but because of its divalency it displaces two sodium ions. Since magnesium is present in small amounts compared to sodium, the increase in concentration of Na^+ in the external solution is negligible and has a negligible effect on the ionic strength. Thus, equilibrium between internal concentration of H^+ and Na^+ and external concentration of H^+ and Na^+ and the rate of movement of Mg^{2+} down the column are all functions of the pK of the resin. A strongly chelating metal could not be used for this method since both pK_1 and pK_2 would be depressed because of chelation (*10*).

RECEIVED for review February 17, 1971. Accepted May 25, 1971. Taken in part from the thesis submitted by George H. Luttrell to the Graduate School of Humanities and Sciences, Southern Methodist University, Dallas, Texas, in partial fulfillment of the requirements for the degree of Master of Science.

Spectrophotometric Determination of Niobium with 4-(2-Pyridylazo)Resorcinol and Colored Complexes Separated from Oxalic and Tartaric Acid Systems

Marija Široki

Laboratory of Analytical Chemistry, Faculty of Science, Institute for Inorganic and Analytical Chemistry, The University, Zagreb, Yugoslavia

Cirila Djordjevic

Department of Chemistry, College of William and Mary, Williamsburg, Va. 23185

Niobium complex species involved in the spectrophotometric determination of Nb(V) with 4-(2-pyridylazo)-resorcinol, (PAR = H_2R), in oxalic and tartaric acid media were separated in solid state. Oxooxalato-4(2-pyridylazo)resorcinol niobate(V) was extracted from aqueous solutions in chloroform by tetraphenyl phosphonium and tetraphenyl arsonium chloride, respectively, and compounds of the formula $(C_6H_5)_4X[NbO-C_2O_4)R]$, where X = P, As; and R = $C_{11}H_7N_2O_2^{2-}$, were obtained. From aqueous tartaric acid solutions, at pH 1–2, a substance corresponding to the formula $NbO(C_4H_4O_6)(HR)\cdot H_2O$ was prepared. The compounds were characterized by analysis, IR and visible spectra, conductivity measurements, and powder photographs. It has been shown that colored species in oxalic and tartaric acid media, absorbing between 560–520 nm, involve mixed ligand spheres, containing coordinated PAR along with an oxalato and tartrato ligand, respectively.

SPECTROPHOTOMETRIC DETERMINATION of niobium with 4-(2-pyridylazo)resorcinol, PAR, and complex species present in different aqueous systems was studied by several authors (*1–6*). Species containing a Nb/PAR ratio of 1/1 have generally been found to exist in solutions, regardless of the presence of other different reagents capable of forming stable complexes with niobium (such as oxalates, tartrates, fluorides, hydrogen peroxide, etc.). It has been observed, however, that the absorption maximum in the visible spectrum is shifted in Nb-PAR aqueous solutions, as dependent upon the presence of a particular additional reagent. These shifts, as well as the instability of the Nb-PAR complex in solutions that do not contain a large excess of tartrates, oxalates, or similar complexing agents, imply the possibility that additional reagents are taking part in the colored Nb-PAR complex formation. However, solution studies alone cannot show if some of the ions present in large excess are coordinated to the metal or not. Therefore, the nature of the Nb-PAR complexes present in the analytical systems was not known. We have undertaken the experiments to separate the colored complexes and characterize them in the solid state and believe that the work described below offers some evidence on the composition and properties of the complexes involved in this analytical method that is becoming increasingly important for analysis of niobium (*7–9*).

EXPERIMENTAL

Reagents and Chemicals. All the chemicals used were Analar grade. Merck monosodium salt of 4-(2-pyridylazo)-resorcinol, Fluka tetraphenylphosphonium and arsonium chloride, BDH niobium pentoxide, and chloroform containing 1% ethanol, were used.

Standard Solution of Niobium. Niobium solutions (about $2 \times 10^{-2} M$) were prepared in 5% tartaric and oxalic acid, respectively. Nb_2O_5 (about 0.7 gram) was fused with $KHSO_4$ (10 grams) in a platinum crucible. The melt was extracted with hot 10% oxalic acid (50 ml). To remove sulfates, niobium was reprecipitated with ammonia and centrifuged and washed three times with ammonium chloride solution (2%) and once with distilled water. Freshly precipitated niobium hydroxide was then dissolved in hot 10% oxalic and tartaric acid (100 ml), respectively. The solutions were heated on a water bath, filtered, and diluted to 200 ml. Solutions were standardized by the tannin or cupferron

(1) T. Belcher, T. V. Ramakrishna, and T. S. West, *Talanta*, **10,** 1013 (1963).
(2) I. P. Alimarin and Han Si-i, *Zh. Anal. Khim.*, **18,** 182 (1963).
(3) S. V. Elinson and L. I. Pobedina, *ibid.*, p 189.
(4) S. V. Elinson, L. I. Pobedina, and A. T. Rezova, *ibid.*, **20,** 676 (1965).
(5) E. Lassner, *Talanta*, **10,** 1229 (1963).
(6) E. Lassner and R. Püschel, *Michrochim. Acta*, **1963,** 950.
(7) R. Z. Bachman and C. V. Banks, ANAL. CHEM., **41,** 112R (1969).
(8) R. G. Anderson and G. Nickless, *Analyst (London)*, **92,** 1093 (1967).
(9) A. I. Busev and V. M. Ivanov, *Zh. Anal. Khim.*, **19,** 1238 (1964).

Table I. Analytical Data

Compound	Calculated, %					Found, %				
	C	H	N	P/As	Nb	C	H	N	P/As	Nb
$NbO(C_6H_4O_6)(HR)\cdot H_2O$	36.8	2.9	8.6	...	19.0	36.3	3.3	8.7	...	19.7
$[(C_6H_5)_4P][NbO(C_2O_4)R]$	59.3	3.6	5.6	4.1	12.4	59.2	3.9	5.8	3.8	12.2
$[(C_6H_5)_4As][NbO(C_2O_4)R]$	56.0	3.4	5.3	9.4	11.7	56.0	4.0	5.1	9.9	11.2

$R = C_{11}H_7N_2O_2$.

method. Solutions of lower concentration were obtained by dilution.

Preparation of $(C_6H_5)_4X[NbO(C_2O_4)R]$, X = P, As. R = $C_{11}H_7N_2O_2$. To the Nb(V) solution (about $2 \times 10^{-2}M$) in 5% oxalic acid (25 ml), an equal volume of an equimolar aqueous solution of PAR was added and the pH was adjusted to 5.5. The solution was heated and an equimolar amount of tetraphenylphosphonium (0.24 gram) and arsonium chloride (0.26 gram), respectively, dissolved in a minimum amount of water was added dropwise. The reaction mixture was transferred into a separatory funnel, extracted with an approximately equal volume of chloroform (50 ml), and the layers separated. The chloroform phase wat transferred into a distillation flask and chloroform was distilled off at 40 °C. The volume was reduced to about half of the initial volume. The solution was then transferred to an Erlenmeyer flask and cooled to 0 °C. To the cool solution an approximataly equal volume of petroleum ether was added dropwise. Leaflet-like crystals which formed were filtered off, washed with petroleum ether, and dried in the vacuum desiccator over calcium chloride. The yield was about 70% and 60% for the phosphonium and arsonium derivative, respectively. Analytical data are given in Table I.

Preparation of $NbO(C_6H_4O_6)(HR)\ H_2O$, HR = $C_{11}H_8N_2O_2$. To the hot Nb(V) solution ($2 \times 10^{-2}M$) in 5% tartaric acid (25 ml), an equimolar amount of PAR dissolved in hot water (5 ml) was added dropwise. After about an hour the precipitate formed coagulated and was centrifuged, washed several times with small amount of water and acetone, and dried in vacuo ($5 \times 10^{-2}M$ Hg) at 50 °C. Analysis is given in Table I.

Analytical Procedures. Niobium. In Compounds Containing Phosphorus or Arsenic. Substance (about 30 mg) was destroyed in a Kjeldahl flask with concd sulfuric acid (1 ml), to which 4–5 drops of concd HNO_3 were added. The procedure was repeated three times. The remaining solution was transferred with 5% oxalic acid (20 ml) in a beaker, diluted to 50 ml, and precipitated by the tannin method.

In Tartrato Compound. The substance (about 30 ml) was dissolved in 0.1*M* NaOH (5 ml). The solution was diluted to 50 ml and heated until the red color of the niobium complex disappeared and the solution became yellow because of the free PAR presence. To the hot solution hydrochloric acid (1:1, 10 ml) was added and the reaction mixture boiled until niobium hydroxide precipitate coagulated. The precipitate was filtered, washed with 2% ammonium chloride solution, ignited at 900 °C, and weighed as Nb_2O_5. Satisfactory results were obtained, too, if the niobium was determined as Nb_2O_5 by igniting the substance in a platinum crucible.

Phosphorous was determined by titration with standard lead nitrate solution and PAR as indicator (*10*), after igniting the sample by the Schöniger method (*11*).

Arsenic was determined iodometrically (*12*), after destroying the sample with concd sulfuric and nitric acid.

(10) R. Püschel, *Michrochim. Acta*, **1960**, 352.
(11) S. W. Schöniger, *Michrochim. Acta*, **1955**, 123; *ibid.*, **1956**, 869.
(12) M. M. Tuckermann, J. H. Hodecher, B. C. Southworth, and K. D. Fleicher, *Anal. Chim. Acta*, **21**, 463 (1959).

Carbon, hydrogen, and nitrogen were determined microanalytically.

Physical Measurements. Visible spectra of the solutions were recorded on a Perkin-Elmer 137 UV Spectrophotometer. Absorbance measurements were carried out on a Beckman Spectrophotometer Model DU-2. IR spectra of nujol mulls of the compounds were recorded on the Perkin-Elmer Spectrophotometer Model 137 and 221 in the region 4000–650 cm^{-1}.

Conductances were measured using a 100-c conductivity bridge and a cell with a cell constant of 0.2 cm^{-1}. Molar conductances in methanol were determined at 25 °C at a concentration of $10^{-3}M$ with a specific conductance of the solvent not greater than 1.33×10^{-6} ohm^{-1} cm^2.

X-Ray powder photographs were obtained in a 0.3-mm capillary with a Phillips 57.54 mm camera, CuK_α radiation, and exposure time of 2 hours.

Experimental work was done at the Faculty of Science, Zagreb, Yugoslavia.

RESULTS

The colored niobium complex formed with PAR in oxalato aqueous solution at pH 5 can be extracted by tetraphenylphosphonium and tetraphenylarsonium chlorides, respectively, in chloroform. This behavior confirms the existence of anionic complexes in aqueous solutions, corresponding by composition to generally used analytical systems. The compounds obtained are only slightly soluble in water, and can be precipitated with onium salts at higher concentration as a fine red-violet solid. However, the substances obtained in this way are impure and cannot be further purified, since they decompose on recrystallization. From chloroform extracts, however, red leaflets of pure complexes, decomposing at 240–245 and 190–195 °C for phosphonium and arsonium derivatives, respectively, are obtained. The analysis agrees with the formula $[(C_6H_5)_4X][NbO(C_2O_4)(R)]$, for X = P, As; R = $C_{11}H_7N_2O_2^{2-}$. The compounds are soluble in alcohols, chloroform, and nitrobenzene. The molar conductivity of methanol solutions was found to be 70–75 ohm^{-1} cm^2, indicating the presence of a 1:1 electrolyte. X-Ray powder photographs of the solids show only diffuse lines.

Visible spectra of the oxalato-PAR-Nb(V) derivatives in aqueous and chloroform solutions are given in Figure 1, as compared to the spectra of the reagents alone. The maxima for the Nb(V) species occur at 545 and 560 nm in aqueous and chloroform solutions, respectively, showing a bathochromic shift from the aqueous to the organic phase. PAR, on the other hand, shows a small hypsochromic shift, the maximum occurring at 410 and 400 nm in water and chloroform, respectively. Visible spectra of the solutions made to correspond with analytical systems and spectra of dissolved complexes are identical. It has been observed, however, that the color intensity of Nb(V)-PAR-oxalato solutions depends upon concentration of PAR, oxalates, and onium salts. For a quantitative extraction, at optimal oxalato and onium salt concentration, a molar ratio of

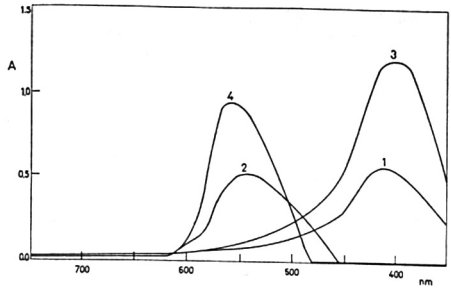

Figure 1. Visible spectra

Aqueous solution, (1) PAR, (2) Nb-PAR-oxalate
Chloroform solution, (3) PAR, (4) Nb-PAR-oxalate

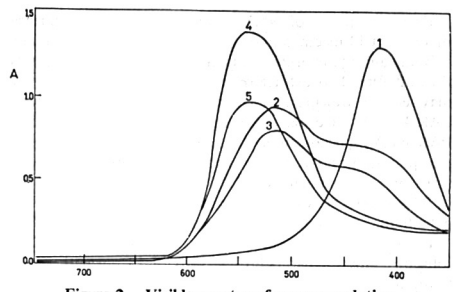

Figure 2. Visible spectra of aqueous solution

(1) PAR, pH 6
System Nb-PAR-tartrates, (2) pH 2; (4) pH 6
$NbO(C_4H_4O_6)HR \cdot H_2O$ in 0.01M tartaric acid, (3) pH 2; (5) pH 6

Nb:PAR of 1:3 is sufficient, and above this value PAR concentration has no effect. Absorbance of the organic phase has been found to increase with the increase of onium salt concentration and only above the molar ratio of Nb:onium salt of 1:50 no further effect on the color intensity was detected. The chloroform solutions are stable (more than 24 hours), but the reproducibility of the absorbance in different samples is poor, dependent strongly upon the oxalate concentration in the aqueous phase. Optimal oxalate concentration amounts to 2×10^{-3} to $6 \times 10^{-3}M$. Reproducibility of the niobium determination is dependent upon the oxalate:PAR ratio as well. Best results are achieved at a Nb:PAR:oxalate molar ratio of 1:10–30:300–400. On comparing the stability of aqueous and chloroform solutions we have observed that the chloroform solutions are more stable, they obey Lambert–Beer's law in a much wider range than aqueous solutions, and the sensitivity of niobium determination is higher in chloroform.

IR spectra of tetraphenylphosphonium and tetraphenylarsonium salts of oxooxalato-PAR niobate(V) are almost identical. Bands at 1715 and 1680 cm^{-1} along with some other characteristic bands indicate presence of coordinated oxalato groups. A strong band at 885 cm^{-1} obviously contains a contribution from the niobyl stretching group (*13*), since it is much more intense than the absorption observed normally for oxalates in this region, because of CO and OCO modes (*14*). Bands at 1570, 1250, and 1211 cm^{-1} could be assigned to coordinated PAR vibrations (*15*).

From acid tartrato aqueous solutions of pH 5–6, which have proved to be most sensitive for niobium determination with PAR, we have not been able to separate complexes in the solid state. They cannot be extracted by organic solvents in the presence of suitable cations and would not precipitate even from concentrated aqueous solutions. However, niobium has been shown to react with PAR in tartaric media even at lower pH (*4*). The complex that forms under such conditions (pH 1–2) is less soluble and can be precipitated from $10^{-2}M$ aqueous solutions. The substance separated in this way has a red-brown color and corresponds according to the analysis to the formula $NbO(C_4H_4O_6)(HR) \cdot H_2O$. It decomposes on heating and does not melt, is soluble in water, and relatively stable in weakly acidic or neutral solutions. In alkaline media the complex is destroyed and PAR ligand released, as shown by spectral evidence. The presence of coordinated PAR and tartrates is confirmed by analysis and other properties of the compound. In weakly alkaline solutions PAR is dissociated off, but niobium hydroxide does not precipitate unless the solution is acidified with hydrochloric acid and boiled. This procedure destroys the tartrato complexes of Nb(V), that are stable in weakly acidic, neutral, and alkaline media. Similar behavior is observed for tartrato Nb(V) solutions alone.

The visible spectrum of the isolated substance in water is identical to the spectrum of solutions corresponding to analytical conditions. For comparison, spectra are shown in Figure 2. Aqueous tartrato solutions of this complex at pH 2 show a maximum at 520 nm, shifted to 540 nm in solutions at pH 6.

The IR spectrum of the oxotartrato-HR-Nb(V) has been helpful for the characterization, confirming the presence of coordinated tartrates, indicated by bands occurring at 1670 and between 1370 and 1200 cm^{-1}. A broad absorption in the region 3500–3000 cm^{-1} is caused by hydrogen bonded OH stretchings. The spectrum is complex, but strong PAR bands are clearly distinguished at 1595, 1585 (doublet), and 1400 cm^{-1}. However, a strong band between 930–850 cm^{-1}, generally observed for a niobyl group stretching (*13*), is not present. A broad background absorption in the wide region between 850–700 cm^{-1} may well be due to Nb-O-Nb vibrational modes, implying a polymeric nature of this substance in the solid state, suggested as well by diffuse X-ray powder photographs.

DISCUSSION

4-(2-pyridylazo)resorcinol (PAR), is an asymmetric azo compound of the formula

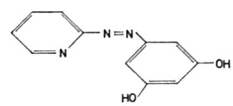

that has been extensively used lately as a spectrophotometric agent for a number of transition metal ions (*7–9*). However, so far there have been no reports on compounds prepared or separated from the aqueous solutions that contain PAR as a ligand in the solid state (*15*).

(13) V. Katovic and C. Djordjevic, *Inorg. Chem.*, **9**, 1720 (1970).
(14) K. Nakamoto, "Infrared Spectra of Inorganic and Coordination Compounds," Wiley, New York, N. Y., 1963, p 211.
(15) M. Široki and C. Djordjevic, *J. Less-Common Metals*, **23**, 228 (1971).

Complex species of Nb(V) with PAR in aqueous tartaric or oxalic acid media cannot be extracted directly by organic solvents and are expected to be anionic in nature. We have thus attempted to extract their salts with large cations that may enable transport into the organic phase. Tartrato-PAR-Nb(V) species have proved nonextractable, but oxalato-PAR-Nb(V) species can be extracted very well by tetraphenylphosphonium and tetraphenylarsonium chlorides in chloroform or some similar solvent, showing a behavior similar to PAR complexes of vanadium, cobalt, gallium, copper, and palladium. Study of these metal systems is in progress.

The visible spectrum of niobium complexes in chloroform solutions shows a bathochromic shift of 15 nm with regard to the corresponding aqueous solution, the maxima occurring at 560 and 545 nm, respectively. The maximum of PAR itself is shifted in chloroform for about 10 nm toward lower wavelength. In this way the separation of maxima of the colored complex and reagent is increased to almost 30 nm. This observation may lead to a spectrophotometric determination of niobium in the organic phase, that should have advantages over the niobium determination with PAR in aqueous solutions.

The optimal pH for Nb-oxalato-PAR complex formation was found to be at 5.5, a region where the oxalato species are unstable and hydrolyze in water. Products of such hydrolytic reactions probably interact with PAR in different ways and have a significant influence on the rate of the niobium-PAR colored species formation, and therefore on time needed to reach equilibrium. Under such conditions a number of factors are critical, for example the amount and sequence of reactants used, and that has actually been observed.

The fact that the complexes are extracted from aqueous solutions under conditions corresponding to the analytical systems, and that the solutions of complexes prepared show the same optical properties as the solutions used for analytical determination, indicate strongly that oxooxalato-PAR-niobate(V) ion characterized in the solid state is the species responsible for the color formation. It has been observed that in more acid Nb(V) oxalato solution, where stable $NbO(C_2O_4)_3^{3-}$ anion is present, PAR does not coordinate to the metal. PAR-onium salts of oxotrisoxalato niobate(V) can be prepared from such solutions, very different in properties from the compounds described above (*15*).

The reaction of Nb(V) with PAR in oxalic systems has been studied less than the reaction in tartaric systems, although oxalates are more suitable for a quantitative transfer of Nb(V) into solution. From the reports published it also seems that tartaric systems perform better in the spectrophotometric determination of niobium with PAR. Such behavior is expected on the basis of lower stability of the tartrato Nb(V) complex species, which are able to react favorably with the azo reagent. Indeed, in oxalato systems, optimal pH for the reaction has been found to be 5.5, where oxalato niobium complexes are less stable and thus more suitable for interaction with an incoming ligand.

In solutions with a pH larger than 5, PAR was found to exist primarily in the form (*16–19*) of HR^-. It is anticipated, too, that PAR acts as a tridentate ligand, with the pyridine and the azo group (the one nearer to the resorcinol ring) (*17*, *20*) nitrogen, and the *o*-hydroxy group oxygen as donor atoms. In more acid tartrato media PAR may thus interact with Nb(V) by forming a neutral molecule. The substance formed under such conditions, as described in the Experimental Section, analyzed to $NbO(C_4H_4O_6)(HR)\cdot H_2O$, containing a PAR and a tartrato ligand. In aqueous solutions, containing an excess of tartrates, the absorption maximum of the complex depends upon pH, and occurs at 520 nm and 540 nm, in solutions with pH 2 and 6, respectively. It is probable that in solutions with pH 2, PAR is coordinated as HR^-, forming the neutral complex described, but at higher pH the R^{2-} form of PAR is coordinated and an anionic complex $NbO(C_4H_4O_6)(R)_{aq}^-$ is present in solution. The shift of spectral maxima in the visible region from 540 to 520 nm may be related to the existence of these different species. The same trend in the shift of absorption maxima is observed for PAR itself, where maxima occur for H_2R, HR^-, and R^{2-} at 385, 415, and 485 nm, respectively.

The work described has shown that colored species involved in the spectrophotometric determination of niobium with PAR in oxalic and tartaric acid media contain a PAR ion coordinated to Nb(V) in addition to an oxalato and tartrato ligand, respectively. This structure explains the instability of color in solutions that do not contain a large excess of tartrates or oxalates. It is very likely that the same situation persists in Nb-PAR systems involving other complexing agents, such as fluorides or hydrogen peroxide, implying that mixed ligand spheres are preferred by niobium(V) in complexes with such simple azo molecules.

RECEIVED for review April 2, 1971. Accepted May 26, 1971.

(16) M. Hniličkova and L. Sommer, *Coll. Czech. Chem. Commun.*, **26**, 2189 (1961).
(17) W. J. Geary, G. Nickless, and F. H. Pollard, *Anal. Chim. Acta*, **26**, 575 (1962); *ibid.*, **27**, 71 (1962).
(18) A. I. Busev and V. M. Ivanov, *Zh. Anal. Chim.*, **22**, 382 (1967).
(19) A. Corsini, I. Mai-Ling Yih, Q. Fernando, and H. Freiser, ANAL. CHEM., **34**, 1090 (1962).
(20) Shun'ichiro Ooi, D. Carter, and Q. Fernando, *Chem. Commun.*, **1967**, 1301.

Gas Chromatographic Determination of Rafoxanide [3′-Chloro-4′-(4-Chlorophenoxy)-3,5-Diiodosalicylanilide] in Plasma by Electron Capture Detection of Its Trimethylsilyl Derivative

Charles P. Talley, Nelson R. Trenner, George V. Downing, Jr., and W. J. A. VandenHeuvel
Merck Sharp & Dohme Research Laboratories, Rahway, N. J. 07065

Experimental conditions have been established for gas chromatography at the submicrogram level of the anthelmintic rafoxanide, 3′-chloro-4′-(4-chlorophenoxy)-3,5-diiodosalicylanilide. The drug is converted to its di-trimethylsilyl derivative (characterized by combined gas chromatography–mass spectrometry) and chromatographed on a 4-in. column with electron capture detection. Rafoxanide, but not the derivative, undergoes a photolytic reaction to form the corresponding mono-iodo compound. A procedure has been developed for the isolation and gas chromatographic determination of rafoxanide in plasma with a sensitivity of 0.01 μg/ml.

GAS CHROMATOGRAPHY coupled with highly sensitive detectors has proved to be an excellent technique for the separation and quantitation of nanogram amounts of materials of biological origin and of exogenous materials in a biological matrix (*1–3*). Unfortunately, many of the more interesting substances associated with biological systems contain one or more groups capable of hydrogen bonding, leading to undesirable adsorption phenomena. The polarity imparted by such groups to a molecule, particularly if it possesses a high molecular weight, precludes direct gas chromatography without prior derivative formation. The substitution of trimethylsilyl (TMSi) groups for active hydrogen atoms has permitted gas chromatography of many high molecular weight, polar molecules (*4–7*). We now report the development of an assay in animal plasma for rafoxanide [3′-chloro-4′-(4-chlorophenoxy)-3,5-diiodosalicylanilide], a new anthelmintic agent (*8*). To detect and quantitate plasma drug levels in the parts per million range soon after oral administration, we have used the technique of gas chromatography with electron capture detection.

EXPERIMENTAL

Apparatus and Chromatographic Conditions. Gas chromatography of nanogram and subnanogram quantities of rafoxanide was carried out with a Glowall Model 320 instrument. The column was a 4-in. × 3-mm i.d. glass U-tube packed with 3% OV-17 coated over 1.5% SE-30 on 80/100 mesh acid-washed and silanized Gas-Chrom P (*9*). The vaporizer was maintained at 300 °C and the column at 250 °C. The carrier gas was high purity, dry N_2 at a flow rate of 75 ml/min. The electron capture detector used was of the Lovelock (*10*) design containing 22.5 μCi of ^{226}Ra coated on the inner surface of a cylindrical platinum foil. The detector was operated at 8 V dc and maintained at 300 °C.

Gas chromatography of microgram quantities of rafoxanide was carried out with a Barber-Colman Model 5000 instrument. The column was a 2-ft × 3-mm i.d. glass U-tube containing the same packing as above. The vaporizer was maintained at 300 °C and the column at 265 °C. The carrier gas was argon at a flow rate of 50 ml/min. Detection was by hydrogen flame ionization.

Combined gas chromatography–mass spectrometry (GC-MS) (*11*) was carried out with an LKB Model 9000 instrument. The column was a 4-ft × 3-mm i.d. glass spiral packed with 1.8% OV-17 on 80/100 mesh acid-washed and silanized Gas-Chrom P (*9*). The vaporizer was maintained at 300 °C and the column at 260 °C. The carrier gas was helium at a flow rate of 30 ml/min. The spectrometer was operated with a source temperature of 270 °C, an electron energy of 70 eV, an accelerating voltage of 3.5 kV, and a trap current of 60 μA.

Reagents. Ethanol (95%) was purchased from U.S. Industrial Chemical Company. Hydrochloric acid (concd) and sodium hydroxide (50% solution) were Merck reagent grade. Spectroquality 2,2,4-trimethylpentane (isooctane) and reagent grade bis-trimethylsilylacetamide (BSA) were purchased from Matheson Coleman and Bell and Pierce Chemical Company, respectively.

Sample Preparation. EXTRACTION. A 1.0-ml aliquot of plasma was treated with 5 ml of 95% ethanol and centrifuged to remove the denatured proteins. The clear supernatant was decanted, acidified with 5 ml of 4% HCl, and extracted twice with 5-ml portions of isooctane. The isooctane layer was extracted twice with 5 ml portions of 1% NaOH. The basic extract (protected from direct lighting) was heated in a steam bath for 1 hr, cooled, acidified with 15 ml of 4% HCl, and extracted twice with 5 ml portions of isooctane. The isooctane extract was evaporated to dryness under a stream of nitrogen.

DERIVATIZATION. The residue from above was taken up in 50 μl of BSA, which served as both reagent and solvent. The mixture was capped tightly, heated in an oil bath at 110 °C for 7 min, cooled to room temperature, and centrifuged. One microliter was injected into the gas chromatograph.

QUANTITATION. Peak areas were measured by height and width at half-height. Quantitation was accomplished by comparison of sample peak area to a standard plot determined each day from a series of standard solutions of derivatized rafoxanide in BSA.

(1) B. J. Gudzinowicz, "Gas Chromatographic Analysis of Drugs and Pesticides," Dekker, New York, N. Y., 1967.
(2) J. A. F. de Silva and C. V. Puglisi, ANAL. CHEM., **42**, 1725 (1970).
(3) E. Townley, I. Perez, and P. Kabasakalian, *ibid.*, p 1759.
(4) A. R. Pierce, H. N. Graham, S. Glassner, H. Madlin, and J. G. Gonzales, *ibid.*, **41**, 298 (1969).
(5) W. E. Wilson and J. E. Ripley, *ibid.*, p 810.
(6) K. Tsuji and J. H. Robertson, *ibid.*, **42**, 1661 (1970).
(7) M. Katz and Y. Lensky, *Experientia*, **26**, 1043 (1970).
(8) H. Mrozik, H. Jones, J. Friedman, G. Schwartzkopf, R. A. Schardt, A. A. Patchett, D. R. Hoff, J. J. Yakstis, R. F. Riek, D. A. Ostlind, G. A. Plishker, R. W. Butler, A. C. Cuckler, and W. C. Campbell, *ibid.*, **25**, 883 (1969).
(9) E. C. Horning, W. J. A. VandenHeuvel, and B. G. Creech, in "Methods of Biochemical Analysis," Vol. XI, D. Glick, Ed., Interscience, New York, N. Y., 1963.
(10) J. E. Lovelock and S. R. Lipsky, *J. Amer. Chem. Soc.*, **82**, 431 (1960).
(11) J. A. McCloskey in "Methods in Enzymology," XIV, Lipids, J. M. Lowenstein, Ed., Academic Press, New York, N. Y., 1969.

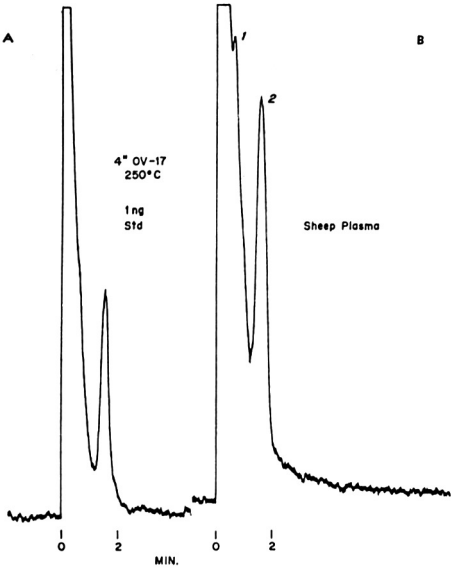

Figure 1. (*A*) Rafoxanide standard (1 ng as the di-TMSi-derivative). (*B*) Plasma of a sheep dosed with rafoxanide. This analysis represents $^1/_{50}$ of the extract from 1 ml of plasma. Peak 1 results from desiodo-rafoxanide produced during sample workup. Details of the chromatographic conditions are given in the Experimental Part, first paragraph

RESULTS AND DISCUSSION

The structure of rafoxanide (I) suggests that this drug might not be particularly well suited to direct gas chromatographic analysis.

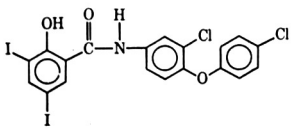

I

Indeed, the compound was not eluted from nonpolar stationary phases such as OV-1 and SE-30 even at high temperatures (300 °C). Trimethylsilylation of rafoxanide with BSA gave a derivative which could be chromatographed at 265 °C on a moderately polar stationary phase composed of OV-17 coated over SE-30.

Characterization of the derivative was accomplished by combined GC-MS. The mass spectrum of this compound, clearly di-TMSi-rafoxanide, exhibited prominent ions at *m/e* 769 (M, molecular ion), *m/e* 754 (M − 15, loss of a methyl radical), *m/e* 680 (M − 89, loss of an OTMSi radical), and *m/e* 642 (M − 127, loss of an iodine radical). Each of these ions displayed the characteristic dichloro isotope cluster. The ion at *m/e* 445 probably possessed the acylium structure II. Trimethylsilylation of rafoxanide results in derivatization of both the phenolic group and the secondary amide group (*12*). Quantitative conversion to this di-TMSi

(12) W. J. A. VandenHeuvel, J. L. Smith, and J. L. Beck, *Anal. Lett.*, **4**, 131 (1971).

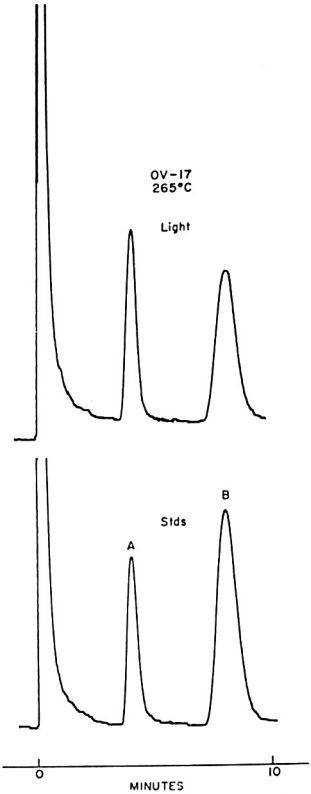

Figure 2. Gas chromatogram (upper) of trimethylsilylation reaction mixture of an aliquot of an ethyl acetate solution (0.1%) of rafoxanide. The ethyl acetate solution had been exposed to ordinary laboratory fluorescent light for three weeks. Gas chromatogram (lower) of a mixture of rafoxanide (*B*) and authentic 3-desiodo-rafoxanide (*A*) as trimethylsilyl derivatives. Details of the chromatographic conditions are given in the Experimental Part, second paragraph

derivative is possible only in a large excess of BSA. This is to be expected since silylated secondary amides are powerful silyl donors (*e.g.*, BSA) (*13*).

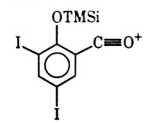

II

A low intensity (~2%) signal at *m/e* 697 is found in the mass spectrum of di-TMSI-rafoxanide. This ion could

(13) A. E. Pierce, "Silylation of Organic Compounds," Pierce Chemical Company, Rockford, Ill. 1968.

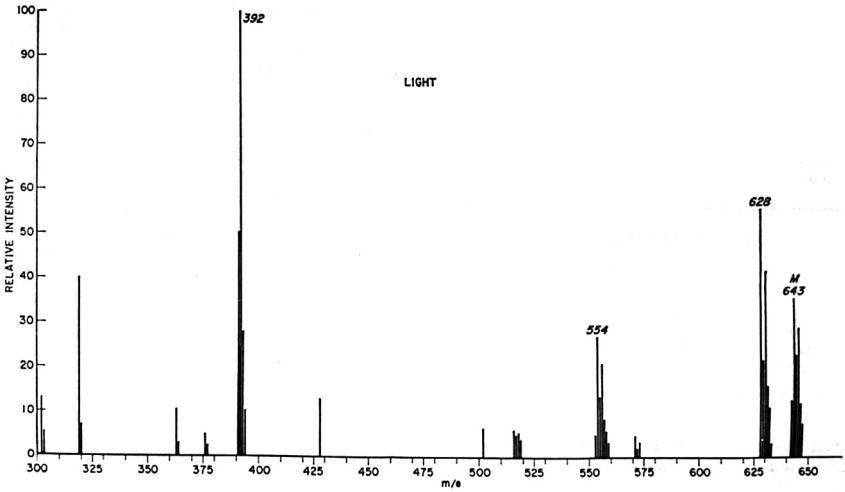

Figure 3. Mass spectrum (m/e 300–650) of the di-TMSi derivative of the product resulting from photolysis of rafoxanide

result from a minor fragmentation path wherein the di-TMSi-rafoxanide loses a $(CH_3)_2SiCH_2$ radical (M − 72). A more likely explanation is that the di-TMSi-rafoxanide reacts with "active sites" in the gas chromatographic packing, exchanging one of its TMSi groups for a hydrogen atom to form mono-TMSi-rafoxanide. The effect is so small with a carefully deactivated gas chromatographic support as to be chromatographically undetectable.

A typical gas chromatogram obtained from a plasma sample (rafoxanide-treated sheep) using the procedure discussed in this paper is seen in Figure 1*b*. The small peak at 0.7-minute retention time corresponds to approximately 2% of the area of the major peak. Control plasma samples spiked with pure rafoxanide and carried through the assay also exhibit this small peak found in samples of biological origin. Rafoxanide loses one iodine atom in a photolytic reaction. Thyroxine has been shown recently to undergo loss of an iodine atom ortho to a phenolic group in the plasma of normal human subjects (*14*). While this is obviously not a photolytic reaction, the interesting aspect is that a second ortho iodine atom is not lost. We have found no evidence for metabolic loss of the one ortho iodine atom or any other type of animal metabolism of rafoxanide in the body fluids examined in the course of this work.

Our efforts to identify this minor component led us to a closer examination of the photolytic behavior of rafoxanide. Gas chromatography of the TMSi derivative of the material resulting from exposure of rafoxanide dissolved in ethyl acetate to ordinary laboratory fluorescent light for three weeks gave the result seen in Figure 2. Characterization of the earlier eluted component as the di-TMSi derivative of "mono-iodo-rafoxanide" (mol wt 643) was accomplished by combined GC-MS. Comparison of its partial mass spectrum (Figure 3) with that of di-TMSi-rafoxanide established the similarity of their fragmentation patterns, ions in the former being shifted 126 amu downfield from those in the latter. This shift corresponded to the replacement of one of the iodine atoms by a hydrogen atom. Several experimental observations indicated that it may have been the iodine atom ortho to the phenolic group (3-position) which was photolytically labile. Identical gas chromatographic retention times were found for the di-TMSi derivative of "mono-iodo-rafoxanide" and authentic 3-desiodo-rafoxanide (lower chromatogram, Figure 2, peak *A*). Spiking of the plasma extract of Figure 1*b* with authentic 3-desiodo-rafoxanide enhanced peak 1 and gave no new peaks. Further, the mass spectra of the di-TMSi photolysis product and of authentic di-TMSi-3-desiodo-rafoxanide were indistinguishable. The 60 MHz NMR spectrum of the photolysis product, indicative of a 1,2,5- rather than a 1,2,3-trisubstituted benzene, was entirely compatible with that of authentic 3-desiodo-rafoxanide. Whereas free rafoxanide in ethyl acetate solution was unstable toward light, di-TMSi-rafoxanide (in BSA) and rafoxanide in 0.5% NaOH solution remained intact even after overnight UV irradiation in a quartz vessel at room temperature. Protection against irradiation was apparently afforded by derivatization of the phenolic group, either as the TMSi ether or as the phenoxide ion. Under the conditions where rafoxanide was photolytically unstable, 3-desiodo-rafoxanide in ethyl acetate solution did not lose iodine. The unavailability of 5-desiodo-rafoxanide precluded a direct comparison with the photolysis product.

The sensitivity requirements of our proposed assay necessitated chromatographic detection at the subnanogram level. On a 2-ft × 3-mm i.d. glass spiral column containing the 3% OV-17/1.5% SE-30 packing, our lower practical detection limit for di-TMSi-rafoxanide was approximately 1 ng per injection. [For comparison, Jaakonmäki and Stouffer (*15*) found that with a 56 μCi ^{226}Ra detector they were able to detect less than 0.5 ng of triiodothyronine methyl ester as the *N,O*-dipivalyl derivative.] Increasing the flow rate at constant column temperature or increasing the temperature

(14) K. Sterling, M. A. Brenner, and E. S. Newman, *Science*, **169**, 1099 (1970).

(15) P. I. Jaakonmäki and J. E. Stouffer, *J. Gas Chromatogr.*, **5**, 303 (1967).

Table I. Recovery of Rafoxanide from Spiked Control Plasma

Rafoxanide added, ppm	Recovery, % GC	Recovery, % Radioactivity
0.19	79	74
0.39	77	77
0.49	76	76
0.80	74	80

Table II. Typical Experimental Data

Animals	Rafoxanide Dose, mg/kg/day	Rafoxanide Plasma level, μg/ml
Rats (4)	0.2	<0.01
Mice (4)	0.2	<0.01
Rats (2)	10	0.16
Mice (4)	10	1.40

at constant flow rate resulted not only in shorter retention times, but also in higher response (peak areas) for di-TMSi-rafoxanide. As the degree of loss could thus be correlated with residence time in the column and as the electron capture detection system is by nature highly selective, the decision was made to use a very short column, one containing only 4 in. of packing. In this respect we are approaching the condition suggested by Purnell, namely, that "the aim of chromatography is elimination of the column" (*16*). Measurable response was obtained with this column from as little as 0.2 ng of rafoxanide (as the di-TMSi-derivative). The plot of detector response (peak area) *vs.* nanograms of rafoxanide as the di-TMSi derivative over the range 0.5 ng to 4 ng yielded a straight line with a relative standard deviation of 1.7%. The line intercepted the abscissa at 0.15 ng, a further indication of irreversible loss on the column (*17*).

Although the electron capture detector exhibited a rather linear response for this small range, over a wider range (0.2 ng to 40 ng) the detector behaved more characteristically and exhibited severe departure from linearity (*18*). This resulted in large measure from the relatively low standing current established in our particular type of detector. Injection of 30 ng produced a peak as high as the standing current; and, as there can be no response greater than the standing current, it was not possible to quantitate above the 30-ng level. Actually, linearity began to fail even below 30 ng. Once a majority of the available electrons in the detector have been absorbed, the few that remain are increasingly less likely to be captured (*19*). Attempts to use a tritium foil detector, which has a more favorable standing current and a wider linear range, failed since it could not be brought to a temperature high enough (maximum temperature of a tritium foil detector is 225 °C) to prevent condensation of the column effluent. The ^{63}Ni detector, probably ideal for our work because of its greater temperature stability, was not available for trial.

Rafoxanide is bound to the albumin in plasma (*20*). The most efficient method of release was protein denaturing with ethanol, a single treatment removing 85% of the drug with the remaining 15% inaccessible to repeated ethanol washings (based on experiments with ^{14}C-labeled rafoxanide). In a preliminary experiment, control plasma was treated with ethanol to denature the proteins (removed by filtration). The ethanolic filtrate was extracted with isooctane, an aliquot of the isooctane extract was evaporated to dryness, and the residue was treated with BSA. Gas chromatography of this solution showed no interfering peaks. Another aliquot of the isooctane extract was spiked with rafoxanide, evaporated to dryness, and treated with BSA. Gas chromatography of this solution resulted in about 30% of the expected detector response for the injected quantity of di-TMSi-rafoxanide. Injection of a standard solution of di-TMSi-rafoxanide immediately following such a run also resulted in a highly attenuated detector response. Column conditioning for more than 2 hr at 290 °C was necessary to restore full response for a standard injection. This effect was not observed when BSA solutions of di-TMSi-rafoxanide spiked with large quantities of nonyl alcohol, α-hydroxystearic acid, or tripalmitin were chromatographed. (The BSA solutions were 1000:1 spiked material:rafoxanide.) Fortunately, the interference was eliminated by hydrolysis of the residue from the isooctane extraction at 100 °C in 1% NaOH solution for one hour; this treatment had no observably deleterious effect on the rafoxanide.

Recovery data were obtained for control plasma samples spiked with ^{14}C-labeled rafoxanide (10,000 cpm/μg) and carried through the assay described above. One-microliter aliquots of the final BSA solution were subjected to liquid scintillation counting and gas chromatography. The results are presented in Table I.

Most of the loss (15%) resulted from the nonquantitative ethanol denaturation step. The additional 5% to 10% discrepancies were caused by losses during the various liquid–liquid partitions and other sample manipulations. Typical data obtained from mice and rats treated with rafoxanide once a day for 4 days (plasma samples collected on day 4) are presented in Table II.

RECEIVED for review March 8, 1971. Accepted May 19, 1971.

(16) J. H. Purnell, *Gas Chromatogr. Biol. Med., Ciba Found. Symp.*, **1969**, 21 (1969).
(17) E. C. Horning, K. C. Maddock, K. V. Anthony, and W. J. A. VandenHeuvel, ANAL. CHEM., **35**, 526 (1963).
(18) J. K. Foreman, T. A. Gough, and E. A. Walker, *Analyst*, **95**, 797 (1970).
(19) D. C. Fenimore and C. M. Davis, *J. Chromatog. Sci.*, **8**, 130 (1970).
(20) N. R. Trenner, Merck Sharp & Dohme Research Laboratories, Rahway, N. J., unpublished results, 1968.

Method for Calculating Cross-Contamination in Column Chromatographic Separation of Radioactive Parent–Daughter Pairs

P. J. Karol

Department of Chemistry, Carnegie-Mellon University, Pittsburgh, Pa. 15213

In the chromatographic separation of two species where one is the radioactive precursor of the other, radioactive transformation while on the column modifies the parent–daughter elution curve from that expected of stable isotopes of the same elements. Precise determination of the amount of daughter species produced by other mechanisms such as nuclear reactions or decay of an alternate (independent) precursor necessitates an accurate calculation of hereditary contamination in the daughter fraction. The extent of this contamination, which can be quite considerable, is a function of the column elution rate and the half-lives of the parent and daughter isotopes. The theoretical plate concept of column chromatography is applied to radioactive systems and used to derive a general expression for the modified elution curve from which the amount of contamination may be determined.

WITH THE CONTINUING improvements in high-resolution chromatography and their efficacious application to rapid radiochemical separations comes the ability to study short-lived isotopes previously inaccessible. For example, among the lanthanides there are presumably many short-lived radioisotopes or isomers which are undiscovered or incompletely analyzed owing to the general inability to achieve satisfactory separation from parent activities in a short amount of time. Rapid column chromatography is doing much to alleviate this deficiency.

An analytical complication occurs, however, when short-lived nuclei are studied using chromatographic separations. This is the distorting effect on the elution curves, especially in the region of cross contamination, caused by radioactive transformation from a species of one element to a species of another element at a rate which is comparable to the separation rate of the two elements on the column. The usual recipe for analyzing cross contamination (*1*) is no longer applicable. A procedure will be derived in detail for calculating the proportionation of the effluent daughter isotope between that produced by parent decay and that produced by alternate parent or independent modes.

For a list of important symbols, see Appendix 3.

THEORY

The basis for the following derivation was suggested by a work of Kallen and Heilbronner (*2*). These authors formulated the solution of an analogous problem—the effect that thermal dissociation of a substance has on its gas chromatogram.

I. Theoretical Plate Concept: Stable Species. The theoretical plate concept (*3*) is based on the successful application of a parameter, the plate height, in describing the spreading of an elution peak by the chromatographic process. The plate height, in turn, is an outgrowth of the theoretical plate model of Martin and Synge (*4*) which was invented to describe the dynamic equilibrium mechanism of column chromatography. These authors define the plate height as "the thickness of the layer such that the solution issuing from it is in equilibrium with the mean concentration of solute in the non-mobile phase throughout the layer." A chromatographic column can then be looked upon as a succession of such plates in which the chromatographic partition process is repeated over and over. If the plate height is H and one has a column of length L, we define another parameter by $L/H = n + 1$ where $n + 1$ is the number of theoretical plates in the column. For a rigorous discussion of the merits and justifications of the theoretical plate concept and its relation to the Martin and Synge model, see Reference *3*.

The elution curve may be derived by considering the mass-balance equation (net change = gain − loss),

$$dN_i = (KN_{i-1} - KN_i)dV \tag{1}$$

where N_i is the number of nuclei (or related variable such as weight or disintegration rate) of a given type in plate i, dN_i represents the change in the number of nuclei in plate i due to repartition by flow of an eluent volume dV through plate i after volume V has already passed, and K represents an effective partition coefficient equal to the fraction of nuclei which is in the solution (mobile) phase per unit volume of solution phase. The first term on the right of Equation 1 is the number of nuclei gained from the effluence of the preceding plate $i - 1$ and the second term represents the loss of nuclei from plate i carried by the advancing eluent fluid.

The function which describes the dependence on effluent volume of the number of nuclei emerging from the column is called the elution curve and is given by $KN_{n+1}(V)$, the number of nuclei per unit volume that issues from the last plate, $n + 1$. (The volume V which has emerged from any plate, the last plate in particular, is related to the volume V' of eluting solution which has entered the column by $V = V' - \epsilon$ where ϵ is the column void volume.)

When eluent flow has not yet started, $V' = V = 0$, and the number of nuclei in the first plate, N_1, is equal to $N(0)$, the original number of nuclei loaded onto the column. Also when $V' = V = 0$, $N_i = 0$ for $i > 1$. By using this information as boundary conditions, Equation 1 may be solved to give

$$N_{n+1}(V) = N(0)\frac{(KV)^n e^{-KV}}{n!} \tag{2}$$

Details of the derivation are contained in Appendix 1. For large values of n, the Poisson distribution in Equation 2 may be approximated by a Gaussian distribution yielding

$$N_{n+1}(V) = N(0)\frac{e^{-(KV - n)^2/2n}}{(2\pi n)^{1/2}} \tag{3}$$

Multiplication of Equations 2 and 3 by K gives the desired

(1) E. Glueckauf, *Trans. Faraday Soc.*, **51**, 34 (1955).
(2) J. Kallen and E. Heilbronner *Helv. Chim. Acta*, **43**, 489 (1960).
(3) J. C. Giddings, "Dynamics of Chromatography," Part I, Marcel Dekker, New York, N. Y., 1965, p 20.
(4) A. J. P. Martin and R. L. M. Synge, *Biochem. J.*, **35**, 91 (1941).

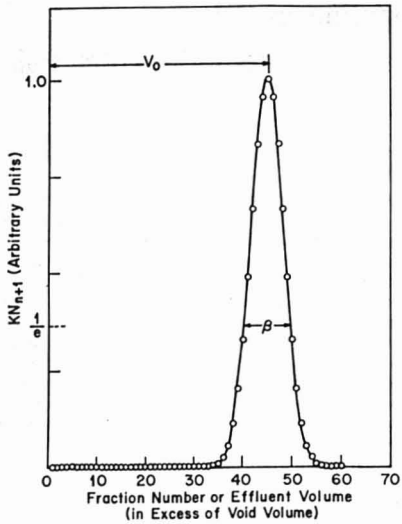

Figure 1. Sample elution peak where the parameter V_e is the volume at which the maximum concentration of eluting species appears and β is the full width of the elution peak at $e^{-1} \times$ height of the peak maximum

elution curve function. A sample elution curve is illustrated in Figure 1.

For both the Poisson and Gaussian forms, V_e, the volume corresponding to the peak maximum is given by

$$V_e = n/K \tag{4}$$

From Equations 3 and 4 the width, β, of the Gaussian elution curve at e^{-1} times the maximum is

$$\beta = \left(\frac{8}{n}\right)^{1/2} V_e \tag{5}$$

Since the parameters V_e and β are known from experiment, the values of $n + 1$ and K can be obtained from Equations 4 and 5.

II. Theoretical Plate Concept: Labile Species. PARENT SPECIES. Consider now the elution of P radioactive nuclei with decay constant λ_P. The mass-balance Equation 1 must now contain an additional term, $-\lambda_P P_i dt$, which accounts for the loss of P by radioactive transformation,

$$dP_i = (K_P P_{i-1} - K_P P_i - \Lambda_P P_i)dV \tag{6}$$

where K_P is the parent partition coefficient and $\Lambda_P = \lambda_P(dt/dV) = \lambda_P/\phi$, where $\phi = dV/dt$ is the constant flow rate of eluent through the column.

The initial conditions used in solving Equation 6 are as follows: At the initiation of the elution process $P_i(V) = P(0)$, [$P(0)$ is not, however, equal to the original number of P loaded onto the column at $t < 0$ but may be obtained from the latter in a straightforward manner]; $P_i(0) = 0$ for $i > 1$. The details of the solution of Equation 6 are given in Appendix 1. The result is

$$P_{n+1}(V) = P(0)\frac{(K_P V)^n e^{-(K_P + \Lambda_P)V}}{n!} \tag{7}$$

differing from Equation 2 only by the presence of the damping factor $e^{-\Lambda_P V}$ which accounts for decay. Equation 7 is approximated by the analog of Equation 3

$$P_{n+1}(V) = P(0)\frac{e^{-(K_P V - n)^2/2n}}{(2\pi n)^{1/2}} e^{-\Lambda_P V} \tag{8}$$

If λ_P is small with respect to the flow rate, *i.e.*, if $\Lambda_P = \lambda_P/\phi \ll 1$, then the damping factor approaches unity and the elution curve approaches that for a stable species as expected for a half-life that is long compared to residence time on the column.

DAUGHTER SPECIES. Daughter nuclei are produced by the decay of P and disappear at a rate determined by decay constant λ_D. Letting $D_i(V)$ represent the number of daughter nuclei in plate i, the mass-balance equation for daughter nuclei generated and consumed by radioactive transformation during elution in a given plate i may be expressed as

$$dD_i = (K_D D_{i-1} + \Lambda_P P_i - K_D D_i - \Lambda_D D_i)dV \tag{9}$$

where P_i is given by Equation 7 with i in place of $n + 1$, K_P is the daughter effective partition coefficient, and $\Lambda_D = \lambda_D/\phi$.

Conditions at the onset of the elution process are used in establishing the solution to Equation 9 as before. When $V = 0$, then $D_1 = D(0)$ and $D_{i>1} = 0$. The solution to Equation 9 contains several terms which will be discussed according to their various origins by use of the following definition:

$$D_i(V) = D_i'(V) + C_i(V) \tag{10}$$

D' represents the number of daughter nuclei which were present in the initial sample loading at the commencement of elution; the number of daughter nuclei which originate as decay products generated during the course of the chromatographic process is denoted by C. From the above definitions, $D(0) = D'(0)$. As shown in Appendix 1, the $D'(0)$ nuclei, hereafter referred to as *primary* daughter nuclei, are chromatogrammed in a manner analogous to $P(0)$, that is

$$D'_{n+1}(V) = D(0)\frac{(K_D V)^n e^{-(K_D + \Lambda_D)V}}{n!} \tag{11}$$

The other daughter nuclei, $C(V)$ will be referred to as *secondary* daughter nuclei.

In deriving an expression for $C_{n+1}(V)$, the only initial condition is that $C_i(0) = 0$ for all i. The derivation of this expression is described in Appendix 1. Definition of several new parameters proves to be convenient at this time:

t_P = the time after elution commences at which the peak in the parent species elution curve emerges $= V_P\Lambda_P/\lambda_P$ (12)

α = parent–daughter separation factor $= V_P/V_D = t_P/t_D = K_D/K_P$ (13)

$$c = (K_P - K_D + \Lambda_P - \Lambda_D)/(K_P - K_D) = 1 + \frac{t_P(\lambda_P - \lambda_D)}{n(1 - \alpha)} \tag{14}$$

The resulting solution is expressible as

$$C_{n+1}(V) = P(0)\frac{\lambda_P t_P e^{\frac{t_P}{1-\alpha}[\alpha\lambda_P - \lambda_D]V/V_P}}{n!c^{n+1}n(1 - \alpha)} \times \left[\gamma\left(n + 1, nc\frac{V}{V_P}\right) - \gamma\left(n + 1, n\alpha c\frac{V}{V_P}\right)\right] \tag{15}$$

where the incomplete gamma function $\gamma(n + 1, u)$ is defined through

$$\gamma(n + 1, u) = \int_o^u e^{-x}x^n \, dx = n!\left(1 - e^{-u}\sum_{j=0}^{n}\frac{u^j}{j!}\right) \tag{16}$$

Equation 15 can be simplified by noting that, for the large values of n routinely encountered in column chromatographic separations, the following asymptotic relationship holds:

$$C^n = \left[1 + \frac{\lambda_P t_P(1 - \lambda_D/\lambda_P)}{1 - \alpha} \cdot \frac{1}{n}\right]^n \sim e^{\frac{\lambda_P t_P(1 - \lambda_D/\lambda_P)}{1 - \alpha}}$$

$$\text{for } n \gg 1 \gg \frac{\lambda_P t_P(1 - \lambda_D/\lambda_P)}{1 - \alpha} \cdot \frac{1}{n}$$

Substituting this expression into Equation 15 gives

$$C_{n+1}(V) = P(0)\frac{\lambda_P t_P e^{\frac{t_P}{1-\alpha}\left[(\alpha\lambda_P - \lambda_D)\frac{V}{V_P} - (\lambda_P - \lambda_D)\right]}}{n!\, cn(1 - \alpha)} \times \left[\gamma\left(n + 1, nc\frac{V}{V_P}\right) - \gamma\left(n + 1, n\alpha c\frac{V}{V_P}\right)\right] \tag{17}$$

A complete description of the elution curve is now possible in terms of its representative components: $K_P P_{n+1}(V)$ describes the elution peak for parent species; $K_D D'_{n+1}(V)$ describes the peak due to *primary* daughter, *i.e.*, daughter in the initial load; $K_D C_{n+1}(V)$ is the function depicting the distribution of *secondary* daughter nuclei which are generated during passage through the column. The latter will emerge at elution volumes lying between those of the Gaussian peaks corresponding to the parent and daughter atoms in the initial load.

One may prefer to express the result in collected fraction number (or drop number) ν rather than volume, in which case V/V_P becomes ν/ν_P, ν_P being the fraction number at which the parent elution curve peaks. The volume per fraction is equal to V_P/ν_P and the number of *secondary* daughter nuclei in a given fraction may be expressed as

$$K_D C_{n+1}(V)\frac{V_P}{\nu_P} = \frac{n\alpha}{\nu_P} C_{n+1}(V) \tag{18}$$

The number of original parent species which has subsequently decayed and been eluted as (*secondary*) daughter species into a given collected fraction is thus equal to

$$\frac{n\alpha}{\nu_P} C_{n+1} = P(0)\frac{n\alpha\lambda_P t_P e^{\frac{t_P}{1-\alpha}\left[(\alpha\lambda_P - \lambda_D)\frac{\nu}{\nu_P} - (\lambda_P - \lambda_D)\right]}}{\nu_P n![n(1 - \alpha) + t_P(\lambda_P - \lambda_D)]} \times \left[\gamma\left(n + 1, nc\frac{\nu}{\nu_P}\right) - \gamma\left(n + 1, n\alpha c\frac{\nu}{\nu_P}\right)\right] \tag{19}$$

Likewise, from Equation 8 the number of undecayed parent nuclei in the given collected fraction is given by

$$\frac{n}{\nu_P} P_{n+1} = P(0)\frac{ne^{-\frac{n}{2}\left(\frac{\nu}{\nu_P} - 1\right)^2}}{\nu_P(2\pi n)^{1/2}} e^{-\lambda_P t_P \frac{\nu}{\nu_P}} \tag{20}$$

and from Equation 11, one obtains a similar expression for the number of undecayed *primary* daughter nuclei:

$$\frac{an}{\nu_P} D'_{n+1} = D(0)\frac{ane^{-\frac{n}{2}\left(\alpha\frac{\nu}{\nu_P} - 1\right)^2}}{\nu_P(2\pi n)^{1/2}} e^{-\lambda_D t_P \frac{\nu}{\nu_P}} \tag{21}$$

SECONDARY CONTAMINATION

At some time T, fractions from ν_{lower} to ν_{upper} are combined to form a consolidated daughter sample which will contain a total of $C^* + D^*$ daughter nuclei as defined below. From Equation 19, the total number of *secondary* daughter nuclei, denoted by the symbol C^*, included in the consolidated sample may be derived yielding the expression

$$C^* = P(0)\sum_{\nu lower}^{\nu upper}\frac{n\alpha\lambda_P t_P e^{\frac{t_P}{1-\alpha}\left[\alpha\lambda_P\frac{\nu}{\nu_P} - (\lambda_P - \lambda_D)\right]} e^{-\lambda_D T}}{\nu_P[n(1 - \alpha) + t_P(\lambda_P - \lambda_D)]} \cdot \frac{\left[\gamma\left(n + 1, nc\frac{\nu}{\nu_P}\right) - \gamma\left(n + 1, n\alpha c\frac{\nu}{\nu_P}\right)\right]}{n!} \tag{22}$$

[The sample consolidation time, T, will have been eliminated from the final expression. See Equation 27.]

Tailing of the parent species elution curve into the daughter fraction will also contribute to the number of *secondary* daughter nuclei in the daughter sample. The amount of tailing may be determined from Equation 8 using the usual radioactive growth and decay expression for parent–daughter pairs and generates an additional term which rigorously should be included in Equation 22. To simplify the ensuing discussion, however, it will be assumed that such normal cross contamination is of much lesser consequence as is usually the case and will be ignored.

The amount of *secondary* daughter, C^*, must be subtracted from the experimental total number of daughter nuclei in the above sample if we want to obtain D^*, the amount of (*primary*) daughter sample in the initial column loading. As is clear from Equation 11, we have

$$D^* = D(0)\sum_{\nu lower}^{\nu upper}\frac{n\alpha e^{-\frac{n}{2}\left(\alpha\frac{\nu}{\nu_P} - 1\right)^2} e^{-\lambda_D T}}{\nu_P\sqrt{2\pi n}\, e^{\lambda_D t_P \frac{\nu}{\nu_P}}} \tag{23}$$

Equations 22 and 23 are the desired results, expressing the proportionation of daughter nuclei in the elution sample between those present in the original parent–daughter mixture loaded onto the chromatograph column (*i.e.*, *primary*) and those produced by parent decay subsequent to the initiation of the separation process (*i.e.*, *secondary*).

Equation 22 contains a factor which involves incomplete gamma functions. These are not amenable to routine calculation without access to either computer facilities or uncommon mathematical tabulations. However, since the number of theoretical plates present in chromatographic columns used for efficacious separations is generally greater than one hundred, the exact bracketed term in Equation 22 may be replaced by one involving the normal probability function which is tabulated in most basic mathematical handbooks (5). Justification for the above substitution is detailed in Appendix 2. Equation 22 becomes

$$C^* = P(0)\sum_{\nu lower}^{\nu upper}\frac{n\alpha\lambda_P t_P e^{\frac{t_P}{1-\alpha}\left[\alpha\lambda_P\frac{\nu}{\nu_P} - (\lambda_P - \lambda_D)\right]} e^{-\lambda_D T}}{\nu_P[n(1 - \alpha) + t_P(\lambda_P - \lambda_D)]} \times \int_{\sqrt{4n\alpha c\nu/\nu_P} - \sqrt{4n + 3}}^{\sqrt{4nc\nu/\nu_P} - \sqrt{4n + 3}} \frac{e^{-\frac{1}{2}z^2}}{\sqrt{2\pi}}\, dx \tag{24}$$

(5) "Handbook of Chemistry and Physics," Chemical Rubber Publishing Co., Cleveland, Ohio.

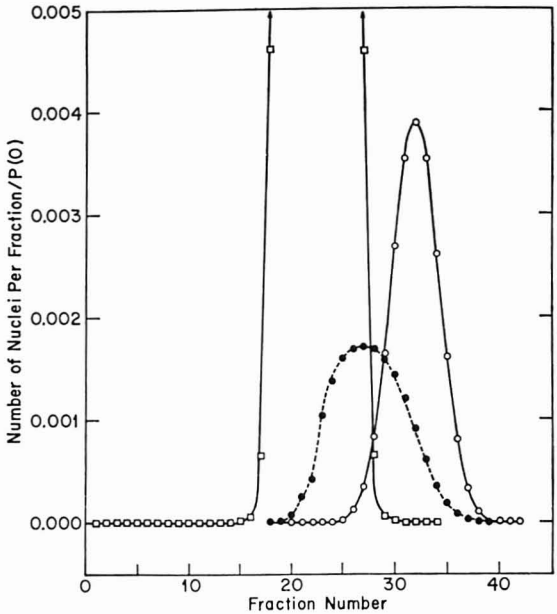

Figure 2. Elution curve calculated for a mixture of ^{166}Tm (7.7 hr) and ^{166}Yb (57 hr) → ^{166}Tm where at the initiation of the elution process there is 40 times as much Yb present as Tm on the column. The flow rate is such that the Yb elution peak occurs after 1 hr of flow. Solid curves represent undecayed ^{166}Yb and ^{166}Tm which were originally part of the sample load. The dotted curve represents ^{166}Tm produced from ^{166}Yb decay during the course of the elution

Equation 24 contains only decay constants, flow rate, peak positions, and peak widths as parameters, all of which are fixed by the particular separation under investigation.

EFFECTIVE TIME OF SEPARATION

The form in which results calculated directly from Equations 23 and 24 appear can be expressed in a more convenient alternative form, in terms of an "effective time of separation" of parent and daughter components by which is meant the following: if one were to have a mixture containing $P(0)$ and $D(0)$ nuclei at time $t = 0$ and an hypothetical instantaneous separation were to occur at some subsequent time $t = \tau_s$, then at time τ_s the number of parent nuclei $P(\tau_s) = P(0)e^{-\lambda_P \tau_s}$, the number of undecayed original daughter nuclei $\bar{D}'(\tau_s) = D(0)^{-\lambda_D \tau_s}$, and the number of decay-produced daughter nuclei $\bar{C}(\tau_s) = \lambda_P P(0)[e^{-\lambda_P \tau_s} - e^{-\lambda_D \tau_s}]/(\lambda_D - \lambda_P)$. The time τ_s is defined by equating the ratio $\bar{D}'(\tau_s)/D(0):\bar{C}(\tau_s)/P(0)$ from the above hypothetical partition to the equivalent ratio calculated from Equations 23 and 24 using data from the actual experimental chromatogram. This ratio is used in order to obviate the necessity of knowing the value for $D(0)/P(0)$. "Effective time of separation" is thus the time at which a hypothetical instantaneous separation of parent and daughter species would yield the same parent–daughter proportionation in a sample as is obtained from the actual column procedure.

From the above discussion

$$\frac{\bar{D}'(\tau_s)/D(0)}{\bar{C}(\tau_s)/P(0)} = \frac{e^{-\lambda_D \tau_s}}{\lambda_P[e^{-\lambda_P \tau_s} - e^{-\lambda_D \tau_s}]/(\lambda_D - \lambda_P)} \qquad (25)$$

where

$$\frac{\bar{D}'(\tau_s)/D(0)}{\bar{C}(\tau_s)/P(0)} = \frac{D^*/D(0)}{C^*/P(0)} \qquad (26)$$

which yields the effective time of separation

$$\tau_s = \frac{1}{\lambda_D - \lambda_P} \ln\left[1 + \frac{\lambda_D - \lambda_P}{\lambda_P} \cdot \frac{C^*/P(0)}{D^*/D(0)}\right] \qquad (27)$$

Equations 23 and 24 can be used to evaluate $C^*/P(0)$ and $D^*/D(0)$ from data. Note that from Equations 23, 24, and 27, T, the time of consolidation of the numerous fractions into a single sample, cancels out when Expression 27 is used, provided normal tailing (cross contamination) is negligible in comparison to hereditary contamination in the sample, as is assumed.

EXAMPLE

As an illustration of the phenomenon under discussion one can consider the following case: cation exchange separation of ^{166}Yb (57 hr) parent from ^{166}Tm (7.7 hr) daughter where at the start of elution there are 40 times as many ^{166}Yb nuclei as ^{166}Tm nuclei, the column contains 200 theoretical plates as determined from the Yb elution curve and Equation 8, and the Yb and Tm maxima elute at fraction numbers 22.5 and 32, respectively. Figure 2 is the calculated elution curve for a flow rate of $2^2/_3$ minutes per fraction, that is, the Yb peaks ~1 hr after elution commences. The solid curves are for ^{166}Yb and (*primary*) ^{166}Tm. The tailing of Yb into Tm is minimal. The dotted curve delineates the amount of parent-produced (*secondary*) ^{166}Tm in each fraction. If one were to consolidate fractions 28 through 38 into a ^{166}Tm sample, 27% of the total ^{166}Tm would be contaminant ^{166}Tm. Alternatively, this result is expressible as an effective time of separation, τ_s of 0.13 hr. If instead one combined fractions 32 through 38, then 15% of the total ^{166}Tm in the sample would be due to hereditary contamination reducing τ_s to 0.06 hr. This example serves to illustrate the magnitude of the hereditary contamination correction only for these specific circumstances.

In the general case a rough estimate of C^*/D^* can be made by an *a priori* argument. If the entire *primary* daughter elution peak were consolidated into the final sample then $D^* \leq D(0)e^{-\lambda_D \tau_r}$ and the number of *secondary* daughter nuclei due to parent decay can be no greater than the number of decayed parent nuclei, *i.e.*, $C^* < P(0)(1 - e^{-\lambda_P \tau_r})$. Taking t_P as a very rough approximation to τ_r, the relative magnitudes of contaminant to indigenous (*secondary* to *primary*) species and hence the practicality of the foregoing method may be extracted from

$$\frac{C^*}{D^*} \sim \frac{P(0)}{D(0)} \frac{(1 - e^{-\lambda_P t_P})}{e^{-\lambda_D t_P}}$$

This is consistent with the preceding rigorous calculation of a specific example.

CONCLUSION

A general method has been devised for calculating the component elution curves in a system where one radioactive species is produced by transformation of a radioactive parent at a rate comparable to the separation rate of the parent and daughter species on a chromatographic column. The result is expressible as a hypothetical instantaneous effective separation time which may be calculated from the half-lives and column elution characteristics of the nuclides.

APPENDIX 1

The differential equations we have to deal with are all of the form

$$\frac{dN_i}{dv} = r_i(v) - \zeta N_i(v) \qquad (i = 1, 2, \ldots, n + 1) \qquad \text{(A1)}$$

where $N_i(v)$ is the number of atoms (or other entity) in the ith plate after volume v of eluent has been passed; $r_i(v)$ is the known rate (per unit volume of eluent) of addition of atoms to the ith plate; and ζ is a known constant.

Equation A1 with t in place of v and λ in place of ζ is the customary equation for a radioactive nuclide of decay constant λ that is being created at rate $r_i(t)$. There are a variety of ways of solving such equations. In the original version of this work, the author solved them by the method of the Laplace Transform. Rubinson (*6*), who was kind enough to read that version critically, then communicated to the author a set of solutions obtained in a more elementary way by the method he had used to derive the equations of radioactive transformation (*7*). The fact that the two methods gave identical results makes it fairly certain that the final equations are mathematically correct. We will follow Rubinson's simpler method in our exposition.

In Equation A1 we recognize that

$$\frac{dN_i}{dv} + \zeta N_i = e^{-\zeta v} \frac{d}{dv} (e^{\zeta v} N_i)$$

so that Equation A1 can be written

$$\frac{d}{dv} (e^{\zeta v} N_i) = e^{\zeta v} r_i(v)$$

Integration of the latter between $v = 0$ and $v = V$ gives a result that can be put in the form

$$N_i(V) = N_i(0)e^{-\zeta V} + e^{-\zeta V} \int_0^V r_i(v)e^{\zeta v} dv \qquad \text{(A2)}$$

This is our basic equation, from which all our solutions are obtained by specialization.

Solution of Equation 1 of Section I and Equation 6 of Section II. These two sets of equations differ only in that in Equation 1 the atoms are nonradioactive, while in Equation 6 they are radioactive. Therefore, the solutions of Equation 1 can be obtained from those of Equation 6 by setting the decay constant in the latter equal to zero.

We write Equation 6 in the form

$$\frac{dP_i(v)}{dv} = K_P P_{i-1}(v) - \sigma P_i(v) \qquad \text{(A3)}$$

where

$$\sigma = K_P + \Lambda_P \qquad \text{(A4)}$$

Explicitly, Equation A3 is the set of differential equations

$$\left.\begin{aligned} \frac{dP_1}{dv} &= -\sigma P_1 \\ \frac{dP_2}{dv} &= K_P P_1 - \sigma P_2 \\ &\cdot \\ &\cdot \\ &\cdot \\ \frac{dP_{n+1}}{dv} &= K_P P_n - \sigma P_{n+1} \end{aligned}\right\} \qquad \text{(A5)}$$

These are to be solved for the case of the initial conditions

$$P_1(0) = P(0), \text{ and } P_i(0) = 0 \text{ for } i > 1 \qquad \text{(A6)}$$

We note that Equations (A5) are of the form (A1) with $\zeta = \sigma$ and

$$r_1(v) = 0; \; r_i(v) = K_P P_{i-1} \text{ for } i > 1 \qquad \text{(A7)}$$

In view of Equations A6 and A7, Equation A2 gives, for $i = 1$,

$$P_1(V) = P(0)e^{-\sigma V} \qquad \text{(A8)}$$

and for $i > 1$,

$$P_i(V) = K_P e^{-\sigma V} \int_0^V P_{i-1}(v)e^{\sigma v} dv \qquad \text{(A9)}$$

For $i = 2$, Equation A9 gives, with use of Equation A8

$$P_2(V) = K_P P(0)e^{-\sigma V} \int_0^V dv = K_P P(0)Ve^{-\sigma V} \qquad \text{(A10)}$$

For $i = 3$, Equation A9 gives, with use of Equation A10

$$P_3(V) = K_P{}^2 P(0)e^{-\sigma V} \int_0^V v dv = P(0) \frac{(K_P V)^2}{2} e^{-\sigma V} \qquad \text{(A11)}$$

Continuing in this way with $i = 4, 5 \ldots, n + 1$ in succession, we obtain

$$P_{n+1}(V) = P(0) \frac{(K_P V)^n}{n!} e^{-\sigma V} \qquad \text{(A12)}$$

which, in view of Equation A4, is Equation 6 of Section II.

To prove Equation 2 of Section I, we note if the species is nonradioactive, then the Λ_P in Equation A4 is equal to zero (see the remark following Equation 6 of Section II), in which case Equation A3 reduces to

$$dP_i/dv = K_P P_{i-1} - K_P P_i \qquad \text{(A13)}$$

(6) W. Rubinson, Chemistry Department, Brookhaven National Laboratory, private communication, 1970.
(7) W. Rubinson, *J. Chem. Phys.*, **17**, 542 (1949).

and Equation A12 reduces to

$$P_{n+1}(V) = P(0)\frac{(K_P V)^n}{n!}e^{-K_P V} \quad \text{(A14)}$$

Except for notation these are identical with, respectively, Equations 1 and 2 of Section I.

Solution of Equation 9 of Section II. We write these equations in the form

$$dD_i/d\upsilon = \Lambda_P P_i + K_D D_{i-1} - \rho D_i \quad (i = 1, 2, \ldots, n+1) \quad \text{(A15)}$$

where

$$\rho = K_D + \Lambda_D \quad \text{(A16)}$$

and solve them for the case of the initial conditions

$$D_i(0) = 0 \text{ for all } i \quad \text{(A17)}$$

i.e., for the case where there is no daughter activity in the initial loading, $D_i = C_i$. Any amount $D_i'(0) = D'(0)$ of daughter activity in the initial loading will pass through the column according to an equation of the same form as that of the parent Equation, A12:

$$D'_{n+1}(V) = D'(0)\frac{(K_D V)^n}{n!}e^{-\rho V} \quad \text{(A18)}$$

and the overall distribution of daughter in the column is obtained by adding this expression to the distribution $C_{n+1}(V)$ of daughter generated from the parent on the column [*cf.* Equation A36 below].

Equation A15 is of the form A1 with

$$r_i(\upsilon) = K_D D_{i-1}(\upsilon) + \Lambda_P P_i(\upsilon), \text{ and } \zeta = \rho \quad \text{(A19)}$$

In view of Equations A17 and A19, Equation A2 gives

$$D_i(V) = e^{-\rho V}\int_0^V [K_D D_{i-1}(\upsilon) + \Lambda_P P_i(\upsilon)]e^{\rho\upsilon}\, d\upsilon \quad \text{(A20)}$$

where $\Lambda_P P_i(\upsilon)$ is known from Equation A12:

$$\Lambda_P P_i(\upsilon) = \Lambda_P P(0)\frac{(K_P\upsilon)^{i-1}}{(i-1)!}e^{-\sigma\upsilon} \quad \text{(A21)}$$

For the case $i = 1$, Equation A20 gives, with use of Equation A21 (note that $D_i(0) = 0$ for $i > 1$)

$$D_1(V) = \Lambda_P P(0) e^{-\rho V}\int_0^V e^{-(\sigma-\rho)\upsilon}\, d\upsilon$$

or, with the abbreviation

$$\omega = \sigma - \rho \quad \text{(A22)}$$

$$D_1(V) = \Lambda_P P(0)\, e^{-\rho V}\frac{(1 - e^{-\omega V})}{\omega} \quad \text{(A23)}$$

For the subsequent deductions, it will simplify matters greatly if we write Equation A21 in the form [*cf.* (A22)]

$$\Lambda_P P_i(\upsilon) = \Lambda_P P(0)\left(\frac{K_P\omega\upsilon}{\omega}\right)^{i-1}\frac{e^{-\omega\upsilon}\, e^{-\rho\upsilon}}{(i-1)!} \quad \text{(A24)}$$

Then with Equations A23 and A24, Equation A20 for the case $i = 2$ is

$$D_2(\upsilon) = \frac{\Lambda_P P(0)}{\omega}\, e^{-\rho V}\int_0^V [K_D(1 - e^{-\omega\upsilon}) + K_P\omega\upsilon e^{-\omega\upsilon}]\, d\upsilon \quad \text{(A25)}$$

Recalling that

$$\alpha = K_D/K_P \quad \text{(13)}$$

and defining

$$x = \omega\upsilon;\ u = \omega V \quad \text{(A27)}$$

Then Equation A25 can be written

$$D_2(V) = \frac{\Lambda_P P(0) K_P}{\omega^2}\, e^{-\rho V}\int_0^u [\alpha(1 - e^{-x}) + xe^{-x}]dx \quad \text{(A28)}$$

The integrals are elementary. Their values and those of subsequent integrals that will arise can be written down directly by noting that by successive partial integrations

$$\int_0^u x^n e^{-x}dx = \int_0^\infty x^n e^{-x}dx - \int_u^\infty x^n e^{-x}dx = n!\left(1 - e^{-u}\sum_{j=0}^{n}\frac{u^j}{j!}\right) \quad \text{(A29)}$$

This is the so-called "incomplete gamma function," conventionally denoted by $\gamma(n+1, u)$ (*cf.* Equation 16).

Evaluation of Equation A28 gives a result that can be manipulated into the form

$$D_2(V) = \frac{\Lambda_P P(0) K_P}{\omega^2}\, e^{-\rho V}[(1 - \alpha)(1 - e^{-u}) + (\alpha - e^{-u})u] \quad \text{(A30)}$$

In the same way Equation A20 can be evaluated for the case $i = 3$ by use of Equations A24 and A30. The result can be put in the form

$$D_3(V) = \Lambda_P P(0)\frac{K_P^2}{\omega^3}\, e^{-\rho V}\, I_3 \quad \text{(A31a)}$$

where

$$I_3 = (1 - \alpha)^2(1 - e^{-u}) + (1 - \alpha)(\alpha - e^{-u})u + (\alpha^2 - e^{-u})\frac{u^2}{2!} \quad \text{(A31b)}$$

Equations A31 display a pattern that leads us to infer that

$$D_{n+1}(V) = \Lambda_P P(0)\frac{K_P^n}{\omega^{n+1}}\, e^{-\rho V}\, I_{n+1} \quad \text{(A32a)}$$

where

$$I_{n+1} = \sum_{j=0}^{n}(1 - \alpha)^{n-j}(\alpha^j - e^{-u})\frac{u^j}{j!} \quad \text{(A32b)}$$

Rubinson (*6*) has proved Equation A32 by mathematical induction, but the proof will not be given here.

We proceed to transform Equation A32 to a form convenient for numerical evaluation. Writing A32b as

$$I_{n+1} = (1 - \alpha)^n\sum_{j=0}^{n}\left[\left(\frac{\alpha}{1-\alpha}\right)^j\frac{u^j}{j!} - \left(\frac{1}{1-\alpha}\right)^j e^{-u}\frac{u^j}{j!}\right]$$

and introducing the new variables

$$y = \frac{\alpha}{1-\alpha}u;\ z = \frac{1}{1-\alpha}u = y + u \quad \text{(A33)}$$

we get

$$I_{n+1} = (1-\alpha)^n \sum_{j=0}^{n} \left[\frac{y^j}{j!} - \frac{z^j}{j!} e^{-(z-y)} \right] =$$

$$(1-\alpha)^n e^y \sum_{j=0}^{n} \left(e^{-y} \frac{y^j}{j!} - e^{-z} \frac{z^j}{j!} \right) \quad \text{(A34)}$$

By the definition of the incomplete gamma function $\gamma(n+1, u)$, (Equation 16)

$$\sum_{j=0}^{n} e^{-u} \frac{u^j}{j!} = 1 - \frac{\gamma(n+1, u)}{n!}$$

so Equation A34 can be written

$$I_{n+1} = (1-\alpha)^n \frac{e^y}{n!} [\gamma(n+1, y) - \gamma(n+1, z)] \quad \text{(A35)}$$

Insertion of Equation A35 into A32a and reversion to our original notation by means of Equations A33, A27, A26, A22, A16, and A4 gives

$$D_{n+1}(V) C_{n+1}(V) = \Lambda_P P(0) \frac{e^{K_D c V}}{(K_P - K_D) c^{n+1} n!} \times$$

$$[\gamma(n+1, K_D c V) - \gamma(n+1, K_P c V)] \quad \text{(A36)}$$

$$c = \frac{\omega}{K_P - K_D} = 1 - \frac{\Lambda_P - \Lambda_D}{K_P - K_D} \quad \text{(A37)}$$

Equation A36 is converted to Equation 15 of the text by means of the appropriate substitutions.

As remarked below Equation A17, the solution, Equation A36, pertains to the case in which there is no daughter activity in the initial load on the column. If the initial load contains an amount $D'(0)$ of daughter activity, then Equation A18 must be added to Equation A36. See Equation 10.

APPENDIX 2

Equation 21 is exact and may be used as such. However, the bracketed term contains the incomplete gamma function for whose evaluation one must resort to Pearson's "Tables of the Incomplete Gamma Function" (*8*) which are useful over a limited range of n. Otherwise numerical determination *via* computer is necessary.

For large values of n such as those routinely encountered in column work, an asymptotic approximation to $\gamma(n+1, u)$ is possible. From the chapter on "Probability Functions" in Reference (*9*) one finds that

$$\gamma(n+1, u) = n![1 - Q(\chi^2|\eta)] \quad \text{(B1)}$$

where $\eta = 2(n+1)$, $\chi^2 = 2u$ and

$$Q(\chi^2|\eta) = \left[2^{\eta/2} \left(\frac{\eta}{2} + 1 \right)! \right]^{-1} \int_{\chi^2}^{\infty} t^{(\eta-2)/2} e^{-t/2} \, dt \quad \text{(B2)}$$

$$(0 \leq \chi^2 \leq \infty)$$

is a chi-square probability function. For $\nu > 100$, that is $n + 1 > 50$

$$Q(\chi^2|\eta) \approx Q(l) \quad \text{(B3)}$$

where

$$Q(l) = (2\pi)^{-1/2} \int_l^{\infty} e^{-z^2/2} \, dx \quad \text{(B4)}$$

and

$$l = \sqrt{2\chi^2} - \sqrt{2\eta - 1} \quad \text{(B5a)}$$

$$= \sqrt{4u} - \sqrt{4n + 3} \quad \text{(B5b)}$$

From the above equations, the following approximation results

$$\frac{[\gamma(n+1, u_2) - \gamma(n+1, u_1)]}{n!} \approx (2\pi)^{-1/2} \int_{l_1}^{l_2} e^{-z^2/2} \, dx \quad \text{(B6)}$$

which is the form used in Equation 24.

APPENDIX 3. LIST OF IMPORTANT SYMBOLS

c = $(K_P - K_D + \Lambda_P - \Lambda_D)/(K_P - K_D)$ see Equations 14 and A37

$C_i(V)$ = number of daughter nuclei in plate i which have been generated during the course of elution by parent decay: *secondary* daughter nuclei in plate i

C^* = number of (*secondary*) daughter nuclei in a sample consolidated from the chromatographic effluent, which nuclei were originally parent species at the time the elution process commenced, *i.e.*, "hereditary contaminant" in final sample; see Equation 22

D^* = number of (*primary*) daughter nuclei in a sample consolidated from the chromatographic effluent, which nuclei have undergone no transmutation during elution; see Equation 23

$D_i(V)$ = total number of daughter nuclei in plate i

$D_i'(V)$ = number of daughter nuclei in plate i which have not undergone radioactive transformation, *i.e.*, are indigenous to the column loading: *primary* daughter nuclei in plate i

$D'(0)$ = number of daughter nuclei in column loading at initiation of elution process

i = index for plate number in column; $1 \leq i \leq n+1$

K = the fraction of all nuclei of given type in the mobile phase per unit volume mobile phase

K_D = the fraction of all daughter nuclei in the mobile phase per unit volume mobile phase.

K_P = the fraction of all parent nuclei in the mobile phase per unit volume mobile phase

$N(0)$ = number of nuclei of particular species on column at initiation of elution process

$n+1$ = number of theoretical plates in the column

$n!$ = n factorial = $n(n-1)(n-2)\cdots 3\cdot 2\cdot 1$

$P_i(V)$ = total number of parent nuclei in plate i

$P(0)$ = number of parent nuclei in column loading at initiation of elution process

t = time elapsed since initiation of eluent flow

t_P = time at which the peak in the elution curve for parent species emerges from the column

T = time at which the fractions comprising the final sample of "daughter species" are combined

V = eluent volume

(8) K. Pearson, "Tables of the Incomplete Γ-Function," University Press, Cambridge, England, 1957.

(9) M. Abramowitz and Irene A. Stegun, Ed., "Handbook of Mathematical Functions," Dover Publications, New York, N. Y., 1965.

V_e = volume at which the peak in the general elution curve emerges; see Figure 1

V_D = volume at which the peak in the elution curve for daughter species emerges

V_P = volume at which the peak in the elution curve for parent species emerges

α = parent-daughter separation factor, *i.e.*, V_P/V_D

β = width of elution curve at e^{-1} times the maximum; see Figure 1

$\gamma(n+1, u)$ = incomplete gamma function; see Equation 16

λ_D = decay constant of daughter species

λ_P = decay constant of parent species

Λ_D = fraction of daughter nuclei per unit volume which decay in the time the unit volume flows, *i.e.*, $\lambda_D dt/dV$

Λ_P = fraction of parent nuclei per unit volume which decay in the time the unit volume flows, *i.e.*, $\lambda_P dt/dV$

ν = fraction number

ν_P = fraction number at which parent species elution curve peaks

τ_s = effective time of separation, *i.e.*, the time at which a hypothetical instantaneous separation of parent and daughter species would yield the same sample as is obtained from the column procedure; see Equation 27

ϕ = column flow rate, dV/dt

ACKNOWLEDGMENT

The author expresses his considerable gratitude to Dr. William Rubinson of Brookhaven National Laboratory for his thorough examination of the mathematical manipulations employed in this work and in particular for his valuable comments and suggestions on simplifying the final form in which these derivations are published.

RECEIVED for review February 25, 1971. Accepted May 19, 1971. Presented in condensed form at the 159th ACS Meeting, Houston, Texas, February, 1970. The author gratefully acknowledges the support of the ACS Petroleum Research Fund, Grant Number 2085-G3, and also partial support by a University Scaife Grant.

Separation of Uranium from Seawater by Adsorbing Colloid Flotation

Young S. Kim and Harry Zeitlin

Department of Chemistry and Hawaii Institute of Geophysics, University of Hawaii, Honolulu, Hawaii 96822

A procedure is described for the separation from seawater of uranium present as the stable tricarbonatouranyl anion by an adsorbing colloid flotation technique which utilizes a collector–surfactant–air system. At pH 6.7 ± 0.1 the uranium is adsorbed effectively on the positively charged ferric hydroxide collector. Upon addition of the anionic surfactant, sodium dodecyl sulfate, and the bubbling of air through the seawater, the colloidal particulates of ferric hydroxide enriched with uranium by absorption are floated within 2–3 minutes to the surface as a stable froth which is easily removed. Uranium was analyzed spectrophotometrically using Rhodamine B. Average recovery of uranium from seawater by this method is 82%.

A RECENT PAPER (*1*) has described the first application of a bubble technique to seawater for the separation of a trace metallic constituent. Under optimal conditions, molybdenum as molybdate is floated to the surface quantitatively and reproducibly in less than five minutes as an easily removable froth by a positively charged iron(III) hydroxide collector, an anionic surfactant (dodecyl sodium sulfate), and air.

The behavior of the collector–surfactant–air system toward a metallic anionic species such as molybdate prompted an investigation to determine whether the flotation method could be applied successfully to other trace metals which exist in seawater as anions. This communication is concerned primarily with the extension of the separation process to uranium believed to be present in seawater as the very stable tricarbonatouranylate ion, $UO_2(CO_3)_3^{4-}$ (*2*) [$K_{diss} = 1.7 \times 10^{-23}$ (*3*)]. Other methods for the separation of uranium in seawater which is present in the 2.9–3.3 μg/l. range include coprecipitation with aluminum phosphate and ferric hydroxide and solvent extraction (*4*). In order to determine the separated uranium spectrophotometrically, a modified procedure was worked out involving Rhodamine B (*5*, *6*) which proves to be comparable to other spectrophotometric and fluorometric methods (*7*, *8*), eliminating the need for a fluorescence attachment. Rhodamine B has not been employed previously for the determination of uranium in natural waters.

EXPERIMENTAL

Apparatus and Equipment. A Beckman DU spectrophotometer was used for absorbance measurements. The absorbances were read in low volume matched quartz cells of 1.0-cm path length. The pH of the solutions was de-

(1) Y. S. Kim and H. Zeitlin, *Separ. Sci.*, in press.

(2) E. D. Goldberg, "The Sea," M. N. Hill, Ed., Vol. 2, Interscience, New York, N. Y., 1966, p 5.
(3) A. G. Klygin and I. D. Smirnova, *Russ. J. Inorg. Chem.*, **4**, 42 (1959).
(4) J. P. Riley and G. Skirrow, "Chemical Oceanography," Vol. 2, Academic Press, London, New York, 1965, pp 391–392.
(5) Frausto da Silva and Legrand de Moura, *Int. Conf. Peaceful Uses At. Energy*, **28**, 537 (1958).
(6) H. H. Ph. Mocken and W. A. H. Van Neste, *Anal. Chim. Acta*, **37**, 480 (1967).
(7) Academy of Sciences of the USSR, "Analytical Chemistry of Uranium," Israel Program for Scientific Translations, 1963.
(8) E. B. Sandell, "Colorimetric Determination of Traces of Metals," 3rd ed., Interscience, New York, N. Y., 1965, p 903.

termined by a Beckman Expandomatic pH meter. Millipore filters, HA 47-mm diameter, were used to filter seawater samples. The flotation unit was similar to that described previously (*1*).

Reagents. All chemicals were of analytical grade. Aqueous reagents were prepared in doubly distilled deionized water. A solution of calcium nitrate tetrahydrate containing EDTA was used as a salting reagent in the extraction of uranium (*9*). Rhodamine B reagent was prepared by the saturation of sodium-dried benzene containing 1% benzoic acid with Rhodamine B. A buffer, pH ~7.5 was prepared from ammonium hydroxide–ammonium nitrate (0.05*M*–0.9*M*). The surfactant was dodecyl sodium sulfate (0.05% in ethanol). A 0.05*M* ferric chloride solution served as the collector. A standard uranium solution was prepared by dissolving 22.8 mg of sodium tricarbonatouranylate, $Na_4[UO_2(CO_3)_3]$, (*10*) in 1 liter of water and adding 1 gram of sodium bicarbonate to stabilize the solution. Ten milliliters of this solution were diluted to 100.0 ml which provided a solution containing 1 μg of U/ml.

Separation of Uranium from Seawater. The flotation setup and procedure were similar to those described previously for molybdenum (*1*). The principal parameters studied were pH of the seawater sample and volume of ferric chloride solution. For this purpose clear uncontaminated nearshore seawater was filtered through a 0.45-μ millipore filter. To the 500 ml samples used in the pH studies were added 3 ml of 0.05*M* ferric chloride and 6.0 μg of uranium. The samples were adjusted to pH 4.0, 4.5, 5.0, 5.5, 6.0, 6.5, and 7.0 (±0.1) with 1*M* hydrochloric acid and 4*M* ammonia. The flow rate of air was adjusted to 10 ± 2 ml/min and allowed to pass for five minutes. Following the flotation, the froth was removed, dissolved in 3–4 ml of 12*M* HCl–16*M* HNO_3 (4:1) and the solution evaporated to a few ml. Uranium was determined by the method described below. The results are given in Figure 1. The optimum volume of ferric chloride solution used as the collector was determined by varying the volume of the 0.05*M* solution and examining the effect on recovery at the previously determined optimum pH of 5.7 ± 0.1 (Figure 2).

Optimum Conditions for Extraction and Determination. When aluminum nitrate was found to be unsuitable as a salting agent for the extraction of uranium, calcium nitrate was substituted satisfactorily. The optimum volume of this reagent was determined by adding, in a series of experiments, 5, 10, 15, 20, and 25 ml of calcium nitrate salting reagent to the near-dry residues contained in vials (see below). Each residue was warmed until it had dissolved. The solution was cooled and 6.0 ml of ethyl acetate were added. Separation of the two layers was carried out with a centrifuge. Five milliliters of the upper organic layer were transferred to a small vial and the solvent evaporated to dryness at 80 to 90 °C. Two drops of dilute nitric acid were added and the evaporation repeated and the residue dissolved in 1 ml of buffer solution (below). In order to obtain the pH for maximum color development of the uranyl–Rhodamine B complex, each residue obtained by extraction with ethyl acetate was dissolved in 1 ml of buffer solution of varying pH (2.2–9.2) and 2.0 ml of Rhodamine B reagent added. The mixture was centrifuged for separation of the two layers. The pink-colored upper layer was transferred to the reduced volume absorption cell by an eye dropper and the absorbance measured against the reagent blank at 555 nm.

Recovery of Uranium. Assessment of recovery was made by comparison of the absorbance obtained from the analysis utilizing the flotation technique under optimal conditions

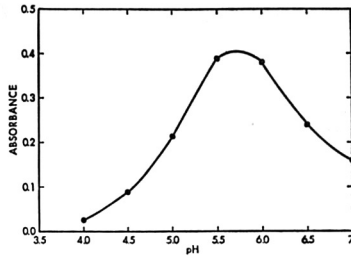

Figure 1. Optimum pH of sample solution for separation by flotation

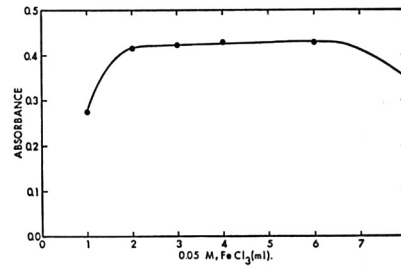

Figure 2. Optimum volume of ferric chloride solution for separation by flotation

with those obtained from the direct analysis of replicate distilled water standards containing 0.0, 2.0, 4.0, and 6.0 μg of uranium in which the coprecipitation and flotation steps were omitted. The latter absorbances were considered to represent 100% recovery of uranium. The results are given in Table I. Interference by the presence of WO_4^{2-} and MoO_4^{2-} which were believed collected by ferric hydroxide was checked by adding these species in amounts four times greater than those in seawater to the Rhodamine B reagent and measuring the effect on the absorbance of the uranium–Rhodamine B complex.

Precision and Reproducibility. An analytical procedure for the determination of uranium in seawater using Rhodamine B was worked out and its precision and reproducibility of recovery measured at one concentration.

Procedure. SEPARATION OF URANIUM FROM SEAWATER. A well-mixed pool of clear uncontaminated seawater filtered through a 0.45-μ millipore filter was used as a source of samples. In order to prepare a working curve, 3 ml of 0.05*M* ferric chloride solution were added to 500-ml samples con-

Table I. Calibration and Working-Curve Data

U, μg	A^a	A'^b	A''^c	Recovery, %
0.0	0.000	0.077	0.000	
2.0	0.124	0.181	0.104	83
4.0	0.255	0.283	0.206	81
6.0	0.374	0.382	0.305	82
				Av 82

[a] Absorbances from standard solutions without coprecipitation and flotation.

[b] Absorbances from 500-ml seawater samples plus added uranium. Reagents solution served as a blank.

[c] $A'' = A' - 0.077$.

(9) T. M. Florence, D. A. Johnson, and Yvonne J. Farrar, ANAL. CHEM., **41**, 1652 (1969).

(10) Academy of Sciences of the USSR, "Complex Compounds of Uranium," I. I. Chernaev, Ed., Israel Program for Scientific Translation, 1966, p 34.

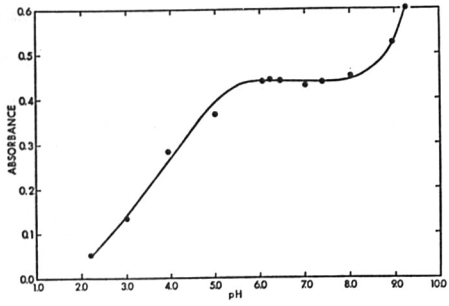

Figure 3. Effect of pH on formation of uranyl–Rhodamine B complex

Table II. Reproducibility of Recovery

Sample No.	Absorbance[a]	Deviation
1	0.377	−0.012
2	0.396	+0.007
3	0.376	−0.013
4	0.391	+0.002
5	0.394	+0.005
Mean	0.389	0.008

[a] From 500-ml seawater samples plus added uranium (6.0 μg). Reagent solution used as a blank.
Standard deviation = 0.010.

taining 0.0, 2.0, 4.0, and 6.0 μg of uranium. The pH was adjusted to 5.7 ± 0.1 with 1*M* hydrochloric acid. The flotation equipment and gas flowrate were similar to that described previously. Two milliliters of 0.05% dodecyl sodium sulfate solution were injected into the cell. After 2 to 3 minutes, the froth was removed and collected into a beaker.

ANALYSIS. The froth was dissolved in 3 to 4 ml of 12*M* HCl–16*M* HNO_3 (4:1). The solution was evaporated carefully to near-dryness and a few milliliters of water together with several drops of dilute nitric acid added. The solution was transferred to a 40-ml capacity borosilicate glass vial and evaporated again gently to dryness with baking avoided. Ten milliliters of the salting agent were added to the vial which was warmed to dissolve all salts. After being cooled to room temperature, the uranium was extracted into 6.0 ml of ethyl acetate by shaking the vial manually for one minute. Separation of the layers was effected by centrifugation for two minutes and exactly 5.0 ml of the top solvent layer was removed and transferred to another vial of 10-ml capacity. The solution was evaporated to dryness, a procedure which was most easily accomplished by insertion of the vial into holes suitably positioned in an aluminum metal block heated to about 90 °C by a hot plate. A few drops of dilute nitric acid were added to the residue and the solution again evaporated to dryness. Upon cooling, 1.0 ml of the buffer was added and residual salts dissolved. Two ml of the Rhodamine B reagent were added and the mixture was shaken for one minute. The mixture was centrifuged for one minute and the reduced volume absorption cell filled with the solution of pink complex with an eye dropper. The working curve was constructed by plotting absorbances read against the reagent blank at 555 nm obtained from the spiked seawater samples *vs.* concentration.

RESULTS AND DISCUSSION

The marked effect of pH on the recovery of uranium from seawater via flotation shown on Figure 1 demonstrates the maximum recovery based on the spectrophotometric determination as obtained between pH 5.5 and 6.0. A pH of 5.7 ± 0.1 was adopted in subsequent work. The results of tests on the effect of the ferric chloride collector on recovery are given in Figure 2. There appears to be no significant difference in the 2- to 6-ml range, and 3 ml of 0.05 *M* ferric chloride solution were chosen for use in the final procedure. The role of ferric hydroxide as a trace metal collector formed from ferric chloride in seawater was recently clarified (*11*). At a low pH, ferric hydroxide, whose charge is pH-dependent, has positive charge density and should adsorb on its active surface sites the stable uranyl carbonate complex through electrostatic attraction. The positively charged ferric hydroxide particulates thus enriched with uranium are attached to the anionic surfactant and floated to the surface through bubble formation. Recovery assessment was carried out by measuring the absorbances, following analysis of distilled water standards containing uranium in which the coprecipitation and flotation were omitted, and comparing them with the absorbances obtained from seawater standards to which uranium was added and determined following coprecipitation and flotation. The results show an average recovery of 82% (Table I). Following separation after according the seawater a similar flotation treatment, approximately 80% of the remaining uranium can be recovered resulting in a combined recovery of about 96%. The recovery data suggest the presence of the following equilibrium system:

$$4\ Fe^{3+}_{(aq)} + 3UO_2(CO_3)_3^{4-}_{(aq)} \rightleftharpoons Fe_4\,[UO_2(CO_3)_3]_{3(s)}$$

It is postulated in accordance with the Paneth–Fajans–Hahn rule (*12*) that the effectiveness of the collector depends upon the ability of Fe^{3+} reacting with the counter ion adsorbed to form a compound of low solubility; in this case, ferric uranyl carbonate with the resulting shift of the equilibrium to the right. However, the forward reaction is not quantitative as evidenced by the 82% recovery. In support of this view, previous work (*13*) has shown that both ferric hydroxide and thorium hydroxide are able to collect molybdenum as molybdate quantitatively from seawater whereas aluminum hydroxide is a very poor collector of molybdate. Solubility tests have shown that ferric and thorium molybdates are insoluble whereas aluminum molybdate is relatively soluble. No information apparently is available on the existence and solubility of ferric uranyl carbonate. An additional factor, as yet unclarified, that may be involved in the recovery of uranium is the effect of pH on the stability of $UO_2(CO_3)_3^{4-}$, particularly at pH 5.7 since the complex may not be stable in acid. Although both mechanisms may be involved to varying degrees it is believed that the former is the more dominant.

The statistical studies on a test series of five replicates for recovery of uranium from seawater spiked with 6.0 μg of uranium show a relative standard deviation of 2.6% (Table II).

In the extraction of uranium from an aqueous system, many workers employ aluminum nitrate as a salting agent (*7, 8*). With its use, the extraction of uranium as shown by the absorbance of the Rhodamine B complex was sharply diminished. This was traced to the small amount of aluminum extracted by the ethyl acetate solvent which precipitated as $Al(OH)_3$ at pH ~7–8. The solid aluminum hydroxide ap-

(11) Y. S. Kim and H. Zeitlin, *Anal. Chim. Acta*, **46**, 1 (1969).
(12) O. Hahn, "Applied Radiochemistry," Cornell University Press, Ithaca, N. Y., 1936.
(13) Y. S. Kim and H. Zeitlin, *Anal. Chim. Acta*, **51**, 516 (1970).

parently adsorbed the uranyl–Rhodamine B complex on its surface, resulting in decreased absorbance. Calcium nitrate which does not cause precipitation was substituted and worked satisfactorily. In the 6- to 8-pH range the degree of extraction and the absorbance of the pink complex are reproducible (Figure 3). The presence of WO_4^{2-} and MoO_4^{2-} revealed no interference in the formation of the Rhodamine B complex.

The calibration data for seawater are given in Table I. The absorbance of 0.077 represented the uranium originally present in the seawater which amounted to 3.2 μg/l., in general agreement with other workers (*4*, *14*).

Of the trace metals in seawater, uranium is considered to be the only one which might command a high enough market price in the foreseeable future to warrant extraction as a commercially attractive possibility (*15*). In excess of 80% of the dissolved uranium can be separated in less than five minutes on a laboratory scale by the flotation technique. A process for the large-scale separation of uranium by means of a filtering bed composed of titanium hydroxide has been tested. Preliminary work, however, has shown that 44% of the dissolved uranium was extracted per cycle which requires four days (*16*). Although the economical extraction of trace metals from seawater appears unlikely at this time, with the possible exception of uranium, the work reported herein suggests that any effort in this direction should consider the use of a flotation technique.

RECEIVED for review February 1, 1971. Accepted May 19, 1971.

(14) Y. Sugimura, *Nature*, **204**, 464 (1964).
(15) R. Spence, *Talanta*, **15**, 1307 (1968).
(16) N. J. Keen, J. H. Miler, and K. Spence, "Conference on the Technology of Sea and Sea-Bed," Vol. 2, S. B. 21, Her Majesty's Stationery Office, London, 1967.

Analysis of Binary Mixtures by Thermometric Titration Calorimetry

Lee D. Hansen and Edwin A. Lewis
Chemistry Department, University of New Mexico, Albuquerque, N. M. 87106

The objective of this study was to determine the feasibility of analyzing, by a single calorimetric titration, a binary mixture of reactants having equal or nearly equal equilibrium constants. The relative error is largely dependent upon the magnitude of the difference in the enthalpy changes for reaction of the two components. Mixtures of sodium acetate and pyridine and of phenol and glycine titrated with perchloric acid and sodium hydroxide, respectively, were used to test the method. The relative error in the method was about 5% for millimolar amounts of each component in the test systems.

BINARY MIXTURES of two reactants can be classified into four general types with respect to the differences in the free energy and enthalpy changes of their reactions with a common titrant. Two of these types, which have nearly equal enthalpy changes and either nearly equal or significantly different free energy changes for reaction with the titrant are of little interest here since the reactants are calorimetrically indistinguishable. The remaining two types of mixtures have enthalpy changes for the reactions which are significantly different. The case where the free energy changes are significantly different has previously been thoroughly studied (*1–3*). In this case, assuming quantitative reactions, the enthalpogram will exhibit a distinct end point for each reactant. The enthalpogram for the case in which the free energy changes are equal (or nearly equal) and the enthalpy changes are significantly different exhibits only one end point. However, a single calorimetric titration provides sufficient information to analyze a binary mixture of this type if the reactions are quantitative. (Calorimetric titration as used here refers to the measurement of heat changes as distinguished from thermometric titration which refers to the measurement of temperature changes.)

The present study reports the results of analysis by calorimetric titration of test mixtures containing sodium acetate ($pK_a = 4.8$, $\Delta H_t \sim 0$) and pyridine ($pK_a = 5.3$, $\Delta H_t \sim 5$), or glycine ($pK_a = 9.8$, $\Delta H_t \sim 11$) and phenol ($pK_a = 10.0$, $\Delta H \sim 6$) (*4*). These particular mixtures were chosen because the two reactants in each case have pK values that differ by less than 0.5, ΔH values that are significantly different, and the mixtures react quantitatively with strong acid and strong base, respectively. The phenol–glycine mixture was also of interest because of the similarity of this system to a polypeptide containing tyrosyl residues and free α or ε amino groups.

THEORY

Since the total number of moles, n_T, and the total heat, Q_T, can be determined in a single calorimetric titration (see Figure 2), simultaneous solution of Equations 1 and 2 with known ΔH values readily yields the number of moles of the reactants A and B, n_A and n_B, respectively, as shown by Equation 3.

$$n_T = n_A + n_B \quad (1)$$

$$Q_T = n_A \Delta H_A + n_B \Delta H_B \quad (2)$$

$$n_A = (Q_T - n_T \Delta H_B)/(\Delta H_A - \Delta H_B) \quad (3)$$

(1) L. S. Bark and S. M. Bark, "Thermometric Titrimetry," Vol. 33, International Series of Monographs in Analytical Chemistry, Pergamon Press, Elmsford, N. Y., 1969.
(2) H. J. V. Tyrell and A. E. Beezer, "Thermometric Titrimetry," Chapman and Hall, Ltd., London, 1968.
(3) J. Jordan, in "Treatise on Analytical Chemistry," I. M. Kolthoff and P. J. Elving, Ed., Part 1, Vol. 4, Wiley-Interscience, New York, N. Y., 1968, pp 5175–5242.
(4) J. J. Christensen and R. M. Izatt, Table, Heats of Proton Ionization and Related Thermodynamics Quantities, in "Handbook of Biochemistry with Selected Data for Molecular Biology," H. A. Sober, Ed., The Chemical Rubber Publishing Company, Cleveland, Ohio, 1968, pp J49–J139.

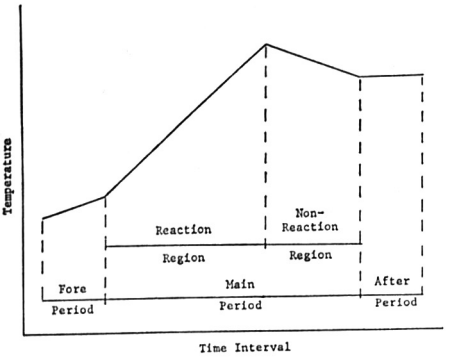

Figure 1. Periods and regions of a thermogram

Error analysis of Equation 3 allows the standard deviation, S, in n_A (or in n_B) due to errors in n_T, Q_T, ΔH_A, and ΔH_B to be calculated (Equation 4).

$$S_{n_A}^2 = \left(\frac{\partial n_A}{\partial n_T}\right)^2 S_{n_T}^2 + \left(\frac{\partial n_A}{\partial Q_T}\right) S_{Q_T}^2 + \left(\frac{\partial n_A}{\partial \Delta H_A}\right)^2 S_{\Delta H_A}^2 + \left(\frac{\partial n_A}{\partial \Delta H_B}\right)^2 S_{\Delta H_B}^2 \quad (4)$$

where:

$$\left(\frac{\partial n_A}{\partial n_T}\right) = [-\Delta H_B/(\Delta H_A - \Delta H_B)]$$

$$\left(\frac{\partial n_A}{\partial Q_T}\right) = [1/(\Delta H_A - \Delta H_B)]$$

$$\left(\frac{\partial n_A}{\partial \Delta H_A}\right) = [-(Q_T - \Delta H_B \times n_T)/(\Delta H_A - \Delta H_B)^2]$$

$$\left(\frac{\partial n_A}{\partial \Delta H_B}\right) = [(Q_T - (\Delta H_A - \Delta H_B) \times n_T - \Delta H_B \times n_T)/(\Delta H_A - \Delta H_B)^2]$$

It is apparent from Equation 4 that the error in n_A (or n_B) is primarily dependent on the inverse of the difference between ΔH_A and ΔH_B.

EXPERIMENTAL

The measurements were made using a Tronac Thermometric Titration Calorimeter, Model No. 1000A, Serial No. 106, which, as used in this study, employed a 6-ml constant rate buret, a single 100-ml Dewar (heat leak constant <0.005 min^{-1} and a thermal equilibration time <0.5 sec) as the reaction vessel, a programmable automatic timer, and digital output. The temperature sensing circuit was modified by changing the temperature sensor from a 5-kohm to a 100-kohm thermistor and the complementary resistor in the Wheatstone bridge from 15 kohm to 100 kohm. (A complete description of the calorimeter can be obtained by writing Tronac, Box 37, Orem, Utah 84057.) The Wheatstone bridge was operated at 12.000 volts and the resulting sensitivity was 139.5 mV/°K which was constant over a 1 °K range. All experiments were done with the buret and reaction vessel immersed in a constant temperature bath maintained at 298.1 ± 0.1 °K and controlled to ±0.0005 °K. A typical run consisted of 15 data points taken in the fore period, 56 data points taken in the main period, and 15 data points taken in the after period at time intervals of 40 seconds. (See Figure 1.) The buret delivery rate selected for this study was 0.1660 ml/minute.

As determined by electrical calibration the two different 100-ml reaction vessels used had energy equivalents of 0.7405 ± 0.0014 and 0.7346 ± 0.0017 cal/mV (± is the standard deviation of the mean) when containing 99.91 ml of H_2O. The energy equivalent was assumed to be the same when a dilute solution was substituted for H_2O. The energy equivalent at each data point in the main period was calculated using Equation 5

$$\epsilon_f = \epsilon_I + C_s V_i/S \quad (5)$$

where C_s is the heat capacity per ml of the solution in the Dewar, ϵ_i is the energy equivalent and V_i the titrant volume added at the ith point, ϵ_I is the initial energy equivalent, and S is the bridge sensitivity. Measurements of the energy equivalent with 105.0 ml of H_2O in the Dewar showed Equation 5 to be valid.

Since the titrant temperature was not the same as the temperature of the solution in the Dewar at the start of the titration, a correction was made by use of Equation 6,

$$Q_{\text{titrant}} = C_T V_i \Delta T \quad (6)$$

where C_T is the heat capacity per ml of the titrant and ΔT is the difference between the titrant temperature (as measured with a 1 °K Beckman differential thermometer) and the temperature inside the Dewar at the beginning of the main period. The heat capacity of the solution in the Dewar, C_s, and the heat capacity of the titrant, C_T, were assumed to be 1 cal/K/ml. These assumptions do not cause any appreciable error since both the corrections to the energy equivalent and for the titrant temperature are small.

The thermograms (*i.e.*, temperature *vs.* time) were converted into enthalpograms (*i.e.*, enthalpy *vs.* moles of titrant added) by the following procedures (5). First, the values of the slopes (mV/time interval) in the fore and after periods and of the temperatures at the beginning and end of the main period were calculated from linear equations obtained by the method of least squares. (Periods and regions are designated in Figure 1.) Since the energy equivalent of the calorimeter was different for the fore and after periods, the slopes were then converted to calories/time interval by use of the initial and final energy equivalents [*i.e.*, $(\partial H/\partial t)_j = \epsilon_j(\partial\theta/\partial t)_j$ where H is heat, θ is temperature, t is time, and j indicates the period]. Second, theoretical values of the rate of heat exchange of the calorimeter system with the surroundings, $(\partial H_E/\partial t)$, were calculated at each temperature–time data point, i, in the main period (Equation 7).

$$(\partial H_E/\partial t)_{\text{main},i} = (\partial H/\partial t)_{\text{fore}} + [(\partial H/\partial t)_{\text{fore}} - (\partial H/\partial t)_{\text{after}}] \times [(\theta_{\text{main},i} - \bar{\theta}_{\text{fore}})/(\bar{\theta}_{\text{after}} - \bar{\theta}_{\text{fore}})] \quad (7)$$

where $\bar{\theta}_j$ is the average temperature in the j period. Third, the heat exchanged with the surroundings during each time interval, Q_{E_i}, was calculated by Equation 8.

$$Q_{E_i} = [(\partial H_E/\partial t)_{\text{main},i} + (\partial H_E/\partial t)_{\text{main},(i-1)}] \times 0.5 \quad (8)$$

Last, the total heat produced from chemical effects to the ith point in the titration, Q_{R_i}, was calculated from Equation 9.

$$Q_{R_i} = \epsilon_{\text{main},i} \times (\theta_{\text{main},0} - \theta_{\text{main},i}) + \sum_i Q_{E_i} - Q_{\text{titrant}} \quad (9)$$

Q_T is obviously equal to Q_R at the end point, and can most easily be determined graphically from the enthalpogram.

(5) J. J. Christensen, R. M. Izatt, L. D. Hansen, and J. A. Partridge, *J. Phys. Chem.*, **70**, 2003 (1966).

Table I. Enthalpy Changes for Reactions Studied

Reactant	Reaction	ΔH kcal/mole[a]
Acetate	$C_2H_3O_2^- + H^+ \rightarrow C_2H_3O_2H$	0.05 ± 0.01[b]
Pyridine	$C_5H_5N + H^+ \rightarrow C_5H_5NH^+$	-4.97 ± 0.01[b]
Glycine	$CH_2(NH_3^+)COO^- + OH^- \rightarrow CH_2(NH_2)COO^- + H_2O$	-2.80 ± 0.01
Phenol	$C_6H_5OH + OH^- \rightarrow C_6H_5O^- + H_2O$	-7.75 ± 0.01

[a] Error limits given are standard deviations of the mean for a series of four runs.
[b] These values were determined in 0.01M Na_2SO_4.

Table II. Results of Analyses of Binary Mixtures

~ Mole %		Moles × 10^3					
		n_A		n_B		n_T	
Sodium acetate (n_A)	Pyridine (n_B)	Taken[a]	Found[b]	Taken[a]	Found[b]	Taken[a]	Found[b]
0	100	...	...	...	4.97 ± 0.04	...	...
10	90	0.52	0.63 ± 0.02	4.97	4.95 ± 0.04	5.49	5.57 ± 0.02
30	70	1.56	1.67 ± 0.03	3.98	3.95 ± 0.03	5.54	5.62 ± 0.02
50	50	2.62	2.75 ± 0.03	2.49	2.45 ± 0.02	5.11	5.20 ± 0.03
70	30	4.19	4.21 ± 0.08	1.49	1.52 ± 0.02	5.68	5.74 ± 0.07
90	10	5.24	5.32 ± 0.13	0.50	0.52 ± 0.03	5.74	5.85 ± 0.02
100	0	...	5.24 ± 0.03	...	...	...	...
Glycine (n_A)	Phenol (n_B)						
0	100	...	...	3.46 (by wt)	3.44 ± 0.01	...	...
10	90	0.40	0.51 ± 0.02[c]	3.46	3.33 ± 0.03[c]	3.86	3.85 ± 0.01[c]
40	60	1.19	1.32 ± 0.01	1.73	1.63 ± 0.02	2.92	2.95 ± 0.02
50	50	1.99	2.02 ± 0.02	1.73	1.65 ± 0.01	3.72	3.67 ± 0.01
70	30	1.99	2.02 ± 0.02[c]	1.04	0.97 ± 0.01[c]	3.03	2.99 ± 0.01[c]
90	10	3.18	3.28 ± 0.02	0.35	0.29 ± 0.01	3.53	3.57 ± 0.01
100	0	3.98 (by wt)	3.96 ± 0.01	...	...	...	...

[a] The moles taken for the sodium acetate–pyridine mixtures were based on the moles found for the respective 100% solutions. The moles taken in the case of glycine–phenol mixtures were based on the weight measurements.
[b] Error limits given are standard deviations for a series of four runs.
[c] Only three runs were made on these mixtures.

All heat change data were corrected for the heat of dilution of the titrant to the ionic strength extant at each data point in the main period. Because the ionic strength of the sodium acetate–pyridine solutions at the end point was a function of n_A and n_B, an iterative calculation procedure was used to correct for the heat of dilution of the titrant. Approximate values of n_A and n_B were calculated using an uncorrected Q_T value. These n_A and n_B values were then used to calculate a value for the ionic strength, which in turn was used to correct Q_T for the heat of dilution of the titrant. This process was reiterated until n_A and n_B remained constant. The iteration procedure was unnecessary for the phenol–glycine mixtures since the ionic strength at the end point was a function only of n_T. All heat of dilution data were taken from reference (*6*) and all computations were done on an IBM 360-67 computer.

The end points, and hence n_T, for all of the titrations were found graphically from the enthalpograms as plotted by a DigiData plotter (4 inches/ml).

The ΔH values for reaction of the individual components were determined by fitting selected points in the reaction region of the main period to a linear equation by the method of least squares. The ΔH value was calculated directly from the slope of the linear equation (cal/time interval) by use of the buret delivery rate (ml/time interval), and the titrant concentration (mmole/ml) (*7*).

Stock solutions of NaOAc (Baker Analyzed Reagent), pyridine (Eastman White Label), glycine (Eastman White Label) and phenol (Allied Chemical C.P.) were prepared using doubly distilled and boiled H_2O. Anhydrous sodium sulfate (Mallinckrodt AR) was added (0.15 g/100 ml) to all solutions containing sodium acetate or pyridine in order to enhance the end-point sharpness for calorimetric titration of the sodium acetate with $HClO_4$ (1.009M). The sodium acetate and pyridine stock solutions were standardized by thermometric titration. The glycine and phenol stock solution were prepared by weight and the concentrations checked by thermometric titration with NaOH solution (0.7042M).

RESULTS

In order to test the procedures and apparatus, the enthalpy of ionization of water was determined by titrating NaOH(aq) with $HClO_4$ (aq) (*7*). The average value of 13.331 ± 0.005 kcal/mole found for $\Delta H_i°$ is in excellent agreement with the value determined by Hale *et al.* (13.335) and Vanderzee and Swanson (13.336) (*8*, *9*).

The enthalpy changes for reaction of the individual components with the respective titrants as determined in this study are given in Table I.

The ΔH values given in Table I apply at the conditions under which the mixtures were analyzed. The values are in good agreement with literature values (*4*) although this is not critical for the purpose of this study since the ΔH values are in principle only calibration constants. The estimated total uncertainty in the values in Table I is ~0.05 kcal/mole.

Typical sets of enthalpograms for pyridine–sodium acetate

(6) V. B. Parker, "Thermal Properties of Aqueous Uni-univalent Electrolytes," NSRDS-NBS 2, U. S. Government Printing Office, Washington, D. C., 1965.
(7) L. D. Hansen and E. A. Lewis, *J. Chem. Thermodyn.*, **3**, 35 (1971).
(8) J. D. Hale, R. M. Izatt, and J. J. Christensen, *J. Phys. Chem.*, **67**, 2605 (1963).
(9) C. E. Vanderzee and J. A. Swanson, *ibid.*, p 2608.

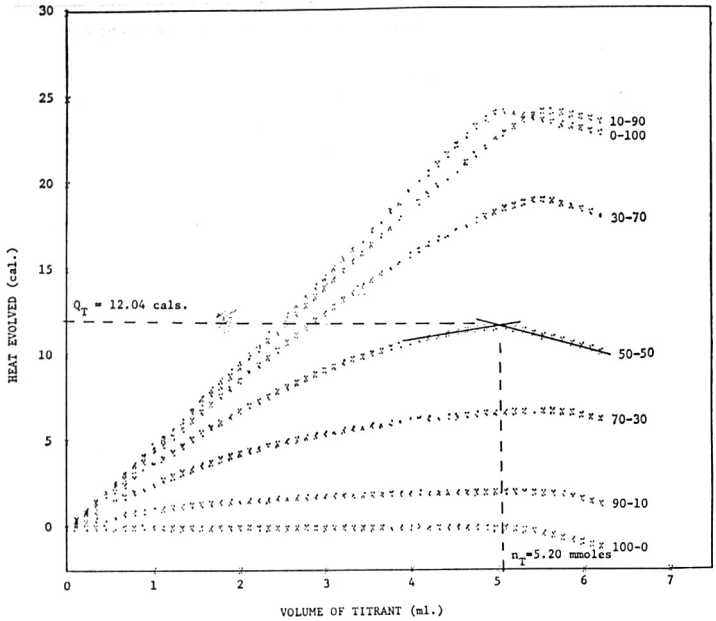

Figure 2. Enthalpograms for titration of pyridine–sodium acetate mixtures with 1.009*M* perchloric acid

Curves are labeled with approximate mol% of acetate and pyridine, respectively. (See Table II.) Sodium sulfate was added to enhance the end points. Titrant delivery rate was 0.1660 ml/minute

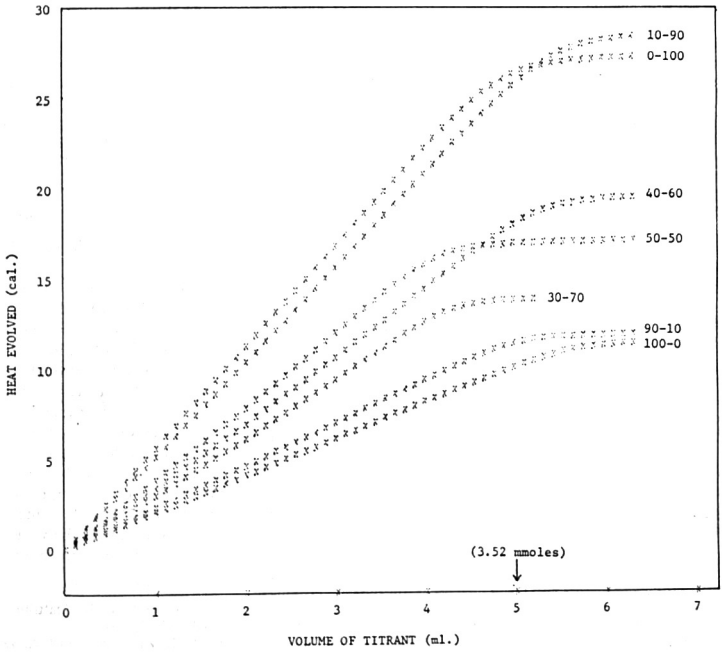

Figure 3. Enthalpograms for titration of phenol–glycine mixtures with 0.7042*M* sodium hydroxide

Curves are labeled with approximate mol % of glycine and phenol, respectively. (See Table II.) Titrant delivery rate was 0.1660 ml/minute

and phenol–glycine mixtures are shown in Figures 2 and 3, respectively. It is immediately obvious from the two series of enthalpograms that the technique is practical. The major difficulty in quantitatively analyzing these data is due to the curvature of the enthalpograms. This curvature, which is a result of the inequality of the equilibrium constants, tends to mask the end points in the systems shown in Figures 2 and 3.

The final results of the analyses of the mixtures of pyridine and sodium acetate and of phenol and glycine are given in Table II.

The difference between the amounts taken and found (Table II) is less than ±0.13 mmole for n_A and n_B in all cases. The precision of the results given in Table II is in some cases as much as one order of magnitude better than the accuracy. This observation would suggest that the accuracy could be improved by running a series of calibration enthalpograms on solutions of known composition and then comparing these to the enthalpogram of the unknown solution.

DISCUSSION

For the systems studied, Table III gives the standard deviation, S, expected in n_A (or n_B) calculated from Equation 4 and estimated errors in n_T, Q_T, ΔH_A, and ΔH_B. The total expected error (Table III) agrees well with the experimental errors in n_A and n_B actually found (Table II).

It has previously been shown that the relative error in n_T cannot be reduced to less than 1% without great effort (*10*). The particular difficulties encountered in determining n_T in this study were due to the curvature of the reaction region of the enthalpograms and the absence of an end point for the reaction of acetate (ΔH_i very small). This second difficulty was overcome by the addition of a thermochemical indicator (*11*), *i.e.*, sulfate, which is a much weaker base ($pK_a \cong 2$) than acetate but which has a sizeable enthalpy change for protonation ($\Delta H \cong -5$ kcal/mole) (*4*). Concave curvature of the enthalpograms as exhibited by the mixtures studied tended to mask the end points. However, the end point would be sharpened by convex curvature, which would result if the component with the larger enthalpy change had the smaller equilibrium constant.

Table III. Calculated Error in n_A

Estimated error	Dependence of n_A on experimental parameters	Sodium acetate–pyridine	Glycine–phenol
S_{N_T} = 0.05 mmole	$\partial n_A/\partial n_T$ =	1.0	1.6
S_{Q_T} = 0.10 cal	$\partial n_A/\partial Q_T$ =	0.2	0.2
$S_{\Delta H_A}$ = 0.05 cal/mmole	$\partial n_A/\partial \Delta H_A$ =	1.0 to 0.0[a]	1.0 to 0.0[a]
$S_{\Delta H_B}$ = 0.05 cal/mmole	$\partial n_A/\partial \Delta H_B$ =	0.0 to 1.0[a]	0.0 to 1.0[a]
	S_{n_A} =	0.07[b]	0.10[b]

[a] The actual value depends on solution composition. Extreme limits are given.
[b] Calculated from Equation 4.

The magnitude of the error in Q_T is determined primarily by the calorimetric equipment and the calculation method used to obtain the enthalpogram from the temperature–time data.

Since the ΔH values must be determined in separate experiments and since they are a function of solution composition, the values obtained may not apply exactly to the reactions as they occur in the mixed solution. However, the correct values can be closely approximated in most cases by using the ΔH values that apply at the ionic strength extant at the end point. The ΔH values would be invalid if any reactions with significant enthalpy changes occurred during the titration of the binary mixtures which did not also occur during the ΔH determinations.

Analysis of binary mixtures by thermometric titration calorimetry could be used for a variety of reactions other than acid–base as exemplified in this work. Redox, precipitation, complexation, and Lewis acid–base reactions could be utilized. Also, the procedure could be expanded to determine three reactants if another quantity such as the mass of the unknown reactant mixture was known.

ACKNOWLEDGMENT

The authors thank Mr. Robert Hill for his help in preparation of solutions.

RECEIVED for review February 8, 1971. Accepted May 19, 1971. This investigation was supported in part by a Public Health Service Research Career Development Award (Number 5-K4-GM-42,545-02) from the National Institutes of Health (L. D. H.) and in part by the Petroleum Research Fund, administered by the American Chemical Society.

(10) M. W. Brown, K. Issa, and A. G. Sinclair, *Analyst (London)*, **94,** 234 (1969).
(11) L. D. Hansen, R. M. Izatt, and J. J. Christensen, "Applications of Thermometric Titrimetry to Analytical Chemistry," in "Modern Titrimetry—A Treatise," J. Jordan, Ed., Marcel Dekker, Inc., New York, N. Y., in press.

Rotated Mercury Cell for Controlled Potential Coulometry

Elimination of Background Current by Digital Normalization

Ray G. Clem, Fredi Jakob,[1] Dane H. Anderberg,[2] and Lawrence D. Ornelas[3]

Nuclear Chemistry Division and Lawrence Radiation Laboratory, University of California, Berkeley, Calif. 94720

A cell which is rotated at high speeds and contains a thin-layer, mercury, working electrode has been developed for controlled potential coulometric determinations. The cell, which is the first successful departure from stirred mercury pool types, has several advantageous features. Constant mercury geometry assures very low noise operation and background currents that are substantially less than most stirred mercury pool cells. A large solution surface area to solution volume ratio results in sparging times that can be as short as 20 seconds. Electrolytic rate constants of 0.020, 0.017, and 0.012 sec^{-1} were obtained for the determination of Pb, Cd, and U, respectively. A unique arrangement of the reference and auxiliary electrodes has been developed. This very compact combination contains both reference and auxiliary electrodes in a single probe configuration. With this electrode, it should be possible to produce scaled down versions of the rotated mercury cell, which currently requires 2 ml of mercury and 2 ml of solution. A new procedure termed "normalization" which requires the use of digital equipment permits the elimination of the continuous background current from individual titrations. The result is improved precision.

To the best of our knowledge, the rotated cell reported in this paper embodies the first successful conceptual departure from the stirred mercury pool design first proposed by Lingane more than 25 years ago (*1*). The reported cell is a cylinder which is closed at the bottom, partially opened at the top, and is mounted on a turntable rotated at 1800 rpm with a synchronous motor. Owing to density differences and the high centripetal force, the mercury phase is held rigidly as a thin film on the wall of the cell, while the solution is forced into a film lying on top of the mercury. Contacting of the solution film with a novel, stationary, fumed-silica (*2*)-reference electrode combination probe generates a very efficient stirring action which, together with the favorable mercury electrode surface area to solution volume ratio provided by the cell geometry, results in the attainment of quite high electrolysis rates. The cell noise level is substantially less than that found in conventional cells since the surface area of the mercury electrode is not free to fluctuate in time. The high solution surface area to solution volume ratio results in very short sparging times. A 20-sec sparging is recommended in the general procedure. Although solution and mercury volumes of 2 ml of each phase are employed presently, there are probably no reasons why cells with much smaller capacities could not be fabricated.

Briefly mentioned in a previous paper (*3*), but detailed here for the first time is a new procedure termed "normalization" which allows the subtraction of the continuous background current from individual controlled potential coulometric titration curves. The precision of the titration results are improved by more than a factor of 4 in the example cited, *i.e.*, the determination of U(VI) in sulfuric acid. Implementation of this normalization procedure requires the use of digital recording equipment, some arithmetic data processing capabilities, and the ability to electronically display the stored data in a log-linear fashion.

EXPERIMENTAL

Instrumentation, Reagents, and Materials. The digital instrumentation used has been described previously (*3*). In addition, a General Radio Model 1538-A strobe light was employed. A Beckman No. 39270 saturated calomel electrode was used as reference.

Stock, 2*M* KCl and 1*M* H_2SO_4 supporting electrolyte solutions were prepared by dilution of reagent grade chemicals. All water used was distilled. Stock, standard metal ion solutions were prepared in the following manner. Weighed, gram amounts of reagent grade cadmium and lead were dissolved individually in nitric acid and converted to the chloride form by repeated evaporations with hydrochloric acid. The excess hydrochloric acid was removed by evaporation to near dryness, and these solutions were made to volume with water. Gram amounts of NBS U_3O_8 (assay 99.95%) were similarly weighed and dissolved in nitric acid, and the excess of this acid was removed by repeated fumings with sulfuric acid. After being cooled, the residue was made to volume with water. Working solutions of the cadmium and lead stock solutions were prepared by dilution with water. Working solutions of the uranium stock solution were made 1*M* in H_2SO_4 and 0.2*M* in sulfamic acid on dilution. All volumetric ware (flasks with T.D. pipets) was of class A tolerance. The calibration of the wash-out micropipets was confirmed by weighing mercury.

The high purity nitrogen employed, to sparge oxygen from the solutions prior to titration, contained nominally less than 10 ppm and averaged 3 ppm oxygen by mass spectrographic analysis. It was necessary to saturate this dry gas with water prior to admitting it to the coulometry cell, to prevent evaporation of the sample solution during the electrolysis.

Masero Laboratories "high-purity," instrument grade mercury was aliquoted into the cell using a luer-tipped, "Tomac" disposable, 2.5-ml hypodermic syringe. The plunger tip of the syringe was sheathed in Teflon (Du Pont), when it was learned from X-ray fluorescence analysis that the original rubber tip contained considerable amounts of metals, notably zinc. Oxide-free mercury can be drawn by inserting the luer tip beneath the mercury surface since the dross has no tendency to cling to the plastic syringe. The need for pinholing the mercury is thus eliminated.

Construction of the Rotated Cell and Assembly. Figure 1 shows an exploded view of the rotated cell apparatus. A set of detailed drawings of the apparatus is available upon request. The following is supplementary information complementary to the drawings.

[1] Permanent address, Chemistry Department, Sacramento State College, Sacramento, Calif. 95819

[2] Glass Shop.

[3] Machine Shop.

(1) J. J. Lingane, *J. Amer. Chem. Soc.*, **67**, 1916 (1945).

(2) R. G. Clem, F. Jakob, and D. Anderberg, ANAL. CHEM., **43**, 292 (1971).

(3) R. G. Clem and W. W. Goldsworthy, *ibid.*, p 918.

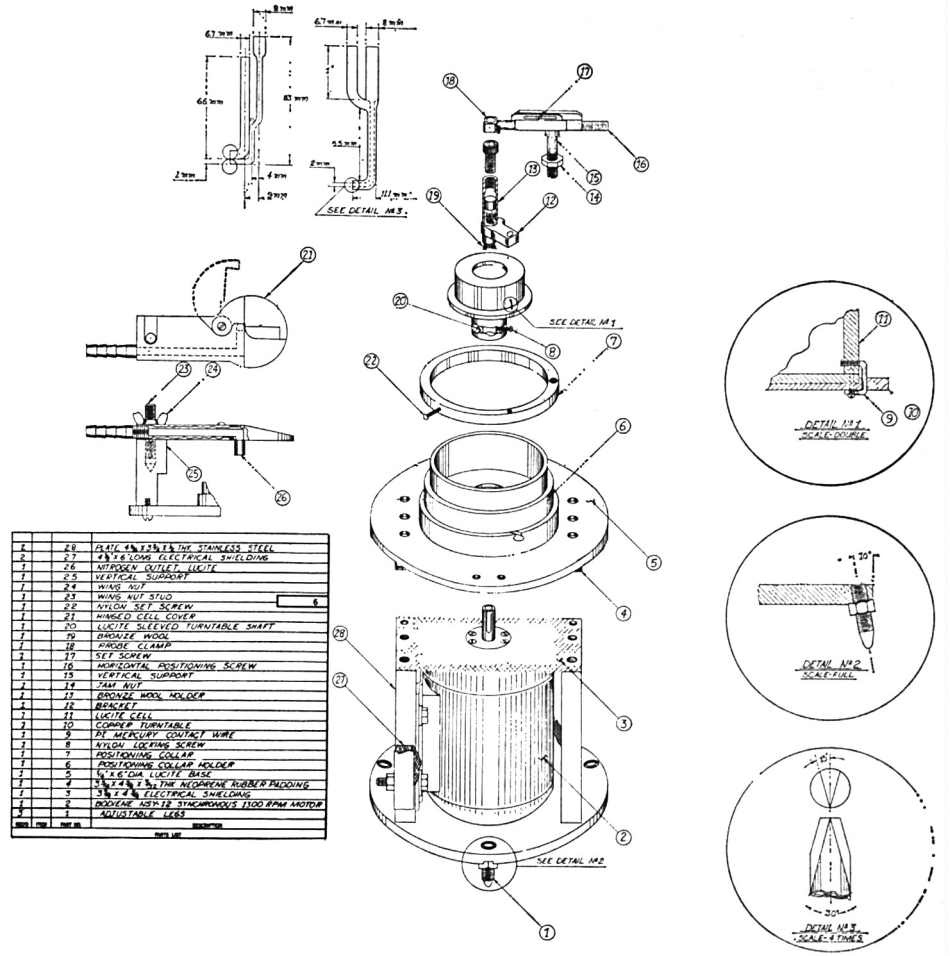

2	28	PLATE 4½ x 3½ x ⅛ THK STAINLESS STEEL
2	27	4½ x 6 LONG ELECTRICAL SHIELDING
1	26	NITROGEN OUTLET, LUCITE
1	25	VERTICAL SUPPORT
1	24	WING NUT
1	23	WING NUT STUD
1	22	NYLON SET SCREW
1	21	HINGED CELL COVER
1	20	LUCITE SLEEVED TURNTABLE SHAFT
1	19	BRONZE WOOL
1	18	FIRGIE CLAMP
1	17	SET SCREW
1	16	HORIZONTAL POSITIONING SCREW
1	15	VERTICAL SUPPORT
2	14	JAM NUT
1	13	BRONZE WOOL HOLDER
1	12	BRACKET
1	11	LUCITE CELL
1	10	COPPER TURNTABLE
1	9	Pt MERCURY CONTACT WIRE
1	8	NYLON LOCKING SCREW
1	7	POSITIONING COLLAR
1	6	POSITIONING COLLAR HOLDER
1	5	6" x 6" DIA. LUCITE BASE
1	4	5½ x 6 DIA. x ½ THK NEOPRENE RUBBER PADDING
1	3	3½ x 6 ELECTRICAL SHIELDING
1	2	BODINE NSY-12 SYNCHRONOUS 1300 RPM MOTOR
4	1	ADJUSTABLE LEGS
QUOTE FROM	PART NO.	DESCRIPTION

PARTS LIST

Figure 1. Rotated cell apparatus—exploded view

Although other materials may be as acceptable and in some instances preferable, the presented cell was constructed from Lucite plastic. This material was selected because it is easy to work when compared to some other materials (*e.g.*, glass) and was thus less expensive of shop time. Also, it is inert to most solutions commonly used as supporting electrolytes in coulometry.

The cell was constructed in the following manner. The wall of the cell was machined to the desired outside diameter from rod stock and center-bored to a specified inside diameter. The resulting cylinder, after polishing to optical transparency, was parted into rings of the required length. Two disks were machined from Lucite sheet. One served as the cell bottom. A hole was center-drilled through the second disk, which became the cell top. The three articles were then united using a glue made by dissolving Lucite shavings in ethylene–dichloride. Commercially available glue should work as well. The cell is now essentially completed, except for the installation of the platinum, mercury-contact wire. A hole is drilled and tapped in the side of the cell a few millimeters from the bottom to receive a finely threaded, platinum wire. The wire is dipped into the Lucite glue, then screwed into the hole until it extends ~1 mm inside. When the glue sets, the excess is scraped away exposing the platinum metal. See Figure 1, Detail 1. The cell must now be subjected to the cleaning and preconditioning procedures given below.

The turntable, to which the cell and its platinum, mercury-contact wire is mounted, is made of copper and is electrically isolated from the motor by sleeving the center of the copper shaft with Lucite and by using a nylon set screw to secure the turntable to the shaft of the 1800 rpm, synchronous Bodine motor, Model NSY-12. It is important that the eccentricity of the cell, when installed on the turntable and mounted on the motor shaft, be less than 2 mils total indicator reading.

Electrical connection to the cell turntable is made through a bronze wool brush contact. Bronze wool is compacted

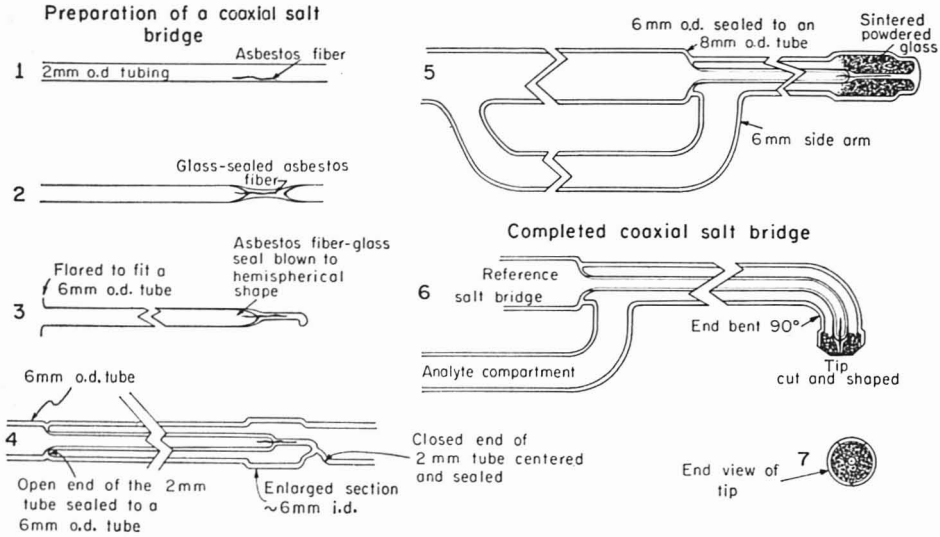

Figure 2. Coaxial probe construction

into the holder using a small screwdriver. The excess wool is cut with shears about $^1/_4$ in. from the end of the holder, and the holder is mounted in the bracket attached to the positioning collar. The brush pressure should be such that the turntable does not heat up, even after prolonged operation.

This contact is relatively trouble free, provided it does not become contaminated with mercury. Amalgamated bronze is a hard substance, completely lacking in resiliency and therefore useless as a contact material. If mercury is spilled on the wool, the entire tuft must be discarded and a new one taken. Contact bounce can occur when using a brush type contact; however, if it does occur in this system, the time width is less than 0.1 μsec. This kind of a contact was developed because we wished to make the cell portable. A mercury contact should work as well.

Note that the brush and all the associated metal parts are ultimately mounted on the Lucite base and are thus electrically isolated from the motor and housing.

The stainless-steel probe holder is made specifically to accommodate a variety of 6-mm or smaller o.d. glass probes and is open at the end to facilitate easy tube mounting and demounting without the necessity of removing the positioning collar or disturbing the probe holder alignment. The probe holder is so designed that the probe cannot move in either the horizontal or the vertical plane when locked.

The Lucite hinged cell cover is mounted less than 10 mils from the top of the rotated cell. In its open position, it permits the aliquoting of the sample and mercury into the cell. In its closed position, it blocks entry of air into the cell. The channel in the cover, which terminates in a short tube, permits the directing of nitrogen into the cell. The exterior of the cell is in contact with the air.

Cell Cleaning and Preconditioning Instructions. Before the cell, if it is made of Lucite, can be used, it is necessary to remove the contaminants introduced during its fabrication. The cell, as received, must be thoroughly washed with dilute hydrochloric acid, rinsed with water, then ethanol. After being dried, the cell is soaked overnight in 2*M* H_2SO_4. The following day, it is washed with water and filled with 0.1*M* $HClO_4$, and the platinum, mercury-contact wire is anodized against another platinum wire for a short time using a 10-V source. This acid is discarded and the cell is refilled with 0.1*M* $HClO_4$. This time, the contact wire is cathodized and, after a few moments, ~0.5 ml of mercury is introduced. The cell is tilted so that the mercury touches the contact wire; the mercury will flow onto and thoroughly coat the exposed platinum. The solution and excess mercury is discarded and the cell is then washed with water, dried, and mounted on the copper turntable. It is now ready for use.

Failure to heed these cleaning and preconditioning instructions will result in very high background currents.

Probe Construction. The two probes used in this work are shown in Figure 1, upper left. The first probe consists of parallel arrangement of the reference anolyte salt bridges. The reference bridge terminates in an asbestos wick, and the anolyte bridge terminates in a glass frit. These parallel probes are easy to construct. The second probe consists of a coaxial arrangement in which the reference bridge is located at the center of the anolyte bridge. This type of probe is more difficult to construct. See Figure 2. Drawings 1 through 5 show the steps required for the fabrication of the coaxial probe, Drawing 6 is a side view of the completed probe, and Drawing 7 is an end view of the tip. The probe tip design is very important and will be discussed below.

Salt Bridge Preparation and Alignment. Both probes are prepared for use in the following manner: the reference electrode salt bridge is filled with 1*M* KCl. Using a polyethylene spitzer, the anolyte compartment is injected, as described in a previous paper (*2*), with either a fumed-silica, gelled solution of 1*M* KCl when titrating cadmium or lead, or a fumed-silica, gelled solution of 1*M* H_2SO_4 when titrating uranium. The anolyte compartment is then filled with the same solution as the gelled one.

Position the arm of the stainless-steel probe holder along an imaginary line passing through the center of the cell, then lock it into this position by tightening the jam nut. Clamp the probe in the holder so that the center of the probe tip is just below the center of the cell and facing toward the probe holder vertical support. Aliquot 4 ml of water

into the cell and start it rotating. Turn the horizontal positioning screw, located in the probe holder arm, counterclockwise until the probe tip just touches the moving wall of water. Orient the probe in such a way that the pointed end of the tip is the first part to contact the water. Continue turning the positioning screw counterclockwise until the entire tip surface contacts the water. When thus correctly positioned, the solution will course around and over the horizontal section of the probe, but no dripping will occur and no spray will be formed. Lock the probe holder in this position by tightening the set screw.

General Procedure. Calibrate the digital integrator to read out directly in nanograms of material titrated by using the voltage equivalent of the nF to atomic weight ratio. Start nitrogen flowing into the cell at a rate of 2.9 l./min or more. The recommended sample size depends upon the type of probe employed and is discussed below. Open the hinged cell cover and aliquot the sample into the cell using a 500-μl pipet. Employing standard microtechniques, rinse the pipet twice by filling it to the miniscus with the 2M KCl stock, supporting-electrolyte solution and once with water when titrating cadmium or lead, or three times with 1M H_2SO_4 when titrating uranium. It is convenient to draw up the rinse from droplets distributed over Parafilm. Add these rinsings to the cell. The total volume of sample plus rinsings must be 2.0 ml. Aliquot 2.0 ml of mercury into the cell, using the plastic syringe; then close the hinged cell cover. Bring the cell up to its designed speed over a 10- to 15-sec interval by slowly increasing the output voltage of a 0 to 120 V Variac.

The solution is sparged of oxygen in part during the aliquoting operation. Allow the cell to rotate for 20 sec to complete the sparging, then apply the pretitration voltage. Cadmium, lead, or uranium is pretitrated at -0.400 V, -0.200 V, or $+0.075$ V *vs.* SCE, respectively. The pretitration electrolysis rates as observed on the rate meter should fall to a value of <5 ng/sec for cadmium or lead and to <10 ng/sec for uranium within 1 to 3 min. After the pretitration, set the appropriate titration voltage and start the titration. Cadmium, lead, or uranium is titrated at -0.825 V, -0.650 V, or -0.275 V *vs.* SCE, respectively. The titration termination times used for the three elements are 7, 8, or 12 min, respectively, provided the current is not initially limited.

The required titration times for the three elements can be reduced to less than 5 minutes, if the empirical chemical calibration approach, suggested by some workers (*4*), is used The titration is terminated at a preselected current level or pulse rate which is higher than background. The titration can be manually terminated when the current or pulse rate falls to the preselected level.

The cell is not conveniently demountable for cleaning between titrations. Remove the titrated solution and mercury from the cell using a polyethylene spitzer connected through a 500-ml filter flask trap to a vacuum line. Rinse the cell several times with water, then aliquot the next sample.

Carry blanks through the above procedure for the element titrated and correct the raw data for the background current.

Normalization Procedure. Normalization of coulometric data contained in the memory of a multichannel analyzer is an alternate and time saving route to coulometric analysis (*3*). After pretitrating the sample, adjust the potentiostat to the required titration potential. Adjust the rate meter to terminate the experiment when the electrolysis rate decreases to 7 ng/sec for cadmium or lead, or 10 ng/sec for uranium. Start the titration and store the digital information in the first half of the memory, using a time-dwell of 3 sec per channel. After the rate meter termination, transfer the stored data, while simultaneously multiplying it by a factor of 10, to the last half of the memory using the data processor. Switch the data processor to its normalize mode of operation and change the storage sense of the analyzer to subtract. While observing the 5-cycle log display of the data on the analyzer oscilloscope, repeatedly initiate the normalization program until all the data points of the curve in the second half of the memory fall on a straight line. Determine the number of channels involved in recording the titration data, using the analyzer peak select function, and multiply this number by one tenth the normalization value per channel. Subtract this product, after rounding to the nearest count, from the total number of counts shown on the accumulate scaler. The scaler data are now corrected for the continuous background current.

If the sample titrated is very small, it will have a significant positive bias owing to the lack of compensation for the charging and the supporting electrolyte impurity currents. Run a blank, normalize these data, and, using the data processor, integrate all non-empty channels. Subtract this integrated value from the scaler data above.

DISCUSSION AND RESULTS

Fundamental considerations, tempered by experimental limitations, served as a guide in the development of the presented cell.

The current–time relationship in a controlled potential coulometric determination, which is free of chemical complications and is carried out at a potential at which the rate of the reaction is limited solely by the rate of mass transfer of the electroactive species to the working electrode, is given by the Lingane equation (*1*, *5*).

$$i = i_o\, e^{-kt} \tag{1}$$

The current i is expressed in milliamperes at some time t expressed in seconds; i_o is the initial current, and k is the electrolysis rate constant. The Nernst diffusion layer concept allows one to relate the electrolytic rate constant to several important experimental parameters. The relationship derived for this model is

$$k = D(A/V)\,(1/\delta) \tag{2}$$

where D is the diffusion coefficient of the electroactive species, A is the working electrode area in square centimeters, V is the volume of solution in milliliters, and δ is the Nernst diffusion layer thickness in centimeters.

Examination of Equation 2 reveals three ways in which the value of k could be increased. The diffusion coefficient could be increased by heating the solution titrated, but the practical consideration of providing some thermostating at the elevated temperature because of shifts in the required control potential militates against this. Also, the background current increases with increasing temperature. Increasing A while decreasing V would increase k. However, space limitations in the cell void restrict the size and the effective area of the auxiliary electrode, thus causing localization of the current distribution pattern. Other probes essential to the operation of the cell must also share the same void. For these reasons, the effective A to V quotient is usually near unity. The third alternative—providing more efficient mass transfer by making δ small through efficient stirring—has attracted the widest attention, because it is the most effective and the easiest to effect.

Making k large is desirable for two reasons: the titration time is reduced, and the contribution of the background current to the total electrolysis current is decreased. The preci-

(4) H. C. Jones, W. D. Shults, and J. M. Dale, ANAL. CHEM., **37**, 680 (1965).

(5) J. J. Lingane, "Electroanalytical Chemistry," 2nd ed., Interscience, New York, N. Y., 1958, pp 224–229.

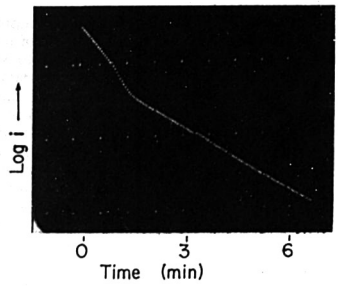

Figure 3. Coulometric titration in which the control potential is exceeded

Taken: 501.5 μg Cd^{2+}. Found: 554.6 μg Cd^{2+}. Conditions: See General Procedure.

sion of the results and the sensitivity of the method is thus improved, provided the cell is free from deleterious potential gradients and the noise level of the cell is low.

A paper by Harrar and Shain (*6*), in which they investigated potential gradients in coulometry cells, was an invaluable guide in the present study. They showed how improper placement of the reference electrode could produce localized excursions of the working electrode potential in which the control potential was sufficiently exceeded to produce undesired reactions. A general conclusion of these workers is that the reference electrode should be placed on a line of minimum separation between the auxiliary and working electrodes.

Cell current noise is caused by stirring which produces electrode-area fluctuations in time. These fluctuations cause variations in the reference to working electrode distances and, if the *iR* drop between the electrodes is appreciable, considerable fluctuations in the control-potential can occur. The net effect is an increase in the background current which decreases the sensitivity of the coulometric method.

The last cell design criterion, sparging time, is largely a matter of convenience although it is of great practical importance if coulometry is to be considered for a control application. Dissolved oxygen interferes with coulometric titrations and must be removed prior to the analysis. The time needed to sparge the coulometry cell of oxygen adds to the total time required for a determination. Sparging time should, therefore, be as short as possible.

The following is an account of the way in which the rotated cell evolved. The rugged, easily fabricated salt bridge described in an earlier paper (*2*) was the precursor of the salt bridge probes developed for this work. Our most difficult developmental problem was that of designing a satisfactory probe with an acceptable tip geometry. Initially, many different tip designs were tested, but were rejected owing to spray formation on contacting the rotated wall of water. Also, with some designs, the water had a tendency to run onto the horizontal probe section and form drops which, upon striking the cell floor, produced spray. Spray formation is objectionable because the droplets can be deposited on the cell cover or probe stem and thus escape titration.

The first problem was overcome when it was observed that a piece of small diameter ($^1/_{32}$ in.) copper wire did not cause spraying or dripping on contacting the water, and produced a wake with the horizontal of about 15° at 1800 rpm. It was reasoned that a much larger diameter object could similarly contact the water without causing the deleterious effects characteristic of the other designs, provided it had a wake-matching 15° triangular shape cut into it. This reasoning proved correct. Although the design shown in Figure 2, Drawing 7 is probably not unique, it was the only one produced by our considerable efforts which met all our requirements. The probe tip surface selected was plane since the ratio of the probe length to the circumference of the cell used for this report was small.

The second problem, drop formation, appears to be related to the diameter of the probe tip. The angular velocity of the solution is diminished in the vicinity of the probe and the corresponding centrifugal force is reduced. The magnitude of this effect is dependent upon the tip diameter. If the use of a larger probe is desirable, the angular velocity of the solution must be increased to avoid drop formation. The foregoing is the reason that a 6-mm o.d. probe tip was selected.

Once a satisfactory probe tip was designed, the next problem was one of selecting the correct geometry for the reference and anolyte probes with respect to the rotating mercury electrode.

In the first titration experiments, two probe holders were employed, mounted on two positioning collars which fitted concentrically on the two stepped collar holder. See Figure 1. The cell used, at this stage of the development, was 4.0 cm in diameter and 4.0 cm in height. These dimensions were selected because they were physically convenient. The cell was charged for each run with 7 ml of mercury and 7 ml of 1*M* KCl containing 200 μg of lead and was sparged of oxygen with a strong jet of nitrogen from a tube inserted through the center of the cell top opening. The angular separation between the probes had an effect on the normalized results. As the angular separation decreased from 180°, the positive titration error decreased, and approached zero as the separation approached 0°. From these results, it was obvious that the control potential was being exceeded sufficiently to cause a secondary electrolysis at wide reference anode separations, hence the high results. See Figures 4 and 6 of Reference *6*. Based upon this experimental information, the parallel probe design was developed and is shown in the upper left corner of Figure 1.

The parallel salt bridges are situated one directly above the other to avoid placing one probe in the compression wake of the first which would be the case if one were allowed to lead the other as, for example, in a side by side configuration. This latter configuration is avoided because it is electronically very noisy. Examination of it with stroboscopic light revealed the cause. Depending upon which probe is allowed to trail, either the control loop or the reference lead is being opened intermittently by the turbulence.

Although these first experiments showed that it was possible to do precision coulometry using a rotated cell provided certain geometrical requirements were met, the electrolytic rate constant for this electrode (*e.g.* 0.006 sec^{-1} for lead in 1*M* KCl) was disappointing. It was reasoned that a considerable area of the mercury electrode was inactive because of the small anode surface area and the probable high collimation of the field. To test this, the cell height was reduced from 4.0 cm to 1.5 cm while keeping the same cell diameter. Upon reducing the rotated electrode surface area by a factor of 2.7 and by decreasing the cell capacity to 2 ml of mercury and 2 ml of solution, the electrolysis constant increased by more than

(6) J. E. Harrar and I. Shain, ANAL. CHEM., **38**, 1148 (1966).

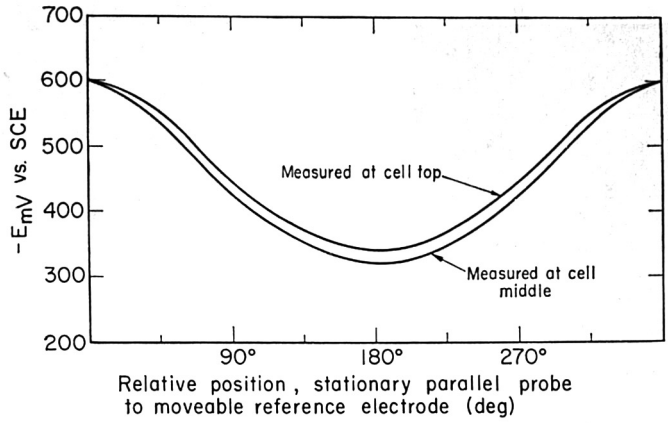

Figure 4. Potential map of the rotated cell

Solution: 0.1*M* KCl

300% to 0.020 sec^{-1}. This increase is due to an increase in the value of k in Equation 2 made possible through a reduction in δ with more efficient stirring, and also is probably due to the fact that the probe diameter now more closely approximates the cell height. One would not expect a change in the cell diameter to affect the stirring efficiency provided the solution film thickness remained constant. Although the geometrical ratio of A to V is 9 to 1 for the 1.5-cm cell, the effective ratio is probably near unity.

Reduction of the cell height and solution mercury volume also reduced the starting inertia of the motor resulting in the entrapment of as much as 20 μl of solution beneath the mercury which led to low titration results. Interposing a transformer between the motor and the line to initially limit the voltage to the motor permitted a much slower and controllable start up and thus eliminated the formation of solution pockets. This was verified by examination of the cell under stroboscopic light. Coincidental with the cell alteration, a more sophisticated means of protecting the cell from the ingress of air became necessary. This took the form of the hinged cell cover.

There is a definite upper limit to the amount of material titrated when using a parallel probe. Figure 3 shows the log i– time behavior for a cadmium sample which exceeds the upper limit. The positive deviation from the expected linear log i– time relation does not conform with the logarithmic form of Equation 1 and is due to the control potential being exceeded sufficiently to cause a secondary electrolysis, hence the high positive error. Again see Figures 4 and 6 of Reference 6. This phenomenon can be explained by assuming that the probe changes from configuration II to configuration III type behavior depending upon the cell current demand. This behavioral transition occurs abruptly so if the upper limit is determined, and care taken that it is not exceeded, a parallel probe can be used without trepidation. Replacement of the parallel probe with the coaxial probe discussed below eliminates these problems.

In conjunction with the above, it seemed advisable to make a potential map of the rotated mercury electrode when it was in its configuration II state. The cell was converted to essentially a constant current operation in the following manner. The cell cover was removed to allow air into the cell, then

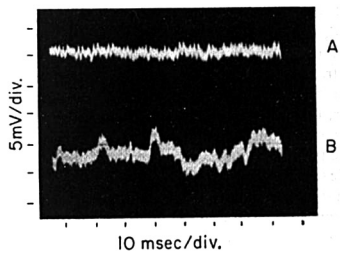

Figure 5. Cell noise

A. **Cell current noise; 1 mV = 1 μA**
B. **Variations in the control potential; 1 mV = 1 mV**
Conditions: 400 μA total current, −600 mV *vs.* SCE, 1*M* KCl

a potential of −0.600 V *vs.* SCE was imposed. The cell current became constant at 400 μA within a short time owing to the equilibrium between the rate of entry of oxygen into the cell with the rate of its reduction. Using the second positioning collar and probe holder as described above, a movable reference probe was introduced into the cell and potential measurements were made against the working electrode at various angular settings with respect to the stationary parallel probe. Figure 4 shows the results. Even though the working electrode potential is less than the control potential over much of the electrode surface, this will not harm the analysis, provided the final electrode potential corresponds to that of complete electrolysis (6), although there are some exceptions (7). The electrode potential of the rotated cell, of course, approaches the control potential at all points on its surface as the current demand approaches zero, a fact confirmed by experiments in which the cell was sparged of oxygen during the potential measurement.

Figure 5, trace A, shows the ac noise superimposed on the 400-μA constant cell current, while simultaneously trace B

(7) J. E. Harrar, *ibid.*, **35**, 893 (1963).

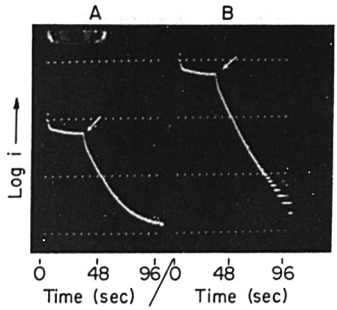

Figure 6. Sparging behavior of the rotated cell

A. Current-time data as recorded
B. Curve *A* expanded by a factor of 10 and normalized
Arrow denotes the point in time at which the N_2 was turned on

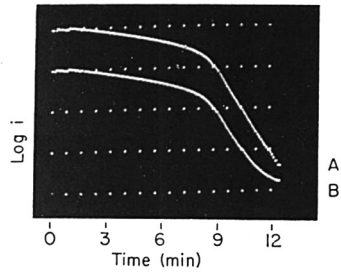

Figure 7. Current limiting behavior of the coaxial probe

A. Curve *B* expanded by a factor of 10 and normalized
B. Current-time data as recorded
1030 μg Cd^{2+} taken, 1032 μg Cd^{2+} found before normalization, curve *B*; 1029 μg Cd^{2+} found after normalization, curve *A*

shows the variation in the control potential. Qualitatively, this cell has one of the lowest noise levels of any efficiently operated, mercury coulometry cell studied by these authors. The cell noise which is due to stirring and/or mechanical shocks transmitted to the mercury by the motor appears to be of a high frequency nature (msec range). Intuitively, however, low frequency noise could occur from a precession in the mercury and would occur if the cell had appreciable eccentricity. A frequency analyzer was, unfortunately, not available for this work.

An outstanding feature of this cell is its outgas characteristics. Figure 6 is in log-linear presentation of the change in the oxygen current with time. Curve *A* is the recorded data, and curve *B* is a normalization of curve *A*. Curve *A* indicates that a solution, initially saturated with air, can be sparged to background in about one minute. It is reasonable to assume that the sparging characteristic of the cell is exponential in nature and that an empirical "sparging constant" could be calculated, since curve *B* is fairly linear. This constant, as might be expected, is related to the volume of the aqueous phase which, in turn, is related to solution thickness. Sparging constants of 0.11, 0.10, and 0.05 sec^{-1} were found for 1.5, 2.0, and 3.0 ml of 1.0*M* KCl, respectively. The thickness of these solutions, in millimeters, is almost identical with the solution volumes. Under the conditions of the general procedure, the sparging time is less than one third that calculated (69 sec) because the sample is being sparged in part during the aliquoting step.

The minimum nitrogen flow rate to maintain the sparging constant of 0.10 is 2.9 l./min. This value is also the minimum flow necessary to maintain an oxygen-free cell environment when the cell cover is mounted 0.01 in. above the rotating cell. A secondary or tight sealing of the cell is not necessary to exclude air. It is being sparged with nitrogen at a minimum rate of 540 dead volumes per minute. Such a high sparging rate in a conventional cell would undoubtedly cause severe splashing with subsequent losses of the sample solution.

Although the parallel probe is easy to construct, the fact that there is an upper limit on the size of the sample titrated impairs its usefulness, if it is to be used in nonroutine work. To circumvent these problems, the coaxial type salt bridge was developed. See Figure 2. Since the reference electrode is located center of and flush with the anolyte bridge, the control potential is reduced by the *iR* drop between the reference and the rotated mercury electrode; therefore, it is impossible to exceed the control potential. This behavior, which limits the cell current to approximately 600 μA in 1*M* KCl is about one third the total current available. If the initial cell current demand is above the current limiting value, the titration time is extended. Figure 7 illustrates this phenomenon. If current limiting is a problem, it can be overcome in one of two ways. An *iR* drop compensator can be installed in the potentiostat or the probe tip can be redesigned in such a way that the reference electrode salt bridge is placed nearer the rotated mercury electrode. It is the considered opinion of the authors that the former suggestion would be the easier to implement.

The two probes compare favorably. The current noise levels of the two probes are the same, but the variations of the control potential (Figure 5) are reduced by roughly 50% through the use of the coaxial probe.

It would be interesting to compare the performance of our cell with that of previous workers. Unfortunately, it has not generally been the practice of past workers to evaluate the electrolysis constants for their cells; rather, the amount of material which can be titrated to background within 15 minutes is usually reported as an upper limit for their methods. If one assumes that the electrolysis current obeys Equation 1 and decays by three orders of magnitude in this time, a constant of 0.008 sec^{-1} is calculated for a typical conventional cell. For this report, a conventional cell is defined as one having a sample volume capacity of from 7 to 10 ml, a sample to mercury volume ratio of unity, a geometrical electrode surface area to solution volume ratio of unity, and one which is continually being sparged with a jet of an inert gas sufficiently energetic to depress the solution surface. The solution–mercury interface is stirred with a disk-type stirrer. In comparison, the measured electrolysis constants for our cell were 0.020, 0.017, and 0.012 sec^{-1} for lead, cadmium, and uranium, respectively. All titrations were performed at the ambient room temperature (~23 °C).

A large value for the electrolysis constant is desirable because, in addition to reducing the time necessary to do a titration, the size of the blank titration is reduced; smaller samples can be titrated with good precision; and, when

Table I. Time Comparison of the Rotated Cell with a Conventional Cell

Operation	Time, minutes: Rotated cell	Conventional cell
Aliquot	1	1
Sparge	0.3	7 to 10
Pretitrate	1 to 3	1 to 3
Titrate[a]	12	15[b]
Time totals	14.3 to 16.3	24 to 29

[a] For U^{6+} in 1M H_2SO_4.
[b] See text.

Table III. Normalization of Uranium Results

Run No.	1	2	3	4	5
Scaler counts	1128373	1128259	1129566	1126863	1126666
Correction	3400	3840	5120	2560	2048
Normalized value	1124973	1124419	1124446	1124303	1124618
Nominal value, μg	1125.0	1124.4	1124.4	1124.3	1124.6
Less charging current U equivalent (1.0 μg)	1124.0	1123.4	1123.4	1123.3	1123.6

Av 1123.5 ± 0.2

Table II. Titration Results

Cd, μg				Pb, μg				U, μg			
Taken	Found	Av dev	No. of analyses	Taken	Found	Av dev	No. of analyses	Taken	Found	Av dev	No. of analyses
1030[a]	1029.9	±1.4	5	1250[a]	1250.0	±0.9	6	1124[a,c,d]	1123.5	±0.2	5
258[b]	257.8	±0.3	5	500[b]	500.2	±0.4	5	562[a,c]	561.7	±0.1	5
26[b]	26.2	±0.2	5	100[b]	99.9	±0.1	5	281[a,c]	280.4	±0.5	6
				10[b]	9.9	±0.2	6	56[a,c]	57.0	±0.2	5

[a] Coaxial probe used.
[b] Parallel probe used.
[c] Normalization procedure used.
[d] Also see Table III.

normalizing data, the uncertainty in the visually determined linearity is greatly reduced because the slope of the titration curve is increased. Table I gives what we consider an objective time comparison of our cell with a conventional cell. The rate of reduction of U(VI) is kinetically controlled and depends upon the rate of disproportionation of the U(V) species (*8*, *9*). The time disparity would be larger, had a diffusionally controlled species been considered.

Calculated electrolysis times of 7, 8, or 12 min for Pb, Cd, or U, respectively, based on the observed rate constants are shorter than those actually employed. The electrolysis was allowed to continue for a time equal to 120% of the calculated value to assure an adequate deviation from the linear log i–time relation to permit the evaluation of the background current by normalization. The selected rate meter termination levels of 7, 7, or 10 ng/sec for cadmium, lead, or uranium were roughly twice as high as the levels to which the integrator count rate would have ultimately decayed, had the titrations been permitted to continue for times greater than those suggested. A computer program which is currently under development will automate this normalization procedure.

Both kinds of probes were used in obtaining the results shown in Table II. A constant titration time interval was used to obtain the reported values for cadmium and lead, whereas the normalization procedure was used for the uranium analyses. Table III details the data reduction steps necessary to arrive at the information shown in the previous Table for uranium at the 1124-μg level. This ability to analyze coulometric titration data for a continuous background current contribution on an individual basis rather than on a statistical basis considerably improves the precision of the final results. Note that the average deviation of 0.2 μg would have been greater by a factor of 4.5 had the average blank correction been used.

Normalization of titration data should also permit the accurate determinations of radioactive elements where the radiolysis products are created at a constant rate, since this technique has rejection for the continuous background current produced by these electroactive products.

FUTURE WORK

Although we have attained our original objectives—a cell having very efficient stirring action, low noise characteristics, a very high sparging rate, and low sample volume requirements—several other studies probably are suggested by this work. If a very low-play, bearing-mount arrangement were developed, it should be possible to scale down the cell size and titrate samples in volumes of 100-μl or less. The probes could be maintained at their present dimensions and thus still be physically easy to handle. Sonic stirring (*10*) could be employed in conjunction with the rotated mercury electrode since the centripetal force would prevent fragmenting of the liquid metal surface.

A fairly large sample volume is generally required for platinum coulometry cells to cover the electrodes. Construction of a rotated platinum gauze or wool electrode would reduce the volume required and make the electrode surface area to sample volume ratio quite favorable and at no increase in the background current over the conventional application. Sonic stirring (*10*) could be applied to this arrangement too.

If by sonic stirring an increase by a factor of 5 in the electrolysis rate constants is realized, potential scanning coulometry would become practical for use in routine analysis.

ACKNOWLEDGMENT

The authors thank Mr. F. T. McCarthy for his help in the initial development of this cell and Dr. E. H. Huffman and Dr. E. K. Hyde for their support in this undertaking.

RECEIVED for review March 17, 1971. Accepted May 19, 1971. Work performed under the auspices of the U. S. Atomic Energy Commission.

(8) G. L. Booman, W. B. Holbrook, and J. E. Rein, ANAL. CHEM., **29**, 219 (1957).
(9) I. M. Kolthoff and W. E. Harris, *J. Amer. Chem. Soc.*, **68**, 1175 (1946).
(10) A. J. Bard, ANAL. CHEM., **35**, 1125 (1963).

Analytical Applications of X-Ray Excited Optical Fluorescence

Direct Determinations of Rare Earth Nuclear Poisons in Uranium at the Part per Giga (1 in 10^9) Level

Arthur P. D'Silva and Velmer A. Fassel

Institute for Atomic Research and Department of Chemistry, Iowa State University, Ames, Iowa

An X-ray excited optical fluorescence method for the direct quantitative determination of Gd, Sm, Dy, Eu, and Pr at the part per giga level (1 in 10^9) in nuclear grade uranium is described. The UO_2 or U_3O_8 samples are incorporated into a quaternary oxide host system, 2 $Li_2O \cdot SrO \cdot UO_2 \cdot 2WO_3$, prepared by heating stoichiometric proportions of Li_2CO_3, $Sr(NO_3)_2 \cdot UO_2$ or U_3O_8, and WO_3 at 825 °C for 3 hours. The internal reference element Er corrects for preparative and excitation variables. The analytical curves extend over the following concentration ranges: 0.005–0.5 ppm Gd, 0.005–0.2 ppm Dy, 0.01–0.5 ppm Pr, and 0.02–0.5 ppm for Eu and Sm.

THE NEUTRON ECONOMY of uranium fueled nuclear reactors may be significantly impaired by the presence of even fractional part per million levels of rare earth impurities (Gd, Sm, Dy, and Eu) possessing high capture cross sections for thermal neutrons (*1*). The direct determination of these rare earths at the fractional part per million level in uranium by spectrometric techniques has so far not been feasible, although attempts to do so at higher concentration levels have met with some success (*2*). Usually these determinations have been effected by appropriate chemical separations and analysis of the concentrates by one of several spectrographic procedures (*3*, *4*). These concentrates have also been analyzed by a ultraviolet excited luminescence technique (*5*).

X-ray excited optical fluorescence of the rare earths (*6*, *7*) has recently emerged as a very sensitive technique for the detection and determination of the rare earths (*8–11*). The application of this technique to the direct determination of fractional ppm amounts of the rare earth 'neutron poisons' in ThO_2, another fertile nuclear material has already been described (*9*, *12*). A recent publication discussed the application of this technique to the determination of the rare earths in uranium and zirconium (*13*). However, in this procedure the prior separation of the rare earths from uranium and zirconium was involved. Thorium tetrafluoride was employed as a carrier for the separation and the final determinations were made in a ThO_2 host. Our efforts to extend the X-ray excited optical fluorescence technique to the direct determination of the rare earths of interest in UO_2 or U_3O_8 have shown that these simple oxides were not suitable hosts for the rare earth activators at the fractional ppm level. However, incorporation of the oxides of uranium into ternary or quaternary oxide systems (*14*, *15*) has led to the positive detection of the rare earths neutron poisons at the ultra-trace level.

In this paper we present a more detailed account on the genesis of these host systems and their application to the determination of Gd, Sm, Dy, Eu, and Pr in uranium at the part per giga (1 in 10^9) level.

EXPERIMENTAL FACILITIES AND PROCEDURES

Apparatus. The basic instrumental facilities utilized in this study have been described (9). Some additional features have been useful in the development of this method. A Jarrell-Ash 0.25 meter monochromator (model 82-410) fitted with two gratings blazed for 3000 Å and 6000 Å and having 250-micron slits was utilized in this investigation. The rotation of the grating selector arm brought either of the two gratings into the optical path without significant wavelength displacement. The wavelength drive was fitted with a system of geared motors (Synchron No. AM-1, No. Q TM17K112 Herbach and Rademan, Inc.) which allowed both forward and backward scans of the spectrum at rates of 100, 200, or 400 Å per 2.5 cm. Even with the low spectral dispersion provided by the spectrometer, 250-micrometer entrance and exit slits provided enhanced powers of detection over the narrower slits.

Preparation of Calibrating Standards and Samples. In our previous communication (*15*) we showed that quaternary oxide phosphor systems with the general formulae $aR_2^{1+}O \cdot bR^{2+}O \cdot bR^{4+}O_2 \cdot cWO_3$ provided powers of detection of the relevant rare earth impurities in the part per giga (part per 10^9) range. The starting materials employed for the preparation of calibrating standards must therefore be highly purified. The UO_2 base material utilized in the preparation of our standards contained detectable Gd and Dy but their concentrations were less than 10 ppg.

(1) C. J. Rodden, *J. Chem. Educ.*, **36**, 459 (1959).
(2) R. Avni and A. Boukobza, *Spectrochim. Acta*, **24B**, 515 (1969).
(3) C. G. Goldbeck in "Analysis of Essential Nuclear Reactor Materials," C. J. Rodden, Ed., U. S. Government Printing Office, Washington, D. C., 1964, pp 959–986.
(4) "Analytical Chemistry of Uranium," Academy of Sciences of the U.S.S.R., Vernadskii Institute of Geochemistry and Analytical Chemistry (Engl. Trans., Israel Program for Scientific Translations (I.P.S.T.), Cat. No. 2057, Jerusalem, 1963.
(5) L. I. Ankina, V. V. Bagreev, T. S. Dobrolyubskaya, Yu. A. Zolotov, A. V. Karyakin, A. Z. Miklishanskii, N. G. Nikitina, P. N. Palei, and Yu. V. Yakoolev, *Zh. Anal. Khim.*, **24**, 1014 (1969).
(6) W. Low, T. Makovsky, and S. Yatsiv in "Quantum Electronics—Paris 1963 Conference," Vol. 1, Columbia University Press, New York, N. Y., 1969, p 655.
(7) V. E. Derr and J. J. Gallagher, *ibid.*, p 817.
(8) R. C. Linares, J. B. Schroeder, and L. A. Hurburt, *Spectrochim. Acta*, **21**, 1915 (1965).
(9) E. L. DeKalb, V. A. Fassel, T. Taniguchi, and T. R. Saranathan, ANAL. CHEM., **40**, 2082 (1968).
(10) R. J. Jaworowski, J. F. Cosgrove, D. J. Bracco, and R. M. Walters, *Spectrochim. Acta*, **23B**, 751 (1968).
(11) W. E. Burke and D. L. Wood in "Advances in X-Ray Analysis," Vol. II, J. B. Newkirk, G. R. Mallett, and H. G. Pfeiffer, Ed., Plenum Press, New York, N. Y., 1968, pp 204–213.
(12) T. R. Saranathan, V. A. Fassel, and E. L. DeKalb, ANAL. CHEM., **42**, 325 (1970).
(13) T. Nakajima, Y. Ouchi, H. Kawaguchi, and K. Takashima, *Bunseki Kagaku*, **19**, 1183 (1970).
(14) E. L. DeKalb, A. P. D'Silva, and V. A. Fassel, ANAL. CHEM., **42**, 1246 (1970).
(15) A. P. D'Silva, E. L. DeKalb, and V. A. Fassel, *ibid.*, p 1846.

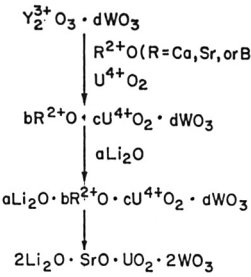

Figure 1. Phosphor genesis

The quaternary oxide phosphor standards or samples were prepared by blending either UO_2 or U_3O_8 with a phosphor base mixture and subjecting the blend to a heating cycle. The U_3O_8 base standards were prepared by dissolving the highly purified UO_2 in nitric acid to prepare a master solution. Appropriate amounts of rare earth nitrate solutions were then added to aliquots of the master solution. The resulting solutions were evaporated to dryness and ignited to 1000 °C for 3 hours to yield a graduated series of U_3O_8 standards.

The host material with the empirical composition $2Li_2O \cdot SrO \cdot UO_2 \cdot 2WO_3$ has been shown (*15*) to yield superior powers of detection for rare earth impurities in the uranium base phosphor. The preparation of the quaternary oxide host system was facilitated by first blending together reagent grade Li_2CO_3 and $Sr(NO_3)_2$ and CP grade WO_3 in the ratio 1.47/2.11/ and 4.64, respectively to yield a phosphor base mixture. The external reference element Er was incorporated into the $Sr(NO_3)_2$ prior to the preparation of the phosphor base mixture; specifically Er in solution was added to a $Sr(NO_3)_2$ solution in the ratio of 30 μg to 2.11 grams, respectively. The resulting solution was evaporated to dryness and the residue dehydrated at 110 °C.

For the analysis of a single sample, 0.270 gram of UO_2 or U_3O_8 was blended with 0.822 gram of the phosphor base mixture in an agate mortar for a few minutes and ignited in a platinum crucible at 825 °C initially for a period of an hour. The phosphor was reground and fired at the same temperature for a further period of 2 hours. It is worth noting that prior dissolution of the UO_2 or U_3O_8 is not necessary, since the internal reference element Er is incorporated into the host through the solid-state reactions discussed above.

Phosphor Genesis. The optical fluorescence of the rare earths in a wide variety of host materials under X-ray or ultraviolet excitation is well documented (*6, 7, 14–16*). The exceptional powers of detection achieved under X-ray excitation can be attributed in large measures to the development of a phosphor system which effectively transfers X-ray energy absorbed by the matrix (the "host") to the fluorescing trace impurities (the "activators") (*14*). Of a large number of such phosphor systems, crystalline compounds with a fluorite or scheelite structure have been found to be excellent hosts for observing rare earth fluorescence under X-ray excitation (*6, 7, 14, 17*). The crystal structures of CeO_2, ThO_2, UO_2, and PuO_2 are known to be of the fluorite type (*18*). Of these only CeO_2 and ThO_2 are known to support rare earth fluorescence (*17*). Our efforts to prepare a UO_2 (or U_3O_8) host capable of supporting rare earth fluorescence even at the 5000-ppm level were unsuccessful. A study of the extensive literature on lanthanide or uranium activated fluorescence in alkaline earth (*19–22*) or rare earth tungstates (*23*) indicated that these offer a more promising host system for the observation of uranium sensitized-rare earth activated fluorescence. Host systems in which uranium sensitizes rare earth fluorescence are known (*24–26*), but our own observations indicate that these hosts are not analytically useful. Of the rare earth tungstates, $Y_2O_3 \cdot 3WO_3$ has been reported to be a good host for observing rare earth fluorescence (*23*). These observations and the knowledge that tungstate phosphors are easily prepared led to the empirically developed phosphor genesis scheme based on preserving charge neutrality. This scheme is shown in Figure 1. Here it can be seen that two Y^{3+} ions are replaced by an alkaline earth and a tetravalent uranium ion pair, thus preserving charge neutrality. In an earlier communication we reported that the phosphor $SrO \cdot UO_2 \cdot 3WO_3$ system provided powers of detection for Sm, Eu, Gd, and Dy in the fractional ppm range (*14*). When Ca is substituted for Sr in this system, a relatively intense background luminescence is developed that reduces the powers of detection of the rare earth impurities in the host. Substitution of Ba for Sr reduces the rare earth line intensities considerably and only the lighter rare earths Pr and Nd can be detected at low concentrations.

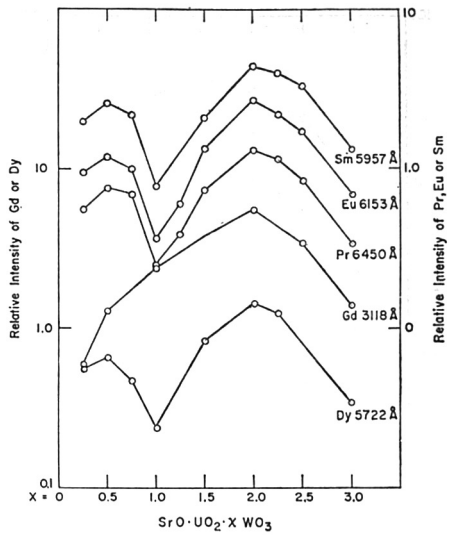

Figure 2. Effect of variation in WO_3 content on rare earth fluorescent line intensities

(16) G. H. Dieke, "Spectra and Energy Levels of Rare Earth Ions in Crystals," Wiley, New York, N. Y., 1968.
(17) R. C Linares, *J. Opt. Soc. Amer.*, **56**, 1700 (1966).
(18) E. S. Makarov, "Crystal Chemistry of Simple Compounds of U, Th, Pu and Np," Consultants Bureau, New York, N. Y., 1959.
(19) F. A. Kroger, "Some Aspects of the Luminescence of Solids," Elsevier Publishing Co., New York, N. Y., 1948, Chap. IV.
(20) H. W. Leverenz, "Luminescence of Solids," John Wiley and Sons, New York, N. Y., 1950.
(21) P. D. Johnson and "Luminescence of Inorganic Solids," P. Goldberg, Ed., Academic Press, New York, N. Y., 1966, Chap. 5.
(22) Yu. S. Leonov, *Opt. Spectrosc. (USSR)*., **9**, 145 (1960); **10**, 357 (1961).
(23) H. J. Borchardt, *J. Chem. Phys.*, **39**, 504 (1963).
(24) Yu. I. Krasilov, Yu. A. Polyakov and Yu. P. Rudnitskii, *Izv. Akad. Nauk SSSR, Neorgan. Mater.*, **3**, 2186 (1966).
(25) G. M. Gaevoi, M. E. Zhabotinskii, Yu. I. Krasilov, Yu. P. Rudnitskii, G. V. Elbert, and V. A. Kizel, *Izv. Akad. Nauk SSSR, Neorgan. Mater.*, **5**, 691 (1969).
(26) M. V. Hoffman, *J. Electrochem. Soc.*, **117**, 227 (1970).

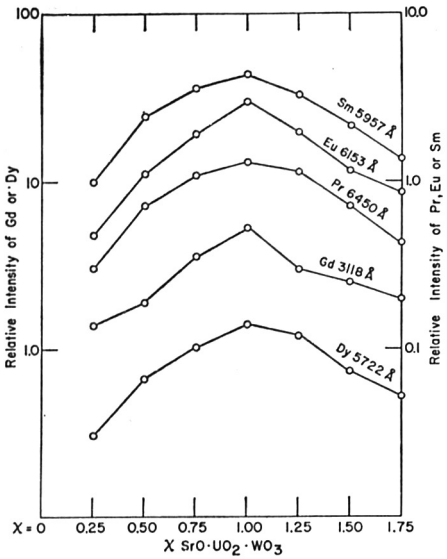

Figure 3. Effect of variation in SrO content on rare earth fluorescent line intensities

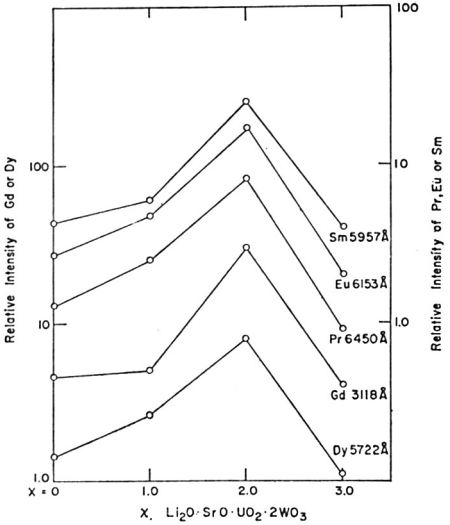

Figure 4. Effect of variation in Li_2O content on rare earth fluorescent line intensities

Since it is known that the molar ratio R_2O_3/WO_3 can vary widely in the rare earth tungstates (*27*), the most logical step was to determine the *b*, *c*, *d* ratio (Figure 1) that would give rise to optimal fluorescent line intensities. The results of these determinations, which are presented graphically in Figures 2 and 3, revealed that the optimal ratios were 1:1:2 rather than the 1:1:3 ratio reported earlier (*14*). A further modification of the $SrO \cdot UO_2 \cdot 2WO_3$ system was suggested by the reports that uranium-activated systems frequently contain lithium as a constituent (*22*, *28*). The beneficial action of Li_2O additions at a molar ratio of 2 to the host material is clearly shown in Figure 4. Thus the system $2Li_2O \cdot SrO \cdot UO_2 \cdot 2WO_3$ has provided the highest powers of detection of the four rare earths of interest in a uranium-containing host. Substitution of lithium by other alkali elements reduced the Gd luminescence appreciably.

The nature of the spectra obtained indicate that the $2Li_2O \cdot SrO \cdot UO_2 \cdot 2WO_3$ host belongs to the scheelite class. The fact that a bright orange colored material is obtained within five minutes of heating the blend of oxides, which by themselves are not orange colored, indicates definite compound formation. The actual host has not been definitely characterized as a single-phase crystalline material. The main emphasis has been to evolve a phosphor with a high degree of reproducibility in preparation and freedom from impurity effects and with the best possible limits of detection for the rare earth neutron poisons.

RESULTS AND DISCUSSION

Fluorescent Spectra. The simple nature of the spectra of rare earth impurities in uranium present in the quaternary oxide phosphor system is evident in Figure 5, which shows the broad background luminescence of this phosphor and the Gd line at 3118 Å at a concentration of 0.1 ppm. The tungstate luminescence extends from 3400–5000 Å, the uranyl ion system from ~5000 to 5800 Å and the uranate ion system from 6400–6800 Å (*29*). The relative intensities of these two systems in our spectra indicate that the uranium occurs predominantly as the uranyl ion in the quaternary oxide host system. The prominent band heads of the second positive system of N_2, which arise from the X-ray excitation of air surrounding the sample are also readily seen (*30*). The spectra of the rare earth impurities of interest present at trace levels are shown in Figure 6. The dotted lines indicate the background from which the relative intensities of the analytical lines are measured. It can be seen from this figure that the simple nature of the spectra gives rise to little spectral interference; the only exception is the Pr 6450 Å line which is not adequately resolved from a sensitive Sm line at 6441 Å. If appreciable Sm occurs in a sample, the relative intensity of the Pr line can be measured above the peak of the Sm 6417 Å line. The concentration of Er, the internal reference element, was arbitrarily set at 10 ppm by weight with reference to the UO_2 component of the host. At this concentration level the intensity of the Er 5507 Å is readily measured and the amount of Er added to each sample is so large that any residual Er in the base mixture at the fractional ppm level makes a negligible contribution to reference line intensity.

All analytical measurements have been based on relating recorded peak height ratios to concentration. In practice the Gd spectrum was scanned first while the 3000 Å blaze grating was in position in the spectrometer.

Analytical Data. The wavelengths of the analytical line pairs, the applicable concentration range, and the estimated

(27) A. Cleve, *Z. Anorg. Chem.*, **32,** 129 (1902).
(28) G. Blasse, *J. Electrochem. Soc.*, **115,** 738 (1968).
(29) H. Gobrecht and W. Weiss, *Z. Physik*, **140,** 139 (1955).
(30) B. Brochlehurst, Atomic Energy Research Establishment, Harwell, C/R **2669**, 1963.

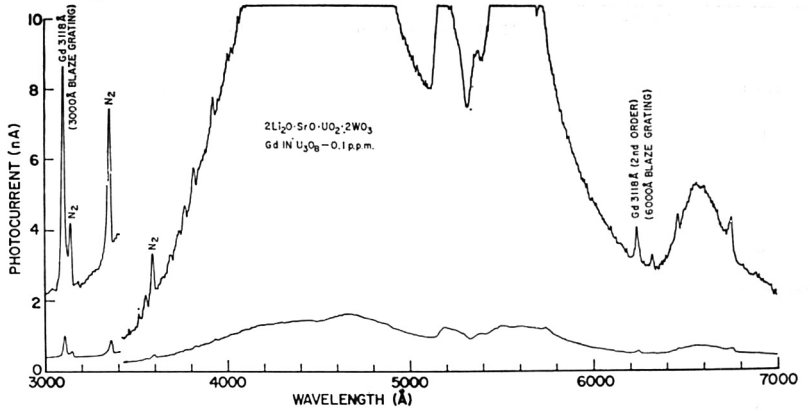

Figure 5. X-Ray excited optical fluorescence spectrum of Gd in $2Li_2O \cdot SrO \cdot UO_2 \cdot 2WO_3$

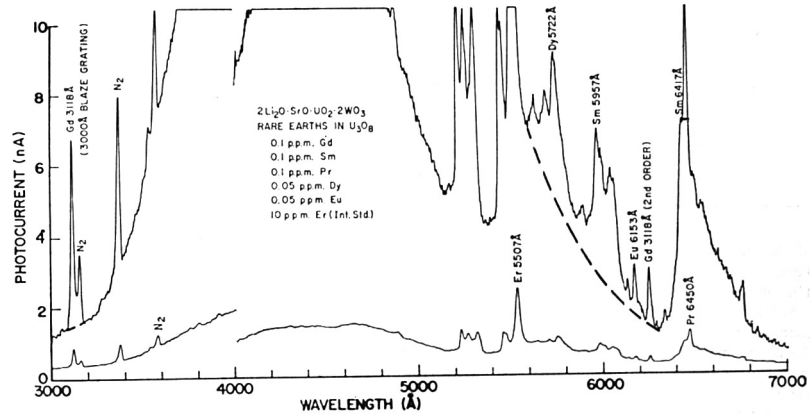

Figure 6. X-Ray excited optical fluorescence spectrum of rare earth impurities and the Er internal reference element in $2Li_2O \cdot SrO \cdot UO_2 \cdot 2WO_3$

Table I. Analytical Data

Element	Analytical line pair, Å	Lowest detectable concentration, ppg	Concentration range in U_3O_8, ppg
Gd	Gd 3118 / Er 5507	2.5	5–500
Sm	Sm 5957 / Er 5507	10.0	20–500
Eu	Eu 6153 / Er 5507	10.0	20–500
Dy	Dy 5722 / Er 5507	2.5	5–250
Pr	Pr 6450 / Er 5507	5.0	10–500

detection limits are summarized in Table I. The detection limits were determined from data obtained from ten different phosphor preparations both of the blank and the lowest standard. From these data the concentrations that would give rise to rare earth line signals equivalent to three times the average peak-to-peak noise in the background spectrum

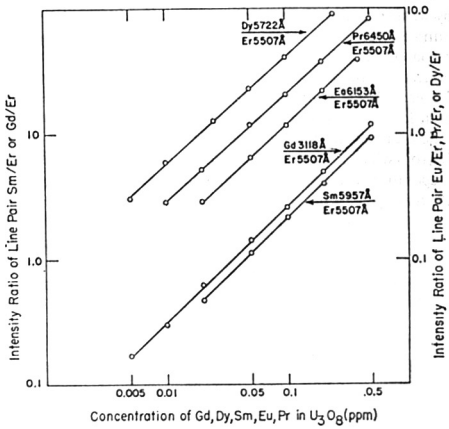

Figure 7. Analytical curves

Table II. Reproducibility of Phosphor Preparation

Sample	Set	Intensity ratio Gd/Er	CV, %	Intensity ratio Sm/Er	CV, %	Intensity ratio Eu/Er	CV, %
	A	0.36		0.26		0.14	
1.	B	0.26	±18.0	0.20	±14.0	0.10	±16.0
	C	0.32		0.24		0.12	
	A	1.50		1.18		0.64	
2.	B	1.39	±16.0	0.98	±15.0	0.45	±17.0
	C	1.42		1.04		0.56	
	A	6.50		5.40		3.2	
3.	B	5.58	±10.0	4.50	±10.0	2.3	±8.0
	C	5.84		5.10		2.6	

Table III. Impurity Effects on the Determination of Rare Earths in U_3O_8

Impurity	Concn in U_3O_8, ppm	Intensity ratio Gd/Er	Sm/Er	Eu/Er	Dy/Er	Pr/Er
...	residual	1.44	1.17	0.54	1.94	1.44
Fe	500	1.46	1.12	0.50	1.90	1.49
	750	1.60	0.92	0.63	1.81	1.60
	1000	1.51	0.98	0.52	2.06	1.46
Ca	500	1.21	1.01	0.63	1.97	1.33
	750	1.36	1.01	0.55	1.95	1.28
	1000	1.41	1.22	0.63	2.08	1.50
Al	500	1.49	1.08	0.47	1.83	1.26
	750	1.50	0.99	0.54	1.78	1.56
	1000	1.62	0.95	0.48	1.58	1.33
Fe + Al + Ca	200 each	1.47	1.06	0.57	1.87	1.32
	500 each	1.37	1.06	0.46	1.76	1.23
	750 each	1.53	1.09	0.46	1.85	1.37

of the blank at the selected wavelengths were calculated. These concentrations are defined as the detection limit. The analytical curves are shown in Figure 7.

Subtle variations in preparative procedures as well as changes in the concentration of extraneous impurities in the sample may affect the analytical line fluorescent intensities in a rather unpredicted manner (*9*, *20*, *21*). However, these intensity changes may be externally compensated by applying the well-known internal reference principle (*9*, *12*).

The reproducibility of phosphor preparation was evaluated by analyzing the rare earth content of three synthetic U_3O_8 samples. Initially, three phosphor base mixtures were prepared from different lots of chemicals, each of which was utilized to prepare five different phosphor samples. Thus for each U_3O_8 sample, 15 phosphor preparations were obtained. The observed coefficients of variation of the intensity ratios calculated for each sample are tabulated in Table II, from which it is evident that the reproducibility of phosphor preparation as measured by the intensity ratios is of the order 10 to 20%.

The deliberate addition of Fe, Ca, and Al, which are typical of the impurities occurring in nuclear grade uranium, has been utilized to study the influence of these impurities either individually or cumulatively on the determination of the rare earths. The data for the relative intensities of each of the rare earths as well as intensity ratios are shown in Table III. The pattern of variations observed is random and no systematic trends are evident, even though the level of impurities added is far in excess of those found in nuclear grade uranium. This significant absence of impurity effects as compared to earlier observations (*9*, *20*) may be a fortuitous characteristic of this particular host. The incorporation of the Er internal reference element, however, is highly desirable because a change in the intensity of the Er reference lines serves to monitor drastic changes in phosphor characteristics as well as instrumental variations.

RECEIVED for review April 12, 1971. Accepted May 19, 1971. Work performed in the Ames Laboratory of the U.S. Atomic Energy Commission, Iowa State University, Ames, Iowa.

Analysis of Mixtures of Isomeric Polynuclear Hydrocarbons by Nuclear Magnetic Resonance Spectrometry

Methylated Derivatives of Anthracene, Benz[*a*]anthracene, Benzo[*c*]phenanthrene, and Pyrene

Larry K. Keefer,[1] Lawrence Wallcave, James Loo, and Ruth S. Peterson

The Eppley Institute for Research in Cancer, University of Nebraska Medical Center, Omaha, Neb. 68105

NMR spectrometry is used for the determination of specific methylaromatic hydrocarbons in mixtures of structurally similar compounds. Identifications are made on the basis of relative chemical shifts, and confirmed using τ_0 values (methyl chemical shift at infinite dilution in a specified solvent system) and peak multiplicity information. Mixtures containing as little as 30–40 μg of each component are quantified by spectral integration. Chemical shift data for authentic specimens of all monomethyl derivatives of anthracene, benz[a]anthracene, benzo[c]phenanthrene, and pyrene are presented. While such reference data are often essential for positive identifications, satisfactory assignments can sometimes be made on the basis of values predicted from structure-shift correlations. The method is applicable to the determination of methylaromatic hydrocarbons in complex environmental mixtures, and the characterization of some petrolatum and asphalt fractions is described.

SINCE THE ISOLATION of benzo[*a*]pyrene (I) from coal tar in 1932 and its identification as a powerful agent for the production of malignant tumors in laboratory animals (*1*), a great deal of effort has been devoted to searching for (I) and related compounds in the human environment (Chart I). The importance of this attempt to establish the "total load of carcinogens" in a given locale as a prerequisite to "planning an effective reduction of the exposure of man to carcinogens" has recently been underscored by the International Union Against Cancer (*2*), and the chromatographic–spectrophotometric procedures (*3*) employed in these studies have accordingly been refined to a level of sophistication such that (I) and several other known polynuclear carcinogens can be routinely determined at levels of a few parts per billion or less.

Nevertheless, the procedures described in the literature as applicable to the study of the distribution of environmental carcinogens all seem to be deficient in at least one critical respect. The chromatographic resolution of most environmental hydrocarbon samples ultimately results in the isolation of many different "alkylaromatic" fractions, each of which may be homogeneous with respect to "ring content" and molecular weight, but which contains a mixture of isomeric compounds. The close similarity of the constituents of these fractions with respect to chemical and physical properties normally precludes analyzing them by the usual chromatographic-spectral methods. Of the numerous reports describing analyses of environmental substances for carcinogenic hydrocarbons, only a few include reliable identifications of specific alkylated polynuclear compounds, and virtually all of these identifications have involved tedious, nonquantitative isolation procedures. The great majority of authors have either drawn conclusions not supported by their data, or have chosen noncommittally to report the total quantities of each compound type (*e.g.*, "alkylpyrene" or "methylpyrene") present in the sample.

The inadequacy of this latter type of analytical information for the purpose of establishing or rationalizing carcinogenicity data becomes readily apparent when one considers the remarkable dependence of the biological properties of these compounds upon the precise nature of their alkyl substitution pattern. Methylation of benz[*a*]anthracene (II) at both the 7 and 12 positions converts a compound which is at most only mildly carcinogenic to one of the most potent tumor-producing agents known. Of the twelve possible monomethyl derivatives, the 6-, 7-, 8-, and 12-isomers are carcinogenic, while the remaining eight have been reported to be inactive (*4*).

Chart I

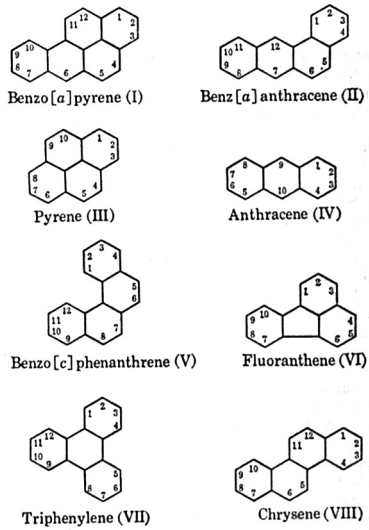

[1] Author to whom inquiries may be addressed, c/o The National Cancer Institute, Bethesda, Md. 20014

(1) J. W. Cook, C. L. Hewett, and I. Hieger, *Nature*, **130**, 926 (1932).
(2) P. Shubik, D. B. Clayson, and B. Terracini, Eds., "The Quantification of Environmental Carcinogens," UICC Technical Report Series, Vol. 4, International Union Against Cancer, Geneva, Switzerland, 1970, p 1.
(3) E. Sawicki, *Chemist-Analyst*, **53**, 24, 56, and 88 (1964).
(4) C. B. Huggins, J. Pataki, and R. G. Harvey, *Proc. Nat. Acad. Sci.*, **58**, 2253 (1967).

Thus an analytical method capable of identifying and quantifying specific alkylaromatic carcinogens in the presence of their biologically inactive isomers on a routine and efficient basis must clearly be made available before the contributions of various environmental factors to the total carcinogenic load can be meaningfully predicted. We have found that nuclear magnetic resonance (NMR) spectrometry, with its nearly unique sensitivity to subtle differences in molecular architecture, goes a very long way toward meeting this requirement. Specifically, information on the chemical shifts, multiplicities, and relative integrals of the peaks found in the methyl region of a sample's NMR spectrum provides a convenient basis for analyzing mixtures of alkylated polynuclear hydrocarbons.

EXPERIMENTAL

Materials. The three methylpyrene samples were purchased from L. Light & Co., Ltd. (Colnbrook, England). 2-Methylanthracene was obtained from Aldrich Chemical Co., (Milwaukee, Wis.), and the 9-methylanthracene was a product of Eastman Organic Chemicals (Rochester, N. Y.). All other methylaromatic compounds were kindly provided by M. S. Newman, of Columbus, Ohio.

The amber petrolatum was an N. F. grade obtained from Arthur S. La Pine and Co., Chicago, Ill. It had a total methylpyrene content of 25 ppm, a dimethyl (and/or ethyl)-pyrene content of 15 ppm, and a methyltriphenylene content of 6 ppm (Unpublished analyses in this laboratory using chromatographic fractionation and UV and mass spectrometry). The asphalt was an 85/100 penetration sample of the grade commonly used in road paving and corresponds to "Asphalt F" of ref. *5*. It had a monomethylpyrene content of 59 ppm and a dimethyl (and/or ethyl)pyrene content of 20 ppm.

Procedure. The entire spectral region of interest was investigated in a single (left-to-right) scan with a Varian Model HA-100 NMR Spectrometer operating in the frequency sweep mode. The sweep width was usually set at 50–100 Hz for maximum horizontal sensitivity. Normal precautions were taken to avoid saturation effects.

The center of each observed peak was located visually, and the pen was swept to that point from left to right. The chemical shift was taken as the average of five successive readings of the V-4315 Frequency Counter, which was set to read the difference to the nearest 0.001 ppm between the pen position and the reference lock signal.

Each set of concentration *vs.* chemical shift data was fitted to a best straight line using a standard least-squares program, which furnished values for the intercept (τ_0), slope, standard error around the line, and the variances in the intercept and slope. The error limits given in Tables I–V are the square roots of these variances.

Decoupling experiments were conducted with the aid of a Hewlett-Packard Model 200 AB Audio Oscillator. Irradiation frequency was determined with the V-4315 Frequency Counter in External mode, and intensity was estimated from the amplitude of the sine wave on the oscilloscope.

Time-averaged spectra were accumulated on a C-1024 Time Averaging Computer.

Error Analysis. Chemical shift values were critically dependent upon solvent effects. The τ_0 value of 4-methylpyrene, for example, was 0.013 ppm smaller in chloroform-*d* than in carbon tetrachloride (*cf.* Table I). The shift data also depended intimately upon the concentration of tetramethylsilane (TMS), which was carefully maintained at 5% of the solvent by weight.

In raising the temperature from −45° to +45 °C, the approximately linear increase in τ for each of the methylpyrenes was only 0.03 Hz/degree, on the average. Therefore, variations in chemical shift due to fluctuations in normal probe temperature (which ranged from 30–36°) were neglected.

The importance of other potential sources of systematic error, *e.g.*, differences among operators in locating centers of peaks, might largely be compensated for by adjusting a given set of readings to a pair of calibration points. The chemical shift of TMS was defined as 10.000 τ by the electronic lock component of our spectrometer, and the chloroform in 95.0:5.0 (w:w) $DCCl_3$:TMS furnished a second reference point of 2.744 τ.

Random errors were estimated by repeatedly determining the chemical shifts for methylpyrene mixtures of four different concentrations throughout the course of a week. The standard deviation for each compound was found to be $\leq$0.15 Hz. This value was taken as an estimate of the standard deviation of chemical shift measurements throughout this study.

The uncertainty in the intercept position could be made as small as necessary. The variance of the τ_0 values can be estimated from the equation

$$V_{\tau_0} = V_\tau \left[\frac{1}{N} + \bar{C}^2 \Big/ \sum_{i=1}^{N} (C_i - \bar{C})^2 \right]$$

where V_τ is the variance for the N chemical shift readings, C_i is the concentration coordinate of the ith reading, and $\bar{C}$ is the arithmetic mean of the C_i's. The standard deviation of a τ_0 value calculated from only two chemical shift readings (for concentrations x and $2x$) can thus be approximated as $\leq$0.34 Hz, which is sufficiently precise for distinguishing with confidence among most of the isomeric compounds described here.

RESULTS AND DISCUSSION

The Methylpyrenes. Initial experiments to determine the applicability of NMR spectrometry to the characterization of environmental alkylaromatic mixtures were with the monomethyl derivatives of pyrene (III). Although these compounds appear not to be particularly interesting from the biological point of view [carcinogenicity tests (*6*, *7*) have thus far yielded negative results], the methylpyrene fractions of petrolatums and asphalts are relatively easily isolated and among the most abundant of their polynuclear components. We therefore determined the spectral properties of the three isomers, using samples obtained from commercial sources.

Our results, although quantitatively somewhat at variance with those of Lewis (*8*), nevertheless confirmed his report that the magnetic environments of the three methyl groups differ substantially. As shown in Figure 1, the methyl resonances all shift toward higher field with increasing concentration, as expected (*9*), but the differences in concentration dependence among the three compounds are relatively small. The methyl spectrum of a mixture of the three methylpyrenes should thus contain three discrete resonances at intervals of 0.09 ± 0.01 ppm, which are due, in the order of increasing field, to the 1-, 4-, and 2-isomers, respectively. This prediction is borne out by the experimental result. The

(5) L. Wallcave, H. Garcia, R. Feldman, W. Lijinsky, and P. Shubik, *Toxicol. Appl. Pharmacol.*, **18**, 41 (1971).

(6) G. Barry, J. W. Cook, G. A. D. Haslewood, C. L. Hewett, I. Hieger, and E. L. Kennaway, *Proc. Roy. Soc., Ser. B*, **117**, 318 (1935).

(7) H. Dannenberg, *Z. Krebsforsch.*, **63**, 102 (1959).

(8) I. C. Lewis, *J. Phys. Chem.*, **70**, 1667 (1966).

(9) J. A. Pople, W. G. Schneider, and H. J. Bernstein, "High Resolution Nuclear Magnetic Resonance," McGraw-Hill Book Company, New York, N. Y., 1959, pp 424*ff*.

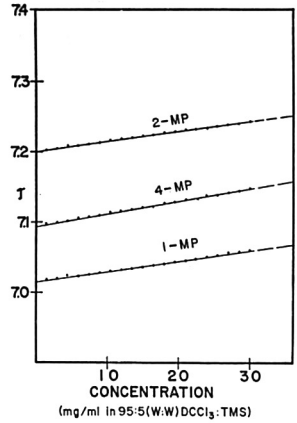

Figure 1. Concentration dependence of methyl chemical shifts of methylpyrenes

spectrum of an artificial mixture (Figure 2) clearly shows all three peaks at the expected relative chemical shifts; integration revealed the three compounds to be present to the extent of 1:1:1, in agreement with the known composition of the mixture.

While unequivocal information on the composition of most methylpyrene mixtures can be deduced from the relative shifts and integrals of the peaks found in a single scan of the methyl region, evidence confirming the identifications may occasionally be required. It may be difficult to distinguish a very concentrated solution of 1- and 4-methylpyrene from a more dilute solution of the 4- and 2-isomers, for example. Figure 2 suggests a powerful means for doing this. The aliphatic protons of a methylaromatic compound might in general be expected to couple measurably with every hydrogen atom attached to the same ring (*10*, *11*). If so, the methyl group of 4-methylpyrene should be coupled to one other proton, and should appear as a doublet, while 2-methylpyrene, the methyl group of which is flanked by two identical ortho protons, should give rise to a triplet in the methyl region. The 1-methyl group of the remaining isomer should be coupled with the meta and ortho protons, and would be expected to appear as a complex multiplet which is difficult to resolve because of the small values of the two different long-range coupling constants. That peak multiplicity data can be used in this way to assign or confirm structures is evident from Figure 2, which clearly shows the expected doublet, triplet, and unresolved multiplet.

A second, even more general way to confirm identifications made on the basis of relative peak positions is to divorce the chemical shift from its concentration dependence by collecting shift information at two or more concentrations in a given reference solvent and extrapolating to infinite dilution (*12*, *13*). The chemical shifts at zero concentration (τ_0) are

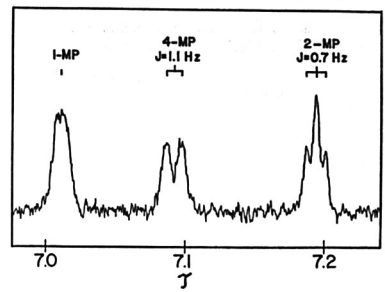

Figure 2. Methyl region NMR spectrum in 95:5 (w : w) $DCCl_3$: TMS of an equimolar mixture of three isomeric methylpyrenes

Table I. Methyl Chemical Shifts of the Methylpyrenes in Two Solvents

Isomer	Solvent[a]	Chemical shift at infinite dilution, τ_0	Slope (S) of plot of chemical shift *vs.* concentration[b]
1	A	$7.022_6 \pm 0.000_4$	$2.24_5 \pm 0.01_8$
	B	$7.015_3 \pm 0.000_7$	$1.48_3 \pm 0.02_7$
2[c]	A	$7.208_1 \pm 0.000_3$	$1.99_1 \pm 0.01_1$
	B	$7.201_0 \pm 0.000_4$	$1.38_9 \pm 0.01_5$
4[d]	A	$7.107_6 \pm 0.000_8$	$2.45_2 \pm 0.04_4$
	B	$7.094_8 \pm 0.000_6$	$1.74_1 \pm 0.02_3$

[a] A = 95:5 (w:w) CCl_4:TMS; B = 95:5 (w:w) $DCCl_3$:TMS.
[b] $S = (\tau - \tau_0)/C$, where C is the solute concentration in grams/ml for any point (C, τ) on the least-squares fitted line defined by these data.
[c] Triplet, J = 0.7 Hz.
[d] Doublet, J = 1.1 Hz.

Table II. Methyl Chemical Shifts of the Methylanthracenes

Isomer	Chemical shift at infinite dilution,[a] τ_0	Slope (S) of plot of chemical shift *vs.* concentration[b]
1	$7.178_9 \pm 0.000_6$	$1.16_9 \pm 0.09_6$
2	$7.456_6 \pm 0.001_3$	$0.87_2 \pm 0.03_7$
9	$6.892_1 \pm 0.000_6$	$1.24_7 \pm 0.01_7$

[a] In 95:5 (w:w) $DCCl_3$:TMS.
[b] $S = (\tau - \tau_0)/C$, where C is the solute concentration in grams/ml for any point (C, τ) on the least-squares fitted line defined by these data.

fully characteristic of even the minor components of a mixture, and identifications can be made or confirmed by comparing experimental τ_0 values with those independently obtained using authentic reference samples. The τ_0 values for the methylpyrenes in two different solvent systems are given in Table I.

Scope and Limitations. The NMR method described for the methylpyrenes is also applicable to problems involving the analysis of other methylated polynuclear compounds. For example, the methyl chemical shifts of the three monomethyl derivatives of anthracene (IV) are separated by intervals more than twice as large as those for the methylpyrenes. Shift data for the former series are summarized in Table II.

The minimum difference in τ_0 among the isomeric methylbenz[*a*]anthracenes (0.016 ppm) is also much larger than the

(10) S. Sternhell, *Rev. Pure Appl. Chem.*, **14**, 15 (1964).
(11) E. Clar, B. A. McAndrew, and Ü. Sanigök, *Tetrahedron*, **26**, 2099 (1970).
(12) N. Jonathan, S. Gordon, and B. P. Dailey, *J. Chem. Phys.*, **36**, 2443 (1962).
(13) P. Durand, J. Parello, and N. P. Buu-Hoï, *Bull. Soc. Chim. Fr.*, **1963**, 2438.

Table III. Methyl Chemical Shifts of the Methylbenz[*a*]anthracenes

Isomer	Chemical shift at infinite dilution,[a] τ_0	Slope (S) of plot of chemical shift *vs.* concentration[b]
1	6.7505 ± 0.0025	2.43 ± 0.14
2	7.3531 ± 0.0008	1.79 ± 0.08
3	7.4436 ± 0.0011	1.42 ± 0.16
4	7.2534 ± 0.0008	2.18 ± 0.26
5[c]	7.2868 ± 0.0009	2.11 ± 0.08
6[c]	7.1945 ± 0.0048	3.74 ± 0.69
7	6.8944 ± 0.0010	4.39 ± 0.46
8	7.1741 ± 0.0018	*d*
9	7.4279 ± 0.0031	1.13 ± 0.42
10	7.4098 ± 0.0023	1.99 ± 0.69
11	7.0687 ± 0.0012	2.93 ± 0.12
12	6.6049 ± 0.0017	3.35 ± 0.73

[a] In 95:5 (w:w) CCl_4:TMS.
[b] $S = (\tau - \tau_0)/C$, where C is the solute concentration in grams/ml for any point (C, τ) on the least-squares fitted line defined by these data.
[c] Doublet, J = 1.2 Hz.
[d] Insufficient sample for accurate measurement of slope.

Table IV. Methyl Chemical Shifts of the Methylbenzo[*c*]phenanthrenes

Isomer	Chemical shift at infinite dilution,[a] τ_0	Slope (S) of plot of chemical shift *vs.* concentration[b]
1	7.5872 ± 0.0007	0.68 ± 0.08
2	7.3488 ± 0.0008	1.05 ± 0.06
3	7.4042 ± 0.0007	1.16 ± 0.12
4	7.1774 ± 0.0006	1.47 ± 0.05
5[c]	7.1964 ± 0.0006	2.12 ± 0.07
6[c]	7.1862 ± 0.0009	2.05 ± 0.05

[a] In 95:5 (w:w) CCl_4:TMS.
[b] $S = (\tau - \tau_0)/C$, where C is the solute concentration in grams/ml for any point (C, τ) on the least-squares fitted line defined by these data.
[c] Doublet, J = 1.0 Hz.

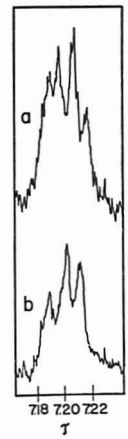

Figure 3. Methyl region NMR spectra in 95 : 5 (w : w) CCl_4 : TMS of an equimolar mixture of 4-, 5-, and 6-methylbenzo-[c]phenanthrene: *a* normal scan; and *b* during simultaneous irradiation at 2.384 τ with 500 mV

experimental error, and it is apparent from the data in Table III that a mixture containing all twelve isomers could be assayed by NMR. The four carcinogenic derivatives (6-, 7-, 8-, and 12-) are particularly easily identified on the basis of their chemical shifts.

The data for 9- and 10-methylbenz[*a*]anthracene illustrate a potential limitation of the method. While their τ_0 values differ substantially (by 0.018 ppm), the rate of increase in τ with concentration is almost twice as large in the isomer which appears at lower field, and their methyl chemical shifts should become identical at an effective concentration of approximately 21 mg/ml.

Several approaches can be taken to circumvent the difficulties arising in specific cases from a chemical shift similarity of this sort. In the example of the preceding paragraph, for instance, an appropriate change in the concentration would permit the mixture to be assayed for the two compounds. Small chemical shift differences could be magnified by determining the spectrum at higher field strength, but, in the absence of this alternative, we have found that decoupling techniques can simplify interpretation by narrowing the peaks; an example of this approach is described later in this section. It might be possible to separate overlapping resonances in some cases by changing the solvent. (Shift values for these compounds at a single concentration in dimethylsulfoxide-d_6 are given in reference *14*). Finally, peaks outside the methyl region might be useful, but somewhat less sensitive, analytical probes.

Data for the monomethylated derivatives of benzo[*c*]phenanthrene (V) are given in Table IV. Three of these compounds are well separated in chemical shift, and thus easily analyzed. The 4-, 5-, and 6-isomers, on the other hand, possess magnetically similar methyl groups, and the spectrum of an equimolar mixture (Figure 3*a*) of the three compounds is accordingly quite complicated. The presence of four peaks in the methyl region can be attributed to the fact that the 5- and 6-methyl groups are both doublets, the downfield half of the former happening to coincide with the upfield half of the latter. Simultaneous irradiation of the aryl protons responsible for the doublets gave rise to sharp singlets for both methyl groups. While the decoupled spectrum (Figure 3*b*) is not ideal for analytical purposes, the occurrence of three peaks with the proper relative chemical shifts clearly reveals the presence of all three isomers, and curve-resolving techniques can be used to estimate the concentrations as approximately equimolar, in agreement with the known composition of the mixture.

The relative methyl chemical shifts of the compounds investigated so far can be rationalized in terms of the structural considerations outlined by Martin (*15*) for the resonances of aromatic protons. Thus β methyl groups (*i.e.*, those with no benzo substituent in the ortho–meta position) appear at significantly higher field than α-methyls (ortho to a single benzo ring), which are in turn significantly shielded with respect to those of the γ-type (ortho to two benzo rings). At lowest field are the α3-methyl groups of compounds such as 1- and 12-methylbenz[*a*]anthracene, in which the angular arrangement of aromatic rings provides an especially strong deshielding influence. Of the methyl shifts given in Tables I–IV, the only one which does not correlate reasonably well with the corresponding aryl proton shift is that of 1-methylbenzo[*c*]-phenanthrene. The anomalously high methyl chemical shift

(14) R. J. Ouellette and B. G. van Leuwen, *J. Org. Chem.*, **34**, 62 (1969).
(15) R. H. Martin, *Tetrahedron*, **20**, 897 (1964), and subsequent papers of that series.

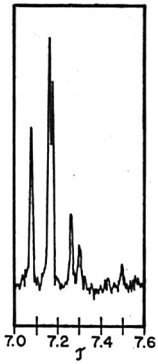

Figure 4. Methyl region NMR spectrum in CCl_4 : TMS of the monomethylpyrene fraction of amber petrolatum

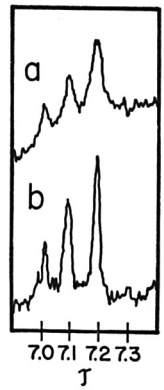

Figure 5. Methyl region NMR spectrum: *a* of *ca.* 220 μg of the monomethylpyrene fraction of asphalt in CCl_4 : TMS (using microcell and computer time-averaging); *b* of a 20 : 38 : 42 mixture of 1-, 4-, and 2-methylpyrene under similar conditions

Table V. Characterization of the Monomethylpyrene Fraction of Amber Petrolatum by NMR

Isomer	(CCl_4[a])	($DCCl_3$[a])	Relative concn, %
1	$7.022_9 \pm 0.001_2$	$7.015_1 \pm 0.001_1$	30
2	$7.207_4 \pm 0.001_2$	$7.202_6 \pm 0.001_0$	15
4	$7.107_3 \pm 0.001_4$	$7.096_0 \pm 0.001_0$	55

[a] Contains 5.0 wt % TMS as internal reference.

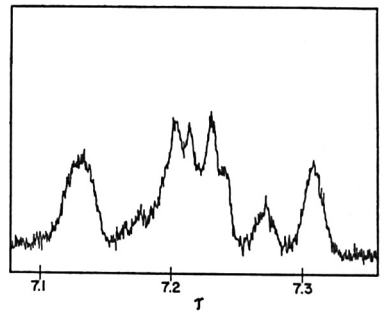

Figure 6. Methyl region NMR spectrum in CCl_4 : TMS of the dimethylpyrene fraction of amber petrolatum

of this compound has been noted and explained (*16*) in terms of the steric displacement of the methyl group from the plane of the aromatic system. In cases not complicated by steric effects, however, the methyl shifts can apparently be crudely predicted on the basis of Martin's rules. The use of these considerations in the identification of a compound for which no reference sample was available is described in the next section.

Applications. Several "alkyl" polycyclic aromatic fractions from amber petrolatum and from a paving grade asphalt were isolated by an appropriate scaling-up of a previously described analytical method (*5*). Although these chromatographic methods cleanly separated the alkylaromatics from the unsubstituted parent compounds, resolution of isomers could not generally be effected and UV methods were not adequate for analysis of the mixtures. The NMR spectrum of the monomethylpyrene fraction contained three peaks in the methyl region (Figure 4) whose relative chemical shifts (7.08, 7.17, and 7.26 τ) demonstrate the presence of all three isomers. The doublet character of the 4-methylpyrene peak can be easily discerned from this spectrum, but the 2-methylpyrene triplet could be resolved only at increased horizontal sensitivity. Further confirmation for these identifications was obtained by extrapolation of the data for several concentrations to infinite dilution. The τ_0 values for these three compounds, which are identical, within experimental error, with those found for the authentic methylpyrenes (*cf.* Table I), are summarized in Table V. The other significant peaks in this spectrum are undoubtedly due to two of the five monomethyl derivatives of fluoranthene (VI), the presence of which had earlier been indicated by the UV spectrum.

All three methylpyrenes were also shown to be present in the asphalt (Figure 5*a*), but the relative proportions were markedly different from those of amber petrolatum. 2-Methylpyrene, which was the least abundant isomer in the petrolatum sample (*cf.* Table V), was the most important constituent of the corresponding fraction of asphalt. The relative concentrations of the 1-, 2-, and 4-isomers in asphalt were estimated from the integral to be 20%, 45%, and 35%, respectively. The assignments of the peaks in this time-averaged, microcell spectrum were "confirmed" by comparison with the spectrum of a synthetic mixture of that composition (Figure 5*b*).

A second sample isolated from amber petrolatum was shown by UV to be an alkylpyrene fraction and by mass spectrometry to consist entirely of molecules with the empirical formula $C_{18}H_{14}$. The assumption that this fraction probably contained ethyl- as well as dimethylpyrenes was not supported by the NMR spectrum (Figure 6), in which no peak attributable to an ethyl group could be detected. From the number of peaks in the spectrum, it was concluded that at least three of the fifteen possible dimethylpyrenes are present in substantial amount, but more specific structural interpretations have not been attempted because of a lack of data for authentic samples.

The last petrolatum fraction investigated was one whose UV and mass spectra had shown a preponderance of a mono-

(16) M. S. Newman, R. G. Mentzer, and G. Slomp, *J. Amer. Chem. Soc.*, **85**, 4018 (1963).

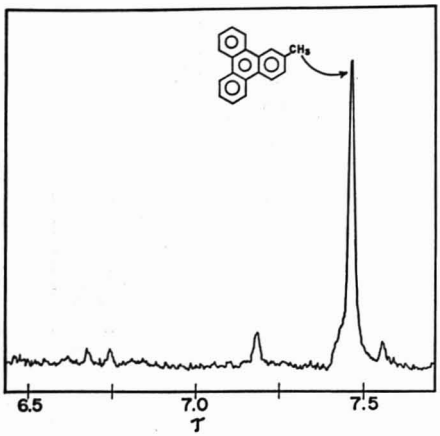

Figure 7. Time-averaged (225 scans) methyl region NMR spectrum in 95 : 5 (w : w) CCl_4 : TMS of the monomethyltriphenylene fraction of amber petrolatum

methyl derivative of triphenylene (VII). The NMR spectrum (Figure 7) of this fraction was dominated by a single peak at 7.46 τ (τ_0 = 7.3996 ± 0.0021). Although shift data for neither methyltriphenylene isomer appear to be available, this peak can rather convincingly be assigned to the 2-isomer, since a methyl group at the 1-position should appear roughly 0.7 ppm toward lower field by virtue of its angular orientation with respect to the benzo ring.

The presence of at least five other compounds is evident from this spectrum. One of the two small peaks at 6.67 and 6.74 τ, each of which integrates to roughly 2% of the mixture, might correspond to 1-methyltriphenylene. Alternatively, since chrysene (VIII) derivatives had been shown by UV to be present to the extent of about 10% in this fraction, these two peaks could be due to 4- and 5-methylchrysene; the latter compound, while reported to be rather strongly carcinogenic (*17*), would, however, be present in the whole petrolatum to the extent of only a few parts per billion.

Finally, the noteworthy sensitivity of the NMR method described in this report can be illustrated using Figure 7. After time-averaging overnight, the peaks at 6.67 and 6.74 τ, each of which corresponds to only 30–40 μg of sample, are quite suitable for quantitative analysis, and it seems likely that the limits of detection could be lowered even further with the appropriate use of Fourier transform and/or microcell techniques.

RECEIVED for review April 12, 1971. Accepted May 19, 1971. Presented in part to the Midwest Regional ACS Meeting, Lincoln, Neb., October 29, 1970. The financial support of the U. S. Public Health Service, Contract No. 43-68-959, is gratefully acknowledged.

(17) G. M. Badger, *Advan. Cancer Res.*, **2**, 73 (1954).

Gas Chromatographic Determination of Aqueous Trace Hydrazine and Methylhydrazine as Corresponding Pyrazoles

L. A. Dee

Air Force Rocket Propulsion Laboratory, Air Force Systems Command, United States Air Force, Edwards, Calif. 93523

A gas chromatographic technique is described in which hydrazine and methylhydrazine are determined simultaneously at concentrations of 0.1 to 50 parts-per-million in aqueous solution. Detector sensitivity to hydrazine and methylhydrazine is enhanced by quantitative formation of the substituted pyrazoles with 2,4-pentanedione prior to chromatographic separation. Unsym-dimethylhydrazine, urea, alanine, iron, copper, and aluminum do not interfere with the analysis.

HYDRAZINE, HYDRAZINE SALTS, and simple organic derivatives are used industrially as fungicides, antioxidants, reducing agents, and as rocket fuels (*1*). A reliable method for the measurement of hydrazine and hydrazine derivatives in dilute aqueous solution is necessary for both industrial and environmental control because even though low concentrations are often effective in processes, these concentrations may be quite toxic (*2*).

Hydrazines are generally powerful reducing agents, and many sensitive tests for their presence are based on this property. Feigl and Dacorso (*3*) reported a number of spot tests based on reduction of metal ions by hydrazine. Sant (*4*) used the reduction of $Ag(NH_3)_2^{1+}$ to Ag^0 to indicate the presence of hydrazine. Weakley *et al.* (*5*) applied the hydrazine reduction of Fe^{3+}, present in excess, to Fe^{2+} and reaction of the remaining Fe^{3+} with 2,2-bipyridine to an indirect spectrophotometric

(1) R. Kirk and D. Othmer, "Encyclopedia of Chemical Technology," Vol. 11, 2nd ed., John Wiley & Sons, New York, N. Y., 1966, p 185.

(2) N. Irving Sax, "Dangerous Properties of Industrial Materials," 3rd ed., Reinhold Book Corp., Albany, N. Y., 1968, p 819.
(3) F. Feigl and G. E. Dacorso, *Chemist-Analyst*, **32**, 28–30 (1943).
(4) B. R. Sant, *Mikrochim. Acta*, **1958**, 169–70.
(5) F. B. Weakley *et al.*, *Microchem. J.*, **7**(2), 185–93 (1963).

determination of hydrazine. McKinnis and Yard (6) measured the nitrogen liberated when KIO_3 was combined with dissolved hydrazine. Such methods are most adequate if the sample is well characterized, but they are sometimes subject to interference if other reducing substances are present.

A number of direct colorimetric tests have been reported. Feigl and Manheimer (7) used the yellow hydrazone from salicylaldehyde to test for hydrazine. Kul'berg and Cherkesov (8) and Riley (9) reacted hydrazine with picryl chloride to produce colored products. Vanags *et al.* (*10–12*) studied the reaction of hydrazine with indanedione derivatives, and others (*13–16*) have used *p*-dimethylaminobenzaldehyde (PDAB) as a colorimetric reagent for hydrazines. Colorimetric methods for hydrazines, although generally more specific than oxidation/reduction methods, still are subject to a number of interferences. Hydroxylamine, urea, amino acids, other hydrazine derivatives, and some amines are typical interferences that have been reported.

Preliminary separation of the desired hydrazine from interfering substances by paper chromatography has been reported by Bremner (*17*) and Hinman (*18*). Reynolds and Thomas (*19*) precipitated interfering proteins with trichloroacetic acid and measured the hydrazine or methylhydrazine content of the supernatant liquid with PDAB. Kalinina (*20*) also used PDAB but overcame the difficulty of interferences by dividing the sample and destroying the hydrazine in one portion prior to a differential spectrophotometric analysis.

Still another approach to interference elimination is through a preliminary reaction followed by separation and measurement of the derivative. Such a method was reported by Neuman and Nadeau (*21*). NaClO added to an aqueous sample liberated methane in proportion to the methylhydrazine content, and the gas was separated and measured by a gas chromatographic technique.

The following method is not affected by earlier reported interferences, and both hydrazine and methylhydrazine can be determined simultaneously. 2,4-Pentanedione is combined with aqueous hydrazine and/or methylhydrazine to form the substituted pyrazoles. Separation and measurement of the pyrazoles from potentially interfering agents is accomplished by gas chromatography. This subsequent separation and measurement by gas chromatography allows the analyst somewhat greater freedom for adjustment of the method to his specific analytical problems.

EXPERIMENTAL

Reagents. *p*-Dimethylaminobenzaldehyde (Eastman) was used without further purification. 2,4-Pentanedione (Aldrich) was distilled through an 18-inch spinning band column (Nestor Faust) and the constant boiling (135 °C at 690 mm) fraction was collected. The hydrazine and methylhydrazine (both from Olin Mathieson) assayed better than 99% and were used without further treatment.

3,5-Dimethylpyrazole. 3,5-Dimethylpyrazole was prepared by combining 0.16 mole of 2,4-pentanedione with 0.16 mole of hydrazine which had been dissolved in 100 ml of distilled water and cooled to 5 °C. Isolation and purification of the pyrazole was accomplished by the method described by Wiley and Hexner (*22*). The melting point was 105–6 °C (found) with 106–7 °C (reported).

1,3,5-Trimethylpyrazole. Methylhydrazine was substituted for hydrazine and 1,3,5-trimethylpyrazole was prepared and purified in a similar manner. The melting point was 36–7 °C (found) with 37 °C (reported). Infrared spectra of the pyrazoles also were used to establish their identity.

Apparatus. A Beckman Model GC-4 equipped with an on-column inlet and a Beckman Model GC-M equipped with a flash vaporizer inlet were used. Both gas chromatographs had dual flame ionization detectors and were used in the conventional manner except that oxygen was used in the detectors instead of air for combustion of the hydrogen. The use of oxygen resulted in a fourfold increase in sensitivity. A Bausch and Lomb Spectronic 20 was used at 460 nm for hydrazine determinations with *p*-dimethylaminobenzaldehyde.

Procedure. Standard Preparation. Stock solutions of 1000 ppm hydrazine and 1000 ppm methylhydrazine were prepared by addition of appropriate amounts of each to separate 1000-ml volumetric flasks containing 150 ml of 0.1*N* H_2SO_4. Dilution to the mark was made with distilled water. In addition, stock solutions containing 3000 ppm 3,5-dimethylpyrazole and 2390 ppm 1,3,4-trimethylpyrazole in distilled water were prepared (equivalent to 1000 ppm hydrazine and 1000 ppm methylhydrazine, respectively). Lower concentrations were prepared by further dilution of aliquots of these stock solutions with distilled water.

Chromatographic Conditions. The columns were either three or six feet in length, constructed of $\frac{1}{8}$-inch stainless steel tubing, and were packed with 60–70 mesh Anakrom ABS (Analabs). The Anakrom ABS was coated with 30% by weight of a mixture containing 16.7% Amine 220 (Applied Science) and 83.3% Apiezon L (Analabs). The flow rate of the helium carrier gas was 25 ml per minute. The temperature of the flash vaporizer inlet was 175 °C and that of the detector oven was 200 °C. The column oven was operated isothermally at 130 °C and the columns were preconditioned at 170 °C with helium flow for 8 hours.

Sample Preparation and Analysis. The pH of an aqueous sample was adjusted to between 6 and 9 with either 1*N* NaOH or 1*N* H_2SO_4 and 50 μl of 2,4-pentanedione were added to a 100-ml portion. The resulting mixture was shaken thoroughly and allowed to stand for at least 1 hour at room temperature. A 5-μl aliquot of the prepared sample or a calibration standard was injected into the gas chromatograph, and the peak height of the desired component was measured.

RESULTS AND DISCUSSION

The 2,4-pentanedione (AA) reactions with hydrazine (N_2H_4) and methylhydrazine (MMH) to form 3,5-dimethylpyrazole (DMP) and 1,3,5-trimethylpyrazole (TMP), respectively, are illustrated by Equations 1 and 2.

(6) H. McKinnis and A. Yard, *U. S. Dept. Com. Office Tech. Serv., P. B. Rept.* 143,914, 13 pp, 1957.
(7) F. Feigl and W. A. Manheimer, *Mikrochim. Ver. Mikrochim. Acta*, **40**, 50–2 (1952).
(8) L. M. Kul'berg and A. I. Cherkesov, *Zh. Anal. Khim.*, **6**, 364–70 (1951).
(9) J. P. Riley, *Analyst*, **79**, 76–81 (1954).
(10) G. Vanags and M. Mackanova, *Zh. Obshch. Khim.*, **25**, 580–3 (1955).
(11) G. Vanags and M. Mackanova, *Zh. Anal. Khim.*, **12**, 149–50 (1957).
(12) G. Vanags and R. Shagata, *Doklady Akad. Nauk SSSR*, **133**, 362–3 (1960).
(13) M. Pesez and A. Petit, *Bull. Soc. Chim. Fr.*, **1947**, 122–3.
(14) H. McKennis and A. Yard, Anal. Chem., **26**, 1960–3 (1954).
(15) R. Freier and G. Resch, *Z. Anal. Chem.*, **149**, 177–81 (1956).
(16) T. Dambrauskas and H. Cornish, *Amer. Ind. Hyg. Ass. J.*, **23** (2), 151–6 (1962).
(17) J. M. Bremner, *Analyst*, **79**, 198–201 (1954).
(18) R. L. Hinman, *Anal. Chim. Acta*, **15**, 125–8 (1956).
(19) B. Reynolds and A. Thomas, *Amer. Ind. Hyg. Ass. J.*, **26**(5), 527–31 (1965).
(20) N. M. Kalinina, *Energetik*, **12**(11), 41–2 (1964).
(21) E. Neuman and H. Nadeau, Anal. Chem., **36**, 640–1 (1964).
(22) R. H. Wiley and P. E. Hexner, "Organic Syntheses," Coll. Vol. IV, N. Rabjohn, Ed., 1963, p 351.

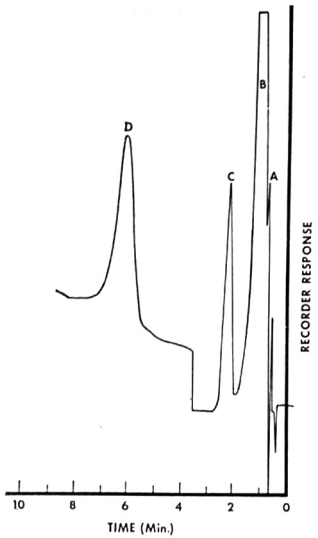

Figure 1. Chromatographic separation of TMP and DMP

A. H_2O (320×)
B. AA (320×)
C. TMP (320×)
D. DMP (160×)

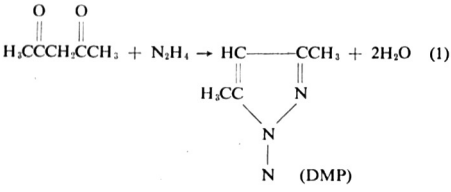

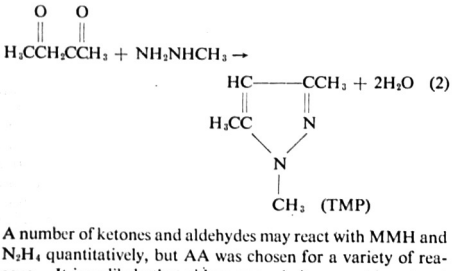

A number of ketones and aldehydes may react with MMH and N_2H_4 quantitatively, but AA was chosen for a variety of reasons. It is unlikely that either pyrazole is present in natural or industrial wastes, and both are relatively nonvolatile and can be easily separated from water, solvents, and volatile natural products. Also these pyrazoles are quite thermally stable and give symmetrical peaks even with only moderately polar substrates. Very dilute (<5 ppm) aqueous solutions of DMP and TMP have been stored in glass for several months with no apparent change in concentration and, therefore, should be useful as permanent gas chromatograph calibration standards. Table I shows the gas chromatograph results obtained for pyrazole artificial standards compared to those of actual N_2H_4 and MMH standards to which 50 μl of AA was added. Over the 0.5 to 50 ppm/wt concentration range, the concentration *vs.* peak height data when plotted result in linear curves which pass through the origin. It is apparent that little accuracy is sacrificed by the use of the more convenient pyrazole artificial standards. In addition, the correlation between the actual and artificial (pyrazole derivative) standards confirms that the reaction is quantitative. Figure 1 is a typical gas chromatogram illustrating the TMP and DMP peaks corresponding to a 5-μl aliquot of an aqueous sample which contained 10 ppm each of MMH and N_2H_4. The baseline shift between *C* and *D* is due to the indicated signal attenuation change. The resolution between the excess AA and the TMP is typical of what can be obtained with the three-foot column described earlier. With a six-foot column of the same packing, the retention volumes of TMP and DMP are approximately doubled, thereby providing somewhat greater resolution between AA and TMP. This increased resolution may be necessary if the sample contains less than 0.5 ppm/wt MMH.

Some hysteresis of the DMP was evident, and several potential sources of this problem were investigated. First, the column material was changed from stainless steel to glass and then Teflon V (Du Pont) was substituted for the diatomaceous earth support, but neither change eliminated the problem. The hysteresis completely disappeared when the inlet was changed from the flash vaporizer to on-column, thus indicating that either dead volume or back diffusion of the sample into cooler portions of the inlet had caused the difficulty.

Many trace hydrazine methods are based on the reaction of a ketone or aldehyde with the hydrazino group, and therefore the use of AA as the reagent offers only a limited advantage (pyrazole formation) unless the reaction products can be

Table I. Detector Response to TMP and DMP Prepared from Concentrated Standards and from Aqueous Trace MMH and N_2H_4 Standards

	Peak height, divisions			
Ppm/wt[a]	MMH	TMP	N_2H_4	DMP
0.1	130	140	170	160
0.5	710	730	390	380
1.0	1440	1480	740	730
2.0	2900	2970	1280	1300
5.0	7600	7550	3300	3100
10.0	15100	15000	6310	6300
20.0	31200	30500	12600	12700
50.0	79700	77200	33000	31800

[a] TMP and DMP are calculated as ppm/wt MMH and N_2H_4, respectively.

Table II. Recovery of N_2H_4 from Samples Which Contain Potential Interferences

Added N_2H_4, ppm/wt	Interference, 100 ppm/wt	Recovered N_2H_4, ppm/wt GC	PDAB
1.0	Urea	1.0	1.1
1.0	1,1-Dimethylhydrazine	1.0	1.1
1.0	DL-Alanine	1.0	1.1
1.0	Fe^{3+}	0.90	0.80
1.0	Cu^{2+}	0.80	1.0
1.0	Al^{3+}	1.0	1.0
1.0	Fe^{3+} + Na_2EDTA	0.97	0.82
1.0	Cu^{2+} + Na_2EDTA	0.97	1.0

separated from or measured in the presence of substances that are indigenous to the sample. Such substances may compete with the AA for N_2H_4, compete with the N_2H_4 for AA, or form a complex with the pyrazole so that chromatographic separation cannot be achieved. Table II shows the analysis results of samples containing 1.0 ppm N_2H_4 and each of several potential interferences at 100 ppm. Of the interferences tested, only Fe^{3+} and Cu^{2+} appear to have a significant effect on the gas chromatographic results. The *p*-dimethylaminobenzaldehyde (PDAB) results are affected by all but Cu^{2+} and Al^{3+}. One-half gram of Na_2EDTA was therefore added to 100-ml portions of the samples which contain the iron and copper prior to addition of the AA, and the pH was adjusted from ~1 to 5.5 with 1*N* NaOH. The gas chromatographic analysis results show that the N_2H_4 was recovered. Na_2EDTA had no effect on the PDAB results.

If a sample contains an impurity that has the same retention time as the pyrazole that is sought, a variety of substrates of varying polarity (*i.e.*, polyethylene glycol, cyanoethylated polyols, Amine 220, Apiezon L on Teflon) can be used for this analysis and at least one of the above substrates should allow separation of the pyrazole from the interference. A blank analysis (injection of an aliquot into the chromatograph prior to addition of the AA) is a less preferable means of overcoming this type of interference problem except when the impurity level is substantially less than that of the pyrazole.

Because of the unique AA/hydrazine reaction and the gas chromatographic separation of the products, the method described herein should be applicable to a variety of analytical problems for which the determination of N_2H_4 and/or MMH is required.

ACKNOWLEDGMENT

The author is grateful to William Robbs for providing many of the analytical data.

RECEIVED for review March 25, 1971. Accepted May 14, 1971

Determination of Mercury in Biological and Environmental Samples by Neutron Activation Analysis

K. K. Sivasankara Pillay, Charles C. Thomas, Jr., James A. Sondel, and Carolyn M. Hyche

Western New York Nuclear Research Center, State University of New York at Buffalo, Buffalo, N. Y. 14214

A neutron activation analysis procedure for the determination of trace levels of mercury in a variety of samples has been developed. Problems associated with mercury losses throughout sampling and analysis have been systematically examined. After neutron activation, the samples are wet ashed with mercury carrier. A preliminary precipitation is followed by further purification, and electrodeposition or precipitation are used to isolate mercury. The radioactivities ^{197}Hg and ^{197m}Hg are measured by scintillation spectrometry using a thin sodium iodide detector. The results of the analysis of several fish species and other aquatic environment samples from Lake Erie are reported. Comparison of the results of this analytical procedure with other techniques has been made.

MERCURY IN THE BIOSPHERE is a very unique pollutant because of its apparent indestructibility and its unusual ability to transform into highly toxic compounds by biological methogenation in nature. The sampling and the analysis of mercury in the environmental and biological samples offer some extremely challenging problems. The minute quantities of mercury present in these samples as well as the volatile nature of mercury and its compounds only add to the problems associated with the complexity of the matrices themselves. The current concern over the environmental contamination by mercury brought out several reviews, reports, and bibliographies on mercury (*1–4*). A bibliography prepared by the U. S. Department of Interior (*2*) lists about 60 papers describing various modifications of mercury determinations using atomic absorption, colorimetry, dithizone titration, X-ray fluorescence, pyrolysis, isotope exchange technique, and neutron activation analysis. The recent edition of the U. S. Atomic Energy Commission publication (*5*)—"Radiochemistry of Mercury"—lists about 80 references describing various applications of neutron activation analysis to mercury determination. However, only a limited number of these procedures can be reliably adapted for the determination of mercury in biological and environmental samples to monitor pollution. The procedures described here were developed for the investigation of the mercury pollution of Lake Erie and its aquatic life. Therefore, the examples presented here are primarily samples from the lake.

Neutron activation analysis is a highly specific and sensitive method for the determination of mercury, provided adequate precautions are taken in aliquoting, handling, storage, and pre-irradiation processing of the samples. The determination of mercury in biological and environmental samples by nondestructive neutron activation analysis is mostly of theoretical interest because there is hardly any environmental sample of interest to pollution studies that could be reliably analyzed by this technique. This is because of the extremely low concentrations of mercury in these samples and the interferences due to radioactivities produced by other components of the matrices.

The mercury present in biological tissues is mostly organic mercurials, while the mercury in other environmental samples is often composed of metallic and ionic mercury with varying amounts of bound organic mercury compounds. The mercury analysis of these samples, therefore, requires the degradation of the organic materials and/or the careful extraction of mercury from the insoluble matrices. Because

(1) "Chemical Fallout," Proceedings of the Rochester Conferences on Toxicity, M. W. Miller and G. G. Berg, Ed., Charles C Thomas, Springfield, Ill., 1969.

(2) "Mercury Contamination in the Natural Environment," U. S. Department of Interior, Office of Library Services, Washington, D. C., 1970.

(3) R. A. Wallace, W. Fulkerson, W. D. Shults, and W. S. Lyon, "Mercury in the Environment—The Human Element," ORNL-NSF-EP-1, Oak Ridge National Laboratory, Oak Ridge, Tenn., 1971.

(4) G. Löfroth, "Methylmercury—A Review of Health Hazards and Side Effects Associated with the Emission of Mercury Compounds into Natural Systems," University of Stockholm, Stockholm, Sweden, 1969.

(5) J. Roesmer, "Radiochemistry of Mercury," Nuclear Science Series NAS-NS-3026, rev, USAEC Division of Technical Information, Oak Ridge, Tenn., 1970.

Table I. Loss of Mercury from Samples during Freeze-Drying[a]

Sample identification	Initial levels of mercury (natural form) in ppm	Loss of mercury, %
A. Fish homogenates		
Fish D-21	1.77	16.4
Fish E-21	0.12	18.3
Fish G-21	4.56	38.8
B. Fish homogenates spiked with radioactive mercury (Hg^{2+} form)		
Fish G-20	...	N.D.[b]
Fish G-40	...	N.D.
Fish G-60	...	N.D.
C. Human brain tissues		
Pons	0.43	56.5
Carona radiata	0.15	24.3
Cerebellar cortex	0.72	18.0
D. Plankton/algae (Lake Erie)		
PL-Cx	17.86	50.0
PL-Cy	17.86	42.1
PL-Cz	17.86	64.3
E. Sediment/silt (Lake Erie)		
s/s-EE	2.30	N.D.
s/s-EF	2.35	N.D.
s/s-EG	2.05	N.D.

[a] VirTis Manifold type and VirTis Model 10-100 freeze-dryers were used.
[b] Not detectable.

of the high volatility of mercury compounds, ordinary combustion processes are not suitable to decompose the bound mercury and to collect them for analysis. Wet oxidation processes are often used to degrade these materials for trace analysis. An excellent discussion of the release of mercury due to volatilization under a variety of wet oxidation conditions was made by Gorsuch (*6*) through his study on the recovery of trace elements in organic and biological materials.

The common procedures using a radioactive tracer to determine recovery and analytical accuracy are not well suited for the analysis of mercury in biological and environmental samples. This is because of the limited knowledge of, and possible variations in the chemical form of mercury present in these samples. Experiments using one particular chemical form of radioactive tracer can only infer that the procedure may work, but it does not necessarily mean that the procedure does work for the forms of mercury actually present in the sample. Recognizing these limitations, an attempt was made to develop a reliable neutron activation analysis procedure to determine trace levels of mercury in a variety of biological and environmental samples.

EXPERIMENTAL

Sample Preparation. In neutron activation analysis using reactor neutrons, it is highly desirable to have the sample compacted, as well as free from excessive amounts of moisture. Since biological samples usually are not too dense and they contain a significant amount of moisture, processes such as oven-drying, freeze-drying, ashing, etc. are often used to prepare samples for reactor irradiation and subsequent handling. During this investigation, a low temperature asher using oxygen plasma for oxidizing tissues, two freeze-dryers (without mercury gauges) and an ordinary laboratory oven were used to investigate the possibility of using them for pre-irradiation sample preparation.

(6) T. T. Gorsuch, *Analyst*, **84**, 135 (1959).

Table II. Loss of Mercury (Hg^{2+} Form) during Low-Temperature Ashing[a]

Sample identification	No. of hours of ashing	Loss of mercury, %
Fish 1	3.5	81.4
Fish 2	3.5	81.9
Fish 3	3.5	91.8
Fish 4	7.0	98.0
Fish 5	7.0	98.0
Fish 6	7.0	98.0

[a] Tracerlab Low Temperature Asher Model No. 505, radio frequency power level = 200 watts (maximum), oxygen flow rate = 100 cc/minute, sample temperature = 110 °C (maximum).

A set of tissue homogenates were mixed with radioactive mercury (Hg^{2+} form) and were homogenized to form a slurry. These samples were aliquoted into freeze-drying flasks and the mercury activity was measured by gamma ray spectrometry using a 10 cm × 10 cm NaI(Tl) detector. The samples were quick-frozen using a mixture of crushed dry ice, liquid nitrogen, and ethyl alcohol. The freeze-drying continued using a similar cold trap. The radioactivity from the mercury was again measured and compared with standards used prior to freeze-drying. The results shown in Table I (Section B) indicate that there is no significant loss of radioactive mercury (Hg^{2+} form) from the fish homogenate.

The freeze-drying processes described above were repeated using a set of fish homogenates, human brain tissues, plankton/algae, and sediment/silt samples previously analyzed for their mercury content by the neutron activation analysis procedure detailed below without any pre-irradiation preparation. The residual samples from the freeze-drying processes were again analyzed for their mercury content by neutron activation analysis. The results of these analyses shown in Table I (Sections A, C, D, and E) indicate that there is significant loss of mercury from all the samples except sediment/silt during the freeze-drying process. Since the use of radioactive tracer indicated that there was no significant loss of Hg^{2+} mercury during freeze-drying, the losses observed here may be attributed to volatile forms of mercury present in the samples.

The investigation of a low temperature asher (Tracerlab Model 505), for preparing analytical samples for neutron activation, involved the use of fish homogenates spiked with radioactive mercury (Hg^{2+} form) as described earlier. The mercury content of the aliquots was measured by gamma ray spectrometry before and after ashing. The results shown in Table II clearly demonstrate that this technique is not suitable for the preparation of ashed samples for neutron activation.

Assuming that it was the volatile organic mercurials that were lost during freeze-drying of the sample, an attempt was made to convert the mercury compounds in the samples to inorganic form by exposure to high radiation doses. The results of these experiments, shown in Table III, indicate that the mercury in biological tissues can be stabilized against loss during freeze-drying by exposure to high doses of high energy nuclear radiation. This procedure, however, is cumbersome for routine application.

An attempt to utilize ordinary laboratory ovens to dry samples of sediment/silt and plankton/algae also revealed that there is significant loss of mercury from these samples even when temperatures of the order of 60 °C were used. The results shown in Table IV are self-explanatory.

From the above mentioned findings and the reported findings of Greenwood and Clarkson (7) regarding storage of samples, it is generally a good practice not to pre-process samples to limit the bulk or to reduce the moisture content and not to store samples in containers that adsorb mercury on their surfaces. The following procedures were used to prepare samples used for reactor irradiation during this investigation:

SOLID BIOLOGICAL TISSUES. The samples of fish and other biological tissues were kept frozen until ready for use. The tissues were homogenized using a blender and/or a grinder made of stainless steel or borosilicate glass. A convenient analytical sample (about 1 to 3 grams) of the homogenized tissue was carefully weighed into a small polyethylene bag (4 × 12 cm size) made of 0.2-mm thick sheets. The air from the bag was squeezed out and the bag was heat sealed, allowing a void space equivalent to at least twice the volume of the wet tissue sample, which allowed room for the gaseous radiation products produced during reactor irradiation. Wet tissue weights of these samples were used for calculating the results.

PLANKTON/ALGAE SAMPLES. The plankton/algae samples were collected using a fine mesh (14 meshes to a centimeter) plankton net. The samples collected in glass bottles were frozen as soon as possible. Prior to sampling for analysis, the contents of glass bottles were allowed to partially thaw to separate most of the ice from the plankton/algae samples. After separating the ice, the plankton/algae samples were transferred into tared polyethylene bags described in the above section. The bags were made to fit into standard 50-ml centrifuge tubes. The polyethylene bags containing the samples, supported in centrifuge tubes, were centrifuged using a high speed centrifuge. The supernatant water was poured out, and the final visible traces of water spots in the bag were removed by a cotton swab. A weighed portion of this sample was taken out into a small aluminum foil dish. The remainder of the sample (about 0.2 to 1 gram) in the bag was weighed along with the polyethylene bag to determine the weight of the wet sample. The aliquot of the sample taken in the aluminum foil dish was dried in a laboratory oven at 60° for 50 hours or until it attained a constant weight. These data were used to calculate the dry weight of the wet sample in the polyethylene bag. The sample was sealed in the bag after squeezing out the air as described earlier.

SEDIMENT/SILT SAMPLES. The sediment/silt samples were collected using two kinds of gear. An Eckman dredge which gathers samples from approximately the top 5 cm of sediment and a Peterson dredge which picks up the materials between 3 and 30 cm below the mud–water interface were employed in collecting the lake sediments. The samples collected in large (2-liter) containers were stored at room temperature until use. Since flint glass surfaces are known to adsorb mercury (7), the analytical samples were aliquoted from the middle part of the container. They were homogenized before the excess water in the samples was removed by centrifuging. The moist samples were contained in polyethylene bags and their dry weight was determined as described for the plankton/algae samples. The equivalent dry weight of the sediment/silt samples were used in calculating the results.

In preparing soil samples, coal, flour, and plant tissues for mercury analysis, the above mentioned procedures can be readily adapted. However, for the determination of mercury in liquid samples, none of the above mentioned pre-irradiation preparations are suitable.

Neutron Activation. The samples encapsulated in heavy duty polyethylene containers along with mercury standards (contained in thin quartz vials) were irradiated at a thermal neutron flux of about 5×10^{12} neutrons cm^{-2} sec^{-1} for 2 hours using a PULSTAR research reactor at the Western New York Nuclear Research Center. Because of the high capture cross section for thermal neutrons (*8*) [3092 barns for $^{196}Hg(n, \gamma)$ ^{197}Hg, and 107 barns for $^{196}Hg(n, \gamma)$ ^{197m}Hg], caution should be exercised to limit the size of the standard to avoid self-shielding and flux pertubation. The samples were allowed to decay for at least 1 hour prior to processing in order to allow the short-lived activities from the matrix to decay.

Wet Ashing and/or Extractive Digestion. The apparatus we have used for the wet oxidation of biological tissues and extractive digestion of soils and sediment samples is a simple version of the apparatus described by Bethge (*9*) and used by

Table III. Effect of Exposure of Fish Homogenates to Radiation Prior to Freeze-Drying

Description of radiation exposure and processing	Mercury content of sample, ppm[a]	Loss of mercury during freeze-drying, %
1. No radiation exposure. No freeze-drying	1.77	None
2. No radiation exposure. Freeze-dried	1.50	15.3
3. Exposed to 1.2 megarads of X-rays using a Van de Graaff machine. Freeze-dried	1.51	14.7
4. Exposed to 2.4 megarads of X-rays using a Van de Graaff machine. Freeze-dried	1.48	16.4
5. Exposed to 2 megarads of gamma rays and 2×10^{16} neutrons per cm^2 in a reactor. Freeze-dried	1.68	5.1
6. Exposed to 5 megarads of gamma rays and 5×10^{16} neutrons per cm^2 in a reactor. Freeze-dried	1.69	4.5

[a] The mercury present in these samples was in the natural form. The results given are the averages of more than two determinations by the neutron activation analysis described.

Table IV. Loss of Mercury from Lake Samples during Low-Temperature Oven Drying[a]

Sample identification	Initial levels of mercury (natural form) in ppm	Loss of mercury, %
A. Plankton/algae (Lake Erie)		
PL-Bx	17.86	51.1
PL-By	17.86	71.7
PL-Bz	17.86	60.6
B. Sediment/silt (Lake Erie)		
s/s-EA	2.25	23.6
s/s-EB	2.25	12.4
s/s-EC	2.25	12.4

[a] 50 hours of drying in a laboratory oven at 60 °C.

(7) M. R. Greenwood and T. W. Clarkson, *Amer. Ind. Hyg. Ass. J.*, **31**, 250 (1970).

(8) W. Seelmann-Eggebert, G. Pfenning, and H. Munzel, "Nuklidkarte," 3rd ed., Der Bundesminister Fur Wissenschaftliche, Forschung, Bonn, 1968.

(9) P. O. Bethge, *Anal. Chim. Acta*, **10**, 317 (1954).

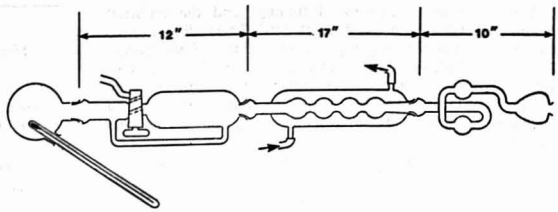

Figure 1. Apparatus used for controlled wet-ashing and/or digestion of samples for mercury analysis

Sjöstrand (*10*) for oxidation of biological tissues. The apparatus shown in Figure 1 can be put together with readily available parts from U. S. distributors.

The irradiated sample contained in the polyethylene bag was removed and the excess bag material around the heat sealed area containing the sample was trimmed to minimize the amount of polyethylene to be ashed. About 200 to 300 mg of bag material that contained the sample was usually ashed along with the sample to prevent any loss of mercury adsorbed or recoiled on to the surfaces of this container. The sample in the polyethylene encapsulation was inserted into the 200-ml distillation flask containing an accurately known amount of mercury carrier (50 mg of Hg/ml as Hg^{2+}) and 10 ml of concd nitric acid. The apparatus shown in Figure 1 was assembled and through the top of the condenser 5 ml of concd sulfuric acid and 5 ml of 70% perchloric acid were added. A volume of 2*M* hydrochloric acid sufficient to cover the lower bent portion of the splash head trap was placed above the condenser. The contents of the flask were simmered (<100 °C) for about half an hour and the temperature was then allowed to rise to 120 °C. The two-way stopcock on the reservoir was closed and the distillate was allowed to accumulate in the reservoir of the reflux column. The temperature rises rapidly from 130 °C, and caution should be exercised to ensure that heating is moderate and the temperature rise is not rapid. A violent reaction can result if the heating is excessive and the polyethylene bag catches fire by the action of perchloric and sulfuric acids. When the temperature reached 150–160 °C, the heating mantle was dropped and the flask was allowed to cool down to below 90 °C.

The condensate in the distillation column was carefully drained into the flask and heating continued. The stopcock was left open to the flask and refluxing continued for another 15 minutes. By this time, all the organic materials including the polyethylene bag had dissolved completely and the solution was clear and free from oily substances from biological tissues. If traces of undissolved or charred tissues and oily suspension remained, the process of heating to 150 °C and subsequent refluxing was repeated. In the case of soils and lake sediment samples, all the organic constituents dissolved leaving aside mostly insoluble silicates. Plankton/algae samples readily dissolve to form a clear solution.

The contents of the flask were allowed to cool. During the cooling period, the stopcock on the reflux column was closed and the splash head trap and the condenser were washed down with one or two 10-ml volumes of water, added to the reservoir on the trap. The washings and the contents of the distillation flask were transferred to a 250-ml beaker. In the case of soil and sediment samples, the insolubles were separated by centrifuging prior to transferring the solutions into beakers.

Separation of Mercury. The excess acids were carefully neutralized using ammonium hydroxide. The solution was then made acidic (about 2*M*) with hydrochloric acid. This solution was warmed and treated with hydrogen sulfide gas until the precipitation was complete. The contents of the beaker were warmed and were allowed to coagulate before centrifuging. The sulfide precipitates were washed with warm 2*M* hydrochloric acid to remove most of the iron, aluminum, chromium, manganese, nickel, cobalt, etc., that may have precipitated along with mercuric sulfide. The precipitates, after washing with warm water, were mixed with 5 ml of ammonium polysulfide and 1 ml of 2*M* sodium hydroxide and were kept warm in a water bath, to allow the dissolution of antimony, arsenic, and tin sulfides, if any. The precipitates were then washed with warm water, followed by 3*M* nitric acid, to remove copper, cadmium, and probably traces of other elements such as gold, platinum, molybdenum, selenium, etc.

The mercuric sulfide precipitate in the centrifuge tube was then mixed with 5 to 10 drops of freshly prepared aqua regia and was kept warm on a water bath for 10 to 15 minutes. It is important here to use the minimum amount of aqua regia and also to remove most of the excess acid by evaporation. Caution should be exercised not to allow the sample to go dry. The mercury salts were then diluted with about 30 ml of water and warmed to coagulate the sulfur. The solution was filtered into a 250-ml beaker using a coarse filter paper. The centrifuge tube was washed and this was also poured through the filter. The solution in the beaker was diluted to about 200 ml and used for electrolysis.

Electrolysis. The electrolytic deposition of mercury was done using platinum anodes and gold foils (2 × 2 × 0.02 cm) as cathodes. The gold foils were properly marked and weighed before electrolysis. The mercury standard irradiated along with the samples was dissolved and a known aliquot was transferred into a 250-ml beaker containing an accurately known amount of mercury carrier (about 50 mg of mercury as Hg^{2+}). Duplicate samples of the standard were also electrolyzed along with the samples. The electrolytic cells were connected in parallel and a dc potential of about 4.5 volts was applied using a constant voltage supply. The total current flow through sixteen cells was usually less than 0.8 ampere. The electrolysis under these conditions allowed an extremely uniform deposition and amalgamation of mercury on the gold surface without too much bubbling and lump formation. Usually the electrolysis was carried out overnight (16 hours or more).

The cathodes, after electrolysis, had a bright silvery appearance. Incomplete chemical separation of other constituents, and excess acidity of the electrolysis solution result in blackened foils and precipitation. The cathodes were identified and rinsed with deionized water before transferring them into 50-ml beakers containing ethyl alcohol, and the excess alcohol adhering to the foils was wiped off with an absorbent tissue paper. The foils were then either air-dried or oven-dried at 60 °C. Oven drying over ten minutes should be avoided as there is a likelihood of loss of mercury from the gold foil. If the foils should be cooled or are to be stored for a short duration, they may be placed in a desiccator containing silica gel.

The mercury deposited on each of the foils was determined by reweighing. The foils were then sealed individually in between very thin polyethylene sheets and were used for

(10) B. Sjöstrand, ANAL. CHEM., 36, 814 (1964).

counting. Radioactive tracers (Hg^{2+} form) used to investigate the processes have shown a one-to-one correspondence between the weights of mercury deposited and the amount of mercury tracer. Generally, the recovery of mercury was in the range of 75 to 90% for an electrolysis period of about 16 hours.

Counting. The gamma and X-ray emissions from ^{197}Hg and ^{197m}Hg were counted using a thin (0.6 × 5 cm) sodium iodide detector with a beryllium window and a 400-channel pulse height analyzer. The advantages and desirability of using a thin crystal for detecting low energy gamma rays and characteristic X-rays have been previously discussed (*11*). The foils were counted using a special sample mount that places the sample in a reproducible geometry close to the detector. Repeat counting of the foils was made, this time reversing the side facing the detector. The pulse height analyzer data were used to calculate the amount of mercury in the original sample. The data from large numbers of samples were processed using Schonfeld's ALPHA-M computer program (*12*).

Alternate Separation of Hg. This procedure is suggested for use only when sufficient time is not available for the electrodeposition of mercury. The solution resulting from dissolution of the mercuric sulfide in aqua regia, evaporation, and subsequent dilution may be used to precipitate mercury as mercuric oxide. The acidity of the solution should not exceed 0.3*M* and it is desirable to have it below 0.1*M*. An excess of 0.5*M* sodium hydroxide solution is added to the solution when mercuric oxide precipitates as a bright yellowish red substance. The precipitate is separated by centrifuging, washed with deionized water and ethyl alcohol, and is collected on a tared filter paper. After drying the precipitate at 60 °C in an oven, it is cooled in a desiccator and weighed as HgO to determine the yield. The sample is mounted face down on a 5-cm plastic ring-disk mount using a thin film of mylar. The radioactivities from the isotopes ^{197}Hg and ^{197m}Hg are counted as described above, along with similarly mounted standards. Nondestructive neutron activation analysis of several samples of the precipitates to determine the mercury content confirms the stoichiometric composition of the precipitate as HgO.

RESULTS

The thermal neutron activation analysis procedures described above were used to survey the mercury levels of the edible tissues of the various fish in Lake Erie. Eleven different species of fish from each of the three basins (Western, Central, and Eastern) caught during the 1970 Fall season were used to prepare analytical samples. Twenty-five individual specimens (or less when sufficient numbers were not available) of each species from each of the three basins of Lake Erie were used to prepare composites of the edible tissues. (Edible tissues here refer to the portions of the fish remaining after removing the head, tail, fins, and all the internal organs.) Large variations in the levels of a given species of fish of the same size and approximate age have been reported by Reynolds and Laarman (*13*). The selection of a sample size of 25 was based on the recent findings (*13*) that an "optimally precise" estimate of the average level in a population of the lake fish can be obtained by preparing a composite of about 25 randomly picked specimens from the group. The results given in Table V are the averages of two or more determinations and are expressed as micrograms of mercury per gram of raw tissue. In general, the fish from the Western Basin of Lake Erie had elevated levels of mercury in their edible tissues when compared with similar species caught from the Central and Eastern basins.

Table V. Mercury Content of Edible Tissues of Lake Erie Fish (1970 Fall Catch)

Species	Mercury content of edible tissues, ppm: Western basin	Central basin	Eastern basin
Walleye	0.79 (25)[a]	0.65 (25)	0.33 (25)
Yellow perch	0.61 (25)	0.49 (25)	0.29 (25)
White bass	0.60 (25)	0.72 (25)	0.43 (25)
Channel catfish	0.36 (25)	0.42 (20)	...
Freshwater drum	0.67 (25)	0.62 (20)	0.30 (25)
Carp	0.23 (25)	0.35 (17)	0.36 (14)
Coho salmon	0.69 (20)	0.58 (10)	0.51 (13)
White sucker	0.55 (24)	0.56 (8)	0.35 (25)
Gizzard shad	0.20 (25)	0.21 (15)	0.26 (18)
Smallmouth bass	...	0.55 (14)	...
Smelt[b]	...	...	0.30 (10)

[a] The numbers in the parentheses refer to the number of fish samples of a particular species used in preparing the composite. [b] Mercury content of the whole fish.

Table VI. Mercury Content of Lake Erie Samples Collected at the Mouth of the Buffalo River

Sample identification[a]	Date of collection	Mercury content in ppm (in terms of dry weight)
A. Sediment/silt		
E-1	7-28-70	2.80
E-2	7-28-70	4.99
P-1	7-28-70	2.59
P-2	7-28-70	3.62
P-1	9-8-70	2.27
P-2	9-8-70	1.95
P-1	10-5-70	2.84
P-2	10-5-70	6.15
E-1	1-15-71	3.69
E-2	1-15-71	5.58
P-1	1-15-71	6.79
P-2	1-15-71	5.57
B. Plankton/algae		
A-1	7-28-70	81.0
A-2	7-28-70	45.9
A-1	9-8-70	51.5
A-2	9-8-70	31.2
A-1	1-15-71	74.3
A-2	1-15-71	63.6

[a] The prefixes E and P for sediment/silt samples refer to samples collected by an Eckman dredge (~5 cm deep) and a Peterson dredge (~30 cm deep) from the water–sediment interface. The suffixes 1 and 2 refer to samples collected from the north and south side of the river, respectively.

Other lake samples that have been analyzed so far include sediment/silt and plankton/algae samples collected from May 1970 to January 1971 from one location in Lake Erie. The results presented in Table VI are in terms of the calculated dry weights of the samples analyzed. Since the wet weights of the samples were liable to change, it is felt that results expressed in terms of dry weights of sediment/silt and plankton/algae will allow for future comparisons. The major industrial mercury waste discharge into the Buffalo River was stopped in April 1970 by Governmental action. However, the

(11) K. K. S. Pillay and W. W. Miller, *J. Radioanal. Chem.*, **2**, 97 (1969).
(12) E. Schonfeld, "ALPHA-M—An Improved Computer Program for Determining Radioisotopes by Least-Squares Resolution of the Gamma-Ray Spectra," USAEC Report ORNL-3975, National Technical Information Service, Springfield, Va., 1966.
(13) J. B. Reynolds and P. W. Laarman, "Estimate of Total Mercury in Lake St. Clair Walleyes," Great Lakes Fishery Laboratory, Ann Arbor, Mich., December 1970.

Table VII. Results of Mercury Analyses Methods Evaluation Program Using Fish Homogenates[a]

Analytical method used	Number of laboratories participated	Range of reported values in ppm Hg		
		Sample D	Sample E	Sample G
Flameless (cold) atomic absorption	13	0.93 to 1.80	0.03 to 0.18	2.80 to 5.21
Flame atomic absorption	5	0.70 to 1.80	<0.05 to 0.49	2.26 to 5.40
Dithizone colorimetry	1	1.31	0.05	3.98
Dithizone titration	1	0.09	<0.03	0.09
Pyrolysis	2	0.47 to 1.52	0.04 to 0.10	2.00 to 4.25
Neutron activation analysis	6	0.95 to 1.77	0.04 to 0.19	2.83 to 4.60
Cold atomic absorption following acid digestion (Fresh Water Institute, Winnipeg, Canada)		1.46	0.04	4.53
Neutron activation analysis with post-irradiation chemical separation (Western New York Nuclear Research Center)		1.77	0.12	4.56

[a] Trace Mercury Analyses Evaluation Program sponsored by the Fresh Water Institute of the Canadian Fisheries Research Board.

Table VIII. Results of Mercury Analyses Methods Evaluation Program Using Soil Samples[a]

Analytical method used	Number of laboratories participated	Range of reported values in ppm Hg		
		Sample Hg 1	Sample Hg 2	Sample Hg 4
Flameless atomic absorption after acid digestion	5	<0.2 to 1.46	<0.2 to 0.35	<0.2 to 6.00
Flameless atomic absorption after direct thermal vaporization of mercury	5	1.40 to 1.90	0.23	1.60 to 5.90
Flame atomic absorption after acid digestion	3	0.56 to 29.0	<0.1 to 0.23	4.87 to 9.40
Dithizone colorimetric	2	2.70	<0.1	4.50 to 8.90
Flameless atomic absorption after acid digestion (Colorado School of Mines)		1.46	0.35	5.93
Neutron activation analysis with post-irradiation chemical separation (Western New York Nuclear Research Center)		1.47	0.41	5.70

[a] Trace Mercury Analyses Evaluation Program sponsored by the Department of Chemistry, Colorado School of Mines, Golden, Colorado.

samples of sediment/silt and plankton/algae collected periodically from Lake Erie at the mouth of the Buffalo River do not show any significant change in their mercury levels during the sampling period.

The analytical method described here was used to determine the base levels of mercury in human brain tissues. The results of the analysis of nearly 70 tissues selected at random from autopsy specimen are reported separately (*14*). These procedures have also been successfully used for the determination of mercury in coal samples, air particulates, and a variety of food materials.

DISCUSSION

The main uncertainty in the determination of mercury using neutron activation analysis described here arises prior to the wet ashing stage, in the presence of carrier mercury. In solution, mercury exchanges rapidly no matter what its oxidation state or the solvent (*15*, *16*). Therefore, the losses of mercury after this stage can be accurately accounted for and corrections made in the final results. The sampling, storing, and resampling for analysis still offer problems; however, the procedures described here seem to be a satisfactory solution.

The investigation of oven-drying, freeze-drying, and oxygen plasma ashing procedures suggests that none of these methods can be reliably used for pre-irradiation sample preparation. The use of high energy radiation exposure of samples to convert volatile organics to less volatile inorganic mercury for freeze-drying seems possible. Independent experiments performed using methyl mercury chloride have shown that a reactor irradiation of 30 seconds under the neutron and gamma flux conditions used in this investigation completely decomposes the methyl mercury compound to inorganic forms of mercury which are nonvolatile to freeze-drying. The 4 to 5% mercury losses (shown in Table III) from samples irradiated in a reactor and freeze-dried subsequently, may not be too significant because of the several additional steps involved in handling these particular samples. Routine application of this procedure to prepare samples for freeze-drying is not advisable.

The use of thick polyethylene bags to contain the samples for neutron irradiation and subsequent dissolution of the bag,

(14) C. A. Glomski, H. M. Brody, and K. K. S. Pillay, "Distribution and Concentration of Mercury in Autopsy Specimens of the Human Brain," *Nature* (in press).
(15) E. L. King, *J. Amer. Chem. Soc.*, **71**, 3553 (1949).
(16) A. C. Wahl and N. A. Bonner, "Radioactivity Applied to Chemistry," John Wiley and Sons, New York, N. Y., 1951.

along with the samples, ensures that there is no loss of mercury from the sample to the surfaces of the irradiation container. The heavy duty polyethylene bags specially chosen and used to prepare the sample containers did not present problems of cross contamination similar to those reported by Bate (*17*) Periodic blank determinations were made to determine the mercury levels of the polyethylene bag. None of the polyethylene sheets we have used so far showed any detectable amount of mercury.

The alternate procedure to precipitate mercury as mercuric oxide suggested here works well only if adequate precautions are taken to ensure that the mercuric sulfide is free from other impurities prior to dissolving it in aqua regia. Other methods of precipitating mercury by a variety of reagents are suggested by Roesmer (*5*).

The repeated counting of the gold foils was done to ensure that there was no uneven absorption of the low energy emissions from the deposited mercury because of preferential deposition on one side of the foil. We have observed two such foils during the counting of over 300 foils, and this was recognized as being due to the foil clinging to the side of the beaker during electrolysis.

The analytical procedures described here were compared with other techniques used for the determination of mercury in biological and environmental samples. The results of two interlaboratory comparison studies using fish homogenates and soil samples are summarized in Tables VII and VIII. The fish tissues analyzed contained only natural forms of mercury and the results of their analyses reflect the problems involved in analyzing these samples.

The accuracy of the analytical procedures detailed here was determined by radioactive mercury (Hg^{2+} form) tracers. These tracer studies showed that the errors of this procedure were less than 15% at 0.01 parts per million level and less than 5% at 2 parts per million level of mercury in biological tissues. The precision of the analysis as determined by repeat analysis of fish samples and sediment samples containing natural forms of mercury showed a standard deviation of less than 5% at 5-ppm levels, less than 7% at 1.5-ppm levels, and less than 17% at 0.01-ppm levels. The results of our analysis identified in Tables VII and VIII have this precision and probably the same accuracy.

Although the procedures described here can yield very reliable mercury values, it is recognized that the art of analysis still plays a significant role as is clearly evidenced from the distribution of results obtained using a particular kind of analytical procedure (Tables VII and VIII). With the recognized elusive nature of mercury, it may be necessary to take all the precautions mentioned here and probably more, to accurately determine the mercury content of environmental and biological samples.

(17) L. C. Bate, *Radiochem. Radioanal. Lett.*, 6 (3), 139 (1971).

ACKNOWLEDGMENT

The authors wish to gratefully acknowledge the assistance of Dr. Wilbur L. Hartman, Bureau of Commercial Fisheries, U. S. Department of Interior, Sandusky, Ohio, and Dr. Robert A. Sweeney, Director, Great Lakes Laboratory, State University College at Buffalo, for their assistance in obtaining various samples used during this investigation.

RECEIVED for review March 18, 1971. Accepted May 11, 1971. Presented at the 161st National Meeting of the American Chemical Society, Los Angeles, Calif., March 1971. This investigation was supported by the Bureau of Sport Fisheries and Wildlife, U. S. Department of Interior.

Low-Resolution Mass Spectrometric Determination of Aromatics and Saturates in Petroleum Fractions

C. J. Robinson

Research and Development Department, American Oil Company, Whiting, Ind. 46394

A new mass spectrometric procedure for determining up to 25 saturated and aromatic compound types in petroleum fractions eliminates the need for a variety of methods to cover wide ranges of boiling points and composition. A base-line technique to resolve the mass spectrum into saturates and aromatics spectra permits analysis of any sample boiling within the range of 200–1100 °F without need for a physical separation or a high-resolution mass spectrum. The entire composition is accounted for in terms of 4 saturated hydrocarbon types, 12 aromatic hydrocarbon types, 3 thiopheno types, and 6 unidentified aromatic groups. The procedure gives reasonable and consistent results on a wide variety of samples.

FOR SEVERAL YEARS low-resolution mass spectrometry has been used to determine hydrocarbon types in petroleum naphthas and middle distillates. The greater complexity of the mixtures boiling in the gas-oil range has ordinarily prevented direct determination of types; instead, the samples are usually separated into saturates and aromatics fractions, which are then examined mass spectrometrically.

To realize the obvious savings in time and money by avoiding such physical separations, Gallegos *et al.* (*1*) have used the resolving power of high-resolution mass spectrometry to obtain separate spectra for saturates and aromatics. In addition, Ferguson and Howard (*2*) have described a low-resolution method to determine 17 hydrocarbon and sulfur types in 400–1000 °F gas oil without prior separation, but they have not published a detailed procedure.

We have now developed a procedure to determine up to 4 saturated and 21 aromatic compound types in gas oils by using only the low-resolution mass spectrum and the number average molecular weight of the unseparated sample. It is an extension of our previously published determination of aromatics in petroleum fractions (*3*) and therefore includes

(1) E. J. Gallegos, J. W. Green, L. P. Lindeman, R. L. LeTourneau, and R. M. Teeter, ANAL. CHEM., **39**, 1833 (1967).
(2) W. C. Ferguson and H. E. Howard, Thirteenth Annual Conference on Mass Spectrometry and Allied Topics, St. Louis, Mo., May 16–21, 1965.
(3) C. J. Robinson and G. L. Cook, ANAL. CHEM., **41**, 1548 (1969).

Table I. Low Mass Patterns of Saturates

z[a] series	Mass[b]	Step 1	2	3	4	5
+1	43[c]	1.00				
	57	0.90	1.00			
	71	0.44	0.52	1.00		
	85	0.27	0.32	0.63		
	99[d]					
0	56	1.00				
	70[c]	0.69	1.00			
	84	0.38	0.57			
−1	55[c]	1.00				
	69	0.69	1.00			
	83	0.51	0.79	1.00		
	97	0.43	0.68	0.87	1.00	
	111	0.24	0.36	0.50	0.58	1.00
	125	0.13	0.19	0.28	0.33	0.54
−2	68	1.00				
	82[c]	1.40	1.00			
	96	1.10	0.83	1.00		
	110	0.66	0.53	0.64	1.00	
	124	0.43	0.35	0.42	0.66	
−3	67	1.00				
	81[c]	1.25	1.00			
	95	1.17	0.94			
−4	80	1.00				
	94[c]	1.00	1.00			
	108	0.90	0.81	1.00		
	122	0.75	0.67	0.83	1.00	
	136	0.63	0.61	0.80	0.96	
−5	79	1.00				
	93[c]	0.86	1.00			
	107	0.64	0.79	1.00		
	121	0.53	0.75	0.90	1.00	
	135	0.52	0.73	0.90	1.00	
	149				0.95	

[a] in C_nH_{2n+z}

[b] The $z = -5$ peaks are monoisotopic; all others are polyisotopic. Lowest mass in each step is a reference peak.

[c] Lowest mass in a series required for $S(M)$.

[d] $S(99)$ = the smaller of: $0.206 \times \{HDI(85) - [H(85) - S(85)]\}$, or $HDI(99)$ where $S(85)$ is the value obtained after completion of Step 3.

the same nomenclature for aromatics, and the same techniques for spectrometer operation, data acquisition, and computer storage and processing of the arrays of polyisotopic $H(M)$ and monoisotopic $HDI(M)$ peaks derived from the mass spectra. The average molecular weight is obtained from distillation data or by any other convenient method, and is stored in the computer for use in the computations.

Low-resolution 70-volt mass spectra of petroleum fractions containing both saturates and aromatics generally have intense peaks due to saturates in the consecutive homologous series from C_nH_{2n+1} through C_nH_{2n-5} below about mass 127. Aromatics contribute heavily to most of the remaining peaks. However, saturates contributions in the aromatics region and aromatics contributions in the saturates region are significant. These cross-contributions are not constant, but depend on the average molecular weight of the fraction and the amounts and kinds of compound types present. An early step in our procedure divides the total sample spectrum into separate spectra for saturates, $S(M)$, and aromatics, $A(M)$ from which much of the interferences has been removed.

Base-line techniques, similar in concept to those described for resolving overlapping aromatic types (*3*), are used in the aromatics regions of C_nH_{2n+1} through C_nH_{2n-5} to resolve saturates and aromatics and to supply some of the peak height values needed for both $S(M)$ and $A(M)$. Remaining values for $S(M)$ are obtained from the saturates region after removing part of the aromatics contributions via a new pattern-fitting procedure. Remaining $A(M)$ values are obtained from the observed peaks in the aromatics region of the total sample spectrum. Although neither $S(M)$ nor $A(M)$ are completely free of interference, a preliminary estimate of composition in terms of group types is made using our aromatics procedure (*3*) on $A(M)$ and a new saturates procedure on $S(M)$. Once this information is obtained the remaining interferences are calculated and a final analysis is reported.

The saturates spectrum containing only the peaks in C_nH_{2n+1} through C_nH_{2n-5} provides insufficient detail to allow a complete resolution of the various cycloparaffin types found in petroleum. Hence, a procedure such as Hood and O'Neal's (*4*) or Lumpkin's (*5*) cannot be used. We have, instead, limited the saturates types to paraffins, noncondensed cycloparaffins, 2-ring condensed cycloparaffins, and 3-ring and greater condensed cycloparaffins. In addition, peak summations for certain cycloparaffins and/or olefins related to steranes and polycyclic triterpanes are determined so that their specific interferences in the aromatics spectrum can be estimated. These types, which we simply call steranes, are limited to compounds of C_nH_{2n-6}, C_nH_{2n-8}, and C_nH_{2n-10} whose molecular weights fall in the range 340–428.

The presence of steranes and polycyclic triterpanes in petroleum is well known. Steranes were observed by O'Neal and Hood (*6*); Meinschein (*7*) mentioned pentacyclic triterpanes and the possible existence of hexacyclic triterpanes. Hills and Whitehead (*8*) have confirmed the presence of the pentacyclic compounds, but there has been no confirmation for the hexacyclics. Nonetheless, we have included C_nH_{2n-10} (possibly hexacyclic) compounds because there is often a small increase in parent peak heights in the C_{25}–C_{31} region.

COMPUTATIONS

All components are initially expressed in terms of their contributions to the total ionization, ΣI, of the sample, where ΣI is defined as the sum of all the polyisotopic peaks heights at whole masses beginning at mass 24 and extending to the end of the spectrum. The fraction of ΣI obtained for aromatics accounts for the total aromatics in the sample. Saturates composition is then normalized to the nonaromatic fraction.

For the computations, a given series of molecular ions is designated $(M)^+$, and the series of ions at each of the next lower masses is expressed as $(M-1)^+$. Polyisotopic peaks are used for the $(M)^+$ series; most, but not all of the $(M-1)^+$ peaks are monoisotopic.

Saturates Spectrum. The saturates spectrum, $S(M)$, consists of all peaks in the consecutive homologous series C_nH_{2n+1} through C_nH_{2n-5} starting with the low mass peaks indicated in Table I and extending to the high-mass end of each series. Peaks at the masses indicated in Table I, in the saturates region of the total spectrum, suffer from two types of aro-

(4) A. Hood and M. J. O'Neal, "Advances in Mass Spectrometry," Vol. 1, J. D. Waldron, Ed., Pergamon Press Ltd., London, 1959, pp 179–192.

(5) H. E. Lumpkin, ANAL. CHEM., **28**, 1946 (1956).

(6) M. J. O'Neal and A. Hood, "Abstracts—American Chemical Society, Division of Petroleum Chemistry," Vol. 1, No. 4, Sept. 1956.

(7) W. G. Meinschein, *Bull. Amer. Ass. Petrol. Geol.*, **43**, 925 (1959).

(8) I. R. Hills and E. J. Whitehead, *Nature*, **209**, 977 (1966).

matics interference: that due to fragmentation processes yielding singly charged ions, and that due to doubly charged ions. The latter can be particularly troublesome in the analysis of cracked stocks. To allow analysis of such stocks without defining the sample source and the consequent use of dual or multiple equation coefficients, we force-fit these peaks to an "average" saturates pattern of relative intensities in each series derived from the spectra of saturates fractions from several sources. This substantially reduces interference from doubly charged ions.

Pattern-fitting is made on a peak-by-peak basis, one series at a time, using reference peaks in each series as starting points. No peak is allowed to exceed the value indicated by the average pattern, but any lower height is retained. After the series is fitted to the given pattern, the reference peak is shifted one carbon number higher and the previously fitted peaks are compared to a new pattern. Again excess peak height is discarded. This stepwise shifting of reference peak and pattern comparison is continued until all peaks have been fitted. Data necessary to perform the pattern fitting are given in Table I.

All remaining peaks for $S(M)$ are obtained by base-line techniques that effectively distinguish between contributions of saturates and aromatics in the aromatics region. The curves of peak heights *vs.* 10^6/mass^2 for the C_nH_{2n+1} through C_nH_{2n-5} series of saturates fractions from petroleum are essentially linear at the higher masses. An example is given in Figure 1 for the C_nH_{2n-1} series of a gas-oil saturates fraction. For clarity some of the peaks at the crowded, high-mass region are not shown, but the linear portion of the curve above mass 251 includes most of the observed peaks in the series. A line drawn from the peak at the highest mass observed, through the linear portion of the curve, to the point X at mass 125 is the base line for this series. The ratio of the height of X at mass 125 to the observed peak height is nearly constant for gas-oil saturates and the ratios of base-line heights to observed heights are also nearly constant at each mass above 125. Thus if the base line of a series is known, it is possible to predict the saturates spectrum of the series in the aromatics region.

The high-mass base point is the peak at the highest observed mass in a series. For samples containing aromatics, it is assumed to be due only to saturates since, at equal boiling points, aromatics peaks occur at lower masses than saturates. The second, low-mass point needed to establish the base line is chosen at a mass where aromatics contribution is small. The peak height at this mass is multiplied by the constant derived from saturates spectra that places the base line on the linear portion of the saturates curve. Values along the base line corresponding to masses in the series are stored in $S(M)$. For the nonlinear portion, base-line values are multiplied by fixed peak-by-peak correction factors and the products replace the original base-line values stored in $S(M)$. Data for establishing base lines are given in Table II and the peak-by-peak correction factors are listed in Table III.

In using base lines and correction factors to derive peak heights, we never allow a calculated peak height to exceed the observed value. Thus, the final operation in preparing $S(M)$ is to compare each calculated peak with the corresponding H or HDI peak and reset each excess value to the observed value.

After these steps are finished, the $S(M)$ array contains all the data needed for further processing. The remaining aromatics interference is removed later from peak summations rather than from individual peaks. Seven of the 14 homologous series for $S(M)$, C_nH_{2n+1} through C_nH_{2n-5}, contain peak height values; the remaining series do not.

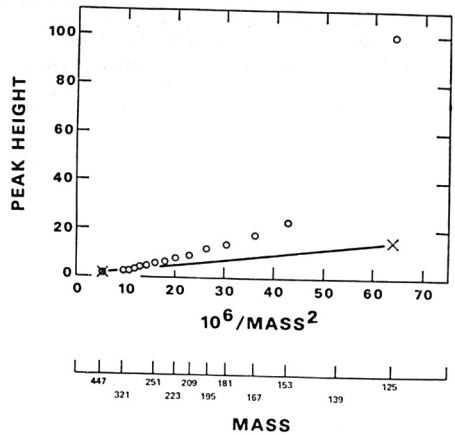

Figure 1. Peak height *vs.* mass for the monoisotopic C_nH_{2n-1} series in the mass spectrum of the saturates fraction from a virgin gas oil

X---X = base points

Table II. Data for Establishing Base Lines

	Low mass base point		
z series	Mass	Abscissa	Ordinate[a]
+1	99	102.03	$1.00 \times HDI(99)$
0	84	141.71	$0.78 \times H(84)$
−1	125	64.00	$0.15 \times HDI(125)$
−2	124	65.04	$0.85 \times H(124)$
−3	95	110.80	$0.21 \times HDI(95)$
−4	136	54.07	$1.16 \times H(136)$
−5	149	45.04	$0.51 \times HDI(149)$

High mass base point

Let $MMAX$ equal the highest observed mass in a series. The coordinates for the high mass base point in that series will be:

Abscissa = $(1000/MMAX)^2$
Odd-mass ordinate[a] = $1.00 \times HDI(MMAX)$
Even-mass ordinate[a] = $1.00 \times H(MMAX)$

[a] Where $HDI(M)$ is the monoisotopic and $H(M)$ is the polyisotopic peak at mass M.

Sterane Identification. For the detection of steranes, the base points given in Table IV are used to establish base lines on the H and HDI spectra for each of the three $(M)^+$ and three $(M-1)^+$ series on scales of linear height peak *vs.* linear mass. Each $(M)^+$ series is first examined in the parent peak region for the presence of steranes, as indicated by H values larger than values represented by the base lines. If they are present, heights measured from the base lines are summed as indicated in Table IV. During the summation any H or HDI value that falls below its base line is ignored. Separate sums representing the three steranes types are retained for correcting the aromatics spectrum.

Aromatics Spectrum. The aromatics spectrum, $A(M)$, consists of the values $H(M)$ minus $S(M)$ for the even-mass series and $HDI(M)$ minus $S(M)$ for the old-mass series.

Table III. Peak-by-Peak Factors to Correct $S(M)$ for Deviation from Base Lines

z series	Mass	Factor	z series	Mass	Factor
+1	113	1.000	−3	207	1.570
	127	0.946		221	1.420
	141	0.896		235	1.400
	155	0.889		249	1.370
	169	0.944		263	1.370
				277	1.200
0	98	1.200		291	1.100
	112	1.230			
	126	1.170	−4	150	0.954
	140	0.930		164	0.875
	154	0.850		178	0.854
	168	0.900		192	0.865
				206	0.870
−1	139	3.200		220	0.900
	153	2.370		234	0.950
	167	2.130			
	181	2.000	−5	163	2.020
	195	2.000		177	1.900
	209	1.570		191	2.020
	223	1.420		205	1.530
	237	1.420		219	1.510
	251	1.330		233	1.370
	265	1.250		247	1.360
	279	1.140		261	1.310
	293	1.070		275	1.220
				289	1.180
−2	138	0.932		303	1.100
	152	0.862			
	166	0.854			
	180	0.900			
	194	0.940			
	208	0.960			
−3	109	3.850			
	123	3.110			
	137	2.540			
	151	2.290			
	165	2.080			
	179	1.900			
	193	1.900			

Table IV. Data for Sterane Summations

Type	Base points[a] Low mass	High mass	Step[b]
C_nH_{2n-6}	330	442	1
	329	441	2
	204	246	2
	203	245	2
	246	274	2
	245	273	2
C_nH_{2n-8}	328	440	1
	327	439	2
	244	272	2
	243	271	2
C_nH_{2n-10}	326	438	1
	325	437	2
	242	270	2
	241	269	2

[a] Base points are peak heights at the masses indicated. Use polyisotopic heights for even masses and monoisotopic heights for odd masses.

[b] Steps 1 are performed first by obtaining sums of heights above the base lines at the masses in each series between the base points. A positive sum confirms the presence of the sterane type and sums from Steps 2 are added to the Step 1 sum. A zero sum in Step 1 indicates absence of the type and Steps 2 are omitted.

Only the peaks required for determining aromatics need be entered in $A(M)$. These consist of the homologous series that include as their lowest masses the first significant $(M)^+$ and $(M-1)^+$ peaks. These first peaks and the values that go into $A(M)$ are given in Table V.

Table V. Peaks Included in the Aromatics Spectrum, $A(M)$

z series	Lowest mass	Value
−6	78	$H(M)$
−7	91	$HDI(M)$
−8	104	$H(M)$
−9	117	$HDI(M)$
−10	130	$H(M)$
−11	129	$HDI(M)$
−12	128	$H(M)$
−13	141	$HDI(M) - S(M)$
−14	154	$H(M) - S(M)$
−15	167	$HDI(M) - S(M)$
−16	166	$H(M) - S(M)$
−17	179	$HDI(M) - S(M)$
−18	178	$H(M) - S(M)$
−19	191	$HDI(M) - S(M)$

Table VI. Factors for Determining Saturates Contributions to Aromatics Summations

	z-series sums: −6 plus −7	−8 plus −9	−10 plus −11
Steranes			
Σ78	1.55	3.41	2.17
Σ104	0.10	4.61	3.41
Σ129	0.02	0.30	4.61
Fractions of saturates total ions	P	CP	CCP
Σ78	0.0010	0.0023	F_{78}
Σ104		0.0005	F_{104}
Σ129			F_{129}

where P = total ions from paraffins
CP = total ions from noncondensed cycloparaffins
CCP = total ions from condensed cycloparaffins
$F_{78} = 0.9 \times 10^{-4} \times MW + 0.0346$
$F_{104} = 0.1542 \times 10^{-4} \times MW + 0.8133 \times 10^{-2}$
$F_{129} = 0.286 \times 10^{-4} \times MW - 0.3726 \times 10^{-2}$

CCP interference in any $(M-1)^+$ series equals:

CCP interference in the summation $\times$ $(M-1)^+/[(M-1)^+ + (M)^+]$

P interference on Σ128[a] equals:

$0.26 \times [S(127) + S(141) + S(155) + \ldots$ to end]

P interference in $(M-1)^+$ of Σ128 equals:

$P \times (0.1675 \times 10^{-4} \times MW - 0.1615 \times 10^{-2})$

[a] No base line is used for $(M)^+$ of Σ128. The paraffin interference is calculated from the C_nH_{2n+1} peak series of the S spectrum.

The resultant $A(M)$ spectrum contains contributions from saturates, including steranes, that must be eliminated before the final analysis. However, these are removed later by correcting summations of peaks rather than individual peaks in the spectrum.

First Aromatics Computation. With only slight modification, the previously described aromatics procedure (*3*) is applied to the $A(M)$ spectrum, and the same terms apply. The only new terms are related to the saturates interferences that must be removed before the final aromatics results are obtained.

Before the peak summations obtained for the class analysis are processed through the inverse matrix, interferences from steranes are removed from the summations representing Classes I, II, and III. The sums obtained for $z = -6, -8$, and -10 steranes, in the formula C_nH_{2n+z}, are each multiplied by the appropriate factors given in Table VI to obtain their total contributions to Σ78, Σ104, and Σ129. Although these factors were derived from a published spectrum of cholestane

(9) and are subject to the errors that can occur when data from a single compound are extrapolated to a class of compounds, the results seem reasonable.

The aromatics procedure (3) yields initial results as contributions of the compound types to total ionization. For samples containing only aromatics, the sum of these contributions may not equal the sum of peak heights at whole masses—a discrepancy probably related to a particular mass spectrometer and its operating conditions. We have found, however, that the ratio of observed to computed total ionization is essentially constant. Consequently, to obtain the agreement in total ionization required for the present method, all the inverse matrix coefficients for aromatics are multiplied by the above ratio, and the diagonal elements of the calibration matrix are divided by the ratio.

(9) American Petroleum Institute, Research Project 44, "Selected Mass Spectral Data," Thermodynamic Research Center, Texas A&M University, College Station, Texas, 1947–1968.

Total ionization contributions due to benzenes, naphthenebenzenes, and dinaphthenebenzenes (Classes I0, II0, and III0) are summed to produce the total ionization from monoaromatics. The total ionization due to polyaromatics includes the sum of contributions from all the remaining classes. These two sums as well as the total ionization for all the aromatics are retained solely for calculating and removing contributions to saturates.

First Saturates Computation. Saturates composition is determined from four peak summations of the $S(M)$ spectrum, which are processed by inverse matrix multiplication to yield total ionization contributions for four compound types. Thirty-three 4 × 4 inverse matrices, one for each carbon number from 8 through 40, are available. The average carbon number of the sample, defined as molecular weight ÷ 14, determines which matrix is to be used. Specifications for peak summations and inverse coefficients are shown in Table VII.

Table VII. Peak Summations and Inverse Matrices for Saturates

Summations:

$\Sigma 43 = 43 + 57 + 71 + \ldots$ to end
$\Sigma 55 = 55 + 69 + 83 + \ldots$ to end
$+ 84 + 98 + 112 + \ldots$ to end
$\Sigma 81 = 81 + 95 + 109 + \ldots$ to end
$+ 96 + 110 + 124 + \ldots$ to end
$\Sigma 93 = 93 + 107 + 121 + \ldots$ to end
$+ 94 + 108 + 122 + \ldots$ to end

Inverses:

		Σ43	Σ55	Σ81	Σ93		Σ43	Σ55	Σ81	Σ93
Paraffins	C_8	+2.0804	−0.2580	+0.0252	+0.0802	C_9	+2.0255	−0.3055	+0.0687	+0.0630
Noncond. Cyclopar.		−0.2017	+2.2795	−0.2228	−0.7089		−0.2546	+2.3236	−0.5224	−0.4791
2-Ring Cond. Cyclopar.		+0.0144	−0.1626	+3.6900	−2.9806		+0.0215	−0.1961	+3.3209	−2.6629
3-Ring + Cond. Cyclopar.		+0.0000	−0.0003	−0.0153	+4.1794		+0.0002	−0.0021	−0.0132	+4.1784
Paraffins	C_{10}	+2.0292	−0.3499	+0.0847	+0.0671	C_{11}	+2.0356	−0.4006	+0.1057	+0.0700
Noncond. Cyclopar.		−0.3046	+2.3634	−0.7735	−0.2875		−0.3570	+2.4144	−1.0474	−0.0819
2-Ring Cond. Cyclopar.		+0.0238	−0.1857	+3.0633	−2.4545		+0.0290	−0.2082	+2.9614	−2.3715
3-Ring + Cond. Cyclopar.		−0.0009	+0.0008	−0.0753	+4.2285		−0.0014	+0.0043	−0.1280	+4.2884
Paraffins	C_{12}	+2.0439	−0.4568	+0.0885	+0.1068	C_{13}	+2.0510	−0.5066	+0.0694	+0.1424
Noncond. Cyclopar.		−0.4033	+2.4505	−1.0453	−0.0982		−0.4418	+2.4898	−1.0582	−0.1030
2-Ring Cond. Cyclopar.		+0.0336	−0.2319	+2.9440	−2.3576		+0.0400	−0.2609	+2.9737	−2.3709
3-Ring + Cond. Cyclopar.		−0.0018	+0.0076	−0.1825	+4.3505		−0.0027	+0.0138	−0.2464	+4.4012
Paraffins	C_{14}	+2.0588	−0.5532	+0.0536	+0.1047	C_{15}	+2.0685	−0.6058	+0.0384	+0.0726
Noncond. Cyclopar.		−0.4812	+2.5338	−1.0732	−0.0918		−0.5204	+2.5837	−1.1001	−0.0714
2-Ring Cond. Cyclopar.		+0.0455	−0.2903	+2.9971	−2.3803		+0.0536	−0.3288	+3.0622	−2.4212
3-Ring + Cond. Cyclopar.		−0.0036	+0.0199	−0.2982	+4.4420		−0.0050	+0.0284	−0.3681	+4.4970
Paraffins	C_{16}	+2.0767	−0.6491	+0.0245	+0.0355	C_{17}	+2.0880	−0.7003	+0.0086	+0.0109
Noncond. Cyclopar.		−0.5653	+2.6356	−1.1368	−0.0407		−0.6061	+2.6959	−1.1667	−0.0437
2-Ring Cond. Cyclopar.		+0.0631	−0.3672	+3.1410	−2.4846		+0.0732	−0.4097	+3.2183	−2.4674
3-Ring + Cond. Cyclopar.		−0.0067	+0.0377	−0.4378	+4.5708		−0.0092	+0.0509	−0.5159	+4.6205
Paraffins	C_{18}	+2.1005	−0.7524	+0.0011	−0.0216	C_{19}	+2.1144	−0.8056	−0.0089	−0.0485
Noncond. Cyclopar.		−0.6474	+2.7543	−1.1992	−0.0429		−0.6905	+2.8154	−1.2370	−0.0393
2-Ring Cond. Cyclopar.		+0.0854	−0.4553	+3.2901	−2.4474		+0.0986	−0.5018	+3.3780	−2.4371
3-Ring + Cond. Cyclopar.		−0.0129	+0.0648	−0.5901	+4.6736		−0.0167	+0.0814	−0.6710	+4.7281
Paraffins	C_{20}	+2.1268	−0.8483	−0.0238	−0.0858	C_{21}	+2.1424	−0.8912	−0.0369	−0.1259
Noncond. Cyclopar.		−0.7352	+2.8794	−1.2758	−0.0320		−0.7814	+2.9426	−1.3090	−0.0243
2-Ring Cond. Cyclopar.		+0.1142	−0.5562	+3.4558	−2.4086		+0.1303	−0.6077	+3.5042	−2.3651
3-Ring + Cond. Cyclopar.		−0.0211	+0.1001	−0.7444	+4.7632		−0.0242	+0.1110	−0.7684	+4.7637
Paraffins	C_{22}	+2.1478	−0.9242	−0.0536	−0.1674	C_{23}	+2.1602	−0.9675	−0.0709	−0.2027
Noncond. Cyclopar.		−0.8169	+2.9924	−1.3387	−0.0209		−0.8620	+3.0770	−1.3826	−0.0169
2-Ring Cond. Cyclopar.		+0.1437	−0.6541	+3.5512	−2.3107		+0.1620	−0.7098	+3.5996	−2.2607
3-Ring + Cond. Cyclopar.		−0.0269	+0.1213	−0.7872	+4.7666		−0.0299	+0.1308	−0.7982	+4.7655
Paraffins	C_{24}	+2.1764	−1.0084	−0.0827	−0.2495	C_{25}	+2.1922	−1.0412	−0.1034	−0.2915
Noncond. Cyclopar.		−0.9101	+3.1464	−1.4208	−0.0071		−0.9522	+3.2167	−1.4621	+0.0046
2-Ring Cond. Cyclopar.		+0.1810	−0.7643	+3.6475	−2.2055		+0.1999	−0.8227	+3.7070	−2.1721
3-Ring + Cond. Cyclopar.		−0.0334	+0.1411	−0.8080	+4.7530		−0.0366	+0.1515	−0.8233	+4.7657

(*Continued next page*)

Table VII. Continued

Summations:

$\Sigma 43 = 43 + 57 + 71 + \ldots$ to end
$\Sigma 55 = 55 + 69 + 83 + \ldots$ to end
$+ 84 + 98 + 112 + \ldots$ to end
$\Sigma 81 = 81 + 95 + 109 + \ldots$ to end
$+ 96 + 110 + 124 + \ldots$ to end
$\Sigma 93 = 93 + 107 + 121 + \ldots$ to end
$+ 94 + 108 + 122 + \ldots$ to end

Inverses:

		Σ43	Σ55	Σ81	Σ93		Σ43	Σ55	Σ81	Σ93
Paraffins	C_{26}	+2.2126	−1.0875	−0.1168	−0.3554	C_{27}	+2.2320	−1.1249	−0.1354	−0.4098
Noncond. Cyclopar.		−0.9998	+3.3017	−1.5021	+0.0140		−1.0492	+3.3783	−1.5430	+0.0350
2-Ring Cond. Cyclopar.		+0.2240	−0.8942	+3.7740	−2.1879		+0.2493	−0.9633	+3.8536	−2.2792
3-Ring + Cond. Cyclopar.		−0.0433	+0.1709	−0.8631	+4.9164		−0.0495	+0.1899	−0.9120	+5.1179
Paraffins	C_{28}	+2.2519	−1.1724	−0.1416	−0.4672	C_{29}	+2.2729	−1.2222	−0.1379	−0.5384
Noncond. Cyclopar.		−1.1024	+3.4776	−1.5959	+0.0387		−1.1444	+3.5560	−1.6452	+0.0449
2-Ring Cond. Cyclopar.		+0.2845	−1.0666	+3.9492	−2.3576		+0.3026	−1.1192	+4.0278	−2.4554
3-Ring + Cond. Cyclopar.		−0.0588	+0.2196	−0.9668	+5.3190		−0.0643	+0.2380	−1.0254	+5.5673
Paraffins	C_{30}	+2.2935	−1.2657	−0.1372	−0.6135	C_{31}	+2.3106	−1.3083	−0.1330	−0.7039
Noncond. Cyclopar.		−1.1964	+3.6525	−1.7029	+0.0586		−1.2370	+3.7423	−1.7630	+0.0754
2-Ring Cond. Cyclopar.		+0.3358	−1.2134	+4.1277	−2.5608		+0.3657	−1.3038	+4.2319	−2.6844
3-Ring + Cond. Cyclopar.		−0.0743	+0.2692	−1.0901	+5.8093		−0.0840	+0.3008	−1.1631	+6.0919
Paraffins	C_{32}	+2.3300	−1.3570	−0.1249	−0.8019	C_{33}	+2.3489	−1.4102	−0.0950	−0.9185
Noncond. Cyclopar.		−1.2801	+3.8393	−1.8301	+0.0916		−1.3269	+3.9498	−1.9116	+0.1112
2-Ring Cond. Cyclopar.		+0.3984	−1.4039	+4.3493	−2.8043		+0.4369	−1.5196	+4.4752	−2.9412
3-Ring + Cond. Cyclopar.		−0.0956	+0.3389	−1.2438	+6.3808		−0.1108	+0.3843	−1.3366	+6.7199
Paraffins	C_{34}	+2.3724	−1.4631	−0.0799	−1.0034	C_{35}	+2.3941	−1.5146	−0.0560	−1.1365
Noncond. Cyclopar.		−1.3796	+4.0670	−1.9840	+0.0838		−1.4368	+4.1819	−2.0627	+0.1061
2-Ring Cond. Cyclopar.		+0.4785	−1.6396	+4.6054	−3.0855		+0.5238	−1.7643	+4.7420	−3.2428
3-Ring + Cond. Cyclopar.		−0.1280	+0.4381	−1.4454	+7.1168		−0.1472	+0.4961	−1.5580	+7.5122
Paraffins	C_{36}	+2.4166	−1.5734	−0.0186	−1.2688	C_{37}	+2.4448	−1.6404	+0.0215	−1.4023
Noncond. Cyclopar.		−1.4912	+4.3096	−2.1574	+0.1244		−1.5536	+4.4490	−2.2572	+0.1358
2-Ring Cond. Cyclopar.		+0.5711	−1.9029	+4.9001	−3.4453		+0.6268	−2.0587	+5.0738	−3.6723
3-Ring + Cond. Cyclopar.		−0.1687	+0.5634	−1.6935	+7.9904		−0.1966	+0.6474	−1.8515	+8.5329
Paraffins	C_{38}	+2.4756	−1.7083	+0.0621	−1.5332	C_{39}	+2.5038	−1.7836	+0.1160	−1.6941
Noncond. Cyclopar.		−1.6263	+4.5961	−2.3510	+0.1017		−1.6930	+4.7519	−2.4584	+0.0745
2-Ring Cond. Cyclopar.		+0.6929	−2.2339	+5.2550	−3.8725		+0.7589	−2.4204	+5.4585	−4.1241
3-Ring + Cond. Cyclopar.		−0.2294	+0.7426	−2.0224	+9.0974		−0.2686	+0.8605	−2.2332	+9.7905
Paraffins	C_{40}	+2.5460	−1.8812	+0.1913	−1.8720					
Noncond. Cyclopar.		−1.7851	+4.9471	−2.5895	+0.0539					
2-Ring Cond. Cyclopar.		+0.8438	−2.6428	+5.6978	−4.4441					
3-Ring + Cond. Cyclopar.		−0.3191	+1.0049	−2.4861	+10.6097					

Before matrix multiplication, it is necessary to correct the summations for aromatic contributions. Because the low-mass peaks include aromatics ions, the original base lines used in obtaining $S(M)$ and $A(M)$ are in error by amounts that depend on the total quantity of aromatics in the sample. Additional aromatics contributions are also present on those low-mass peaks that were previously pattern-fitted.

Corrections for base-line error are made by first calculating the fraction of aromatics on each low-mass base peak, assuming that this fraction is constant for all peaks determined by the base line, and, finally, by removing the total contribution found from the saturates summation and adding it to the aromatics summation. The base-line technique assumes that the highest mass peak in a series, $S(MMAX)$, is aromatic-free. Therefore, all calculations for base-line error are made on values of $S(M) - S(MMAX)$. Data to determine aromatics on the low-mass base peaks, given in Table VIII-A, were obtained from the spectra of a number of aromatic fractions. The product of the factor, F, times aromatics total ions is the contribution from aromatics at a low-mass base peak.

Aromatics contributions to the pattern-fitted peaks in the saturates summations depend on both the average molecular weight of the sample and the amounts of mono- and poly-aromatics. The fractions of total ions for the two aromatics groups are calculated from the equations given in Table VIII-B. These equations are relatively simple and, admittedly, can only approximate the aromatics contributions to saturates, but they fit most of our spectra of aromatics fractions.

After the correction steps have been completed, the saturates summations are processed by inverse matrix multiplication, which yields approximate values of total ions for the four saturates types. These are used to correct the various aromatics summations. For such corrections, total ions for the two condensed-ring cycloparaffin types are combined and used as a single type.

Final Aromatics Computation. Contributions from saturates to Σ78, Σ104, Σ129, and Σ128 are arbitrarily divided into two categories: those that must be removed from the $(M)^+$ plus $(M-1)^+$ sums, and those that interfere specifically with the $(M-1)^+$ sums used to resolve overlapping aromatic types. Data to remove contributions from the $(M)^+$ plus $(M-1)^+$ sums are given in Table VI. The corrected sums are next multiplied by the 7×7 inverse matrix coefficients to obtain final values of total ions in each of the seven classes.

Table VIII. Fractions of Aromatics Total Ions Appearing on the Low-Mass Base Peaks and on Low-Mass Peaks in the Saturates Summations

A. On low-mass base peaks:

Base peak	Equation[a]
99	$F = 0.159 \times 10^{-3} + 0.892 \times 10^{-6} \times MW$
84	$F = 0.948 \times 10^{-3}$
125	$F = 0.326 \times 10^{-3} + 0.178 \times 10^{-5} \times MW$
124	$F = 0.153 \times 10^{-3} + 0.100 \times 10^{-5} \times MW$
95	$F = -0.0013 + 0.1717 \times 10^{-4} \times MW$
136	$F = 0.147 \times 10^{-3} + 0.124 \times 10^{-5} \times MW$
149	$F = 0.356 \times 10^{-3} + 0.187 \times 10^{-5} \times MW$

B. On low-mass peaks in saturates summations:

Summation	Equation[a]
Σ43	$FM = 0.415 \times 10^{-3} \times MW - 0.0611$
	$FP = 0.282 \times 10^{-2} \times MW - 0.0538$
Σ55	$FM = 0.354 \times 10^{-3} \times MW - 0.0548$
	$FP = 0.129 \times 10^{-3} \times MW - 0.0197$
Σ81	$FM = 0.056 \times 10^{-2} \times MW - 0.0061$
	$FP = 0.019 \times 10^{-3} \times MW - 0.0030$
Σ93	$FM = 0.046 \times 10^{-3} \times MW - 0.0027$
	$FP = 0.014 \times 10^{-3} \times MW - 0.0004$

[a] MW is average molecular weight of sample. F is fraction of total ions for all aromatics. FM is fraction of total ions for all monoaromatics FP is fraction of total ions for polyaromatics.

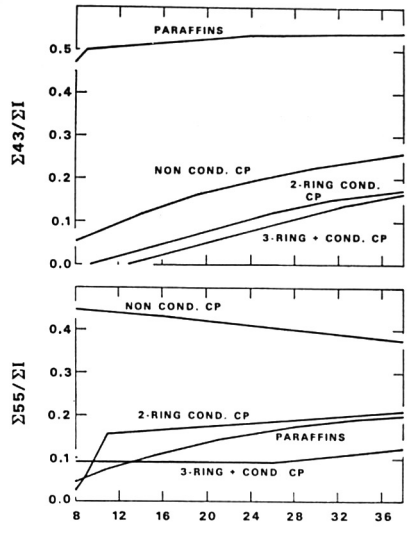

Figure 2. Σ43/ΣI and Σ55/ΣI *vs.* average carbon number for saturated hydrocarbon types

Condensed-ring cycloparaffins contribute significantly to the $(M - 1)^+$ series of Classes I, II, and III, and paraffins contribute to the $(M - 1)^+$ series of Class IV. It is necessary first to calculate the total interference to a series (Table VI), and then to distribute this quantity among the nominal, first, and second overlaps. The spectra of a number of saturates fractions have shown that about 0.0317 of the total ions from condensed-ring cycloparaffins is on the $(M - 1)^+$ peaks for the nominal, I0, type of Class I. This value is subtracted from the total condensed-ring interference in $(M - 1)^+$ of Class I to yield the interference to the overlap sums. Half of such interference is subtracted from the first overlap and half from the second overlap. Negative results, if found, are set to zero. Amounts of interference in Classes II0 and III0 are equal to the amount in Class I0 multiplied by the ratios F_{104}/F_{78} and F_{129}/F_{78}, respectively (Table VI). Again, the remaining interferences are divided equally between the first and second overlaps, and negative results are set to zero before continuing.

The entire $(M - 1)^+$ contribution from paraffins to Class IV is removed from the second overlap. For Class I the small contribution from paraffins is subtracted from the nominal type. Similar contributions from noncondensed cycloparaffins to Classes I and II are deducted from the respective nominal types. Any negative results are set to zero.

When steranes are present, corrections for their contributions to the $(M - 1)^+$ series of Σ78, Σ104, and Σ129 are obtained by multiplying the total interferences as calculated from the data in Table VI by $(M - 1)^+/[(M - 1)^+ + (M)^+]$. The results are then assigned 17% to the nominal type and 83% to the second overlap type.

The total corrections to the $(M - 1)^+$ series also must include those for aromatics (*3*). Once all these corrections have been made, total ion contributions of the aromatic types are calculated. Since the total ionization is approximately proportional to the liquid volume of sample charged to the mass spectrometer (*10*), the ratio of total ionization for each aromatic type to the total ionization of the sample is its fractional liquid volume concentration in the sample.

Final Saturates Computation. The entire procedure for the first saturates computation is repeated with the new values obtained in the final aromatics computation. The results are in terms of total ionization (and, consequently, relative liquid volumes) for each of the four saturates types. These values are normalized to the total saturates value represented by sample minus total aromatics.

RESULTS AND DISCUSSION

Saturates. The procedure to determine saturates uses most of the peaks available in the saturates spectrum. In any scheme using summations the choice of peaks to be summed for a group type is dictated not only by the spectral features of the compounds included in the group, but also by the features of all other compounds likely to be present in the sample. The objective is to maintain high and constant sensitivity for the compounds in the group, but low and constant sensitivities for compounds in other groups. Inclusion of all $(M - 1)^+$ peaks, and $(M)^+$ peaks for cycloparaffins, results in higher sensitivities than are obtained with only a few peaks in each sum. Inclusion of masses 43 and 57 for paraffins and 55 for noncondensed cycloparaffins keeps sensitivities high at low carbon numbers.

Inverse matrices for saturates are derived from calibrations containing interpolated and extrapolated data principally from published spectra (*9*). These data, in the form $\Sigma x/\Sigma I$, where Σx is a summation and ΣI is the sum of all peak heights at whole masses, are shown as functions of average carbon number in Figures 2 and 3. We have included matrix co-

(10) A. Hood, ANAL. CHEM., **30**, 1218 (1958).

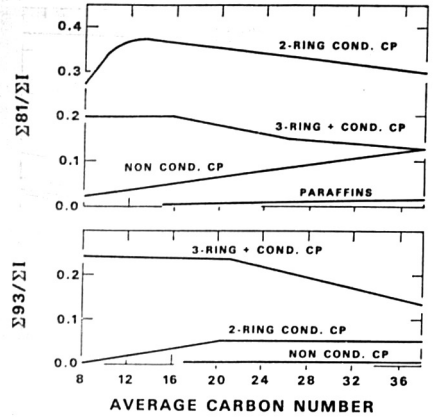

Figure 3. Σ81/ΣI and Σ93/ΣI *vs.* average carbon number for saturated hydrocarbon types

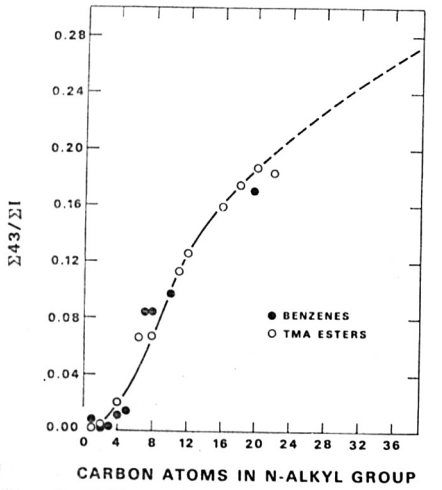

Figure 4. Σ43/ΣI *vs. n*-alkyl chain length for *n*-alkylbenzenes and *n*-alkyl trimellitic anhydride esters

efficients for 3-ring+ condensed cycloparaffins at C_8; because low average carbon number samples often contain these compounds as heavy ends, it would be wrong to exclude them.

The curves representing interferences at Σ43 are of particular interest. At the higher carbon numbers, long *n*-alkyl side chains apparently cause interfering contributions that increase with increasing chain length. As shown in Figure 4, to obtain better data, we plotted Σ43/ΣI for *n*-alkylbenzenes (*9*) and for 4-*n*-alkyl esters of trimellitic anhydride (*11*) *vs.* chain length. The data for the two compound types are in good agreement and a curve representing the TMA esters is smooth enough to extrapolate with some confidence. When applied to the cycloparaffins, values from the curve supplement data from published spectra and permit extension of Σ43/ΣI to high carbon numbers.

(11) Unpublished spectra from this laboratory.

Table IX. Analysis of Aromatic-Free and Saturate-Free Samples

	Liquid volume %: Acid-treated white oil (389 MW)	Liquid volume %: Aromatics fraction (353 MW)
Paraffins	19.8	0.0
Noncondensed cycloparaffins	44.9	2.8
2-Ring condensed cycloparaffins	19.2	0.4
3-Ring+ condensed cycloparaffins	14.8	2.7
Total saturates	98.7	5.9
Benzenes	0.0	7.8
Naphthenebenzenes	0.0	10.4
Dinaphthenebenzenes	0.0	13.6
Naphthalenes	0.0	4.4
Acenaphthenes, dibenzofurans	0.2	9.8
Fluorenes	0.1	10.9
Phenanthrenes	0.1	6.5
Naphthenephenanthrenes	0.0	5.1
Pyrenes	0.0	4.7
Chrysenes	0.0	2.5
Perylenes	0.1	1.0
Dibenzanthracenes	0.3	0.6
Benzothiophenes	0.0	3.4
Dibenzothiophenes	0.0	3.1
Naphthobenzothiophenes	0.2	0.9
Unidentified	0.3	9.4
Total aromatics	1.3	94.1
Calculated total ionization, %	97.5	100.5

Table X. Total Aromatics in Gas Oils and in Catalytically Reformed Naphtha

	MW	Aromatics—liquid vol. %: This method	Aromatics—liquid vol. %: Silica gel
Gas Oil A	253	21.9	19.6
Gas Oil B	340	38.9	39.8
Gas Oil C	297	46.2	45.1
Gas Oil D	339	17.6	19.6
Gas Oil E	278	29.6	29.9
Gas Oil F	298	38.5	39.2
Naphtha	129	32.5	32.0[a]

[a] Mass spectrometric naphtha type analysis.

Sulfur Compounds. Of the several sulfur compound types often found in petroleum, our procedure specifically considers only the thiopheno types. In some oils thiaalkanes and dithiaalkanes may be present in significant amounts. Since the mass spectra of these compounds (*9*) show that many of their large peaks are at low masses not included in *S*(*M*) or *A*(*M*), the calculated total ionization should be less than ΣI. However, since the saturates are normalized to sample minus aromatics, the result is that much of the sulfur is distributed among the saturated types.

Olefins and Cracked Stocks. In the development of this procedure, we did not consider the possible presence of olefins. We believe that the presence of nonaromatic olefins would lead to errors in the saturates values while the presence of aromatic olefins would lead to errors in the aromatics values. Most of the olefins produced by catalytic cracking of petroleum appear in the gas and naphtha fractions. Products boiling above gasoline do not usually contain large amounts of olefins and we have had no difficulty in using the procedure on such materials.

Typical Analyses. Our analyses of several typical petroleum samples are summarized in Tables IX through XIII.

Table XI. Comparison of Aromatics Compositions

	Liquid vol. %: Virgin gas oil MW = 278		Coker gas oil MW = 297	
	Whole oil	Arom. frac.[a]	Whole oil	Arom. frac.[a]
Benzenes	4.9	4.8	5.2	5.3
Naphthenebenzenes	4.6	4.8	5.8	5.5
Dinaphthenebenzenes	4.6	4.6	6.0	5.6
Naphthalenes	4.3	4.2	3.3	3.3
Acenaphthenes, dibenzofurans	2.8	2.9	4.3	4.8
Fluorenes	2.4	2.4	3.9	4.4
Phenanthrenes	1.7	1.7	2.3	2.8
Naphthenephenanthrenes	0.3	0.0	1.5	0.0
Pyrenes	0.7	0.4	2.0	2.0
Chrysenes	0.1	0.1	0.6	0.6
Perylenes	0.0	0.1	0.3	0.4
Dibenzanthracenes	0.0	0.0	0.1	0.1
Benzothiophenes	1.9	2.2	5.3	6.1
Dibenzothiophenes	1.3	1.4	4.0	4.3
Naphthobenzothiophenes	0.0	0.0	1.1	1.1
Unidentified	0.0	0.0	0.6	0.0

[a] Normalized to the total aromatics found for the whole oil.

Table XII. Composition of a Wide Boiling West Texas Gas Oil and Its Distillate Fractions in Liquid Volume Per Cent

	Cut 1	Cut 2	Cut 3	Cut 4	Cut 5	Cut 6	Cut 7	Cut 8	Calculated	Analyzed
Volume % of whole feed	13.5	12.2	13.2	12.2	12.8	12.5	10.4	13.2	100.0	100.0
Boiling range, °F	345–632	562–684	665–730	727–782	778–847	830–893	868–944	909–1180		408–1086
Average molecular weight	211	249	281	307	344	379	414	468		351
Composition:										
Paraffins	32.7	29.2	21.8	20.3	18.0	15.7	10.6	6.5	19.6	19.1
Noncondensed cycloparaffins	25.7	21.7	19.2	17.7	18.8	19.8	18.5	20.2	20.3	20.0
2-Ring condensed cycloparaffins	11.0	9.4	9.0	9.2	8.8	9.4	7.9	6.8	9.0	9.2
3-Ring + condensed cycloparaffins	6.0	6.1	5.9	5.6	7.8	11.0	10.2	11.4	8.0	8.2
Total saturates	75.4	66.4	55.9	52.8	53.4	55.9	47.2	44.9	56.9	56.5
Benzenes	7.3	5.2	5.4	4.8	4.0	3.9	3.8	3.7	4.8	4.9
Naphthenebenzenes	4.5	4.0	4.4	4.4	3.3	2.5	3.9	4.0	3.9	4.5
Dinaphthenebenzenes	3.3	5.5	5.4	5.5	5.0	4.6	5.4	6.0	5.1	5.8
Naphthalenes	5.5	4.7	3.4	2.6	2.0	2.3	1.2	0.5	2.8	3.5
Acenaphthenes, dibenzofurans	1.1	4.3	5.0	5.1	4.9	4.2	4.0	3.0	3.9	4.4
Fluorenes	0.7	2.3	4.0	4.5	5.1	4.5	4.7	4.7	3.8	3.5
Phenanthrenes	0.2	1.3	3.3	3.8	3.1	2.5	2.4	1.8	2.3	2.1
Naphthenephenanthrenes	0.0	0.4	1.2	2.4	1.7	0.5	3.7	3.7	1.6	2.1
Pyrenes	0.1	0.7	1.7	2.8	2.9	2.3	2.5	1.8	1.8	1.9
Chryenes	0.0	0.1	0.8	1.2	1.5	1.6	1.8	1.1	1.0	0.9
Perylenes	0.0	0.0	0.2	0.3	1.0	1.2	1.4	1.6	0.7	0.3
Dibenzanthracenes	0.0	0.0	0.0	0.1	0.6	0.7	0.5	0.8	0.3	0.2
Benzothiophenes	1.9	3.3	3.3	3.4	3.3	2.9	2.9	2.6	2.9	3.2
Dibenzothiophenes	0.0	1.7	5.9	4.5	3.0	2.5	2.4	2.3	2.8	2.7
Naphthobenzothiophenes	0.0	0.1	0.1	0.2	1.8	2.5	1.7	1.5	1.0	0.8
Unidentified	0.0	0.0	0.0	1.6	3.4	5.4	10.5	16.0	4.5	2.7
Total aromatics	24.6	33.6	44.1	47.2	46.6	44.1	52.8	55.1	43.2	43.5
Calculated total ionization, %	95.4	99.4	101.4	102.6	98.6	95.2	100.8	100.5	...	98.3

For example, Table IX shows results for a highly acid treated (aromatics free) white oil and an aromatics (saturates free) fraction. Despite such extreme ranges in concentrations, the results are reasonable and good balances are obtained for the total ionization of both samples.

As shown in Table X, total aromatics determined on several gas oils agree with data obtained for fractions separated on silica gel, and the value obtained for a catalytically reformed naphtha agrees with that determined by a naphtha type analysis. Likewise, as shown in Table XI, the aromatics determined in whole distillates agree well with the results obtained by our analysis for aromatics only (*3*).

The results in Table XII illustrate that the method clearly distinguishes changes in the concentrations of various compound types with boiling range. These samples were obtained from a wide-boiling virgin gas oil that had been distilled to give eight cuts of approximately equal volume. The increase in noncondensed cycloparaffins with boiling range above cut 4 may be due to an increase in isolated multiring structures (*4*). Also, we believe that the sharp increase in 3-ring+ condensed cycloparaffins that occurs above cut 4 is due, at least partly, to steranes. The appearance of polynuclear aromatic structures in what seems to be the proper boiling range order is gratifying. An apparent anomalous increase in naphthenephenanthrenes in the last two cuts is attributed to unidentified Class I aromatics. However, the good agreement between the calculated and analyzed composition of the whole oil indicates that the method is consistent over various boiling ranges.

Table XIII shows the composition of the SAE-10 distillate fraction and all the other products obtained during the solvent extraction and dewaxing of a Louisiana crude. These data substantiate prior general knowledge of such materials. For example, the extract contains 76% of the aromatics and only 15% of the saturates, while the wax contains 18% of the saturates (including 50% of the paraffins) and slightly more than 2% of the aromatics. Table XIII also includes two compositions calculated for the distillate from the data for extract plus waxy raffinate and for extract plus wax plus base stock. The close agreement with the composition of the original distillate confirms the consistency of the method over a range of compositions.

Table XIII. Compositions of Products from Processing SAE-10 Lousiana Distillate for Lubricating Oil Base Stock

	Liquid volume, %						
	Distillate	Waxy raffinate	Extract	Wax	Base stock	Extract + waxy raffinate	Extract + wax + base stock
Distillate, %	100.0	72.4	27.6	14.4	58.0	100.0	100.0
Paraffins	21.3	26.1	7.1	73.2	15.5	20.9	21.6
Noncondensed cycloparaffins	27.1	32.5	13.5	12.9	36.7	27.2	26.9
2-Ring condensed cycloparaffins	14.8	16.4	8.1	5.0	17.6	14.1	13.1
3-Ring + condensed cycloparaffins	15.4	17.3	12.2	5.2	21.1	15.9	16.3
Total saturates	78.6	92.3	40.9	96.3	90.9	78.1	77.9
Benzenes	2.6	0.7	5.7	0.2	1.1	2.1	2.2
Naphthenebenzenes	1.6	0.0	4.4	0.1	0.0	1.2	1.2
Dinaphthenebenzenes	3.0	0.8	7.4	0.3	0.8	2.6	2.6
Naphthalenes	2.1	1.4	4.7	0.4	1.7	2.3	2.3
Acenaphthenes, dibenzofurans	1.6	0.8	5.3	0.7	1.0	2.0	2.1
Fluorenes	2.1	0.7	6.7	0.0	1.2	2.4	2.6
Phenanthrenes	1.6	0.0	4.9	0.1	0.0	1.4	1.4
Naphthenephenanthrenes	0.4	0.0	3.0	0.0	0.0	0.8	0.8
Pyrenes	0.9	0.0	4.4	0.0	0.0	1.2	1.2
Chrysenes	0.4	0.0	2.1	0.0	0.1	0.6	0.6
Perylenes	0.5	0.1	0.9	0.0	0.2	0.3	0.4
Dibenzanthracenes	0.7	0.6	0.9	0.2	0.6	0.7	0.6
Benzothiophenes	0.6	0.1	1.5	0.0	0.2	0.5	0.5
Dibenzothiophenes	0.5	0.0	1.5	0.4	0.0	0.4	0.5
Naphthobenzothiophenes	0.4	0.3	1.1	0.0	0.3	0.5	0.5
Unidentified	2.4	2.2	4.6	1.3	1.9	2.9	2.6
Total aromatics	21.4	7.7	59.1	3.7	9.1	21.9	22.1
Calculated total ionization, %	99.0	97.3	101.0	97.8	97.0	...	...

CONCLUSION

An important feature of our procedure is its applicability to most, if not all, samples encountered in petroleum processing. Thus, it is now possible to use a single method to determine compound types in fractions ranging in volatility from heavy naphthas to heavy gas oils and in composition from all saturates to all aromatics. This is not only an advantage for the analyst, but, of more significance, it avoids the discontinuities in data that can occur when separate methods are used.

In our method, agreement between calculated and observed total ionization is about ±5% for samples boiling in the range of 400–1000°F and increases only slightly if the range extends to 200–1100°F. When compared with the method of Hood and O'Neal for saturates (*4*), in the applicable carbon number range, it gives about equal results on paraffins, but somewhat higher noncondensed and 2-ring condensed cycloparaffins at the expense of 3-ring+ compounds. We have found no need for separate inverses to accomodate predominantly *n*-paraffinic and isoparaffinic samples.

COMPUTER PROGRAM

The computer program in use in this laboratory, written in Fortran IV, will be available to prospective users of our procedure. Details may be obtained from the author.

RECEIVED for review January 28, 1971. Accepted May 13, 1971.

Spectrofluorimetric Determination of Orthophosphate as Rhodamine B Molybdophosphate

G. F. Kirkbright, R. Narayanaswamy, and T. S. West
Chemistry Department, Imperial College, London, S.W.7., U.K.

Between 0.04 and 0.6 μg of phosphorus is determined as orthophosphate *via* formation of the ion-association complex of molybdophosphate with the basic dyestuff Rhodamine B. After extraction of excess dye reagent into chloroform, the Rhodamine B molybdophosphate is extracted into chloroform:butanol (4:1 v/v) and the intensity of the fluorescence in this solvent measured at 575 nm with excitation at 350 nm. Optimal conditions for the determination have been established, and the effects of 100-fold excesses of each of 37 foreign ions have been examined. The determination is highly selective; large amounts of silicate do not interfere, and As(III) and V(V) are tolerable at 25- and 50-fold weight excesses, respectively. The structure of the ion-association complex has been examined.

COMMONLY EMPLOYED METHODS for the determination of orthophosphate are based on the absorption spectrophotometry in solution of molybdophosphoric or molybdovanadophosphoric acids, or of their reduction products in aqueous or organic media. These methods are neither highly sensitive nor selective, although the latter may be attained by solvent extraction of the heteropoly acid or the use of masking agents (*1–4*). Sensitive and selective procedures have been described for the determination of orthophosphate by indirect amplification, in which the twelve molybdate ions associated with each phosphate ion in the heteropoly acid are determined by molecular or atomic absorption spectrophotometry after

(1) C. Wadelin and M. G. Mellon, ANAL. CHEM., **25**, 1668 (1953).
(2) J. Paul, *Anal. Chim. Acta*, **23**, 178 (1960).
(3) J. Paul, *Mikrochim. Acta*, **1965**, 830.
(4) R. A. Chalmers and A. G. Sinclair, *Anal. Chim. Acta*, **34**, 412 (1966).

its extraction from excess molybdate reagent (*5–8*). Orthophosphate has been determined fluorimetrically by utilizing its quenching effect on the fluorescence of the complex formed between aluminium and morin (*9*). Sensitive spectrofluorimetric methods for phosphate have been described which are based on conversion to glucose-6-phosphate of glycogen in the presence of inorganic phosphate, activated phosphorylase, and phosphoglucomutase. The glucose-6-phosphate then reacts with the oxidized form of triphosphopyridine nucleotide (*10*) or nicotinamideadenosinediphosphate (*11*) to yield their reduced forms whose fluorescence is measured. Babko and coworkers (*12*) have studied the use of a range of basic dyestuffs for the extraction and spectrophotometric determination of phosphorus; procedures based on the use of iodine green and crystal violet were reported. A spectrophotometric method based on the formation of a complex between malachite green and molybdophosphoric acid has also been reported (*13*). In an attempt to exploit the potentially high sensitivity of solution spectrofluorimetry, while retaining the selectivity for the determination of phosphorus available from earlier work with its determination by indirect amplification methods, we have investigated the reaction of molybdophosphoric acid (MPC) with the fluorescent dyestuff Rhodamine B (RhB). In the method for the determination of phosphorus described here, the fluorescence of the ion-association complex formed between molybdophosphate and Rhodamine B is measured after its extraction into chloroform–butanol. When optimized conditions for the formation and extraction of the molybdophosphate are employed, a selective and sensitive method for the determination of phosphate is obtained.

EXPERIMENTAL

Apparatus. A double monochromator spectrofluorimeter (Aminco-Bowman, American Instrument Co., Silver Spring, Md.) fitted with a high intensity xenon arc lamp and an RCA IP28 photomultiplier was used in conjunction with an X-Y recorder (Bryans, England, Model 21000). Fused quartz cells (10 × 10 × 48 mm) were employed. In order to obtain maximum sensitivity 5-mm slits, corresponding to *ca.* 50-nm bandpass were used (Aminco slit arrangement No. 5) in both the excitation and analyzing monochromators.

One-hundred milliliter separating funnels fitted with ground glass stoppers and taps were used throughout. These were cleaned thoroughly in chromic–nitric acid mixture after each use.

Reagents. Standard Phosphorus Solution. Dissolve 0.0324 gram of sodium dihydrogen phosphate dihydrate, $NaH_2PO_4 \cdot 2H_2O$, (AR grade) in distilled water and dilute to 250 ml. This solution contains 25 μg P per ml, and was diluted as required to 1 μg P/ml with distilled water.

Molybdate Solution. Dissolve 30 grams of sodium molybdate dihydrate (AR grade) in distilled water and dilute to 1 liter. Using this solution, prepare the reagent for use by the following procedure: To a 250-ml volume of the molybdate solution, add an equal volume of distilled water and sufficient concentrated hydrochloric acid (AR grade) to make the solution approximately 1*M* with respect to acid. Allow the solution to stand for 10 minutes and then shake twice with 100-ml aliquots of chloroform–butanol extractant reagent. Allow the phases to separate, discard the organic phase, and shake the aqueous phase four times with 100-ml aliquots of chloroform. Allow the phases to separate, discard the chloroform phase and retain the aqueous phase for use as the molybdate reagent.

Rhodamine B Solution. Dissolve 0.115 gram of Rhodamine B (CI 45170) (Hopkin and Williams, Chadwell Health, U. K.) in distilled water and dilute to 1 liter.

Extractant. A 4:1 v/v mixture of analytical reagent grade chloroform and butanol was used.

Diverse Ions. Stock 1000-ppm solutions of foreign ions were prepared by dissolution of their analytical reagent grade salts in distilled water or dilute hydrochloric acid.

Calibration Graph for Phosphorus. To 100-ml separating funnels, add 5 ml of prepared molybdate reagent solution, 0.5 ml concentrated hydrochloric acid, and 5 ml of Rhodamine B solution. Add 0, 0.04, 0.1, 0.2, 0.4, and 0.6 μg of phosphorus in 2 ml of aqueous solution to the funnels. Mix the solutions and allow to stand for 10 minutes. Add 10 ml of chloroform to each funnel and shake vigorously. Allow the phases to separate and carefully separate and discard the chloroform phase. Repeat the chloroform extraction. Add 10 ml of the chloroform–butanol extractant solvent to the aqueous phase and extract the Rhodamine B molybdophosphate. Separate the phases and transfer the organic phase to a clean dry spectrofluorimeter cell. Measure the fluorescence intensity at 575 nm with an extraction wavelength of 350 nm. After subtraction of the reagent blank fluorescence, obtained simultaneously, the calibration graph is linear and passes through the origin.

RESULTS AND DISCUSSION

Rhodamine B is extracted readily into most organic solvents from acid solutions. The fluorescence characteristics of the ion-association complex formed between molybdophosphate (MPC) and Rhodamine B (RhB) are similar to those of RhB itself. When the Rhodamine B molybdophosphate (RhBMPC) is to be extracted prior to measurement of its fluorescence, therefore, the excess RhB reagent must first be selectively extracted from the solution. We have found that chloroform is an effective solvent for this purpose. Although the distribution coefficient for RhB between chloroform and water is not very high at the acidity employed, so that several extractions are required, chloroform does not extract the RhBMPC complex. In preliminary experiments two extractions with chloroform (10 ml) were found to reduce the reagent blank to a low constant value. In all experiments concerned with the establishment of optimum conditions for the phosphate determination, therefore, after formation of RhBMPC in the presence of excess molybdate and RhB in acid medium, the excess RhB was removed by extraction with two 10-ml aliquots of chloroform before extraction of RhBMPC into chloroform–butanol and measurement of its fluorescence.

Spectral Characteristics. The fluorescence excitation and emission spectrum for a 2.4 × 10^{-6}*M* RhB solution in chloroform:butanol (4:1 v/v) after extraction from 1*M* HCl is shown in Figure 1*a*. The absorption band at 350 nm is used to stimulate fluorescence at 565 nm; when the higher wavelength band at 550 nm is employed for excitation, high blank readings due to scattered light are obtained when the fluorescence emission at 565 nm is measured with wide slit

5) V. Djurkin, G. F. Kirkbright, and T. S. West, *Analyst*, **91,** 89 (1966).
(6) F. Umland and G. Wunsch, *Z. Anal. Chem.*, **213,** 186 (1965).
(7) G. F. Kirkbright, A. M. Smith, and T. S. West, *Analyst*, **92,** 1096 (1967).
(8) W. S. Zaugg and R. J. Knox, Anal. Chem., **38,** 1759 (1966).
(9) D. B. Land and S. M. Edmonds, *Mikrochim. Acta*, **1966,** 1013.
(10) D. W. Shultz, J. V. Passonneau, and O. H. Lawry, *Anal. Biochem.*, **19,** 300 (1967)
(11) W. M. Kirsch, J. W. Leitner, and D. Schulz, *ibid.*, **21,** 39 (1967).
(12) A. K. Babko, Y. F. Shkaravskii, and V. I. Kulik, *Zh. Anal. Khim.*, **21,** 196 (1966).
(13) K. Itaya and M. Ui, *Clin. Chim. Acta*, **14,** 361 (1966).

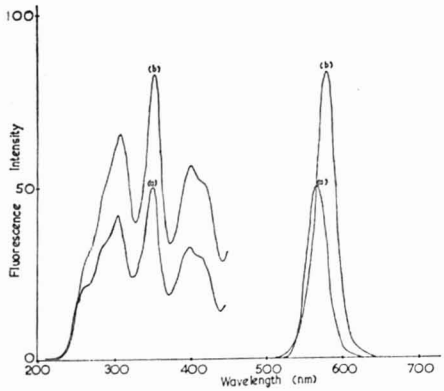

Figure 1. Uncorrected excitation and emission spectra in butanol/$CHCl_3$ of:

(*a*) Molybdophosphate RhB complex (equivalent to 0.5 μg of P), and (*b*) Reagent (RhB) alone (2.4×10^{-6} *M*)

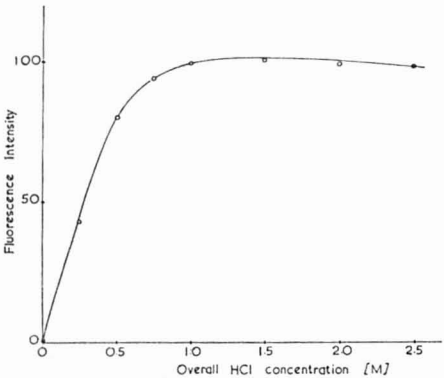

Figure 2(*a*). Effect of hydrochloric acid concentration on fluorescence in chloroform–butanol

widths. In addition, the wavelength of the 550-nm excitation maximum varies considerably with the RhB concentration. Figure 1*b* shows the fluorescence excitation and emission spectrum of the RhBMPC extracted into chloroform–butanol after formation in a 1*M* HCl solution containing 0.5 μg P. The appearance of the spectrum is similar to that of RhB itself, there being only a slight shift in the fluorescence emission maximum to 575 nm. This might suggest that the fluorescence measured for analytical purposes is that of free RhB itself, after its liberation from the RhBMPC ion-association complex on extraction into chloroform–butanol. Alternatively, if the RhBMPC complex is stable in chloroform–butanol, the inference is that the ion-association between RhB and the molybdophosphate anion does not alter the spectral absorption or emission characteristics of the RhB significantly. In practice, the similarity of spectral excitation and emission characteristics of RhB and its molybdophosphate does not constitute a disadvantage by the existence of a

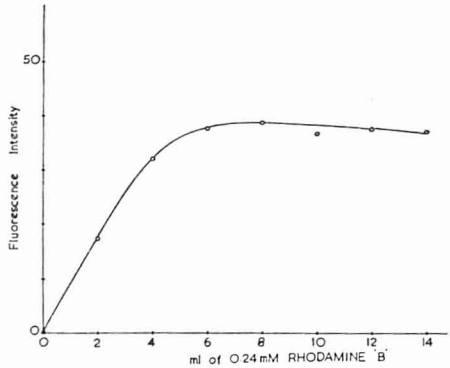

Figure 2(*b*). Effect of Rhodamine B reagent concentration on fluorescence in chloroform–butanol

high blank fluorescence, as the excess RhB is extracted into chloroform before extraction of the RhBMPC into chloroform–butanol.

Effect of Acid, Rhodamine B, and Molybdate Concentrations. The conditions employed initially for the formation of MPC were similar to those used by Wadelin and Mellon (*1*). The effect of hydrochloric acid concentration in the aqueous phase on the formation of RhBMPC was studied using the general experimental procedure described above. The experiments were conducted using 7.5 μg of P in 0.3 ml of aqueous solution to which 10 ml of 0.24m*M* RhB solution and 20 ml of diluted molybdate reagent solution (1:1) were added in the presence of varying molarities of hydrochloric acid. The effect of the hydrochloric acid molarity in the original solution on the fluorescence intensity measured in the final chloroform–butanol extract is shown in Figure 2*a*. A concentration of 1*M* HCl was chosen as the optimum in the initial solution and was used in all further work.

The optimum RhB concentration was determined similarly using 12.5 μg of P in 0.5 ml of aqueous solution, 20 ml of the diluted reagent (1:1), and an overall acidity of 1*M* HCl. The excess RhB, if any, was removed as described above by three extractions with 10-ml aliquots of chloroform before the final extraction with 25 ml of chloroform–butanol. As shown in Figure 2*b* the fluorescence increases up to 8 ml of 0.24m*M* RhB and this remains constant when the reagent concentration is increased further. Ten milliliters of 0.24m*M* RhB solution was therefore chosen for use; this represents an approximately 75-fold weight excess over 1 μg of P. This Rhodamine B concentration was used for further work, although to permit the determination of small weights of phosphorus the volume of all the reagents was halved compared to the above experiments.

A significantly lower reagent blank was obtained in the procedure if the molybdate reagent was prestripped of phosphate impurities before use. This was accomplished by the preliminary extraction procedure described in the experimental section. The molybdate reagent concentration employed was that shown in earlier work (*7*) to result in quantitative formation of molybdophosphoric acid with microgram amounts of phosphorus. Thus 5 ml of 56m*M* molybdate reagent solution was used in all experiments.

Extraction of Excess Rhodamine B Reagent and Rhodamine B Molybdophosphate. In order to obtain low blank fluores-

cence in the phosphorus determination, it was necessary to remove the excess RhB reagent before extraction of RhBMPC into chloroform–butanol. The number of chloroform extractions required to reduce the reagent blank to a low value was determined. With optimum conditions of acidity and RhB and molybdate concentrations, and in the absence of phosphorus, the fluorescence of the RhB reagent was measured in the organic phases obtained on repetitive extraction with 10-ml aliquots of chloroform. As shown in Figure 3, the excess RhB is extracted from the blank solution effectively with two 10-ml aliquots of chloroform. It is also evident from Figure 3 that when the experiment is repeated in the presence of 0.5 μg of phosphorus, the fluorescence in the chloroform phase is still appreciable after two extractions and then decreases slowly with further extractions. It appears that after extraction of the excess free RhB by two extractions with two 10-ml aliquots of chloroform, RhB formed by progressive dissociation of RhBMPC is removed when further chloroform extractions are made. The ion-association complex itself is not extracted into chloroform; no molybdenum was detectable in the chloroform phase after extraction. After two extractions with 10-ml aliquots of chloroform, the highest net fluorescence signal intensity ratio was observed in the final chloroform–butanol extract. We observed that a single extraction with a 10-ml aliquot of chloroform–butanol extractant solvent was sufficient to extract the RhB and its associated molybdophosphoric acid quantitatively from the residual aqueous phase after the chloroform extractions.

Order of Addition of Reagents and Time of Complex Formation. The order of addition of the reagents which was found to enable rapid complex formation is as described in the experimental procedure. In this method, the phosphorus sample solution is added after the acid, molybdate, and RhB solutions. Under these conditions, complex formation is complete in the initial aqueous solution after 5 minutes, so that the excess RhB may be extracted at any time after this. In practice, when several sample and standard solutions are to be treated, it is convenient to allow 10 minutes after mixing reagents before the excess reagent is extracted.

Calibration Graph, Sensitivity, and Precision. With the optimum conditions used in the procedure described, the calibration graph is linear in the range 0.04 to 0.6 μg of phosphorus in the original 2-ml sample solutions, *i.e.*, 0.02 to 0.3 ppm. The blank fluorescence is low and reproducible; the use of prestripped molybdate reagent, from which phosphate impurity has been removed, results in a considerably lower blank value than when untreated reagent is employed. Appreciable curvature of the calibration graph toward the concentration axis occurs when more than 0.6 μg of P is determined under the recommended conditions. The use of higher molybdate and Rhodamine B concentrations does not extend this upper limit; concentration quenching of the rhodamine B fluorescence appears to be responsible for this effect. The recommended procedure was applied to the repetitive determination of 0.5 μg of phosphorus. The ten determinations produced a coefficient of variation of ±3.9%.

Effect of Foreign Ions. The effect of 100-fold weight excesses of 37 foreign ions on the fluorescence intensity obtained in the final chloroform–butanol extract for 1 μg of phosphorus determined by the recommended procedure was investigated. A foreign ion was considered to interfere when it produced an error in fluorescence intensity compared to that for 1 μg of P alone of greater than twice the coefficient of variation (*i.e.*, 8%). The following ions did not interfere at the 100-fold weight excess level under these conditions: Ag,

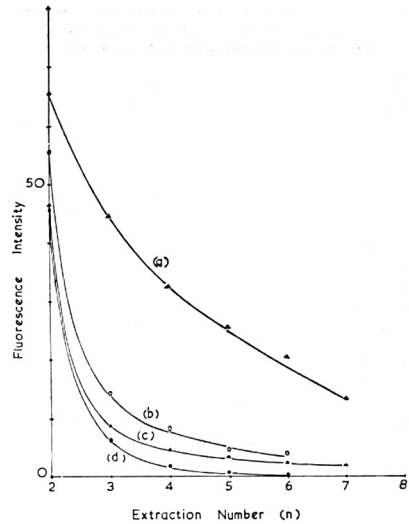

Figure 3. Variation in fluorescence intensity with number of extractions with chloroform

(*a*) Fluorescence intensity obtained for *n*th extraction into butanol/$CHCl_3$ (10 ml) after ($n - 1$) extractions with chloroform (10 ml) from sample containing 0.5 μg of P
(*b*) Successive $CHCl_3$ extractions (10 ml) from sample containing 0.5 μg of P. Fluorescence measured in *n*th chloroform extract
(*c*) Blank for (*a*), no phosphorus
(*d*) Blank for (*b*), no phosphorus

Al, Au, Bi, Ca, Cd, Ce(IV), Co(II), Cu(II), Fe(III), Ge, Hg(II), Mg, Mn(II), Ni, Pb, Sb(III), Se(IV), Si, Sn(IV), Te(IV), Ti(IV), Tl(III), Th, W(VI), Zn, Zr, F^-, NO_3^-, SO_4^{2-}, ClO_4^-, and EDTA. The presence of a 100-fold excess of the following ions caused the error given in parentheses: As(V), (+150%); As(III), (+28%); V(V), (+20%); Cr(VI), (+16%); Cr(III), (−12%). The presence of As(III) and V(V) was tolerable at 25-fold and 50-fold weight excesses, respectively, whereas As(V) interferes seriously even when present only at equal weight with phosphorus, *i.e.*, 1 μg. Chromium(III) may be present at 50-fold excess without interference. Silicon as silicate does not interfere; the acidity employed (1*M*) is unfavorable for the formation of molybdosilicate, and chloroform–butanol (4:1) is known not to extract this heteropoly acid even if it is formed (*1*).

Accuracy. A measure of the accuracy of the method was obtained by the determination of phosphorus in synthetic solutions containing foreign ions which were treated as unknown samples. The results of these analyses are shown in Table I.

Nature of Ion Association Complex. Mole ratio and continuous variations procedures with the established optimum conditions of acid concentration etc., and using the recommended extraction procedure, reveal a combining ratio of 3 moles of Rhodamine B to 1 mole of molybdophosphate in the ion-association complex. This is in accordance with the formation of an uncharged complex of the type $[RhB^+]_3[PMo^{3-}]$. An estimate of the apparent overall formation constant for the complex was obtained *via* experiments in

Table I. Determination of Phosphorus in Synthetic Mixtures Treated as Unknowns

Phosphorus taken, μg	Phosphorus found, μg[a]	Error, %	Foreign ions present (weight excess over P)
0.150	0.152	+1.33	Ca(20), Fe(10), Cu(15)
0.300	0.295	−1.67	Al(30), Si(30)
0.300	0.296	−1.33	Zn(30), Pb(20)
0.400	0.420	+5.00	As^{III}(10), Cd(20)
0.250	0.260	+4.00	Se(20), Te(20)
0.200	0.200	0.0	Bi(15), Cu(20)
0.350	0.335	−4.30	W(20), Sb(25), Ge(25)
0.080	0.079	−0.62	Si(15), Ni(10)

[a] Each result is the average of two determinations in good agreement.

which the Rhodamine B recovered in the final butanol–chloroform phase from the complex after its formation from known amounts of phosphorus was determined fluorimetrically. Allowance for depletion of the Rhodamine B concentration in the final chloroform–butanol phase due to the chloroform extractions, which promote the dissociation of the complex by removal of the excess reagent, was made. The overall cumulative formation constant, K, defined as [RhB-MPC]/[MPC][RhB]^2, under these conditions was estimated to be $1.6 \pm 0.3 \times 10^{11}$ liter^2 mole^{-2}.

Conclusions. High sensitivity is obtained for the determination of phosphorus by the spectrofluorimetric method developed. The sensitivity achieved is higher than that for most other methods based on the formation of molybdophosphoric acid, and compares favorably with that of more complex enzymatic methods. High selectivity is achieved with the optimum conditions established. Of the ions investigated, only arsenic(V) interferes seriously, by formation and extraction of the corresponding Rhodamine B molybdoarsenate; arsenic (III), however, may be tolerated when present in moderate excess with respect to phosphorus.

RECEIVED for review April 9, 1971. Accepted May 14, 1971. We thank the Government of Ceylon for the award of a scholarship to one of us (R.N.), the University of Ceylon for the grant of study leave (R.N.), and the Science Research Council for the award of a grant for the spectrofluorimeter.

Application of an Iodide-Specific Resin to the Determination of Iodine in Biological Fluids by Activation Analysis

Michel Heurtebise and W. J. Ross

Sección Química, Instituto Venezolano de Investigaciones Científicas, Apartado 1827, Caracas, Venezuela

A reliable method has been developed for the determination of iodine in biological fluids that incorporates the high sensitivity of neutron activation analysis with a very simple, economical, and rapid radiochemical separation procedure. Through the use of a novel and specific "iodinated" resin, ^{128}I is separated from all other radioactive components of an activated sample. The high degree of isolation achieved permits the determination of this isotope with the maximum sensitivity that can be attained by means of gamma spectrometry. The method has been applied to the routine analysis of urine, blood serum, PBI, and saliva.

OF THE MANY TYPES of clinical analyses performed each year, one of the most difficult and expensive is the determination of iodine in biological fluids. The analytical method most commonly used is based on the catalytic effect of trace amounts of iodine on the oxidation of As(III) by Ce(IV) (*1*, *2*). This method is not only complex for routine application but there remain potential sources of error due to both the loss of iodine and to the interferences of other trace elements and organic constituents on the catalytic reaction (*3*).

Because of the importance of this analysis, especially in the physiopathology of the thyroid, continual efforts have been made to improve the reliability of this colorimetric method and to adapt it to automated application (*4*). During the past decade, efforts also have been made to avoid the problems inherent in the catalytic method through the use of neutron activation analysis (*5*, *6*). These latter studies have culminated in the development of a fully-automated system based on the measurement of ^{128}I after isolation of this isotope from other radioactive components produced during neutron irradiation of biological fluids (*7*).

Even though this nuclear method affords more reliable results, it has not been adopted on a large scale because of the requirements of a nuclear reactor and a sophisticated separation system. Nuclear reactors, however, are becoming increasingly more available to analytical chemists in all parts of the world. Consequently, increased simplification of the separation procedure should lead to greater acceptance of this method. One effort in this direction has been the development of a semi-automated separation system much less elaborate and expensive than previously available (*8*). This paper describes a new concept in chromatographic separation that is specific for iodide and which offers even greater simplicity and economy for large scale routine application of the nuclear approach.

Essentially every known separation technique has been investigated for separating iodine from biological fluids. The

(1) E. B. Sandell and I. M. Kolthoff, *Mikrochim. Acta*, **1**, 9 (1937).
(2) H. Hoch and C. G. Lewallen, *Clin. Chem.*, **15**, 204 (1969).
(3) H. Hoch, S. L. Sinett, and T. H. McGavack, *ibid.*, **10**, 799 (1964).
(4) E. Comoy, *Rev. Fr. Etudes Clin. Biol.*, **12**, 189 (1967).
(5) C. Kellershohn, D. Comar, and C. Le Poec, *Int. J. Appl. Radiat. Isotop.*, **12**, 87 (1961).
(6) E. M. Smith, J. M. Mozley, and H. N. Wagner, *J. Nucl. Med.*, **5**, 828 (1964).
(7) D. Comar and C. Le Poec, International Conference on Modern Trends in Activation Analysis, IAEA, College Station, Texas, 1965.
(8) M. Heurtebise, *J. Radioanal. Chem.*, **7**, in press (1971).

use of anion exchange resins is the most suitable for the nuclear method and the most amenable to automation. A very well-known method for the separation of mineral iodide from the protein-bound-iodine (PBI) is based on the adsorption of the former on anion exchange resin and has been made the basis of a method for the determination of PBI by neutron activation analysis (*9*). Comar and Le Poec (*10*) observed that neutron activation of a biological liquid ruptures the organic iodine ligand so that total retention of iodine can subsequently be achieved by anion exchange chromatography. This phenomemon eliminates the need for ashing the sample to liberate the organic iodine. Consequently, iodide can be isolated from other radioactive species (principally ^{24}Na, ^{38}Cl, ^{42}K, ^{80}Br, ^{82}Br) through retention on Dowex-2 and subsequent selective elution with nitrate solutions (*11*). Since the induced radioactivity of the major components is very large, high decontamination factors ($\sim 10^5$ for ^{24}Na and ^{38}Cl) are required to permit accurate measurement of ^{128}I. Such efficiency can be achieved only by relatively lengthy elution procedures.

Sansoni (*12*) has reported that molecular iodine and its complexes I_n^- are adsorbed very strongly on anion resins probably through a molecular adsorption mechanism. The degree of retention is not a function of pH, extraneous ions, type of solvent, or basicity of the resin. In this paper it is demonstrated that an anion exchange resin that is saturated by a concentrated solution of $I^-/I_2/I_n^-$ exhibits specific retention for iodide ion. This characteristic has been made the basis of a method for the selective and rapid separation of ^{128}I from all other radioactive components of irradiated biological fluids.

EXPERIMENTAL

Resin Column. Resin columns are prepared individually by placing 150 mg of Dowex 2-X8 (200–400 mesh) in a suitable tube and washing the resin with an iodine reagent until no difference can be observed between the colors of the influent and effluent. Ten milliliters of reagent are usually sufficient. An additional 5 ml of reagent is then passed through the resin column to ensure complete saturation. The resin is held in the tip of the tube by means of a small wad of glass wool so that the resin bed is approximately 1 cm high and 0.5 cm in diameter. The iodine reagent is prepared by dissolving 25 g of iodine in 1 liter of 1*M* KI to form a solution nearly saturated in I_2. When not in use the resin columns are stored in the iodine reagent. While separations are being performed, the resin holders are connected to a source of vacuum by small-diameter tubing.

Preparation of Sample. SALIVA AND URINE. Two-milliliter aliquots are combined with 0.1 ml of 0.05% $K_2S_2O_5$ solution and sealed in a polyethylene irradiation tube.

BLOOD SERUM. One-milliliter aliquots are diluted with 2 ml of distilled water and 0.1 ml of 0.05% $K_2S_2O_5$ and then encapsulated.

PBI. This fraction is separated by anion exchange (*8*, *9*) and subsequently treated in the same manner as serum.

IODINE STANDARD. Solutions that contained 10 to 100 ng of iodine per ml were prepared from potassium iodide or commercial lyophilized serum solutions (Versatol). Two-milliliter aliquots and 0.1 ml of 0.05% $K_2S_2O_5$ were normally used.

Irradiation of Samples. All irradiations were performed in the RV-1 Reactor at a thermal neutron flux of $\sim 5 \times 10^{12}$ n cm^{-2} sec^{-1}.

Counting Equipment. Gamma measurements were made with a 3-in. × 3-in. NaI(Tl) well detector coupled to a 400-channel pulse-height analyzer.

Procedure. Groups consisting of three samples and one standard are irradiated in a single container for 25 minutes. During this period the resin columns are purged of excess iodine reagent by washing them with 1 ml of water. The irradiated solutions are transferred, with minimum delay, to the resin columns that are connected to water aspirators. The radioactive eluent is collected in a trap or is flushed into a "hot" drain. A flow rate of 1 to 4 ml per minute is maintained by regulation of the aspirator. After the sample has completely drained, the resin is washed twice with 2-ml volumes of water and then twice with 5-ml portions of water or, preferably, 2% NaCl solution. When the column is dry the tube is disconnected from the vacuum line and placed in the counting facility where it is counted for 2 minutes. The activity of each sample, corrected for decay, is compared with that of the standard of its group, that has been processed in the same manner, to obtain the weight of iodine in the sample.

RESULTS AND DISCUSSION

Retention of Components of Urine and Blood. Initial studies of the retention characteristics of the "iodinated" resin were performed by adding, one at a time, radioactive tracers (^{24}Na, ^{38}Cl, ^{42}K, ^{82}Br, ^{131}I) to two milliliters of inactive urine or blood serum and then passing these solutions through a resin column. The resin was subsequently washed with 2-ml portions of water. Flow rates of 1 to 4 ml per minute were employed. A large percentage (~90%) of all of these elements, except iodine, passed directly through the resin. More than 99% of the extraneous ions are eliminated by washing the resin only twice with 2 ml of water. Only 0.1 to 0.2% of the ^{131}I activity was found in the sample eluate and none was detected in seven subsequent wash solutions. It was interesting to observe that chloride and bromide are not retained to any greater degree than sodium or potassium. The anion exchange properties of the original resin (Dowex 2-X8) seem to have disappeared after saturation with iodine and its complexes. Contrariwise, the retention of ^{128}I is essentially quantitative and unaffected by water washes. Since >99% of the ^{24}Na and ^{38}Cl are removed by washing the resin with only 4 ml of water, a satisfactorily high decontamination factor is obtained by washing with an additional 10 ml. No loss of iodine from the resin has been observed after successive washes of 2 ml of water.

Similar tests were conducted with samples of PBI fraction and, once again, the retention of iodine was observed to be 99.6% after the resin had been washed seven times.

It was possible to eliminate essentially all trace of ^{24}Na or ^{38}Cl activity from the resin columns and to achieve an even greater decontamination factor by substituting 2% NaCl solution for water in the last 5 washes. No loss of iodine occurs during these NaCl elutions.

Effect of pH. To estimate the effect of the pH on the retention characteristics of the resin, solutions that contained 3 μg of iodide and known quantities of ^{131}I tracer were prepared at different pH. The retention of iodide was at least 99.8% when the pH of the solution was ≤ 7. Approximately 1% of the iodide was lost when the pH was 9.2; however the retention dropped sharply to 86% at pH 10.5 and 84% at pH

(9) C. W. Fang and R. H. Tomlinson, Nuclear Activation Techniques in the Life Sciences, IAEA Symposium, Amsterdam, May 1967.
(10) D. Comar and C. Le Poec, Symposium on Radiochemical Methods of Analysis, IAEA, Salzburg, Austria, 1964.
(11) R. C. De Geiso, W. Rieman, and S. Lindenbaum, ANAL. CHEM., **26**, 1840 (1954).
(12) B. Sansoni, *Angew. Chem.*, **73**, 493 (1961).

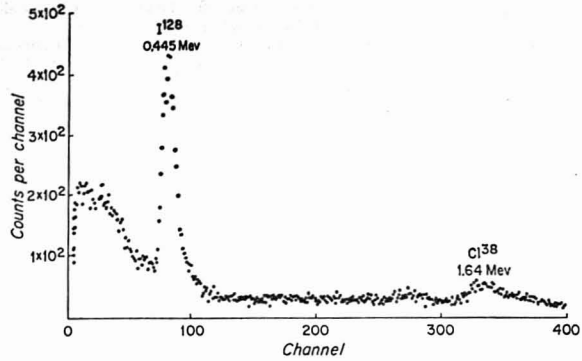

Figure 1. Spectrum of blood sample after separation

(Iodine = 58 ppb)
Flux: 5×10^{12} n cm^{-2} sec^{-1}
Irradiation time: 25 min
Decay time: 10 min
Counting time: 1 min

12. It is known that I_2 is not stable in basic solution but disproportionates slowly to IOH and I^-. IOH is subsequently converted rapidly to IO^-_3 and I^-. This transformation begins at pH 9.5 and is total near pH 11 (*13*). The decrease in retention of iodide when the pH is >9 can probably be explained by deterioration of the resin through alteration of the iodine species.

Effect of the Amount of Iodide on the Resin. The effect of the amount of iodide in a sample solution was established with solutions that contained ^{131}I tracer and iodide of different concentration at a pH of 6.5. Complete retention was attained with carrier-free ^{131}I and when as much as 2.5 mg of I^- was passed through the column. However, when 25 mg of I^- was present in the initial solution, only 73% was retained during passage at a rate of 2 ml per minute.

Effect of Reducing Agent. Iodide has been reported to be oxidized during neutron irradiation (*10*). This would cause negative errors due to the inability of this "iodinated" resin to retain free iodine. Such oxidation and consequent loss of iodine can readily be prevented by adding a small amount of reducing agent to the sample before irradiation. To establish the effect of a reducing agent on the "iodinated" resin, retention studies were performed with 2-ml solutions of $K_2S_2O_5$ of different concentrations (at pH 6.5) to which 3 μg of iodide and ^{131}I tracer were added. The retention of the iodide was 97.5%, 99.0%, 99.2%, and ~100% when the concentration of $K_2S_2O_5$ was 0.4%, 0.2%, 0.1%, and 0.05%. As expected, a slight decrease in retention was observed as the concentration of the $K_2S_2O_5$ solution was increased because of the reduction of free iodine and its complexes on the resin. However, when 2 ml of 0.05% $K_2S_2O_5$ solution is used, no interference on the retention characteristics of the resin is observed. The introduction of only 0.1 ml of 0.05% $K_2S_2O_5$ solution to each sample during preparation is sufficient to counteract any oxidation during irradiation. This precaution probably is unnecessary when body fluid samples are analyzed because identical results have been achieved with and without the reductant. Because of the simplicity of the precautionary measure, this step has been retained in the procedure.

Repetitive Use of a Resin Column. Even though a relatively insignificant expense of time or money is involved in the preparation of a resin column, it was considered worthwhile to establish if such a column can be used repetitively. Consequently, one column was used for the analysis of seven urine and four blood samples which had been "spiked" with ^{128}I. After each analysis, the resin was washed with ~2 ml of iodine reagent and stored in this reagent when not in use. The ^{128}I activity in the eluates was measured and always found to be negligible (<0.2%). Before each new use of the column, the resin was washed with 1 to 2 ml of water to eliminate excess iodine. In each test the retention of the ^{128}I tracer was >99.8%. The cumulative amount of iodine in these eleven samples was negligible (~1 μg) in relation to the quantity (2.5 mg) that such resin can completely retain. This resin was subsequently used in the routine analyses of many irradiated samples, and the selectivity was observed to be the same as that of a new column.

Accuracy and Precision. A value for the overall precision of this method was established through seventeen repetitive determinations of the iodine content of one sample of urine. The average result of these determinations was 107 ppb iodine with a relative standard deviation of 6.5%. When various aliquots (0.2 to 2 ml) of this urine specimen were taken for analysis, a linear relationship was achieved between the weight of iodine found and the volume of the sample. An estimation of the accuracy was made through comparative analyses of four urine samples by this method and by a semi-automated method of proved accuracy which involves the chromatography of I^- on a Dowex 2-X8 column (*8*). In Table I is shown the comparison of the results.

Sensitivity. The sensitivity of all techniques that use neutron activation analysis, radiochemical separation, and gamma spectrometry is a function of the following controllable factors: the neutron flux that is used; the yield of the radiochemical procedure; its rapidity, if the half-life of the measured isotope is short; and the degree of purity with which this radionuclide can be isolated. One of the limitations of gamma spectrometry is the accuracy with which a photopeak

Table I. Comparative Analysis of Urine

Sample	Ppb of Iodine: Semi-automated method	This method
1	120	109
2	164	170
3	127	126
4	84	83

(13) G. Charlot, "L'Analyse Qualitative et Les Réactions en Solution" 334 Masson et Cie, Paris, 1963.

can be distinguished from the background caused by Comptons of higher energy radionuclides. In Figure 1 is presented a spectrum of iodine, separated from an irradiated blood sample, which demonstrates the high degree of decontamination achieved by this method. Isolation of ^{128}I from urine samples is equally evident from spectral data. This fulfills one prerequisite for a sensitive method. In addition this procedure has a radiochemical yield of >99% and can be performed in less than 5 minutes. Therefore, this technique appears to offer the maximum sensitivity that can be achieved through use of activation analysis and gamma spectrometry for ^{128}I. The spectrum in Figure 1 was obtained during the analysis of a sample of serum that contained 58 ng of iodine. As little as 4 ng of iodine, irradiated and measured under the same conditions, would have been sufficient to yield ^{128}I activity equal to that of the background which is essentially due to ^{38}Cl contamination.

The high decontamination that is attained by this procedure also permits accurate measurements of iodine at normal concentrations in biological fluids with a single-channel analyzer, thereby reducing equipment cost and facilitating data reduction. The background, primarily ^{38}Cl Compton, is prohibitively large only when the concentration of iodine is <10 ppb. One remaining limitation for routine clinical application of this technique is the difficult radioprotection problem encountered when as many as 100 samples (irradiated at flux such as 5×10^{12} n cm^{-2} sec^{-1}) are treated every day.

The amount of ^{128}I activity required to achieve the desired sensitivity could be reduced by a factor of fifteen if the beta activity of this isotope were counted. Such enhancement over the sensitivity achieved by gamma counting is due to both the greater abundance of beta particles and the higher efficiency of beta detectors. Consequently, shorter irradiations or lower neutron fluxes could be employed, thereby reducing the total amount of radioactivity per sample. This refinement awaits the development of an efficient and rapid procedure for counting the "iodinated" resin beads in a GM detector and such a program is now being carried out in our laboratory.

RECEIVED for review January 25, 1971. Accepted May 7, 1971.

Qualitative Studies of Trace Constituents by Plasma Chromatography

Francis W. Karasek
University of Waterloo, Waterloo, Ontario

Wallace D. Kilpatrick and Martin J. Cohen
Franklin GNO Corporation, P.O. Box 3250, West Palm Beach, Fla. 33402

By using an ion-molecule reactor and ion-drift spectrometer, the plasma chromatograph produces a plasmagram pattern characteristic of a trace constituent in a gas. Concentrations of 1 ppb and less are detected. The qualitative aspects of the positive and negative plasmagrams obtained for the organic compounds of benzoic acid, salicylaldehyde, phenethyl alcohol, acetophenone, and naphthalene are presented. An interpretation is made of the plasmagrams in terms of the type of ion-molecule complexes formed, concentration effects, and a measure of their molecular weight. When the reactant ions $(H_2O)_2H^+$ and $(H_2O)_2O_2^-$ are used, plasmagrams characteristic of the sample molecules, their concentration, and reactivity with the reactant ion are obtained.

THE TECHNIQUE of plasma chromatography permits characterization and analysis of trace constituents in a gaseous mixture at atmospheric pressure. The instrumentation involves a positive and negative ion-molecule reactor coupled with an ion-drift spectrometer. Reactions occur between a generated reactant ion and the trace molecule to be detected. The ion-molecule complexes formed are separated in the ion-drift spectrometer and arrive at the spectrometer detector as ion peaks which are recorded as a plasmagram. Individual peaks can be directed into a quadrupole mass spectrometer for mass identification.

Fundamental to the sensitivity and selectivity of the technique are the characteristics of the ion-molecule reaction selected to produce the detected species. Ion-molecule reactions have very high reaction rates and form stable ion-molecule complexes. The sensitivity to trace compounds arises from the fact that the ion-molecule reaction occurs at atmospheric pressure, where the probability of reaction is high because of the short mean-free-path and the many millions of collisions possible.

The first publications on the Plasma Chromatograph ™(PC) appeared only recently. Karasek (*1*) described the basic features of the method. Considerations attendant to coupling a gas chromatograph to the system are a subject of a recent paper by Cohen (*2*). A further paper by the above authors presents a study of the plasmagrams obtained for the compounds 1-octanol and 1-nonanol (*3*). An experimental correlation of plasmagram time of an ion-molecule complex to its mass has been reported by Karasek (*4*) and is further described by Kilpatrick (*5*). This method will be used for interpretation of the results obtained in this study. Cram (*6*)

(1) F. W. Karasek, *Res./Develop*, **21**, (3), 34 (1970).
(2) M. J. Cohen and F. W. Karasek, *J. Chromatogr. Sci.*, **8**, 330 (1970).
(3) F. W. Karasek and M. J. Cohen, *J. Chromatogr. Sci.*, **9**, 390 (1971).
(4) F. W. Karasek, *Res./Develop.*, **21**, (12), 25 (1970).
(5) W. D. Kilpatrick, "An Experimental Mass-Mobility Relation for Ions in Air at Atmospheric Pressure," Proceedings of the 19th Annual Conference on Mass Spectrometry, May 1971, Atlanta, Ga.
(6) S. P. Cram, W. D. Kilpatrick, and M. J. Cohen, "Inorganic Analyses by Plasma Chromatography," presented at the Pittsburgh Conference on Analytical Chemistry and Applied Spectroscopy, March 1971, Cleveland, Ohio.

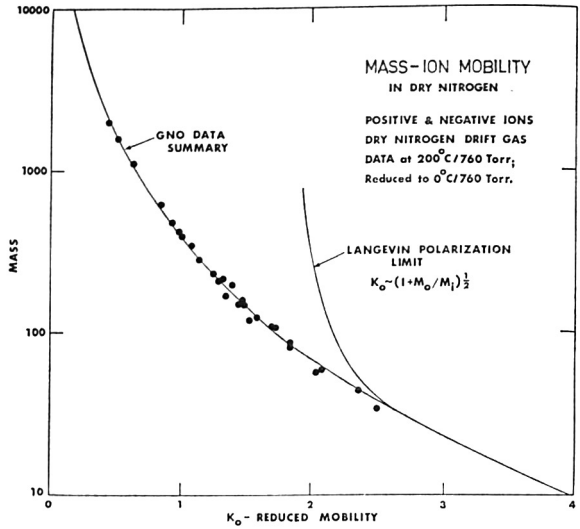

Figure 1. Comparison of the Langevin equation and experimental data in the PC

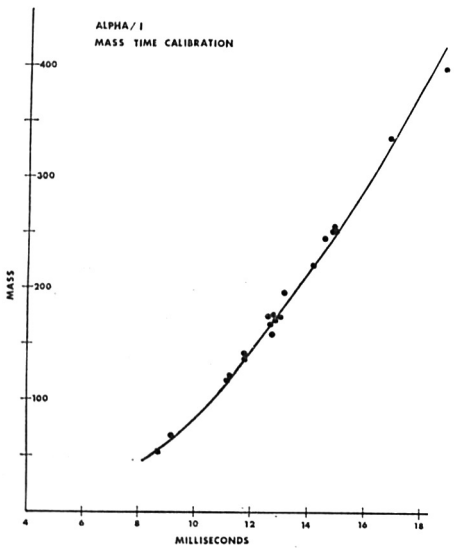

Figure 2. Experimental correlation of ionic mass vs plasmagram time

recently described experiments with the PC in which metal chelates of Al and Cr were identified as ion-molecule complexes with molecular weights as high as 2500 AMU. For a more complete description of the instrumentation, one is referred to previous work (*1*, *2*).

This study was undertaken to determine the qualitative aspects of the plasmagrams obtained for a series of compounds of very similar molecular weights but different molecular structures and functional groups. The molecular weights ranged from 120 to 128. These compounds were selected also to provide further data on the ion-drift behavior as a function of molecular weight.

Separation of the ion-molecule complexes formed is brought about by their different mobilities as they move through an inert gas at 760 Torr under the influence of an electrical field. The detailed quantitative treatment of the mobility for simple ions under these conditions was given by Langevin in 1905. His equation (7), established for simple atomic ions at low pressures, predicts a polarization mobility limit that begins below a molecular weight of 100 as shown in Figure 1. A plot of a large amount of mass-identified mobility data taken in the plasma chromatograph–mass spectrometer indicates that this limit does not occur for the ion-molecule complexes studied. Mobility actually follows a curve inversely proportional to the ion-molecule mass. Using a more complete form of the mobility equation, Carroll and Mason (*8*) were able to show that the mobility of these ion-molecule complexes should be a function of ionic radius and can be expected to follow the experimental curve shown in Figure 1.

This experimental and theoretical evidence for the validity of the curve of ion-mobility *vs.* mass provides a basis for interpretation of the times of the plasmagram peaks in terms of mass units and the ion-molecule complex corresponding to that mass. For a given set of operating parameters in a plasma chromatograph the data of Figure 1 can be plotted as shown in Figure 2. The known values fall within 5% of the curve in Figure 2. This curve was used to assign a mass value to the peaks obtained in the plasmagrams and led to interpretation of the most probable ion-molecule complex present.

(7) E. W. McDaniel, "Collision Phenomena in Ionized Gases," John Wiley & Sons, New York, N. Y., 1964, p 755.
(8) D. I. Carroll and E. A. Mason, "The Theoretical Relationship Between Ion Mobility and Mass," Proceedings of the 19th Annual Conference on Mass Spectrometry, May 1971, Atlanta, Ga.

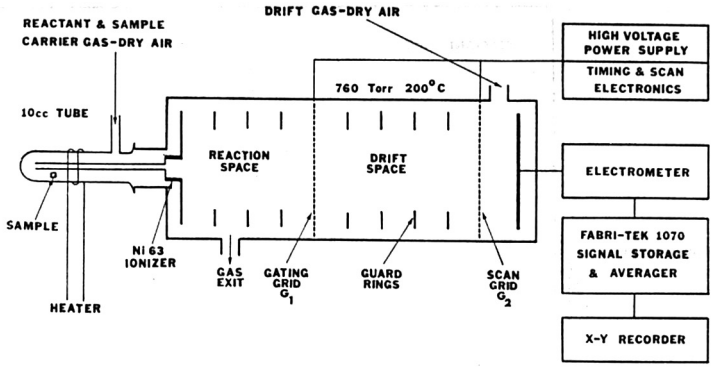

Figure 3. Schematic diagram of the plasma chromatograph

EXPERIMENTAL

Instrumentation. The basic instrumentation and its functions have been described previously (*1–4*) in detail. The PC version used for this work is shown schematically in Figure 3. While it is possible to record a plasmagram directly from the electrometer output, it is more useful and convenient to store the plasmagram in channels of a Fabri-Tek Signal Averaging Computer (Fabri-Tek AN-FT-1072, Fabri-Tek Instruments, Inc., 5225 Verona Road, Madison, Wis. 53711). The data can then be displayed on an oscillograph, plotted on a recorder, or processed through this unit as desired for the experimental objectives. All data plotted here were obtained in this way.

Timed injection and scan pulses are used to produce a smoothed scan for a recording that averages several minutes of the 20-millisecond individual plasmagram scans. At grid G_1 a short 0.25-millisecond pulse injects a cluster of ion-molecule complexes into the drift region. This region is 8 centimeters in length with an electrical field of 214 V/cm. A single plasmagram can be recorded at the ion collector in a 20-millisecond span. To produce this same plasmagram in minutes for recording ease, a gating grid is used prior to the collector. This grid is opened for transmission of the ions by a 0.25-millisecond pulse, at times delayed from the injected pulse so as to move it at a controlled rate across the 20-millisecond plasmagram. If the delay and gate opening are coincident with arrival of a given set of ion-molecule complexes, they will reach the collector for recording. If this delay grid takes 2 minutes to cover its range, a 2-minute plasmagram will be recorded, the sum of all the 20-millisecond individual plasmagrams occurring during the two minutes. The resolution obtained in the plasmagram is directly related to the width of these two pulses on the injection and scanning grids. The 0.25-millisecond width chosen for this study provides the highest resolution consistent with an adequate ion current.

Procedure. Because of the qualitative nature of this study and the variability of responses from these compounds, three different sampling methods were used, all of which produced trace concentrations adequate for the purposes of this study. For the solids benzoic acid and naphthalene a very small crystal, less than 1 milligram in weight, was placed in the sample holder and heated slowly. The amount reaching the reaction region depended upon the heating rate and vapor pressure of the compound. As soon as sufficient vapor was present to obtain a response, the sample tube was removed and replaced with a clean, empty one. This procedure was necessary so as not to saturate the instrument with concentrations greater than ppm. The liquid samples can be admitted by injection with a 1-microliter syringe, usually in very dilute water solution. However, sufficient sample for most compounds can be obtained by insertion of a liquid-wet rod into the sample inlet tube and permitting the vapors to diffuse into the tube for 3–5 seconds. This latter method was used for the acetophenone, phenethyl alcohol, and salicylaldehyde samples. Samples admitted in these manners were sufficient for several hours of data-taking with the instrument. It can be estimated that these techniques produced trace concentrations at the ppb or less level.

Initial concentrations were usually too high, as evidenced by disappearance of the reactant ion. As the sample concentration became reduced by the action of the flowing carrier gas, its changes could be followed by the appearance and growth in intensity of the reactant ion peak. Sequential plasmagrams were taken during these changes and chosen to describe concentration effects. Table I lists the experimental conditions for this work.

Table I. Experimental Parameters for Plasmagrams Obtained with Compounds Studied

Sample temperature:	25–200 °C
Sample gas flow:	170 cc of dry air/minute
Drift gas flow:	500 cc of dry air/minute
Ion-drift space:	8 cm
Electric field:	214 V/cm
Injection pulse:	0.25 millisecond
Gating pulse:	0.25 millisecond
Recorded scan:	2-minute sweeps—4 averaged
Compounds:	CP reagent grade with greater than 99.9% purity
Sample and Drift Gas:	Linde high pressure cylinder, 79% N_2, 21% O_2, suitable for breathing, dried by a metal trap 24-in. × 2-in. diameter packed with Linde Molecular Sieve 3A

RESULTS AND DISCUSSION

Reactant Ions. Reactant ions are formed from the direct, primary ionization of components in the air used as a carrier for introducing the sample. A drying procedure leaves sufficient water vapor, about 10 ppm, in the air to provide the major source of reactant ions. The incoming gas mixture passes adjacent to a 10-millicurie nickel-63 radioactive beta source which ionizes the gas species in proportion to concentration. As a first step, positive nitrogen and oxygen ions and electrons are formed, creating a weak plasma of equal numbers of

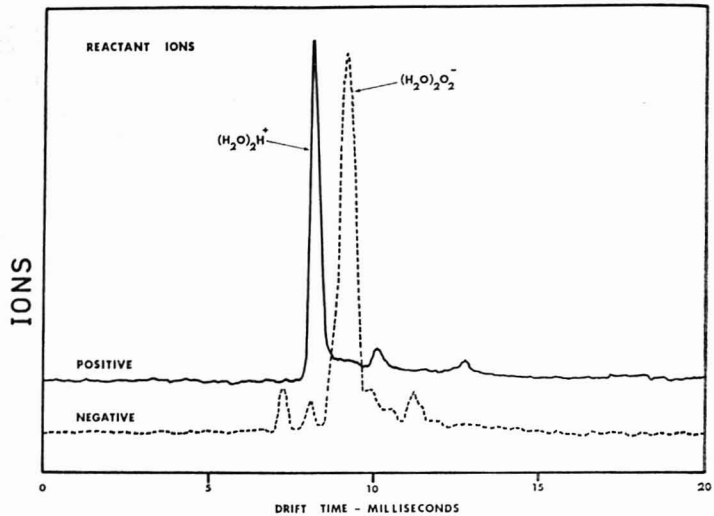

Figure 4. Plasmagram of reactant ions

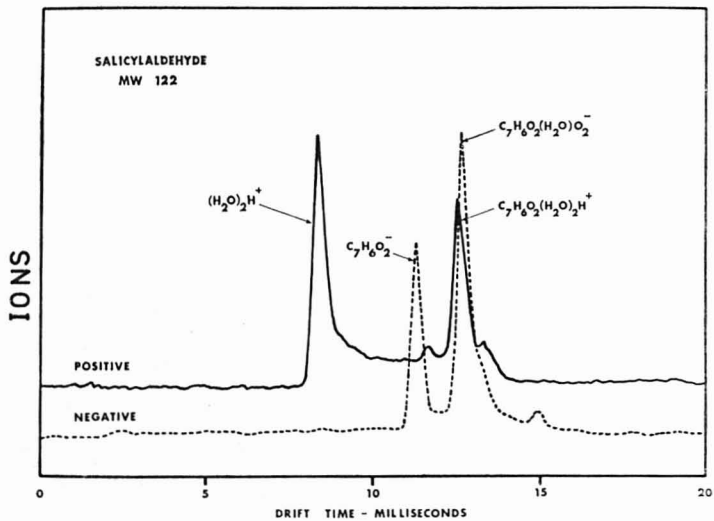

Figure 5. Comparative positive and negative plasmagrams of salicylaldehyde

positive and negative charges. The behavior of the electrons in the reaction space, in the absence of a sample component, consists of energy moderation by inelastic collisions to quickly reach temperature equilibrium with the gas. Then, an electron attachment reaction takes place with the predominant electronegative oxygen species to form hydrated negative oxygen ions of the nature $(H_2O)_nO_2^-$. Mohnen (9), in studies of the troposphere, finds the terminal tropospheric negative ion to be $(H_2O)_nO_2^-$ where n shows an equilibrium distribution with a maximum around 3 or 4. At the 760-Torr cell pressure, these reactions occur within a fraction of a millisecond and within millimeters of the position of the electron generation adjacent to the source electrode. The value of n is a function of the water concentration and cell temperature. At 200 °C and the 10-ppm water concentration cited above, n typically has the values 0, 1, 2, 3. For the positive reactant ion, the probable sequence of reactions starting with N_2^+ and O_2^+ eventually produces $(H_2O)_nH^+$ ions. The existence of such water cluster ions under these conditions is well known and their properties have been studied. Burke (*10*) has observed

(9) V. A. Mohnen, *J. Geophys. Res.*, **75**, 1717 (1970).

(10) R. R. Burke and W. J. Miller, "Effects of Electric Fields and Sample Expansion on Ion Sampling at High Pressure," Proceedings of the Seventeenth Annual Conference on Mass Spectrometry and Allied Topics, May 1969, Dallas Texas, paper No. 54, p 163.

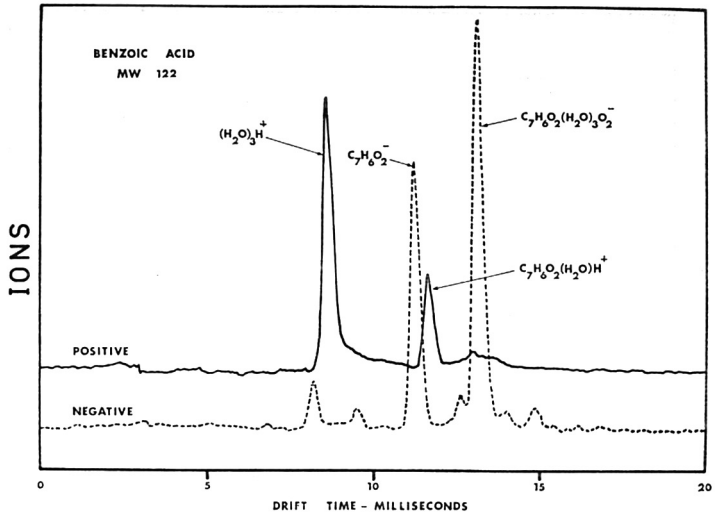

Figure 6. Comparative positive and negative plasmagrams of benzoic acid

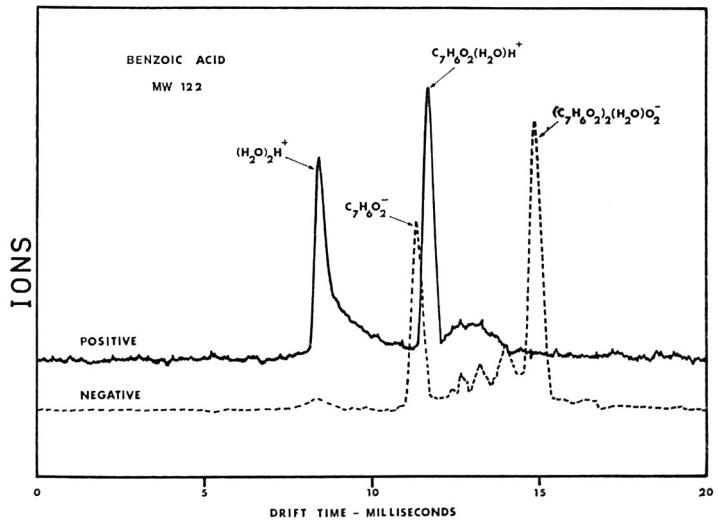

Figure 7. Comparative positive and negative plasmagrams of benzoic acid—concentration higher than in Figure 6

mixtures of these ion clusters with water molecules varying from 1 to 19. Ion transformations to produce hydrated protons have also been observed under vacuum conditions up to several Torr pressure by Shahin (*11*) and Good (*12*).

The primary reactant ion for formation of positive ion-molecule complexes is a mixture of the hydrated protons $(H_2O)_2H^+$ and $(H_2O)_3H^+$. The predominating species in any given sample run depends upon the concentration of water vapor reaching the reaction cell that arises from both the sample carrier gas and sample itself. The reactant ions giving rise to the negative plasmagrams are predominantly the $(H_2O)_2O_2^-$ ions. Both positive and negative reactant ions are shown in the plasmagrams of Figure 4.

Plasmagrams of Compounds. The data obtained for these compounds are indicated in the positive and negative plasma-

(11) M. M. Shahin, *J. Chem. Phys.*, **45**, 2600 (1966).
(12) A. Good, D. A. Durden, and P. Kebarle, *ibid.*, **52**, 212 (1970).

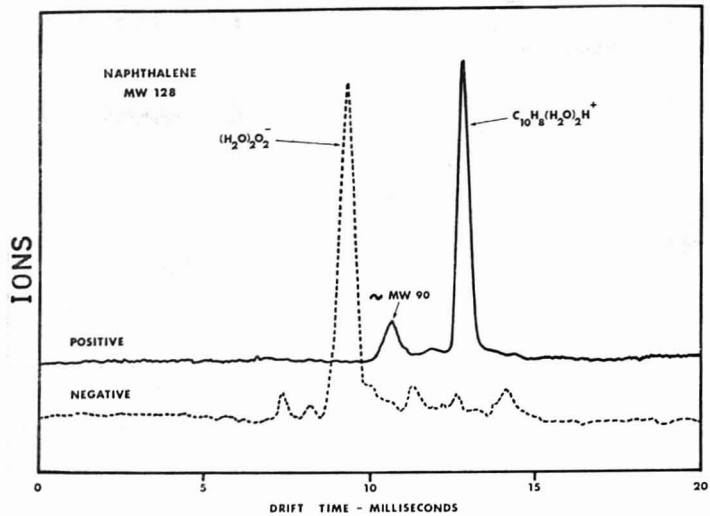

Figure 8. Comparative positive and negative plasmagrams of naphthalene

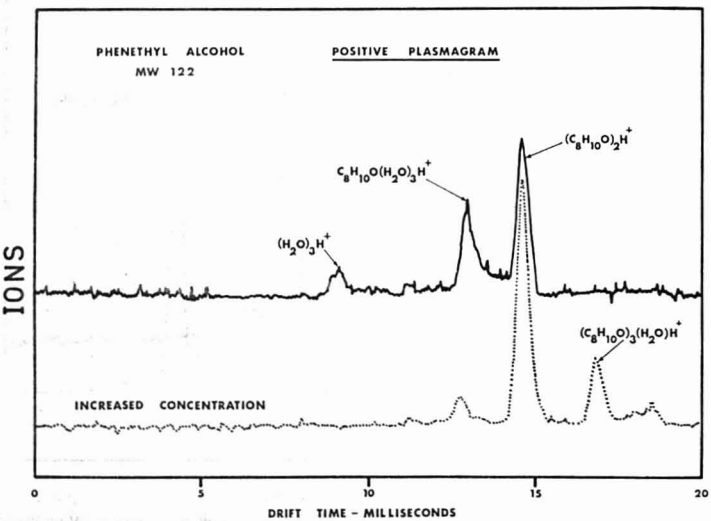

Figure 9. Plasmagram of two different concentrations of phenethyl alcohol

grams shown in Figures 5–10. Mass assignments for the individual ion-molecule peaks were made from the correlation curve in Figure 2. Structures consistent with these masses, to within a 5% correlation, and with the most probable ion-molecules present, from considering the reactions involved in their creation, were assigned.

The positive plasmagrams of salicylaldehyde, benzoic acid, naphthalene, acetophenone, and phenethyl alcohol show that when concentrations are low, as is indicated by the continued presence of a strong reactant ion peak, a single peak of the ion-molecule complex is formed. The data suggest benzoic acid forms ion-molecule complexes with the $(H_2O)H^+$, the salicylaldehyde and naphthalene with $(H_2O)_2H^+$, and acetophenone and phenethyl alcohol with $(H_2O)_3H^+$.

As either the concentration or reactivity of the organic molecule increases, the reactant ion-peak will decrease and even disappear, with the resultant formation of higher molecular weight ion-molecule complexes containing multiples of the

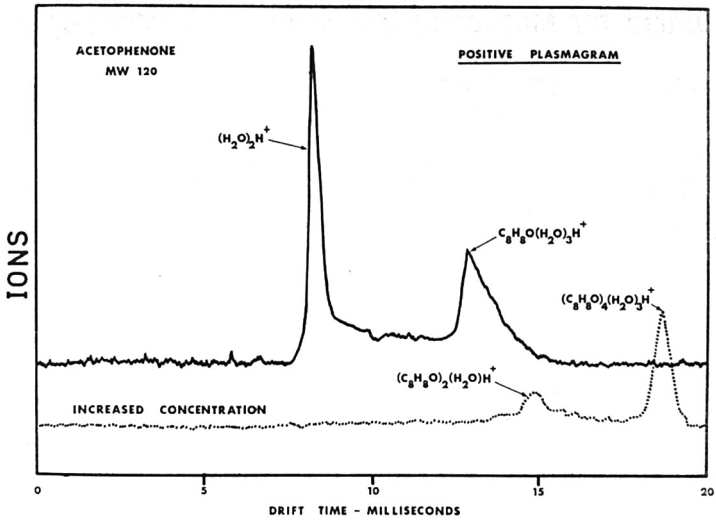

Figure 10. Plasmagram of two different concentrations of acetophenone

trace molecules. This appearance of dimers and trimers at higher concentrations was also found to occur by Karasek (*3*) in a study of 1-octanol and 1-nonanol where the ion-molecule complexes were mass-identified in a quadrupole mass spectrometer. A similar concentration effect is also found to occur in chemi-ionization spectra (*13*). This occurrence can be seen in the plasmagrams of benzoic acid (Figure 7), phenethyl alcohol (Figure 9), and acetophenone (Figure 10). The higher concentration of acetophenone in Figure 10 appears to have four molecules of the compound associated with the hydrated proton.

Negative plasmagrams were studied for the compounds salicylaldehyde (Figure 5), benzoic acid (Figures 6, 7), and naphthalene (Figure 8). Both salicylaldehyde and benzoic acid show that the molecular negative ion is formed by electron transfer, while the major ion-molecule species appear as different complexes formed with water molecules and the negative oxygen molecule.

The plasmagrams in Figures 6 and 7 show the behavior one obtains with benzoic acid at two different concentrations. The concentration of benzoic acid in Figure 6 is less than that in Figure 7, as indicated by the greater amount of positive reactant ion shown. In both cases the molecular ion appears by electron transfer, but the higher concentration of benzoic acid in Figure 7 leads to the formation of a negative dimer complex. These two figures also reveal that the ion-molecule reactions are much more favorable for the negative than the positive.

The plasmagrams for naphthalene (Figure 8) show a behavior that is exactly opposite to that found for benzoic acid. The positive ion-molecule reactions are the most favored. At a concentration of naphthalene sufficiently high to leave no reactant ion in the positive mode, there are no apparent negative ion-molecule reactions occurring. The negative plasmagram differs little from the reactant ion plasmagram of Figure 4. This behavior is consistent with that observed in the electron capture detector where hydrocarbons have little sensitivity. It is also supported by recent work of the author where it was found that negative plasmagram response of a series of polychlorinated biphenyl compounds was directly related to their electron capture detector response (*14*).

CONCLUSIONS

All compounds studied give plasmagrams in both the positive and negative modes. The plasmagrams are not only characteristic of the sample molecules involved, but are a sensitive function of concentration. They provide an indication of relative reactivity between reactant ion and sample under positive and negative reactant ion conditions. The ability to observe both positive and negative plasmagrams concurrently gives one a more certain identification, since one mode appears to predominate for a given molecular structure. Quite clearly, only the surface of the potential of this method has been explored here. A study of the selectivity and sensitivity possible when one uses different reactant ions for analysis of specific trace compounds promises to broaden the scope of the method considerably. Work is now in progress in this area as well as a more definitive study of the quantitative aspects of the method.

RECEIVED for review March 30, 1971. Accepted June 16, 1971. Presented in part at the Pittsburgh Conference on Analytical Chemistry and Applied Spectroscopy, Cleveland, Ohio, March 1971.

(13) F. H. Field, Rockefeller Institute, New York, N. Y., personal communication, 1971.

(14) F. W. Karasek, "Plasma Chromatography of the Chlorinated Biphenyls," unpublished work, Waterloo, Ontario, April 1971.

An Instrument for Measuring the Hydrogen Content of Metals

J. B. Condon, R. A. Strehlow, and G. L. Powell
Union Carbide Corporation, Nuclear Division, Oak Ridge, Tenn. 37830

An instrument has been developed to measure the hydrogen content of metals in the range from 0.01 to 100 weight parts per million (wppm). The instrument requires a 0.1-gram to 5.0-gram sample size and records, as a function of time, both the rate at which hydrogen is thermally evolved from the sample and the total amount of hydrogen evolved.

Low concentrations of hydrogen in metals can have a dramatic effect on their physical properties. Hydrogen is known to contribute significantly to hardness and embrittlement of stainless steels and transition metals in general. Stress corrosion cracking in titanium and other transition metal alloys has been attributed to hydrogen charging. A determination of low concentrations of hydrogen in the one weight-part-per-million (wppm) range and lower has become increasingly important to the study of this phenomenon.

Often along with a knowledge of the hydrogen content, the diffusion properties and distribution of hydrogen in the metal or alloy is of vital concern. This would be especially important in the progression of stress corrosion cracking induced by hydrogen charging. A knowledge of the hydrogen diffusion rate also makes possible the establishment of reasonable control specifications in metal and alloy processing.

High sensitivity instruments for hydrogen analysis have been reported in the literature (*1–7*). Most have relied on the vacuum hot extraction or fusion method. The most sensitive (*8–11*) utilized the high sensitivity of a gas chromatograph on a collected volume of gas obtained by vacuum fusion. A few methods utilized a mass spectrometer and hot extraction to obtain both high sensitivity and instantaneous readout (*12–14*).

The instrument described in the present article was designed to perform the following functions: To measure the hydrogen content of a metal in the range from 0.01 wppm to 100 wppm using a specimen size ranging from 0.1 gram to 5.0 grams; to measure the hydrogen evolution rate from the metal; to analyze for gases other than hydrogen; and to be operated under routine analytical laboratory conditions.

Hydrogen evolution rate measurements could be used to determine the diffusion rate of hydrogen in metals as well as to time-resolve "surface hydrogen" from hydrogen distributed uniformly throughout the bulk of the metal. "Surface hydrogen" could be atomic or molecular hydrogen adsorbed on or near the surface of the metal or hydrogen combined in water or organic compounds adsorbed on the metal surface. For most transition metals, these compounds would react with the metal to produce molecular hydrogen during the early stages of the hot-extraction process. This "surface hydrogen" could contribute up to one wppm to the total hydrogen content of a one-gram metal specimen.

(1) C. R. Masson, *Metallurg. Rev.*, **12,** 147, (1967).
(2) M. W. Mallett, *Talanta*, **9,** 133–144 (1962).
(3) J. Fischer, Fresenius' *Z. Anal. Chem.*, **209,** 163–176 (1965).
(4) W. Baum and S. Eckhard, *ibid.*, pp 188–197.
(5) N. A. Gokcen and E. S. Tankins, *J. Metals*, **14,** 584–87 (1962).
(6) W. G. Guldner, *Talanta*, **8,** 191–202 (1961).
(7) S. Matsuo, T. Hirata, *Nippon Kinzoku Gakkaishi*, **31,** 590–3 (1967).
(8) F. Sperner and K. H. Kock, *Metall*, **18,** 701–704 (1964).
(9) Richard Lasser and H. Gruber, *Z. Metallk*, **51,** 495–501 (1960).
(10) Richard Lasser, *Trans. Nat. Vac. Symp.*, **8,** 782–787 (1961).
(11) J. J. Schmidt-Collerus and A. J. Frank, *WADD TR*, 60-482, Denver Research Institute, University of Denver, Denver, Colo., 1961.
(12) H. Hintenberger, *Fresenius' Z. Anal. Chem.*, **209,** 176–187 (1965).
(13) L. A. Ferguson, D. E. Seizinger, and C. H. McBride, *U. S. At. Energy Rept.* MCW-1462 (1961).
(14) V. I. Fistul, *Kom Anal. Khim. Akad. Nauk SSSR, Inst. Gcokhim Anal. Khim.*, **10,** 71–81 (1960) (URRL-Trans-1377).

EXPERIMENTAL

Principles of Operation. The principle of operation of the hot-extraction method used here was as follows. A sample was allowed to drop into a hot zone in a high vacuum system. The hydrogen and other gases were evacuated through an orifice into a detection chamber which was equipped with a residual gas analyzer (a small mass spectrometer or RGA). Proper control over the pumping speeds of the extraction chamber and the detection chamber allowed a calculation to be made of the total amount of hydrogen evolved as a function of time. In this system there was a constant pumping speed, S_1, determined by an orifice from the furnace chamber. The detection chamber was evacuated by a constant pumping speed, S_2. According to kinetic theory, the pressure in the detection chamber (P_2) was related to the pressure in the furnace chamber (P_1) by the following equations:

$$\frac{dP_1}{dt} = \frac{RT}{V_1}\frac{dn_1}{dt} - \frac{S_1}{V_1}(P_1 - P_2) + \frac{L_1}{V_1} \quad (1)$$

and

$$\frac{dP_2}{dt} = (P_1 - P_2)\frac{S_1}{V_2} - \frac{S_2}{V_2}P_2 + \frac{L_2}{V_2} \quad (2)$$

where n designates the amount of hydrogen evolved, L designates the inherent leak rate of the system which is constant and shows up as a base pressure, and V is the volume of the respective chambers.

Upon integration and rearrangement, the following is obtained:

$$\frac{RT}{V_1}n = \left(1 + \frac{V_2}{V_1} + \frac{S_2}{S_1}\right)P_2 + \frac{S_2}{V_1}\int P_2 dt - \frac{L_2 + L_1}{V_1}t - \frac{L_2}{S_1} + \frac{V_2}{S_1}\frac{dP_2}{dt} \quad (3)$$

If $S_2 \gg S_1$ and $V_2 \cong V_1$, then $1 + V_2/V_1 + S_2/S_1 \cong S_2S_1$. The last two terms in Equation 3 are extremely small and the third term is the base pressure correction. Letting $P_2 = Ai$ where i is the RGA signal, $N = A(S_2/S_1)(V_1/RT)$, and subtracting out the base pressure correction Equation 3 reduces to:

$$n = N[i + S_1/V_1 \int i dt] \quad (4)$$

Equation 4 is also the solution to Equation 1 for the case where i is proportional to P_1 and $P_2 \gg P_1$. Under these conditions, the mass spectrometer could be used to measure P_1 in a very passive manner.

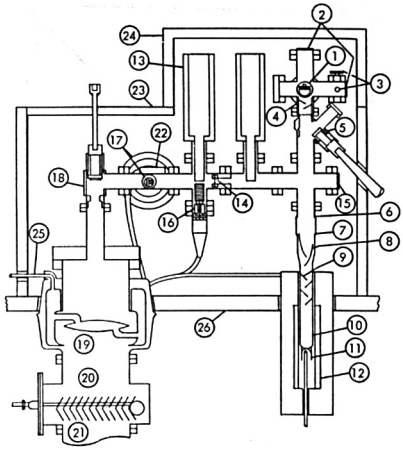

Figure 1. High Vacuum Hydrogen Analyzer

1. Sample feed mechanism
2. Windows
3. Gas injection calibration system (Nupro Type-H valves)
4. Optically dense baffles
5. Bakeable ultra-high vacuum straight-through valve (Varian)
6. Kovar-to-borosilicate glass graded seal
7. Borosilicate glass-to-quartz graded seal
8. Stainless steel mesh baffles to reduce sample impact on quartz baffles
9. Quartz baffles
10. Quartz furnace chamber
11. Quartz thermocouple well with thermocouple
12. Standard 1-inch-i.d. combustion tube furnace (element insulated with firebrick contained in SS)
13. Reentrant-type liquid nitrogen dewars
14. Aluminum foil orifice mounted between Mini-ConFlat flanges
15. Orifice observation window
16. Nude ionization Gauge
17. Mass spectrometer (EAI QUAD 150)
18. Bakeable ultra-high vacuum L-valve (Varian)
19. Liquid nitrogen cold trap (Granville-Phillips)
20. Refrigerated (−33 °C) baffle (Torr Vacuum Prod)
21. Mercury diffusion pump (Torr Vacuum Prod)
22. Temperature controls for bake-out mantle
23. Bake-out mantle with 5000 watts heating capability
24. Bake-out mantle cover (removed during operation of instrument)
25. Liquid nitrogen fill tube
26. Color Ceran table top (Johns-Manville)

All components made of 304 Stainless Steel with exception of those noted. All flanges above the liquid nitrogen cold trap were of the ConFlat type with which OFHC copper gaskets were used

Apparatus. The instrument was constructed mostly from ultrahigh-vacuum components readily available from commercial vendors. Figure 1 is a complete diagram of the instrument. Evacuation of the system was accomplished by a diffusion pump and a mechanical forepump. Use of ion pumps was unsatisfactory since the pumps re-evolved hydrogen and were easily saturated. The orifice, S_1, consisted of a thin aluminum foil barrier containing a hole. A hole size of 0.030-inch diameter was found to be optimum. For convenience, this foil was mounted on the inside of the standard ($1^1/_2$-inch i.d.) ultrahigh-vacuum "T" fitting by welding a Mini-ConFlat (Varian Associates) flange on the inside. The foil was then fixed in place with a mating MiniConFlat flange.

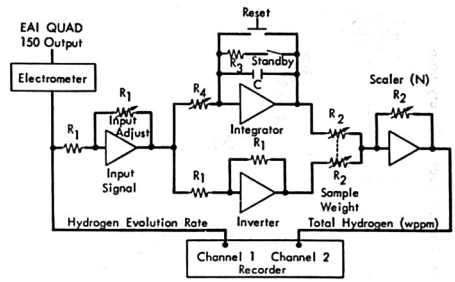

Figure 2. Analog device for computing total hydrogen (wppm) from mass spectrometer output

Philbrick-Nexus operational amplifiers powered by a PR-30C power supply were used. All fixed resistors were rated 1% and all variable resistors were rated 3%, 0.2% linear. Component designations were as follows:

Integrator-SP-65AU
All other amplifiers P-35AU

R_1 − 50 KΩ
R_2 − 100 KΩ
R_3 − 1 KΩ
R_4 − 1 MΩ
C − 20 μf

To admit the sample to the hot zone, a mechanical manipulator (a bellows-type rotary-linear feed-through) was used to shove samples off the end of a platform. To ensure separation, a sliding board with holes in it was used to contain the samples. When a sample was admitted, it fell through a set of stainless steel baffles, through a straight-through valve, and through another set of quartz baffles into the quartz tube hot zone. The function of the latter set of baffles was to prevent sublimation pumping. The potential gettering action that some metals will produce by the sublimation of the metal to form an active thin film in the cooler portions of the extraction tube could significantly reduce the evolution of gases from the furnace tube. Titanium is especially effective in this respect and each metal must be examined on an individual basis to determine the severity of the problem. In most instances the problem can be solved by a series of baffles leading into the hot zone. Generally, metals will condense at a temperature sufficiently high that the sticking coefficient for hydrogen is very low, and pumping action will not occur with successive layer deposition. The purpose of the former set of baffles was to prevent premature heating of the samples by radiation from the quartz tube hot zone. The straight-through valve was extremely convenient for it isolated the sample chamber from the rest of the vacuum system. Sample loading could therefore be done without disturbing the rest of the vacuum system. A separate sorption pump was used on this area for pumpdown after loading.

The quadrupole residual gas analyzer used with this instrument was an EAI QUAD 150 (Electronics Associates, Inc.). The signal was amplified with an electrometer (Keithley 417, Keithley Instruments, Inc.) which had a current suppressor to substract out the background signal. The signal was then routed through an analog device whose schematic is shown in Figure 2. The analog device carried out the calculations indicated in Equation 4, taking into account the weight of the sample, the time constant, S_1/V_1, for the vacuum system, and displayed the total amount of hydrogen evolved from the specimen in weight parts per million as a function

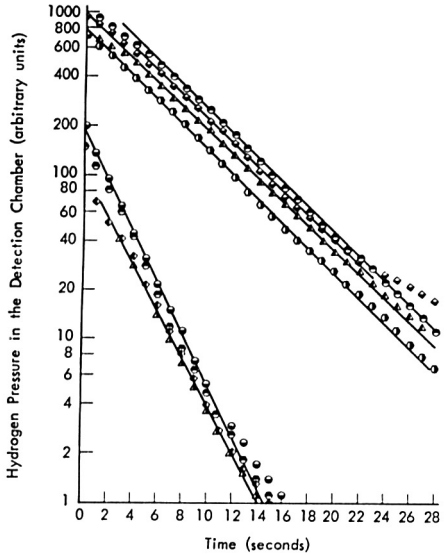

Figure 3. Pump-down curves for hydrogen through two different orifices in the hydrogen analyzer

Orifice 1	Orifice 2
◓ S/V = 0.172 sec^{-1}	◒ S/V = 0.349 sec^{-1}
▲ S/V = 0.169 sec^{-1}	Δ S/V = 0.342 sec^{-1}
◇ S/V = 0.170 sec^{-1}	◇ S/V = 0.316 sec^{-1}
○ S/V = 0.174 sec^{-1}	○ S/V = 0.338 sec^{-1}
S/V av = 0.171 sec^{-1}	S/V av = 0.336 sec^{-1}
σ = 0.002 or 1.3%	σ = 0.014 or 4.2%

of time on a strip-chart recorder. A two-channel (Brush 220, Gould Brush, Inc.) recorder was used.

The second channel was used to display the mass spectrometer output which was approximately the hydrogen evolution rate from the sample. The analogue device had three variables that could be programmed. Two of the variables were N and (S_1/V_1) found in Equation 4. The third variable was a scaler for the weight of the sample to give direct readout in wppm. The value of N and (S_1/V_1) was determined by expanding a known amount of hydrogen from a "trapping" volume. A calibrated, "trapping" volume was attached to the furnace chamber through an all-metal, bellows-type valve (Nupro SS-4H-SW, The Nupro Company). A second valve (Nupro SS-4H-SW) connected this volume to a hydrogen source and a quartz Borden Gauge (Texas Instrument). Absolute pressure measurements in the range of 1.00 torr to 50.0 torr could be made with 1% accuracy. The Oak Ridge Y-12 Plant Standards Laboratory determined the "trapping" volume to be 2.10 ± 0.05 cm^3. This calibration was traceable to the National Bureau of Standards.

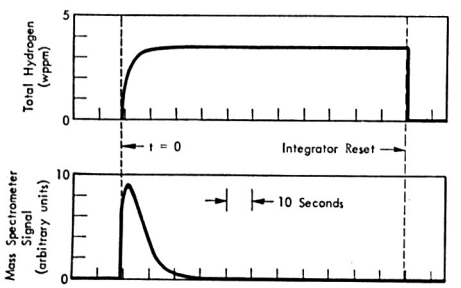

Figure 4. Typical calibration measurement

(Trapping volume pressure, 15.6 torr, *i.e.*, 3.5 μg; assumed sample weight, 1.00 gram)

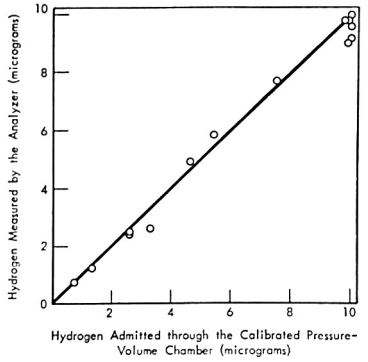

Figure 5. Experimental determination of accuracy of the hydrogen analyzer

RESULTS AND DISCUSSION

The S_1/V_1 term could be evaluated experimentally from the pumpdown rate. Typical pumpdown curves determined by this method can be seen in Figure 3, showing S_1/V_1 values of 0.34 ± 0.02 sec^{-1} and 0.171 ± 0.002 sec^{-1} for two different orifices. After the value of S_1/V_1 was programmed into the analog device, the value of N was determined by adjusting the analog device to read directly on the recorder the amount of hydrogen in wppm released from the trapping volume for an assumed sample weight. Figure 4 shows typical results of the calibration procedure. Before each analysis the base pressure correction was adjusted until the analog device drifted at a rate of less than 0.001 wppm per minute. Repeated calibrations of the system over a large range (Figure 5) confirm that the precision was better than 10%. A typical hydrogen analysis of a 0.50-gram uranium cube containing 2.5 wppm hydrogen is given in Figure 6.

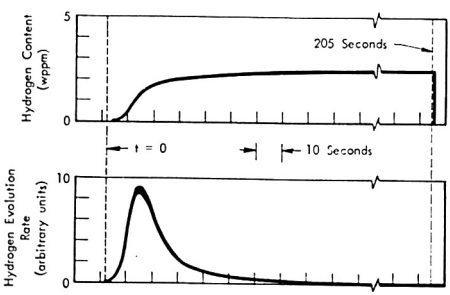

Figure 6. Hydrogen analysis of a 0.4-gram uranium specimen

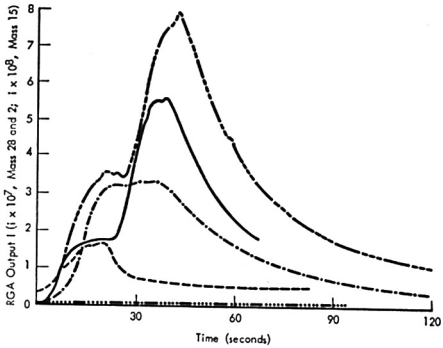

Figure 7. Gaseous evolution observed on the RGA for uranium alloy rods

Mass 2 (without trap)
Mass 2 (with trap)
Mass 15 (without trap)
Mass 28 (without trap)
Mass 18 (no increase without trap)

Another factor taken into account is the formation of hydrogen by the reaction of the hot metal with the residual water or hydrocarbon vapor pressure. At the high temperature of extraction, the interdiffusion of metal and metal oxide could be very rapid and therefore affords exposure of free metal atoms at the sample surface to react rapidly with the water vapor to produce hydrogen. Since it was convenient in many cases to run the system at 10^{-6} or 10^{-7} Torr rather than ultrahigh vacuum, the production of hydrogen from this reaction for an extraction of a 1-gram sample for a 1-hour duration would be nearly 2×10^{-6} mole which corresponds to a determinate error of +4 ppm. The problem was effectively eliminated by exposing the extraction chamber to a liquid nitrogen cold finger with a pumping speed 1000 times greater than the orifice. This reduced the above error to ±0.004 ppm.

The liquid nitrogen trap in the extraction chamber was a re-entrant dewar with approximately a ten-square-inch cold area exposed to the vacuum. With a background pressure of 10^{-6} Torr the analyzer without the trap cooled yielded an answer that was at least twice as high as it should have been for 32 wppm Ti standards. Even with a low background pressure of 10^{-8} Torr or better a high answer was obtained. The size of the error was, of course, a function of the metals analyzed and the speed by which the surface was poisoned; it was best, however, to eliminate the error by use of the cold trap.

Another error which may arise is from the cracking patterns of low molecular weight hydrocarbons. The origin of these hydrocarbons is probably from specimen handling and should, therefore, not be counted as part of the hydrogen content. Figure 7 presents the time dependence of masses 2 (hydrogen), 15 (methane and other hydrocarbons), 18 (water), and 28 (CO, N_2, and hydrocarbons) for some uranium alloy rods of nearly identical weight and treatment which were dropped in the hot zone without the liquid nitrogen dewar cooled. An overnight pumpdown of the system was used in an effort to remove surface water. Another trace of mass 2 was made with the re-entrant dewar cooled showing a marked decrease in the first hydrogen peak. The difference could be accounted for by the assumption that it was the mass 2 fragment from

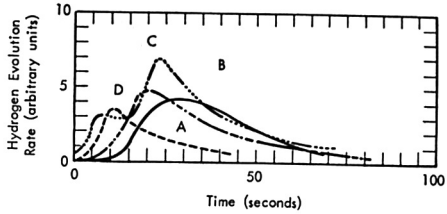

Figure 8. Effect of various treatments on hydrogen content and distribution in a uranium alloy (all samples were 0.50-gram cubes)

A. ——— Machined uranium alloy (32 wppm hydrogen) (attenuated ×20)
B. – – – – Machined uranium alloy (1.76 wppm hydrogen)
C. — · — · — Machined uranium alloy etched with 10% aqueous HNO_3 for 10 min (2.2 wppm hydrogen)
D. – – – – – Machined uranium alloy high vacuum degassed at 1000 °C and water quenched (0.82 wppm hydrogen)

Table I. Typical Set of Hydrogen Analyses as Run

Specimen	Specimen description	Specimen weight, grams	Hydrogen content total, wppm
1	5.0 μg H_2 gas (47 torr cc)	1.000[a]	5.1
2	5.0 μg H_2 gas (47 torr cc)	1.000[a]	4.8
3	5.0 μg H_2 gas (47 torr cc)	1.000[a]	5.1
4	Titanium NBS Standards Rated, 32 wppm	0.054[b]	35
5	Titanium NBS Standards Rated, 98 wppm	0.047[b]	98
6	Uranium Alloy No. 1	0.378[b]	2.7
7	Uranium Alloy No. 2	0.091[b]	42
8	Uranium Alloy No. 1	0.435[b]	1.9
9	Uranium Alloy No. 2	0.098[b]	44
10	Titanium NBS Standards Rated, 32 wppm	0.050[b]	41
11	Titanium NBS Standards Rated, 98 wppm	0.036[b]	107

[a] Assumed.
[b] Extraction temperature 1000 °C.

hydrocarbons. With liquid nitrogen dewar pumping, no increase was observed for masses 15, 18, and 28. Without the trap, no water evolution was observed indicating that the overnight high-vacuum pumpdown was sufficient to remove superficial water from the sample surfaces.

As can be seen from Equation 4, a time plot of i was very nearly proportional to a time plot of the instantaneous gas evolution (dn/dt) from the sample. Given a sufficiently high pumping speed from the furnace chamber, these plots would be proportional. In practice, the only place where i (or H_2 pressure in the detection chamber) and dn/dt differ significantly was where the pressure was changing rapidly. Since the plot of i was generally used to qualitatively evaluate the distribution of hydrogen in the sample, this difference between i and dn/dt was of little consequence. When a rigorous curve shape analysis of i was used to determine diffusion coefficients and activation energies, the mass spectrometer output (i) was taken digitally and corrected to dn/dt by computer. Figure 8 demonstrates the effect of sample history on the rate that hydrogen was evolved from the furnace chamber. Hydrogen generated by surface effects significantly contributed to the total amount of hydrogen determined for a specimen containing less than 10 wppm hydrogen.

Table II. Hydrogen Determinations in wppm for Uranium and Uranium Alloy Specimens[a]

Specimen	Sample[b] 1	2	3	4
Uranium-1[c]	1.6	2.3	1.5	...
Uranium-2[c]	2.5	2.5	2.2	...
Uranium Alloy-1[d]	33	31	30	33
Uranium Alloy-2[d]	32	28	28	27
Uranium Alloy-3[d]	2.3	2.0	2.4	2.0
Uranium Alloy-4[d]	3.0	2.9	2.4	2.2

[a] Extraction temperature 1000 °C.
[b] Each sample was cut from an adjacent position along a 1/8-inch by 1/8-inch rod.
[c] Uranium specimens were from different billets of high-purity derby uranium.
[d] Uranium alloy specimens were from different batches of similar materials except uranium alloys 3 and 4 had been vacuum-heat treated.

Some hydrogen determinations for titanium, uranium, and uranium alloys were performed. Tables I and II demonstrate the precision of the instrument when used as a routine analytical device. During these analyses, the samples were degreased in acetone, and the samples were allowed to accumulate in the furnace chamber until all eight samples were analyzed. Samples from a given specimen were analyzed on two different days in order to demonstrate the stability of the instrument.

CONCLUSIONS

The instrument described in this article has been satisfactory for the determination of hydrogen in metals over the concentration range from 0.01 wppm to 100 wppm with a precision of 10%. Diffusion parameters, surface reactions, and the distribution of hydrogen in the sample can be evaluated using the hydrogen evolution rate data and the thermal history of the sample after it is dropped into the furnace.

Micromole quantities of other gases can also be determined; thus, the instrument can be used to study a great variety of thermally activated gas evolution processes.

RECEIVED for review March 16, 1971. Accepted June 7, 1971. Work performed at Oak Ridge Y-12 Plant under contract W-7405-eng-26 with the U. S. Atomic Energy Commission.

Effect of Atmosphere on Spectral Emission from Plasmas Generated by the Laser Microprobe

William J. Treytl, Kenneth W. Marich, James B. Orenberg, Peter W. Carr,[1] D. Craig Miller, and David Glick
Division of Histochemistry, Department of Pathology, Stanford University School of Medicine, Stanford, Calif. 94305

The effects of various atmospheres on laser-induced optical emission of plasmas from solid samples have been investigated. Atmospheres of argon, air, oxygen, nitrogen, helium, and also vacuum, were used. Samples of iron in steel and in iron oxide-coated tape, and of magnesium in aluminum foil, human serum, and liver were employed. Laser energies of approximately 1.2, 3.6, and 8.0 mJ were used. Signal-to-background ratios were not found to vary systematically with atmosphere and laser energy, but significantly larger values occurred in vacuum at 1.6-mJ laser energy. Signal intensities were greater in denser atmospheres at 3.6 and 8 mJ, but approximately the same at 1.2 mJ. Signal intensities varied directly with these laser energies, except in vacuum where the signal was independent of laser energy. Metallic and nonmetallic targets behaved similarly.

SINCE THE INNOVATIONS in laser microprobe instrumentation reported by Peppers *et al.* (*1*), efforts have been directed to optimization of conditions for analysis of elements. The effect of composition of the sample on the laser-induced emission signal has been studied (*2*). The present investigation concerns the effects of various atmospheres on signal intensity from laser-generated plasmas.

Effects on emission spectra of atmospheres in which plasmas are generated by a dc arc have been reported (*3–7*). Vallee (*3, 4*) demonstrated that an argon-atmosphere enhanced spectral line emission without significantly increasing the background. In contrast, increased signal-to-noise ratio was achieved with helium by suppression of the background (*3*). Undesirable cyanogen bands were reduced by use of noble gases. Rates of volatilization of elements in a sample varied with the composition of the atmosphere. Vallee (*3*) concluded that, for particular metals, certain atmospheres could be used to enhance the sensitivity of analysis.

The use of inert gases with the Stallwood jet increased signals, diminished background, reduced selective volatilization, and produced a more stable dc arc (*8*). Stabilization of the ac arc was also achieved by Sukhnevich (*9*) with inert gases.

More recently, use of controlled atmospheres in spark excitation showed improved precision and accuracy, higher sensitivity, and reduced inter-element effects (*10, 11*).

[1] Present address, Department of Chemistry, University of Georgia, Athens, Ga. 30601

(1) N. A. Peppers, E. J. Scribner, L. E. Alterton, R. C. Honey, E. S. Beatrice, I. Harding-Barlow, R. C. Rosan, and D. Glick, ANAL. CHEM., **40**, 1178 (1968).
(2) K. W. Marich, P. W. Carr, W. J. Treytl, and D. Glick, *ibid.*, **42**, 1775 (1970).
(3) B. L. Vallee, C. B. Reimer, and J. R. Loofbourow, *J. Opt. Soc. Amer.*, **40**, 751 (1950).
(4) B. L. Vallee and S. J. Adelstein, *ibid.*, **42**, 295 (1952).
(5) B. L. Vallee and S. J. Adelstein, *Spectrochim. Acta*, **6**, 134 (1954).
(6) Z. L. Szabo and I. Toth, *Magy. Kem. Foly.*, **74**, 394 (1968).
(7) C. K. Matocha and J. Petit, *Appl. Spectrosc.*, **22**, 562 (1968).
(8) A. J. Mitteldorf, "Trace Analysis: Physical Methods," G. H. Morrison, Ed., Interscience Publishers, New York, N. Y., 1965, p 200.
(9) V. S. Sukhnevich, *Z. Prikl. Spektrosk.*, **9**, 199 (1968).
(10) R. R. Boyd and A. Goldblatt, *Appl. Spectrosc.*, **19**, 22 (1965).
(11) J. Kashima and M. Kubota, *Rep. Cast. Res. Lab., Waseda Univ.*, **1967**, No. 18, pp 9–19.

Buravlev (*12*) observed a strong dependence of sampling rate on the arc discharge atmosphere, and greater reproducibility of the effect of sample matrix in noble gas atmospheres.

Laser-induced plasmas and the effects of ambient conditions on them have been studied extensively. Minck (*13*) measured gas breakdown thresholds in air, argon, helium, hydrogen, and neon at various pressures. Browne (*14*) explained this breakdown as an inverse bremsstrahlung process triggered by an unspecified multiphoton interaction. Daibler and Winans (*15*) studied the laser-induced emission spectrum of nitrogen and argon, and Litvak and Edwards (*16*) observed emission from hydrogen in the vicinity of the 6563 Å Balmer line. Both groups observed intense continuous emission from the central portion of the plasma and considerable Stark broadening of the lines.

The nature of the interaction of focused laser radiation with solid materials and their resulting vapor plasmas have also been investigated. These studies, however, have been primarily concerned with the physics of rapid absorption of laser energy in condensed media (*17–20*), thermal distribution and equilibration at the surface (*19*, *21–24*), and the equations of state of the gas dynamics which describe the evolution, expansion, and properties of the plasmas generated by the ejection of atoms, ions, and electrons from the target (*17–19*, *21*, *25*).

While the formation of plasmas by focused laser beams has been studied, the effects of ambient atmospheres on the optical emission properties of these plasmas have not been investigated from an analytical standpoint. In the present work the effects of atmospheres of argon, helium, nitrogen, oxygen, and air, and partial vacuum on optical emission from laser-induced plasmas, as a function of three laser energy densities were investigated. Metallic, nonmetallic, and biological samples were employed.

EXPERIMENTAL

Apparatus. The laser microprobe assembly, the spectrograph, and the photoelectric detection system employed in this study were described in detail in previous publications (*1*, *2*, *26*). The widths of the entrance and exit slits on the spectrograph were 50 microns. Oscilloscope tracings of the photomultiplier anode signals were photographed with a Polaroid camera mounted on a Tektronix (No. 454) oscilloscope.

The 3020 and 2802 Å lines of iron and magnesium, respectively, were chosen for the present work because of their relatively high intensities and lack of interference from other lines in the emission spectra from laser-induced plasmas. Iron and magnesium hollow cathode lamps (Perkin-Elmer) were used for spectral alignment.

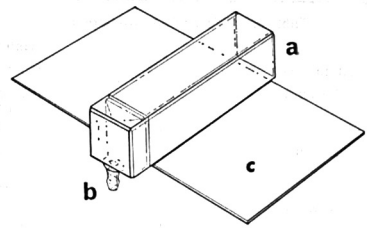

Figure 1. Evacuable glass cuvette (12.5 × 12.5 × 45 mm) with (*a*) open end facing spectrograph, (*b*) gas inlet tube, and (*c*) plastic support slide

The atmosphere chamber consisted of a removable quartz window on an evacuable glass cuvette (Flow Cell No. 480, Scientific Cell Co., Forest Hills, Long Island, N. Y.) fastened to a plastic slide with expoxy cement (Figure 1). High-vacuum silicone grease was applied to the ground edges of the cuvette at its open end and the quartz window was firmly sealed to the opening by application of vacuum (~5 Torr)

Materials. The argon, helium, nitrogen, and oxygen gases used were USP grade. The gas was passed through a column of Drierite before entering the chamber. The iron samples used were from a block of NBS (No. 462) standard steel and Memorex (MRX-3) magnetic tape. The tape was composed of a ferric oxide coating, 10 microns thick, deposited on a polyester backing, 38 microns thick. Heavy duty aluminum foil, human serum and liver were used for the magnesium samples.

Procedure. Alignment of spectral lines was performed by centering lines from the hollow cathode lamps in the slits in front of the photomultiplier tubes by rotation of the spectrograph grating. The sample was placed in the cuvette near the opening and then the quartz window was mounted. The chamber was evacuated, checked for leaks with a manometer, and then gas was introduced. After each laser discharge, the chamber was evacuated before it was refilled with a fresh atmosphere to prevent the previous atmosphere from influencing the spectral emission of the succeeding sample. Light from the laser-induced plasma was focused on the slit of the spectrograph by a quartz lens as previously described (*1*).

Samples of 40 nl of serum were deposited on plastic cover slips with a precision pipetting device (Oliver Instrument Company, Sunnyvale, Calif.) employing a 1-μl Hamilton syringe and air-dried as reported earlier (*2*). Five-micron thick sections of formalin-fixed, paraffin-embedded, deparaffinized liver tissue were mounted on plastic slides.

RESULTS AND DISCUSSION

The integrated optical emission data from the steel and iron oxide samples are given in Tables I and II. In general, the signal intensities showed a marked dependence on incident laser energy and atmosphere conditions, the strongest signals being produced in argon at high laser energies. Signal-to-background ratios (S/B) did not exhibit systematic trends. The exception occurred in vacuum where the S/B varied inversely with laser energy, an approximately fourfold increase being obtained at 1.2 mJ, although the signal intensity did not vary regularly. A small laser energy independent increase in S/B was found for steel in argon. These observa-

(12) Yu M. Buravlev, *Zh. Prikl. Spektrosk.*, **6**, 583 (1967).
(13) R. W. Minck, *J. Appl. Phys.*, **35**, 252 (1964).
(14) P. F. Browne, *Proc. Phys. Soc.*, **86**, 1323 (1965).
(15) J. W. Daibler and J. G. Winans, *J. Opt. Soc. Amer.*, **58**, 76 (1968).
(16) M. M. Litvak and D. F. Edwards, *IEEE J. Quantum Electron.*, **QE-2**, 486 (1966).
(17) J. F. Ready, *J. Appl. Phys.*, **36**, 462 (1965).
(18) H. Klocke, *Spectrochim. Acta*, **24B**, 263 (1969).
(19) A. Caruso, B. Bertotti, and P. Guipponi, *Nuovo Cimento*, **45B**, 176 (1966).
(20) W. G. Griffin and J. Schluter, *Phys. Lett.*, **26A**, 241 (1968).
(21) Yu V. Afans'ev and O. N. Krokhin, *JETP*, **25**, 639 (1967); **52**, 966 (1967).
(22) J. M. Baldwin, *Appl. Spectrosc.*, **24**, 429 (1970).
(23) V. P. Veiko, Ya. A. Imas, A. N. Kokora, and M. N. Libenson, *Soc. Phys. Tech. Phys.*, **12**, 1410 (1968).
(24) S. Namba, P. H. Kim, S. Nakayama, and I. Ida, *Jap. J. Appl. Phys.*, **4**, 153 (1965).
(25) N. G. Basov, V. A. Boiko, V. A. Dement'ev., O. N. Krohkin, and G. V. Sklizko, *JETP*, **24**, 659 (1967); **51**, 989 (1966).
(26) E. S. Beatrice and D. Glick, *Appl. Spectrosc.*, **23**, 260 (1969).

Table I. Effect of Atmosphere and Laser Energy on Laser-Induced Optical Emission from Iron in Steel[a]

(Integrated Photoelectric Data)

Atmosphere	N[b]	Laser energy, mJ	Signal[c]	S/B[d]
Vacuum	14	1.05 ± 0.06	5.99 ± 0.56	18.5 ± 3.9
	10	3.63 ± 0.26	10.3 ± 0.4	8.07 ± 1.14
	10	8.09 ± 0.86	6.83 ± 0.33	4.79 ± 0.64
Helium	11	1.27 ± 0.06	11.1 ± 1.3	5.77 ± 1.13
	12	4.38 ± 0.47	45.7 ± 4.4	4.67 ± 0.80
	10	9.09 ± 0.56	102 ± 9	4.19 ± 0.53
Nitrogen	11	1.19 ± 0.06	15.4 ± 1.6	5.60 ± 0.77
	12	4.33 ± 0.42	103 ± 14	6.69 ± 1.49
	10	8.48 ± 0.68	230 ± 40	6.89 ± 0.74
Air	10	1.12 ± 0.06	16.2 ± 1.9	5.39 ± 1.06
	10	3.96 ± 0.20	137 ± 19	7.92 ± 1.32
	10	8.86 ± 0.46	182 ± 25	7.12 ± 1.10
Oxygen	13	1.57 ± 0.05	24.9 ± 3.4	5.41 ± 1.00
	11	4.82 ± 0.16	109 ± 16	5.79 ± 0.98
	12	7.86 ± 0.72	244 ± 40	7.25 ± 1.54
Argon	11	1.15 ± 0.07	57.6 ± 7.7	11.5 ± 2.1
	13	4.01 ± 0.20	276 ± 48	9.7 ± 3.5
	11	7.63 ± 0.61	608 ± 49	10.8 ± 1.4

[a] National Bureau of Standards (NBS No. 462).
[b] Number of laser shots.
[c] Background-corrected, arbitrary units, ± std dev.
[d] Signal-to-background ratio, ± std dev.

Table II. Effect of Atmosphere and Laser Energy on Laser-Induced Optical Emission from Iron in Magnetic Tape[a]

(Integrated Photoelectric Data)

Atmosphere	N[b]	Laser energy, mJ	Signal[c]	S/B[d]
Vacuum	12	1.39 ± 0.10	5.22 ± 0.31	20.5 ± 4.4
	12	3.89 ± 0.33	9.30 ± 0.69	9.20 ± 1.36
	13	8.40 ± 1.44	9.70 ± 1.01	5.34 ± 1.20
Helium	12	1.28 ± 0.08	8.12 ± 1.07	4.99 ± 0.94
	11	3.84 ± 0.25	35.8 ± 3.1	4.36 ± 1.81
	12	8.17 ± 1.17	67.9 ± 6.8	4.85 ± 2.95
Nitrogen	12	1.13 ± 0.09	3.04 ± 0.77	3.69 ± 1.28
	11	3.75 ± 0.22	28.5 ± 2.2	3.43 ± 0.63
	11	7.86 ± 0.31	76.1 ± 9.0	4.07 ± 0.66
Air	11	1.16 ± 0.09	5.05 ± 1.05	3.53 ± 1.05
	10	3.89 ± 0.24	42.7 ± 8.3	4.20 ± 1.10
	10	7.47 ± 0.34	86.6 ± 12.2	4.39 ± 0.84
Oxygen	11	1.06 ± 0.05	4.45 ± 0.89	3.17 ± 1.06
	10	3.62 ± 0.21	43.3 ± 6.2	4.14 ± 0.71
	10	7.78 ± 0.28	96.8 ± 7.3	4.40 ± 0.52
Argon	10	1.21 ± 0.09	12.9 ± 1.9	4.45 ± 0.85
	10	3.93 ± 0.19	105 ± 12	4.72 ± 0.62
	10	7.94 ± 0.15	229 ± 23	4.42 ± 0.54

[a] Memorex (MRX-3) (Memorex Corp., Santa Clara, Calif.).
[b] Number of laser shots.
[c] Background-corrected, arbitrary units, ± std dev.
[d] Signal-to-background ratio, ± std dev.

tions are quite different from those reported in dc arc studies (*3*, *4*). Under the conditions giving the highest S/B values (vacuum, 1.2 mJ laser energy), the actual signals were reduced by a factor of 100 (steel) and 50 (iron oxide) from the largest signals observed (argon, 8 mJ).

A typical oscillograph of direct photomultiplier anode pulses is shown in Figure 2. In the signal channel trace, the rapid continuum portion (prepulse), and the longer discrete signal pulse are clearly discernible. The background channel trace shows only the prepulse. Measurements from oscillographs for the steel and iron oxide tape samples are shown in Tables III and IV, respectively. Inherent imprecision of measuring the parameters from the oscillographs gives semiquantitative results.

The most striking feature of the oscillographic data was the enhanced amplitude of signal pulses obtained in helium atmospheres, approximately twice those of corresponding pulses in other atmospheres. No systematic differences were observed in signal pulse duration for air, oxygen, and nitrogen, but argon generally supported longer pulses and helium shorter ones. Plasmas produced in vacuum were both shorter and less intense, except at the lowest laser energy. Tables I–IV reveal that signal intensities at 1.2 mJ were less sensitive to changes in atmosphere than at higher laser energies.

The enhanced signal and S/B values obtained in argon from iron in steel, relative to iron in iron oxide, indicate a possible effect of metallic *vs.* nonmetallic matrices. The emission of

Table III. Effect of Atmosphere and Laser Energy on Laser-Induced Optical Emission from Iron in NBS Steel (Oscillographic Data)

Laser energy[a], mJ	Atmosphere	Signal height, mA	Signal ½ BW, μsec[b]	Prepulse height, mA	Prepulse ½ BW, μsec[b]	Signal area[c]	Prepulse area[c]	S/B[d]
1.21 ± 0.15	Vacuum	43.3	0.23	17.2	0.03	9.97	0.70	14.2
	Helium	59.2	0.34	52.5	0.03	20.1	2.25	8.92
	Nitrogen	23.3	0.34	24.2	0.03	7.93	1.20	6.61
	Air	41.7	0.40	60.4	0.05	16.7	2.37	7.04
	Oxygen	37.5	0.35	43.1	0.03	13.1	1.67	7.87
	Argon	41.7	0.58	60.4	0.03	24.2	1.33	18.2
4.00 ± 0.35	Vacuum	49.3	0.30	58.3	0.04	14.8	1.73	8.54
	Helium	176	0.44	243	0.05	77.4	8.27	9.36
	Nitrogen	76.0	0.75	145	0.04	57.0	6.59	8.65
	Air	67.7	0.90	257	0.06	79.0	11.7	6.73
	Oxygen	79.0	0.70	182	0.03	55.3	4.85	11.4
	Argon	117	1.10	260	0.04	129	6.73	19.1
8.14 ± 0.49	Vacuum	64.2	0.28	106	0.05	18.0	4.71	3.82
	Helium	304	0.58	425	0.06	176	19.6	8.96
	Nitrogen	132	0.75	425	0.03	98.7	17.1	5.76
	Air	132	0.90	700	0.05	118	31.0	3.82
	Oxygen	132	1.00	480	0.03	131	14.1	9.36
	Argon	146	1.35	840	0.05	197	28.6	6.91

[a] Means for 12 samples ± std dev.
[b] Band-width at half-height.
[c] Product of signal height and ½ BW.
[d] Ratio of signal area to prepulse area.

magnesium, present as an impurity in aluminum foil, was measured in different atmospheres (Table V) and exhibited the same trends as iron in steel.

The degree of sample vaporization is largely dependent on the amount of laser energy incident to the sample. A plasma generated by a focused laser beam (*13–16*, *25*, *27–30*) can absorb laser light strongly; e.g. 80% absorption of incident light has been reported (*31*). Acceleration of plasma expansion rates due to additional energy absorption has also been observed (*25*, *27*, *32*). Because of the triggering effect of electrons and ions ejected by a solid target (*13*, *28*, *29*, *33*), atmosphere breakdown occurs at substantially lower laser energy densities than with omission of the target. Large prepulses should indicate strong "shadowing" of the target by the plasma, and therefore reduced laser energy density and direct sampling efficiency. In competition with shadowing, the hot plasma itself can produce more sampling (*34*), and material vaporized into the plasma will share in its energy by elastic and inelastic collisions. Since plasma expansion is sensitive to pressure and density (*29*), expansion against a dense atmosphere could confine the sample vapor and prolong the emission.

Helium has a 21.3 eV metastable state while the other atmospheres have metastable states of ~12 eV. Ion kinetic energies are ~10 eV (*25*, *35*, *36*). This energetic helium level should result in increased sample excitation (*37*). The higher ionization potential could also permit more efficient sampling by the laser beam. The lower density and mass of helium would lead to more rapid plasma expansion. The net result would be a signal with a larger amplitude but shorter duration as shown by the iron-in-helium data Tables III and IV. The inverse applies to the iron-in-argon data while the other atmospheres give intermediate results. Although it is difficult to explain the relative invariance of signal intensity with changing laser energy in vacuum (Tables I–IV), a rapid plasma expansion against the vacuum could be responsible. The interactions in laser-generated plasmas are complex, and the data are not sufficient to permit exhaustive or rigorous theoretical interpretation.

Magnesium emission from human serum and liver tissue

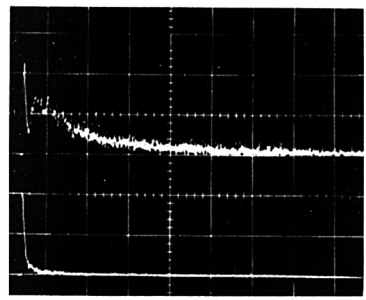

Figure 2. Typical photomultiplier anode pulses

Upper trace is signal channel at 3020 Å and lower trace is background channel at 3015 Å. Horizontal scale 1 μsec/div, vertical scale 4 mA/div. Conditions: iron in NBS steel sample, air atmosphere, 4.0 mJ laser energy

(27) E. Archbald, D. W. Harper, and T. P. Hughes, *Brit. J. Appl. Phys.*, **15,** 1321 (1964).
(28) V. V. Korobkin, S. L. Mandel'shtam, P. P. Poshkin, A. V. Prokhindeev, A. M. Prokhovrov, N. K. Sukhodrev, and N. Ya Shchlev, *JETP*, **26,** 78 (1968).
(29) Yu V. Afans'ev and O. N. Krokhin, *ibid.*, **25,** 639 (1967).
(30) E. Piepmeier and H. Malmstadt, ANAL. CHEM., **41,** 700 (1969).
(31) P. Nelson, P. Veyrie, M. Berry, and Y. Durand, *Phys. Lett.*, **13,** 226 (1964).
(32) H. Weichel and P. V. Avizonis, *Appl. Phys. Lett.*, **9,** 334 (1966).
(33) E. Bernal G., J. F. Ready, and L. P. Levine, *IEEE J. Quantum Electron.*, **QE-2,** 480 (1966).
(34) A. W. Ehler, *J. Appl. Phys.*, **37,** 4962 (1966).
(35) E. W. Sucov, J. L. Pack, A. V. Phelps, and A. G. Engelhardt, *Phys. Fluids*, **10,** 2035 (1967).
(36) D. W. Koopman, *ibid.*, p 2091.
(37) H. E. Taylor, J. H. Gibson, and R. K. Skogerboe, ANAL. CHEM., **42,** 1569 (1970).

Table IV. Effect of Atmosphere and Laser Energy on Laser-Induced Optical Emission from Iron in Memorex Magnetic Tape

(Oscillographic Data)

Laser energy,[a] mJ	Atmosphere	Signal height, mA	Signal ½ BW, μsec[b]	Prepulse height, mA	Prepulse ½ BW, μsec[b]	Signal area[c]	Prepulse area[c]	S/B[d]
1.21 ± 0.15	Vacuum	37.5	0.22	4.97	0.04	8.25	0.75	11.0
	Helium	60.6	0.23	35.0	0.03	13.9	1.27	11.0
	Nitrogen	29.2	0.20	43.1	0.03	5.83	1.12	5.19
	Air	29.2	0.20	31.1	0.04	5.83	1.03	5.65
	Oxygen	41.7	0.30	34.5	0.03	12.5	1.67	7.50
	Argon	29.2	0.28	25.9	0.04	8.17	1.08	7.54
4.00 ± 0.35	Vacuum	56.3	0.26	37.9	0.04	14.6	2.25	6.50
	Helium	199	0.44	164	0.04	87.7	4.22	20.8
	Nitrogen	91.4	0.50	195	0.03	45.7	4.39	10.4
	Air	102	0.56	242	0.04	57.3	6.43	8.91
	Oxygen	102	0.60	274	0.02	61.4	8.80	6.98
	Argon	102	0.56	153	0.06	57.3	6.43	8.91
8.14 ± 0.49	Vacuum	64.2	0.20	57.6	0.04	12.8	3.25	3.95
	Helium	235	0.54	231	0.05	127	8.80	14.4
	Nitrogen	133	0.70	623	0.03	93.0	4.98	18.7
	Air	150	0.70	276	0.03	105	17.8	5.87
	Oxygen	99.7	0.86	467	0.04	85.7	15.0	5.70
	Argon	188	1.00	646	0.04	188	27.1	6.94

[a] Means for 12 samples ± std dev.
[b] Band-width at half-height.
[c] Product of signal height and ½ BW.
[d] Ratio of signal area to prepulse area.

Table V. Effect of Atmosphere on Laser-Induced[a] Optical Emission from Magnesium in Aluminum Foil[b] and Correlation with Iron Samples

(Integrated Photoelectric Data)

Atmosphere	Signal[c]	S/B[d]	R_1[e]	R_2[f]
Vacuum	51 ± 12	1.1 ± 0.3	7.3 ± 2.2	8.4 ± 2.6
Air	720 ± 140	1.3 ± 0.3	6.1 ± 1.7	3.2 ± 1.0
Argon	1070 ± 180	1.3 ± 0.3	7.5 ± 3.0	3.6 ± 0.9

[a] Laser energy = 3.6 ± 0.2 mJ.
[b] Alcoa Wrap, Aluminum Co. of America, New Kensington, Pa.
[c] Mean for 10 samples ± std dev.
[d] Signal-to-background ratio, ± std dev.
[e] R_1 = (S/B) Fe Steel/(S/B) Mg, ± std dev.
[f] R_2 = (S/B) Fe Tape/(S/B) Mg, ± std dev.

Table VI. Effect of Atmosphere on Laser-Induced[a] Optical Emission from Magnesium in Serum and Liver

(Integrated Photoelectric Data)

	Signal		S/B[d]	
Atmosphere	Serum[b]	Liver[c]	Serum	Liver
Vacuum	4.5 ± 1.3	1.6 ± 0.3	2.3 ± 1.0	5.7 ± 1.9
Air	20.3 ± 2.8	10.5 ± 1.6	1.8 ± 0.5	3.7 ± 1.0
Argon	34.1 ± 7.6	36.2 ± 7.9	1.1 ± 0.4	4.2 ± 1.1

[a] Laser energy = 3.6 ± 0.2 mJ.
[b] Human blood serum; air dried 40-nl samples, (approx. 400 μ dia.) mean for 10 samples ± std dev.
[c] Formalin-fixed, paraffin-embedded, and deparaffinized tissue sections, 5 μ thick.
[d] Signal-to-background ratio, ± std dev.

samples (Table VI) was measured for comparison with magnesium in a metallic matrix, aluminum foil. The data show that in the different atmospheres, the serum and aluminum foil exhibited a similar trend of S/B, while liver and aluminum matrices did not. A possible matrix effect (*2*) due to differences in sample structure and composition between liver and serum may be indicated by the significantly lower background intensities observed in liver.

At 1.2-mJ laser energy, significant enhancement of S/B was obtained in a 5-Torr vacuum with little loss of signal intensity. At higher laser energies, S/B values behaved irregularly with atmosphere variation. Argon gave appreciably higher signals while vacuum conditions yielded reduced signals. The results suggest that it may be advantageous in certain cases to select an appropriate atmosphere in order to optimize S/B or signal intensity, but in general the atmosphere composition did not appear to affect the S/B sufficiently to warrant changing to atmospheres other than air in time-integrated laser microprobe emission spectrometry.

RECEIVED for review March 29, 1971. Accepted June 7, 1971. Studies in Histochemistry, No. CXIV. Supported by Grants GM 16181, GM 09227, HE 06716, and 5K6AM18513 (to D. G.), from the National Institutes of Health, U. S. Public Health Service.

Improved Enzyme Electrode for Amygdalin

R. A. Llenado and G. A. Rechnitz

Department of Chemistry, State University of New York, Buffalo, N. Y. 14214

An enzyme electrode for amygdalin is constructed by immobilizing β-glucosidase in a polymer gel layer coupled to a cyanide-sensing membrane electrode. The characteristics of a novel inverted electrode configuration are shown to be superior to earlier designs and to permit analyses of samples as small as 0.2 ml. Optimum operating conditions for the enzyme electrode system are described.

THE ARRAY of useful ion-selective membrane electrodes and their applications continues to multiply (*1–3*). Recently the use of biological materials in membrane electrodes has resulted in the development of the valinomycin-based potassium electrode (*4–6*) and enzyme electrodes for urea (*7*) and for amino acids (*8*).

In a recent preliminary communication (*9*), we reported a new kind of enzyme electrode made by coupling the enzyme β-glucosidase to a cyanide-responsive membrane electrode. This novel electrode, responsive to amygdalin, is the first successful example of a potentiometric enzyme electrode utilizing a nonglass membrane and will find applications in agricultural chemistry and plant biochemistry.

The electrode is prepared by mechanically coupling a thin membrane of polyacrylamide gel containing immobilized β-glucosidase with the polycrystalline sensing element of the solid state cyanide electrode. When this electrode system is exposed to aqueous solutions of amygdalin, the immobilized β-glucosidase catalyzes the hydrolysis of amygdalin at the membrane according to

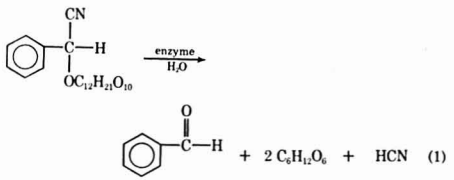

The cyanide ion, produced in stoichiometric proportion to the concentration of amygdalin in the sample solution, gives rise to the potentiometric response of the electrode system. We now report a detailed study of the properties of this enzyme electrode and propose an improved electrode system configuration designed for optimum convenience and utility. It will be seen that the characteristics of the present electrode system are even more attractive than those described in our preliminary report (*3*).

EXPERIMENTAL

Chemicals and Reagents. The enzyme β-glucosidase, emulsin type, prepared from almonds, was obtained from Sigma Chemical Co., St. Louis, Mo. 63118. Its activity was reported as 3.7 units per mg. This enzyme can be stored under refrigeration with little loss of activity.

Solutions of amygdalin (Sigma) were prepared by sequential dilution of a stock solution with borax/NaOH buffer, 0.1*M*, to keep pH and ionic strength constant. Solutions were freshly prepared for each measurement except when used for studying solution aging effects. Solution deterioration can also be minimized by refrigeration.

Polymer solutions with varying percentages of total monomer (5–15%) and cross-linking agent (4–16%) of the total monomer) were made by dissolving appropriate amounts of acrylamide (Eastman) and *N,N'*-methylenebisacrylamide (East man) in deaerated distilled and deionized water. Dissolved oxygen, which inhibits polymerization, was removed by nitrogen bubbling. Potassium persulfate and riboflavin (Eastman) were added as redox catalysts. Polymer solutions are stable when kept in the dark and refrigerated except when the redox catalysts have already been added.

Preparation of the Enzyme Membrane. Normally, 100 mg of β-glucosidase was dissolved per milliliter of polymer solution. The solution was kept in the dark and refrigerated until dissolution of the enzyme was complete. The enzyme–polymer solution was then transferred into a Plexiglas-Teflon (Du Pont) syringe-type chamber (Figure 1*a*) where photopolymerization was carried out (*10–12*) to form the membrane gel.

After photopolymerization, slices of polyacrylamide membranes containing immobilized enzyme are obtained by cutting the material as it is extruded by the Teflon plunger (Figure 1*b*). With practice one can conveniently and uniformly slice membranes having thicknesses as thin as 300 ± 100 μ. No attempts were made to cut with better precision because swelling of the gel contributes significantly to the uncertainty. With 1 ml of polymerized material, one can cut 10–20 slices depending on the thickness desired. The sliced membrane is transferred onto a porcelain spot plate and stored under refrigeration until used (Figure 1*b*).

Preparation of the Enzyme Electrode. A thin enzyme membrane is mechanically coupled to the sensing element of an Orion 94-06 cyanide electrode (Figure 2*a*). The Plexiglas cap serves to hold the enzyme membrane rigidly in place and is also the sample cell for the potentiometric measurement. When properly prepared and preconditioned, the enzyme membrane swells to fit its space snugly and prevents solutions from creeping into the sides of the holder. Silicone oil applied to the body of the electrode facilitates the positioning and removal of the Plexiglas cap. This method of assembly was superior to direct polymerization of the gel on the electrode sensing element as described in our preliminary communication (*9*).

Potentiometric Measurements. Figure 2*b* shows how potentiometric measurements were carried out with the enzyme electrode connected to the imput terminal of a Corning Model 10 pH meter. The reference electrode, Orion 90-01 sleeve type, fits precisely into the assembly to form a solution

(1) G. A. Rechnitz, *Accounts Chem. Res.*, **3**, 69 (1970).
(2) R. A. Durst, Ion Selective Electrodes, NBS Special Publication No. 314, U. S. Government Printing Office, Washington, D. C., 1969.
(3) E. Pungor and K. Toth, *Analyst*, **95**, 625 (1970).
(4) M. S. Frant and J. W. Ross, Jr., *Science*, **167**, 987 (1970).
(5) G. A. Rechnitz, ANAL. CHEM., **41** (12), 109A (1969).
(6) G. A. Rechnitz and M. S. Mohan, *Science*, **168**, 1460 (1970).
(7) G. G. Guilbault and J. G. Montalvo, Jr., *J. Amer. Chem. Soc.*, **92**, 2533 (1970).
(8) G. G. Guilbault and E. Hravankova, ANAL. CHEM., **42**, 1779 (1970).
(9) G. A. Rechnitz and R. A. Llenado, *ibid.*, **43**, 283 (1971).
(10) P. Bernfeld and J. Wan, *Science*, **142**, 678 (1963).
(11) G. Hicks and S. Updike, *Nature*, **214**, 986 (1967).
(12) G. G. Guilbault and J. Das, *Anal. Biochem.*, **33**, 341 (1970).

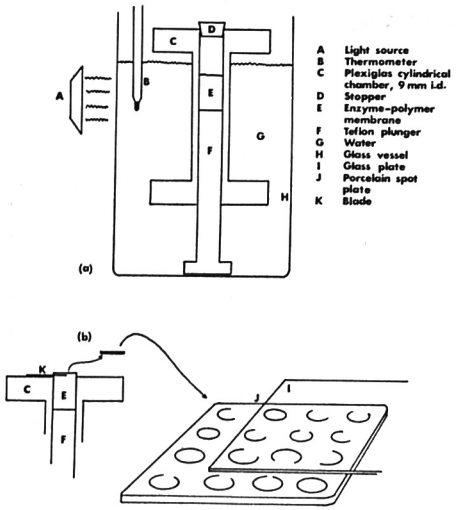

Figure 1. (*a*) **Photopolymerization of enzyme–acrylamide solution**
(*b*) **Slicing of enzyme–polycrylamide membrane**

space requiring as little as 0.20 ml of sample. Millivolt readings are taken at 25 °C with the amygdalin sample solutions preequilibrated at 25.0 ± 0.1 °C in a constant temperature bath. Readings were monitored on a Varicord Model 43 recorder.

RESULTS AND DISCUSSION

Effect of Substrate Concentration. The electrode system senses the cyanide produced at the membrane via the β-glucosidase catalyzed hydrolysis of amygdalin. Because of the stoichiometry of Reaction 1, the potential of the electrode is dependent on the amygdalin concentration.

$$E = E^\circ - 2.3RT/F \log^a CN \quad (2)$$

and

$$E = E^\circ - 2.3RT/F \log[\text{Amygdalin}] \quad (3)$$

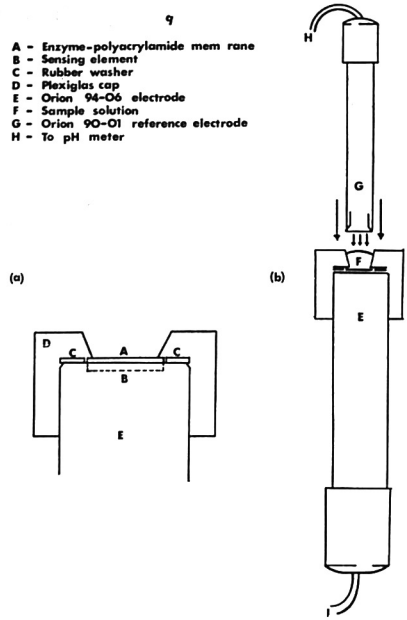

Figure 2. (*a*) **Cross-section of enzyme electrode**
(*b*) **Potentiometric measurement setup**

However, the response is not completely Nernstian, having a slope of 48 mV per decade change of amygdalin concentration at the linear portion of the calibration plot shown in Figure 3. This is so because not all of the cyanide produced reaches the electrode surface. Reasonable reproducibility of potentials is observed as shown in Table I.

Below $10^{-5}M$ amygdalin concentration, enzymatic hydrolysis is extremely slow and the electrode response is too sluggish to be of analytical value. Above $10^{-2}M$, the calibration curve levels off because a steady state is reached and the reaction is zero order with respect to the substrate concen-

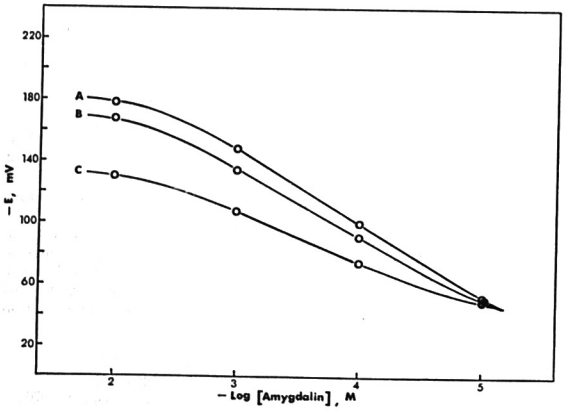

Figure 3. Amygdalin concentration curve

pH 10.4, 25 °C, and 10 mg of enzyme per membrane. Curve (*A*) fresh, (*B*) 3 days old, (*C*) 18 days old

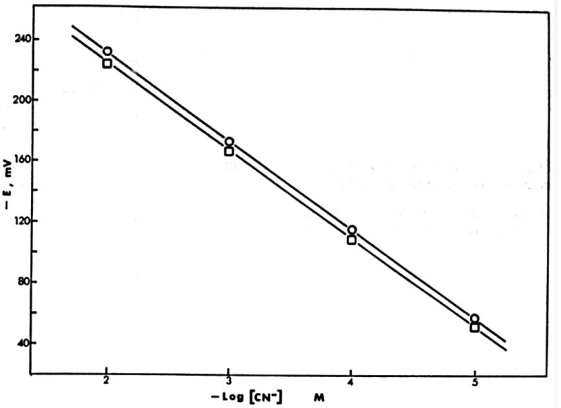

Figure 4. Comparison of Orion 94-06 cyanide electrode response with and without a 600-μ polyacrylamide membrane

All measurements were made at pH 10.4, 25 °C, and ionic strength held constant at 0.1M

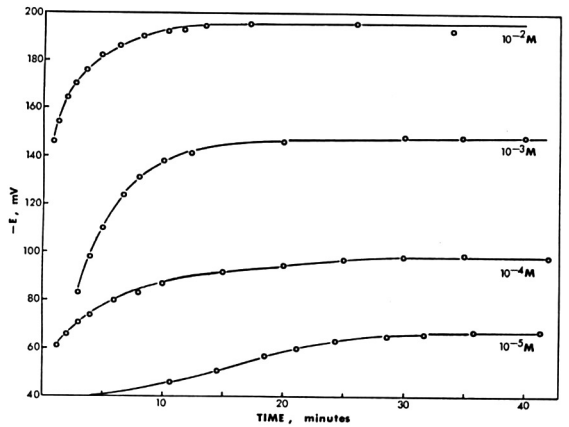

Figure 5. Elecrode response times with fresh amygdalin solutions and 10 mg of enzyme per membrane

tration. The absolute validity of our amygdalin calibration curve is shown by comparison with the calibration of the electrode using aqueous solutions of cyanide (Figure 4). Typical electrode response times are shown in Figure 5.

Effect of Solution and Enzyme Age. Amygdalin solutions deteriorate with time to yield progressively lower potentials and lower calibration slopes. These effects are shown in Figures 6 and 3. Solution deterioration is retarded by storing under refrigeration. When older solutions are measured for cyanide ion, no free cyanide ion is observed showing that other hydrolytic products are formed, extensive solvation occurs, or conformational changes retard the rate of the enzymatic reaction.

The results of continuous electrode use are shown in Figure 7. The enzyme electrode was satisfactory only for four days under such extreme use because of leaching of the enzyme from the gel layer. Longer lifetimes can be achieved by increasing the concentration of the enzyme immobilized in the gel layer or by storing the electrode between measurements. It is also possible to increase electrode lifetimes by interposing a cellophane film between the sample and the electrode, but this leads to retardation of electrode response

Table I. Reproducibility of Potential[a]

	Amygdalin concentration			
Trials	$10^{-2}M$	$10^{-3}M$	$10^{-4}M$	$10^{-5}M$
1	−195 mV	−148 mV	−99 mV	−58 mV
2	−196	−148	−100	−58
3	−191	−150	−96	−56
4	−194	−147	−101	−54
5	−191	−148	−104	−52
Mean	−193	−148	−100	−56
Std dev	2.35	1.12	2.92	2.6
Rel std dev	1.22%	0.756%	2.92%	4.6%

[a] Readings were made at pH 10.4, T = 25 °C, 10 mg of enzyme per membrane with freshly prepared amygdalin solutions.

(*7*, *13*). Because the immobilized enzyme can be stored indefinitely under refrigeration (*12*), it is easily possible to prepare enough gel material for 100 determinations or more by immobilizing 100 mg of enzyme in 1 ml of polymer.

(13) K. K. Stewart and L. C. Craig, ANAL. CHEM., **42**, 1257 (1970).

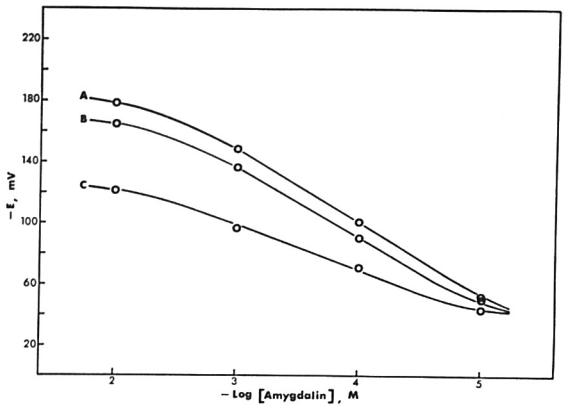

Figure 6. Effect of solution age and storage of immobilized enzyme membrane

pH 10.4, 25 °C, and 6 mg of enzyme per membrane. Curve (*A*) fresh, (*B*) 4 days old, (*C*) 14 days old

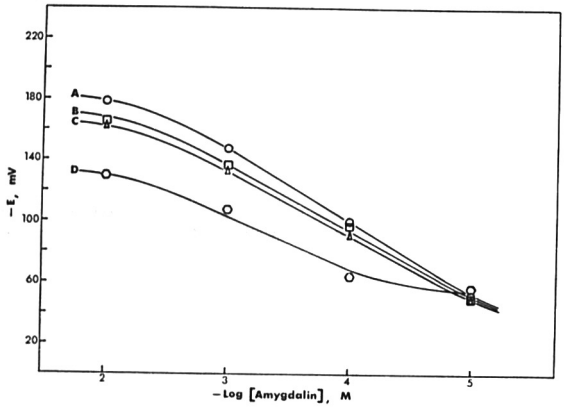

Figure 7. Continuous measurements

(*A*) first day, (*B*) second day, (*C*) third day, (*D*) fourth day

Effect of Amount of Enzyme in the Membrane. Little difference was observed when the amount of enzyme in the membrane was changed from 3 mg to 6 mg to 10 mg. This is so because the amount of enzyme is always much greater than the amount of substrate per 0.20 ml of sample, except at $10^{-2}M$ amygdalin where the amount of substrate and enzyme are such that the response becomes zero order with respect to the substrate and the curve levels off.

Effect of Buffer, Temperature, and pH. The behavior of the enzyme electrode is dependent on the pH of the solution to which the system is exposed because the sensing element of the cyanide electrode responds only to the activity of the cyanide ion (*14*) and not to any HCN formed ($K_a = 4 \times 10^{-10}$). At pH 9.2, 50% of the cyanide is free; above pH 10.3, 90% of the cyanide is free; and at pH 12, virtually all the cyanide is in the free form.

For this enzyme electrode, the pH range of 10–11 seems to be optimum. Working above pH 11 exposes the immobilized enzyme to irreversible deactivation while resulting in only negligible improvements on the overall electrode response and at pH < 10 sensitivity is lost because of HCN formation.

Borax/NaOH, $NaHCO_3$/NaOH, and Na_2HPO_4/NaOH buffer systems were investigated. The borax system was best for use with the electrode. The others gave high blanks and poor reproducibility due to reaction with silver ion from the electrode crystal or to inhibition of the enzyme.

Best results were obtained by working at room temperature. While higher temperatures speed up electrode response somewhat, they also result in more rapid deterioration of amygdalin solutions and enzyme gels.

Effect of Diverse Ions. Ions capable of forming insoluble silver salts will interfere because of the formation of a precipitate on the membrane surface; substances capable of reducing silver ion will also interfere. Thus, direct enzyme immobilization on the sensing elements is less attractive than mechanical coupling of the gel membrane because the latter permits rapid cleaning of the crystal surface and replacement of the enzyme layer when necessary. Certain transition and heavy metal ions form very stable cyanide complexes and, hence, will interfere. Some metals like Cu, Cd, and Hg may serve to inactivate the enzyme. However, common impurities like Cl^- and Br^-, and the ordinary constituents of many biological samples can be tolerated.

(14) Orion Cyanide Electrode Instruction Manual, Orion Research Inc., Cambridge, Mass. 02139.

CONCLUSION

The electrode described represents a new variation of potentiometric enzyme systems. We have succeeded in coupling an enzyme membrane to a polycrystalline non-glass membrane. The principle involved is generally applicable since there are literally thousands of enzymes with high activity and selectivity which can be coupled to existing potentiometric sensors (*5*). It may also be possible to adapt these systems to the determination of the β-glucosidase enzyme rather than the substrate. Such efforts are currently under way and, if successful, would lead to new sensors useful for enzyme analysis and for the diagnosis of certain disease states involving enzyme abnormalities.

RECEIVED for review March 25, 1971. Accepted June 8, 1971. We gratefully acknowledge the support of the National Institutes of Health.

Correction

Identification of Barbiturates by Chemical Ionization Mass Spectrometry

In this article by H. M. Fales *et al.* [ANAL. CHEM., **42,** 1432 (1970)] there is an error on page 1434. Figure 2 shows a line in the E.I. spectrum at *m/e* 140. This should be *m/e* 141, and therefore a revised Figure 2 is shown below.

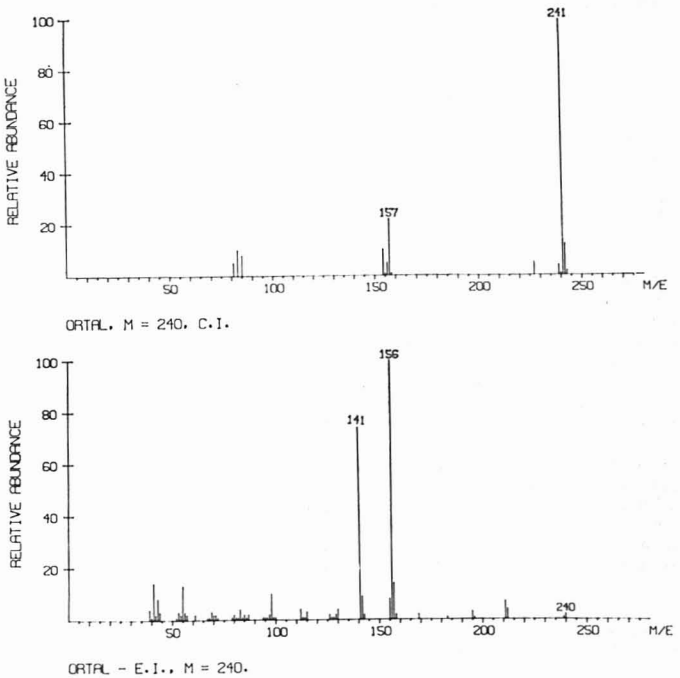

Figure 2. Electron impact and chemical ionization mass spectra of ortal

Membrane Probe–Spectral Emission Type Detection System for Mercury in Water

Robert S. Braman

Department of Chemistry, University of South Florida, Tampa, Fla. 33620

A new method for mercury detection and analysis is presented. Mercury compounds are reduced to metallic mercury, diffused into a helium carrier gas stream through a rubber diaphragm immersed in sample solutions and then passed through a dc discharge. The 2537 Å mercury emission line intensity is observed. The lower limit of detection is 4 parts per trillion for a concentration sensing probe and is 4×10^{-10} gram in a batchwise analysis modification of the technique. Since only volatilized mercury diffuses through the diaphragm, both free and total mercury may be determined on the same sample. Dimethyl mercury is detected. Operating characteristics, calibration, and use of the method for the analysis of some environmental samples are presented. The membrane technique holds promise as a new analytical procedure for volatile materials in solution.

Owing to the toxicity of mercury and its compounds, interest in their detection and determination has been of long standing. Much of the older analytical work is aimed at trace analysis. Considerable current interest lies in the analysis of environmental samples for traces of mercury. Low concentrations of mercury or small amounts are determined largely by spectrophotometric methods using the dithizone mercury complex (*1–4*). Spectrophotometric techniques are often complicated by separation or masking steps to eliminate interferences. When these techniques are applied to very small sample sizes, blank errors or background corrections can become troublesome, particularly if considerable preconcentration is required. Lower limits of detection are approximately 0.5 μg of mercury. A catalytic method developed by Pavlovic and Asperger (*5*) is subject to similar separation and interference problems and has similar sensitivity. Neutron activation analysis has been used (*6*, *7*) for detection of microgram sized samples but the procedures are inconvenient, especially when interferences must be removed. Flame emission and conventional atomic absorption analysis do not have very low limits of detections, approximately 2.5 ppm and 10 ppm, respectively (*8*).

The most sensitive methods for low concentrations to date have been based upon absorption by mercury of UV radiation from a mercury vapor lamp. Early work was reported by Woodson (*9*). A number of what are essentially modifications of the same method have been reported (*10–13*) and are now called flameless atomic absorption methods. Concentration limits of detection for these range from 0.02 to 1.0 μg per liter depending upon sample sizes taken. The lower limit of detection on an analyte weight basis is 5 to 10 nanograms (*14*). Metals other than mercury are not an interference in this method but volatilized materials absorbing in the 2537-Å region are, if present.

The dc discharge spectral type detector (*15*) is useful for the analysis of small amounts of heteroatom-containing organic compounds; lower limits of detection range from 10^{-10} to 10^{-14} gram for many compounds. Because of this and the high degree of selectivity available in emission type detection systems, the method was chosen for application to mercury detection and analysis. In order to use an emission type detector, mercury metal vapor or a volatile mercury compound must be separated from its sample matrix materials. It must then be passed through an electrical discharge in helium carrier gas and the 2537-Å Hg emission line observed in an appropriate optical system. The analysis of water or air samples by total sample injection onto a gas chromatography column of appropriate type appears feasible. Nevertheless, the analysis of large water samples is clearly a problem because of the need for eventual removal of 1 ml or more of water from the column. The analysis of 10-μl size samples would be more suitable, but the 10^{-9} to 10^{-12} gram of mercury in the samples could be lost in the separation process.

Two techniques for separating mercury from aqueous samples were investigated prior to study of the membrane. Vacuum evaporation of water samples, and reduction of the residue with sodium borohydride in a small tube was first tried with some success. Mercury vapors were readily detected but reproducibility was poor, largely because water from the reducing agent solution interfered in discharge operation. A direct volatilization method similar to that used in the flameless atomic absorption method was next tried. Helium carrier gas was passed through a sample solution treated with sodium borohydride and then through a drying tube and into the detector cell. Larger sample sizes could be accomodated and limits of detection were low but sample handling, necessity for replacement of the drying tube, and time required for analysis rendered this approach less convenient than the membrane-emission detector probe technique subsequently developed.

Selection of the diffusion of mercury through a membrane from air or water solution into the carrier gas stream was based upon prior reported work. Volatile materials are well

(1) Yikimura and V. L. Miller, *Anal. Chim. Acta*, **27**, 325 (1962).
(2) W. H. Gutenmann and D. J. Lisk, *J. Agr. Food Chem.*, **8**, 306 (1960).
(3) "Official Methods of Analysis," 8th Ed., Association of Official Agricultural Chemists, Washington, D. C., 1955.
(4) E. B. Sandell, "Colorimetric Determination of Traces of Metals," 3rd ed., Interscience, New York, N. Y., 1965.
(5) D. Pavlovic and S. Asperger, Anal. Chem., **31**, 939 (1959).
(6) B. Sjostrand, *ibid.*, **36**, 814 (1964).
(7) C. K. Kim and J. Silverman, *ibid.*, **37**, 1616 (1965).
(8) H. H. Willard, L. L. Merritt, Jr., and J. A. Dean, "Instrumental Methods of Analysis," 4th Ed., Van Nostrand, Princeton, N. J., 1965.
(9) T. T. Woodson, *Rev. Sci. Instrum.*, **10**, 308 (1939).
(10) C. W. Zuehlke and A. E. Ballard, Anal. Chem., **22**, 953 (1950).
(11) O. Lindstrom, *ibid.*, **31**, 461 (1959).
(12) M. J. Fishman, *ibid.*, **42**, 1462–3 (1970).
(13) W. R. Hatch and W. L. Ott, *ibid.*, **40**, 2085 (1968).
(14) L. P. Morgenthaler, "The Determination of Trace Quantities of Mercury by Atomic Absorption Spectrometry," McKee-Pedersen Instruments, Applications Notes, Vol. 5, Nov. 1970.
(15) R. S. Braman and A. Dynako, Anal. Chem., **40**, 95 (1968).

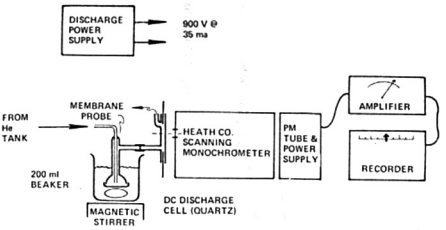

Figure 1. Apparatus arrangement for membrane probe—emission type detector

known to diffuse through membranes. Some uses of membranes in analysis have been reported. Oxygen diffuses through thin layers of Teflon (Du Pont) in the polarographic membrane electrodes (*16*). Membranes are also used to separate carrier gases from eluant in interfacing mass spectrometers with gas chromatography systems (*17, 18*). Carbon dioxide membrane electrodes are used (*19*).

An entire latex rubber balloon was used in initial experiments with promising results. Probe designs providing more control over membrane surface area and more convenient to use were then constructed and used throughout the study. The membrane probe technique reported here for the determination of mercury has eventually proved to be more selective with lower sample size limits of detection than any other method for this element.

EXPERIMENTAL

Apparatus. The apparatus arrangement used is shown in Figure 1. It consisted of the helium carrier gas source, a membrane type probe (or batchwise cell) and emission type detector cell, and a conventional optical and electronic system. The probe type cell design is shown in Figure 2*a*. Latex rubber balloons, 1.7 cm in diameter (not inflated) and 18.5 cm long and 4 mils thick were cut off to 2 inches long and pulled over the glass probe end. The balloons fit tightly enough over the 4-cm diameter probe end so as to serve as their own leak-tight seal. A short end of the balloon tip extended below the probe. Although the membrane area influences the total rate of mercury diffusion, difficulties arising from the elasticity of the rubber were not observed. The carrier gas inlet pressure was kept just above ambient. Helium carrier gas flowed over the inner surface of the rubber diaphragm and carried diffused mercury and other diffused vapors into the quartz DC discharge cell shown in Figure 2*b*. This cell was constructed entirely of quartz for optical transmission and to minimize absorption of mercury on metal surfaces. Polyethylene tubing, $^1/_4$-in. o.d., was a convenient connector. It stretched tightly over the 6-mm glass tubing.

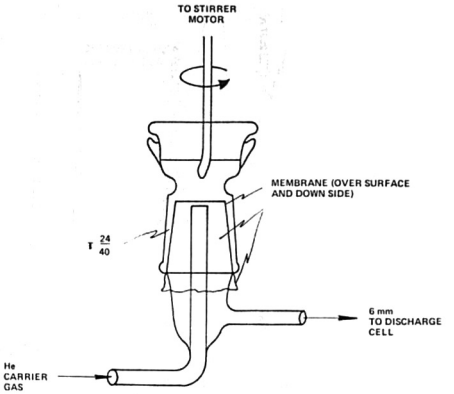

Figure 3. Batchwise cell (half size)

A batch analysis type cell was also constructed and is shown in Figure 3. It was easily substituted for the concentration probe cell by using the polyethylene connectors. The same carrier gas, monochromator, and electronic equipment were used. A Heath Company scanning monochromator, Model EU 701-30 photomultiplier module (1P28 tube), a model EU 703-31 Heath amplifier, and a 0–10 mV strip chart recorder were used. An unregulated discharge power supply, a voltage doubler followed by a pi filter, was constructed.

(16) D. E. Carritt and J. W. Kanwisher, ANAL. CHEM., **31**, 5–9 (1959).
(17) S. R. Lipsky, D. G. Horvath, and W. J. McMurray, *ibid.*, **38**, 1585 (1966).
(18) J. T. Watson and K. Biemann, *ibid.*, **36**, 1135 (1964).
(19) J. W. Severinghaus and A. F. Bradley, *J. Appl. Physiol.*, **13**, 515 (1968).

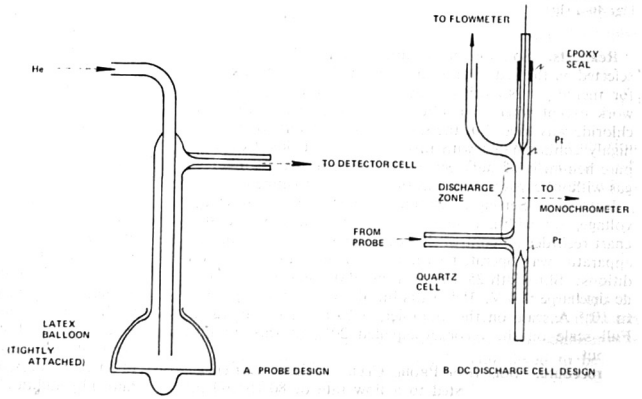

Figure 2. Probe cell and discharge design

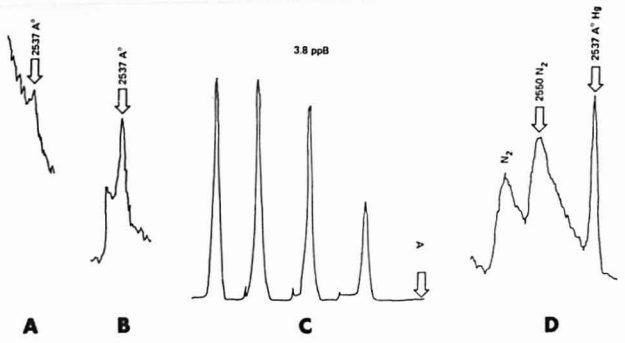

Figure 4. Selected response recordings

A. Tap water, λ scan, 0.036 ppb (10^{-7} A scale)
B. Standard, λ scan, 0.096 ppb (10^{-7} A scale)
C. Standard, λ scans, 3180 ppb (10^{-6} A scale)
D. Standard, λ scan, approximately 0.2 ppb (10^{-7} A scale)

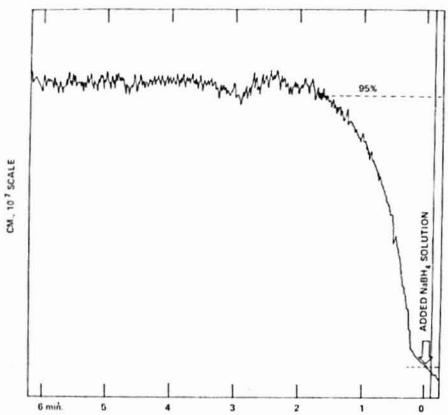

Figure 5. Mercury detection system response rate

Continuous scan at 2537 Å Hg line, 23 °C, 10^{-7} A scale, 0.48 ppb Hg, 40-μ slit)

Reagents. Sodium borohydride from Alfa Inorganics, selected as the reducing agent, exhibited a zero blank value for mercury. No other reagents were necessary for most work except where pH adjustments were made. Stannous chloride was tried, but the sample on hand was found to be highly contaminated with mercury. J. T. Baker Co. ultrapure helium is of sufficient purity to permit use as a carrier gas without cryogenic purification or other treatment.

Instrument Settings. Photomultiplier voltage, discharge voltage, slit width, amplifier gain, and range of the strip chart recorder all control the total signal gain. The present apparatus was operated with the following ranges of conditions: Slit width 25–100 microns, PM voltage 750–800 V., dc discharge 900 V, 31.5 watts/lineal inch of discharge, 10^{-6} to 10^{-8} A scale on the amplifier, 0–10 mV recorder range. Full scale on the recorder equaled 20% of the amplifier output.

Procedure. Solution Probe Cell. Helium carrier gas is turned on and adjusted to a flow rate of 80 to 100 ml/minute. The outlet of the detector cell is restricted by a pinch clamp so as to raise the internal pressure of the system to slightly above ambient. This helps to decrease diffusion of air into the carrier gas through small leaks, but does not affect detector response. After 3–5 minutes, the system is sufficiently flushed out with helium to permit the dc discharge to remain on. A determination of residual mercury can be made on the system by placing distilled water (or tap water) in the sample beaker and scanning the 2537-Å region. A peak will occur at 2537 Å superimposed on the N_2 4th positive band system (see Figure 4). Residual mercury, if present from previous analyses, rapidly decreases to a low value or zero.

Analysis of aqueous samples is accomplished by placing 200-ml samples in a 400-ml beaker, 3 to 10 drops of 2% $NaBH_4$ in distilled water is added, and the emission response is recorded. Solutions are stirred during the analysis. Response at 2537 Å rises to a maximum in 2 to 3 minutes after addition of the reducing agent as is shown in Figure 5. Data may be taken by recording response at 2537 Å as a function of time or by scanning through the 2537-Å region several times over a 2- to 6-minute period. The scanning method appears best for the 0- to 0.2-ppb range so that a base-line technique of emission peak area may be used to calculate responses. This also affords observation of any background radiation which may be present. Dissolved nitrogen is usually present. At higher mercury concentrations changes in background will be sufficiently small as to be negligible. Examples of the types of data obtained are shown in Figure 4.

A decrease in the response of 2537 Å is observed after the initial rise to a maximum. This is due to the removal of mercury from the sample during analysis. The maximum response is usually constant over several minutes before the decay is observed. Response values taken in this time period are used in calibration based upon concentration and analysis. After each analysis the cell is washed with distilled water and is allowed to stand with a blank water solution for 3–5 minutes, or until residual mercury is cleared from the system. The apparatus is then ready for the next sample. If the interior of the diffusion cell and detector cell become overloaded with mercury or if cleaning is desired, bromine water wash may be used followed by water. Solvents may be used but the last wash should be with water. Organic layers absorb nearly completely 10- to 100-nanogram amounts of mercury passed through the system. Calibration is obtained by addition of appropriate volumes of dilute (10 ppm)

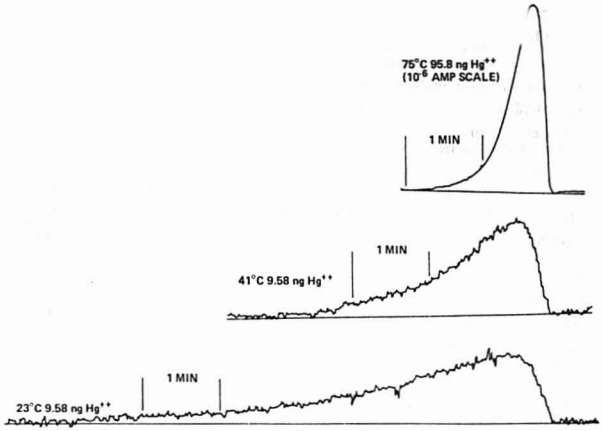

Figure 6. Effect of temperature on batchwise cell response

Top curve: 75 °C, 95.8 ng Hg^{2+}, 10^{-6}-A scale
Middle curve: 41 °C, 95.8 ng Hg^{2+}, 10^{-7}-A scale
Bottom curve: 23 °C, 95.8 ng Hg^{2+}, 10^{-7}-A scale

$HgCl_2$ solutions to 200 ml of distilled water and then analysis by this procedure. Sample volumes down to 50 ml have been used with the probe.

BATCHWISE ANALYSIS CELL. Samples may be analyzed by diffusing all the mercury in a small sample volume through a membrane. From 2 to 5 ml of sample solution is placed on top of the membrane in the batchwise analysis cell shown in Figure 3. The cell is heated to 60–80 °C by means of an electrical tape wound around the cell. A stirrer is mounted above the cell. One or two drops of 2% $NaBH_4$ solution are added to the sample. The emission response at 2537 Å is recorded as a function of time. Data of the type shown in Figure 6 are obtained. The area under the curve is proportional to the total amount of mercury in the sample. Calibration is obtained by simply adding known amounts of mercury from dilute solutions to a blank water sample.

RESULTS AND DISCUSSION

Response Curves, Precision, and Limits of Detection. Several response curves were obtained in the study of the technique. Samples of known mercury content were prepared by injecting microliter volumes of an approximately 10 ppm (as Hg) standard mercuric chloride solution into water of nil or very low mercury content just prior to analysis. Local tap water was found to be very low, 10 ppt or less, in mercury and served as a convenient blank source. One microliter of the 10 ppm Hg solution contains 10 nanograms (ng) of mercury and produces a solution at 50 ppt Hg when added to 200 ml water.

Table I gives the experimental conditions, least squares line equations and pertinent statistical data from the response curve study. Precision of the slopes ranged from 2 to 5% relative and is a fair measure of the precision of the method for the concentration ranges and sample sizes used.

Series 1 was carried out using sample volumes measured by filling the sample cell to the 200-ml mark, a less precise method than the sample weighing procedure used in series 2. The improved precision of the technique is reflected in the 0.01 ppb estimate of the standard deviation of the individual values.

Series 3 affords an evaluation of the lower limit of detection of the method on a concentration basis. The standard deviation in the individual points is near 4 parts per trillion. The standard deviation in the individual points for the batchwise analysis method is 3.8×10^{-10} gram.

The approximate flow rate of mercury through the detector was calculated from data on the decrease in the signal as a function of time. This was found to be 1.7×10^{-10} g/sec at $Ct = 0.7$ ppb. At a carrier gas flow rate of 43 ml/minute and with a detector active volume of 0.32 ml, 5.3×10^{-11} gram of mercury is present in the detector at time t. Since the concentration limit of detection for 200-ml sample volumes is on the order of 2×10^{-11} g/ml, this should yield a flow rate of 5×10^{-10} g/sec with 1.5×10^{-12} gram in the detector active volume at the limit of detection. This is in fair agreement with the sample size limit of detection of 3.8×10^{-10} gram over a 30-second response time, calculated from the response curves series 4 in Table I.

Membrane Function. Membrane operation is analogous to the plating out of a metal at an electrode. The rate of diffusion of mercury across the membrane is the effect controlling the detector response in a stirred solution. If dN/dt is rate of mercury loss to the carrier gas inside the probe, then from Fick's law:

$$\frac{dN}{dt} = DA\frac{dC}{dX} \tag{1}$$

Where A is the membrane area, dC/dX is the concentration gradient across the membrane, and D is the diffusion coefficient for mercury metal in the membrane. If dC/dX is linear across the diffusion layer, then

$$\frac{dC}{dX} = \frac{C_{sol.} - C^\circ}{d} \tag{2}$$

where d is the thickness of the layer and C° the mercury concentration at the water-carrier gas interface. The diffusion layer includes the membrane but possibly also solution outside the membrane. If C° may be considered to be very small, then

Table I. Response Curves and Statistical Data for Mercury in Water Analyses

	Response curves		Conditions
Series 1	0.1 to 1.4 ppb Hg, probe type cell ng/200 ml = 15.94 cm (peak right) − 20.2 s (slope) = 0.30 s (ng/200 ml) = 0.08 n = 12	23½ °C	24-μ slit, 800 V, PM, 10^{-7}-A scale range, chart speed 1 in./minute, 80–100 ml/min, He
Series 2	0.1 to 1.0 ppb, probe type cell ppb = 0.04594 × cm (peak height 0 + 0.01 s (slope) = 0.00176 s (intercept) = 0.02 n = 9	23½ °C	40-μ slit, 740 V, PM, 10^{-7}-A scale range, chart speed ½ in./minute, 122 ml/min, He
Series 3	0.001 to 0.100 ppb, probe type cell cm² (peak area) = 18.90 × ppb + 0.21 s (slope) = 0.99 s (intercept) = 0.052 s (area) = 0.074 cm² s (ppt) = 4 n = 7	23½ °C	40-μ slit, 740 V, PM, 10^{-7}-A scale range, chart speed ½ in./minute, 122 ml/min, He Scan rate 0.02 Å/sec
Series 4	0–10 ng, batchwise cell cm² (peak area) = 0.574 × ng + 0.16 s (slope) = 0.027 s (intercept) = 0.15 s (area) = 0.22 cm² s (ng) = 0.38 n = 7	75 °C	35-μ slit, 740 V, PM, 10^{-7}-A scale range, chart speed ½ in./minute, 122 ml He/min, Scan rate 0.05 Å/sec

Table II. Effect of He Flow Rate on Response (96 ng/200 ml sample)

Flow rate, ml/min	Peak height, cm, 10^{-6} scale
114	6.4
100	6.4
72	6.5
64	6.4
46	6.4
35	6.3

$$\frac{dN}{dt} = \frac{AD\,C_{sol}}{d} \qquad (3)$$

and the rate of mercury transfer to the carrier gas stream is a linear function of the concentration of mercury metal in the sample solution. This was confirmed by experiment. Values of D for mercury were calculated from experimental data and found to be 1.2×10^{-4} cm²/sec for an assumed 4-mil value of d and 20 cm² for A.

The technique operates in a manner similar to controlled potential coulometry in the batchwise analysis technique. Mercury leaves the system through diffusion and thus:

$$Ct = Coe^{-\frac{DAt}{V}} \qquad (4)$$

gives the concentration at any time t where Co is the mercury concentration at time $t = 0$, A is membrane area, V is sample volume, and D is the apparent diffusion coefficient. Figure 6 which illustrates a typical response for the batchwise type cell indicates conformance of experimental results to Equation 4.

Only one type of membrane material other than latex rubber was tested. Saran wrap, 1 mil thick, was used in a few experiments in the batchwise analysis cell. Saran diffused mercury much more rapidly than the latex rubber, probably because of its decreased thickness. It will be suitable for use in batchwise analyses but is more fragile.

As predicted from Equation 3, response is a function of membrane area. Comparison of calibration plots for two different balloons, approximate areas 18 and 23 cm² indicated a linear relation of mercury diffusion rate to membrane area.

Detection System Characteristics. Equation 3 predicts that carrier gas flow rate or pressure will have no influence on the rate of diffusion. The rate of mercury transfer across the diffusion membrane layer, then, controls the rate of flow of mercury through the discharge.

If the detector responds to rate of flow, then carrier gas flow rate should have no effect on response. This was found to be the case experimentally as shown in Table II. Nevertheless, it was expected that the detector would be concentration sensitive since the excitation process does not destroy mercury. Further investigation is clearly needed to evaluate detector operation.

Stirring rate influences response but only if very slow rates are used. If stirring is halted altogether, the rate of mass transport of mercury through the solution to the diffusion layer becomes important. An increase in slit width increases response. Slit widths larger than 200 microns admit too much background radiation.

Temperature Effects. Temperature influences the diffusion rate of mercury. Consequently, the concentration sensing probe must be operated under temperature controlled conditions. All calibration runs were made at 23.5–24.0 °C, room temperature. To determine the temperature effect on probe response, several duplicate samples were analyzed in the range 24–50 °C. The temperature effect from 24 to 40 °C was to increase the probe signal by 2.04% per °C increase in temperature, the expected temperature effect on diffusion coefficients. The decay rate of the peak signal was increased by increasing the temperature. At 50 °C, water diffusion through the membrane starts to quench the discharge.

The batchwise analysis cell operation is also influenced by temperature. Temperature increases decrease the analysis

time because of the increased diffusion rate. Figure 6 shows the sharpening effect of elevated temperature on the Hg response *vs.* time curve. Batchwise analyses were carried out at 70–80 °C to take advantage of the improved response time. The response of the system in terms of area per ng Hg is not influenced by temperature. Quenching of the discharge was not observed at the elevated temperatures, presumably because of the smaller membrane area than was present in the probe cell temperature study.

Limitations and Interferences. The mercury detection and analysis technique is subject to the chemical limitation that mercury must be mercury metal or a volatile compound. Sodium borohydride is capable of reducing mercurous and mercuric compounds in mildly acidic to alkaline media. Acidic solutions rapidly hydrolize sodium borohydride and even though some reduction occurs, there may be reoxidation of mercury prior to detection. This may be avoided by buffering the solution with borax prior to using sodium borohydride. Alternatively, a different reducing agent, providing it is sufficiently low in mercury content, can be used.

The following materials did not interfere with the analysis technique: sea water, dissolved organic solvents, EDTA, oxalic acid, NO_3^-, $H_2PO_4^-$, CN^-, Fe^{3+}, Zn^{2+}, and borax. Oxidizing agents which react with sodium borohydride will interfere unless additional sodium borohydride is added to reduce these materials.

Mercury not in solution or not readily convertible to mercury will not be detected. Dimethyl mercury diffuses rapidly enough for easy detection, but a paint fungicide, di(phenylmercury)dodecenylsuccinate, diffused too slowly through the membrane for easy analysis. Prior oxidation of this type of mercury compound will apparently be needed before analysis.

Applications. Samples from natural water sources in and around the Tampa Bay area were analyzed using the concentration probe cell. Analyses required approximately five minutes per sample. Mercury concentrations ranged from 0.01 to 0.16 ppb. Samples ranged in quality from fresh river water to highly polluted salt water from port areas. No interferences were detected based upon recovery of added known amounts of mercury prior to analysis.

Several commercial chemical products were analyzed after suitable sample preparation. Commercial bleach was found to contain 125 ppb Hg. Sufficient reducing agent was added to reduce the hypochlorite content of the sample and to provide an excess for mercury reduction.

Highly acidic waster water samples were analyzed after addition of sufficient borax solution to the sample to adjust the pH to 7–8. The borax solution contained insignificant amounts of mercury.

It is particularly important to check on the mercury content of reagents used in sample preparation. There may also be wide variations in mercury content of reagents from different sources. For example, one source of $SnCl_2$ had 2.5 ppb Hg, another had 0.3 ppm Hg. The analysis of some common laboratory reagents were as follows: EDTA 2.0 ppm Hg; concd H_2SO_4, 4.4 ppb; concd HNO_3, 5.1 ppb; $(NH_4)_2S_2O_8$, 55 ppb; $KMnO_4$, 80 ppb; NaOH, 34 ppb; $K_2Cr_2O_7$, less than 1 ppb, and NH_4OH, less than 1 ppb.

Several urine samples and a pooled blood serum sample were directly analyzed by the technique. No interferences were observed. Mercury in the urine samples ranged from 3 to 10 ppb.

The method was also suitable for the determination of dimethyl mercury in low concentration in aqueous solutions. Dimethyl mercury is detected without reduction by sodium borohydride with the same sensitivity as mercury.

SUMMARY

Combination of a membrane probe with a dc discharge emission type detector has expanded its capabilities. Extraction, preconcentration, and gas chromatographic separations are avoided. Separation by means of a membrane permits transfer of analytes directly from samples into the helium carrier gas stream of the detector. Diffusion of water and dissolved gases is insufficient to quench the discharge. Thus, the dc discharge detector can be used for analysis of aqueous samples directly without separation for any diffusible material with a specificity limited only by the emission wavelength specificity available in the dc discharge detector.

The technique has been applied here to the determination of mercury in water. The method is specific, comparatively free of interferences, rapid, and convenient to perform. Limits of detection are equal to 10 to 20 times lower than those of the flameless atomic absorption methods (depending upon the published limits of detection used for comparison.) Both concentration measurements and batchwise analyses can be made.

The technique has been applied to the detection of mercury in fresh water, sea water, laboratory chemicals, commercial chemical products, food samples, and urine. Limitations are based upon the necessity for converting all mercury compounds into mercury metal by reduction (except those mercury compounds which diffuse through the membrane). Complexing agents do not prevent the reduction of mercuric or mercurous salts to mercury metal.

The diffusion technique described here obviously serves as a model for many other water or air analysis applications. Dissolved oxygen, nitrogen, sulfur dioxide, carbon dioxide, nitrogen oxides, and many volatile organic compounds are detectable. Certain inorganic compounds are also detectable. The potential uses are multifarious. The technique is being studied further.

RECEIVED for review April 8, 1971. Accepted June 8, 1971. Presented at the Meeting-in-Miniature, Florida Section, American Chemical Society, May 1971. Equipment used in this research was provided by National Science Foundation Grant GP 8598.

Direct Enthalpimetric Determination of Olefins

Donald W. Rogers

Chemistry Department, The Brooklyn Center, Long Island University, Brooklyn, N.Y. 11201

We have constructed an apparatus which permits direct enthalpimetric determination of olefins through the heat given off upon catalytic hydrogenation of an unknown sample. Under the conditions described, hydrogenation takes place in 10–30 seconds permitting rapid and routine estimation of unsaturation. Sample size is in the vicinity of 10^{-6} to 10^{-4} mole and the average error is about 1–2%. We have presented data for 1-hexene, cyclohexene, cyclopentene, phenylacetylene, linoleic acid methyl ester, and linoleic acid ethyl ester.

HYDROGENATION has long been a preferred method of analysis of olefins (*1–3*). Brown and coworkers have developed the method to a high degree of accuracy and sensitivity by their method of *in situ* generation of catalyst and hydrogen (*4, 5*). Their method has been modified by Curtis and Baker (*6*) for samples containing sulfur impurities and has been automated by Szakasits (*7*). Recently, Curran and coworkers have developed a sensitive method employing pressure transducers (*8, 9*). Their method is semi-automated and is capable of determining μmolar quantities of olefinic compounds.

The enthalpy change on hydrogenation of an olefin has been widely studied by Kistiakowsky, Turner, Skinner, and their coworkers. See reference (*10*) for a survey of the literature on the thermochemistry of hydrogenation.

The heat of hydrogenation of many compounds is known to be about 30 kcal/mole for unstrained, unconjugated double bonds. The quantitative nature of most hydrogenations and their high heat output make them ideal for direct enthalpimetric study by methods described by Jordan, Ewing, and others (*11–13*). To date, however, direct injection enthalpimetric (DIE) determination of olefins has not been used because of the complexity of the apparatus, the need to dissassemble the apparatus after each run, and the slowness of the hydrogenation reaction, reported, in the thermochemical literature, to be from 20 minutes to several hours.

We have constructed a calorimeter in which hydrogenation may be made to take place in 10 to 30 sec allowing rapid recording of the heat of reaction of replicate samples as they are injected into the calorimeter at four- or five-minute intervals. These characteristics make the direct enthalpimetric determination of olefins a practical technique.

The principle of the method is simple. If one knows how much heat is liberated on hydrogenation of a pure olefin, then liberation of any fraction of that amount of heat on hydrogenation of an unknown sample leads to the per cent composition of the sample.

While both Brown's and Curran's methods produce results of high accuracy and are very sensitive, we think that direct enthalpimetric determination of olefins may eventually prove to be competitive with both methods in both respects. A major advantage is in the simplicity of instrumentation and operation. Moreover, the method is well suited to rapid, routine determinations and produces a permanent record in the form of a temperature *vs.* time plot for each substance hydrogenated. As Jordan and coworkers have observed (*11*), "DIE is readily adaptable to process stream control".

EXPERIMENTAL

Apparatus. The reaction chamber is shown in Figure 1 and described in detail in reference (*10*). Samples are injected through the rubber plug using a microsyringe. With the use of silicone grease, it is possible to inject replicate samples of olefin into the reaction chamber in much the same way that one injects samples into a GLC column. Hydrogen leakage through the punctured stopper was nil. The syringe was of the fixed needle type, of 25-μl capacity and had a Chaney adaptor (Hamilton Syringe Co., P. O. Box 307, Whittier, Calif., 90608). The thermistor (Y.S.I. Components Div., Yellow Springs, Ohio) protruded to the bottom of the thermistor well which contained *n*-butyl phthalate to facilitate heat transfer. The thermistor leads were connected across a Wheatstone bridge (Leeds and Northrup 4760) and potential across the arms of the bridge was registered on a recorder (Microcord 44, Photovolt Corp., 1115 Broadway, New York, N. Y., 10010), which showed full scale deflection for a 0.5-mV potential difference. Constant potential was maintained across the bridge by a 6-V lead storage battery. A variable series resistance (Leeds and Northrup 4775, 0 to 10,000 ohms) between the battery and the bridge controlled the sensitivity of the temperature sensing apparatus.

The reaction chamber, containing a magnetic stirring bar, rested in a cavity cut into a styrofoam insulating block. The removable top of the insulating block was cut with a hole to facilitate cooling the reaction chamber as described below. The hydrogen inlet needle was connected to a hydrogen tank by a leak proof "twist type" luer joint (Microlab, L.S. 1101, Mountain View, Calif.). A magnet spinning just below the reaction chamber to activate the magnetic stirring bar within was powered by an external motor, thermally well shielded from the chamber. The drive shaft was made of a fibrous plastic to prevent heat transfer from the motor to the chamber. Stirring speed is not crucial but a good area is in the vicinity of 400–500 rpm.

Reagents. Cyclopentene and phenylacetylene were obtained from Aldrich Chemical Co. Hexene, cyclohexene hydrogen, and 5% palladium catalyst on charcoal were obtained from Matheson, Coleman and Bell. Olefins were shown to be more than 99% pure by GLC or were so purified by standard GLC trapping methods (*14*). Both esters were obtained from Nutritional Biochemicals Corp. and certified to be 99% pure by the manufacturer.

Procedure. Twenty or twenty-five ml of glacial acetic acid were placed in the reaction chamber along with the

(1) S. Siggia, "Quantitative Organic Analysis *via* Functional Groups," 2nd ed., Wiley, New York, N. Y., 1954, Chap. 6.
(2) A. Polgar, and J. L. Jungnickel, in "Organic Analysis", Interscience, New York, N. Y., 1956.
(3) M. Sidlak, ANAL. CHEM., **38,** 1503 (1966).
(4) C. A. Brown, S. C. Sethi, and H. C. Brown, *ibid.*, **39,** 823 (1967).
(5) C. A. Brown, *ibid.*, p 1882.
(6) J. L. S. Curtis and M. O. Baker, *ibid.*, **42,** 279 (1970).
(7) J. J. Szakasits, *ibid.*, p 1708.
(8) D. J. Curran and J. L. Driscoll, *ibid.*, p 813.
(9) D. J. Curran and J. E. Curley, *ibid.*, **43,** 118 (1971).
(10) D. W. Rogers and F. J. McLafferty, *Tetrahedron*, in press.
(11) J. S. Wasilewski, P. T.-S. Pei, and J. Jordan, ANAL. CHEM., **36,** 2131 (1964).
(12) G. J. Ewing and C. J. Mazak, *ibid.*, **38,** 1575 (1966).
(13) J. C. Wasilewski and C. D. Miller, *ibid.*, p 1750.
(14) A. B. Littlewood, "Gas Chromatography," Academic Press, New York, N. Y., 1962, p 260 ff.

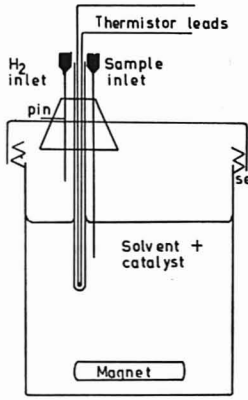

Figure 1. Reaction chamber

The body of the chamber is plastic, the inlet ports protrude through a rubber stopper, and the cap is tightened down over a coating of sealant

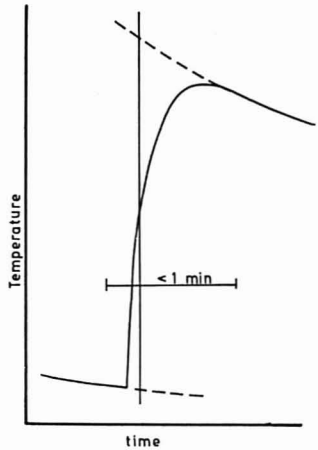

Figure 2. Typical temperature *vs.* time curve

The vertical axis is proportional to temperature

stirring bar and 0.6 gram of 5% Pd catalyst on charcoal. The threads of the reaction chamber were coated with quick drying sealant (Silastic 732, Dow Chemical Co., Midland, Mich., 48640) and its cap was firmly tightened over the sealant. After ten minutes drying time, the reaction chamber and charge were placed in the insulating block and the insulating top was clamped in place. The reaction chamber was now ready for use; it needed only to be connected with the external circuitry.

Catalyst Preparation. Hydrogen was admitted to the reaction chamber at a pressure of 2 atm, the valve on the hydrogen tank was closed, and an outlet valve was opened to bleed off the excess pressure, thereby sweeping out most of the air. Residual air remaining after flushing the chamber once did not interfere with the remainder of the procedure. During hydrogenation, the tank valve remained open so as to maintain a constant pressure of 2 atm. As hydrogen was admitted, a considerable amount of heat was produced which drove the recorder off scale. The recorder was brought back on scale by reducing the resistance of the variable arm of the Wheatstone bridge by one ohm. If a one-ohm change of the bridge setting caused the recorder to go off scale at the low temperature end, the sensitivity of the temperature sensing circuit was reduced by increasing the series resistance.

In these experiments adsorption of hydrogen caused a temperature change of about one degree which necessitated a change of 3 to 4 ohms on the Wheatstone bridge at an input voltage 600 to 700 mV. After hydrogen adsorption was complete (in about 3 min), the recorder stopped its rapid advance to the high temperature end of the scale and started a slow drift downward due to heat leak away from the reaction chamber.

Ambient temperature was restored by holding a small piece of dry ice over the hole cut in the top of the insulation block for that purpose. Cold carbon dioxide flowing down over the reaction chamber caused a rapid drop in temperature which was compensated for by stepwise increase of the bridge resistance to keep the recorder on scale. In less than a minute, the original bridge setting had almost been reached. The dry ice was removed and the reaction chamber began a slow drift toward temperature equilibrium indicated by an approximately logarithmic approach of the recorder to a steady reading. Two or three minutes generally sufficed to establish a relatively steady base line as shown at the bottom of Figure 2. The entire catalyst preparation took about 10 minutes.

Hydrogenation. The hydrogenation procedure began by injecting a sample of pure olefin or a standard of known concentration and noting the scale deflection. The series resistance was adjusted so as to give nearly full scale deflection for the standard. At this point it is convenient to set the voltage divider switch of the Wheatstone bridge at "0.1" so as to be able to vary the bridge resistance in steps of 0.1 ohm. The bridge resistance and the "zero adjust" control on the recorder may now be used in conjunction to establish any base line desired.

After each hydrogenation, the reaction chamber was cooled by the dry ice procedure just described and temperature equilibrium was reestablished. After the proper series resistance had been found, fifteen samples of the same olefin containing varying amounts of an inert hydrocarbon diluent were hydrogenated.

RESULTS AND DISCUSSION

Reaction Time. The success of DIE determination of olefins depends on short reaction times. Reaction times of the simple olefins reported here were from 10 to 30 seconds as contrasted to several hours reported for similar hydrogenations under different conditions (*3*, *15*). These short reaction times make errors from instrumental drift negligible and minimize extrapolation errors in Figure 2. Watt and Walling (*16*) have shown that hydrogenation of higher monoolefins proceeds by a zero order reaction on reduced Pd catalyst. Hence the small sample size in these experiments is an advantage because reaction times are directly proportional to amount of olefin, all other things being equal. Zero order reactions are frequently limited by the catalyst surface area available to the reactants, hence it is not surprising that by using an overwhelming excess of catalyst adsorbed on acti-

(15) R. B. Williams, *J. Amer. Chem. Soc.*, **64**, 1395 (1942).
(16) G. W. Watt and M. T. Walling, Jr., *J. Phys. Chem.*, **59**, 7 (1955).

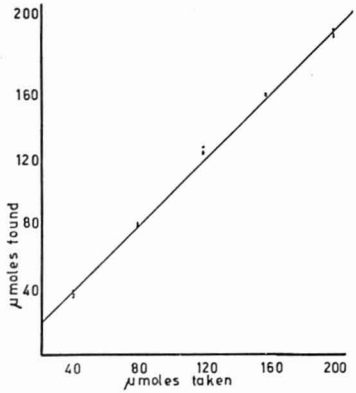

Figure 3. Micromoles found *vs.* micromoles taken for cyclohexene

Standard deviation = 3.0%

Table I. Enthalpimetric Determination of Unsaturation

Compound	Amount, μmoles	Replicate samples	Inert diluent	Std dev, %
1-Hexene	32–160	15	Hexane	1.5
Cyclopentene	46–228	16	Hexane	1.2
Phenylacetylene	15–75	15	Ethylbenzene	0.9
Phenylacetylene[a]	3.2–15	15	Ethylbenzene	2.3
Linoleic acid, Methyl ester	12–61	15	Hexane	1.8
Linoleic acid Ethyl ester	11–57	15	Hexane	1.4

[a] Series resistance 600 ohms, input voltage about 3 volts.

vated charcoal in the form of a stirred slurry, we achieved a considerable reduction in reaction time. In other experiments we have used a variety of solvents but we have not noticed the usual variation of reaction time with stirring rate (*17*) or with solvent (*2*).

The practical value of any analytical technique is, in part, determined by its rapidity. We were able to go through the entire preparation and hydrogenation process for 15 samples in about $2^1/_2$ hours.. Deterioration of the catalyst is not a problem with pure olefins. We have hydrogenated as many as 40 samples on the same catalyst charge with no decrease in reaction rate and no evidence of incomplete reaction.

Extrapolation of the Temperature-Time Curve. Figure 2 is, in effect, a temperature–time curve familiar from classical calorimetry except that the temperature axis is in units of recorder scale deflection instead of degrees. That we do not know how many units of scale deflection equal one degree is immaterial because all measurements are relative to a known standard or a calibration curve constructed therefrom.

We attribute the maximum in Figure 2 to rapid transfer of heat generated by the reaction to the stirred reaction mixture followed by slow transfer of heat from the reaction mixture to the reaction chamber and its fittings. Because of this, Figure 2 is not strictly comparable to the cases treated in the literature (*9*), and we have not attempted to extrapolate this curve in the usual way by truncating the maximum. Instead, we have used the extrapolation shown in Figure 2 which includes the maximum. This amounts to extrapolating out the heat capacity of the reaction chamber and fittings and comparing temperature increments of the stirred solutions independent of the reaction chamber. Heat rise is measured by the vertical in Figure 2 in accord with Skinner's recommendation for fast reactions (*18*).

Microanalysis. The determination of synthetic unknowns of cyclohexene in *n*-hexane is shown in Figure 3 in the form of a plot of micromoles of unknown taken as a function of micromoles of unknown found. The series resistance was 6500 ohms. Cyclopentene in *n*-hexane and 1-hexene in *n*-hexane are shown as the first two entries in Table I. The series resistance was 5000 ohms for cyclopentene and 5500 ohms for 1-hexene. The last column in Table I is the relative standard deviation from the "best" straight line through the data, as computed by a linear regression technique.

Ultramicro Analysis. We felt that at series resistance of 5000 ohms and more (bridge input voltage, 600 mV or less) we were not taking advantage of the full potential of the apparatus. Therefore we decided to select one substance and to decrease its concentration to the limit of the apparatus.

In connection with some other work, we had become interested in phenylacetylene; hence, we selected it as our test substance. Selection of an acetylene instead of a monoolefin ensures a twofold increase in sensitivity because two pi bonds are hydrogenated rather than one (nothing happens to the ring). We feel, however, that the great increase in sensitivity shown in the fourth entry in Table I and the respectable level of error show that direct enthalpimetric determination of unsaturation at the ultramicro level is a method of considerable promise. We do not feel that the concentrations shown in Table I represent the ultimate limit of sensitivity and we are presently redesigning the apparatus to improve this feature of the method.

The need for improved sensitivity is evident from the last two entries in Table I. These esters have a high molecular weight; consequently, they give off a relatively small amount of heat per mole. Moreover, they are viscous and difficult to handle in the pure state using microvolumetric equipment. Improved sensitivity would enable one to handle dilute solutions of high molecular weight compounds and to extend the method to solid compounds containing double bonds which may have limited solubility in the calorimeter fluid.

Disadvantages. Like all methods of great generality, DIE methods are nonspecific; one cannot, in general, determine one olefin in the presence of another. An exception is the determination of normal unsaturation in the presence of an aromatic compound as in the case of cyclohexene in benzene or even differentiation between normal and aromatic unsaturation in the same molecule as in the hydrogenation of the acetylenic double bond in phenylacetylene while not disturbing the ring.

Some heats of hydrogenation differ from others even for compounds containing only one double bond. One must, therefore, have a pretty good idea of what olefins are present for the DIE method to be useful. Reasons for differences in heat output are generally related to steric strain.

Compounds contaminated by sulfides can be expected to poison the catalyst.

(17) T. Flirtcroft, H. A. Skinner, and M. C. Whiting, *Trans. Faraday Soc.*, **53**, 784 (1957).

(18) H. A. Skinner, in "Biochemical Microcalorimetry," H. D. Brown, Ed., Academic Press, New York, N.Y., 1969, p 6.

Although the compounds reported here and twenty or thirty others we have investigated are fast reacting, we have run across a few which are not. Pinene does not react rapidly under these conditions and the DIE method is not applicable.

We have encountered one case of a strained diolefin in which one double bond is hydrogenated while the other is not (*10*). While this poses some interesting structural problems, it does not effect the DIE method.

Heat of Solution. The linear calibration curve of scale deflection *vs.* concentration does not, in general, pass through the origin. This is because of the heat of solution of the inert diluent and the heat of solution of the reaction product obtained on hydrogenating the olefin. Thermochemical analysis (*12*, *16*) shows that even the heat of hydrogenation of a pure olefin must be corrected for the heat of solution of the reaction product. Wide variation in the nature of the inert diluent can cause some error. Thus, if the calibration curve were constructed using solutions of olefin in hexane and unknowns were olefin in decane, a small error would result. Our heat of solution studies (*19*) indicate that this error would be 1–2% in the most unfavorable cases and would vanish as the nature of the inert solvent is known and unknown samples become more similar.

ACKNOWLEDGMENT

The author wishes to acknowledge the sabbatical leave granted by Long Island University during which this work was done.

RECEIVED for review March 12, 1971. Accepted June 8, 1971.

(19) E. Bretschneider and D. W. Rogers, *Mikrochim. Acta*, **1970**, 482.

Automated Data Acquisition System and Computer Analysis for Sedimentation Equilibrium Experiments

A. C. Beckwith, H. C. Nielsen, and R. O. Butterfield

Northern Regional Research Laboratory, Northern Marketing and Nutrition Research Division, Agricultural Research Service, U. S. Department of Agriculture, Peoria, Ill. 61604.

A method is presented which shows that commercially available digital voltmeters and high speed paper tape punches can be used to digitize the analog output from a photoelectric scanner attachment on the analytical ultracentrifuge. Equations which are used in a computer analysis of the digital information are developed. Computer output can be presented in a variety of ways for the convenience of the experimenter, but most generally is shown as apparent molecular weight *vs.* concentration The method provides better than a 30-fold decrease in the time required to carry out a complete analysis over manual methods while using at least a 10-fold increase in the amount of information across the solution column at equilibrium.

OF THE TWO GENERAL ultracentrifuge methods, the equilibrium method is probably the best for determining the molecular weights and molecular weight distributions of macromolecules. In the equilibrium method, tedious measurements must be made before the output from the optical systems on the centrifuge can be converted to values of concentrations and radii and these variables, in turn, must be manipulated in rather involved calculations before obtaining molecular weight values.

Many computer programs are available which perform the required calculations. The more general of these programs have been reviewed by Trautman (*1*). However, with these programs, the task of converting the optical output to a form which can be accepted by a computer still remains.

The development of the scanning absorbance optics for the ultracentrifuge (*2*) made it possible to devise equipment that would convert raw data from the centrifuge to a form directly readable by a computer. Spragg (*3*) and Spragg and Goodman (*4*) have automated the data acquisition using an ultracentrifuge–computer on-line operation.

The results presented in this paper were obtained with an integrating digital voltmeter and paper tape punch to collect the raw data from an absorbance scanner attachment. A computer converted this information into units of concentrations and radii and calculated apparent molecular weight values at many points within the solution column at sedimentation equilibrium. The data acquisition system to be described permitted the use of conventional double sector cells in multiplaced rotors so that parameters such as solvent and initial solute concentration could be varied in a single equilibrium experiment. A rapid computer analysis of the data made it possible to use the ultracentrifuge routinely to explore the sedimentation behavior of paucidispersed, associating–dissociating, or ideal macromolecular solutions.

THEORETICAL

The general starting point used in preparing the computer analysis considers a solution of nonelectrolyte polymer in an incompressible solvent at sedimentation equilibrium. The polymer consists of n components capable of having different molecular weights. The fundamental equation of interest which applies to any component j in this system is given by Equation 1.

$$M_j c_j (1 - \bar{v}_j \rho) w^2 r c_j / RT = dc_j/dr + M_j c_j \sum_{k=1}^{n} B_{jk}(dc_k/dr) + \ldots \quad (1)$$

(1) R. Trautman, "Fractions," Bull. No. 2, Spinco Inc., Palo Alto, Calif., 1966.
(2) L. Lamers, F. Putney, I. Z. Steinberg, and H. K. Schachman, *Arch. Biochem. Biophys.*, **103** 379 (1963).
(3) S. D. Spragg, *Anal. Chim. Acta*, **38**, 137 (1967).
(4) S. D. Spragg and R. F. Goodman, *Ann. N.Y. Acad. Sci.*, **164**, 294 (1969).

The theoretical development and standard meanings for the terms in Equation 1 can be found in reference (*5*). Terms containing higher powers of concentration for all components have been neglected. Since it is generally assumed that the partial specific volumes are the same for all components, the subscript on $\bar{v}$ is not needed.

For subsequent testing purposes, it was convenient to represent the coefficients B_{jk} in Equation 1 in terms of an average value B and a deviation from the average Δ_{jk}. Making this substitution and using the standard definitions, $c = \sum_{l=1}^{n} c_l$ and $\bar{M}_w = \sum_{l=1}^{n} M_l c_l/c$, where c is the total concentration and $\bar{M}_w$ the weight average molecular weight, Equation 1 is summed over j from 1 to n to yield after some rearrangement

$$[1 + B\bar{M}_w c]d\ln c = \lambda\bar{M}_w d(r^2) - \sum_{j=1}^{n} M_j \sum_{k=1}^{n} \frac{\Delta_{jk} c_j dc_k}{c} \quad (2)$$

where $\lambda = (1 - \bar{v}\rho)\omega^2/2\,RT$.

Since an absorbance profile gives information pertaining only to total concentration, the integral of 2 is most directly applied to scanner signal values. Because of electronic and other forms of signal noise, Equation 2 is not easily and rapidly evaluated by numerical integration methods. To obtain an approximation to the integral of 2 which could later be used in a standard regression analysis, it is noted that other workers (*6*, *7*) have represented the total concentration at any radius in the solution column by a sum of exponential terms of the form:

$$C_l = b_l e^{a_l r^2} \text{ and } C = \sum_{l=1}^{n} b_l e^{a_l r^2} \quad (3)$$

which can be derived from 1 by first equating all B_{jk}'s to zero.

Since Equation 2 already contains an estimate for thermodynamic nonideality, it is assumed that Equation 3 can be used to approoximate the ratios appearing within the second summation on the right in Equation 2. However, before carrying out the integration, the exponential terms can be expanded as their Taylor series and coefficients having similar powers of the radius collected. After carrying out the indicated division with the series approximations, the integration produces

$$\ln c + B\bar{M}_w c = I + (\lambda\bar{M}_w - K_0)r^2 - \sum_{l=1}^{m} K_l r^{2l+2} \quad (4)$$

I is a general constant of integration and the K's arise as a result of using Taylor series approximations for exponential functions.

Finally, in order to relate Equation 4 to absorbance or digital signal, it must be assumed that some average absorptivity value applies for all components. For paucidispersed systems this assumption may not be valid, but for ideal systems and simple systems undergoing association-dissociation reactions, the assumption should not introduce a serious error (*7*). Therefore, if Y represents the absorbance or the corrected digital signal across the solution column, the equation in Y corresponding to Equation 4 has the form

$$\ln Y + A_3 Y = A_1 + A_2 r^2 + \sum_{k=4}^{m} A_k (r^2)^{k-2} \quad (5)$$

Additional comments pertaining to the use of Equation 5 appear in later sections.

EXPERIMENTAL

Equipment A Spinco Model E analytical ultracentrifuge equipped with an RTIC unit, a photoelectric scanner attachment, and a multiplexing accessory was used in these studies. The multiplexing accessory permitted direct photoelectric scanning of absorbance profiles from one to five double-sector cells during a single experiment.

An Infotronics Corp. Model CRS-30 integrating digital voltmeter was connected directly to the output of the photoelectric scanner (at the recorder input terminals). This mode of connection took full advantage of the multiplexing accessory when using multiplaced rotors. The high impedance CRS-30 is designed to average a voltage for a selected period of time and then punch the average voltage, expressed in relative units of selected full-scale voltage, onto paper tape with a precision of 1 to 2 parts per 100,000.

A Teletype BPRE-II paper tape punch, capable of punching up to 110 characters per sec, was connected to the output of the CRS-30. A five-digit number and an end-of-line character was punched in standard IBM 8-channel paper tape code.

A system of relays designed to control the operational conditions of the CRS-30 and tape punch were actuated from a single stack on the step function switch of the scanner.

An IBM-1130 computing system with 8K core, disk, paper tape reader, card reader, printer, and plotter was used to analyze all results of the equilibrium experiments.

Materials. Proteins that have been used for testing the procedure were bovine hemoglobin (Hb) (2× crystallization) obtained from Pentex Inc., sperm whale myoglobin supplied by the Mann Research Laboratories, Inc., and ribonuclease A purchased from the Sigma Chemical Co. A sample of gamma-3 wheat gliadin was provided by K. R. Sexson of the Northern Laboratory.

L-Tyrosine purchased from the National Biochemical Corp. served as an absorbance standard at 278 nm for testing the photoelectric scanner in its function as a spectrophotometer.

Other chemicals used in preparing solutions were commercially available reagent-grade chemicals.

Methods. Five standard solutions of L-tyrosine were prepared in 0.01*N* HCl and the ultraviolet spectra of the solutions were determined on a Cary 14 spectrophotometer with quartz cells having a 10-mm pathlength. The measured absorbance at 278 nm for these solutions was corrected for the 12-mm light path of the double-sector centrifuge cells. Five double-sector cells, each containing a tyrosine solution of a different concentration and also 0.01*N* HCl solvent, were used in a six-place rotor along with the scanner's reference cell. Absorbance profiles at 278 nm across the cells were determined at 25 °C and at three different rotor speeds: 10,589; 17,250; and 27,690 rpm.

Stock solutions of ribonuclease and myoglobulin were prepared in 0.15*M* KCl; a solution of Hb, in 0.1*M* NaCl; and a solution of wheat gamma-3 gliadin, in 3*M* urea–0.15*M* KCl. These stock solutions were dialyzed against solvent for 24 hours at 4 °C before preparing dilutions for sedimentation equilibrium determinations.

Equilibrium runs were made at 20.9 °C and 17,250 rpm for ribonuclease and myoglobin; at 16.5 °C and 10,589 rpm for Hb; and at 16.6 °C and 15,220 rpm for gamma-3 gliadin. Scanner response for each solution was converted to digital values on punched paper tape as soon as the rotor reached the desired speed in order to obtain information relating to initial protein concentrations. The digitizing process was repeated after reaching the equilibrium state. In accordance with the recommendations of Barlow *et al.* (*8*), high speed profiles

(5) H. Fujita, "Mathematical Theory of Sedimentation Analysis," Academic Press, New York, N. Y., 1962.
(6) T. H. Donnelly, *J. Phys. Chem.*, **70**, 1862 (1966).
(7) S. J. Edelstein, M. J., Rehmar, J. S. Olson, and G. H. Gibson, *J. Biol. Chem.*, **245**, 4372 (1970).
(8) G. H. Barlow, L. Summaria, and K. C. Robbins, *J. Biol. Chem.*, **244** 1138 (1969).

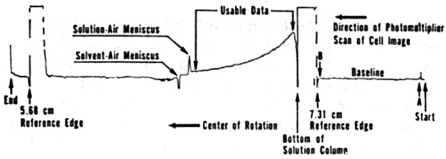

Figure 1. Tracing of photoelectric scanner recording, indicating reference points and work data described in text

(39,460 rpm for Hb and gamma gliadin; 59,780 for ribonuclease and myoglobin) were digitized in order to prepare proper base-line corrections. However, the scanner response was not sampled until the rotor speed was slowly reduced to that of the equilibrium determination.

The permanent records of the experiments in the form of punched paper tapes were then analyzed on the IBM 1130 computing system.

Numerical Analysis For practical reasons, the upper limit of the index k in Equation 5, while extending to infinity, was taken as $m = 8$. With this upper limit, a total of seven mathematical models can be generated from Equation 5 which were used in a standard form of regression analysis to test the data within the solution column.

$$\begin{aligned}
&\text{(a)}\ \ln Y = A_1 + A_2 r^2 \\
&\text{(b)}\ \ln Y + A_3 Y = A_1 + A_2 r^2 \\
&\text{(c)}\ \ln Y + A_3 Y = A_1 + A_2 r^2 + A_4 r^4 \\
&\quad \cdots \\
&\text{(g)}\ \ln Y + A_3 Y = A_1 + A_2 r^2 + \sum_{k=4}^{8} A_k (r^2)^{k-2}
\end{aligned} \tag{6}$$

Once estimates of the coefficients were obtained, calculated values of Y were found by a Newton–Rapheson iteration procedure. The choice of which model best fit the data was made on the basis of an F ratio test. The chosen model was then used to calculate the quantities.

$$d\ln Y/d(r^2) = d\ \ln c/\mathrm{d}(r^2) \text{ and } M_{w\ \mathrm{app}} = \frac{2RT}{(1 - \bar{v}\rho)\omega^2}\, d\ln Y/d(r^2) \tag{7}$$

at a large number of discrete points across the solution column. $M_{w\ \mathrm{app}}$ is the apparent weight average molecular weight at concentration c.

In Equation 7, values for $\bar{v}$ were taken from the literature for Hb, myoglobin, and ribonuclease (*7*, *9*, *10*) and estimated from amino acid composition (*11*) for gamma gliadin. The density of dilute salt solutions was taken to be that of water at the specified temperature whereas the solvent density was used for urea solutions.

RESULTS AND DISCUSSION

The absorbance data for solutions of nonsedimenting L-tyrosine at 278 nm had standard deviation amounting to less than 2% of the average count value. The term count refers to the net digital signal after substracting base-line corrections. At a given rotor speed the average count value across the tyrosine solutions was linear with absorbance measured on the Cary 14 spectrophotometer. The results clearly indicated, however, that the scanner response changed slightly with changes in rotor speed. This change amounted to 48 counts per absorbance unit for each 1000-rpm increase in rotor speed. Because of this change, all data sampling for protein solutions was done at the speed of the equilibrium determination.

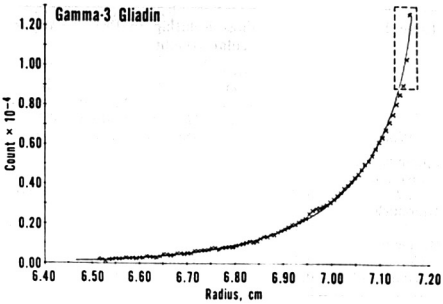

Figure 2. Calculated curve (——) using best fitting equation through every other digitizer count (xxx) in working area of data

A traced scanner recording of signal changes is shown in Figure 1 for a solution of Hb at sedimentation equilibrium. The initial protein concentration was 0.146 mg/ml. Depending upon the size of the cell image at the phototube slit, the integrating digital voltmeter averages the signal some 800–1000 times between start and end (Figure 1). All points bearing labels in Figure 1 are isolated out of the digital record by the computer which also assigns radial distances to the reference hole edges. The information between A and B in Figure 1 establishes a digital base-line average and the variance of the data is used for F ratio tests. Since the anomalies in the profile at the solution air meniscus and near the bottom of the cell prohibit the use of information in these regions, the portion of the profile labeled Usable Data in Figure 1 was used in the regression analysis. Estimates of apparent molecular weights and quantities proportional to concentration at the meniscus and bottom of the cell must be obtained by extrapolation procedures to determine the weight average molecular weight for the undistributed solute.

Treating any system as being composed of solvent and a single macromolecular solute, Equation 1 was developed along similar lines as that described by Nordby and Oncley (*12*) as the equation would apply to absorbance optics. In terms of the variable Y, defined earlier, Equation 6b can be shown to represent the simplest form of this equation. As was expected, the mere introduction of higher powers of the dependent variable did not improve the general applicability of 6b.

By first equating the Bjk's to zero, a general equation consisting of a series of exponential expression can be derived from Equation 1 (*6*, *7*). Curve fitting with this general type of equation proved very time-consuming since it was assumed that prior knowledge about the number of components and the size of the components was unavailable.

Equations 6a–6g circumvented the above difficulties and gave more reliable estimates for extrapolated derivative quantities and concentration values than did simple or orthogonal

(9) H. K. Schachman and S. J. Edelstein, *Biochemistry*, **5**, 2681 (1966).
(10) K. E. Van Holde and R. L. Baldwin, *J. Phys. Chem.*, **62**, 734 (1958).
(11) T. L. McMeekin, M. L., Groves, and N. J. Hipp, *J. Amer. Chem. Soc.*, **7** 3298 (1949).
(12) G. L. Nordby and J. L. Oncley, "Biophysics Research Reports—Number 1," University of Michigan, Ann Arbor, Mich., 1964.

Table I. Computer Findings Relating to Protein Apparent Molecular Weights

Protein	Initial concn., mg/ml	Equation used for fitting	M_{app} at meniscus	M_{app} at bottom of cell	$\bar{M}_w$ for undistributed solute
Sperm whale myoglobin (*9*, *13*)	0.080	6a	...	...	16,000
Ribonuclease (*10*)	0.171	6a	...	...	13,830
Bovine hemoglobin (*7*, *9*)	0.146	6b	39,550	55,960	46,420
γ_3-Gliadin (*14*)	0.320	6c	36,650	101,500	47,250

polynomials. In support of this claim, a portion of the computer results for gamma-3 wheat gliadin is presented in Figure 2. This protein preparation contained an impurity with a 260-nm absorbance maxima and represented an example of a paucidispersed system. The X's in Figure 2 represent every other count in the usable data (Figure 1). The smooth curve in Figure 2 was obtained with an equation similar to 6c. The curve as presented in Figure 2 has not been extrapolated to the bottom of the cell whereas the extrapolation to the meniscus is shown. The effects upon the analysis due to the presence of a small amount of high molecular weight impurity can be detected and evaluated by deleting a few data points at the bottom of the cell as indicated by the dashed rectangle in Figure 2. The ordinate in Figure 2 is in units of Y described earlier.

Table I summarizes the results obtained with the proteins used for this presentation. As seen from Table I, both myoglobin and ribonuclease showed ideal sedimentation behavior. The molecular weight shown for ribonuclease is in the range found by Van Holde and Baldwin (*10*). The molecular weight of myoglobin shown in Table I is from a single experiment only and is somewhat lower than the values given in the references (*9*, *13*). Within the estimated error for a single experiment, the observed molecular weight reported in Table I could be as large as 16,400. Schachman and Edelstein (*9*) and Edelstein *et al.* (*7*) have described the concentration dependence for the molecular weight of Hb. The results presented in (*7*) clearly indicate the effect of solvent upon molecular weight values obtained. The number average molecular weight for the Hb used here has been reported as 68,500 + 1900 (*15*). The results in Table I for Hb clearly suggest that a monomer–dimer type of association could be present in the system at sedimentation equilibrium. The choice of Equation 6b shown in Table I means that an equation of the form 6b describes the usable data in Figure 1 to within the uncertainty of the base line at a 95% confidence limit. Expressed in terms of concentration units (mg/ml), Equation 6b for Hb is

$$\ln c - 0.978\,c = -14.0 + 0.245\,r^2 \qquad (8)$$

Equation 8 can now be used to estimate initial values for a monomer molecular weight at zero concentration as well as provide an initial estimate for the constant representing thermodynamic nonideality. The values obtained are 38,300 grams/mole and −0.0000256 ml/mg, respectively. It is to be noted that the general approach taken here cannot be expected to describe accurately those features which may be characteristic for special systems. However, the results obtained with this method can serve as an excellent starting point for further detailed analyses, with Hb representing a good example of this feature. At this point the reader is referred to the theoretical discussions of Adams and Fujita (*16*). For a monomer–dimer type of association–dissociation, Equation 22 in (*16*) can be integrated to yield an expression for the total concentration:

$$M_1(r^2 - r_m^2)\frac{(1-\bar{\nu}\rho)^2}{RT} = \ln\frac{c}{c_m} + 2BM_1(c - c_m) + \ln\left.\frac{\sqrt{1+4K_2c}-1}{\sqrt{1+4K_2c}+1}\right|_{c_m}^{c} \qquad (9)$$

r_m and c_m are the radius value and total concentration at the meniscus and K_2 is a dissociation constant. Other terms in Equation 9 have their usual meaning. Equation 9 is presented here only to point out that if an unknown system at sedimentation equilibrium is suspected of undergoing a monomer–dimer interaction, the Equations 6b–g can be used to obtain the best estimate for c_m as well as initial values for M_1 and B in Equation 9. The usable data can now be reanalyzed in terms of Equation 9 using an iterative procedure to obtain best values for M_1, B, and K_2. This has not been done for the purpose of this presentation in the case of Hb.

By using the standard deviation obtained from the regression analysis, the weight average molecular weight for the undistributed proteins has an uncertainty of ±2.5% or less. The uncertainty is about twice this value for estimates of apparent molecular weights at the meniscus and less than half this uncertainty for molecular weights at the bottom of the cell.

Finally, options have been built into the computer analysis so that reciprocal quantities such as $M_w^{-1}{}_{app}$ can be printed and plotted as a function of Y or concentration. Advantages for using the results in this form can be found in any treatise relating to sedimentation theory.

CONCLUSIONS

The main objective of this work has not been to report molecular weight values for well characterized protein systems, but rather to describe briefly a method that provides a rapid analysis of sedimentation equilibrium data. Relatively inexpensive and commercially available components have served to interface the centrifuge with a computer, thereby eliminating the tedium of data gathering. The software used in no way limits the use of other absorbance scanner accessories. Molecular weights for a particular system can still be examined as a function of concentration or solvent in a single equilibrium experiment. A computer analysis rapidly converts experimental results into meaningful apparent molecular weight values for a wide variety of sedimenting systems.

RECEIVED for review March 15, 1971. Accepted June 11, 1971. The Northern Regional Research Laboratory is headquarters for the Northern Marketing and Nutrition Research Division, Agricultural Research Service, U.S. Department of Agriculture. Mention of firm names or trade products is for identification only and does not imply endorsement by the Department.

(13) E. J. Cohn and J. T. Edsall, "Proteins, Amino Acids, and Peptides," Reinhold Publishing Corp., New York, N. Y., 1943.
(14) R. W. Jones, G. E. Babcock, and R. J. Dimler, *Cereal Chem.*, **42**, 210 (1965).
(15) Y. V. Wu, J. E. Cluskey, and K. R. Sexson, *Biochim. Biophys. Acta*, **133**, 83 (1967).
(16) E. T. Adams, Jr., and H. Fujita, in "Ultracentrifugal Analysis in Theory and Experiment," J. W. Williams, Ed., Academic Press, New York, N. Y., 1963, Part II, p 119.

Simplified Rapid Procedure for Determination of Agmatine and Other Guanidino-Containing Compounds

Millicent C. Goldschmidt[1] and Betty M. Lockhart

Department of Clinical Pathology, The University of Texas M. D. Anderson Hospital and Tumor Institute at Houston, and The University of Texas Graduate School of Biomedical Sciences, Houston, Texas 77025

This paper presents an adaptation of two methods into a single rapid and sensitive micro-quantitative and/or -qualitative procedure for use in the routine laboratory analyses of guanidino compounds. Agmatine can be quantitatively or qualitatively detected in the presence of arginine or creatine following a differential extraction with an alkaline *n*-butanol solution. 80–85% of the agmatine is removed from an aqueous solution by this procedure. The agmatine is quickly visualized (within 3 min) by the addition of a modified diacetyl reagent to the butanol layer. As little as 5–10 μg/ml of agmatine can be detected. Differential extraction of several other guanidino and related compounds is discussed. In addition, the same reagent can be used to quantitate agmatine, arginine, creatine, and other guanidino-containing compounds over a range of 2–90 μg/ml. Time concentration curves are also presented.

AGMATINE, the amine formed by decarboxylation of arginine, is usually determined in biological systems either by the production of CO_2 (*1*), a color change in an indicator (*2*), or fluorometric analysis (*3*). Sakaguchi's reagent (*4*, *5*), diacetyl (*6–8*), and phenanthrequinone (*9*) have also been used to detect guanidino-containing compounds (*10*).

This paper presents a rapid and sensitive micromethod for the qualitative and quantitative determination of agmatine, arginine, and several other guanidino-containing compounds. In combination with a modified differential procedure, agmatine can be determined in the presence of arginine. A simplified diacetyl reagent quickly allows the visualization of these compounds on either a qualitative or quantitative basis.

EXPERIMENTAL

Reagents and Equipment. All chemicals were reagent grade unless otherwise specified and the solvents were spectro quality. Glass distilled water was used. Solutions of 1-naphthol and diacetyl (2,3-butanedione) were stored in dark (amber) glass bottles in the cold. Pre-coated Silica Gel thin-layer chromatography (TLC) plates without fluorescent indicator (E. Merck AG, Darmstadt, Germany) were obtained from Brinkmann Instruments, Inc. A DK-2A Ratio Recording Spectrophotometer (Beckman Instruments, Inc.) and a Zeiss Spectrophotometer PMQII (Brinkmann Instruments, Inc.) were used.

Procedures. DIACETYL REAGENT. The diacetyl reagent consisted of a combination of two solutions which were stored separately and mixed together before use. Solution A: 60 μl of diacetyl were diluted to 100 ml with distilled water and refrigerated in a dark glass bottle for periods not exceeding 2 weeks. Solution B: 1 gram of 1-naphthol, 6 grams of NaOH, and 20 grams of NaCl were dissolved in distilled water, diluted to 100 ml and stored in a dark glass bottle at −5 °C for periods not exceeding 3–4 weeks. This solution remains a liquid at this temperature. The solutions were freshly mixed daily in the proportions of 2 parts A + 3 parts B. It was also possible to add each solution individually to the sample in these proportions. Three milliliters of the diacetyl reagent were added to each 6-ml sample. The appearance of a red-purple color within 3–5 min indicated the presence of a guanidino containing compound.

DIFFERENTIAL EXTRACTION PROCEDURE. The procedure used by Cohn and Shore (*3*) to extract agmatine from a mixture of arginine and agmatine has been greatly simplified and modified. A salt-saturated KOH solution was prepared by adding sufficient solid NaCl to 10% KOH so that an excess of NaCl remained in the flask. Equal proportions of the sample and this solution (2 ml of each) were mixed in 125- × 16-mm screw cap test tubes. The differential extraction was completed by adding 2 ml of *n*-butanol to each tube. The tubes were then agitated for 1–2 min and centrifuged or allowed to settle. Then, 0.5 ml of the top butanol layer was removed and mixed with the diacetyl reagent to detect the appearance of colored derivatives in this layer. If only a qualitative estimation was desired, it was not necessary to remove the butanol layer from the reaction tube. The diacetyl reagent was added directly to the butanol layer, the tube agitated slightly, and this layer observed for color formation.

THIN-LAYER CHROMATOGRAPHY. Ascending one-dimensional chromatograms were obtained using Silica Gel thin-layer chromatography plates. These were preactivated by heating for 30 min at 100–110 °C and could be stored for several months in a desiccator chamber without further reactivation. The solvent system consisted of a mixture of phenol, acetic acid, and water in a ratio of 6:1:6. The plates were dried at 100–110 °C before developing. Several spray reagents were used to observe the positions of the compounds on the plates. These were prepared as follows:

Ninhydrin Spray Reagent Ninhydrin, 0.1 gram, was dissolved in a small volume of 95% ethanol and brought to a final volume of 100 ml with chloroform. The plates were then heated to 100–110 °C just until the purple-orange color developed.

Diacetyl Spray Reagent. Soution A was sprayed on the plates. After air drying, solution B was sprayed on the plates. The plates were then heated to 100–110 °C just until the red-orange color developed.

Sakaguchi Spray Reagent. The thymine, 1-naphthol, and thiosulfate solutions were combined as indicated in the pro-

[1] Present address, The University of Texas Graduate School of Biomedical Sciences at Houston, 109 Herman Professional Building Garage, 6410 Fannin, Houston, Texas 77025

(1) E. F. Gale in "Methods of Biochemical Analysis," D. Glick, Ed., Vol. 4, Interscience, New York, N.Y., 1957, p 285.
(2) V. Moller, *Acta. Pathol. Microbiol. Scand.*, **34**, 102 (1954).
(3) V. H. Cohn and P. A. Shore, *Anal. Biochem.*, **2**, 237 (1961).
(4 S. Sakaguchi, *J. Biochem.*, **37**, 231 (1950).
(5) J. F. Van Pilsum, R. P. Martin, E. Kito, and J. Hess, *J. Biol. Chem.*, **222**, 225 (1956).
(6) A. H. Ennor and L. A. Stocken, *Biochem. J.*, **55**, 310 (1953).
(7) H. Rosenberg, A. H. Ennor, and J. F. Morrison, *ibid.*, **63**, 153 (1956).
(8) L. Meites, "Handbook of Analytical Chemistry," McGraw-Hill, New York, N.Y., 1963, pp 10–83.
(9) B. E. Magun and J. W. Kelly, *J. Histochem. Cytochem.* **17**, 821 (1969).
(10) J. E. Bonas, B. D. Cohen, and S. Natelson, *Microchem. J.*, **7**, 63 (1963).

Table I. Qualitative Determination of Guanidino-Containing Compounds before and after Differential Butanol Extraction

	Before extraction					After extraction				
	In tube		On chromatogram			In tube[a]		On chromatogram[a]		
Compound	Da	Sak	Da	Sak	Nin	Da	Sak	Da	Sak	Nin
Agmatine	+	+	+	+	+	+	+	+	+	+
L-Arginine	+	+	+	+	+	−	−	−	−	−
L-Homoarginine	+	+	+	+	+	−	−	−	−	−
Creatine	+	−	+	−	−	−	−	−	−	−
Creatinine[b]	+	−	+	−	−	−	−	−	−	−
Spermine	−	−	−	−	+	−	−	−	−	+
Spermidine	−	−	−	−	+	−	−	−	−	+
L-Citrulline	−	−	−	−	+	−	−	−	−	−
L-Canavanine[c]	+	−	+	+	+	−	−	−	−	−
4-Guanidinobutyl-1-amine	+	+	+	+	+	+	+	+	+	+
1,4-Diguanidobutane sulfate	+	+	+	+	−	+	+	+	+	−

+ = red-purple or orange color indicating presence of guanidino compounds.
− = no color or absence of these compounds.
Extraction = treatment with NaCl saturated 10% KOH followed by agitation with *n*-butanol.
Sak = Sakaguchi reagent.
Da = Diacetyl reagent.
Nin = Ninhydrin reagent.

[a] = *n*-Butanol layer.
[b] = Very very weak diacetyl reactions.
[c] = Very weak Sakaguchi reaction on chromatogram.
20 to 40 micrograms were used to spot the chromatograms; 80–100 micrograms/ml were added to the tubes in these reactions.

cedure of Bonas *et al.* (*10*) except that the NaOCl was not added. The plates were sprayed with this solution and heated to 100–110 °C for 1–3 min. While still hot, they were sprayed with NaOCl (undiluted commercial Clorox) to develop the orange color associated with guanidino groups.

SPECTROPHOTOMETRIC DETERMINATIONS. Samples for spectrophotometric determinations were dissolved in distilled water and reacted with the diacetyl reagent. Similar samples were differentially extracted and the butanol layer reacted with the diacetyl reagent. The samples were then pipetted into cuvettes and placed in the Beckman DK-2A Ratio Recording Spectrophotometer to obtain the characteristic absorption curves. Quantitative measurements were also made on these solutions using a Zeiss Spectrophotometer model PMQII. The wavelength used depended on the absorption characteristics of the compounds and is so indicated in the data.

RESULTS AND DISCUSSION

Guanidino compounds are important metabolic precursors of many substances including ornithine, urea, and creatinine. Agmatine has been mentioned as one of the classical substrates of diamine oxidase (*3*). In addition, one test used in the identification of Gram-negative bacteria involves a lengthy monitoring of arginine decarboxylase and dihydrolase activity. Thus, a rapid method of detecting and quantitating several important guanidino compounds, especially agmatine, would be of value to the microbiologist and the biochemist. Attempts to develop a rapid routine method for detection of arginine decarboxylase activity in microbial cultures resulted in the adaptation and modification of a differential extraction procedure and a diacetyl reagent into this single method for the rapid detection of agmatine in the presence of arginine. The use of this procedure in the routine detection of agmatine produced by various bacteria (media, pH, and other growth parameters) will be published in a separate paper (*11*).

Qualitative Determinations. Diacetyl and Sakaguchi reagents have been used to detect certain guanidino compounds (*4*, *7*, *8*). However, the Sakaguchi reagent is only specific for monosubstituted guanidino derivatives (*10*). In addition, the control blank is colored, thus making the detection of small amounts very difficult. We have modified the diacetyl reagent so that amounts as low as 2–10 μg of guanidino compounds such as agmatine and arginine can be detected. Related compounds such as citrulline, spermine, and spermidine were also tested to determine the specificity of the reaction with the modified reagent. These data are presented in Table I.

Chromatograms were run on pre-coated thin-layer silica gel plates to observe the position of the different compounds. Although DiJeso (*12*) reported the use of hand-prepared cellulose TLC plates using several different solvent systems followed by many different spray reagents, ours was a simple procedure for these compounds. Duplicate samples were differentially extracted and the butanol layer was tested for compounds which would react with diacetyl and Sakaguchi reagents. Chromatograms similarly monitored the differential extraction process and indicated the presence of only a few guanidino compounds in the butanol layer. These were agmatine, 1,4-diguanidobutane sulfate and 4-guanidinobutyl-1-amine. Chromatograms were also sprayed with ninhydrin to detect the compounds with NH_2 groups and observe their presence before and after differential extraction. A summary of these experiments is presented in Table I. As can be seen, the extraction procedure also removed spermine and spermidine from the mixture.

Meites (*8*) indicated that creatinine gave a positive reaction with diacetyl reagent. However, we observed only a weak reaction with our modified reagent (Table I) and could not detect a reaction with the concentrations used in the recording spectrophotometer (Figure 1). Therefore, this reagent is not recommended for the determination of small amounts of

(11) M. C. Goldschmidt and B. M. Lockhart, *Appl. Microbiol.*, in press.

(12) F. DiJeso, *J. Chromatogr.*, **32**, 269 (1968).

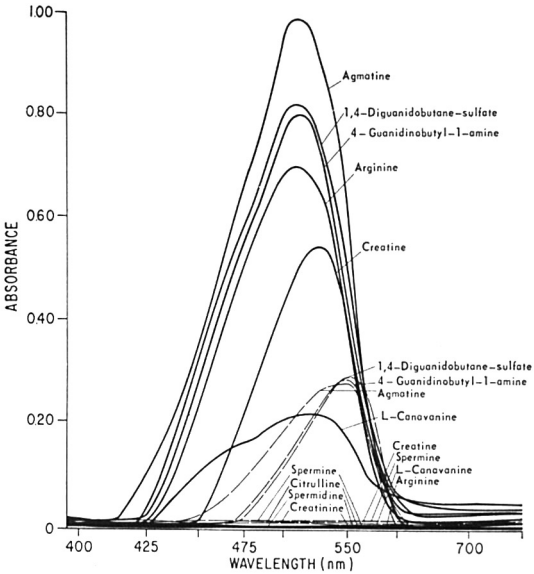

Figure 1. Absorption spectra of various compounds after reacting with the modified diacetyl reagent in water (——) and in the *n*-butanol layer following the differential extraction procedure (- - -)

creatinine (20–50 μg). Addition of 0.1 ml of dimethylsulfoxide per 3 ml of diacetyl reagent slightly intensified the color reaction. The absorption spectra of several guanidino derivatives produced during the reaction with the diacetyl reagent were recorded and reproduced in a composite figure (Figure 1). Several other compounds, such as citrulline, spermine, and spermidine were included in order to observe possible interference and areas of maximal absorbance. The spectral curves for the guanidino derivatives again provided supportive data since they indicated that only agmatine, 1,4-diguanidobutane sulfate, and 4-guanidinobutyl-1-amine were present after the differential extraction procedure with butanol. Since different initial amounts were used in these experiments, the relative proportions before and after extraction cannot be determined from the data. Actually, about 80–85% agmatine was extracted by this method.

Quantitative Determinations. There are several methods reported in the literature for quantitative determinations of various guanidino compounds. Cohn and Shore (*3*) presented a sensitive fluorometric assay for agmatine. Unfortunately, the derivative lost its stability 15 min after the reaction was completed. Several modifications of Sakaguchi's procedure have been published (*4*, *5*, *10*). Hutzler, Odievre, and Dancis (*13*) reported an indirect method for detecting agmatine using dinitrofluorobenzene. However, many of these procedures have high color control blanks or are too lengthy and complicated for routine laboratory procedures. Figures 2–5 show the time-concentration curves for arginine, creatine, agmatine, and 1,4-diguanidobutane sulfate in water, respectively. No one has reported the use of diacetyl in the quantitative determination of agmatine. Ennor and Stocken (*6*) used a diacetyl reagent to assay creatine in the urine. Rosenberg, Ennor, and Morrison (*7*) used a modification of their method for arginine and other guanidino compounds (but not agmatine) and added propanol to increase the sensitivity. The former authors reported that a tenfold increase in the concentration of arginine was needed to produce any results comparable to those obtained with creatine. They further stated that the arginine reaction showed no signs of reaching completion even after 50 min. Our modification lowered the value for arginine to a 2.6-fold equivalency compared to creatine and

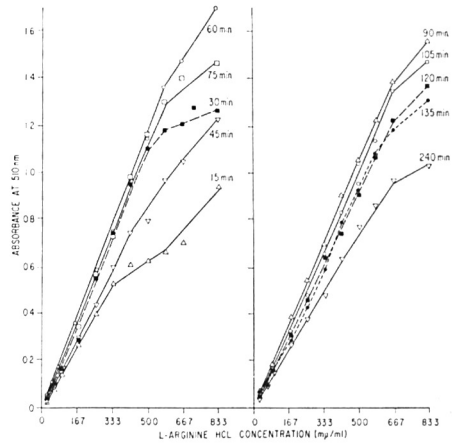

Figure 2. Time course of development, intensity, and stability of the colored derivative formed from the reaction of arginine with the modified diacetyl reagent

(13) J. Hutzler, M. Odievre and J. Dancis, *Anal. Biochem.*, **19**, 529 (1966).

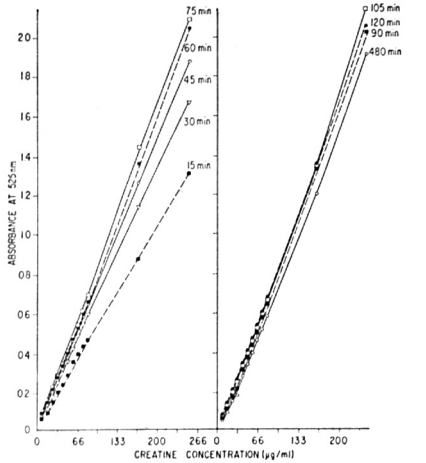

Figure 3. Time course of development, intensity, and stability of the colored derivative formed from the reaction of creatine with the modified diacetyl reagent

the time curves straightened out after 30 min (Figure 3). The results with agmatine (Figure 4) were similar. 1,4-Diguanidobutane sulfate was the least sensitive of the four compounds (Figure 5). As can be seen, these curves had not straightened out by 2 hours. Under our conditions, propanol did not enhance the time or intensity of the color reaction as might possibly be expected from the report of Rosen *et al.* (7). Of all the compounds tested here, creatine was the most sensitive to this reagent as much lower amounts (2 μg/ml) were detected compared to the other compounds. In addition, all time curves were straight even from the earliest assay period of 15 min (Figure 3).

The last four figures showed that the reaction with diacetyl first intensified and then slowly faded with time. However,

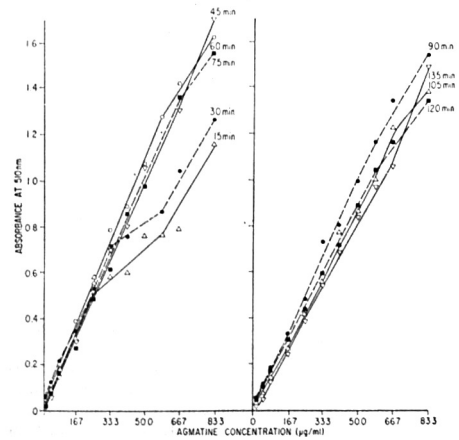

Figure 4. Time course of development, intensity, and stability of the colored derivative formed from the reaction of agmatine with the modified diacetyl reagent

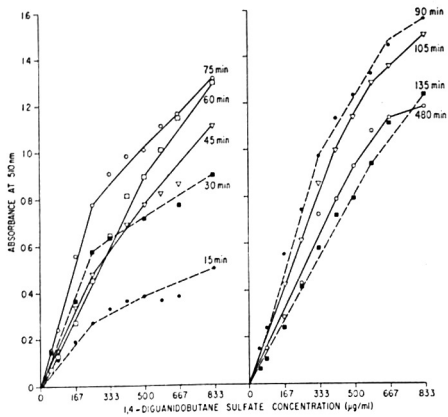

Figure 5. Time course of development, intensity, and stability of the colored derivative formed from the reaction of 1,4-diguanidobutane sulfate with the modified diacetyl reagent

as long as concurrent standards are run, any straight portion of the curves or any standard time could be used for the assay procedure. Probably 35–40 min would be the most convenient.

We next investigated the possibility of diluting the derivatives after a 30- to 40-min color development so that those samples with high values could be determined more accurately on the spectrophotometer. If this were possible, it would save time needed to rerun unknowns with an initial concentration higher than 80 μg/ml. If the samples of agmatine or arginine were diluted with the color control "blank" (Extra color control blanks were prepared for this purpose at the beginning of these experiments.), an average error of 3–6% lower than the theoretical value occurred. When the samples were diluted with water and read against an undiluted color control, the error was 35% above the theoretical value. If both sample and color control were diluted with water, an average error of 7–12% higher than the theoretical value was noted. Errors observed with creatine were very high (25–35%) with any of these procedures. 1,4-Diguanidobutane sulfate was not run. Therefore, only an approximation of the value can be obtained by diluting samples of arginine or agmatine after color development regardless of the diluent employed.

The concentration of agmatine in the butanol layer could also be determined. Since only 80–85% was removed in the first extraction, a second extraction with 2 ml of butanol was necessary to remove the remainder. The two extractions removed 98–99%. When colored derivatives obtained from reacting diacetyl with the guanidino compounds extracted into the butanol layer were run, the samples eventually became cloudy. Results were more accurate when the agmatine was first removed from the butanol layer with water before forming the colored derivatives. Tests showed that all of the agmatine was removed by this method.

CONCLUSIONS

The combination of a differential extraction procedure with a modified diacetyl reagent allowed the rapid detection

of agmatine in the presence of arginine. The method is simple and convenient to perform and would be easily adaptable for routine automated procedures employing autoanalyzers or flow-through cuvette systems now available with many spectrophotometers. In addition, the procedure can be used to quantitate guanidino-containing compounds in general. It should be of value both in routine monitoring of arginine decarboxylase activity or other systems in which agmatine is present in the presence of arginine as well as the detection and assay of other guanidino-containing compounds in general.

RECEIVED for review April 19, 1971. Accepted June 14, 1971. This research was supported, in part, by a research grant from the National Institutes of Health (NCI) No. CA-06939.

On-Line Interactive Data Processing

I. As Applied to Mass Spectrometry and Gas Chromatography

J. W. Frazer, L. R. Carlson, A. M. Kray, and M. R. Bertoglio[1]
Lawrence Radiation Laboratory, University of California, Livermore, Calif. 94550

S. P. Perone
Chemistry Department, Purdue University, Lafayette, Ind. 47907

An interactive computer system used for simple instrument control, data acquisition, and interactive data reduction is described. Emphasis is placed on the interactive data reduction aspects. The approach taken establishes convenient and effective communications links between the processing digital computer and the experimenter–operator such that the computer can execute a variety of tedious processing operations under the continuous guidance of the operator. Thus, the operator can impose his experienced judgment on the net processing procedure by interacting with the computer during data reduction. The operator can oversee the processing functions by graphical communications with the computer through an oscilloscopic display terminal. Applications to spark-source mass spectrometry and gas chromatography are illustrated.

THE WORK PRESENTED here and in the following paper (*1*) provides a description of our interactive computer system used for simple instrument control, data acquisition, and interactive data reduction. The emphasis here will be placed on the interactive data-reduction aspects of this automation. The work describes data reduction of nonroutine data by means of operator interaction with digitized waveforms generated as outputs from chemical instrumentation. Eventually, the work reported here will help support the development of a real-time interactive system for experimentation.

For routine data reduction applications, where the boundary conditions are well defined, it is usually preferable to provide computerization *via* predetermined algorithms. However, it is difficult to incorporate completely into a computer program the complex interpretive processes required to analyze the nonroutine data obtained from research and development projects. These waveforms, obtained as transducer outputs or from the correlation of the data, are often very complex and noisy; the information obtained is often unpredictable in form at the onset of the work; and the waveforms often have drifting or abruptly changing backgrounds. Under those conditions the ability to have dynamic interactive capabilities for the retrieval of information is advantageous.

The data processing approach developed here involves establishing a convenient and effective communications link between the processing digital computer and the experimenter–operator such that the computer can execute a variety of tedious processing operations under the continuous guidance of the operator. Thus, the operator can impose his experienced judgment on the net processing procedure by interacting with the computer during data reduction.

The interactive system developed here incorporates the experimenter–operator into the data processing system in a most efficient manner. The computer is programmed to carry out control functions, data acquisition, and the tedious and difficult computational handling of the data, whereas the operator is required to make judgments regarding the selection of regions of the data to be analyzed and how the analysis should proceed for maximum benefit. These functions are readily selectable by the operator through an oscilloscopic display system which allows graphical communication with the computer. Because of this dynamic computer–display–operator interaction, it is also possible to obtain unique visual perspectives on experimental data. The operator quickly makes a selection, by visual methods, and by mathematical tests, of the best approach for data reduction.

The principal interaction capability is provided by an oscilloscope, a Graf-Pen (Science Accessories Corporation, 65 Station Street, Southport, Conn.), and a special function panel. The Graf-Pen permits the input of information in a manner similar to that provided by a light pen. The special function panel consists of several switches and push buttons which are used by the operator to communicate with the software program to call special calculational, control, and display functions.

Data-processing software will vary with the requirements of various analytical tasks to be performed. Therefore, software was developed such that all programming for data processing was done in the FOCAL language (FOCAL is a trademark of the Digital Equipment Corporation, Maynard,

[1] Present address, Chemistry Department, University of Illinois, Urbana, Ill.

(1) S. P. Perone, J. W. Frazer, and A. M. Kray, ANAL. CHEM., **43**, 1485 (1971).

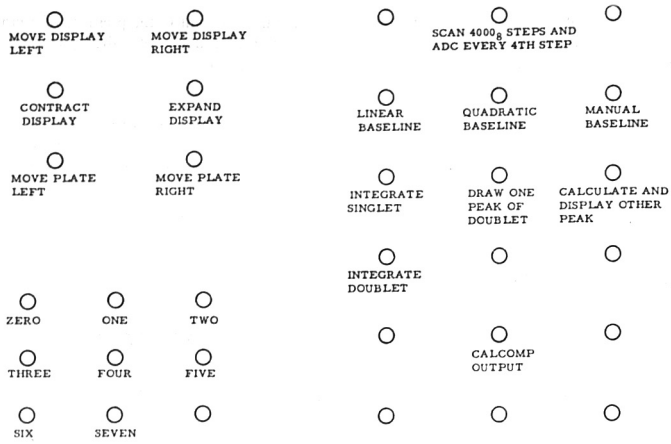

Figure 1. Schematic of the function panel

Mass.). FOCAL is a high-level interpretive language that provides a wide degree of flexibility and convenience. The FOCAL interpreter was modified to provide communication between the interactive display software and the FOCAL data-processing programs. This modification allowed operator interaction through the display system to be transmitted to the FOCAL data-processing programs wherever appropriate. Conversely, it also allowed processing information to be transmitted to the interactive display software.

The use of an interpreter in this application has two effects. First, all computations proceed at a slower rate than would occur with assembly language programs. Second, the effort required for the development of applications programs for data reduction and interactive display is reduced by a couple orders of magnitude. Furthermore, changes in the computational procedures are readily accomplished.

The interactive data processing illustrated here includes methods for handling the variety of base lines encountered, deconvolution of doublets, measurement of peak areas, and the necessary mathematical calculations required to reduce these data, together with calibration data, to quantitative results. In addition, the introduction of deliberate errors in the processing procedure was tested to further demonstrate the applicability of interactive data processing.

EXPERIMENTAL

Computer System. The system consisted of three basic units: a data acquisition system, computer, and interactive terminals. All data acquisition functions were under direct computer control. The display and interactive units consisted of an oscilloscope, special function panel, and a teletypewriter (TTY).

The computer used was a Digital Equipment Corporation (DEC) PDP 8/I with 8K words of core memory and a 32K word magnetic disk. In addition, there was an extended arithmetic unit to provide high speed calculational capabilities, a real-time clock, high speed paper tape reader and punch, and a KSR 33 teletypewriter. The analog-to-digital converter (A/D) was a standard 12-bit DEC AFO1.

The principal interactive terminal was a Tektronix Model 611 large screen oscilloscope, together with a Graf-Pen. The oscilloscope was interfaced so that three modes of operation were available under computer control: (1) Non-store mode, which required continuous refreshing of the display, (2) Store mode, which retained the image for an extended period of time, and (3) Write-Thru mode, which also required continuous refreshing of the display. The write-thru mode allowed transient data to be displayed in conjunction with stored data (*2*).

The Graf-Pen provides the means of operator interaction with the data displayed on the oscilloscope. The display was implemented to have a resolution of 512 in the X direction and 1024 in the Y direction.

The operator communicates with the software through the special function panel. The computer senses when one of the buttons or switches is closed and after identifying the element, gives control to the subroutine (written in assembly language or FOCAL) which is responsible for performing the requested service. A layout of the function panel is shown in Figure 1 together with the functions implemented for the applications described in this paper.

SOFTWARE

The software generated to operate this system falls into two categories: the interactive display program which provides the various functions indicated in Figure 1, and allows the interactive communication between operator, display, and computer; and the data processing software. The data processing software can be written easily in FOCAL by the operator and can be oriented toward the specific type of data he is interested in processing routinely (*e.g.*, electrochemical, gas chromatographic, spectrographic, etc.).

In addition to the function-panel capabilities, a total of 17 additional new linking functions to the display software (Table I) was implemented to improve the interactive capabilities. The use of a high-level interpreter together with these additional capabilities provides a very powerful system that can be modified easily to handle new requirements as they arise.

Large effective processing programs may be implemented by swapping program segments from the disk during program execution. In addition, the disk may be used for storage of program variables or experimental data. It is particularly useful

(2) Nick Stadfeld, "Information Display Systems," Tektronix, Inc., Beaverton, Ore., 1968.

Table I. Linking Functions to the Display Software

FD(OS, T, T ....)	STORE TABLES ON SCREEN—RETURN
FD(OWT, T, T ....)	WRITE THRU TABLES—DOTS
FD(ONS, T, T ....)	NON-STORE
FD(OV)	VANISH THE CRT
FM(OI, N)	SET INCREMENT
FM(CZ, T, T ....)	ZERO TABLES
FM(ODP, T)	DRAW LINE INTO TABLE ONLY THIS LINE AND THE DOTS WILL BE DISPLAYED IN WRITE THRU MODE, SO BE SURE TO DISPLAY EVERYTHING ELSE IN THE STORE MODE.
FM(OD, OV)	VANISH DOTS
FM(OD, OX, N)	GET X VALUE OF THE N, TH DOT
FM(OD, OY, N)	GET Y VALUE OF THE N, TH DOT
FM(OD, OL)	GET LEFT EDGE
FM(OD, OR)	GET RIGHT EDGE
FM(OGD)	GET DATA INTO TABLE O
FM(OT, T)	SET TABLE FOR FG—FP
FM(OCC, T, T, T ....)	PLOT TABLES AND DOTS ON CALCOMP
FG(X)	GET DATA FROM T SET BY FM(OT, T)
FP(X, Y)	PUT DATA INTO T SET BY FM(OT, T)

to be able to save the original data and any intermediate display for future reference.

INTERACTIVE OPERATION

The interactive operation will be described for the data reduction of the spectra recorded on photo plates by a spark source mass spectrograph. Data reduction for gas chromatograms proceeded in a similar manner.

Mass Spectrometer System. The spark source mass spectrograph, Consolidated Electrodynamics Corporation, Model 21-110, is used for the simultaneous determination of up to 45 different elements in rocks and soil samples. A representative sample is ground to a fine powder (<300 mesh), dried to a constant weight, blended in a 1:1 ratio with spectrograde graphite powder, and pelletized. The pellet is sparked at 100 kV and the discrete mass/charge beams are recorded covering a total ion current range of from 10^{-13} to 10^{-17} coulomb. Calibration curves are obtained by analyzing standard samples consisting of similar matrices to the unknown.

The transmittance data are obtained automatically from a Grant recording microphotometer operating under computer control. The photomultiplier signal is amplified and filtered in a data-conditioning amplifier prior to being sent to the A/D at the computer. Two stepping motors are installed to position the Grant photoplate carriage in the X and Y planes. These stepping motors are driven by a special interface in the computer. In order to reduce the inertia load on the stepping motor, the mechanical indicators are disengaged from the feed screw by means of electric clutches. Positioning of the photoplate carriage on the Grant can be accomplished manually or by the computer.

After the mass spectra are obtained, the chemist manually marks the lines (m/e) of interest for ease of location. The photo plate is positioned on a Grant microphotometer, and control is passed to the computer. Further positioning of the photo plate under the optical reader is performed by depressing one of two buttons (Move Grant Left or Move Grant Right, Figure 1) on the function panel. When a line to be read is in position, it is identified by inputting on the TTY its chemical symbol. The button marked Digitize Data is then pressed. This action results in the computer digitizing and recording 512 points with a four-micron resolution across the area of interest. At the completion of the data-acquisition cycle, the information is displayed on the oscilloscope. Adjustment of the display can be obtained easily by depressing the required buttons (see Figure 1).

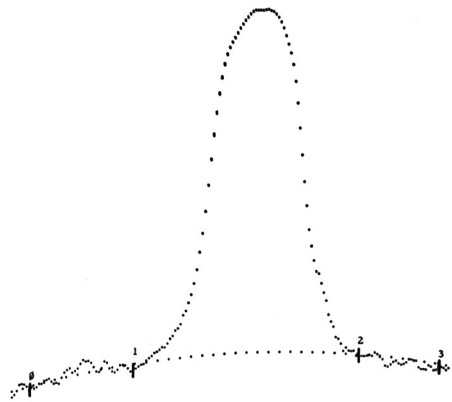

Figure 2. Quadratic least squares fit to base-line data

The operator next selects the base-line regions he believes to be most representative of the background. Starting at the left side of the display, two selected regions are marked by means of the Graf-Pen and function panel. These regions are bounded by the 4 appropriate cursor points. The most appropriate base line is selected by depressing the corresponding button. The base-line is then computed and displayed. Figure 2 is an example of a singlet m/e peak displayed together with the boundary conditions designated (dots 0 through 3) and a quadratic base-line fit projected through the regions 0–1, 2–3, and the peak.

The area under the peak is determined and typed on the TTY by selecting the Integrate Singlet function. Finally, the analytical result in PPM by weight is determined and printed on the TTY.

When the required information is contained in one or both of the lines comprising an unresolved doublet, the first stages of processing are similar to that required for a singlet (Figure 3*a*). After the base-line determination is completed, the function "Draw One Peak of Doublet" is initiated. The operator is able to draw on the screen what he feels to be the best representation of *one* of the peaks (Figure 3*b*). The boundaries of the manually drawn curve are set with dots 4

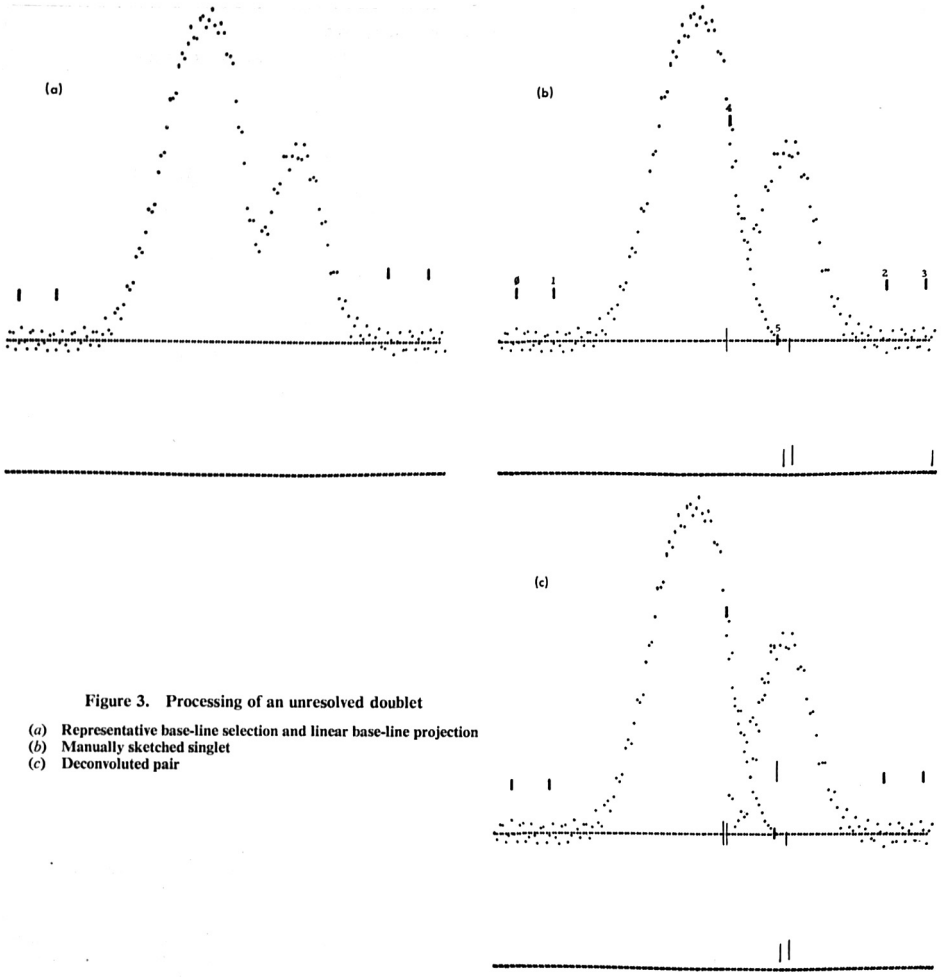

Figure 3. Processing of an unresolved doublet

(*a*) Representative base-line selection and linear base-line projection
(*b*) Manually sketched singlet
(*c*) Deconvoluted pair

and 5 and the function "Calculate and Display Other Peak" is then selected. These actions result in the computer subtracting the new information in the channels bounded by dots 4 and 5 from the original waveform and displaying the difference (Figure 3*c*). This particular doublet contains considerable noise which is readily apparent in the resultant waveform of the second peak. In many applications it would be desirable to filter the original data by means of an analog filter or digital smoothing techniques (*3*). (Note the difference between this example, Figure 3*c*, and Figure 4 where the data are relatively smooth.)

The final analysis is completed in a manner similar to that described above.

Gas Chromatographic System. A Varian Aerograph Model 1200 gas chromatograph equipped with a flame ionization detector was used throughout this study. The column (6-feet long by 0.085-inch i.d. stainless steel) was packed with 80/120 mesh PAR No. 1. Injection port and detector oven temperatures were maintained at 200 and 300 °C, respectively. The nitrogen and hydrogen flows were 35 cc per minute and the air flow was 400 cc per minute.

The flame ionization detector output was not compatible with the A/D converter. Therefore, the signal was amplified by means of two Hewlett Packard 2470A Data Amplifiers connected in series. Flame ionization response factors used were obtained from work performed by W. A. Dietz (*4*).

To evaluate the effectiveness of interactive data processing, two samples were prepared. The first was a mixture of 33.74% methanol, 32.53% ethanol, and 33.73% 2-propanol by weight. Operating under the conditions defined above and a column temperature of 140 °C, the components were only partially

(3) A. Savitzky and M. J. E. Golay, ANAL. CHEM., **36**, 1627 (1964).

(4) W. A. Dietz, *J. Gas Chromatogr.*, **5**, 68–71 (1967).

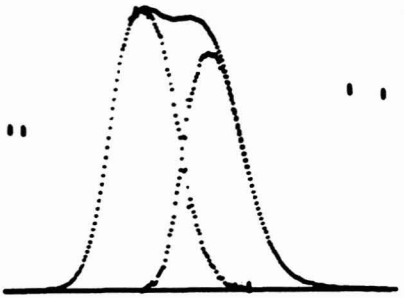

Figure 4. Chromatographic doublet, manually deconvoluted

resolved (Figure 5). The second sample was a mixture of 51.29% ethanol and 49.71% 2-propanol run at a column temperature of 125 °C. Again the components were not resolved (Figure 4).

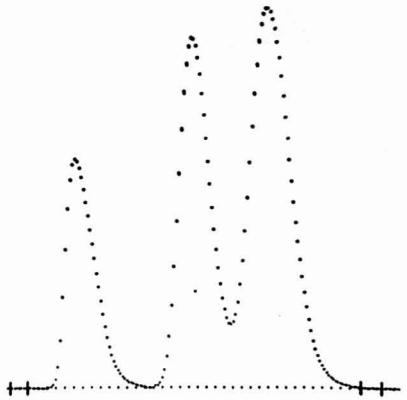

Figure 5. Chromatogram of methanol, ethanol, and 2-propanol as run on a 6 ft PAR-1 column at 140°C

RESULTS

Gas Chromatography. The deconvolution of overlapping peaks was a typical use to which the interactive data-reduction system was applied. For doublets, the procedure described in the Experimental Section was followed. The deconvoluted doublet obtained from the mixture of 51.29% ethanol and 48.71% 2-propanol mixture, shown in Figure 4, was typical of results obtained with the interactive system. For 10 totally independent analyses of the mixture, an average per cent composition of 51.25% for ethanol and 48.71% 2-propanol was obtained, with a standard deviation of 0.15% absolute. Another estimate of the reproducibility was obtained by making ten separate interactive data-processing analyses of one chromatogram for which the results were 51.15% ethanol and 48.85% 2-propanol, with a standard deviation of 0.24% absolute. Both the accuracy and precision are quite adequate for most nonroutine determinations.

To evaluate further the accuracy obtainable with the interactive system, partially resolved (Figure 5) chromatograms of the mixture of 33.74% methanol, 32.53% ethanol, and 33.73% 2-propanol were analyzed. Analyses from nine independent runs gave the following results: methanol 33.74%, std dev = 0.34%; ethanol 32.57%, std dev = 0.15%; 2-propanol 33.69%, std dev = 0.27%. Again, it is interesting to note the accuracy of the means which indicates that the errors encountered were random in nature. Furthermore, the standard deviations, on an absolute basis, are quite acceptable and represent, on a relative basis, precision of 0.3 to 1.0%, which compares well with the data usually obtained on isolated peaks.

Another way to demonstrate the power of interactive data processing is to examine improper processing of data similar to those presented above. Figure 6*a* shows the results of one type of error that can occur when attempting to deconvolute two fused peaks. Any chemist experienced in gas chromatography will immediately note the following anomalies: the trailing edge of the second peak is still unnaturally convex with respect to the Y-axis; and the tail as drawn on the first peak was terminated too soon and does not show the same general exponential decay as the second peak. (The values obtained were in error by approximately 2% relative.)

Another type of error that can easily occur is shown in

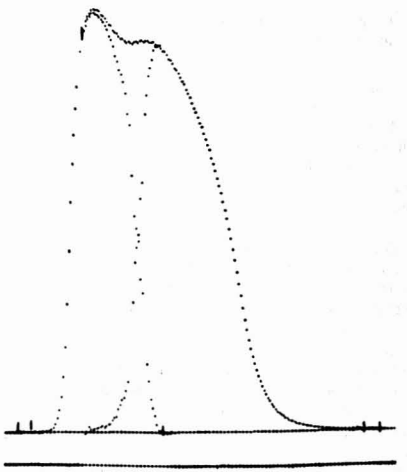

Figure 6*a*. Poor deconvolution due to lack of extension of the tail of the first peak

Figure 6*b*. The first peak has been sketched such that the peak top is too low. Note the resulting anomalous small hump on the front of the second peak. Similar results are observed if the shape factors are approximately correct but the peak half-width of the hand-drawn peak was deliberately drawn too narrow.

Mass Spectrographic Results. The processing of data obtained from spark source mass spectrometry requires three basic functions: identification of the *m/e* peaks to be analyzed, deconvolution of doublets, and precise measurement of peak areas. For the determination of trace impurities in rocks and soils, the determinations are complicated by the fact that a great deal of the photoplate is fogged due to space-charge effects. This fogging results in a range and variety of nonlinear base lines that are difficult to process for quantitative analytical data. Also the data are usually very noisy and often

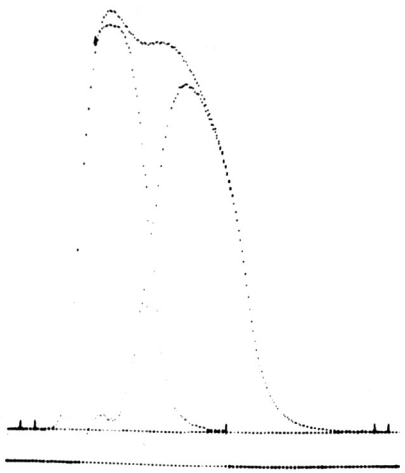

Figure 6*b*. Poor deconvolution due to excessive shortening of the first peak

the signal-to-noise ratio of important individual lines is low (often the S/N was less than 5).

The non-alignment of the individual spectra is an additional difficulty encountered when a non-interactive (*5*) computerized system is used for data reduction. Also, it is found to be very difficult to develop and program the algorithm for making the decision as to which line(s) of which exposure to use to obtain the required determination for each element.

When the interactive system is used for data reduction, the above difficulties are easily accommodated. The availability of three methods (linear, quadratic, and manual sketching) for base-line determination is especially useful. The *m/e* line shown in Figure 2 is typical of peaks requiring nonlinear projection of base lines through the peak. In some instances the composite base line as represented by areas on both sides of the peak is of such a nature that the best estimate is that obtained by manually sketching a proposed base line. Polynomial equations often produce poor results under these circumstances.

Spark source mass spectrometry analysis of trace impurities in rocks and soil does not have the accuracy required to adequately evaluate interactive data processing. The inaccuracies are due to inherent errors in obtaining reproducible sparks, sample matrix effects, and photoplate beam monitoring capabilities, along with lesser error contributions (*6*, *7*). However, as one test of the merit of this procedure two NBS geological samples, W-1 and G-1, were analyzed and a correlation of the Ti in the two rock standards is given in Figure 7. These results, including the two poor G-1 values, obtained *via* on-line interactive data processing are typical of the spark-source mass spectrometric technique.

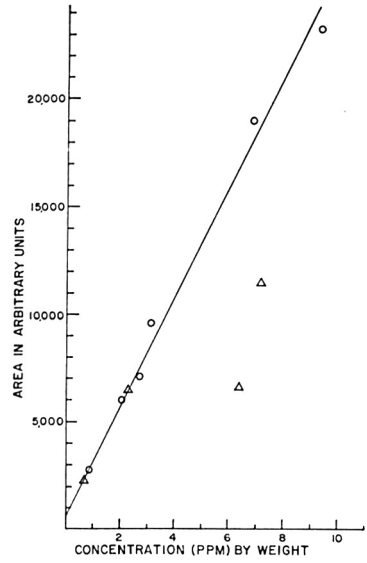

Figure 7. Titanium isotope calibration data for NBS Standards W-1 (○) and G-1 (△) normalized to exposure

The interactive data reduction of the mass spectrographic data requires approximately 10 minutes time per 15 determinations. In practice, the non-interactive computerized system (*5*) required more operator time to determine and enter the required initializing parameters than is required to *completely* reduce the data by means of the interactive system described here.

RECEIVED for review January 18, 1971. Accepted June 16, 1971. This work was performed under the auspices of the U. A. Atomic Energy Commission. Partial support was provided also for one of the authors (S.P.P.) by the National Science Foundation, Grant No. GP-8677.

(5) C. A. Bailey, R. D. Carver, R. A. Thomas, and R. J. Dupzyk, "A Computer-Controlled System for Automatically Scanning and Interpreting Photographic Spectra," "*Developments in Applied Spectroscopy*," E. L. Grove and A. J. Perkins, Ed., Plenum Press, New York, N. Y., Vol. 7A, 1968, p 294.

(6) G. D. Nicholls, A. L. Graham, E. Williams, and M. Wood, ANAL. CHEM., **39**, 584 (1967).

(7) R. K. Skogerboe, A. T. Kashuba, and G. H. Morrison, *ibid.*, **40**, 1096 (1968).

On-Line Interactive Data Processing

II. Processing Voltammetric Electrochemical Data

S. P. Perone
Chemistry Department, Purdue University, Lafayette, Ind. 47907

J. W. Frazer and Arthur Kray
Lawrence Radiation Laboratory, University of California, Livermore Calif. 94550

This work illustrates the application of a computerized interactive processing system for analysis of voltammetric data. A small digital computer forms the heart of the system. The operator can oversee data processing functions by graphical communication with the computer through an oscilloscopic display terminal. Processing is programmed in a high-level conversational language. Applications to single-sweep and cyclic-sweep data are illustrated.

ANALYTICAL ADVANTAGES of digital data acquisition and subsequent computer processing of voltammetric data have been amply demonstrated (*1–3*). However, computer processing of voltammetric data presents a nontrivial problem for the electrochemist. It is difficult to incorporate completely into a computer program the complex interpretive processes required by the expert electrochemist to analyze nonroutine voltammetric data. Typical problems include: overlapping peaks; nonlinear base lines; non-ideal electrolytic behavior (irreversibility, adsorption, etc.); and discrimination between real and anomalous processes. For cyclic voltammetric studies, the problems are compounded by the fact that the voltage sweep is reversed during the experiment and both positive and negative peaks must be analyzed. Moreover, because cyclic experiments are generally applied to systems where peak shapes are distorted due to chemical kinetic complications, data processing can be particularly difficult.

This work describes the application of an *interactive* computerized data processing approach to electroanalytical data. The basic philosophy and features of this approach have been described previously (*4*). The interactive system incorporates the experimenter–operator into the computer data processing operation. While the computer is programmed to carry out the tedious and difficult computational handling of data, the operator can impose his expert judgements regarding the selection of data regions to be analyzed and specific analysis procedures. Interaction with the processing computer is through an oscilloscopic display system which allows graphical communication.

EXPERIMENTAL

Electrochemical Instrumentation. The electrochemical instrumentation used for the voltammetric studies reported here has been described previously (*2, 5*). (The 20-Hz low-pass output filter was bypassed for the work reported here.) The instrument used was a general-purpose voltammetric device constructed from solid-state operational amplifier modules and was designed to perform single- and cyclic-sweep voltammetric experiments with regular current or derivative readouts. The instrument provided timing circuitry for synchronization of voltammetric experiments with the dropping mercury electrode, so that experiments could be run during the latter portion of the drop-life. All data were obtained at a scan rate of 1.0 V/sec.

The electrochemical cells and electrodes used have been described in detail previously (*2, 5*). The apparatus involved two matched cells with dropping mercury electrode (DME) systems, providing synchronized drop dislodgment at timed intervals. It was possible to make measurements on either cell independently, or to make differential measurements. Saturated calomel reference electrodes and platinum wire counter electrodes were employed.

The solutions used in this work were prepared from analytical reagent grade chemicals and deionized water. Specific solution compositions are given in the text. All solutions were deaerated with high purity nitrogen. Cell temperatures were thermostated at 25.00 ± 0.02 °C.

Computerized Real-Time Data Acquisition System. The electrochemical data acquisition system is identical to that described in detail previously (*2*). It involved using a DEC (Digital Equipment Corporation, Maynard, Mass.) PDP-8/S computer for acquiring, storing, and limited processing of experimental data. In addition, the computer could transfer the experimental data to a permanent punched paper tape buffer for later data processing. Data acquisition was carried out at a 250-Hz rate for all experiments described here.

Data Processing System. The computerized interactive data processing system has also been described in detail elsewhere (*4*). It involved the use of a DEC PDP-8/I computer with 8 K of core memory and a 32-K magnetic disk storage capability. The oscilloscopic display system included a Tektronix Model 611 large screen oscilloscope. Coupled with the oscilloscopic display was a hard wired control panel. Although the previously reported work employed a Graf-Pen (Science Accessories Corporation, South Port, Conn.), the control panel used here had associated with it a "joystick" (*6*) which could be manipulated to control the positioning of a cursor point projected on the oscilloscope screen. It was possible to rotate the joystick in a complete 360° arc and position the cursor point anywhere on the face of the screen. The oscilloscopic interactive display program could readily translate the joystick-positioned cursor points into X, Y information available to the data processing programs as described below.

The control panel provided several pushbutton switches, the status of which could be monitored by the interactive program, and be interpreted in a variety of ways (*4*). For example, one could depress a button which would instruct the computer to acquire real-time data and display the data on the oscilloscope screen. Another button could be de-

(1) W. F. Gutknecht and S. P. Perone, ANAL. CHEM., **42**, 906 (1970).
(2) S. P. Perone, J. E. Harrar, F. B. Stephens, and R. E. Anderson, *ibid.*, **40**, 899 (1968).
(3) G. Lauer, R. Abel, and F. C. Anson, *ibid.*, **39**, 765 (1967).
(4) J. W. Frazer, *et al.*, *ibid.*, **43**, 1479 (1971).
(5) F. B. Stephens, E. Behrin and J. E. Harrar, *U. S. At. Energy Comm. Rep.*, **UCRL-50374** (1968).
(6) *Tekscope*, Art Anderson, Ed., Vol. 2, No. 3, Tektronix, Inc., Beaverton, Ore., June 1970.

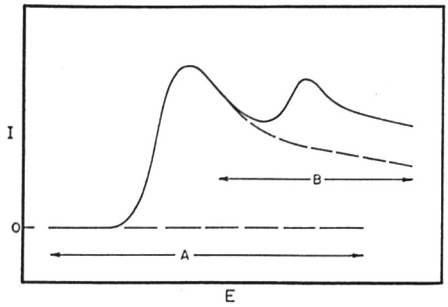

Figure 1. Types of base lines for voltammetric data

A. **Linear region**
B. **$1/(t^{1/2})$ extrapolation region**

Table I. Basic Control Functions for Interactive Processing System

Mode	Function
I	Initialize system and/or take real-time data
II	Display data and cursor point; operator selects base-line and peak regions with joystick and display markers
III	Process data as selected by Mode II operation
IV	Subtract extension of preceding peak or base line and display rest of curve
V	Manually sketch base line
VI	Save currently displayed intermediate data on disk, and/or scale current data
VII	Restore intermediate data saved on disk in mode VI
VIII	Restore original data from disk, or take new data from paper tape; display; save on disk
IX	Acquire background "blank" data and correct original data

pressed whenever the operator wanted to display several markers on the displayed data which would establish reference points for any of the data processing routines. A summary of the functions available through the control panel used in this work is provided in Table I.

The interactive display software, which provides the various functions outlined in Table I and allows the interactive communication between operator, display, and computer, has been described previously (*4*). The data processing software is done by the operator in the FOCAL language (Digital Equipment Corporation). The FOCAL interpreter was modified for operator interaction through the display system (*4*).

VOLTAMMETRIC DATA PROCESSING

Requirements. The processing of voltammetric data requires two basic functions: recognition and precise location of reduction peaks; and precise measurement of peak heights. These measurements are complicated in single- or cyclic-sweep voltammetry by the fact that a variety of nonlinear base lines are required to process various peak regions. Thus, the computerized data processing scheme developed here had to include methods for handling the variety of base lines encountered, as well as for precise location of peaks. The mathematical foundation for such processing depends on the nature and validity of the theoretical equations describing electrochemical voltammetric phenomena.

The basic approach used was to define the most common kinds of base lines which would be encountered in voltammetric data and the kinds of peak information that would be processed, and to incorporate the appropriate mathematical descriptions of these data regions into the processing programs. Then, using the computerized interactive display system, the operator would acquire the data, instruct the computer to display the data on the ocsilloscope screen, observe the general nature of the data (*i.e.*, where the base line and peak regions occurred), use the joystick on the control panel for placing markers on the display screen defining specific regions of the data, and then instruct the computer to apply the appropriate mathematical handling of the selected data regions to locate and properly measure peaks.

The normal voltammetric background current can generally be attributed to the combination of capacitive charging current and current due to reduction of minor impurities in solution. Unfortunately, the background current is generally not linear, but can only be represented by a very complicated and varied shape. It would be impossible to provide some standard mathematical function which fit background currents in general. Therefore, it is assumed that any voltammetric data processed would be corrected for background current first. Thus, in the system developed here, provision is made for automatically acquiring and subtracting background currents from the voltammetric data. Alternatively, the voltammetric data could be acquired from a differential system (*2, 5*), and therefore be presented for data processing in a background-corrected form. In either case the remaining background contribution or base line would be zero or linear in nature. Both approaches were used in this work and will be discussed later.

Because voltammetric data were corrected for background, the processing program could assume that only two kinds of base lines need be considered to make peak height measurements: linear base lines, and the base line afforded by the extension of the diffusion-controlled reduction peak. These two regions are specified in Figure 1. The linear region corresponds to potentials preceding any reduction steps. The second kind of base line indicated in Figure 1 is really the extension of the tail of a preceding reduction wave. This tail should follow a current–time function which decays with $1/(t)^{1/2}$, where t is time (*7, 8*). The diffusion-limited $1/(t)^{1/2}$ current on the tail of a peak is a general and well defined characteristic of voltammetric reduction waves. There are some exceptions, however. These exceptions include cases where surface phenomena complicate the reduction step or where the kinetics of coupled chemical reactions influence the current along the tail of a reduction wave. With the former case (surface complications), the most common problem is that the reduction process will be limited by surface coverage. In that case the peak current will generally return to the base line established by the preceding process. Therefore the base line defined by the preceding process will continue to define the base line for steps following the surface-limited reduction peak. For the latter case (chemical kinetic complications), there is no general way for predicting base-line effects. These would have to be handled on an individual basis. The computerized interactive system described here has the capability to allow the operator to sketch in the projected base line by manipulation of the joystick. This could be used whenever it was apparent that neither of the approaches to defining the base line shown in Figure 1 seemed adequate.

Mathematical Approaches. For the region marked off by the operator as defining a linear base-line region, the

(7) A. Sevcik, *Collect. Czech. Chem. Commun.*, **13**, 349 (1948).
(8) R. S. Nicholson and I. Shain, ANAL. CHEM., **36**, 706 (1964).

computer applies a linear least squares analysis to determine the equation for the best straight line fitting those data points (*9*, *10*). The linear segment is projected through the selected data points across the entire data display.

The computer program for handling the extrapolated diffusion current base line established by a preceding reduction peak is computed by an iterative approach. This approach simply assumes that the data in the region marked off by use of the joystick follow a $1/(t^{1/2})$ dependence as shown in Equation 1. The only unknown in the equation is t_o. (i_o = current at t_o; t = time past t_o.)

$$i_{(t+t_o)} = i_o\left[\frac{t_o}{t+t_o}\right]^{1/2} \qquad (1)$$

The program attempts to fit the data to the $1/(t)^{1/2}$ function by finding the correct t_o to obtain an adequate fit. [The approach is similar to that described by Polcyn and Shain (*11*).] The criterion for selection of t_o involves establishing a fit, within 1%, to the latter data points in the region, based on the values of the earlier data points in the region. If the data do not follow a $1/(t^{1/2})$ dependence, the iterative procedure will not converge rapidly, if at all. Thus, the operator will know immediately if the $1/(t^{1/2})$ dependence does not fit the data.

The third type of processing computations involves analysis of the data region selected by the operator as containing the peak information. The program to handle these data involves fitting a quadratic equation to the data in the peak region by employing a linear least squares procedure (*9*, *10*). The peak data are corrected for base-line contributions due to either linear or $1/(t^{1/2})$ functions *before* the quadratic curve-fitting step. Therefore, peak measurements are not distorted by superimposed base-line trends. Once the least squares quadratic fit is determined, the peak maximum is established by evaluating the first derivative and setting equal to zero. The current value at the peak maximum is computed from the quadratic equation.

The validity and effectiveness of these theoretical approaches to processing single- and cyclic-sweep voltammetric data will be evaluated in the following sections.

OPERATING PROCEDURES AND SYSTEM DESCRIPTION

When the experimental voltammetric data are available (in computer memory) for processing, the interactive processing system can be implemented. The operator has at his disposal three means of communication with the computer; visual oscilloscopic display of the data and auxiliary information—such as base lines, marker points, and the cursor point; a push-button control panel and joystick—where the joystick can manipulate the cursor point on the scope display, and the push-button controls can select various modes of computer operation; and a teletype for results output and operator information input. The various modes of operation—selectable from the control panel—are summarized in Table I. Additional information requested by the computer to be entered through the teletype include: the number of data to acquire; the data density; whether data correspond to *sample blank*, or *blank-corrected* data; the scaling factors desired for the data display; and the values (in mV) of initial and switching potentials. The computer also types out informational comments such as when a disk block transfer has been completed and the next stage of operation can be executed.

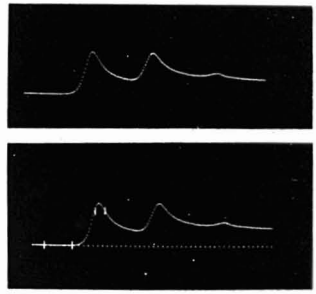

Figure 2. Processing first peak in single-sweep polarogram

A. **Display of blank-corrected data (differential dual-cell measurement). 1.2 × 10^{-4} *M* Pb(II), 1.0 × 10^{-4}*M* Cd(II) in 1.0*M* KCl (3rd peak undefined)**

B. **Data with 4 cursor points selected by operator and joystick. First 2 define base-line region; 2nd 2 bracket peak. Projected line is computed linear base line**

The exact operating procedure can vary depending on the kind of data to be analyzed. This is one of the advantages of the approach taken. To provide some insight to the procedural aspects and the capabilities of the interactive system, two specific applications are described here. One of these involves the processing of the single-sweep polarogram for a simple 2-component mixture; the other involves processing an uncomplicated cyclic polarogram.

Analysis of Single-Sweep Polarogram. Figure 2*A* presents a typical polarogram to be analyzed. The first 2 peaks correspond to 1.2 × 10^{-4}*M* Pb(II) and 1.0 × 10^{-4}*M* Cd(II), respectively. The small third peak is an anomalous peak of unknown origin. Figure 2*B* represents the same trace after the operator has executed Mode II (Table I) and marked off two distinct regions using the joystick and the corresponding displayed cursor point (also shown as an isolated dot on the photograph). The first two points define the base-line region. The second two points bracket the first peak.

Figure 2*B* also shows the computed base line displayed after Mode III has been executed. The computations involve, first, generating a linear base line by a least squares fit to the data included within the base-line markers. Next, a quadratic equation is fit to the data in the peak region. The peak potential and the base-line-corrected peak height are computed and printed out. The use of the least squares fitting technique here minimizes problems associated with noisy data and provides more accurate peak measurements than a linear interpolation approach.

Figure 3*A* shows the display after the operator has returned to Mode II, selected the base line and peak regions for the next peak, and executed Mode III again. In this case he tells the computer (*via* a push-button on the control panel) that the base line should correspond to a $1/(t^{1/2})$ decay function. Figure 3*A* displays the extrapolated decay function fit to the data between the base-line markers. In addition, the computer has calculated the base-line-corrected peak height and peak potential for the 2nd peak (just as for the first peak). These results are printed on the teletype.

(9) P. R. Bevington, "Data Reduction and Error Analysis for the Physical Sciences," McGraw-Hill, New York, N.Y., 1969.
(10) W. E. Groves, "Brief Numerical Methods," Prentice-Hall, Inc., Englewood Cliffs, N. J., 1966.
(11) D. S. Polcyn and I. Shain, ANAL. CHEM., **38**, 370 (1966).

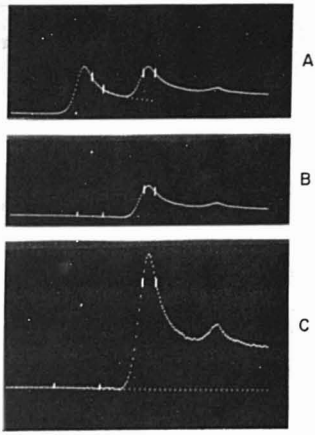

Figure 3. Processing second peak in single-sweep polarogram

A. Data with new placement of 4 cursor points. First 2 define diffusion-controlled base-line region ($1/(t^{1/2})$ dependence); 2nd 2 points bracket peak. Projected line is computed base line for 2nd peak
B. Display of data after subtracting extrapolated contribution of first peak. Markers placed on curve to define new linear base line
C. Same data as in *B* above, except scaled ×4. The new linear base line has been computed and displayed. (Necessary only when the preceding linear base line is nonzero)

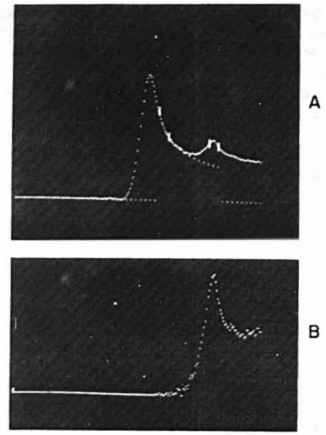

Figure 4. Processing and extracting succeeding peaks in single-sweep polarogram

A. Tail of 2nd peak is processed to establish base line for 3rd peak. (Peak height and peak potential of 3rd peak are computed and printed out on teletype.)
B. 3rd peak extracted (and scaled ×5) by subtracting extrapolated contribution of 2nd peak

Figure 3*B* shows the display that results when Mode IV is executed next. The computer subtracts the extrapolated first peak from all the data and displays the results. The operator can scale the result by an appropriate factor, as demonstrated in Figure 3*C*. (The operator might also choose at this point to save the intermediate data on the disk in case future manipulations do not turn out well.) Also shown in Figures 3*B* and 3*C* are the operator's placement of markers. Figure 3*C* shows the new computed linear base line.

Figure 4 illustrates the sequence of operations which one can follow next to eventually extract each succeeding peak in the voltammetric curve—assuming each reduction step reaches diffusion control before the start of the next step. The quantitative information obtained becomes less accurate for succeeding steps, particularly if several larger peaks have preceded. The two limitations are: the dynamic range of the digitized data (*e.g.*, 0 to 1023 for a 10-bit conversion); and the propagation of computational errors where succeeding calculations are affected by the accuracy of preceding steps.

For the data analyzed in Figures 2 to 4, only a qualitative perspective on the 3rd peak was required. The question was whether the anomalous peak arose from a diffusion-limited process, or from a surface-limited process such as adsorption pre-wave or post-wave (*12*). The fact that the extracted curve in Figure 4*B* gives the appearance of a typical diffusion-limited reduction process could not have been ascertained readily from the original data displayed in Figure 2*A*. Moreover, the apparent location of the third peak on the potential axis was distorted in the original display (Figure 2*A*) due to the decaying base line. The best estimate to E_p from Figure 2*A* was -0.830 ± 0.005 V *vs.* SCE. The peak extracted in Figure 4*B* had a computed E_p of -0.839 ± 0.001 V.

Analysis of Cyclic Polarograms. The analysis of cyclic voltammetric data is demonstrated in Figure 5. All the capabilities outlined above can be applied to these data also. Essentially the same operating procedures are followed. In addition, the computation of particularly useful quantities such as the separation of peak potentials, ΔE_p, and the ratio of reverse to forward peak currents, I_R/I_F, is provided. It is also useful to be able to extract the reverse peak and display it, corrected for the theoretical extrapolated base line, as shown in Figure 5*C*.

RESULTS AND DISCUSSION

Various experimental studies were carried out with the objective of evaluating the interactive processing system for voltammetric data processing. The systems studied included: uncomplicated reversible reduction processes; multicomponent mixtures of metal ions; and dilute solutions of reducible species. It was hoped that observing this variety of voltammetric systems would provide an adequate evaluation of the capabilities and limitations of the interactive processing system applied here.

Single-Sweep Voltammetric Studies with Multicomponent Mixtures. These studies were designed to evaluate the ability to make accurate reproducible, quantitative analytical measurements on a variety of simple mixtures of electroactive species. Several replicate processing runs were performed on each set of data. The results of these studies are summarized in Table II.

Three different mixtures were studied. One of these was a mixture of $2 \times 10^{-4}M$ Pb(II), $2 \times 10^{-5}M$ Cd(II), and $4 \times 10^{-5}M$ Zn(II) in $1.0M$ KCl. The peak height measurements obtained agreed with those predicted from standards within

(12) R. H. Wopschall and I. Shain, ANAL. CHEM., **39**, 1514 (1967).

Table II. Quantitative Results from Single-Sweep Experiments

Component	E_p (V *vs.* SCE)	Std[d] dev	$I_p \times 10^4$, μA/M	Std[d] dev
Cd (std)	−0.645	0.001	0.432	0.004
Cd[a]	−0.645	0.001	0.426	0.007
Cd[b]	−0.644	0.001	0.441	0.003
Cd[c]	−0.652	0.001	0.447	0.007
Pb (std)	−0.440	0.002	0.219	0.003
Pb[b]	−0.438	0.002	0.218	0.002
Pb[c]	−0.443	0.001	0.202	0.002
Zn (std)	−1.083	0.002	0.210	0.002
Zn[c]	−1.077	0.005	0.213	0.007

[a] $1 \times 10^{-4}M$ Pb(II), $1 \times 10^{-4}M$ Tl(I), $1 \times 10^{-4}M$ Cd(II), 1.0*M* KCl.
[b] $1 \times 10^{-4}M$ Pb(II), $2 \times 10^{-5}M$ Cd(II), 1.0*M* KCl.
[c] $2 \times 10^{-4}M$ Pb(II), $2 \times 10^{-5}M$ Cd(II), $4 \times 10^{-5}M$ Zn(II), 1.0*M* KCl.
[d] Reported precision reflects repeatability of results for at least three replicate processing operations.

Table III. Quantitative Results of Cyclic Voltammetric Studies

Solution	I_R/I_F	Std[a] dev	ΔE_p, mV	Std dev, mV[a]
$5 \times 10^{-4}M$ Fe(III), oxalate buffer	0.997[b]	±0.015	60.2	0.5
$2 \times 10^{-4}M$ Pb(II), 1*M* KCl	1.05[b]	±0.01	28.7	0.7
$2 \times 10^{-4}M$ Tl(I), 1*M* KCl	1.04[b]	±0.03	59.4	1.4
$2 \times 10^{-4}M$ Zn(II), 1*M* KCl	1.693[b]	±0.012	114.2	2.0
$2 \times 10^{-4}M$ Zn(II), 1*M* KCl	1.331[c]	±0.035	117.2	1.7
$1.2 \times 10^{-4}M$ Pb(II), 1*M* KCl	0.885[c]	±0.06	31.4	0.5

[a] Results based on 4–7 replicate runs on representative data.
[b] Using extrapolated $1/(t)^{1/2}$ base line.
[c] Using manually sketched extrapolated base line.

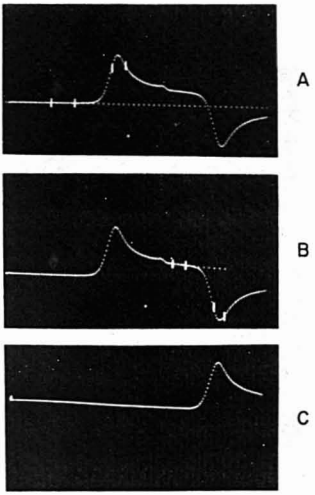

Figure 5. Processing cyclic voltammetric data

$1.2 \times 10^{-4}M$ Pb(II) in 1.0*M* KCl; $E_i = -0.103$ V *vs.* SCE; $E_s = -0.585$ V *vs.* SCE; 1.0 *V*/sec sweep

***A*. Data and linear base line displayed for cathodic peak**

***B*. Data and $1/(t^{1/2})$ base line displayed for anodic peak**

***C*. Anodic peak extracted and displayed, corrected to zero base line and inverted**

0.5 to 3.5% in each case. The measured peak potentials in the mixture agreed within 3 to 7 mV with the standards in each case.

Another solution studied was an equimolar mixture of Pb(II), Tl(I), and Cd(II) in 1.0*M* KCl. The reduction peaks for Pb(II) and Tl(I) overlapped so badly (ΔE_p = 45 mV) that it was not possible to use the data processing approach described here to analyze for either the Tl(I) or the Pb(II). Nevertheless, it was possible to determine the amount of Cd(II) in the mixture by using the combined tails of the Tl(I) and Pb(II) reduction peaks as the base line for the Cd(II) peak. The same approach as outlined above was used except that no attempt was made to analyze quantitatively for the Tl(I) or Pb(II) species. The results for the Cd(II) peak are within 0.5% of the predicted value. However, it can be shown that the combined tail should follow a simple $1/(t^{1/2})$ dependence only when t_0 is identical for both processes. For cases where the peaks are as close as seen here, the fit is adequately close as long as the operator selects the base-line determining region close to the foot of the peak to be analyzed.

Quantitative Analysis of Cyclic Polarograms. One system studied with cyclic voltammetry was $5 \times 10^{-4}M$ Fe(III) in oxalate buffer (0.20*M* $K_2C_2O_4$, 0.25*M* $H_2C_2O_4$), presumably a reversible system (*13*). The results obtained are included in Table III, along with results of other cyclic experiments. The ratio of peak currents is very nearly unity, as predicted by theory (*8*). The computer-evaluated peak separation, ΔE_p, is 60.2 mV, very nearly equal to the value predicted for a one-electron reversible system (*8*). More important here is the fact that the standard deviations for the determinations of peak ratio and peak separation are quite small. Other reverisble systems studied with cyclic voltammetry included $2 \times 10^{-4}M$ Pb(II) and $2 \times 10^{-4}M$ Tl(I) in 1*M* KCl. The results of processing those data are also given in Table III. Close correspondence to predicted correlations was observed.

Other cyclic voltammetric experiments were run to illustrate the capability of the interactive processing system to handle relatively "messy" data. One of these is the cyclic study of $2 \times 10^{-4}M$ Zn(II) in 1.0*M* KCl. The type of data obtained is illustrated in Figure 6*A*. Obviously the Zn(II) reduction step is considerably more drawn-out than the reverse oxidation step. Moreover, the tail of the reduction step does not follow a $1/(t^{1/2})$ diffusion-controlled decay. This can be seen from Figure 6*A*, where the result of an attempt to impose a $1/(t^{1/2})$ decay function on the tail of the reduction peak is illustrated. The explanation for the non-ideal behavior is probably that the reduced Zn does not diffuse into the Hg electrode. This may be due to intermetallic complex formation between the Zn and Hg (*14*). In any event the fact that the Zn does not diffuse into the Hg accounts for the drawn-out cathodic peak as predicted for such a case (*15*). The reverse peak is quite sharp, however, because the Zn is concentrated near the surface of the electrode and is re-oxidized into solution quite rapidly. Figure 6*B* illustrates how the alternative manual method for estimating a base line was utilized in this case for the reverse peak. The results obtained in each case are summarized in Table III.

(13) S. P. Perone, ANAL. CHEM., **38,** 1158 (1966).

(14) W. Kemula, "Advances in Polarography, Proceedings International Congress," I. S. Longmuir, Ed., Pergamon Press, New York, 1960, Vol. 1, pp 105–143.

(15) S. P. Perone and K. K. Davenport, *J. Electroanal. Chem.*, **12,** 269 (1966).

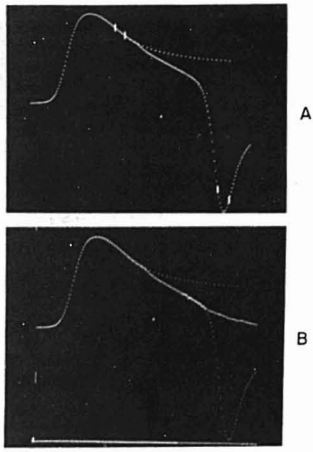

Figure 6. Cyclic voltammetric data for Zn(II) in KCl

$2.0 \times 10^{-4}M$ Zn(II) in $1.0M$ KCl; $E_i = -0.800$ V *vs.* SCE; $E_s = -1.295$ V *vs.* SCE. (Display starts at -0.880 V *vs.* SCE)
***A.* Result of attempted $1/(t^{1/2})$ fit to cathodic peak decay current**
B. Display of manually sketched base line for anodic peak

Still another cyclic voltammetric study carried out involved looking at a very low concentration of Pb(II) ($1.2 \times 10^{-6}M$) in $1.0M$ KCl. Because it was difficult to match the dual cells adequately at this sensitivity for a valid differential measurement, it was necessary to correct the single cell measurement for a blank cyclic polarogram run in the same cell under the same conditions. Figures 7*A* and 7*B* show the data displayed before and after blank correction. Figure 7*C* shows the blank-corrected data after computer scaling. Obviously, this kind of data handling would be extremely difficult to perform accurately on cyclic experiments where data were obtained by photographic recording. With the computerized system described here, the blank correction is very conveniently and accurately carried out. The processing of these data is illustrated in Figures 8*A* and 8*B*. It was necessary to use a manual sketch of the base line for the reverse peak because the data were too noisy to allow convergence of the program which fits a $1/(t^{1/2})$ function to the tail of the cathodic peak.

CONCLUSIONS

The computerized interactive system described here illustrates a particular approach to quantitative processing of chemical data. The approach has certain established advantages—such as allowing the superposition of human judgment on computer data processing functions. The specific application reported here provides a reliable, rapid, and versatile tool for processing voltammetric data. The reliability of the system is reflected in the repeatability of the results. At least an order of magnitude decrease in processing time required compared to manual analysis has been observed. Finally, the variety of processing situations allowed attests to the versatility of the approach.

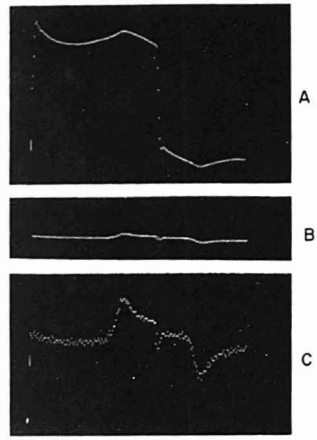

Figure 7. Cyclic voltammetric data for dilute Pb(II) in KCl

$1.2 \times 10^{-6}M$ Pb(II) in $1.0M$ KCl; $E_i = -0.100$ V *vs.* SCE; $E_s = -0.585$ V *vs.* SCE
***A.* Single cell measurement**
***B.* After subtracting blank**
***C.* Data from *B* scaled $\times 10$**

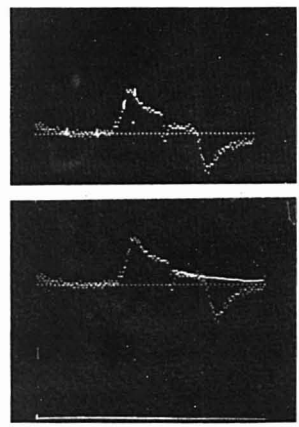

Figure 8. Processing cyclic data for dilute Pb(II) solution. (Same data as Figure 7)

***A.* Analyzing cathodic peak**
***B.* Using manually-sketched base line for anodic peak**

ACKNOWLEDGMENT

The authors thank Jackson Harrar and Fred Stephens for invaluable assistance in carrying out the voltammetric studies.

RECEIVED for review January 18, 1971. Accepted June 16, 1971. Work performed under the auspices of the U. S. Atomic Energy Commission. Partial support was provided also for one of the authors (S.P.P.) by the National Science Foundation, Grant No. GP-8677.

Molecular Interactions of Asphalt

Tentative Identification of 2-Quinolones in Asphalt and Their Interaction with Carboxylic Acids Present

J. C. Petersen, R. V. Barbour, S. M. Dorrence, F. A. Barbour, and R. V. Helm

Laramie Energy Research Center, Bureau of Mines, U. S. Department of Interior, P.O. Box 3395, University Station, Laramie, Wyo. 82070

The tentative identification of 2-quinolones has been made in a Wilmington (Calif.) asphalt. These compounds, which exist predominantly in the *N*-unsubstituted form, were concentrated in an asphaltic resin fraction and are largely responsible for the 1655 cm^{-1} infrared absorption band in the asphalt. A strong hydrogen-bonding association between the 2-quinolones and carboxylic acids in asphalt is reported. The association complexes between the 2-quinolines and the carboxylic acids in asphalt and between the model compounds 2-quinolone and cyclohexanecarboxylic acid were studied by infrared spectrometry using a silylation reaction in which the 2-quinolones and carboxylic acids reacted at different rates. The ability of two solvents, methylene chloride and tetrahydrofuran, to break up hydrogen-bonded molecular complexes is shown. The diagnostic value of these solvents in infrared spectrometry for identification of carbonyl functional group types has been demonstrated, and use of these solvents for molecular association studies in asphalts is reported.

THE CARBONYL STRETCHING region of the infrared spectra of asphalts (approximately 1620–1800 cm^{-1}) is generally broad and irregular in shape and has not been exploited in asphalt composition studies. The lack of exploitation of this region probably results from the complexity of the absorption bands caused by the presence of a large variety of functional groups. These groups are polar; and many are capable of forming intermolecular complexes, often through hydrogen bonding, thus further complicating the spectra. Intermolecular hydrogen bonding in asphalts has been studied in the hydrogen-stretching region of the infrared spectra at 3100–3700 cm^{-1} (*1*) but has not been related to interactions involving the carbonyl group. In the present study, molecular complexes formed through hydrogen bonding interactions to carbonyl groups are reported. The complexity of asphalt precludes, from a practical standpoint, the possibility of isolating the compounds containing these interacting groups; therefore it is necessary to devise techniques to study specific functional group types in the presence of many others. We have followed this approach by applying selective chemical reagents and solvents capable of forming association complexes to asphalt fractions and interpreting the results using infrared spectrometry.

Most asphalts show a major band maximum in the infrared spectra at about 1700 cm^{-1} which has been attributed to the carbonyl group absorption of such functional groups as carboxylic acids, acid anhydrides, ketones, esters, etc. (*2–5*). In many asphalts, however, an absorption in the carbonyl region centered at about 1655 cm^{-1} is observed. This band varies widely in intensity in different asphalts and is absent in some. The band was reported by Stewart (*6*) in an asphaltic resin fraction, and he suggested that it might result from amides or amines, although no attempt was made to confirm the speculation. The band at 1655 cm^{-1} is difficult to observe because in many instances it is overlapped on one side by the carbonyl absorption centered at 1700 cm^{-1} and on the other by the so-called aromatic band at about 1600 cm^{-1}.

In the present paper we report that 2-quinolones and their association complexes with carboxylic acids have tentatively been identified as major contributors to the 1655 cm^{-1} band in asphalts. 2-Quinolones have been identified in the high-boiling fractions of petroleum crude oils (*7, 8*), and the carboxylic acids in petroleum have received considerable study (*9*). However, 2-quinolones have not previously been identified in asphalts nor has their association with carboxylic acids been recognized. 2-Quinolones in asphalt and their interaction products with the carboxylic acids present were studied in this work by selectively silylating the quinolones and carboxylic acids. Similar studies were conducted on the model system, 2-quinolone and cyclohexanecarboxylic acid. The effects of associating solvents on the acid–quinolone interactions; on the interactions of carbonyl groups in an asphalt fraction; and on the carbonyl stretching frequencies of model acids, esters, ketones, and amides were also studied.

Because the molecular interactions of 2-quinolones and carboxylic acids with themselves and with each other result from strong hydrogen bonds (*10*), the probable importance of these interactions as significant contibutors to asphalt physical properties is suggested.

EXPERIMENTAL

Materials. Three asphaltic samples were used in the analytical work: Wilmington (Calif.) asphalt described in previous studies (*1, 11, 12*), a molecular distillation fraction from this asphalt (*4*), and an asphaltic resin fraction obtained by the Kleinschmidt (*13*) separation procedure from the molecular distillation fraction. The asphaltic resin fraction from the Kleinschmidt procedure is that portion of deasphaltened asphalt not removed from fuller's earth with pentane or methylene chloride (CH_2Cl_2) but removed with methyl ethyl ketone. The molecular distillation fraction,

(1) J. C. Petersen, *Fuel*, **46**, 295 (1967).
(2) J. Knotnerus, *J. Inst. Petrol., London*, **42**, 355 (1956).
(3) P. G. Campbell and J. R. Wright, *J. Res. Nat. Bur. Std.*, **68C**, 115 (1964).
(4) R. V. Helm and J. C. Petersen, ANAL. CHEM., **40**, 1100 (1968).
(5) R. V. Helm, *ibid.*, **41**, 1342 (1969).
(6) J. E. Stewart, *J. Res. Nat. Bur. Std.*, **58**, 265 (1957).
(7) E. C. Copelin, ANAL. CHEM., **36**, 2274 (1964).
(8) L. R. Snyder, B. E. Buell, and H. C. Howard, *ibid.*, **40**, 1303 (1968).
(9) W. K. Seifert and W. G. Howells, *ibid.*, **41**, 554 (1969) and references cited therein.
(10) J. Claine Petersen, *J. Phys. Chem.*, **75**, 1129 (1971).
(11) T. C. Davis, J. C. Petersen, and W. E. Haines, ANAL. CHEM., **38**, 241 (1966).
(12) J. W. Ramsey, F. R. McDonald, and J. C. Petersen, *Ind. Eng. Chem. Prod. Res. Develop.*, **6**, 231 (1967).
(13) L. R. Kleinschmidt, *J. Res. Nat. Bur. Std.*, **54**, 163 (1955).

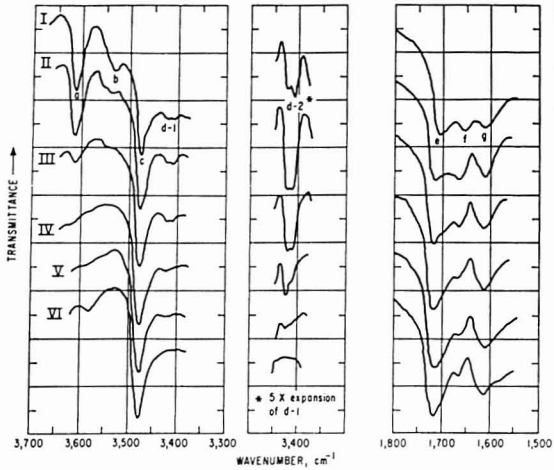

Figure 1. Infrared spectra during silylation of asphaltic resins from molecular distillation fraction, Wilmington asphalt

0.10 g/15 ml in CCl_4, 3600–3400 cm^{-1} region in 1.06-cm cell, 1800–1600 cm^{-1} region in 0.10-cm cell, solvent and reagent compensated; Curve I, before addition of HMDS; II, 1 hr at 25 °C after addition of HMDS; III, an additional 18 hr at 46 °C; IV, V, VI, an additional 30 min, 30 min, and 7 hr at 72 °C, respectively

which had an average molecular weight of 710 (vapor pressure osmometry in carbon tetrachloride), was distilled from the whole asphalt and represented 6.4% of the charge. Thirty per cent of the molecular distillation fraction appeared as asphaltic resins. Hexamethyldisilazane, HMDS, [bis(trimethylsilyl)amine] used in the silylation reactions was from Pierce Chemical Co. The carbon tetrachloride (CCl_4) and methylene chloride (CH_2Cl_2) were Baker and Adamson ACS reagent grade. Tetrahydrofuran (THF) was from Eastman Chemical Co. and was stabilized with 0.025% butylated hydroxytoluene. The small amount of stabilizer caused no significant interference in the infrared spectra. For use as a spectral solvent, THF must be free of hydroperoxides which, if present, spontaneously decompose at the slightly elevated temperatures in the infrared cell and give rise to spurious carbonyl absorption bands. Cyclohexanecarboxylic acid was Eastman Practical grade, and 2-quinolone was Eastman white label; each was of better than 95% purity. Materials used to determine the carbonyl frequencies of the infrared spectra of the model compounds were obtained from laboratory supply houses and were of unknown purity.

Infrared Spectra. Infrared spectra were obtained on a Perkin-Elmer Model 521 infrared spectrophotometer. Solutions from the silylation experiments were examined directly without solvent removal in 1.06-cm (NH and OH region) and 0.1-cm (carbonyl region) cells equipped with potassium bromide windows. The spectrum of excess HMDS was nulled by a CCl_4 solution of the reagent in a variable pathlength cell placed in the reference beam. Scale expansion (5×) was used where necessary is observing weak absorption bands. Solution concentrations used are noted on the respective figures showing the spectra. Conditions under which the spectra of the model carbonyl compounds and the molecular distillation fraction were obtained are noted in the corresponding table and figures.

Silylation Reaction. Asphalt or asphaltic resins (0.1 g/15 ml) or a mixture of 2-quinolone and cyclohexanecarboxylic acid (5 mg and 20 mg, respectively, per 100 ml) was dissolved in CCl_4. To 15 ml of the above solution was added 0.15 ml of HMDS, and the mixture was allowed to stand at room temperature, warmed, or refluxed as described later. Samples (cooled when necessary) were transferred from the reaction flask directly to the infrared cell for determination of the infrared spectra.

RESULTS AND DISCUSSION

The 1655 cm^{-1} infrared absorption band is weak in most asphalts and occasionally missing or barely discernible in others. Consistent with Stewart's observation (*6*), we found that the types of compounds in asphalt which absorb in this region are concentrated in the asphaltic resins. The 1655 cm^{-1} absorbing material can also be concentrated from a molecular distillation fraction of asphalt by elution from a silica gel column (*5*) with benzene–methanol (1:1) following prior elution of the column with benzene. The silylation studies reported in this paper were conducted on asphaltic resins separated on fuller's earth; however, confirming experiments were run on asphaltic resins from silica gel and on several whole asphalts, including the asphalt from which the asphaltic resins were derived.

Evidence for 2-Quinolone in Asphalt. Several preliminary chemical tests were run on a sample of asphaltic resins to classify the functional group type giving rise to the 1655 cm^{-1} band. The band was not affected by attempted hydrolysis with either 10% sodium hydroxide or 10% hydrochloric acid. No reduction occurred using zinc and 10% sodium hydroxide, but reaction with lithium aluminum hydride removed the 1655 cm^{-1} band. These tests indicate that the 1655 cm^{-1} band results from a carbonyl functional group which is resistant to hydrolysis and to all but vigorous reduction conditions. 2-Quinolones exhibit chemical properties similar to those indicated by the classification tests and, further, show strong carbonyl absorption bands in the 1655 cm^{-1} region.

On the assumption that the compound type, of which 2-quinolone is typical, might be responsible for the 1655 cm^{-1} band in asphalts, the compound 2-quinolone was chosen as a model compound for study in this work. 2-Quinolone rather than 2-pyridone, which has similar properties, was chosen as a model compound because it is likely that 2-quinolones would predominate over the lower molecular weight 2-pyridones in a high-molecular-weight petroleum residue like asphalt. Copelin's (*7*) identification of 2-quinolones in heavy gas oil supports this assumption. Infrared spectra of the functional groups

and thermodynamic data of 2-pyridone (*14*) and 2-quinolone (*10*) are quite similar, and conclusions based on the chemical reactivity and interactions of one should apply generally to the other.

Further evidence suggesting that the 1655 cm^{-1} band in asphalt might result from 2-quinolones was obtained by comparing the spectra of pure 2-quinolone with the spectra of asphaltic resins in the NH-stretching region. The free NH band of 2-quinolone appears at 3408 cm^{-1} in CCl_4 solution but is weak even in highly dilute solutions, and its intensity is concentration dependent because of strong intermolecular hydrogen bonding (*10*). Asphaltic resin also shows a weak band at about 3410 cm^{-1} which is also concentration dependent, indicating a hydrogen capable of hydrogen bonding.

With indirect evidence suggesting 2-quinolones and because of the near impossibility of isolating pure compounds from asphalt, specific reactions were sought by which this compound type could be confirmed in the presence of the many other functional types present. 2-Quinolone (A) was found to react with silylating reagents such as hexamethyldisilazane (HMDS) through its hydroxy tautomer to yield a silyl ether (B) as follows:

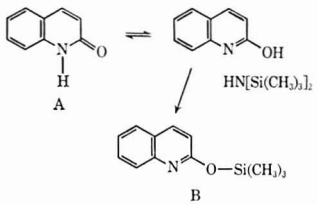

A similar reaction with 2-pyridone has been reported (*15*). The reaction is easily followed by infrared spectrometry because both the NH and carbonyl absorptions disappear simultaneously upon silylation.

Results of the application of the silylation reaction to the asphaltic resin fraction from a Wilmington (Calif.) asphalt molecular distillation fraction are shown in the series of spectra reproduced in Figure 1. Spectrum I of Figure 1 shows the absorption bands of interest in the unreacted resins. Bands previously assigned are the free phenolic OH (*1*) at 3610 cm^{-1} (*a*), the free carboxylic acid OH (*16*) at 3540 cm^{-1} (*b*), the free pyrrolic-type NH (*1*) at 3480 cm^{-1} (*c*), the carbonyl group (*6*) at about 1700 cm^{-1} (*e*), and the so-called aromatic band (*6*) at about 1600 cm^{-1} (*g*). Band *d*-2 is a 5× expansion of band *d*-1 and is a doublet with frequencies at about 3410 and 3422 cm^{-1}. Band *f* is the 1655 cm^{-1} band discussed previously. Upon addition of HMDS to the asphaltic resin solution (spectrum II), band *b* rapidly decreased accompanied by a significant increase in band *d*-2. Also noted was an apparent increase in frequencies of bands *e* and *f* and an increase in the valley between bands *f* and *g*. After 18 hour at 46 °C (spectrum III), band *b* nearly disappeared, band *a* decreased considerably, and bands *d*-2 and *f* began to decrease. Spectra IV, V, and VI show that with the increasing temperature and reaction times indicated in the figure, bands *d*-2 and *f* decreased simultaneously, leaving only a small band at *f* which was resistant to further change after the disappearance of band *d*-2.

(14) N. Kulevsky and W. Reineke, *J. Phys. Chem.*, **72**, 3339 (1968).
(15) L. Birkover, A. Ritter, and H. Kuhlthau, *Chem. Ber.*, **97**, 934 (1964).
(16) S. M. Dorrence and J. C. Petersen, ANAL. CHEM., **41**, 1240 (1969).

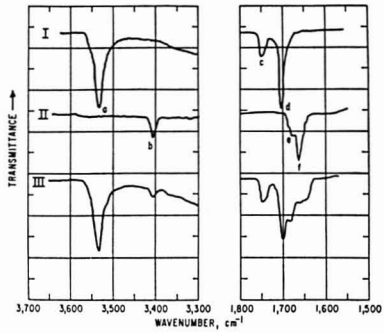

Figure 2. Infrared spectra of cyclohexanecarboxylic acid (I), 2-quinolone (II), and their mixture (III)

I, 20.0 mg/100 ml; II, 5.0 mg/100 ml; III, 20.0 mg I and 5.0 mg II in 100 ml; all solutions in CCl_4, 3600–3400 cm^{-1} region in 1.06-cm cell, 1800–1600 cm^{-1} region in 0.10-cm cell, solvent compensation

These silylation results are interpreted as follows: upon addition of HMDS to the asphaltic resins, the carboxylic acids are rapidly silylated at room temperature, yielding the silyl ester of the acid. This results in the disappearance of the free acid OH band (*b*) and the formation of a silyl ester carbonyl band which has a slightly higher frequency than the bonded acid carbonyl. The formation of the silyl ester carbonyl band causes the apparent increase in frequency of the 1700 cm^{-1} band (*e*). Silylation of the phenols results in a decrease in the free phenolic OH band (*a*). The disappearance of the phenolic and carboxylic acid OH bands in asphalt upon silylation has previously been reported by this laboratory (*16*). Silylation of the carboxylic acids also causes the increase in the free NH band (*d*-2) attributed to 2-quinolones through liberation of the 2-quinolones which previously were strongly associated with the carboxylic acids. The increase in the valley between bands *f* and *g* and the increased frequency of band *f* result from loss of the quinolone carbonyl involved in the association complex between the 2-quinolones and carboxylic acids and the corresponding production of quinolone carbonyl which absorbs at a higher frequency. Finally, the 2-quinolones silylate with the simultaneous disappearance of their NH (*d*-2) and carbonyl (*f*) bands. Note that the band at 3410 cm^{-1} silylates at a faster rate than the one at 3422 cm^{-1}, suggesting the presence of at least two structurally different compounds capable of tautomerism. Based on the nearly complete disappearance of bands in the 1655 cm^{-1} region, it is concluded that most 2-quinolones present are *N*-unsubstituted. This is consistent with the work of Copelin (*7*), who concluded that over 75% of the 2-quinolones in a gas-oil fraction from a Wilmington crude were *N*-unsubstituted.

The interpretation presented above was tested using the model compounds 2-quinolone and cyclohexanecarboxylic acid, the infrared spectra of which are shown in Figure 2. Spectra I and II are those of the acid and quinolone and show the free OH (*a*) and NH (*b*) bands, the free carbonyl bands (*c* and *e*), and the bonded carbonyl bands (*d* and *f*), respectively. The spectrum of a mixture of 2-quinolone and cyclohexanecarboxylic acid at the same initial concentration (spectrum III) shows decreases in the free NH and OH bands and complex changes in the carbonyl region in which bands attributed to the individual species decrease and additional

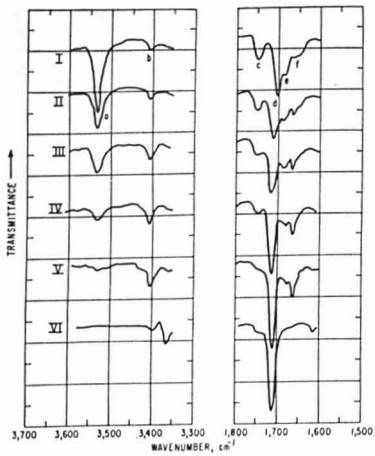

Figure 3. Infrared spectra during silylation of a mixture of 2-quinolone and cyclohexanecarboxylic acid

20.0 mg cyclohexanecarboxylic acid and 5.0 mg 2-quinolone/100 ml in CCl_4, 3600–3400 cm^{-1} region in 1.06-cm cell, 1800–1600 cm^{-1} region in 0.10 cm cell, solvent and reagent compensated; curve I, before additionof HMDS; II, 1 hr at 25 °C after addition of HMDS; III and IV, successive warming to 60 °C for a few minutes; V and VI, an additional 3 min and 15 hr at 72 °C, respectively

bands appear. The complexity of the carbonyl region of the mixture has been shown (*10*) to result from the following equilibria:

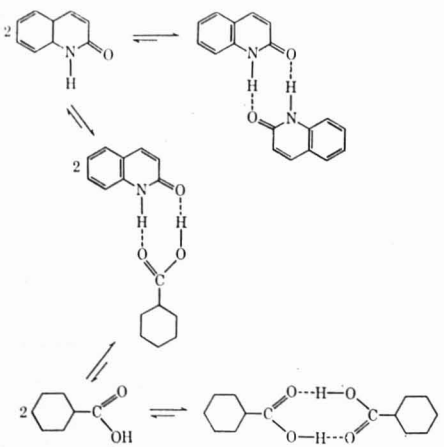

Not only do the acid and 2-quinolone strongly self-associate, but they also associate strongly with each other to form a mixed dimer. As a result, the carbonyl region of the spectra is composed of six individual carbonyl bands, some of which are not readily observable because of band overlap. These bands are the free and bonded (dimer) acid bands at 1752 cm^{-1} and 1706 cm^{-1}, the free and bonded (dimer) quinolone bands at 1680 cm^{-1} and 1664 cm^{-1}, and the bonded acid and bonded quinolone bands of the mixed dimer at 1689 cm^{-1} and 1651 cm^{-1}, respectively (*10*).

Changes in the absorption bands on silylation of a model quinolone–acid mixture are shown in Figure 3. Similar to the acids in the resins, the free acid OH of cyclohexanecarboxylic acid silylated rapidly (band *a*), forming the silyl ester (compare with Figure 1). The formation of the ester carbonyl band at 1712 cm^{-1} and the simultaneous loss of the bonded acid carbonyl band *d* appear as an apparent increase in the frequency of the bonded acid carbonyl band (spectra I through IV). As expected, silylation also resulted in the loss of the free acid carbonyl band *c*. Silylation of the carboxylic acid caused an increase in the concentration of free and dimer 2-quinolone as evidenced by an increase in the absorbances of the free NH (*b*) and bonded carbonyl (under *f*) bands. Loss of the bonded acid and 2-quinolone carbonyls involved in the mixed dimer is evidenced by changes in the area of band *e* and loss of the shoulder on the low frequency side of band *f*, respectively. Refluxing the mixture (curve VI) finally caused the 2-quinolone NH (*b*) and carbonyl (*f*) bands to disappear. A mixture of 2-pyridone and cyclohexanecarboxylic acid was found to silylate in a similar manner.

In addition to the evidence already presented for the presence of 2-quinolones in asphalt, their presence in asphalt was also indicated by high-resolution mass spectrometry. Parent peaks characteristic of the unsubstituted 2-quinolone and of substituted 2-quinolones were observed in the asphaltic resin fraction. Moreover, the P − 28 ions were also observed. These ions result from the loss of carbon monoxide from the parent ions as previously described (*17*). This fragmentation is characteristic of the conjugated lactam structure.

Solvent Effects on Molecular Interactions. Because 2-quinolones, carboxylic acids, and possibly other carbonyl-containing molecules in asphalt associate strongly in neat samples and in CCl_4 solutions, their characterization by infrared spectrometry without supplementary chemical evidence is difficult. The infrared spectra are further complicated by the variety of carbonyl types present, thus producing broad carbonyl absorptions composed of many overlapping bands. Figure 4 shows the ability of associating solvents to reduce the complexity of the carbonyl absorption bands of 2-quinolone and cyclohexanecarboxylic acid. Both the acid (I) and quinolone (II) are in equilibrium with their cyclic dimers in CH_2Cl_2 as evidenced by two carbonyl absorptions for each compound. The lower frequency in each case is assigned to the bonded carbonyl of the dimer and the higher frequency to free carbonyl of the monomer. Although these compounds associate in CH_2Cl_2, the tendency to form a cyclic dimer is much less in CH_2Cl_2 than in CCl_4. This can be seen by comparing spectra I, II, and III in Figure 4 with those in Figure 2. The ability of CH_2Cl_2 to reduce the association of carboxylic acids has previously been noted (*4*). Methylene chloride has also been shown to reduce intramolecular hydrogen bonds in certain amides (*18*). The ability of CH_2Cl_2 to reduce association in hydrogen-bonded complexes probably results from the interaction of its electron deficient hydrogens with the hydrogen-bonding bases, thus competing with the bonding hydrogens in the complex. The tendency of halogenated hydrocarbons such as CH_2Cl_2 (*18*), chloroform (*18–20*), and even

(17) J. Moller and O. Buchardt, *Acta Chem. Scand.*, **21**, 1668 (1967).
(18) W. Barbieri and L. Bernardi, *Tetrahedron*, **21**, 2453 (1965).
(19) F. Takahashi and C. L. Norman, *J. Phys. Chem.*, **69**, 2950 (1965).
(20) H. Suhr, *J. Mol. Struct.*, **1**, 295 (1968).

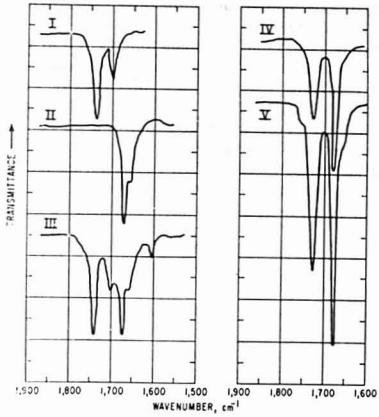

Figure 4. Infrared spectra of cyclohexanecarboxylic acid and 2-quinolone in methylene chloride and tetrahydrofuran

Curves I, II, and III, cyclohexanecarboxylic acid, 2-quinolone, and their mixture, respectively, in CCl_4; Curves IV and V, mixture of cyclohexanecarboxylic acid and 2-quinolone at two concentrations in THF; all spectra are dilute solutions in 0.10-cm cells, concentrations unknown

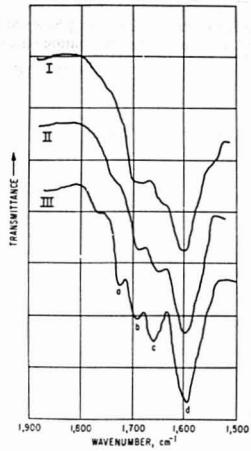

Figure 5. Infrared spectra of molecular distillation fraction from Wilmington asphalt in carbon tetrachloride (I), methylene chloride (II), and tetrahydrofuran (III)

0.1 g/10 ml in 0.05-cm cell, solvent compensated

CCl_4 (*21*), to form association complexes with electron donors has been reported. In spite of the reduced association of 2-quinolone and carboxylic acids in CH_2Cl_2 when compared with CCl_4, the spectrum of the mixture is still complex and overlapped (Figure 4, III) and is composed of the six bands representing the free and bonded carbonyls of the pure compounds plus the bonded carbonyls of the mixed dimer similar to those described for the mixture in CCl_4 solution.

Electron donating solvents such as tetrahydrofuran (THF) have been reported to form 1:1 complexes with electron acceptors (*22*) and to break up molecular associations between the ketone oxygen and the magnesium in chlorophyll-like materials (*23*). The ability of THF to reduce molecular association and thus simplify the carbonyl absorption region in the 2-quinolone–cyclohexanecarboxylic acid mixture is shown in spectra IV and V, Figure 4, in which the spectra at two different concentrations in THF are reproduced. Instead of six carbonyl bands, only two are present. THF completely prevented the association of the acid or quinolone, as either dimer or mixed dimer; and only the free carbonyl bands at 1728 cm^{-1} for cyclohexanecarboxylic acid and 1678 cm^{-1} for 2-quinolone are apparent. This probably results from the strong association of the oxygen of the THF molecule with the bonding hydrogens in the acid and quinolone, thus liberating the carbonyl groups. Any possible equilibrium toward dimer formation is overwhelmed by the preponderance of solvent molecules.

The ability of CH_2Cl_2 and THF to break up the molecular association of carbonyl groups in the molecular distillation fraction from Wilmington asphalt is shown in Figure 5. Spectrum I is a reference trace in CCl_4. Note the broad carbonyl band at about 1700 cm^{-1} and the weak shoulder in the 1665 cm^{-1} region. The spectrum in CH_2Cl_2 (II) shows increased resolution of the 1700 cm^{-1} band with a slight solvent shift to a lower frequency and an increased resolution of the 1655 cm^{-1} region. There is a weak shoulder at about 1720 cm^{-1} which probably results from the free carbonyl of carboxylic acids. Finally, spectrum III shows the absorption bands of the fraction in THF. A strong free carboxylic acid carbonyl band (*a*) is now apparent. Band *b* is probably caused by ketones plus possibly some associated acids, and band *c* is well resolved and probably results primarily from 2-quinolones.

The electron donating ability of THF is further demonstrated by its ability to completely associate with the electron deficient or acidic phenolic OH and pyrrolic NH groups in asphalt. The free phenolic OH and pyrrolic NH bands, normally observed at 3610 cm^{-1} and 3480 cm^{-1} in CCl_4 (*1*), are not observed in THF solutions. These groups both show a broad absorption band of the association complex in THF with a band maximum of about 3300 cm^{-1}. The model compounds phenol and indole both give association bands in THF at the same frequency (3300 cm^{-1}). These results further confirm the previous assignment in asphalts (*1*) of the phenolic OH and pyrrolic NH bands at 3610 and 3480 cm^{-1}, respectively.

Associating solvents such as CH_2Cl_2 and THF can be most useful in the resolution of the carbonyl band; however the asphalt components must be soluble in the THF or CH_2Cl_2 solvent for dissociation of the asphalt molecules to occur. Meaningful resolution of the carbonyl band is complicated by the presence of an increasing number of carbonyl types with differing absorption frequencies. Therefore, the use of associating solvents to simplify the carbonyl region will be less suc-

(21) H. Wolff and R Wuertz, *Ber. Bunsenges Phys. Chem.*, **72**, 101 (1968).
(22) M. A. Slifkin, *Spectrochim. Acta*, **25A**, 1037 (1969).
(23) L. J. Boucher and J. Katz, *J. Amer. Chem. Soc.*, **89**, 4703 (1967).

Table I. Carbonyl Stretching Frequencies of Selected Classes of Carbonyl-Containing Compounds

Compound	Frequency,[a] cm^{-1} in CH_2Cl_2	in THF	Frequency shift from CH_2Cl_2 to THF
Acids			
Stearic acid	1707 (1742)[b]	1734	−8
Cyclohexanecarboxylic acid	1703 (1740)	1728	−12
Benzoic acid	1692 (1730)	1721	−9
Cholanic acid	1706 (1742)	1731	−11
Esters			
Cyclohexyl acetate	1722	1732	+10
Methyl stearate	1730	1740	+10
Phenyl stearate	1751	1760	+9
Methyl benzoate	1719	1725	+6
Coumarin	1730	1736	+6
Ketones			
Cyclohexanone	1706	1710	+4
Acetophenone	1683	1687	+4
Laurophenone	1682	1686	+4
Benzophenone	1658	1662	+4
Anthrone	1660	1666	+6
Fluorenone	1713	1717	+4
Amides			
1-Naphthylacetamide	1682	1690	+8
Benzamide	1679	1683	+4
n-Methyl-2-phenylacetamide	1667	1680	+13
N,N-Diphenylacetamide	1665	1679	+14
Oxindole	1730 (1710) (1753)	1732	+2
6-Methyl-4-quinolone	1641	1646	+5
2-Quinolone	1673 (1660)	1678	+5
2-Pyridone	1672 (1654)	1678	+6

[a] Spectra are of dilute solutions contained in a 0.05-cm cell using solvent compensation in the reference beam.

[b] Frequencies in parentheses are those of bands of minor intensity. For the acids, this is the free carbonyl band; for 2-quinolone, the associated carbonyl band; and for oxindole, type unknown.

cessful with whole asphalts than with asphalt fractions that are more homogeneous.

To support the interpretation of this work and to provide reference frequencies for future studies of the carbonyl region in asphalt, the infrared spectra of several classes of compounds containing the carbonyl group were obtained in CH_2Cl_2 and THF. Results are shown in Table I. Spectra were obtained in dilute solutions using a 0.05-cm cell and compensating with solvent in the reference beam. In some instances two or more carbonyl bands were observed, and the weaker bands are reported in parentheses. The higher frequencies of the acids and 2-quinolone in CH_2Cl_2 result from the free carbonyls; the lower frequencies result from the bonded carbonyls. The reason for the multiple carbonyl peaks of oxindole is unknown.

Carbonyl solvent shifts on going from CH_2Cl_2 to THF are also shown in Table I. With self-associated species, shifts of the free carbonyl are reported. All classes of carbonyls investigated shifted to a higher frequency on going from CH_2Cl_2 to THF except the carboxylic acids free C=O bond which showed a decrease in frequency. This behavior can be useful in distinguishing between carboxylic acids and ketones formed in asphalt components on oxidative aging. Care must be taken, however, to distinguish between the bonded and free carbonyl bands in CH_2Cl_2. This decrease in frequency of free acid carbonyl in THF probably results from the inductive effect of the strong hydrogen bond formed between the THF and the acid OH group.

Significance of Molecular Interactions in Asphalt. It is tempting to speculate on the significance of the interactions of 2-quinolones and carboxylic acids on the physical properties of asphalts. Upon examination of the 1655 cm^{-1} absorption band in several asphalts, and based on molar absorptivities for 2-quinolone (*10*), it is estimated that the concentration of 2-quinolones in some asphalts may approach 0.5 weight per cent. Carboxylic acids initially present and formed on oxidation by oxidative weathering may exceed this value several fold based on acid numbers determined in our laboratory. Thermodynamic studies of model compounds (*10*) have shown that the equilibrium constants (1 mol at 22 °C in CCl_4) for the self-associations of 2-quinolone and cyclohexanecarboxylic acid and for the association of quinolone and acid to form the mixed dimer are 3.34×10^4, 3.84×10^3, and 2.52×10^4, respectively; hydrogen-bond strengths ($\Delta H°$, kcal/mol dimer) for the respective dimers are −8.69, −11.1, and −10.3. These data show a high degree of association and the formation of strong hydrogen bonds. 2-Quinolones and carboxylic acids in asphalt would be expected to behave similarly. This is evidenced by the infrared spectra of neat asphalt samples which show the 2-quinolones and carboxylic acids to be highly associated. These and other molecular interactions, therefore, must play an important part in determining the rheological or flow properties of asphalt, both initially and as they change during oxidative weathering.

Received for review February 15, 1971. Accepted May 3, 1971. Presented at the Division of Petroleum Chemistry, 161st National Meeting, American Chemical Society, Los Angeles, Calif., March 1971. The work upon which this report is based was done under a cooperative agreement between the Bureau of Mines, U. S. Department of Interior, and the University of Wyoming. Mention of specific brand names or models of equipment is made for information purposes only and does not imply endorsement by the Bureau of Mines.

Application of Rapid Infrared Spectrometry to Air Pollution Research

Joseph R. Comberiati

Morgantown Energy Research Center, Bureau of Mines, United States Department of the Interior, Morgantown, W. Va.

LABORATORY RESEARCH of methods being studied for the removal of sulfur dioxide in stack gases from coal-burning electric powerplants requires the application of rapid and continuous analysis for type and concentration of constituents. Several methods under investigation for removing sulfur dioxide (*1–4*) from gas streams, for instance, involve chemical transformation of sulfur dioxide into other gases that must subsequently be identified and their concentration established. Slow-scan standard spectrophotometers and a 1-compound, single-wavelength infrared monitor in general use are not adequate. Moreover, infrared spectra of pure permanent gases are not as widely available in the literature as are spectra of liquid compounds (*5–8*). Also, few collections of pure compound gases are available. Pierson and coworkers (*9*) compiled infrared spectra of 66 gases and vapors. Accordingly, application was made of a rapid-scan infrared spectrophotometer that gives a complete spectrum of gases in 12.5 seconds, thus providing positive identification of all gaseous compounds, except the elemental gases, without flow interruption and without time-consuming delay for sampling and analysis.

EXPERIMENTAL

Equipment. Several fast-scan infrared spectrophotometers are marketed that could have been used for this investigation, but a Beckman IR-102 was available and suitable for the purpose. (Trade names are included to facilitate understanding and do not imply endorsement by the Bureau of Mines.) The IR-102 is a single-beam instrument with automatic repetitive scanning in 5 or 12.5 seconds of wavelengths in three divisions—2.5 to 4.5 microns; 4.4 to 8.0 microns; and 7.9 to 14.5 microns—with interference filters. The sample cell has a gold-plated interior, 30-cm pathlength, holds 9 cc, and is used in a flow-through manner. Coupled to the spectrophotometer is a high-speed hot-stylus oscillographic recorder.

Both instruments rest on a table fitted with 5-inch diameter wheels and two shelves containing accessories and tubing. The assembly is compact and can readily be moved from one laboratory to another. A simple switching arrangement permits monitoring of three gas streams: helium to provide an inert atmosphere in the sample cell for a background trace, gas to a reaction vessel, and gas from a reaction vessel.

Gases and Gas Mixtures. Standard gas mixtures were prepared gravimetrically rather than by pressure, although other mixtures were also made by pressure for comparative purposes. Individual gases were obtained in lecture size bottles with grade and purity as follows: SO_2, commercial grade, 99.9%; CH_4, CP grade, 99.1%; CO_2, bone-dry grade, 99.8%; CO, CP grade, 99.5%; and COS, 96%.

Qualitative Analysis. Since the spectrophotometer is a single-beam instrument, bands in the spectrum from CO_2 and moisture in the air are corrected by means of a background trace before and after each analysis. Spectra are obtained by simultaneously passing the pure gas and dilution gas (helium or nitrogen) through the gas cell in a flow-through manner. Scanning is begun and the dilution gas flow is adjusted until suitable spectra are obtained. Spectra are recorded for all constituents in the gas stream except the elemental gases. The complete spectrum is quite small—2 inches × 5½ inches—so an illuminated magnifier and a millimeter rule are used to determine the wavelengths of the bands.

Quantitative Analysis. The small spectra makes it essential that measurement of band absorbance be accurate. Therefore, part of the standard infrared absorbance scale is redrawn, photographed, and reduced to the size of the instrument spectra. A transparent plastic overlay is then placed over the spectra and the absorbance of the individual band is measured. With the aid of the illuminated magnifier, readings can be obtained with an accuracy of ±0.05 to ±0.1 and good reproducibility.

After the spectra of gas mixtures of known concentrations are obtained and the band absorbance is measured, the latter values are plotted against corresponding concentrations to make a calibration curve. Gases in trace amounts can be determined if multiple interference is no problem and only simple mixtures with little overlapping of bands are analyzed.

RESULTS AND DISCUSSION

Figures 1 (*A*) and 2 (*C*) show spectra of sulfur dioxide and carbonyl sulfide, each diluted with helium. (Background traces of all spectra were raised to avoid overlap of the two traces.) Apparent bands in the 4 to 5 micron and the 8-micron regions are actually the result of filter changes.

Table I gives infrared absorption bands for the common gases found in flue and producer gas, except for elemental gases that do not absorb in the 2.5 to 14.5 micron range. Only the bands used to identify the gases are listed. Relative

(1) D. Bienstock, L. W. Brunn, E. M. Murphy, and H. E. Benson, *BuMines Inf. Circ.* **7836** (1958).
(2) P. G. Marvin and J. Jonakin, *Chem. Eng.*, **77** (9), 173 (1970).
(3) J. G. Stites, Jr., W. R. Horlacker, Jr., J. L. Bachofer, Jr., and J. S. Bartman, *Chem. Eng. Progr.*, **65** (10), 74 (1969).
(4) S. T. Cuffe, R. W. Gerstle, A. A. Orning, and C. H. Schwartz, *J. Air Poll. Control Ass.*, **19** (9), 353 (1964).
(5) S. Ochiai and S. Yoshio, *Bunseki Kagaku*, **17**, 1025 (1968); *Chem. Abstr.*, **69** (26), 109597*a* (1968).
(6) R. Cameroni and A. Albasini, *Il Farmaco*, **19** (5), 227 (1964); *Chem. Abstr.*, **64**, 1248*a* (1966).
(7) J. W. Birkeland and J. H. Shaw, *J. Opt. Soc. Amer.*, **49**, 637 (1959).
(8) R. L. Bowman and J. H. Shaw, *Appl. Opt.*, **2**, 176 (1963).
(9) R. H. Pierson, A. N. Fletcher, and E. St. C. Gantz, ANAL. CHEM., **28**, 1218 (1956).

Table I. Absorption Bands for Constituents in Flue and Producer Gases

Gaseous compound	Band vibration[a]	Wavelength, μ	Frequency, cm^{-1}
SO_2	C	4.05 (w)	2,470 (w)
	AS	7.25 (s)	1,380 (s)
	AS	(Not resolved)	
	AS	7.45 (s)	1,340 (s)
	SS	8.60 (m)	1,160 (m)
	SS	8.85 (m)	1,130 (m)
CH_4	AS (CH_3)	3.30 (m)	3,030 (m)
	AS (CH_3)	3.40 (m)	2,940 (m)
	SB (CH_3)	7.35 (s)	1,360 (s)
	SB (CH_3)	7.50 (s)	1,330 (s)
CO_2		2.60 (w)	3,850 (w)
		2.70 (w)	3,700 (w)
	AS	4.30 (s)	2,320 (s)
CO	S	4.60 (s)	2,170 (s)
	S	4.70 (s)	2,130 (s)
COS	C	3.50 (m)	2,860 (m)
	AS (C=O)	4.95 (s)	2,020 (s)
	AS (S=C=O)	9.80 (m)	1,020 (m)
	SS (S=C=O)	12.00 (s)	830 (s)
CS_2		4.60 (w)	2,170 (w)
	AS	6.55 (s)	1,530 (s)

[a] C, combination; AS, asymmetric stretching; SS, symmetric stretching; SB, symmetric bending; S, stretching.

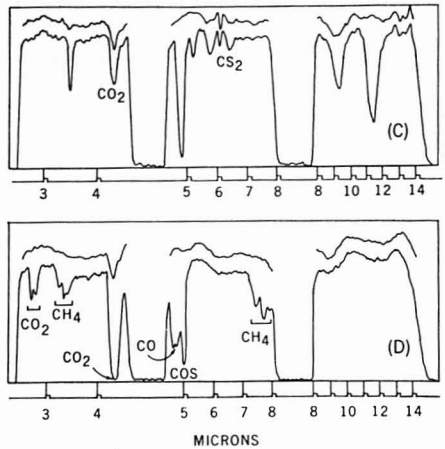

Figure 2. (*C*) **Carbonyl sulfide (impurities carbon dioxide and carbon disulfide)**
(*D*) **Gas mixture No. 4 used as standard for quantitative analysis**

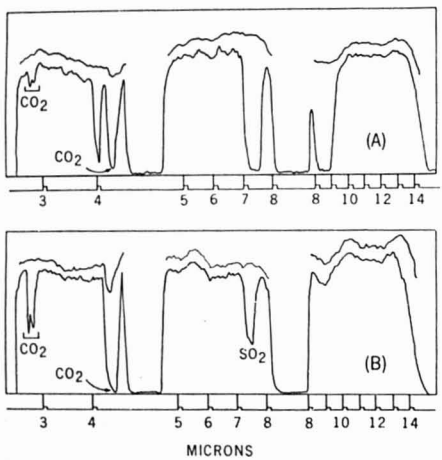

Figure 1. (*A*) **Sulfur dioxide (impurity carbon dioxide)**
(*B*) **Gas mixture No. 1 used as standard for quantitative analysis**

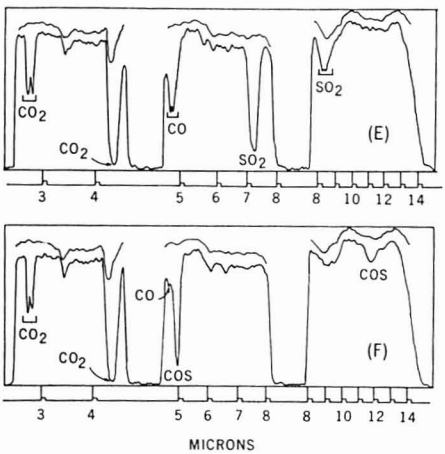

Figure 3. Reaction of SO_2 with CO in the presence of catalyst: (*E*) inlet gas stream, (*F*) outlet gas stream

intensities are designated as strong (s), medium (m), or weak (w). Included in the list is carbon disulfide, a common impurity of carbonyl sulfide. Spectra were made for oxides of nitrogen and several other gases, but none were found in the gases that were monitored.

Figures 1 (*B*) and 2 (*D*) show traces for two gas mixtures that were used as standards for quantitative analysis and converted into calibration charts. Charts were made for all gases of interest. A linear relationship usually existed over a small range, *e.g.*, four gas mixtures containing concentrations of sulfur dioxide from ≈300 ppm up to ≈4000 ppm showed a straight line relationship for sulfur dioxide's most intense bands at 7.25 and 7.45 microns. The relationship above this concentration was not determined for sulfur dioxide. Accuracy of the infrared analyzer for sulfur dioxide was determined by comparing with analyses of a flue gas mixture of unknown sulfur dioxide concentration by gas chromatograph and mass spectrometer. Results of these analyses were as follows: gas chromatograph, 2500 ppm; mass spectrometer, 2300 ppm; infrared analyzer, 2580 ppm.

Application of Method. Infrared monitoring was conducted of the inlet and outlet gas streams in three different research investigations of sulfur dioxide removal from flue gas by chemical reaction or absorption. Spectra of gases in these three studies are shown in Figures 3–5, with com-

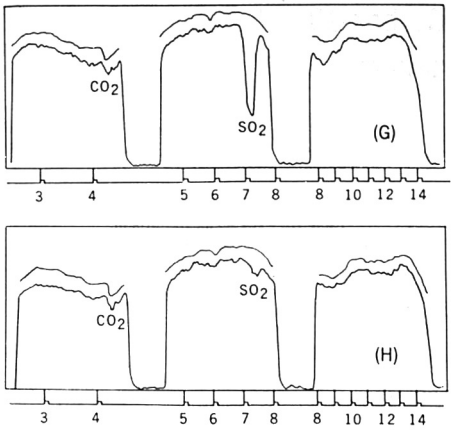

Figure 4. Reaction of SO_2 with FeS: (*G*) inlet gas stream, (*H*) outlet gas stream

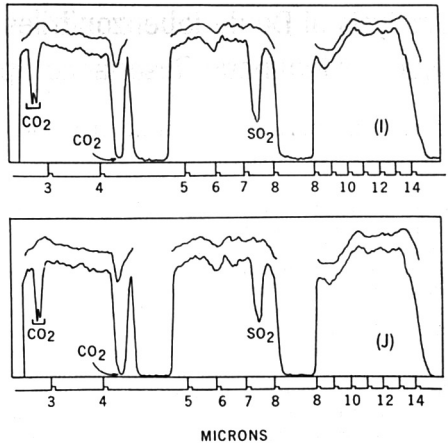

Figure 5. Absorption of SO_2 on eastern oil shales: (*I*) inlet gas stream, (*J*) outlet gas stream

parison of inlet and outlet gases given in each instance. It is quite apparent that chemical reaction took place. In Figure 3, for example, carbon dioxide, carbon monoxide, and sulfur dioxide are present in the inlet gas stream; in the outlet stream, the carbon dioxide concentration is about the same, but the carbon monoxide content is about one fourth of what it was before. Moreover, carbonyl sulfide bands are present but the sulfur dioxide bands are not. In this work, the reaction between flue gas and producer gas was being investigated. The objective was to precipitate elemental sulfur and convert carbon monoxide to carbon dioxide. In the initial experiments, a small amount of sulfur was formed, but 4 to 6 hours was required for each experiment. The first few tests with the in-line infrared analyzer showed that the carbon monoxide was completely converted to carbon dioxide within a few minutes and the sulfur dioxide concentration remained relatively unchanged. In a later test under different conditions, the spectra shown in Figure 3 (*F*) was obtained after two minutes of operation. In this case, sulfur dioxide was converted to carbonyl sulfide, as evidenced by the bands at 4.95 and 12.00 microns. The test was discontinued because the objective was not met, thus saving 4 to 6 hours of running time.

Figure 4 shows the sulfur dioxide (diluted with nitrogen) concentration of inlet and outlet gas streams to be about 3700 and 370 ppm, respectively—a reduction of about 90 per cent. Figure 5 shows a small decrease in sulfur dioxide content, representing a little more than 25 per cent removal.

CONCLUSIONS

Qualitative and quantitative analyses of gas mixtures are obtainable in 5 to 10 minutes by repeated, rapid scanning with an infrared spectrometer. Rapid analysis permits evaluation of chemical reactions during an experiment and provides a basis for stopping the experiment or continuing it.

Portability of the analytical system makes possible the monitoring of research studies in different laboratories. Practical use of the method is limited to laboratory research studies with clean dry gases; it cannot be used in the plant to analyze actual stack gases.

Analyses at temperatures up to 100 °C resulted in good spectra, although analyses have been made at temperatures up to 300 °C. At the higher temperature, the silicone gaskets had to be replaced with aluminum gaskets. Sensitivity of the instrument was lower, however, and the background trace dropped down to less than 50 per cent transmittance.

RECEIVED for review January 28, 1971. Accepted May 25, 1971.

Analysis of Deuteriobenzonitriles by Carbon-13 Nuclear Magnetic Resonance Spectrometry

G. L. Lebel, J. D. Laposa, B. G. Sayer, and R. A. Bell

Department of Chemistry, McMaster University, Hamilton, Ontario, Canada

In connection with a study of the positional variation of the contribution of C–H out-of-plane bending modes to the radiationless deactivation processes from the triplet state of benzonitrile, we required a number of deuterium substituted benzonitriles. The characterization of the specific isomers by infrared spectrometry is complex (*1*) and suffers from the serious liability of being unable to adequately determine the presence of isomeric impurities. Likewise proton magnetic resonance spectrometry, although in principle adequate to characterize the pure isomers, is tedious and time consuming and requires the computer simulation of a four spin system where the nuclei have very similar chemical shifts. (The total chemical shift range of the protons of benzonitrile at 100 MHz is only 30 Hz.) In addition, the presence of isomeric impurities is very difficult to detect. On the contrary, the analysis of the proton decoupled ^{13}C magnetic resonance spectrum of benzonitrile, as described below, is straightforward and simple, and yields both qualitative and quantitative information about the isotopic composition of the required compounds.

EXPERIMENTAL

Preparation. The monodeuteriobenzonitriles were prepared by reductive removal of bromine from the corresponding bromobenzonitrile (supplied by Aldrich Chemical Co.) with zinc in the presence of acetic anhydride and deuterium oxide (*1*). The derivatives were all obtained in close to 100% isotopic purity and with less than 5% of rearranged isomers. Commercial benzonitrile (Aldrich Chemical Co.) was vacuum distilled, prior to use. Perdeuteriobenzonitrile was used as received from Merck, Sharp and Dohme of Canada; its isotopic purity was better than 99%.

Apparatus. Spectra were recorded with a Varian Associates HA-100 spectrometer operating at 23.5 kG and 25.1 MHz. The operating probe temperature was +55 °C. Field/frequency stabilization was achieved by use of an external (1.5-mm capillary) $^{13}CH_3I$ lock, and chemical shift measurements were made initially relative to internal benzene and thence relative to internal tetramethylsilane. Samples of 0.2–0.3 ml of the neat benzonitriles were used in a 5-mm o.d. sample tube, and normally a signal accumulation of 9 to 16 scans with a Varian Associates C-1024 time averaging device was sufficient to give an adequate signal-to-noise enhancement. As a typical example, for benzonitrile itself a signal accumulation of 9 scans gave a signal to noise ratio of 34:1 for the single para carbon and a linewidth at one-half peak height of 1.2 Hz. Proton decoupling was carried out using a Varian Associates V-3512-1 noise decoupler.

RESULTS AND DISCUSSION

In the proton decoupled ^{13}C magnetic resonance spectrum of benzonitrile (*2*), all six ring carbon atoms are significantly different in chemical shift (see Table I), with the ortho carbons separated from the para carbon by 0.7 ppm and from the meta carbons by 2.9 ppm. Such chemical shift differences make the analysis of deuteriobenzonitriles an exceedingly simple task; as a typical case the spectrum of *o*-D-benzonitrile is shown in Figure 1. The carbon bearing the deuterium is split into a triplet by coupling with the deuterium nucleus [$J_{^{13}C,D}$ = 25.0 Hz (*3*)], and from the chemical shift of 134.2 ppm of the center line of the triplet it is obvious as to which carbon the deuterium is bound. The signal intensities in proton decoupled ^{13}C spectra are normally altered because of the intramolecular nuclear Overhauser effect (*4*). However in the present case the ortho, meta, and para carbons will all show the same Overhauser enhancements for a given experiment since each carbon is directly bonded to a single proton, and the dipolar relaxation effect of this proton will completely outweigh the relaxation effects of the more distance protons on adjacent carbon atoms because of the $1/r^6$ dependence (*5*, *6*). Unequivocal experimental evidence for this has been found in intensity measurements performed on a series of polynuclear aromatic hydrocarbons (*7*) where all carbon atoms bearing one hydrogen showed identical areas irrespective of their position in the molecule. Thus, for the specific example of *o*-D-benzonitrile, the observed signal intensity of the meta carbons at 131.5–131.6 ppm can be used to obtain a standard area for a single carbon and this can then be compared with the observed area of the undeuterated ortho carbon at 134.45

Table I. ^{13}C Chemical Shifts of Benzonitrile and Deuterated Derivatives

	Carbon, ppm[a,b]		
	ortho	meta	para
C_6H_5CN	134.45	131.55	135.20
o-DC_6H_4CN	133.20	131.50	135.00
	134.20	131.60	
	135.20		
	134.45[c]		
m-DC_6H_4CN	134.30	130.25	135.10
	134.45	131.25	
		132.25	
		131.55[c]	
p-DC_6H_4CN	134.45	131.45	133.65
			134.70
			135.65
C_6D_5CN	133.05	130.05	133.70
	134.05	131.05	134.70
	135.10	132.05	135.65

[a] Carbon-1 and the nitrile carbon absorbed at 114.65 and 120.95 ppm, respectively.
[b] All shifts are negative (downfield) relative to internal tetramethylsilane (TMS) and are accurate to ±0.05 ppm.
[c] Unsubstituted carbon.

(1) B. Bak and J. T. Nielsen, *Z. Elektrochem.*, **64**, 560 (1960).
(2) F. W. Wehrli, J. W. de Haan, A. I. M. Keulemans, O. Exner, and W. Simon, *Helv. Chim. Acta*, **52**, 103 (1969).
(3) F. J. Wiegert and J. D. Roberts, *J. Amer. Chem. Soc.*, **89**, 2967 (1967).
(4) E. G. Paul and D. M. Grant, *ibid.*, **86**, 2977 (1964).
(5) K. F. Kuhlmann and D. M. Grant, *ibid.*, **90**, 7355 (1968).
(6) R. A. Bell and J. K. Saunders, *Can. J. Chem.*, **48**, 1114 (1970).
(7) A. J. Jones, D. M. Grant, and K. F. Kuhlmann, *J. Amer. Chem. Soc.*, **91**, 5013 (1969).

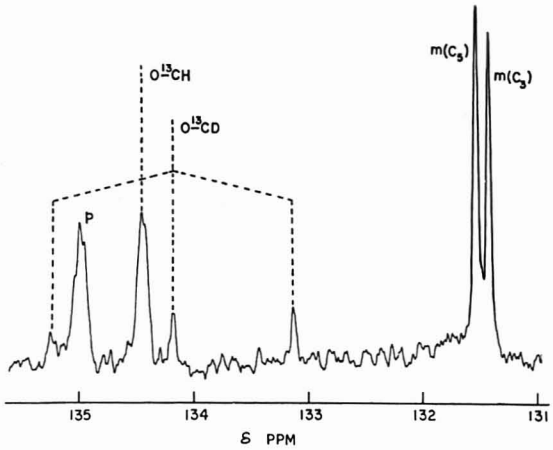

Figure 1. ^{13}C spectrum of *ortho*-monodeuteriobenzonitrile; 25 scans

The two high field ^{13}C–D lines have a $^1/_2$ peak height linewidth of 1.0 Hz and a signal to noise ratio of 12 : 1. The meta carbon, C_3, is moved upfield by a second order isotope shift (*9*)

ppm. Any increase over the standard area can therefore be attributed to proton contamination of the deuterium-bearing carbon. The presence of deuterium on other carbons could be ascertained by a careful search for the triplets in their characteristic positions. In practice a limit of 5% isomeric impurity could be detected by this method although in theory smaller quantities of other deuterated isomers should be detectable by increasing the number of time averaging scans.

The isotope shift of 0.2–0.5 ppm to higher field in the ^{13}C chemical shift induced by the directly bonded deuterium is normal (*8*). More interesting are the second atom isotope shifts of 0.15 ppm induced by the deuterium substituent. This effect is the origin of the apparent "splitting" of the meta carbons in *o*-D-benzonitrile in Figure 1 and while the effect has been observed for other nuclei (*9*), the magnitude of the shifts caused by the deuterium is larger than that of the shifts caused by substitution of the isotopes of other elements (*10*).

RECEIVED for review February 1, 1971. Accepted May 25, 1971.

(8) G. E. Maciel, P. D. Ellis, and D. C. Hofer, *J. Phys. Chem.*, **71**, 2160 (1967).

(9) H. Batiz-Hernandez and R. A. Bernheim, *Progr. Nucl. Magn. Resonance Spectrosc.*, **3**, 63 (1967).

(10) J. Bacon and R. J. Gillespie, *J. Chem. Phys.*, **38**, 781 (1963).

Differential Reduction and Atomic Absorption Determination of Selenium

Wladislaw Reichel

Canadian Copper Refiners Limited, Montreal East, Quebec, Canada

THIS TECHNIQUE was developed as a result of the inaccuracy of gravimetric determination of selenium in high purity material (*1*), and the success of the atomic absorption technique for the determination of selenium in selenium-bearing metallurgical by-products.

Many volumetric procedures for the determination of selenium require the absence of interfering elements and small sample weight. To overcome the last difficulty, Barabas and Bennett (*2*) separated approximately 97% of the selenium under controlled conditions from a relatively large sample, and potentiometrically titrated the remaining selenium. Intended for the analysis of pure selenium, their procedure was seriously affected by interference from impurities when applied to lower grade materials.

Suseela (*3*) has shown that selenium(IV) reacts stoichiometrically with hydrazine sulfate. The reduction of selenium by hydrazine sulfate is nonspecific. Among other elements, As(V) and Fe(III) are preferentially reduced to lower oxidation states if hydrazine sulfate is deficient with respect to

(1) S. Barabas and W. C. Cooper, ANAL. CHEM., **28**, 129 (1956).
(2) S. Barabas and P. W. Bennett, *ibid.*, **35**, 135 (1963).

(3) B. Suseela, *Z. Anal. Chem.*, **147**, 13 (1955).

selenium content. Hence, in the present study it was essential to separate selenium quantitatively from these interfering elements prior to differential precipitation.

EXPERIMENTAL

Apparatus. A filter stick (consisting of a length of glass tubing, the lower part of which was packed with glass wool held in place by a constriction in the tube) was used to remove the solution after the first precipitation of selenium by hydrazine sulfate.

Atomic absorption measurements were made with a Techtron Model AA-100 unit, equipped with a 10-cm slot laminar-flow burner head Type AB-41. Fuel and supporting gas were acetylene and air at 12 and 15 psi, respectively. The 1960.26 Å selenium resonance line was used for measurement.

Reagents. Reagent grade chemicals were used: sulfuric–nitric acid mixture, prepared by mixing equal volumes of water, sulfuric, and nitric acids; hydrazine sulfate; and selenium of 99.99% purity.

Procedure. Separation of Selenium from Interfering Elements. Weigh accurately into a 400-ml beaker a sample containing 1.9–2.0 grams of selenium. Add 30 ml of sulfuric–nitric acid mixture to samples of elemental selenium or 10-ml of sulfuric acid and 10 ml of 1:1 nitric acid to samples of selenium salts. Cover and digest until completely dissolved. Remove the cover partially and evaporate the remaining nitric acid (at not more than 105 °C), that is, until the cover is dry. Cool, dilute with distilled water to 200 ml, and add 3.50 grams of hydrazine sulfate. Cover, increase the temperature slowly, and boil to complete the coagulation of the elemental selenium. Cool to about 60 °C. Aspirate the solution from the beaker through a filter stick packed with glass wool. Wash the beaker wall and the selenium residue four times with 1% v/v sulfuric acid. Leave the filter stick in the beaker and with the cover on, add slowly 20 ml of nitric acid. Digest on a hot plate to dissolve the precipitate completely. Wash the filter stick 3 times with water, applying pressure by a rubber bulb at the outlet to remove all the solution from the glass wool. Add the washings to the beaker, and remove the filter stick. Add 10 ml of sulfuric acid and mix well. Uncover partially and evaporate the excess nitric acid as above. Cool and dilute with distilled water to 100 ml.

Run three selenium standards, containing exactly 1.9200, 1.9600, and 2.0000 grams of high purity selenium, respectively, through the entire procedure.

Differential Precipitation of Selenium. To the cold solution (now free from interfering elements) add 3.150 grams of accurately weighed hydrazine sulfate. Wash the beaker wall, dilute with distilled water to 200 ml, and cover. Boil to complete the coagulation of the elemental selenium. Cool to room temperature. Filter the remaining unreacted selenious acid solution through Whatman No. 541 filter paper into a 250-ml volumetric flask. Wash the beaker, selenium residue, and filter paper several times with water, collecting the washings in the volumetric flask. Dilute to the mark with distilled water.

Atomic Absorption Determination of Selenium. Read absorbances of selenium standards. Construct a calibration curve by plotting absorbances of selenium standards against their original concentration.

Read the sample absorbance to establish the corresponding selenium value in grams from the calibration curve.

$$\text{Se } \% = \frac{\text{selenium found (g)}}{\text{sample weight (g)}} \times 100 \text{ (1)} \qquad (1)$$

RESULTS AND DISCUSSION

Sample Weight. An advantage of the differential technique is the use of a larger sample. As the quantity of the reductant must be deficient, it is important to know the approximate selenium concentration for materials of uncertain composition. Sample must contain at least 1.90 grams of selenium.

Purification of Selenium. There are no known specific reagents for selenium reduction. Selenium must be separated from interfering elements before the use of the differential reduction technique.

Hydrazine sulfate can be used for this initial separation. An excess of hydrazine sulfate in dilute (5% v/v) sulfuric acid reduces selenium(IV) quantitatively to elemental selenium. Interfering elements are reduced to a lower oxidation state, remain in the solution, and are easily removed by aspiration through a filter stick. The purified selenium is redissolved in the original beaker to avoid losses due to transfer and filtration. The elements Si, Ag, Sn, Sb, Te, Au, Hg, Pb, and Bi coprecipitate with selenium, but with the exception of Ag and Sn do not interfere with the differential precipitation. Spectrographic examination of the purified selenium did not show significant amounts of other impurities. Very impure materials require double purification to remove coprecipitated and occluded interferents. Four consecutive separations have been performed on the same synthetic sample without noticeable loss of selenium. When the selenium is free from elements reducible by hydrazine sulfate, the purification may be omitted.

Differential Precipitation of Selenium. To reduce the relative error (2–4%) in atomic absorption concentration measurement, 95–99.5% of the selenium present in the samples was precipitated with a calculated deficiency of hydrazine sulfate. In a series of experiments, after purification by the described procedure, the amount of selenium precipitated by the same quantity (3.150 grams) of hydrazine sulfate was remarkably constant. According to the equation:

$$H_2SeO_3 + N_2H4.H_2SO_4 \rightarrow Se + N_2 + 3H_2O + H_2SO_4 \quad (2)$$

3.150 grams of pure hydrazine sulfate (certified as 99.0%) precipitates 1.892 grams of selenium. The average weight of precipitated selenium was 1.893 grams in close agreement with the calculated value.

Atomic Absorption Determination of Selenium. The differential reduction of selenious acid leaves 5 to 100 mg per 250 ml dissolved selenium in solution, together with any tellurium present in the original sample. Since tellurium interferes in most volumetric procedures for determination of selenium (*2*, *4*) and since potentiometric titration covers a relatively narrow concentration range (*1*), the selective atomic absorption technique is more suitable for the determination of the residual dissolved selenium.

The atomic absorption calibration curve was established by running three selenium standards throughout the procedure. The absorbance due to unreacted selenium was plotted against the original concentration of the standards.

The calibration curve adhered to Beer's law in the range studied (0–500 μg Se/ml). Since the total selenium in the sample in grams was read from the calibration curve, any error in atomic absorption concentration measurement was decreased markedly as it affected only a small portion of the original sample.

Interference. Nitric acid interferes, and must be removed by the procedure described. Nevertheless, traces of residual nitric acid do not effect the results.

A treatment with methanol (*2*) to destroy the residual traces of nitric acid did not improve the precision of the procedure.

(4) I. M. Kolthoff and P. J. Elving, "Treatise on Analytical Chemistry," Part II, Vol. 7, Interscience Publishers, a division of John Wiley & Sons, New York-London, 1961, p 196.

Table I. Recovery of Selenium from Synthetic Standards

Se present, %	Foreign elements, %	Se found, %	Se recovered, %
95.00	5.0 Na	95.0	100.00
70.00	30.0 Na	69.9	99.86
95.00	5.0 Al	95.0	100.00
95.00	5.0 Si	95.0	100.00
95.00	5.0 Ca	94.9	98.89
95.00	5.0 Cr	95.1	100.11
95.00	5.0 Mn	95.1	100.11
95.00	5.0 Fe	95.1	100.11
95.00	5.0 Co	95.0	100.00
95.00	5.0 Ni	94.9	99.89
95.00	5.0 Cu	95.0	100.00
95.00	5.0 Zn	95.0	100.00
95.00	5.0 As	95.2	100.21
90.00	10.0 As	90.1	100.11
95.00	5.0 Sb	94.9	99.89
95.00	5.0 Te	94.9	99.89
98.00	2.0 Hg	97.8	99.80
95.00	5.0 Pb	94.9	99.89
98.00	2.0 Bi	97.9	99.90
		Average % recovery:	99.98

Table II. Precision. Comparative Results by Differential Reduction Atomic Absorption Determination and Classical Gravimetric Method

Material	Differential reduction A.A. determination	Gravimetric determination
High purity selenium, 99.99%	No. of determinations, 24	n = 24
	Mean Se %, 99.98	102.1
	Std dev, 0.077	0.449
Crude Se, Lot No. 41-E	No. of determinations, 24	n = 24
	Mean Se %, 98.82	100.5
	Std dev 0.095	0.660

The direct differential reduction may be applied only to selenium materials free from substances reducible by hydrazine sulfate. In all other cases purification is necessary.

A set of synthetic samples, each containing 95% selenium and 5% of a foreign element were analyzed by the proposed procedure. The elements studied were Na, Al, Si, Ca, Cr, Mn, Fe, Co, Ni, Cu, Zn, As, Ag, Sn, Sb, Te, Hg, Pb, and Bi. Silver and tin were the only interfering elements after purification by hydrazine sulfate.

The interference from silver was eliminated by precipitation with a small excess of hydrochloric acid before hydrazine reduction. Tin interferes by forming metastannic acid, which coprecipitates with selenium prior to hydrazine reduction. Small amounts of tin salts (up to 10 mg) and metallic tin (which does not dissolve) can be tolerated.

The atomic absorption measurement of selenium in the final 5% v/v sulfuric acid solution is interference-free because all foreign salts with the exception of tellurium have been removed during purification. Tellurium up to 500 μg/ml causes no interference.

Accuracy and Precision. Accuracy of the procedure was evaluated by recovery experiments on synthetic samples. Recovery was established by dissolving high purity selenium to which calculated amounts of impurities were added, and treating the samples as described (Table I). The average recovery was 99.98%.

Precision was evaluated on selenium samples of different purity (Table II). The samples were also analyzed by the classical gravimetric procedure (*5*). In precision, the recommended method is superior to the gravimetric procedure. Standard deviation for sets of 24 results obtained in 12 separate runs made during two months was 0.095% for the differential procedure compared to 0.660 for gravimetry (Table II).

Other Applications. The procedure was applied successfully to selenium dioxide, sodium selenite, and selenium mixtures.

The use of high purity selenium standards makes the procedure applicable to the indirect determination of the purity of hydrazine sulfate.

ACKNOWLEDGMENT

The author is indebted to I. Krzisnik who conducted most of the experimental work.

RECEIVED for review February 18, 1971. Accepted May 12, 1971.

(5) W. W. Scott, "Standard Methods of Chemical Analysis," Fifth Edition, Vol. I, D. Van Nostrand Company, Inc., New York, N.Y., 1939, p 787.

Filters for X-Ray Spectrometry Prepared by Thin-Layer Electrodeposition

Basil H. Vassos, Roland F. Hirsch, and Donald G. Pachuta

Chemistry Department, Seton Hall University, South Orange, N. J. 07079

FILTERS serve several purposes in analytical methods utilizing X-rays. When the filters are placed in the primary beam of an X-ray spectrometer, they help to improve sensitivity by reducing the background (*1–3*). Filters are used in energy-dispersive X-ray spectrometry to simplify mathematical analysis of the spectra (*4*). Balanced pairs of filters permit monochromatization of X-ray beams for diffractometry (*5, 6*).

These filters must be thin if a satisfactory amount of the radiation of the desired wavelength is to be transmitted. Furthermore, the thickness of the filters must be carefully controlled if they are to serve as balanced pairs. Among the

(1) R. Jenkins and J. L. de Vries, "Practical X-Ray Spectrometry," 2nd ed., Springer, New York, N. Y., 1969, p 175.
(2) J. T. Gilmore, ANAL. CHEM., **40**, 2230 (1968).
(3) S. Caticha-Ellis, A. Ramos, and L. Saravia, *Advan. X-Ray Anal.*, **11**, 105 (1968).
(4) E. P. Bertin, "Principles and Practice of X-Ray Spectrometric Analysis," Plenum Press, New York, N. Y., 1970, pp 258ff.
(5) W. Bol, *J. Sci. Instrum.*, **44**, 736 (1967).
(6) M. Berman and S. Ergun, *Rev. Sci. Instrum.*, **41**, 870 (1970).

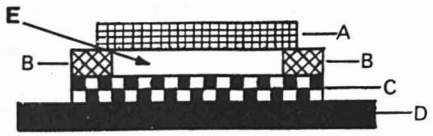

Figure 1. Thin layer electrolysis cell

A, pyrolytic graphite cathode; *B*, phase separation paper mask; *C*, filter paper; *D*, anode of metal being deposited; *E*, electrolyte

methods for preparation of X-ray filters described in the literature are pack-rolling metal foils (*7*), spreading a film of a dispersion of the powdered filter material in a plastic binder (*7*), and pressing the filter material with a binder into a slab (*6*).

These methods of preparing X-ray filters have several disadvantages. Some metals are brittle and others are difficult to roll to the desired thickness. The range of compounds which can be incorporated into films or slabs with binders is greater, but there still is a problem in obtaining uniform films (*7*).

This report describes a new method for obtaining X-ray filters: plating the desired element onto a thin disk of pyrolytic graphite. The filters prepared by this method are reproducible and uniform in thickness and stable. The support material is transparent to X-rays, unlike other plating materials. The use of the new filters in X-ray spectrometry is discussed.

EXPERIMENTAL

Preparation of Plated Filters. Thin sheets of pyrolytic graphite were cleaved from 2.5 × 2.5-cm blocks. The sheets were further reduced in thickness by polishing them on fine sandpaper. The final thickness was about 0.25 mm.

The metal was deposited by thin-layer electrolysis in the arrangement shown in Figure 1. The electrolysis cell consists of a sheet of filter paper (Schleicher and Schuell No. 589 Black Label) impregnated with electrolyte. Around the edges of the cathode is a piece of phase separation paper (Schleicher and Schuell No. 2498). This paper has a hole cut in it in the shape desired for the deposit. Being water repellent, it provides a sharply defined boundary around the deposit and, at the same time, prevents any electrolyte from leaking out of the cell. The assembly was laid upon a graphite block serving as contact for the anode and a stainless steel rod was pressed against the graphite electrode serving as electrical contact for the cathode.

The electrolytes used were: 100 g/l. $CuSO_4 \cdot 4H_2O$ and 20 g/l. concentrated H_2SO_4 for copper, and 300 g/l. $NiSO_4$, $7H_2O$, 50 g/l. $NiCl_2 \cdot 6H_2O$, and 1 g/l. boric acid, adjusted to pH 4, for nickel.

The metal was plated at constant current, using a Sargent Model IV Coulometric Current Source. During electrolysis an equal amount of the metal dissolves from the anode. An electrodeposition rate of 0.1 microequivalent/cm²/sec was usually found to be satisfactory.

After deposition was completed, the graphite sheet was rinsed with deionized water and air dried. The deposit was protected from abrasion by coating it with a layer of Krylon 1301 spray (*8*). This coating material does not attenuate the X-ray beam noticeably.

The filters were tested in a General Electric XRD-5 X-ray spectrometer. The standard sample holders were modified, as shown in Figure 2, to accept the graphite–metal filters.

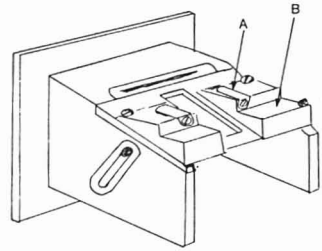

Figure 2. Modified sample holder for General Electric XRD-5 X-ray spectrometer

A, clip to hold primary beam filters; *B*, aluminum support

RESULTS AND DISCUSSION

One of the advantages of electrodeposition as a means of preparing X-ray filters is that the thickness of the metal film or foil can be adjusted to any desired value by choosing the proper current and time of electrolysis. The thickness (T, in mg/cm²) of the deposit is given by

$$T = M/A = WIt/nFA \quad (1)$$

where M is the weight of metal deposited in milligrams, A is the area of the deposit in cm², W is the gram atomic weight of the metal, t is the deposition time in seconds, I is the (constant) current in milliamperes, n is the number of electrons required to deposit one metal atom, and F is the faraday (96,500 coulombs/equivalent).

The length of time required to yield the desired thickness of the filter is

$$t = TnFA/WI \quad (2)$$

For example, to obtain a 1.00-cm² copper filter with a thickness of 25.0 mg/cm², at a current of 10.0 mA (about 0.1 microequivalent/sec) requires

$$t = \frac{25.0 \times 2 \times 96{,}500 \times 1.00}{63.5 \times 10.0} = 7600 \text{ seconds} \quad (3)$$

The validity of these calculations depends on two factors. First, the current efficiency (the fraction of the current which actually produces the desired electrolysis reaction) must be 100%. This is true for the metals studied under the conditions given in the Experimental section of this paper, as well as for many other metals, for example, cobalt, gold, and silver (*8*).

Second, the deposit must be uniform in thickness, with no significant variation from one point to another. The thin-layer electrolysis cell used in this work assures uniformity of the deposit. To show this, a 1.5 mg/cm² electrodeposited copper filter was placed in the sample position in the spectrometer under a mask with a 4-mm² opening. Ten-second readings at $2\theta = 45.0$ taken with various portions of the filter exposed to the X-ray beam gave 12,310 ± 260 counts. This is a relative standard deviation of ±2.1%, compared to the counting precision of about ±0.9%. The variation in the filter thickness is thus at most about ±1.5%. (A thick piece of copper sheet in the same sample holder gave 150,600 counts in ten seconds. The filter tested for uniformity was thus far from the critical thickness beyond which any filter would appear uniform regardless of how much the thickness actually varied.)

Discussion of the Electrodeposition Technique. For thin deposits (under 50 microequivalents/cm²), one can dispense

(7) F. O. Halliday *et al.*, *J. Appl. Phys.*, **38**, 1874 (1967).
(8) B. H. Vassos, F. J. Berlandi, T. E. Neal, and H. B. Mark, Jr., ANAL. CHEM., **37**, 1652 (1965).

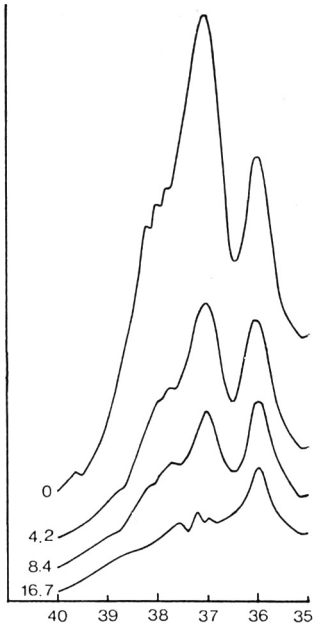

Figure 3. Effect of copper primary beam filter thickness on X-ray spectrum

Numbers indicate the thickness of the filter in mg/cm². The spectra are for a 0.001 *M* mercuric nitrate sample solution

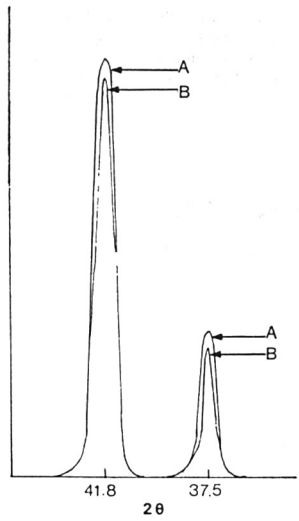

Figure 4. Effect of pyrolytic graphite on zinc X-ray spectrum

***A*, no graphite in beam; *B*, 0.25 mm thick graphite disk in beam**

with the phase separation paper mask. The simple sandwich of metal–paper–graphite is very easy to handle, and the deposits are homogeneous. When thicker deposits are made, they tend to include fibers from the filter paper. In this case, the use of the mask is essential. For very thick deposits evaporation of the electrolyte is a problem, since only a few drops of electrolyte are used. An inverted plastic cup was used successfully to cover the electrolysis cell to minimize evaporation. In some cases, however, it was advisable to demount the cell and add a drop of electrolyte every two hours or so.

If the current efficiency is not 100%, some water may be electrolyzed. This happens when high current densities are used. For nickel, the current had to be reduced to 0.01 microequivalent/cm²/sec in order to eliminate this problem entirely. The occurrence of water electrolysis can easily be detected by the presence of bubbles and constitutes a satisfactory test of the current efficiency.

For those metals which cannot be readily deposited, there is another alternative to the conventional techniques of X-ray filter preparation. An ion of the element which will act as the X-ray absorber can be exchanged onto a cation or anion exchange membrane or filter paper. Campbell, Green, and coworkers (*9*, *10*) have used ion exchange papers to collect traces of ions for determination by X-ray spectrography. If the ion exchanger is loaded with an ion and then placed in the primary or secondary beam, it acts as an effective filter for the X-radiation. We have obtained satisfactory results with zinc and copper filters prepared from Ionac MC-3470 cation exchange membrane. Since the thickness of the filter is limited to those values that result using one or two or three layers of membrane, the technique is less versatile than electrodeposition. It may be useful when filters include elements such as Rb, Cs, Ba, Th, U, or Se, which are difficult to deposit electrochemically.

An example of the use of electrodeposited filters is given in Figure 3, which shows the determination of mercury using its L_{α_1} line. The copper filters in the primary beam serve to reduce the amount of scattered radiation from the X-ray tube. The degree of attenuation depends on the thickness of the filter. The ease of preparing a filter of exactly the desired thickness by the electrodeposition technique is therefore a significant advantage when trying to achieve the optimum signal-to-background ratio for an analysis. The same advantage holds for the preparation of balanced filters for monochromatization of X-ray beam. For example, copper–nickel filters were successfully prepared for use with zinc Kα radiation.

Graphite as a Filter Support. Pyrolytic graphite has several advantages as a support for the metal film which acts as the filter. It is easy to prepare flat plates of pyrolytic graphite by cleavage and a small amount of polishing. Thin plates (0.25 mm in this work) of the graphite are strong, chemically inert, and unaffected by the X-ray beam.

As shown in Figure 4, the graphite itself reduces the X-ray beam intensity only slightly, hardly by 5% for the zinc radiation. If this loss were significant, thinner plates (0.1 mm) could be cleaved and used as filter supports with only

(9) W. J. Campbell, E. F. Spano, and T. E. Green, ANAL. CHEM., **38**, 987 (1966).
(10) T. E. Green, S. L. Law, and W. J. Campbell, *ibid.*, **42**, 1749 (1970).

slightly greater care in handling needed to prevent breakage. In addition, pyrolytic graphite is highly pure carbon and therefore does not itself add any background radiation to the X-ray spectrum. These properties are all in sharp contrast to those of other possible support materials for electrodeposited filters.

RECEIVED for review April 12, 1971. Accepted May 28, 1971. This work was supported by Undergraduate Research Participation Grant No. GYO-7516 from the National Science Foundation. D. G. P. was a National Science Foundation Undergraduate Research Participant, 1970, at Seton Hall University, while a student at Montclair State College.

Hydrated Porosity of Macroreticular Cation Exchange Resins via Nuclear Magnetic Resonance

L. S. Frankel

Rohm and Haas Company, 5000 Richmond Street, Philadelphia Pa. 19137

CONVENTIONAL GEL ION EXCHANGE resins consist of a continuous network of quasi-homogeneous copolymer (*1*). Macroreticular resins have two discrete phases, a gel phase as described above and a phase composed of large pores or voids which are occupied in the hydrated state by water molecules (*2*). One of the most important physical characteristics of a macroreticular ion exchange resin is its porosity, or the fraction of the total volume of the resin occupied by the pores. The porosity is conventionally obtained in the dry state *via* a mercury porosimeter or a helium densitometer (*2*). However, of greater interest is the porosity of the hydrated resin and a subsequent comparison with the porosity of the dry resin. There is to our knowledge no simple way of determining the hydrated porosity.

The determination of the hydrated porosity requires knowledge of the distribution of the total water between the gel phase and the pores. The only significant contribution to this problem we are aware of utilizes a mercury porosimeter and studies the porosity as a function of hydration. These results have been interpreted to indicate that the hydration of the gel phase is complete prior to any water entering the pores *via* capillary action (*2*). Our attention was called to this problem during our study of the nuclear magnetic resonance (NMR) spectra of ion exchange resins (*3–16*). We wish to show how the hydrated porosity may be obtained from the NMR spectra and the resin moisture holding capacity. Data for a gel resin and a macroreticular resin, both of which contains 5% DVB cross-linking, are reported.

EXPERIMENTAL

All measurements were made on a Varian H.R. 60 spectrometer operating at 56.4 MHz. The true density or skeletal density of the dry macroreticular copolymer was obtained on a helium densitometer. The apparent density or the density of the entire mass of dry macroreticular resin was determined in a modified mercury porosimeter (*2*).

Experimental bead copolymers of both the gel and macroreticular type were prepared using commercial grade monomers. The divinylbenzene contained 58.2% DVB as a mixture of *ca.* 70% *m*- and 30% *p*-isomer. The major impurities in the DVB were isomers of ethylvinylbenzene. A stock monomer solution containing 5% by weight of DVB and 95% by weight of styrene and ethylvinylbenzenes was used for the synthesis of all polymers. The copolymers and resins were prepared by standard techniques (*17*)

DISCUSSION AND RESULTS

The NMR spectra of ion exchange resins will generally show sets of peaks. One peak originates from solvent or counter ions inside the ion exchange resin (interior peak); the other (exterior peak) is from the molecules in the volume of the NMR tube not occupied by the resin beads (void volume of column). The solid resin backbone does not contribute any peaks to the spectrum since its molecular motion is highly restricted.

In several previous reports on gel resins, the chemical shift of the hydrogen and sodium form have been shown to be linear functions of the internal molality, $\bar{m}_r$, of the resin, $\bar{m}_r = (QW)(100 - \% H_2O)/\% H_2O$. QW is the dry weight capacity of the resin and % H_2O is the weight per cent water or moisture holding capacity. Molal chemical shifts in the hydrogen form of 0.287 ppm (*6*), 0.321 ppm (*7*), and 0.337 ppm (*8*) have been reported. These values are slightly less than that reported for the effect of hydrogen ion on water, 0.344 ppm (*18*). The molal chemical shift for the 5% DVB gel resin was 0.339 ppm and for the 5% DVB macroreticular resin, 0.345 ppm. A similar analysis is applicable to the sodium form although the analytical sensitivity is much less.

(1) W. Rieman III and H. F. Walton, "Ion Exchange in Analytical Chemistry," Pergamon Press, New York, N. Y., 1970, p 13.
(2) K. A. Kun and R. Kunin, *J. Polym. Sci., Part C*, **16**, 1457 (1967).
(3) J. E. Gordon, *J. Phys. Chem.*, **66**, 1150 (1962).
(4) D. Reichenberg and I. J. Lawrenson, *Trans. Faraday Soc.*, **59**, 141 (1963).
(5) R. H. Dinius, M. T. Emerson, and G. R. Choppin, *J. Phys. Chem.*, **67**, 1178 (1963).
(6) J. P. deVilliers and J. R. Parrish, *J. Polym. Sci., Part A*, **2**, 1331 (1964).
(7) T. E. Gough, H. D. Sharma, and N. Subramanian, *Can. J. Chem.*, **48**, 917 (1970).
(8) R. W. Creekmore and C. N. Reilley, ANAL. CHEM., **42**, 570 (1970).
(9) L. S. Frankel, *Can. J. Chem.*, **48**, 2432 (1970).
(10) R. W. Creekmore and C. N. Reilley, ANAL. CHEM., **42**, 725 (1970).
(11) A. Dařílková, D. Doskočilová, Š. Svvčik, and J. Štamberg, *J. Polym. Sci., Part B*, **8**, 259 (1970).
(12) L. S. Frankel, ANAL. CHEM., **42**, 1640 (1970).
(13) D. G. Howery and M. J. Kittay, *J. Macromol. Sci., Part A*, **A(4)**, 1003 (1970).
(14) D. G. Howery and B. H. Kohn, *Anal. Lett.*, **3**, 89 (1970).
(15) H. Sternlicht, G. L. Kenyon, E. L. Packer, and J. Sinclair, *J. Amer. Chem. Soc.*, **93**, 199 (1971).
(16) H. D. Sharma and N. Subramanian, *Can. J. Chem.*, **49**, 457 (1971).
(17) J. A. Marinsky, "Ion Exchange," Marcel Dekker, New York, N. Y., 1969, Chapter 6.
(18) J. C. Hindman, *J. Chem. Phys.*, **36**, 1000 (1962).

Macroreticular resins do not show separate water resonances for pore and gel phase water (*19*). The intensity of the interior water peak has been shown to account for all of the internal water (*19*). This implies that the water in the two internal phases undergoes rapid exchange. Under rapid exchange conditions the observed chemical shift from the exterior water, δ, is given by (*20*)

$$\delta = X_G\delta_G + X_P\delta_P \quad (1)$$

where X_G is the mole fraction of the total water present in the resin in the gel phase of the macroreticular resin, δ_G is the chemical shift of the water in the gel phase, X_P and δ_P are similarly defined for the pore phase. If one assumes that the chemical shift between water in the pore phase and water in the void volume of the column is zero, the ratio δ/δ_G gives X_G from which the hydrated porosity may be calculated.

We believe the assumption $\delta_P = 0$ is reasonable since the water in the pore phase is not influenced by any ionic groups which are all in the gel phase and the fact that the average pore diameter is large compared to the size of a water molecule. It is pertinent to note that the macroreticular copolymer does not show resolvable interior and exterior water peaks. All previous studies suggest that dispersion interactions with the copolymer do not greatly affect the chemical shift (*3*).

The chemical shift between the gel water and the exterior water must now be considered. We will attempt to show that δ_G is the same as that of the gel resin of the same cross-linking density. This is equivalent to saying that the internal molality of the gel phase of the macroreticular resin is identical to that of a conventional gel resin having the same cross-linking density. The values of QW (Table I) are virtually identical and are typical for complete monosulfonation of the copolymer. These values are, however, not distinctive of any particular cross-linking density of up to approximately 20% DVB. What is needed is an independent physical measurement which is sensitive to the gel phase cross-linking density of the macroreticular resin but yet totally insensitive to the other unique properties of macroreticular ion exchange resins such as surface area and pore size distribution (*2*). Associated with a certain cross-linking density is a certain water content (*21*). Therefore it is sufficient to show that the cross-linking density of the gel phase of the macroreticular resin is identical to that of the conventional gel resin. It has previously been reported that the line width at half height of the counter ion NMR resonance of the $N(CH_3)_4^+$ ionic form of cation gel resins is strongly dependent on the cross-linking density (*3*). As the cross-linking density is increased, the counter ion rotational freedom decreases and the transverse relaxation rate, and hence the line width, increases. Since all the counter ions are in the gel phase, the counter ion line width should depend on the gel phase cross-linking density and be independent of other physical properties. The counter ion line widths at half height for both 5% DVB resins were identical, 4.5 Hz, and we therefore conclude that the cross-linking density and hence the moisture holding capacities are identical. (The counter ion line width of the $N(CH_3)_4^+$ ionic form of a 4.75% DVB and an 8.0% DVB gel resin was 3.5 and 14.0 Hz.) The synthetic method for preparing these cation resins would support the fact that the cross-linking densities are similar. If the dry weight capacity and the moisture holding capacity of the gel phase are equal, the internal molality of the gel resin and the gel phase of the macroreticular resin are equal. Therefore, δ_G is given by the conventional gel resin chemical shift. The distribution of the gel water is then readily calculated from Equation 1.

Table I. Summary of Results

	H^+ form	Na^+ form
Dry weight capacity of gel resin meq/g dry resin, QW	5.22	4.67
Dry weight capacity of macroreticular resin, meq/g dry resin, QW	5.19	4.65
Chemical shift of gel resin, Hz	55.0	12.0
Chemical shift of macroreticular resin, Hz	36.5	8.0
Mole fraction water present in gel phase of macroreticular resin, X_G	0.644	0.67
Per cent water in gel resin	64.4	57.5
Per cent water in macroreticular resin	73.5	68.0
Hydrated density of macroreticular resin, g/cc hydrated resin	1.10	1.16
Porosity of hydrated macroreticular resin *via* NMR, cc pores/cc hydrated resin	0.288	0.26
Porosity of hydrated macroreticular resin *via* per cent water, cc pores/cc hydrated resin	0.282	0.288
Skeletal density of dry macroreticular resin, g/cc[a]	1.437	1.497
Apparent density of dry macroreticular resin, g/cc[b]	1.121	1.108
Porosity of dry macroreticular resin, cc pores/cc dry resin	0.220	0.260
Porosity of dry macroreticular resin, cc pores/g dry resin	0.196	0.239

[a] The skeletal density is the density of just the solid copolymer backbone.
[b] The apparent density is the density of the entire volume of the macroreticular resin.

The data are summarized in Table I. The hydrated porosity in cc of pores/cc of hydrated resin, per cent of volume occupied by the pores, is calculated from ($\%$ H_2O)X_PD where D is the density of the hydrated resin.

After establishing that the gel phase of the macroreticular resin and the gel resin are identical, the hydrated porosity may be calculated from the total moisture holding capacity of the two resins. Consider 1 cc of pore water and calculate the number of grams of hydrated gel phase, Z, that must be added to give the observed weight fraction water in the macroreticular resin, W_{MR},

$$W_{MR} = (1 + W_GZ)/(1 + Z)$$

W_G is the weight fraction water in the gel phase. The hydrated porosity, P, in per cent by volume, is then calculated from

$$P = D/(1 + Z)$$

Excellent agreement is obtained *via* the above procedure and the NMR chemical shift data (Table I); however, this should not be regarded as independent confirmation. The calculation of Z involves $W_{MR} - W_G$. Each of the above quantities can generally be obtained to within a few tenths of a per cent. For the hydrogen form of the resin, the chemical shift data are analytically more sensitive; for the sodium form, the moisture capacity data have greater analytical sensitivity.

(19) L. S. Frankel, *J. Phys. Chem.*, **75**, 1211 (1971).
(20) J. A. Pople, W. G. Schneider, and H. J. Bernstein, "High-Resolution Nuclear Magnetic Resonance," McGraw-Hill, New York, N. Y., 1959, Chapter 10.
(21) T. R. E. Kressman and J. R. Millar, *Chem. Ind. (London)*, **1961**, 1833.

The porosity of a dry resin is typically expressed on a dry volume or dry weight basis. We wish to compare the porosity of a hydrated resin with that of a dry resin. To make this comparison, it is necessary to express the results from the dry resin on the basis of a hydrated resin. The porosity of the dry resin must be expressed in cc of pores/cc of hydrated resin assuming no swelling occurs; therefore, the volume of pores does not increase upon hydration. This assumption is clearly not valid but is made to allow the above comparison. Assuming no swelling occurs, the porosities of the hydrated macroreticular resins are 0.052 and 0.075 cc pores/cc hydrated resin for the hydrogen and sodium ionic form. The correct hydrated porosities are summarized in Table I. The correct hydrated porosities are approximately four times that of the dry porosities.

ACKNOWLEDGMENT

The author wishes to acknowledge Mr. K. Treger and Dr. J. Barrett for the synthesis of the ion exchange resins.

RECEIVED for review April 6, 1971. Accepted June 7, 1971.

Ultraviolet Refractive Indices of Aqueous Solutions of Urea and Guanidine Hydrochloride

J. R. Krivacic and D. W. Urry

Division of Molecular Biophysics/Laboratory of Molecular Biology, University of Alabama Medical Center, 1919 Seventh Avenue South, Birmingham, Ala. 35233

IN STUDYING PROTEINS AND POLYPEPTIDES, it is often necessary to use denaturants such as urea and guanidine hydrochloride. In evaluating the nature of the unfolding or dissociation of these macromolecules, optical rotatory dispersion (ORD) is often the tool of choice for following such phenomena. To evaluate the results in a meaningful manner, a parameter is required which is independent of the solvent system used. Since the ORD of molecules depends on the background contributions and the field in which the molecule resides, it becomes necessary to adjust the ORD spectra for these variables. The Lorentz field correction, applied to such spectra, yields a solvent independent molar rotation. Applying such a correction requires knowledge of the refractive index, as a function of wavelength, of the solvent.

Furthermore, knowledge of refractive index dispersion is necessary for a wider understanding of light scattering phenomena. In our laboratory, distortions in circular dichroism spectra due to light scattering and self absorption of particulate systems can be corrected by using Mie or Rayleigh–Gans approximations for estimating the scattered light and by employing the absorption flattening considerations of Duysens. To apply such corrections, refractive index dispersion of the solvent system and of the particulate system are necessary (*1–3*). The construction of particle refractive indices has been demonstrated by Urry *et al.* (*1,2*).

The refractive indices herein reported have been determined by variable angle single reflection spectrometry. The general principles have been elaborated on by Harrick (*4*) and Hansen (*5*). Specific details are presented in our previous works (*6,7*). Previously, refractive index data in the ultraviolet have been limited with little or no data available at wavelengths shorter than 265 mμ. This is particularly true of highly absorbing solutions. It is, in fact, shorter wavelengths that are of the most direct interest to studies on proteins and polypeptides—studies which often employ urea and guanidine hydrochloride solutions. To our knowledge, the method used herein provides the first direct measurements of refractive indices for urea and guanidine hydrochloride solutions to wavelengths of 2000 Å. These direct measurements are compared to fitting the long wavelength data to a Sellmeier-type equation which is commonly extrapolated to shorter wavelengths. Also, the direct measurements are least squares fitted by a general dispersion expression.

EXPERIMENTAL

Reagents. Urea was supplied by J. T. Baker Chemical Co. as a "Baker Analyzed" reagent and was recrystallized from aqueous ethanol. Guanidine monohydrochloride was also supplied by J. T. Baker as a "Baker Grade" reagent and was twice recrystallized from aqueous ethanol. Both reagents were stored in the cold and solutions were freshly prepared.

Final concentrations were determined by refractive index on a Bausch & Lomb Model 3L Abbé Refractometer and compared to the data of Warren and Gordon (*8*) for urea and of Kielley and Harrington (*9*) for guanidine hydrochloride.

Apparatus. Reflection spectra were run on the Cary Model 14 Spectrophotometer using the Harrick Scientific Model RMVA-1 variable angle reflectance attachment with a sapphire hemicylinder (*10*). We have previously described the use and calibration of this particular device (*7*).

Procedure. The optical constants are determined from two spectral scans at different angles of incidence. The first angle is above the sapphire–sample critical angle and the second is below the critical angle. Both angles must be above the sapphire–air critical angle. Optical constants are calculated for the samples at 50-Å intervals using the equations

(1) D. W. Urry and J. Krivacic, *Proc. Nat. Acad. Sci. U. S.*, **65**, 845 (1970).
(2) D. W. Urry, T. A. Hinners, and J. Krivacic, *Anal. Biochem.*, **37**, 85 (1970).
(3) D. W. Urry, L. Masotti, and J. R. Krivacic, *Arch. Biochem. Biophys.*, in press.
(4) N. J. Harrick, "Internal Reflection Spectroscopy," Interscience Publishers, New York, N. Y., 1967, pp 32, 182–188.
(5) W. N. Hansen, *Spectrochim. Acta*, **21**, 815 (1965).
(6) J. R. Krivacic and D. W. Urry, ANAL. CHEM., **42**, 596 (1970).
(7) J. R. Krivacic and D. W. Urry, *Anal. Biochem.*, in press.
(8) J. R. Warren and J. A. Gordon, *J. Phys. Chem.*, **70**, 297 (1966).
(9) W. W. Kielley and W. F. Harrington, *Biochim. Biophys. Acta*, **41**, 414 (1960).
(10) N. J. Harrick, ANAL. CHEM., **37**, 1445 (1965).

Table I-a. Refractive Indices of Aqueous Urea Solutions

Wavelength, Å	Concentration (molarity) 0.678	1.078	2.136	4.218	6.242	8.163
5900	1.3401	1.3460	1.3565	1.3684	1.3815	1.3986
$Na^{22}{}_D$[a]	1.3385	1.3418	1.3504	1.3676	1.3843	1.4000
4500	1.3445	1.3513	1.3620	1.3744	1.3877	1.4060
3500	1.3522	1.3594	1.3692	1.3834	1.3980	1.4197
2900	1.3814	1.3870	1.3922	1.4220	1.4340	1.4546
2650	1.3927	1.3966	1.4053	1.4349	1.4473	1.4701
2500	1.3855	1.3931	1.4028	1.4324	1.4467	1.4716
2400	1.3925	1.3969	1.4070	1.4381	1.4534	1.4785
2300	1.3986	1.4028	1.4137	1.4471	1.4630	1.4884
2200	1.4030	1.4080	1.4192	1.4549	1.4717	1.4979
2100	1.4113	1.4148	1.4287	1.4692	1.4892	1.5133
2000	1.4296	1.4352	1.4497	1.4934	1.5179	1.5446

Table I-b. Refractive Indices of Aqueous GuHCl Solutions

Wavelength, Å	Concentration (molarity) 0.532	1.052	2.090	4.131	6.143
5900	1.3481	1.3562	1.3715	1.4015	1.4310
$Na^{22}{}_D$[a]	1.3426	1.3511	1.3681	1.4015	1.4344
4500	1.3542	1.3636	1.3801	1.4095	1.4398
3500	1.3625	1.3732	1.3905	1.4234	1.4544
2900	1.3994	1.4063	1.4260	1.4794	1.5061
2650	1.4111	1.4178	1.4396	1.4951	1.5266
2500	1.4038	1.4104	1.4338	1.4903	1.5244
2400	1.4077	1.4142	1.4400	1.4978	1.5353
2300	1.4126	1.4214	1.4485	1.5084	1.5495
2200	1.4202	1.4272	1.4573	1.5185	1.5649
2100	1.4299	1.4380	1.4715	1.5367	1.5871
2000	1.4528	1.4603	1.5035	1.5792	

[a] Determined on Bausch & Lomb Model 3L Abbé Refractometer.

Table II. Analysis of Dispersion Equation

Urea	Coefficients of dispersion eq.[a] A	$C \times 10^{11}$	Wavelength range of greatest error	Maximum error of fit, %[b]
0.678*M*	0.33086	9.09221	4000–2650	±0.9
1.078*M*	0.33676	9.05982	4000–2100	±0.6
2.136*M*	0.34786	8.32994	4000–2650	±0.7
			2000–1950	+0.9
4.218*M*	0.35622	10.9292	4000–2650	±0.9
			2000–1950	+0.4
6.242*M*	0.36900	10.8252	4000–2650	+0.9
			2050–1950	+0.9
8.163*M*	0.38548	11.2257	4000–2650	+0.9
			2150–2000	+0.6
GuHCl				
0.532*M*	0.33747	10.5029	4000–2650	+1.1
			2450–1950	−0.9
1.052*M*	0.34589	10.2561	4000–2650	+1.0
			2450–1950	−0.9
2.090*M*	0.35977	11.0754	4000–2050	±0.9
			2000–1950	+0.7
4.131*M*	0.38513	13.6032	4000–2000	±1.4
6.143*M*	0.41406	13.0376	4000–2650	±1.2

[a] At 23 °C.
[b] + Experimental value above equation. If greater accuracy is required, use experimental values directly listed in Table I.

of Hansen (*5*, *11*). The refractive indices are least squares fitted to a general dispersion equation,

$$n_\lambda = 1 + A\lambda^2/\lambda^2 - C \qquad (1)$$

where λ is the wavelength in centimeters. All spectra were run at 23 °C.

RESULTS AND DISCUSSION

The refractive index data are presented in Table I. For comparison, sodium D line data are also included. Coefficients A and C of Equation 1 are given in Table II along with the regions of maximum error of fit. A more detailed explanation for the errors in the least squares fitted equation in the region of 4000 to 2650 Å has been presented elsewhere (*7*). The maximum error is usually in the 3500 to 3000 Å region where the rising absorption of the sapphire–UV mirrors unit makes reflectivity measurements of sample unit *vs.* air unit less accurate. The errors in this region tend to make the dispersion equation fit well in high absorption regions where anomalous dispersion occurs. While the present method is the first to give far UV data for highly absorbing samples, the increasing absorption of the unit does decrease the signal to

(11) W. N. Hansen, *Spectrochim. Acta*, **21**, 209 (1965).

Table III. 8*M* Urea at 20 °C[a]

	A	$C \times 10^{11}$	3500	2900	2650	2200	2000
3[b]	0.38835	10.2636	1.4239	1.4423	1.4548	1.4929	1.5224
5[c]	0.38818	10.3604	1.4240	1.4427	1.4554	1.4939	1.5239
6[d]	0.38794	10.4943	1.4243	1.4433	1.4561	1.4954	1.5259

[a] See reference 12.
[b] Points fitted 5461 Å – 1.4022; 4358 Å – 1.4105; 3131 Å – 1.4340.
[c] Plus 3650 Å – 1.4208 and 2894 Å – 1.4433.
[d] Plus 2655 Å – 1.4572.

noise ratio which decreases accuracy in reflectivity measurements.

The attenuation index, κ, in the 2300 to 1950 Å region varies from 0.01 to 0.05 for both guanidine monohydrochloride (6*M*) and urea (8*M*). While these indices appear small in magnitude when compared to typical indices obtained by reflection studies in the infrared regions, one must recall that, in general, the penetration depth varies directly with wavelength which results in a much shorter penetration depth in the ultraviolet regions. The penetration depth also increases as the relative refractive index approaches one (*4*). The sapphire hemicylinder has a refractive index of approximately 1.9 in the far UV region and thus is sufficiently different from that of bulk solutions. (A suprasil hemicylinder, on the other hand, has a refractive index of approximately 1.6, such that the relative refractive index with the solutions of interest is very nearly one.) Thus, the attenuation indices obtained are reasonable in these wavelength regions.

Even with such values of the attenuation index, well defined critical angles are not observed. Thus the two angle method for obtaining the optical constants becomes an important procedure in slightly to highly absorbing regions.

One of the reasons for providing the data in Tables I and II has been alluded to in the introduction. This reason, the Lorentz field correction, can be clarified by the following example. Frequently refractive indices are obtained at three or four wavelengths in a non-absorbing region by refractometric means and then fitted to a dispersion equation. The dispersion equation is then used to compute the refractive indices into absorbing regions where the anomalous rotatory dispersion occurs, but this is, of course, a region where anomalous ordinary dispersion also occurs. It is in this region that the dispersion equation underestimates the true refractive index. For 8*M* urea (*12*) fitted to Equation 1 using three, five, and six points, we present in Table III the coefficients and refractive indices in the far UV region for comparison with our data in Tables I and II. Clearly, the fitting of long wavelength dispersion data can underestimate the true refractive index, in this case by approximately 2%.

The dips in *n* observed in Table I, a and b, between 2650 and 2400 Å are due to changes in the angle of incidence for continuing the spectra into the far UV region where net absorption due to the reflecting mirrors and sample are higher. The purpose is to optimize the angles of incidence (*13*). Several changes of angles of incidence are required throughout the spectral region studied (6500-1950 Å).

Agreement of our data with those of Warren and Gordon (*8*) has also led us to conclude that the birefringence of the sapphire hemicylinder has a negligible effect. Harrick Scientific supplies a sapphire hemicylinder which has an optical axis coinciding with the hemicylinder axis.

The accuracy of the method has been discussed by many authors. Analysis of the equations described elsewhere (*6*) yields maximum errors in the refractive index of the sample of 0.5 to 0.6%. These errors are based on reading the absorption to ±0.006; the angle of incidence to ±0.1° of arc; and assuming a constant polarization of the beam, *i.e.*, $\gamma = I_{\parallel}/I_{\perp}$, to within ±10%. There are inherent systematic errors also in the technique, such as supplying reflectivities to only three decimal places, thus introducing an error of 1.3% in *n* (*13*), and determining γ to ±10% yields a maximum error in the reflectivity of 2% (*14*). The refractive index data are presented with a maximum possible error of ±2 to 3%. However, comparison of the sodium D line data, presented in Table I, a and b, with our 5900 Å results gives a standard deviation of 0.0082 and 0.0099, respectively. Comparison at 2650 Å gives a deviation of 0.012. On this basis the expected error is 0.6 to 0.8%.

This note presents the refractive indices of aqueous solutions of urea and guanidine monohydrochloride as a function of concentration and wavelength for the 6500 to 2000 Å region. Coefficients of a least squares fitted dispersion equation using 90 to 92 points are presented for generating the refractive indices. Experimental values of the refractive index were determined from variable angle single reflection spectrometry.

RECEIVED for review April 14, 1971. Accepted May 19, 1971.

(12) J. Foss, Y. Kang, and J. Schellman, in G. D. Fasman, "Methods of Enzymology," S. P. Colowick and N. O. Kaplan, Ed., Academic Press, New York, N. Y., 1963, Volume 6, Chapter 126.

(13) J. Fahrenfort and W. M. Visser, *Spectrochim. Acta*, **18**, 1103 (1962).

(14) A. C. Gilby, J. Barr, Jr., W. Krueger, and B. Crawford, Jr., *J. Phys Chem.*, **70**, 1525 (1966).

Determination of Mercury by a Combustion Technique Using Gold as a Collector

D. H. Anderson, J. H. Evans, J. J. Murphy, and W. W. White

Industrial Laboratory, Kodak Park Division, Eastman Kodak Company, Rochester, N. Y. 14650

INCREASED INTEREST in testing materials that contain mercury has intensified the search for analytical methods that are simple and selective. The use of cadmium sulfide as a collecting agent for mercury was reported by Ballard and Thornton (*1*) in 1941 and has been used extensively in this laboratory.

In essence, material containing mercury is oxidized using nitric acid or other suitable oxidants to convert mercury into a water soluble ionic form. The solution is neutralized with ammonium hydroxide and then trickled through a cadmium sulfide–asbestos pad which collects the mercury as mercury (II) sulfide. Mercury is volatilized from the pad by thermal decomposition and determined using the Resonik Selective Mercury Analyzer as described by Ling (*2*).

This paper describes a method involving combustion of materials containing mercury and the collection of nanogram quantities of mercury on a thin film of gold. The gold is heated at 500 °C and the volatilized mercury is determined using resonance absorption of the 253.7-nm wavelength line with background correction. The detection limit is 0.001 μg of mercury. The total time of an analysis for mercury in hair or tissue such as fish is less than 15 minutes. Lengthy acid digestion periods are unnecessary, and the many days of elapsed time involved in neutron activation are likewise not needed. Airborne elemental mercury can also be monitored using this collection technique.

EXPERIMENTAL

Reagents. Gold-coated asbestos is prepared by adding 2 grams of gold(III) chloride to 15 grams of acid-washed asbestos fibers with sufficient water to make a slurry. The mixture is dried and ignited in a muffle furnace at 600 °C for 1 hour to produce a dispersed film of metallic gold.

Gold-coated fritted glass disks 10 mm in diameter, 1 mm thick, medium porosity are prepared by immersion into a solution containing 1 gram/ml of gold(III) chloride. It is necessary that the gold solution penetrate the fritted glass disk. Warming or evacuating the solution will aid in displacing the air in the disk. The disks are removed from the solution and warmed to drive off moisture. The disks are heated in a muffle furnace as described in the gold-coated asbestos preparation.

General Procedure. Twenty-five to 50 mg of sample is wrapped in aluminum foil and placed in a quartz or other heat resistant tube as shown in Figure 1.

The tube is approximately 35 cm in length and the fritted disks at each end are held by plastic tubing. Heat is applied electrically with a heating coil or gas burner slowly, at first, and then to 850 °C. The combustion tube should be long enough so that the gold-coated disks remain essentially at room temperature. The flow of air through the tube is approximately 100 cc/min.

Ignition normally takes less than five minutes. The disk containing mercury is rinsed with acetone and dried before being placed in the Resonik Selective Mercury Analyzer.

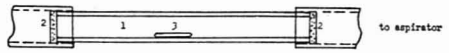

Figure 1. Combustion apparatus for collecting mercury

1. Quartz tube
2. Gold-coated fritted disk
3. Sample

The disks are used repeatedly and are reignited occasionally to ensure freedom from mercury.

A 100-mg plug of gold-coated asbestos was used in the initial experiments to collect mercury. However, it was found that a gold-coated disk has the advantage of being easier to manipulate and place in the Resonik Mercury Analyzer.

Airborne elemental mercury is readily collected by passing a known quantity of air through a gold-coated disk at a rate of 2 cu ft/hr using a light weight, low volume air pump. The mercury on the disk is determined as previously described.

Calibration of Instrument. A calibration curve is prepared by thermally decomposing known quantities of mercury(II) sulfide. Alternatively a calibration curve can be prepared by adding tin(II) chloride to a solution containing 2 to 40 ng of mercury as mercury(II) chloride. The solution is aerated using a bubble dispenser for several minutes. The exhaust air which contains elemental mercury vapor is passed through a gold-coated disk which collects the mercury. The disk is prepared for analysis by rinsing with acetone and drying as described in the procedure.

RESULTS AND DISCUSSION

It was found that elemental mercury in air or in the vapors coming from burning tissue is more effectively collected on gold. We prefer the gold-impregnated glass disks for this purpose. The loose, fluffy asbestos impregnated with cadmium sulfide is best suited for the collecton of mercury in aqueous solutions where it reacts with the sulfide ion and precipitates as mercuric sulfide. The cadmium sulfide asbestos pad is, of necessity, prepared fresh each time, whereas the gold impregnated glass disk can be used repeatedly.

Table I contains mercury values in air found in typical sampling locations. The effectiveness of the collection technique was demonstrated by placing three disks in series and passing air through them. When the disks were checked, only the first disk contained mercury.

Table II shows a comparison of mercury results found in spiked gelatin samples using several different methods. Gelatin was found to be a satisfactory matrix for mercury. Por-

Table I. Elemental Mercury in Air

Sample location	Mercury found, g/cu m
Outdoor atmosphere	$<2 \times 10^{-9}$
General lab work area	1.2×10^{-8}
Polarographic work area	8.0×10^{-7}
Suggested maximum (public health) limit for Hg in air	1×10^{-4}

(1) A. E. Ballard and C. D. W. Thornton, IND. ENG. CHEM., ANAL. ED., **13,** 893 (1941).
(2) C. Ling, ANAL. CHEM., **40,** 1876 (1968).

Table II. Comparison of Mercury Results Found in Gelatin Using Diverse Methods

	Au collection method (Resonik Analyzer), ppm	Rel std dev, %	CdS collection method (Resonik Analyzer), ppm	Rel std dev, %	Atomic absorption, ppm	Neutron activation,[a] ppm
Sample A	1.3	21	1.2	13	1.4	1.2
Sample B	0.13	15	0.11	9	0.14	0.09

[a] Data, courtesy of Dr. R. E. Jervis, University of Toronto.

Table III. Comparison of Mercury Results Found in Soil Using Diverse Methods

	Au collection method (Resonik Analyzer), ppm	CdS collection method (Resonik Analyzer), ppm	Atomic absorption, ppm[a]	Neutron activation, ppm[a]
Sample 1	1.0	1.2	1.5	1.5
Sample 2	0.3	0.2	0.4	0.4
Sample 3	5.1	6.0	6.0	5.7

[a] Data, courtesy of Dr. K. W. Edwards, Colorado School of Mines.

Table IV. Comparison of Mercury Values in Various Substances Using Gold and Cadmium Sulfide Collection Methods

Sample	Au, ppm	CdS, ppm
Fish 1	0.20	0.21
Fish 2	0.23	0.20
Fish 3	0.50	0.58
Fish 4	1.8	1.5
Human hair	1.9	1.8
Sugar	0.05	0.05
Coal	0.20	0.19
Wood	0.05	0.03

tions of these spiked samples are analyzed regularly to ensure operator and instrument reliability.

The combustion gold collection method has been checked twice by neutron activation analysis. One trial involved the spiked gelatin samples which were tested by Dr. R. E. Jervis at the University of Toronto. A second trial was with soil samples supplied by Dr. K. W. Edwards of the Colorado School of Mines. The results shown in Table III are in good agreement. The precision of the gold collection method is not as good as the cadmium sulfide method but the convenience and analytical time required to determine mercury by the former more than compensates for the loss in precision.

Table IV gives data from a variety of samples that have been analyzed for mercury using the gold and cadmium sulfide collection methods.

Materials such as fish tissue and hair are directly combusted after wrapping in aluminum foil. Organics such as sugar, coal, and some cellulosics tend to form a tar when ignited. The addition of sodium carbonate aids in minimizing tar formation during combustion. However, for these types of materials, it is recommended that a two-stage heating device be used. A microcombustion apparatus containing primary and secondary furnace sections makes an efficient unit. The tube in the secondary section of the unit is packed with quartz wool and also heated to 850°C to further break down volatilized organics. The quartz wool acts to retard the flow of vapors and provides additional heating surface.

Mercury which has been collected on a gold-coated disk or gold-coated asbestos can also be separated from the gold by distillation into a nitric acid solution and measured colorimetrically using dithizone. This technique represents an inexpensive and convenient method of analysis for samples containing relatively large quantities of mercury. The cost of the gold is not a significant factor since the coated disks are used repeatedly. When necessary, the gold can be recovered by well-established procedures.

RECEIVED for review November 4, 1970. Accepted May 25, 1971.

High-Speed Ion Exchange Chromatography of Several Monosubstituted Pyridine Isomers

Charles P. Talley

Merck Sharp & Dohme Research Laboratories, Rahway, N. J. 07065

A SIMPLE, RAPID, and efficient technique for the separation and quantitation of mixtures of the more polar monosubstituted pyridine isomers has been lacking in the literature. Nicotinic acid has been determined by the methods of polarography (*1*) and aqueous (*2*, *3*) and nonaqueous (*4*) titration, none of which was isomer specific. Gas chromatography has been useful for the separation of the isomeric picolines (*5*), the cyanopyridines (*6*), and the esters of the pyridinecarboxylic acids (*7*). The amides of these acids have been eluted directly from the gas chromatograph (*8*, *9*), but there

(1) V. A. Serazetdinova, A. D. Kagarlitskii, D. K. Semba'ev, R. U. Umarov, F. A. Ivanovskaya, and B. V. Suvorov, *Vestn. Akad. Nauk Kaz. SSR*, **24**, 68 (1968).
(2) G. M. Belousova, M. D. Prokhorenko, and G. N. Al'Tshuler, *Khim. Farm. Zh.*, **4**, 51 (1970).
(3) O. C. Saxena, *Chim. Anal. (Paris)*, **52**, 647 (1970).
(4) V. K. Kondratov and E. G. Novikov, *Zh. Anal. Khim.*, **22**, 1881 (1967).
(5) L. D. Gluzman, V. M. Efimenko, and Y. A. Slachinskii, *Coke Chem., USSR*, **1969**, (11) 37.
(6) I. I. Kan, D. K. Semba'ev, and B. V. Suvorov, *Zh. Anal. Khim.*, **25**, 374 (1970).
(7) H. Liliedahl, *Acta Chem. Scand.*, **20**, 95 (1966).
(8) J. D. Ashby and J. C. Deavin, *J. Pharm. Pharmacol.*, **21**, 52S (1969).
(9) V. I. Trubnikov, L. M. Malakhova, and E. S. Zhdanovich, *Zh. Anal. Khim.*, **23**, 1546 (1968).

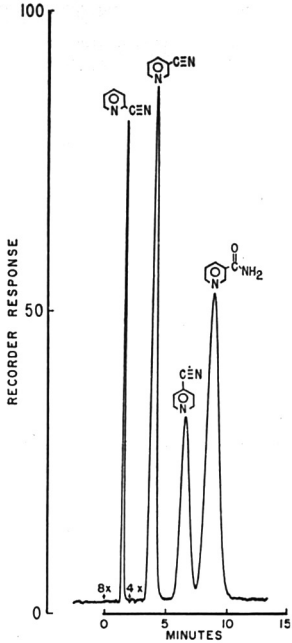

Figure 1. Chromatogram of the three nitrile isomers

The attenuation settings 8× and 4× correspond to 0.08 and 0.04 absorbance units full scale, respectively. The peaks in the order of elution represent: *A*, 0.96 μg picolinonitrile; *B*, 1.99 μg nicotinonitrile; *C*, 2.16 μg isonicotinonitrile; *D*, 1.75 μg nicotinamide, the internal standard

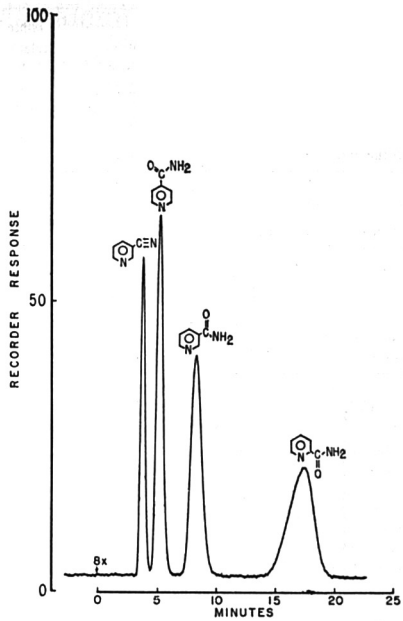

Figure 2. Chromatogram of the three amide isomers

The attenuation setting 8× corresponds to 0.08 absorbance unit full scale. The peaks in the order of elution represent: *A*, 2.50 μg nicotinonitrile, the internal standard; *B*, 2.40 μg isonicotinamide; *C*, 2.50 μg nicotinamide; *D*, 2.80 μg picolinamide

has been no report of a system which has resolved nicotinamide and isonicotinamide (*9*, *10*). This difficulty has traditionally been avoided by dehydration of these amides to their corresponding nitriles with phosgene (*9*, *10*), phosphorus pentoxide, thionyl chloride, or *p*-toluenesulfonylchloride (*11*). The inconvenience in handling these reagents and the nonquantitative, often isomer-dependent nature of reaction yields have made this approach less than satisfactory.

Although several reports have appeared on the use of high-speed, high-resolution liquid chromatography (HSLC) for the analytical scale separation of some polar compounds (*12–15*), none have given detailed examples of its use as a quantitative tool. This paper presents an HSLC method for the separation of isomeric mixtures of the cyano-, carboxamido-, and carboxy-substituted pyridines yielding quantitative results with a relative standard deviation of about 1%. Semi-quantitative measurements can be made down to 0.01% of an isomer within a substituent group.

(10) V. I. Trubnikov, L. M. Malakhova, E. S. Zhdanovich, and N. A. Preobrazhenskii, *Khim. Farm. Zh.*, **1**, 14 (1967).
(11) C. P. Talley and T. Y. Cheng, Merck Sharp & Dohme Research Laboratories, Rahway, N. J., unpublished results, 1971.
(12) M. W. Anders and J. P. Latorre, ANAL. CHEM., **42**, 1430 (1970).
(13) R. E. Majors, *J. Chromatogr. Sci.*, **8**, 338 (1970).
(14) C. G. Scott and P. Bommer, *ibid.*, p 446.
(15) J. Churáček and P. Jandera, *J. Chromatogr.*, **53**, 69 (1970).

EXPERIMENTAL

Apparatus. A Du Pont Model 820 liquid chromatograph equipped with an ultraviolet absorption detector set at 254 nm was used. The column, operated at 27 °C, was 1 m × 2.1 mm i.d. precision bore stainless steel tubing packed with 1% SCX (a 1% sulfonated fluorocarbon) on Zipax glass beads. Since the high acidity of the eluent tended to dissolve the porous nickel frits supplied with the column, a small glass wool plug at the column inlet and a porous Teflon frit at the column outlet were used and found to be more durable substitutes. The eluent was an aqueous solution of sodium nitrate (0.1*N*) and phosphoric acid (0.1*N*). Flow through the column was 1.70 ml/min at a column inlet pressure of 1500 psig. A Honeywell Model 194 strip chart recorder was used at a chart speed of 5 min/in.

Reagents. Methanol, phosphoric acid (85%), and sodium nitrate were Merck reagent grade. Picolinonitrile (Aldrich Chemical Co.), picolinamide (Matheson, Coleman and Bell), picolinic acid (Aldrich Chemical Co.), isonicotinonitrile (Aldrich Chemical Co.), nicotinonitrile (Nepera Chemical Co.), and isonicotinic acid (Eastman Organic) were used as received without further purification.

Procedure. Mixtures were prepared by weighing from about 1 to 100 mg (to the nearest 0.1 mg) of each isomer within a substituent group into a 100-ml volumetric flask which contained a known amount of internal standard. Eluent was added to the mark and 5-μl aliquots were injected with a conventional 10-μl Hamilton syringe against the

Table I. Retention Data

Isomer	Absolute retention		Relative retention	Isomer	Absolute retention		Relative retention
	Time, min	Volume, ml			Time, min	Volume, ml	
Picolinonitrile	1.25	2.13	1.00	Isonicotinamide	5.15	8.76	4.12
Nicotinonitrile	3.71	6.31	2.97	Picolinic Acid	2.90	4.93	2.32
Isonicotinonitrile	6.44	10.9	5.15	Nicotinic Acid	7.15	12.2	5.72
Picolinamide	18.8	32.0	15.0	Isonicotinic Acid	4.10	6.97	3.28
Nicotinamide	8.40	14.3	6.72				

Table II. Analysis of Nitrile Mixtures

No.	Picolinonitrile, mg		Nicotinonitrile, mg		Isonicotinonitrile, mg	
	Found	Present	Found	Present	Found	Present
1	27.7	28.2	4.5	4.7	90.2	90.4
2	109.0	109.7	2.5	2.1	2.7	3.1
3	22.1	22.4	92.9	92.7	1.1	0.9
4	77.6	76.4	50.1	50.4	...	...
5	25.9	25.5	11.6	11.6	59.0	58.6
Relative standard deviation, %	±1.35%		±0.73%		±0.77%	

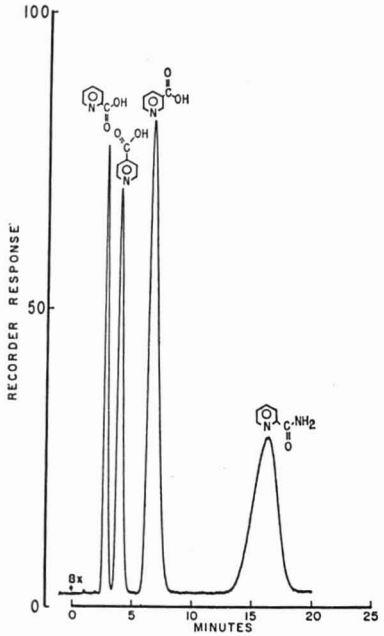

Figure 3. Chromatogram of the three acid isomers

The attenuation setting 8× corresponds to 0.08 absorbance unit full scale. The peaks in the order of elution represent: *A*, 1.25 μg picolinic acid; *B*, 2.70 μg isonicotinic acid; *C*, 4.40 μg nicotinic acid; *D*, 3.35 μg picolinamide, the internal standard

column inlet pressure of 1500 psig. No syringe failure or leakage was experienced. Each mixture was injected three times and for each isomer average values of the peak areas, determined by peak height and width at half-height, were plotted against weight of that isomer.

RESULTS AND DISCUSSION

Figures 1, 2, and 3 represent chromatograms of the isomeric nitriles, amides, and acids, respectively. As a result of the high resolution exhibited here, it was possible in each case to choose as the internal standard for one substituent group an isomer from another substituent group. Resolution was not sufficient, however, to permit base-line separation of all nine isomers in one test mixture. Table I lists retention data for each isomer under conditions such that solvent breakthrough occurred in 1.10 minutes, corresponding to a column dead volume of 1.87 ml. The isomeric picolines and pyridine itself are not eluted under these conditions within an hour. They have been separated on a column packed with 1% BOP (β,β'-oxydipropionitrile) on Zipax with isooctane containing 1% ethanol as eluent (*16*, *17*).

For each isomer, the plot of

$$\frac{S}{S_0} = k\frac{W}{W_0} + C \qquad (1)$$

where S = isomer peak area
S_0 = internal standard peak area
W = mass of isomer injected
W_0 = mass of internal standard injected
k = slope
C = intercept

exhibited a linear mass dependence over the range 50 ng to 5 μg. [Other experiments (*11*) have shown that there is also a linear dependence from 50 ng to 0.5 ng, the approximate limit of detection. Possible extension beyond 5 μg has not been investigated.] The best straight lines determined by a least squares analysis of the data points passed through the origin so that $C = 0$ in all cases.

Table II shows the results of analyses on five mixtures of the isomers in the nitrile group. Experimental values (averages of triplicate runs) and actual values are expressed as milligrams per 100 ml of solution. These data were determined over a range of less than 1% to more than 95% composition by weight. Treatment over a narrower range would give correspondingly greater accuracy.

ACKNOWLEDGMENT

The author is indebted to Carlos Rosas and Miss Yolanda Karockay of these laboratories for the samples of nicotinamide, isonicotinamide, and nicotinic acid used in this work.

RECEIVED for review March 19, 1971. Accepted May 11, 1971.

(16) R. E. Majors, presented at the January 1971 meeting of the North Jersey Chromatography Discussion Group, Celanese Research Co., Summit, N. J.
(17) C. P. Talley, unpublished results, 1971.

Determination of Water Associated with Metal Chelates by Gas Chromatography

Dennis Gaede and Clifton E. Meloan

Department of Chemistry, Kansas State University, Manhattan, Kan. 66502

When metal chelates are extracted from an aqueous solution, in certain cases water molecules are associated with the chelates in the organic phase (*1–3*). The number of water molecules associated with these chelates was first determined by Meloan and Brandt (*1*) using the Karl Fischer titration technique. This technique has also been employed by Gere and Meloan (*2*) and by Burchett and Meloan (*3*).

Since the Karl Fischer method can become quite expensive and time consuming, it was decided to investigate the possibility of determining water associated with metal chelates by gas chromatography as shown by several workers (*4–9*). Two approaches were tried: A direct measurement and a differential measurement.

EXPERIMENTAL

Apparatus. Two chromatographs were used for this study, a Micro-Tek model GC-2500R and a Wilkens Aerograph model A-350-B. Both were dual column instruments employing thermal conductivity detection. A 10-μl Hamilton syringe equipped with a Chaney adapter was used to obtain reproducible sample sizes.

Column. A packing of 20% Carbowax 20 M on 30/60 mesh Chromosorb T (Teflon 6) was prepared. The Teflon was treated with special caution as described by Kirkland (*10*). The material was packed into a 3-foot by $^1/_4$-inch o.d. copper tube. The column was preconditioned overnight with helium carrier gas at a temperature of 200 °C.

Preparation of Chelates. The extraction of tris(1,10 phenanthroline)-Fe(II) chelate from water into nitromethane was performed in the manner of Burchett and Meloan (*3*).

A final chelate concentration range of $1.65 \times 10^{-4} M$ to $13.20 \times 10^{-3} M$ in nitromethane was used. Higher concentrations could not be analyzed since chelate precipitation from the nitromethane began to take place.

The extraction of iron(III)-benzohydroxamic acid chelate from water into 1-decanol was performed according to the procedure of Meloan and Brandt (*1*).

RESULTS AND DISCUSSION

The sensitivity factors were found to be 118 mm² per microgram of water for the Micro-Tek instrument and 37 mm² per microgram of water for the Aerograph instrument. This is adequate sensitivity for the differences in water concentrations required, differences of the order of 1 μg.

Retention times under the set of conditions used for the tris(1,10-phenanthroline)-Fe(II)–nitromethane system were 1.2 minutes for water and 2.5 minutes for nitromethane with base-line separation. Thus, a single analysis is complete in less than four minutes. The nonvolatile metal chelate remains in the fore-part of the column as shown by the red coloration and gives no peak or interference.

The retention time of water under the set of conditions used for the iron benzohydroxamic acid chelate–1-decanol, which remained in the column, was eluted by increasing the temperature to 220 °C.

The results of the determination of the number of water molecules associated with each chelate molecule are shown in Table I. From the average area computed for each chelate concentration, the area obtained for the blank was subtracted. This corrected area was then multiplied by the sensitivity factor, which gave micrograms of water. Conversion of micrograms to micromoles and division by sample volume (μl) gave the molar concentration of associated water. The number of water molecules associated with each chelate molecule was obtained by dividing the molar concentration of associated water by the known molar chelate concentration.

By averaging the water per chelate values obtained and calculating the standard deviation, the number of water molecules associated with each chelate molecule is 5.9 ± 1.7 for tris(1,10-phenanthroline)-Fe(II) in nitromethane and 10.5 ± 2.2 for the iron(III)-benzohydroxamic acid chelate in 1-decanol. These are the same values obtained by Karl Fischer titrations (*1–3*).

The variation in the number of waters per chelate molecule can be accounted for on the basis of random or statistical error. In the case of the iron(III)-benzohydroxamic acid system, the apparent decrease in the number of waters per chelate at the higher chelate concentrations can be explained on the basis of reported decreased chelate solubility in 1-decanol at concentrations greater than $5 \times 10^{-3} M$ (*1*).

Sample size was varied to see if the splitting off of water molecules might be affected by the amount of chelate injected. It was found that the sample volume chosen for analysis is not critical from 2-μl to 10-μl sample sizes.

The effect of carrier gas flow rate on area response was determined. From the data obtained, it is evident that flow rate control is essential to the analysis. At a flow rate of 30 ml/min, area responses varied by about 100 mm² for a change of only 5 ml/min in flow rate. The dependence of peak areas on flow rate is that expected for a thermal conductivity detector (*11*).

The effect of injection port temperature was determined. Through the range of 135 to 315 °C, injection port temperature had essentially no influence on the water split off the chelate.

Differential Method. Included in this investigation was a study of the feasibility of determining water on chelates by a

(1) C. E. Meloan and W. W. Brandt, *J. Inorg. Nucl. Chem.*, **24**, 1645–50 (1962).
(2) D. R. Gere and C. E. Meloan, *ibid.*, **25**, 1507–14 (1963).
(3) A. S. Burchett, Doctoral Thesis, Kansas State University, Manhattan, Kansas.
(4) W. M. Schwecke and J. H. Nelson, Anal. Chem., **36**, 689–90 (1964).
(5) N. H. Stein and J. M. Ambrose, *ibid.*, **35**, 550–2 (1963).
(6) A. A. Calstrom, C. F. Spencer, and J. F. Johnson, *ibid.*, **32**, 1056 (1960).
(7) G. M. Neuman, *Fresenius' Z. Anal. Chem.*, **244**, 302–5 (1969).
(8) A. N. Beresenev, *et al.*, *Zh. Anal. Khim.*, **24** (20), 280 (1969).
(9) G. Bender and C. E. Meloan, *J. Chromatogr.*, **45**, 220 (1969).
(10) J. J. Kirkland, Anal. Chem., **35**, 2003 (1963).
(11) S. Dal Nogare and R. S. Juvet, "Gas Liquid Chromatography," Interscience, New York, N. Y., 1962, p 260.

Table I.

Water on Tris(1,10-Phenanthroline)-Fe(II) Chelate

[Chelate] (μl)	Av area, mm²	Blank area, mm²	Corrected area, mm²	[H_2O] (μl)	[H_2O]/[Chelate] (μ/M)	Dev from average	(Dev)²
1.65×10^{-3}	4725	4560	165	7.75×10^{-3}	4.69	−1.25	1.5625
5.00×10^{-3}	5340	4560	780	36.54×10^{-3}	7.31	+1.37	1.8769
10.00×10^{-3}	5940	4560	1380	64.64×10^{-3}	6.46	+0.52	0.2704
13.20×10^{-3}	6054	4560	1494	69.98×10^{-3}	5.30	−0.64	0.4096
							4.1194 Total
						$\sigma = \pm 1.17$	

Water on Iron(III)-Benzohydroxamic Acid Chelate

0.002	5921	5826	95	0.0282	14.1	+3.6	12.96
0.004	5977	5826	131	0.0388	9.7	−0.8	0.64
0.006	6049	5826	223	0.0662	11.0	+0.5	0.25
0.008	6076	5826	250	0.0742	9.3	−1.2	1.44
0.10	6111	5826	285	0.0846	8.5	−2.0	4.00
							19.29 Total

$$\sigma = \frac{(\text{Dev})^2}{n-1} = \pm 2.2$$

differential process. The large background water, due to the high solubility of water in the organic solvent, greatly limits the precision of the analysis. Two identical columns were prepared and the flow rates were adjusted equally through both columns of the dual column instrument. Through one column was injected the chelate solution while the water-saturated solvent solution was injected through the other column simultaneously. The area of the resulting peak was due to water associated with the chelate.

The differential method increased the precision of the analysis but it was difficult to establish equal flow rates. Geometry differences in the outlet block of the two channels resulted initially in "peaks" on both sides of the base line.

This was due to the particular design of the detector used. Since the detecting element on the reference side was recessed, there was a time lag between its response and the sample side of the detector. In addition, the length of the column from the packing to the detector was longer for one column than the other. When an additional short piece of column was added to the short side, the peaks were normal again.

The differential technique is superior to the direct method because some solvents have large water solubilities and it is difficult to accurately detect small differences between relatively large numbers. 1-Decanol is a perfect example of this with its large water background and this is why it was used here to evaluate the method.

The main disadvantage of the differential technique was the difficulty of establishing equal flow rates through both sides. However, once equal flows were established, many injections could be made without having to readjust the flow rates. The difficulty of preparing exactly identical columns was not as great as anticipated since a slight difference in column packing or length could be compensated for by a flow rate adjustment.

RECEIVED for review August 26, 1966. Resubmitted April 7, 1970, and May 10, 1971. Accepted May 17, 1971. This research was supported by funds from the National Science Foundation and by the National Defense Education Act and this assistance is gratefully appreciated.

Gas Chromatographic Separation and Determination of Isomeric Methylbenzene Tricarbonylchromium Complexes

Janet S. Keller,[1] Hans Veening, and Bennett R. Willeford

Department of Chemistry, Bucknell University, Lewisburg, Pa. 17837

SINCE ARENE TRICARBONYLCHROMIUM complexes were first synthesized in 1957 by Fischer and Öfele (*1*), much experimentation has been carried out involving synthesis, identification, and reactions of these compounds. Recent work in these laboratories has shown that gas chromatography (GC) can be used as a fast and accurate method for the separation and analytical determination of arene tricarbonylchromium complexes in mixtures (*2*). A combined mode of gas chromatography–mass spectrometry provides a convenient means for the identification of the separated compounds (*3*). GC has also been used to determine the cis-trans isomer ratios of alkylindane tricarbonylchromium complexes (*4*, *5*), and the isomer distributions for the Friedel–Crafts acetylation of alkylbenzene tricarbonylchromium complexes (*6*).

We report here the extension of the GC technique to include the separation and determination of ring isomeric methylbenzene tricarbonylchromium complexes. The compounds

[1] Present address, Department of Clinical Pediatrics, Hahnemann Hospital, Philadelphia, Pa.

(1) E. O. Fischer and K. Öfele, *Chem. Ber.*, **90**, 2532 (1957).
(2) H. Veening, N. J. Graver, D. B. Clark, and B. R. Willeford, ANAL. CHEM., **41**, 1655 (1969).
(3) W. J. A. VandenHeuvel, J. S. Keller, H. Veening, and B. R. Willeford, *Anal. Lett.*, **3**, 279 (1970).
(4) D. E. F. Gracey, W. R. Jackson, W. B. Jennings, and T. R. B. Mitchell, *J. Chem. Soc. (B)*, **1969**, 1204.
(5) D. E. F. Gracey, W. R. Jackson, C. H. McMullen, and N. Thompson, *ibid.*, p 1197.
(6) W. R. Jackson and W. B. Jennings, *ibid.*, p 1221.

studied include the isomeric di-, tri-, and tetra-methylbenzene tricarbonylchromium complexes.

EXPERIMENTAL

Samples. The following complexes (I–IX) were prepared by methods similar to those described in the literature (*7*, *8*).

I	1,2-dimethylbenzenetricarbonylchromium (*o*-XTC)
II	1,3-dimethylbenzenetricarbonylchromium (*m*-XTC)
III	1,4-dimethylbenzenetricarbonylchromium (*p*-XTC)
IV	1,2,3-trimethylbenzenetricarbonylchromium (1,2,3-TBTC)
V	1,2,4-trimethylbenzenetricarbonylchromium (1,2,4-TBTC)
VI	1,3,5-trimethylbenzenetricarbonylchromium (1,3,5-TBTC)
VII	1,2,3,4-tetramethylbenzenetricarbonylchromium (1,2,3,4-TMTC)
VIII	1,2,3,5-tetramethylbenzenetricarbonylchromium (1,2,3,5-TMTC)
IX	1,2,4,5-tetramethylbenzenetricarbonylchromium (1,2,4,5-TMTC)

In general, the compounds are synthesized by refluxing chromium hexacarbonyl with the deaerated ligand in an inert solvent such as diglyme under nitrogen. The complexes are removed by precipitation and filtration and are purified by vacuum sublimation. Each of the complexes was characterized by melting point, infrared and NMR spectra, and elemental analysis.

Apparatus and Instrumental Conditions. A Perkin-Elmer Model 900 gas chromatograph equipped with a flame ionization detector was used to separate and detect the complexes. A Leeds and Northrup (1 mV) recorder with a disc integrator was used to record and integrate the chromatograms. Helium was used as a carrier gas, and prepurified hydrogen and air were used to operate the flame ionization detector.

Two types of columns were employed for this work. One of these was a 6-ft (or 12-ft) length of borosilicate glass tubing, 2 mm i.d., packed with 100–120 mesh Gas Chrom-Q coated with 3.6% SE-30; the second column consisted of a 100-ft × 0.5-mm i.d. stainless steel, support coated open tubular (SCOT) column coated with *m*-bis(*m*-phenoxyphenoxy) benzene and Apiezon L (Perkin-Elmer). The injection block for the SCOT column was equipped with a split ratio restrictor of 1:4. The hydrogen flow rate was 24 ml/min while that of air was 300 ml/min. Other conditions of operation are given in the tables and figures.

Procedure. Solutions of the complexes were prepared in spectral grade benzene or carbon tetrachloride solvents, which were deaerated with prepurified nitrogen before use in order to minimize oxidation of the chromium complexes. The flow rate for the SCOT column was determined by injecting 40 to 50 μl of methane and measuring the time of elution. The resultant linear gas velocity in ft/sec was then converted to volume flow rate in ml/min by the appropriate conversion factors. Flow rates for the packed column were determined by use of a soap-film flow meter.

For quantitative studies, the internal standard method described previously (*2*) was employed, except that peak areas were measured by means of a disc integrator. Chromium complexes which did not interfere with the determination under study were used as internal standards in the calibration solutions and in the synthetic mixtures. Calibration graphs used for the analysis of synthetic mixtures were constructed by drawing a computer calculated least squares straight line through the experimental points obtained by plotting ratios of peak areas (sample to internal standard) *vs.* concentration of metal complex (g/ml).

(7) B. Nicholls and M. C. Whiting, *ibid.*, **1959**, 551.

(8) E. O. Fischer, K. Öfele, H. Essler, W. Fröhlich, J. P. Mortensen, and W. Semmlinger, *Chem. Ber.*, **91**, 2763 (1958).

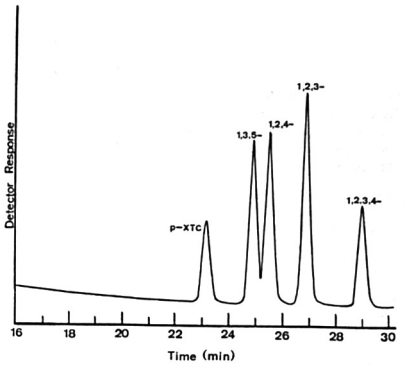

Figure 1. Separation of 1,3,5-TBTC, 1,2,4-TBTC, and 1,2,3-TBTC on a packed column

Internal standards: *p*-XTC and 1,2,3,4-TMTC
Column temp: 80 to 200 °C, programmed at 4°/min
Inj. port temp: 145 °C
Column flow: 11 ml/min
Amounts injected: 1.49 μg 1,3,5-TBTC
1.68 μg 1,2,4-TBTC
2.09 μg 1,2,3-TBTC

Table I. Determination of Isomeric Trimethylbenzene–tricarbonylchromium Complexes in Mixtures

Column, 6-ft packed; column temp, programmed from 80 to 200 °C; programming rate, 4°/min; carrier gas, helium; column flow rate, 11 ml/min; inj. port temp, 145 °C; detector temp, 150 °C; internal standard, 1,2,3,4-TMTC

	Sample, g/ml × 10^4		
Complex	Taken	Found	Error, %
1,3,5-TBTC	2.02	2.20	+8.9
	3.03	3.48	+14.8
	5.05	5.25	+4.0
	10.04	10.20	+1.6
	12.37	13.63	+10.2
1,2,4-TBTC	2.30	2.22	−3.5
	3.46	3.85	+11.3
	5.76	5.97	+3.6
	10.00	9.92	−0.8
	14.00	13.95	−0.4
1,2,3-TBTC	2.51	2.71	+8.0
	3.77	4.17	+10.6
	6.28	6.38	+1.6
	10.70	10.47	−2.1
	17.46	16.96	−2.9

Average error = ±5.6%.

RESULTS AND DISCUSSION

It was found that the isomeric trimethylbenzene complexes, 1,2,3-TBTC, 1,2,4-TBTC, and 1,3,5-TBTC could be separated and determined on the packed column as shown in Figure 1. 1,2,3,4-TMTC and *p*-XTC were included in this mixture and served as the internal standards. Identification of the peaks was accomplished by trapping the eluted components in hexane and recording a UV spectrum of the resulting solution. In each case, the UV spectrum of the eluted sample was identical with that of the known compound. Quantitative results obtained for the determination of the isomeric trimethylbenzene complexes on a packed column in mixtures are given in Table I. In each case, the calibration plots used for the analysis of synthetic mixtures were found to be linear between 2.0×10^{-4} and 2.0×10^{-3} g/ml. The accuracy of

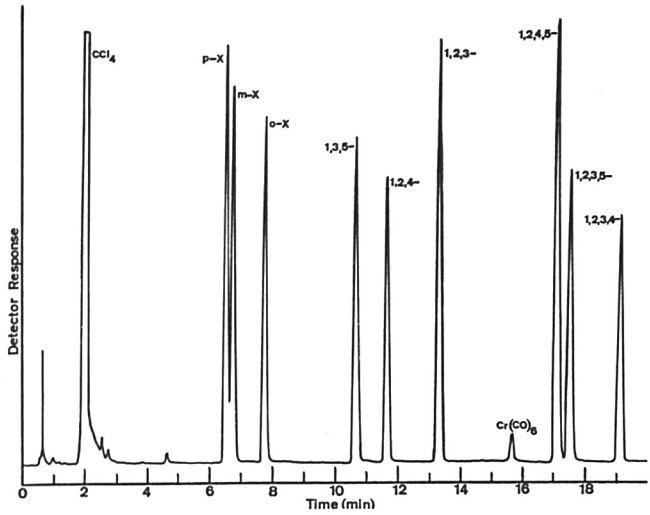

Figure 2. Gas chromatogram of the peaks resulting from the injection of the di-, tri-, and tetramethylbenzene-tricarbonylchromium complexes on a SCOT column

Column temp: 80 °C for 2 min. Programmed to 150 °C at 4°/min
Inj. port temp: 180 °C
Column flow: 6.2 ml/min

Complex	Amount injected, μg
p-XTC	2.23
m-XTC	2.06
o-XTC	2.07
1,3,5-TBTC	2.06
1,2,4-TBTC	1.76
1,2,3-TBTC	2.76
1,2,4,5-TMTC	3.20
1,2,3,5-TMTC	1.84
1,2,3,4-TMTC	1.69

the determination is good to within ±5.6% relative error. It should be noted that synthetic mixtures containing *ca.* 3.5×10^{-4} g/ml of complex gave consistently high positive errors; this causes a relatively high overall error. Omission of these data results in an over relative error of ±4.0%, more nearly comparable to results obtained in other experiments.

While arene tricarbonylchromium complexes survive gas chromatographic analysis intact on a packed glass column, elution of these compounds on the SCOT column resulted in complete decomposition. The peaks resulting from complex pyrolysis were those of the hydrocarbon ligands. A temperature programmed chromatogram showing the peaks for the eluted ligands resulting from decomposition of a nine-component mixture of all the complexes in CCl_4 solution on the SCOT column is shown in Figure 2. An additional peak at 15.8 minutes was identified as $Cr(CO)_6$. The chromatogram obtained when the complexes are injected is identical to that obtained when a mixture of the free ligands is eluted under

Table II.[a] Pyrolytic Determination of Isomeric Di-, Tri-, and Tetramethylbenzenetricarbonylchromium Complexes in Mixtures

	Dimethylbenzenes[b] Sample, g/ml × 10^4				Trimethylbenzenes[c] Sample, g/ml × 10^4				Tetramethylbenzenes[d] Sample, g/ml × 10^4		
Complex	Taken	Found	Error, %	Complex	Taken	Found	Error, %	Complex	Taken	Found	Error, %
p-XTC	1.96	1.85	−5.6	1,3,5-TBTC	2.03	1.96	−3.4	1,2,4,5-TMTC	2.31	2.35	+1.7
	2.95	2.85	−3.4		3.04	3.08	+1.3		3.47	3.56	+2.6
	2.95	2.89	−2.0		4.06	3.74	−7.9		4.63	4.88	+5.4
	3.93	3.57	−9.2		5.07	5.04	−0.6		5.79	5.94	+2.6
	7.86	7.66	−2.5		8.11	7.77	−4.2		5.79	5.68	−1.9
	10.00	9.80	−2.0		11.56	12.15	+5.1		9.26	9.50	+2.6
									12.11	11.95	−1.3
m-XTC	2.02	1.91	−5.4	1,2,4-TBTC	2.08	2.03	−2.4				
	3.03	2.99	−1.3		2.08	2.14	+2.9	1,2,3,5-TMTC	2.31	2.45	+6.1
	3.03	3.04	+0.3		3.12	2.96	−5.1		2.31	2.48	+7.4
	5.05	4.77	−5.5		5.19	5.33	+2.7		2.31	2.19	−5.2
	8.08	7.76	−4.0		8.31	7.68	−7.6		3.46	3.52	+1.7
	10.65	10.57	−0.8		13.24	14.03	+6.0		5.77	5.64	−2.2
									9.22	9.24	+0.2
o-XTC	2.04	1.87	−8.3	1,2,3-TBTC	2.01	2.10	+4.5		14.96	15.09	+0.1
	2.04	2.03	−0.5		2.01	2.06	+2.5				
	3.05	2.88	−5.6		3.01	3.04	+1.0	1,2,3,4-TMTC	2.60	2.61	+0.4
	4.06	4.24	+4.4		4.02	4.01	−0.2		2.60	2.62	+0.8
	8.13	7.85	−3.4		8.04	7.24	−10.0		3.89	3.95	+1.5
	11.10	11.19	+0.8		13.70	14.84	+8.3		5.19	5.03	−3.1
									10.38	9.91	−4.5
									14.83	14.99	+1.1
Average error = ±3.6%				Average error = ±4.2%				Average error = ±2.6%			

[a] SCOT column, helium carrier gas.
[b] Column temp, 80 °C; flow rate, 3.9 ml/min; inj. port temp, 180 °C; detector temp, 210 °C; internal standard, toluenetricarbonylchromium.
[c] Column temp, 120 °C; flow rate, 4.1 ml/min; inj. port temp, 190 °C; detector temp, 192 °C; internal standard, *p*-XTC.
[d] Column temp, 115 °C; flow rate, 5.8 ml/min; inj. port temp, 170 °C; detector temp, 180 °C; internal standard, *o*-XTC.

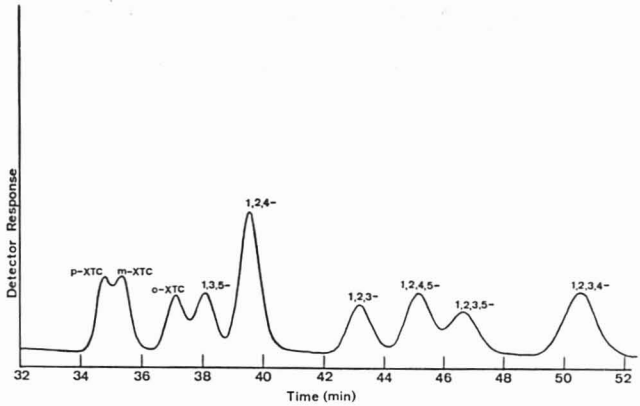

Figure 3. Partial separation of the di-, tri-, and tetramethylbenzenetricarbonylchromium complexes on a 12-foot packed column

Column temp: 80–180 °C at 6°/min
Inj. temp: 145 °C
Column flow: 10 ml/min
Amounts injected: approximately 1 μg of each complex

Table III. Relative Retention Data

Compound	SCOT column temp. programmed (hydrocarbon peaks from pyrolyzed complexes) Ret time, min	SCOT column temp. programmed (hydrocarbon peaks from pyrolyzed complexes) Rel retention (*p*-XTC = 1.00)	Packed column (SE-30, 12-ft) temp. programmed (eluted complexes) Ret time, min	Packed column (SE-30, 12-ft) temp. programmed (eluted complexes) Rel retention (*p*-XTC = 1.00)
p-XTC	6.6	1.00	34.8	1.00
m-XTC	6.8	1.03	35.4	1.02
o-XTC	7.8	1.18	37.2	1.07
1,3,5-TBTC	10.7	1.62	38.1	1.09
1,2,4-TBTC	11.7	1.77	39.6	1.14
1,2,3-TBTC	13.4	2.02	43.2	1.24
1,2,4,5-TMTC	17.2	2.60	47.2	1.35
1,2,3,5-TMTC	17.6	2.66	48.7	1.40
1,2,3,4-TMTC	19.2	2.91	52.5	1.51

identical conditions, with the sole exception of the appearance of the $Cr(CO)_6$ peak.

Though the observed peaks are those of pyrolysis products, the quantitative determination of these complexes in mixtures has been shown to be feasible. Table II shows the quantitative results obtained for the analysis of synthetic mixtures of the di-, tri-, and tetramethylbenzenetricarbonylchromium complexes. Toluenetricarbonylchromium (TTC), *p*-XTC, and *o*-XTC served as internal standards for these three groups of compounds. The average errors found in these three analyses were ±3.6, ±4.2, and ±2.6%, respectively; this indicates that pyrolysis was quantitative when using the SCOT column.

It is likely that the decomposition of these compounds occurred in the open tubular column injection accessory rather than in the column. Contact of the gaseous complexes with heated stainless steel is prolonged in the injection block. Decomposition on the column is thought to be unlikely because the retention times were reproducible under a given set of conditions, and because the column was internally coated with powdered quartz and stationary phase.

While it was possible partially to separate and elute all the complexes without decomposition on a packed glass column, the resolution for the di- and tetramethylbenzene complexes was not sufficient to warrant a quantitative study. The elution order for the nine alkylbenzenetricarbonylchromium complexes studied was *p*-XTC < *m*-XTC < *o*-XTC < 1,3,5-TBTC < 1,2,4-TBTC < 1,2,3-TBTC < 1,2,4,5-TMTC < 1,2,3,5-TMTC < 1,2,3,4-TMTC. A temperature-programmed chromatogram of these complexes on a 12-foot packed column is shown in Figure 3. It is interesting to note that, for each group of isomers, the most symmetrically substituted complex elutes first, whereas the vicinally substituted complex elutes last.

The retention times and relative retentions of all the complexes on the packed column compared to those found for the pyrolysis products on the SCOT column are shown in Table III. It is worth noting that the differences in relative retentions for isomers within each group are far more pronounced for the SCOT column than for the packed column, indicating the superior resolution obtained on the former. Also, the pyrolysis technique is much faster.

The analytical determination of isomeric methylbenzenetricarbonylchromium complexes by their elution from a packed column, and by measurement of the eluted hydrocarbon peaks obtained from metal complex injections on a capillary column has been found to be a fast, accurate, and reliable method. Satisfactory analytical results obtained, whether or not the complexes retain their integrity, have shown that the use of GC has greatly facilitated the determination of metal π-complexes of this type.

RECEIVED for review March 19, 1971. Accepted June 2, 1971. Paper taken in part from the M.S. thesis of J.S.K. Presented at the 161st National Meeting, American Chemical Society, Los Angeles, Calif., March 1971. Work supported by the National Science Foundation Grants GP-8938 and GP-18755.

Polarimetric Studies of Alkali Metal Ion Complexes of *l-trans*-1,2-Diaminocyclohexane-*N,N,N′,N′*-Tetraacetic Acid

James D. Carr and D. G. Swartzfager

Department of Chemistry, University of Nebraska, Lincoln, Neb. 68508

RECENTLY SEVERAL REPORTS have appeared on the formation of weak 1:1 complexes between the alkali metal ions and the aminocarboxalate multidentate ligands: ethylenediaminetetraacetic acid (*1*), propylenediaminetetraacetic acid (*2–4*) and *trans*-1,2-diaminocyclohexane-*N,N,N′,N′*-tetraacetic acid (*5*). In the present study the optical rotatory properties of *l-trans*-1,2-diaminocyclohexane-*N,N,N′,N′*-tetraacetic acid (abbreviated here as *l*-CyDTA or Cy) have been employed as a convenient and accurate method of monitoring the formation of these weak complexes.

EXPERIMENTAL

Apparatus. Polarimetric measurements were performed at 365 nm in a 10-cm cell thermostated at 25 °C in a Perkin-Elmer Model 141 polarimeter. All pH measurements were made with a Corning Model 12 expanded scale pH meter.

Reagents. All solutions were prepared with deionized water and stored in polyethylene bottles. The *l-trans*-1,2-diaminocyclohexane-*N,N,N′,N′*-tetraacetic acid was prepared by the method of Reinbold and Pearson (*6*). A 0.5% aqueous solution of the active acid gave a specific rotation of −53.1 at the sodium D line. Stock solutions of the cations sodium, potassium, cesium (Alfa Inorganics) and tetramethylammonium (Southwestern Analytical) were prepared from their respective hydroxides. Solutions of lithium and tetraethylammonium hydroxide were prepared via ion exchange of their chloride salts.

Procedure. Working solutions were prepared volumetrically from the stock solutions. The initial concentration of *l*-CyDTA was about $2.0 \times 10^{-2} M$ in all runs. After the alkali metal ion was added (in the hydroxide form), the ionic strength was adjusted to 0.5 with tetramethylammonium hydroxide which gave an initial pH of about 13.4. The optical rotation of the solution was determined at approximately 0.2 pH unit intervals as the pH was lowered by the addition of concentrated HCl. The observed molar rotation was then calculated according to Equation 1 after the total concentration of the active species was corrected for dilution.

$$[\alpha]_{obs} = \alpha_{obs}/bc \qquad (1)$$

where α_{obs} = the observed rotation (degrees)
b = cell length (centimeters)
c = concentration (moles per liter)

RESULTS AND DISCUSSION

The effect of a large excess of each of the cations on the observed molar rotation over the pH range from 1.5 to 13.5 is illustrated in Figure 1. Since the observed molar rotations in the presence of both tetramethylammonium and tetraethylammonium were identical within experimental error over the entire pH range, it is assumed that these cations do not interact with CyDTA. The behavior in the high pH region (10 to 13.5) is generally consistent with the known complexation of lithium, sodium, and potassium. Between pH 5 and 10 there are rather dramatic differences in the molar rotations observed in the presence of sodium and lithium. This is ascribed to the formation of the protonated complexes of these metal ions. Although less obvious, it is apparent that potassium also forms a protonated complex of some stability. Only below pH 5 do the curves all become congruent indicating complete dissociation of any associated species of CyDTA and the alkali metal ions.

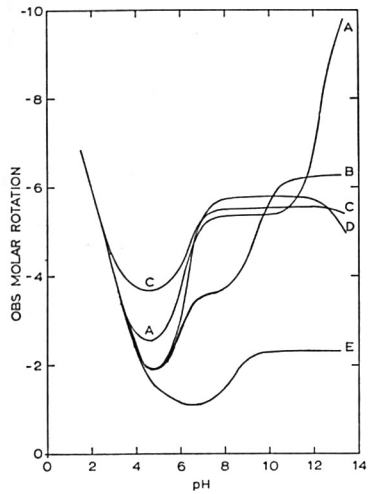

Figure 1. Effect of a large excess (0.35*M*) of each of the various cations on the observed molar rotation of *l*-CyDTA

(*A*) potassium, (*B*) sodium, (*C*) cesium, (*D*) tetramethylammonium and tetraethylammonium, (*E*) lithium

The effect of varying the concentrations of the metal ions: lithium, sodium, and potassium are shown in Figures 2, 3, and 4, respectively. The constraints on the system are represented by Equations 2–7.

$$K_3 = \frac{[H^+][HCy^{3-}]}{[H_2Cy^{-2}]} \qquad (2)$$

$$K_4 = \frac{[H^+][Cy^{4-}]}{[HCy^{3-}]} \qquad (3)$$

$$K_{MCy} = \frac{[MCy^{3-}]}{[M^+][Cy^{4-}]} \qquad (4)$$

(1) G. Anderegg, *Helv. Chim. Acta*, **50**, 2333 (1967).
(2) J. L. Sudmeier and A. J. Senzel, ANAL. CHEM., **40**, 1693 (1968).
(3) J. L. Sudmeier and A. J. Senzel, *J. Amer. Chem. Soc.*, **90**, 6860 (1968).
(4) J. D. Carr and D. G. Swartzfager, ANAL. CHEM., **43**, 583 (1971).
(5) *Ibid.*, **42**, 1238 (1970).
(6) P. E. Reinbold and K. H. Pearson, *Inorg. Chem.*, **9**, 2325 (1970).

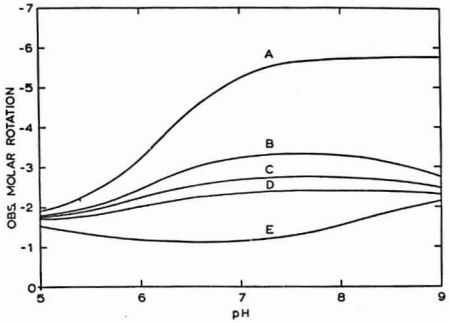

Figure 2. Effect of varying the lithium ion concentration

Concentration of lithium: (*A*) 0, (*B*) 0.048, (*C*) 0.072, (*D*) 0.094, (*E*) 0.212

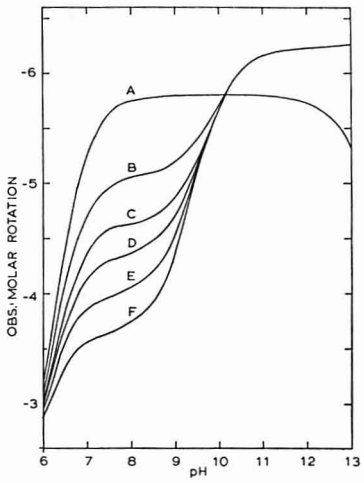

Figure 3. Effect of varying the sodium ion concentration

Concentration of sodium: (*A*) 0, (*B*) 0.059, (*C*) 0.099, (*D*) 0.148, (*E*) 0.237, (*F*) 0.355

$$K_{MHCy} = \frac{[MHCy^{2-}]}{[M^+][HCy^{3-}]} \tag{5}$$

$$F_f + F_c = 1 \tag{6}$$

$$[M^+] = [M]_T - [Cy]_T F_c \tag{7}$$

where F_f and F_c are identified as follows:

$$F_f = \frac{[Cy^{4-}] + [HCy^{3-}] + [H_2Cy^{2-}]}{[Cy]_T} \tag{8}$$

$$F_c = \frac{[MCy^{3-}] + [MHCy^{2-}]}{[Cy]_T} \tag{9}$$

Utilizing Equations 2–7 and Equation 10,

$$[\alpha]_{obs} = [\alpha]_f F_f + [\alpha]_c F_c \tag{10}$$

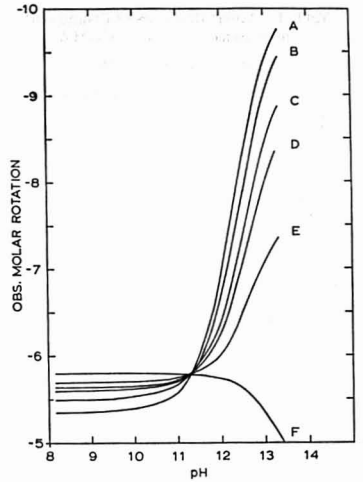

Figure 4. Effect of varying the potassium ion concentration

Concentration of potassium: (*A*) 0.375, (*B*) 0.166, (*C*) 0.083, (*D*) 0.055, (*E*) 0.028, (*F*) 0

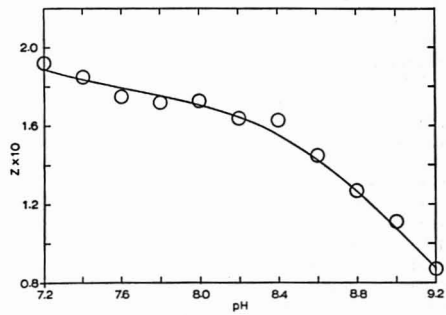

Figure 5. Comparison between experimental values of *Z* and the fitted curve for sodium data

which relates the observed molar rotation at a given pH to the molar rotations of the free ligand $[\alpha]_f$, (taken as the observed molar rotation in the presence of tetramethylammonium ion) and the complexed ligand $[\alpha]_c$ at the same pH, the following expression was derived.

$$[\alpha]_{obs} = [\alpha]_c - \frac{Z([\alpha]_{obs} - [\alpha]_f)}{[M^+]_T - [Cy]_T F_c} \tag{11}$$

where the quantity Z is identified as follows:

$$Z = \frac{[H^+]^2 + K_3[H^+] + K_4K_3}{K_4K_3K_{MCy} + K_3K_{MHCy}[H^+]} \tag{12}$$

and F_c is expressed in the following terms:

$$F_c = \frac{[\alpha]_{obs} - [\alpha]_f}{[\alpha]_c - [\alpha]_f} \tag{13}$$

Table I. Molar Reactions of Complexed and Protonated Forms of CyDTA

μ = 0.5, T = 25 °C, λ = 365 nm

Species	(l-deg/cm-mole)
$LiCy^{3-}$	−2.30
$NaCy^{3-}$	−6.27
KCy^{3-}	−10.2
$LiHCy^{2-}$	−0.4
$NaHCy^{2-}$	−2.6
$KHCy^{2-}$	−5.2
CsH_2Cy^{1-}	−4.4
Cy^{4-}	−4.4
HCy^{3-}	−5.80
H_2Cy^{2-}	−1.87

Table II. Stability Constants of CyDTA with Alkali Metal Ions[a]

T = 25 °C, μ = 0.5

$K_{LiCy} = 1.3 \pm 0.3 \times 10^6$
$K_{NaCy} = 4.6 \pm 1.0 \times 10^4$
$K_{KCy} = 68 \pm 8$
$K_{LiHCy} = 14 \pm 1$
$K_{NaHCy} = 5.5 \pm 0.5$
$K_{KHCy} = 6 \pm 3$
$K_{CsH_2Cy} = 7 \pm 1$
$pK_4 = 13.09 \pm 0.09$
$pK_3 = 6.22 \pm 0.08$

[a] Uncertainty quoted is one standard deviation.

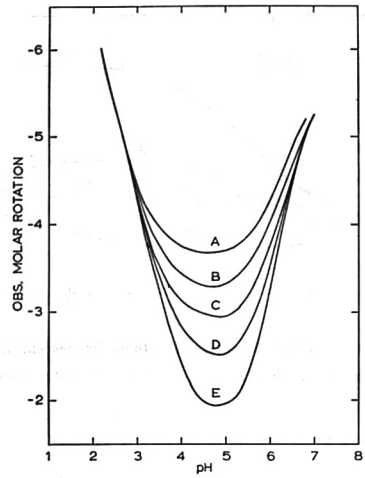

Figure 6. Effect of varying the cesium ion concentration

Concentration of cesium: (*A*) 0.348, (*B*) 0.212, (*C*) 0.107, (*D*) 0.053, (*E*) 0

Utilizing Equations 11 and 13, the values of $[\alpha]_\epsilon$ and Z were calculated at several values of the hydrogen ion concentration with the aid of a computer program by an iterative least squares procedure involving successive approximations for $[\alpha]_\epsilon$.

The values of the various protonation and stability constants were determined by a computer assisted regression analysis of the hydrogen ion dependence of Z. A graphical comparison between the experimental points and the fitted curve (for the sodium data) is shown in Figure 5.

In the case of potassium where useful values of Z could be determined only above pH 11, the first term in the numerator of Equation 12 was dropped since it was insignificant compared to other terms. Similarly in the case of sodium and lithium the third term was dropped since it is insignificant below pH 10 where the most accurate values of Z could be obtained.

The values of $[\alpha]_\epsilon$ and the various protonation and stability constants are presented in Tables I and II.

The values of K_{NaCy} and K_{KCy} reported in this work are somewhat higher than those reported previously (*5*). These differences are in part due to the assumption, made in the previous work, that the protonated species of these complexes were non-existent.

The effect of the various alkali metal ions on the observed molar rotation at low pH is illustrated in Figure 1. These effects are consistent with the reported behavior of *l*-propylenediaminetetraacetic acid under the same conditions. The presence of lithium or sodium appears to have little or no effect on the observed molar rotation. In the case of potassium the effect proved too small for meaningful calculations. The effect of varying the cesium ion concentration is shown in Figure 6. Assuming that the stoichiometry of the complex is 1:1, it can be show that Equations 6, 7, 10, and 12 still apply. The quantity Z is now further complicated by the addition of several terms. However, the observed effect indicates that the interaction is predominately with the diprotonated form of the ligand. Thus if the quantity Z is evaluated at a pH of 4.9 where the species H_2Cy^{2-} is the predominate form of the free ligand, then the quantity Z simply reduces to the inverse of the stability constant of the complex (CsH_2Cy^{1-}). The values of K_{CsH_2Cy} and $[\alpha]_\epsilon$ are presented in Table I.

RECEIVED for review May 3, 1971. Accepted June 2, 1971. The authors thank the Eastman Kodak Company for the graduate fellowship under which this work was carried out.

Titration Errors in Chelometric Titrations Employing Ion-Selective Indicator Electrodes

Franklin A. Schultz

Department of Chemistry, Florida Atlantic University, Boca Raton, Fla. 33432

TWO RECENT REPORTS (*1*, *2*) have described the error in potentiometric titrations which employ ion-selective indicator electrodes in the presence of interfering ions. These ions, when either present in the sample or introduced with the titrant, are sensed by the electrode and distort the titration curve, causing the inflection point to fail to coincide with the equivalence point. Previous treatments considered the case of precipitation titrations. This work reports the titration error in chelometric titrations and considers the effect of interfering ions bearing a charge different than that of the sample ion. This is a common circumstance in chelometric titrations of divalent metal ions where univalent cations may be employed in a buffer or as the counter ion in the titrant.

THEORY

The chemical equilibrium is represented as the dissociation of the complex MY

$$MY \rightleftarrows M + Y \tag{1}$$

which has the equilibrium constant

$$K = K_d = \frac{[M][Y]}{[MY]} \tag{2}$$

In the titration $V_M°$ ml of a $C_M°F$ solution of M are titrated with V_Y ml of a C_YF solution of complexing agent. Solving the appropriate mass-balance equations for M and Y yields the following equation for metal ion concentration during the titration

$$M = [M] = \frac{\beta + \sqrt{\beta^2 + \frac{4KC}{(1 + rf)}}}{2} \tag{3}$$

where

$$\beta = \frac{(1 - f)C}{(1 + rf)} - K \tag{4}$$

In these equations C is the initial sample concentration ($C_M°$), r is the dilution factor ($C_M°/C_Y$), and f is the fraction titrated ($C_YV_Y/C_M°V_M°$). An expression equivalent to Equations 3 and 4 was presented originally by Meites and Meites (*3*).

Potentiometric interferences occur as terms of the form $k_i(C_i)^{n/z_i}$, where k_i, C_i, and z_i are the selectivity coefficient, concentration, and charge, respectively, of the interfering ion, and n is the charge of the metal ion. C_i is an instantaneous value which varies throughout the titration as a result of dilution. For interfering ions present initially in the sample, the potentiometric interference is given by

$$\sum_i k_i(C_i)^{n/z_i} = \sum_i A_i \left(\frac{V_M°}{V_M° + V_Y}\right)^{n/z_i} = \sum_i \frac{A_i}{(1 + rf)^{p_i}} \tag{5}$$

where A_i is the value of $k_i(C_i)^{n/z_i}$ at the beginning of the titration ($V_Y = 0$) for each ion, and p_i is the metal ion to interfering ion charge ratio (n/z_i). For interfering ions present in the titrant

$$\sum_i k_i(C_i)^{n/z_i} = \sum_i L_i \left(\frac{V_Y}{V_M° + V_Y}\right)^{n/z_i} = \sum_i L_i \left(\frac{rf}{1 + rf}\right)^{p_i} \tag{6}$$

where L_i is the value of $k_i(C_i)^{n/z_i}$ for each ion in the titrant solution. A complete expression for electrode potential during the chelometric titration of M with a metal ion-selective electrode is therefore

$$\frac{n(E - E')}{S} = \log\left[M + \sum_i \frac{A_i}{(1 + rf)^{p_i}} + \sum_i L_i \left(\frac{rf}{1 + rf}\right)^{p_i}\right] \tag{7}$$

where S is the Nernst factor, $2.303RT/F$.

An expression similar to Equation 7 may be used to calculate the error of precipitation titrations in the presence of ions of various charge types. For the precipitation titration of X with an X-ion selective electrode, the expression for M in Equation 7 is replaced by the expression for $[X^{n-}]$ in Equations 10 and 11 in Reference *1*. In all treatments, activities are equated with concentrations, and variations in ionic strength and liquid junction potential are neglected.

Titration errors are calculated as described previously (*1*) using an IBM 360/40 computer. An explicit equation for the second derivative of Equation 7 (d^2E/df^2) is examined at increments of $f = 0.001$ for a change of sign. Linear extrapolation is used to estimate the titration error to the nearest 0.01%.

RESULTS AND DISCUSSION

Table I compares titration errors of chelometric and precipitation titrations. Under equivalent experimental conditions the error is significantly smaller in a chelometric titration. This is consistent with the greater precision inherent in a chelometric titration relative to an ion-combination titration (*3*).

Consideration of the ion charge ratio, p, becomes important only when dilution strongly influences the titration error. For interfering ions in the sample solution the difference between the errors at $p = 0.5$, 1.0, and 2.0 is slight. When interfering ions are introduced with the titrant, the dilution factor and ion charge ratio become important variables since the interference term for this case is of the form r^pL. Table I shows that the error is larger when a divalent ion

(1) F. A. Schultz, ANAL. CHEM., **43**, 502 (1971).
(2) P. W. Carr, *ibid.*, p 425.
(3) L. Meites and T. Meites, *Anal. Chim. Acta*, **37**, 1 (1967).

Table I. Titration Errors in Chelometric and Precipitation Titrations with Ion-Selective Indicator Electrodes[a]

Interfering ions in sample

	Precipitation titration			Chelometric titration	
A	$p = 0.5$	$p = 1.0$	$p = 2.0$	$p = 1.0$	$p = 2.0$
0	−0.01%	−0.01%	−0.01%	0.00%	0.00
10^{-5}	−0.19	−0.18	−0.17	−0.09	−0.09
10^{-4}	−0.93	−0.91	−0.86	−0.27	−0.26
10^{-3}	−2.70	−2.64	−2.52	−0.59	−0.58
10^{-2}	−6.46	−6.13	−5.61	−1.30	−1.20

Interfering ions in titrant

	Precipitation titration			Chelometric titration	
L	$p = 0.5$	$p = 1.0$	$p = 2.0$	$p = 1.0$	$p = 2.0$
0	−0.01%	−0.01%	−0.01%	0.00%	0.00%
10^{-5}	−0.07	−0.03	−0.01	−0.02	0.00
10^{-4}	−0.46	−0.19	−0.03	−0.09	−0.02
10^{-3}	−1.71	−0.94	−0.18	−0.27	−0.09
10^{-2}	−4.79	−2.94	−0.92	−0.65	−0.26

[a] $C = 1.0 \times 10^{-2}$; $K = K_{sp} = K_d = 1.0 \times 10^{-8}$; $r = 0.10$.

Table II. Effect of Sample Ion Concentration and Equilibrium Constant on the Titration Error in Chelometric Titrations[a]

Sample ion concentration varied

C	$K = 1.0 \times 10^{-10}$	$K = 1.0 \times 10^{-8}$
1.0×10^{-1}	−0.10%	−0.15%
3.0×10^{-2}	−0.10	−0.29
1.0×10^{-2}	−0.16	−0.59
3.0×10^{-3}	−0.29	−1.30
1.0×10^{-3}	−0.59	−2.68

Equilibrium constant varied

K	$C = 1.0 \times 10^{-2}$	$C = 1.0 \times 10^{-3}$
1.0×10^{-12}	−0.10%	−0.16%
1.0×10^{-10}	−0.16	−0.59
1.0×10^{-9}	−0.29	−1.25
1.0×10^{-8}	−0.59	−2.68
1.0×10^{-7}	−1.23	−5.71
1.0×10^{-6}	−2.52	−12.09

[a] $A_1 = 5.0 \times 10^{-4}$; $A_2 = 5.0 \times 10^{-4}$; $L_1 = 0.0$; $L_2 = 1.0 \times 10^{-4}$; $r = 0.10$; $p_1 = 1$; $p_2 = 2$.

interference is added to a univalent ion sample than when a univalent interference is added to a divalent sample. The latter case is the normal circumstance in chelometric titrations. In usual experimental practice, the error in chelometric titrations contributed by interfering ions introduced with the titrant should be negligible.

Variation of the titration error with sample ion concentration and equilibrium constant (the inverse of the conditional formation constant) is shown in Table II. Values of C, K, A, and L are chosen to correspond to conditions encountered in the analysis of calcium in sea water (*4*). The approximate sodium and magnesium ion concentrations in sea water are 0.5M and 0.05M, respectively, and the optimum selectivity coefficients of a calcium ion electrode for these ions are $k_{Ca,Na} \cong 1.6 \times 10^{-3}$ and $k_{Ca,Mg} \cong 1 \times 10^{-2}$ (*5*). These values combined with the above concentrations give $\sum_i A_i \cong 10^{-3}$. Therefore, if one maintains $\sum_i A_i \leq 10^{-3}$, $C \geq 10^{-2}$, and $K \leq 10^{-8}$, the titration error is always less than 1%. If electrode selectivity diminishes (*6*), however, the titration error increases correspondingly. From Table I, it can be seen that a tenfold increase in A increases the error by about a factor of two.

The variables C and K also affect the titration error. A threefold decrease in C and a tenfold increase in K each increases the error by a factor of two.

Titration errors arising from potentiometric interferences, as discussed in this and previous work (*1*, *2*), are most serious when the end point is evaluated from the usual presentation of electrode potential *vs.* titrant volume. These errors can be circumvented by application of the Gran plot technique (*7*, *8*). In this approach the end point is located by extrapolation from points early in the titration where the ratio of sample ion to interfering ion concentration is more favorable than it is at the equivalence point.

ACKNOWLEDGMENT

Paul Viebrock wrote the computer programs for this work.

RECEIVED for review March 25, 1971. Accepted June 2, 1971.

(4) M. Whitfield, J. V. Leyendekkers, and J. D. Kerr, *Anal. Chim. Acta*. **45**, 399 (1969).

(5) J. W. Ross, Jr. in "Ion-Selective Electrodes," R. A. Durst, Ed., NBS Special Publication 314, U. S. Government Printing Office, Washington, D. C., 1969, Chapter 2.

(6) G. A. Rechnitz and Z. F. Lin, ANAL. CHEM., **40**, 696 (1968).

(7) G. Gran, *Analyst*, **77**, 661 (1952).

(8) *Specific Ion Electrode Technology Newsletter*, Orion Research Inc., Cambridge, Mass., November–December 1970, pp 49–55.

Automated Method for Determination of Mercury

B. W. Bailey and F. C. Lo

Division of Laboratories and Research, New York State Department of Health, Albany, N.Y. 12201

THE GENERALLY accepted procedure for determination of trace amounts of mercury is the cold vapor atomic absorption technique originally described by Hatch and Ott (*1*). This method, however, is relatively time-consuming and the receipt of a considerable number of samples for mercury determination at the authors' laboratory (prompted by the current concern with mercury pollution) led to the development of an automated version of the Hatch and Ott method which is described.

EXPERIMENTAL

Equipment. The equipment used in this work was a Varian Techtron atomic absorption spectrophotometer model AA5 with auto sampler, curve corrector, digital indicator, and digital printer, together with a Technicon Mark II peristaltic action pump and associated glassware and tubing.

Reagents. STANDARD MERCURY SOLUTION. A 1000-ppm mercury stock solution is prepared by dissolving 1.3538 grams of mercuric chloride in a small amount of water, adding 7 ml of concentrated sulfuric acid to avoid hydrolysis of the mercury salt, and finally diluting the mixture to 1 liter with deionized water. By proper dilution, a fresh 10-ppm stock solution is prepared daily from which a 1-ppm solution is prepared twice a day to provide mercury standards.

STANNOUS CHLORIDE SOLUTION. A fresh solution is prepared daily by dissolving 100 grams of stannous chloride in a small amount of water, adding 14 ml of concentrated sulfuric acid, and then diluting with deionized water to make a 10% solution.

HYDROXYLAMINE HYDROCHLORIDE–SODIUM CHLORIDE SOLUTION. Sixty ml of 25% hydroxylamine hydrochloride are mixed with 50 ml of 30% sodium chloride and diluted to 500 ml with deionized water.

POTASSIUM PERMANGANATE SOLUTION. Fifty grams of potassium permanganate are dissolved in deionized water to make a 5% solution.

Procedure. Basically, the procedure followed is the same as the manual version in that the sample is digested to destroy organic matter and get the mercury into solution in the mercuric state. To this solution permanganate is added, followed by hydroxylamine hydrochloride and stannous chloride. This latter step reduces the mercury to the metal which can then be liberated as a vapor by aerating the solution with air or nitrogen. The absorbance of the mercury vapor so liberated is then measured.

RESULTS AND DISCUSSION

The system used is shown schematically in Figure 1. The major difference from the Hatch and Ott manual procedure is that the closed system they employ for the aeration and subsequent liberation of the mercury vapor is not feasible in an automated method. In the manual method, the rate of aeration of solution is not particularly critical while in the automated system it is. For a given set of experimental conditions, the sensitivity decreased with increasing flow rate. However, with slower flow rates, it takes a longer time for the signal to return to the base line between samples. Thus, a compromise must be made between sensitivity and speed of analysis. Under the experimental conditions described, a flow rate of 120 cc/min provided more than adequate sensitivity and it took 1 minute for the signal to return to the base line after a sample.

The sampler, as supplied by the manufacturer, is intended for use in conventional atomic absorption spectrometry and has a very short sample time (25 sec/sample, maximum). This was modified by paralleling the capacitor in the timing circuit of the sampling cycle with a 5-μf capacitor which increases the sampling time to 1.1 minutes. Toward the end of the sampling cycle, the auto sampler triggers the printer. To ensure that the signal being produced is synchronized with the cycle, a simple adjustment is made in the lengths of tubing in the mixing stage of the procedure.

In the system described, the signal attained a maximum about 2 minutes after sampling. Thus the output of the printer is always one sample behind the auto sampler. Since it takes a minute for the signal to return to the base line after a sample, a blank of deionized water is placed between each sample. The automatic control which is activated by the sampler zeroes the instrument between samples. This ensures compensation for base-line drift caused by lamp fluctuations or electronic variation between sample readings. The auto zero triggers after each sample cup on the auto sampler and will thus trigger twice between samples. After a sample has been read, the trigger will adjust the gain of the amplifier so that signal will correspond to zero; as the sample is purged, the signal on the amplifier will not be activated until mercury is completely dispelled from the system. At this point the auto zero will trigger again and the gain on the amplifier will be adjusted to give zero signal. This is best appreciated by monitoring the output on a recorder; an example is shown in Figure 2.

The sample size required for analysis is 7 ml of solution. The concentration range in which the authors were working was 0.001 to 0.01 ppm in which a scale expansion of about 7 × was used. It is thus possible to work in higher or lower concentration ranges by varying the scale expansion. The digital corrector allows adjustment to be made for any deviations from Beer's law. However, in the concentration range

Table I. Printer Output of Automated Mercury Analyses

Sample No.[a]	Reading, ppm	Sample No.[a]	Reading, ppm
0001	00.28	0027	00.26
0003	00.57	0029	00.53
0005	00.88	0031	00.87
0007	01.17	0033	01.21
0009	00.23	0035	00.24
0011	00.59	0037	00.52
0013	00.86	0039	00.90
0015	01.16	0041	01.18
0017	00.23	0043	00.26
0019	00.54	0045	00.50
0021	00.91	0047	00.90
0023	01.20	0049	01.18
0025	00.26		

[a] Even numbered samples are water blanks. The corresponding readings are all 0.00.

(1) W. R. Hatch and W. L. Ott, ANAL. CHEM., **40**, 2085 (1968).

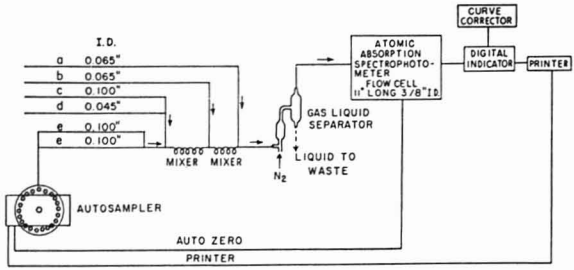

Figure 1. Schematic of equipment used for automatic analysis of mercury

a. 10% stannous chloride in 0.5*N* sulfuric acid
b. 3% hydroxylamine hydrochloride–3% sodium chloride
c. air
d. 5% potassium permanganate
e. sample

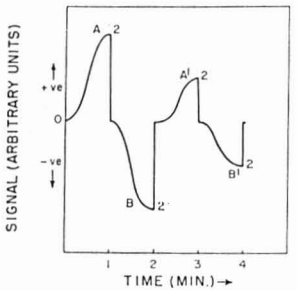

Figure 2. Output of automated system for analysis of mercury

A and *A*¹ correspond to signal peaks
2 indicates triggering of auto zero
B and *B*¹ are negative signals resulting from purging after gain has been zeroed on peaks *A* and *A*¹

mentioned, it was unnecessary. The digital indicator unit enables the output of the amplifier to be displayed in terms of concentration.

To determine the precision of the method, a series of standards was run in replicate. The standards contained 0.3, 0.6, 0.9, and 1.2 μg mercury in 150 ml (*i.e.*, 2 to 8 ppb). The concentration readout was adjusted to display the output in terms of the amount of mercury present in the original solution. The printer output is shown in Table I. The coefficients of variation calculated from these results at the 2, 4, 6, and 8 ppb levels are 7.6, 6.1, 2.3, and 1.6%, respectively.

The procedure described combines rapidity, it is possible to analyze 22 samples per hour, and a high degree of precision and has the added advantage of requiring only a small sample for analysis. It has been satisfactorily applied to a wide variety of samples including water, coal, oil, blood, urine, hair, fish, and other foodstuffs.

A comparison of results obtained with the procedure described, and independent laboratories, using manual procedures, is shown in Table II, together with some results of replicate analyses of blood and coal samples.

Table II. Results of Duplicate Analyses by Automated Procedure and Comparisons with Manual Procedure

	Hg concentration, ppm		
Sample	I[a]	II[b]	III[c]
Brine 1	0.0077	0.0071	
2	0.0078	0.0076	
3	0.0041	0.0044	
Fish 1	0.07		0.06
2	0.4		0.4
3	0.8		0.6
4	1.2		1.0
Blood[d]	0.055		
	0.062		
Coal[d]	0.48		
	0.45		
	0.50		
	0.52		

[a] I. Automated procedure.
[b] II. Beckman Mercury Vapor Monitor (Industrial Lab).
[c] III. Beckman Mercury Vapor Monitor (Government Lab).
[d] Replicate analyses.

While the work described in this article was in progress, an automated procedure for determining mercury was presented at the Technicon Symposium (2). However, that procedure was developed for the continuous monitoring of water with a recorder output.

ACKNOWLEDGMENT

The authors would like to acknowledge the technical assistance provided by Mr. E. Le Gere and Mr. T. Moran.

RECEIVED for review April 1, 1971. Accepted June 7, 1971.

(2) P. D. Goulden and B. K. Afghan, presented at the Technicon International Congress, New York, N. Y., November 1970.

Countercurrent Distribution as a Tool for Purification of Hypothalamic Hormones on a Preparative Scale

A. V. Schally, R. M. G. Nair, and W. H. Carter

Endocrine and Polypeptide Laboratories, Veterans Administration Hospital and Department of Medicine, Tulane University School of Medicine, New Orleans, La. 70140

THE ISOLATION of hypothalamic-releasing hormones involves tremendous efforts in which hundreds of thousands of hypothalami have to be processed to obtain even meager amounts of material for use in the study of composition and structure (*1–3*). Consequently, such an endeavor requires the selection of several purification techniques, the consecutive use of which would reduce the bulk of several kilograms of extracts (*2, 3*) to quantities more easily handled by usual laboratory procedures. In connection with such projects Guillemin *et al.* (*4*) stated that partition chromatography on Sephadex, by the method of Yamashiro (*5*), has much higher limits of capacity and produces a better degree of resolution than the countercurrent distribution technique of Craig (*6*). We have successfully used the technique of partition chromatography for the purification of thyrotropin-releasing hormone (TRH) (*2*) and luteinizing hormone-releasing hormone (LH-RH) (*7, 8*), and we find it particularly useful when small amounts of material of the order of a few milligrams are involved. We wish to correct here the report (*4*) about the so-called limitations of counter-current distribution and relate our recent experiences with the use of this valuable and elegant method for the purification of LH-RH on a preparative scale.

EXPERIMENTAL

Materials. Fragments of 250,000 ventral hypothalami of pigs (dry weight = 5.67 kg) were defatted with acetone and petroleum ether and then extracted with 2*N* acetic acid as described previously (*2*), yielding 2.05 kg of lyophilized extracts. The LH-RH activity in this extract was concentrated by gel filtration on a column of Sephadex G-25 (15.5 × 180 cm) in batches of 80 grams (*2*). The fractions with LH-RH activity were lyophilized (yield 731 grams) and extracted with 4 l. of phenol (*2, 7*). The LH-RH active material was recovered from phenol by re-extraction into the aqueous phase, after the addition of 35 l. of redistilled diethyl ether (*2, 9*). The phenol extract (yield 179.9 grams), which showed LH-RH activity at doses of 10–100 μg was used as the starting material for countercurrent distribution.

Apparatus. Countercurrent distribution (CCD) was carried out in an automatic all glass apparatus (H.O. Post Scientific Co.). The model C-2 liquid–liquid fractionator (CCD) containing 100 cells with 50-ml capacity in each phase was utilized. The time periods allowed for decantation and transfer were both increased from 20 sec to 45 sec. This was accomplished by substituting a new adjustable three-piece metal flap attached to the timing disk (*10*) driven by the Haydon timing meter (We are grateful to Mr. K. Schuerger, H.O. Post Scientific Instrument Co., Inc., for the construction of the metal flap with 3 adjustable fingers which we substituted in place of the original three-pronged metal strip). The mixing was accomplished in 12 strokes.

Procedure. The CCD system consisted of 0.1% acetic acid–1-butanol–pyridine (11:5:3) as recommended by Craig *et al.* (*11*) and utilized previously for purification of TRH (*2*). The partition coefficient *K* of LH-RH in this solvent system is 2.0 (*7*). Analytical grade pyridine (Baker) was redistilled over sodium hydroxide pellets. 1-Butanol (Baker) was treated with zinc powder and redistilled. Glass distilled water was used for making up the solvent and for washing all glassware.

After the run, both phases remaining in the CCD train were removed by suction. The active fractions were then recovered by adding 2–4 volumes of redistilled benzene (*2*) to displace all of the materials into the lower phase, which was then flash-evaporated to a small volume and lyophilized.

The separation pattern brought about by the CCD run was followed by dry weight, Folin–Lowry reaction (*12*) and bioassays for LH-RH and pressor activity. The migration of the maximal concentration of activity (center of gravity of solute), *N*, was calculated according to an equation proposed by Williamson and Craig (*13*)

$$N = nKr/Kr + 1$$

where *n* is the number of transfers applied, *r* is the ratio of the upper and lower phase, and *K* is the partition coefficient. The whole operation was performed at a temperature of 70 ± 1 °F.

Assays. The LH-RH activity was measured by stimulation of release of LH in ovariectomized rats pretreated with estrogen and progesterone (*14, 15*). Serum LH-levels were estimated by a radioimmunoassay procedure (*16*). The pressor activity was determined as recommended by Dekanski

(1) A. V. Schally, A. Arimura, C. Y. Bowers, A. J. Kastin, S. Sawano, and T. W. Redding, *Recent Progr. Horm. Res.*, **24**, 497 (1968).
(2) A. V. Schally, T. W. Redding, C. Y. Bowers, and J. F. Barrett, *J. Biol. Chem.*, **244**, 4077 (1969).
(3) R. Burgus, T. F. Dunn, D. Desiderio, D. N. Ward, W. Vale, and R. Guillemin, *Nature*, **226**, 321 (1970).
(4) R. Guillemin, R. Burgus, E. Sakiz, and D. N. Ward, *C. R. Acad. Sci*, **262**, 2278 (1966).
(5) D. Yamashiro, *Nature*, **201**, 7677 (1964).
(6) L. C. Craig, *J. Biol. Chem.*, **155**, 519 (1944).
(7) A. V. Schally, A. Arimura, A. J. Kastin, J. J. Reeves, C. Y. Bowers, and Y. Baba, "Mammalian Reproduction," H. Gibian and E. J. Plotz, Ed., Springer-Verlag, Berlin, 1970, pp 45–83.
(8) A. V. Schally, A. Arimura, Y. Baba, R. M. G. Nair, H. Matsuo, T. W. Redding, L. Debeljuk, and W. F. White, *Biochim. Biophys. Res. Comm.*, **43**, 393 (1971).
(9) A. V. Schally, C. Y. Bowers, W. F. White and A. I. Cohen, *Endocrinology*, **81**, 77 (1967).
(10) L. C. Craig and D. Craig, "Technique of Organic Chemistry," A. Weissberger, Ed., Vol. III, Interscience New York, N. Y., 1956, pp 149–332.
(11) L. C. Craig, T. P. King, and W. Konigsberg, *Ann. N. Y. Acad. Sci.*, **88**, 571 (1966).
(12) O. H. Lowry, N. J. Rosebrough, A. L. Farr, and R. J. Randall, *J. Biol. Chem.*, **193**, 265 (1951).
(13) B. Williamson and L. C. Craig, *ibid.*, **168**, 687 (1947).
(14) V. D. Ramirez and S. M. McCann, *Endocrinology*, **73**, 193 (1963).
(15) A. V. Schally, A. Arimura, C. Y. Bowers, I. Wakabayashi, A. J. Kastin, T. W. Redding, J. C. Mittler, R. M. G. Nair, P. Pizzolato, and A. J. Segal, *J. Clin. Endocrinol. Metab.*, **31**, 291 (1970).
(16) G. D. Niswender, A. R. Midgley, Jr., S. E. Monroe, and L. E. Reichert, Jr., *Proc. Soc. Exp. Biol. Med.*, **128**, 807 (1968).

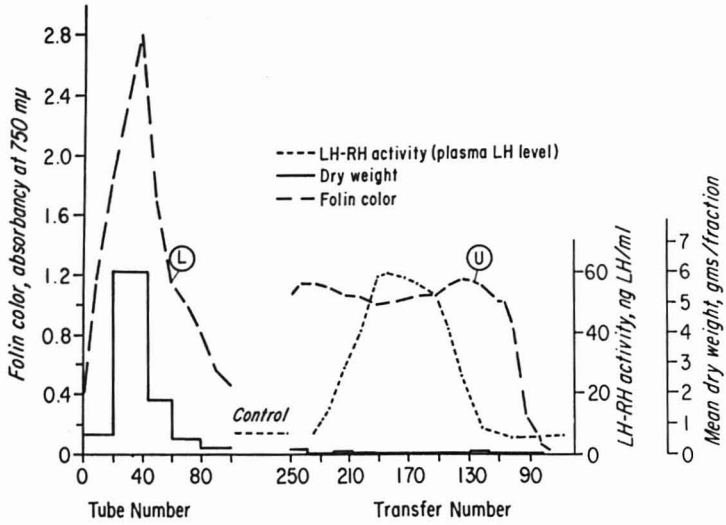

Figure 1. Preparative countercurrent distribution of 171.3 grams of LH-RH concentrate in a system of 0.1% acetic acid : 1-butanol:pyridine = 11:5:3, by the single withdrawal method

171.3 grams of material was loaded in tubes No. 0–19. 100-cell train was filled with 50 ml lower phase and 25 ml upper phase. 250 transfers were performed. Folin–Lowry analyses were carried out on 10 μl lower phase (L) and 25 μl upper phase (U). LH-RH activity was determined in 1-μl aliquots of upper phase, equivalent to approximately 0.8 μg dry weight

Table I. Biological Activity of Hypothalamic Fractions before and after CCD

Fraction No.	Dose, μg	LH-releasing activity, ng LH/ml ± SE	P
Before CCD	...	12.2 ± 1.2	...
Control			
Phenol extract	10	27.0 ± 2.4	0.01
Phenol extract	100	75.0 ± 6.6	0.001
After CCD			
Control	...	9.4 ± 1.2	...
Fraction 149–157, Figure 1	0.2	43.9 ± 0.9	0.001
Fraction 189–197, Figure 1	0.2	27.2 ± 2.9	0.01
Fraction 20–42, Figure 1 (inactive)	20	11.6 ± 2.3	N.S.

(*17*). Follicle stimulating hormone-releasing hormone (FSH-RH) activity was measured as described previously (*7*, *8*).

RESULTS AND DISCUSSION

As the starting material (179.9 grams) for the countercurrent distribution was incompletely soluble, it was extracted 7 times with lower phase (140 ml each time) and upper phase (70 ml each time) of the CCD solvent. This was followed by centrifugation. The residue (8.6 grams) showed no LH-RH activity at doses of 100 μg. The extracts were combined, and the upper phase was made up to 500 ml and the lower phase to 1000 ml, so that the average concentration of the solute was 11.4%. This was introduced into the first 20 cells of the CCD train so that each of these cells contained 50 ml of lower phase and 25 ml of upper phase. The fore-run consisted of pre-equilibration with upper phase of about 20 tubes in front of the advancing solute bands. Co-current was set at about 0.5 ml. The distribution for 250 transfers was started using the single withdrawal method (*18*) to remove the LH-RH activity from the train and increase the chances of separation. The settling time was set at 1 hour for the first 20 transfers, then reduced to 29 min for the remaining 230 transfers. After 80 transfers were completed and the upper phase began to emerge from the CCD train, eight to 10 fractions were collected together into 1000-ml conical flasks, using the exit tube for manual operations. These flasks were changed every 4 hours. The collected fractions were immediately acidified with glacial acetic acid to pH 4.

The pattern of separation as determined by dry weight, peptide analyses by the Folin–Lowry method (*12*), and bioassays is shown in Figure 1. In agreement with calculations the LH-RH activity was transferred out of the train with the emerging upper phases and was found in fractions No. 130–230. The band width and the location of LH-RH activity were in good agreement with theoretical computations. The increase of decantation and transfer periods to 45 sec allowed for an adequate draining of the viscous upper phase. The K value for LH-RH, determined to be 2.0 in two analytical runs in this solvent system, did not change in this run even in spite of very large amounts of material used. When the CCD separation of TRH was carried out on a preparative scale with 16-gram amounts, some change in K value was

(17) J. Dekanski, *Brit. J. Pharmacol.*, **7**, 567 (1952).

(18) T. P. King and L. C. Craig, "Methods of Biochemical Analysis," D. Glick, Ed., Vol. 10, Interscience, New York, N. Y., 1964, pp 201–228.

found in this solvent system as compared with analytical runs with 1 gram of material (*2*). This was thought to be possibly due to incomplete draining during the decantation and transfer stages. When the fractions were flash-evaporated and lyophilized, the combined dry weight of the LH-RH active area was 2.7 grams. Thus a purification of over 60-fold resulted in this run, with an excellent recovery of biological activity which was estimated to be essentially quantitative. The proportionate increase in the specific biological activity was evident from bioassays for LH-RH shown in Table I. The pressor activity was found in fractions 60–99 (mean K = 0.76). Since LH-RH contains an inherent activity of FSH-releasing hormone (FSH-RH) (*7, 8*), this activity was also found in tubes No. 130–230. The fractions which remained in the CCD train contained the bulk of the dry weight and were devoid of LH-RH and FSH-RH activity at doses of 20 μg.

This experiment is an example of the successful application of the technique of countercurrent distribution for the purification of a biologically active material from the hypothalamus on a preparative scale. The versatility of the apparatus is also apparent as the approach can be conveniently modified to suit one's purpose.

Similar CCD techniques could be used for the purification of other biologically active substances as stated many times by Craig and associates (*6, 10, 11, 13, 18*). The advantages and suitability of the CCD method for this type of separation are once more confirmed. It may be pertinent also to mention that a modification of CCD called the "counter double countercurrent distribution" (CDCD) has a still much larger capacity (*19*).

ACKNOWLEDGMENT

We are deeply grateful to Professor Lyman C. Craig, Rockefeller University, New York, for generous advice on the techniques of CCD. We wish to thank Mr. K. Schuerger, H. O. Post Scientific Instrument Co., Inc., for his cooperation in constructing the adjustable metal flap for the timing disk.

RECEIVED for review April 14, 1971. Accepted May 28, 1971. Supported in part by USPHS Grant AM-07467 and The Population Council, New York, N. Y.

(19) O. Post and L. C. Craig, ANAL. CHEM., **35**, 641 (1963).

Solvent Isotope Effects on Decomposition of *N,N*-Dialkyldithiocarbamic Acids

K. I. Aspila, S. J. Joris,[1] and C. L. Chakrabarti[2]

Department of Chemistry, Carleton University, Ottawa, Ontario, K1S 5B6, Canada

STUDIES ON THE DECOMPOSITION of dithiocarbamates in D_2O have appeared recently in the literature (*1, 2*). It was shown that the rate of decomposition of C-*N,N*-tetramethylenedithiocarbamic acid at pH 1.0 is 2.6 times faster (*1*) in D_2O than in H_2O; and that the pD dependence of the decomposition of *N,N*-diethyldithiocarbamic acid is similar to its pH dependence (*1, 2*).

In this paper, solvent isotope effects on decomposition rates of several dialkyldithiocarbamates are compared. The synthesis of the dithiocarbamates used in this study was described in an earlier paper (*3*). D_2O was 97% pure. Rate measurements were done spectrophotometrically (*3*) at 15 ± 0.1 °C and at pH (or pD) values of 1 ± 0.2. In this range of acidity the rates of decomposition of dithiocarbamates are independent of pH (pD) since nearly 99% of the dithiocarbamate anions are converted to the unstable acid form (*1, 3*).

It appears from Table I that the magnitude of the solvent isotope effect is related to the substituent in the dithiocarbamate molecule. An inversion of isotope effect is observed in the case of diisopropyl-dithiocarbamate for which the rate of decomposition is slower in D_2O than in H_2O.

Table I. Solvent Isotope Effects on the Decomposition of *N,N*-Dialkyldithiocarbamic Acids

(Temp = 15.0 ± 0.1 °C, pH = pD = 1)

Dithiocarbamic acid	Decomposition rate constants, sec^{-1}		Ratio of decomposition rate constants
	K_{D_2O}	K_{H_2O}	K_{D_2O}/K_{H_2O}
Dimethyl	0.0506	0.0180	2.80
Diethyl	0.0922	0.0363	2.54
Dibutyl	0.0272	0.0150	1.81
Diisopropyl	0.0352	0.0827	0.42

It was shown (*4*) that dithiocarbamic (DTC) acids are formed by protonation of a sulfur atom of the dithiocarbamate anion (models I and II). Through subsequent redistribution of electron densities in the acid molecule (*5*), the nitrogen atom accepts (*3*) a hydrogen bond. As the dithiocarbamate anion picks up only one proton (*4*), the hydrogen bond formed at the nitrogen atom is either intramolecular

[1] Postdoctoral research fellow. Present address, Noranda Research Centre, 240 Hymus Boulevard, Pointe Claire, Quebec, Canada.

[2] Correspondence should be addressed to this author.

(1) K. I. Aspila, V. S. Sastri, and C. L. Chakrabarti, *Talanta*, **16**, 1099 (1969).
(2) S. W. Dale and F. Fishbein, *J. Agr. Food Chem.*, **18**, 713 (1970).
(3) S. J. Joris, K. I. Aspila, and C. L. Chakrabarti, *J. Phys. Chem.*, **74**, 860 (1970).
(4) S. J. Joris, K. I. Aspila, and C. L. Chakrabarti, ANAL. CHEM., **41**, 1441 (1969).
(5) D. M. Miller and R. A. Latimer, *Can. J. Chem.*, **40**, 246 (1962).

(model III) or is the result of solvent participation in the transfer of the proton from the sulfur atom to the nitrogen atom of the DTC acid (model IV). Solvent participation is likely to occur in the case of DTC acids with small alkyl substituents (*e.g.*, dimethyl- or diethyl-DTC acid) as the studies with mixed solvents indicated (*3*) that for these DTC acids the solvent is able to approach closely the N–C bond (See Scheme 1).

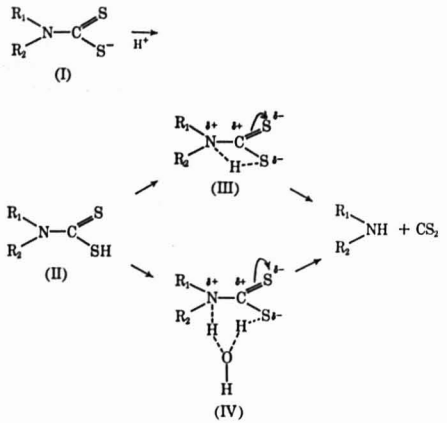

Scheme 1

The present authors propose that the solvent isotope effect observed in the decomposition of DTC acids containing small alkyl substituents is mainly due to the difference in position of either the deuteron or the proton in the hydrogen bond. Indeed, in agreement with zero point energy considerations, the probability of finding the deuteron close to the nitrogen atom is larger than the equivalent probability for a proton (*6*). As a result, the fractional charge on the nitrogen atom (model IV) will be larger when a deuteron rather than a proton occupies the "hydrogen bond." We have shown previously how an increase of fractional charges in the DTC acid molecule enhances the decomposition rate (*3*).

However, in the case of DTC acids containing large alkyl groups (*e.g.*, diisopropyl-DTC acid), the solvent is less able to approach the N–C bond as is reflected in the great instability of these acids (*3*). The lower decomposition rate of diisopropyl-DTC acid in D_2O suggests that the rate-determining step in the decomposition of that compound is the transfer of proton from the sulfur atom to the nitrogen atom (model III). Indeed, the transfer of a deuteron from one base to another occurs at a slower rate than that of a proton.

The opposite solvent isotope effects seen in Table I thus lead to the conclusion that, depending on the availability of a solvent molecule near the N–C bond, the rate-determining step in the decomposition of DTC acids is either the proton (or deuteron) transfer from the sulfur to the nitrogen atom or the decomposition of the intermediate IV. The solvent isotope effect in the decomposition of dibutyl-DTC acid (Table I) clearly illustrates the competition between these two possible rate-determining steps.

If the above arguments are a true interpretation of the experimental results, the solvent isotope effect may be regarded as confirming the conclusion reached by studies in mixed solvents (*3*); namely, that the rates of decomposition of DTC acids are primarily governed by the ease of approach of the solvent to the N–C bond. Solvent isotope effects have the peculiarity to throw light on the influence of the proton transfer on the overall reaction rate.

ACKNOWLEDGMENT

The authors are grateful to Dr. P. M. Laughton and Dr. C. H. Langford, Carleton University, for helpful discussions.

RECEIVED for review March 22, 1971. Accepted June 7, 1971. This paper constituted a part of the M.Sc. thesis of K. I. Aspila. The authors are grateful to the National Research Council of Canada for research grants.

(6) R. E. Rundle, *J. Phys.*, **25**, 487 (1964).

Gas Chromatographic Determination of Penicillins

Charles Hishta, David L. Mays, and Michael Garofalo[1]

Bristol Laboratories, Division of Bristol-Myers Company, Syracuse, N. Y.

NUMEROUS CHEMICAL METHODS are available for the quantitative determination of penicillins; the identity of the penicillin must usually be determined by a different procedure, such as infrared spectrophotometry or thin-layer chromatography. Official microbiological methods for determining penicillins suffer from high variability and time-consuming procedures.

A gas chromatographic procedure for the indirect identification of penicillins was reported by Kawai and Hashiba (*1*). Organic acids produced by alkaline cleavage were converted to methyl esters and separated on a 3.5% SE-30 column. Wolfe (*2*) and coworkers chromatographed the methyl ester of L-phenethicillin. A single peak without evidence of column decomposition was obtained from two columns coupled in series, 1% SE-30 on glass beads (70 cm) followed by 5% NGS on Chromosorb (40 cm). The chromatography of methyl esters of several 6-amino penicillanic acid derivatives was reported by Evrard (*3*) in 1964. Some of these derivatives were separated on a 0.4% SE-52 column

[1] Present address, Xerox Corporation, Rochester, N. Y.

(1) S. Kawai and S. Hashiba, *Bunseki Kagaku*, **13**, 1223 (1964).

(2) S. Wolfe, Queens University, Kingston, Ontario, personal communication, 1964.

(3) E. Evrard, M. Claesen, and H. Vanderhaeghe, *Nature*, **201**, 1124 (1964).

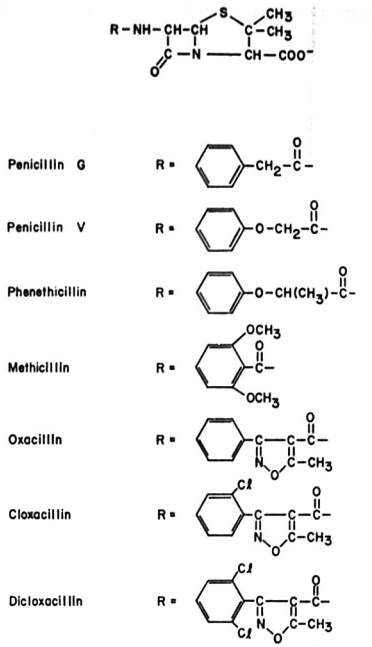

Figure 1. Structure of penicillins

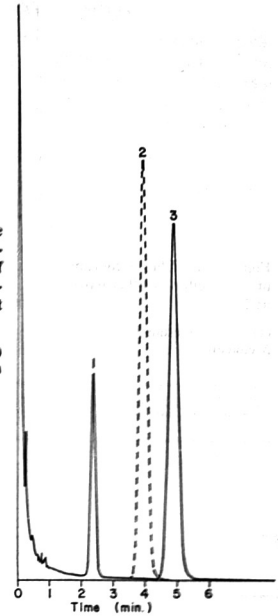

Figure 2. Composite chromatograms indicating the separation of penicillin G and penicillin V isothermally at 245 °C

(1) 5-α-Cholestane, (2) Penicillin G, (3) Penicillin V

without evidence of decomposition. Martin (*4*) pioneered the detection of trace quantities of penicillins G and V by gas–liquid chromatography of the methyl esters.

Other antibiotics, including Neomycin, Paromomycin, and Kanamycin, have recently been gas chromatographed (*5*, *6*). This paper reports the separation and quantitative determination of several penicillins by gas chromatography.

EXPERIMENTAL

Apparatus. A Varian Aerograph Model 2100 gas chromatograph equipped with flame ionization detector was used with gas flow rates of 165 to 215 ml/min for helium, 85 ml/min for hydrogen, and 260 ml/min for air. Column oven temperatues of 245 and 275 °C were used; injector and detector temperatures were maintained at 275 °C.

Column. A 4-mm i.d. × 660-mm glass U-tube column was packed with 2% OV-17 (Applied Science Laboratories, State College, Pa.) on 80–100 mesh Supelcoport (Supelco, Inc., Bellefonte, Pa.). The column packing was prepared by the standard slurry-filtration method. Before it was packed, the empty glass column was thoroughly rinsed with methanol and acetone, dried, conditioned 30 min with a 5% (w/v) HMDS (Ohio Valley Specialty Company, Marietta, Ohio) solution in toluene to silylate reactive sites, and again rinsed with methanol and acetone, and dried. The packed column

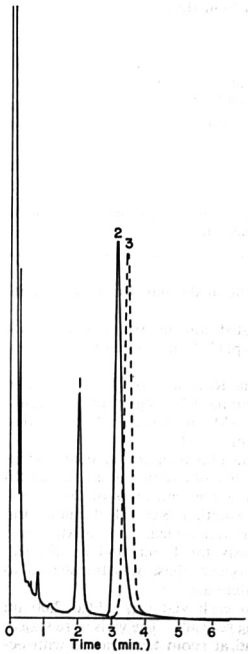

Figure 3. Composite chromatograms indicating the separation of D-phenethicillin and L-phenethicillin isothermally at 245 °C

(1) 5-α-Cholestane, (2) D-Phenethicillin, (3) L-Phenethicillin

(4) J. Martin, R. Robinson, and R. Bezjian, "The Determination of Sub-Microgram Amounts of Penicillin by Gas Chromatography," presented at the 17th Annual Pittsburgh Conference on Applied Spectroscopy, Pittsburgh, Pa., Feb. 1966.
(5) K. Tsuji and J. H. Robertson, ANAL. CHEM. **41**. 1332 (1969).
(6) *Ibid.*, **42**, 1661 (1970).

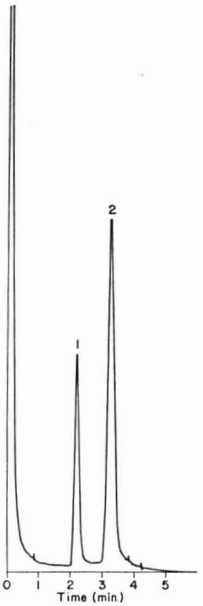

Figure 4. Chromatogram of methicillin isothermally at 275 °C

(1) 5-α-Cholestan-3-one, (2) Methicillin

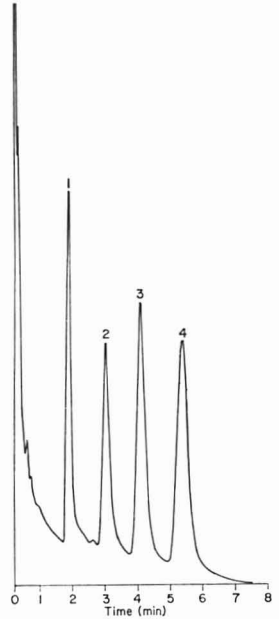

Figure 5. A single chromatogram showing the separation of oxacillin, cloxacillin, and dicloxacillin isothermally at 275 °C

(1) 5-α-Cholestan-3-one, (2) Oxacillin, (3) Cloxacillin, (4) Dicloxacillin

Table I. Calibration Data for 245 °C and 165 ml/min Carrier Flow Rate

Compound	Relative retention time	Relative response factor	Relative standard deviation of response factor, %[a]
5-α-Cholestane	1.00 (2.3 min)	1.0	...
Penicillin G	1.65	2.5	1.5
D-Phenethicillin	1.60	2.4	1.0
L-Phenethicillin	1.71	2.4	1.3
Penicillin V	2.05	2.5	1.7

[a] Relative standard deviations were calculated from the response factors obtained before rounding off.

Table II. Calibration Data at 275° and 215 ml/min Carrier Flow Rate

Compound	Relative retention time	Relative response factor	Relative standard deviation of response factor, %[a]
5-α-Cholestan-3-one	1.00 (2.0 min)	1.0	...
Methicillin	1.51	2.6	2.4
Oxacillin	1.58	2.5	2.5
Cloxacillin	2.16	2.7	2.1
Dicloxacillin	2.83	3.3	2.3

[a] Relative standard deviations were calculated from the response factors obtained before rounding off.

had a theoretical plate height of 0.6 mm for silylated Penicillin V.

Buffer Solution. A saturated aqueous solution of ammonium sulfate was adjusted to pH 2.2 with concentrated sulfuric acid.

Internal Standard–Silylating Reagent. A 50% v/v solution of HMDS in pyridine containing 0.375 mg/ml of 5-α-cholestane or 5-α-cholestan-3-one (Mann Research Laboratories, Inc., New York, N. Y.) was prepared.

Reference Standards. Penicillin reference standards (Figure 1) (Bristol Laboratories Control Division house standards) were dissolved in water at a concentration of 20 mg/ml. To 2.00 ml of the standard solution, 8.00 ml of chloroform and 2.0 ml of pH 2.2 buffer were added. The mixture was immediately shaken vigorously for 1 min and centrifuged. A 2.00-ml aliquot of the organic phase was transferred to an 8.2-ml serum vial for silylation.

Silylation Procedure. To each vial was added 2.00 ml of internal standard-silylating reagent. The vials were sealed, mixed, and allowed to stand at room temperature with occasional shaking. Silylation was essentially complete within 10 minutes for penicillin G, penicillin V, D- and L-phenethicillin, and methicillin. Oxacillin, cloxacillin, and dicloxacillin required up to 60 minutes for complete silylation. Two microliters were injected into the chromatograph.

RESULTS AND DISCUSSION

The merit of the gas chromatographic determination of penicillins is the capability to separate, identify, and quantitate penicillins in a single procedure. Unfortunately, two pairs in the set of penicillins tested have similar retention times

under the experimental conditions. Typical chromatograms indicating the separation of several penicillins are shown in Figures 2 to 5. Relative retention times, as well as response factors and their relative precision, are shown in Tables I and II. Precision was determined for each compound by calculating the relative standard deviation of response factors obtained from six separate preparations of reference standard. Response factors were calculated from peak areas of internal standards and reference standards, measured by the peak-height times half-width method.

An LBK 9000 gas chromatograph–mass spectrometer was used to confirm the identity of the silyl derivatives of each penicillin. Chromatographic peaks were shown to be the trimethylsilyl esters of the intact penicillins by observation of their molecular ions.

CONCLUSIONS

Good precision of response factors of reference standards indicates the direct applicability of the procedure to penicillin prime bulk material. Combined with suitable sample preparation the method could be extended to include bulk blends, tablets, syrups, and other commercial preparations.

ACKNOWLEDGMENT

The supply of purified D- and L-phenethicillin from the Bristol Laboratories Research Division is acknowledged. R. D. Brown of the Control Division performed the mass spectrometric analyses.

RECEIVED for review April 22, 1971. Accepted June 7, 1971.

CORRESPONDENCE

The Internal Reflection Probe

SIR: Double-pass internal reflection plates for Internal Reflection Spectrometry (IRS) (*1*) permit a light beam to enter and exit through one and the same end of the plate. These plates can then be used as "Internal Reflection Probes" for recording spectra of liquids and powders and for reaction monitoring since the free end can be immersed into the sample material (Figure 1*a*), thus eliminating the need for special cells (*2*).

The double-pass geometry was conceived to overcome the difficulty of building vacuum chambers, dewars, and ovens having two optical windows, such as used in IRS surface studies with single-pass plates. The double-pass geometry requires only one optical window. This geometry also simplifies the design of the transfer optics for their use in spectrometers and, furthermore, permits use of reflection plates of any length without altering the optics.

Studies were made for NASA on the potential use of such a probe for dipping into the surface of the moon to record spectra of moon dust. The advantage that IRS offers is that particulate matter, regardless of size, does not scatter light in its interaction with the evanescent wave (*3*), and, therefore, spectra of powders can be recorded without elaborate sample preparation.

The prisms (or equivalent mirrors) in Figure 1*a* rotate the slit image from the usual vertical orientation to a horizontal orientation, and the mirrors direct the light beam at the required angle so that light will travel *via* multiple reflection, vertically along the length of the reflection plate. A more sophisticated structure, the vertical double-pass plate, was developed (*4*) to minimize the number of optical components required to achieve the same result. The VDP plate, shown in

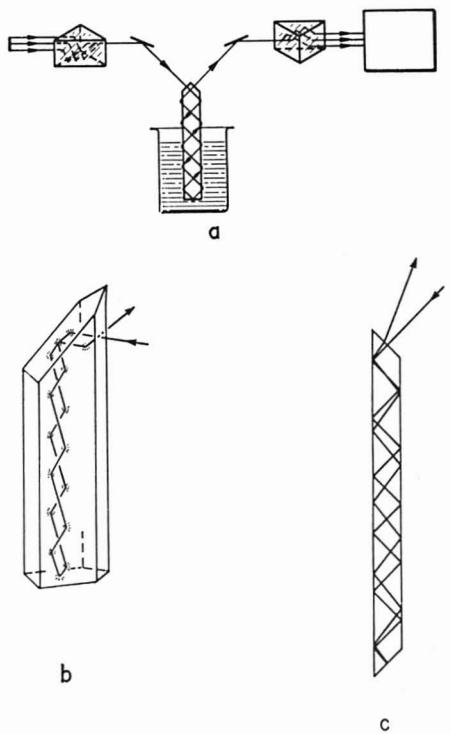

Figure 1. Internal reflection probes

a. **Double-pass plate; *b*. Vertical double-pass plate; *c*. Double-pass, double-sampling plates. The free end can be dipped into liquids, powders, etc. for recording spectra**

(1) N. J. Harrick, "Internal Reflection Spectroscopy," Interscience, Division of J. Wiley & Sons, New York, N. Y., 1967.
(2) N. J. Harrick, ANAL. CHEM., **36,** 188 (1964). Flexible optical fibers may also be used for this purpose as demonstrated by W. N. Hansen, *ibid.*, **35,** 765 (1963).
(3) N. J. Harrick and N. H. Riederman, *Spectrochim. Acta*, **21,** 2135 (1965).
(4) N. J. Harrick, *Appl. Opt.*, **5,** 1 (1966).

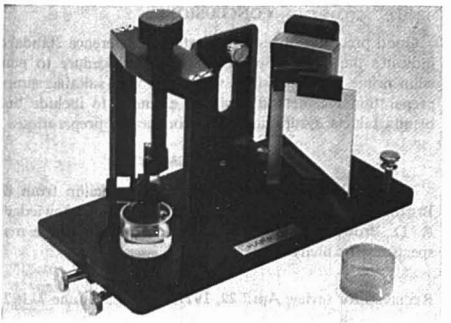

Figure 2. Vertical double-sampling internal reflection plate with versatile reflection attachment can be adapted to most commercially available spectrometers

Figure 1*b*, is the equivalent of the double-pass plate, the mirrors, and the two prisms of Figure 1*a*. These more sophisticated internal reflection plates require precision in fabrication but with careful fabrication high performance is achieved.

Double-pass plates are not limited to a roof-top bevel at one end. The light may, for example, be introduced through the sampling surface and deflected internally *via* the bevel (*1*). Because of sensitivity and aperture size considerations, double-pass, double-sampling plates were developed. In this case the light enters and exits *via* the same aperture and the light beam strikes each point on the surface twice. In order to separate the entrance and exit beams, the opposite bevel is cocked slightly and metallized so that the light beam is reflected back down the length of the plate at a slightly different angle of incidence. A horizontal double-sampling plate is shown in Figure 1*c*.

Vertical double-sampling plates can also be made by providing a single bevel (rather than a roof-top bevel) along one edge of the plate and cocking and metallizing the bevel at the end of the plate. Such an internal reflection probe (IRP) with transfer optics that can be adapted to most spectrometers is shown in Figure 2. [This accessory, the Versatile Reflection Attachment (VRA), is a multi-purpose attachment that in addition to its use with the IRP, can be used for internal reflection spectrometry with double-sampling reflection plates of any length or with double-sampling plates having the sampling surface in a horizontal position. It can also be employed for specular reflection (low angle of incidence, $\theta = 12°$, as required in epitaxial film thickness measurements) and with the addition of a retro-mirror accessory (*5*), such measurements can be made over a wide range of angles of incidence. This is useful for studying thin films on metals and measuring both refractive index and film thickness (*6*).] In this reflection plate the average angle of incidence is 45°, there are approximately 15 reflections

(5) N. J. Harrick, ANAL. CHEM., **37**, 1445 (1965).
(6) N. J. Harrick, *Appl. Opt.*, in press.

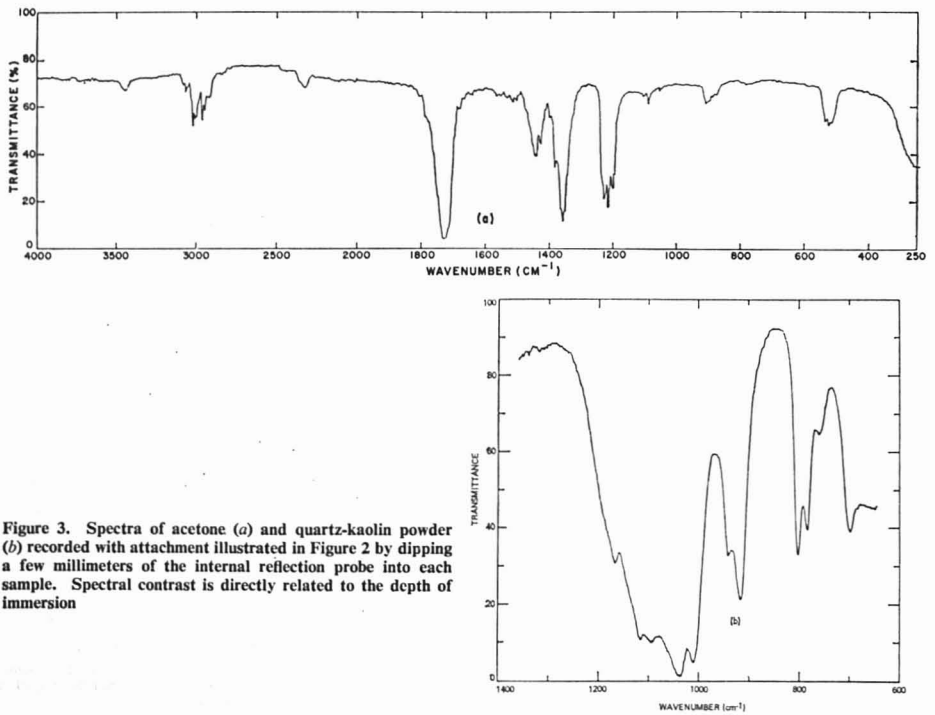

Figure 3. Spectra of acetone (*a*) and quartz-kaolin powder (*b*) recorded with attachment illustrated in Figure 2 by dipping a few millimeters of the internal reflection probe into each sample. Spectral contrast is directly related to the depth of immersion

per cm length of the plate and about 3 cm (45 reflections) can be employed if necessary.

There are many applications of the Internal Reflection Probe. As originally illustrated, it eliminates the need of special cells for studying liquids and powders. It is also useful for viscous media and turbid solutions where suitable cells cannot be made. The spectra of acetone and quartz-kaolin powder were recorded by dipping a few millimeters of the end of the IRP into the sample and are shown in Figure 3. Spectral contrast can be controlled by adjusting the depth to which the IRP is immersed into the sample. Of particular interest is the use of the IRP for reaction monitoring as required in process control. The Internal Reflection Probe can readily be combined with a low cost commercially available instrument for this purpose. Although the use of the internal reflection probe has been demonstrated only for the IR, it can be adapted to any spectral region from the UV to the far IR.

N. J. HARRICK

Harrick Scientific Corporation
Ossining, N. Y. 10562

RECEIVED for review May 11, 1971. Accepted June 22, 1971

Changes of Drop-Shapes on Freezing

SIR: Davis and Bartell (*1*) determined the surface tension of molten materials by measurement of the shapes of solidified pendent drops, obtaining reasonable results for a variety of substances, including metals. Their method requires that the shape of the drop not change during "cooling." This is at least a two-stage process, except for glasses—namely freezing, followed by cooling of the solid to room temperature. They suggest that for isotropic substances the second stage should cause no trouble, but they do not comment on the first stage.

Unless customary precautions are taken, metal castings, on solidification, commonly form depressions at the free surface, or even deep pipes into the body of the casting, owing to shrinkage on freezing. The reverse phenomenon occurs with water and materials such as type-metal, which expand on freezing. The effect of this on drop-shape can invalidate the method unless solidification occurs superficially first, and the interior is frozen in such a way that the volume change is in some way vented. Cheng (*2*) has reported the ejection of microdroplets during freezing of a supercooled water drop. An experimental arrangement to allow this venting in a more controlled way can be imagined but it is difficult to see that this was achieved in the method as originally described.

A clear example of the distortion that can occur may be seen in the photographs, Figure 1. Three drops of water are shown, each resting in a shallow depression on top of an aluminium rod, the bottom of which dips into freezing mixture. As each drop is frozen from below, a change of shape occurs, leading ultimately to the formation of a cusp. In other experiments, when water drops were placed directly in depressions in pieces of Dry Ice, the form of the frozen drop resembled (in cross section) a Gothic arch. These more Byzantine forms were always obtained when the aluminum rod was used.

The general features of the distortion of a drop on freezing in this way may be understood by assuming that the original shape of the unfrozen drop is spherical, and that the solid advances in a front of some particular form. If the advance creates a volume $d\upsilon$ of solid, the amount of liquid removed will not be $d\upsilon$, but $d\upsilon' = d\upsilon\ \rho_s/\rho_l$. For water $d\upsilon' < d\upsilon$, so a small extra volume $d\upsilon'' = d\upsilon(1 - \rho_s/\rho_e)$ is generated. If this is accommodated in the liquid, its volume is slightly increased over that contained in the original envelope. If this envelope is more than a hemisphere, its radius of curvature R will be increased. It it is less than a hemisphere, R will be decreased. Thus the lower portion of an originally spherical drop should become more gently, and the upper portion more sharply curved.

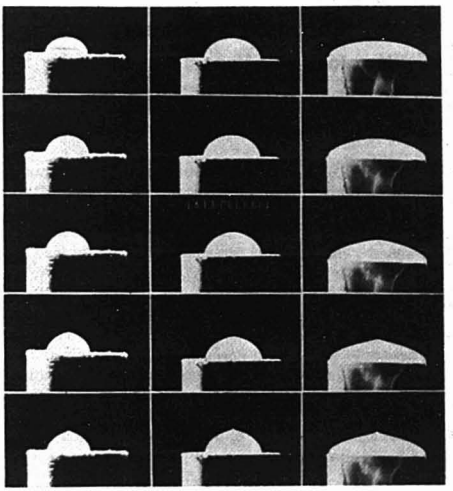

Figure 1. Three water drops being frozen from below

In each sequence (from top to bottom) it may be seen that the extra volume generated on freezing accumulates at the top of the drop (scale in millimeters)

Attempts to carry out this calculation showed that the outer form depends on the shape of the advancing front in a critical way. When it was taken to be flat, the predicted form for the frozen drop was egg-shaped. with the small end up. Assumption of a spherical interface meeting the free surface at right angles led to a cusp, but no reverse curvature.

When freezing was interrupted by blowing off the liquid with a puff of air, exposing the interface, it was found to be saucer-shaped, with the center flatter, and the outer portion more curved, than a spherical surface. We did not attempt to use an interface of this form in the calculations. In all versions, the assumption was made that the free surface of the

(1) J. K. Davis and F. E. Bartell, ANAL. CHEM., **20,** 1182 (1948).
(2) R. J. Cheng, *Science*, **170,** 1395 (1970).

liquid was continuous through the intersection with the interface, and that no change in slope occurred at this line. This appears to be approximately justified by the photographs, though we expected that the requirement of mechanical equilibrium of the surface and interfacial tensions would require a change of slope.

It is clear from these considerations that the calculation of surface tensions from the form of frozen drops is fraught with dangers. The established method (*3*) involving photography of liquid sessile or pendent drops is to be preferred.

(3) W. D. Harkins and A. E. Alexander, in "Physical Methods of Organic Chemistry," A. Weissberger, Ed., 3rd ed., Interscience, New York, N. Y., 1959, pp 805–809.

ACKNOWLEDGMENT

This work was performed while the author was a guest of the Chemistry Department, University of California, Berkeley. For their hospitality, and for the generous assistance of Paul L. Chambré with the calculations, he is most grateful.

R. A. STAIRS

Department of Chemistry
Trent University
Peterborough, Ontario
Canada

RECEIVED for review May 3, 1971. Accepted June 15, 1971.

AIDS FOR ANALYTICAL CHEMISTS

New Use for a 0.5-Nanometer Molecular Sieve Gas Chromatography Column

W. A. McAllister and W. V. Southerland

Department of Chemistry, East Carolina University, Greenville, N. C. 27834

THE USE OF 0.5-nm molecular sieve columns in gas chromatography for separation of diatomic gases is routine. At this laboratory, however, it has been used for the separation of CO_2 and N_2O at 250 °C. This has been a valuable asset, allowing the use of a simple gas chromatograph for the separation and detection of CO, N_2, NO, CO_2, and N_2O without a column change or modifications to the chromatograph. The literature (*1–6*) and commercial firms all propose using series columns, parallel columns, or elaborate column switching devices to separate this group of gases. These particular gases result from our studies of some catalyzed oxidation–reduction reactions between CO and NO at 1 atmosphere. The detection limit is satisfactory in that a 0.5-ml sample provides a detectable limit of about 1 part per thousand on the 3-ft × $^1/_4$-in. column.

EXPERIMENTAL

The gas chromatograph used in these measurements was a Gow-Mac Model 69-500 with a 1-mV recorder. Helium flow gas was used with a flow rate of 60 ml per minute and the detector current was 150 mA. The 60–80 mesh 0.5-nm molecular sieve was obtained from Fisher Scientific Company. It had been refined by Coast Engineering Laboratory and was from their lot 81170. It was packed manually in $^1/_4$-in. copper tubing (approximately 4 grams per foot) and was conditioned for 1 hour at 250 °C by purging with helium.

RESULTS AND DISCUSSION

One can only obtain complete separation of the diatomic portion of the gaseous mixture at 250 °C by using an inordinately long column. However, complete separation is not absolutely necessary for our reaction studies because the ratios of peak heights for the diatomic species on the three- and six-foot columns are sufficient to give an approximate indication of how the reaction is proceeding. The temperature can be lowered to 100 °C occasionally to obtain accurate diatomic concentration from peak area measurements.

Table I. Retention Times for 0.5-Nanometer Molecular Sieve GC Columns

Temp, °C	Gas	Column length: 3-ft Retention time, min:sec	Column length: 6-ft Retention time, min:sec
100	O_2	0:30	0:42
	N_2	0:53	1:12
	NO	1:20	2:00
	CO	2:25	3:45
250	N_2O	2:50	4:05
	CO_2	4:00	5:35

The data for typical operation are given in Table I. An unsuccessful attempt was made to separate SO_2 and NO_2. Ballistic temperature programming was also unsuccessful, apparently because of the slow rate at which the temperature of the column increases. A more sophisticated instrument or a modification of this instrument oven with an additional heater should work if the temperature rise is rapid enough. The 250 °C temperature seems to be the minimum for separation of the triatomic gases and must be reached fairly quickly while still allowing time for greater separation of the diatomics at lower temperatures. Six feet seems to be the minimum column length for this mode of operation.

(1) W. M. Graven, ANAL. CHEM. **31,** 1197 (1959).
(2) E. Heftmann, "Chromatography," Reinhold Publishing Corp., New York, N. Y., 1961.
(3) P. G. Jeffery and P. J. Kipping, "Gas Analysis by Gas Chromatography," The Macmillan Company, New York, N. Y., 1964.
(4) E. W. Lard and R. C. Horn, ANAL. CHEM. **32,** 879 (1960).
(5) R. Stock and C. B. F. Rice, "Chromatographic Methods," Reinhold Publishing Corp., New York, N.Y., 1963.
(6) D. H. Szulczewski and T. Higuchi, ANAL. CHEM., **29,** 1541 (1957).

RECEIVED for review May 13, 1971. Accepted June 14, 1971. This work was supported in part by the National Air Pollution Control Administration, Consumer Protection and Environmental Health Service, Public Health Service Grant Number APO1085-01.

Platinum Group Metals and Compounds

ADVANCES IN CHEMISTRY SERIES NO. 98

Eleven papers from a symposium by the Division of Inorganic Chemistry of the American Chemical Society chaired by U. V. Rao.

What new complexes of the platinum group metals have been synthesized? Here is a collection of 11 symposium papers presenting data on chalcogenides, oxides, nitrido and hydrido complexes, as well as the catalytic properties of these metals and their alloys. Information is included on

- synthesis
- structure
- magnetic susceptibility
- double bond migration

The platinum group metals are considered from the viewpoints of both industry and research. Their magnetic and thermodynamic properties are explored, as well as recent chemistry of σ- and π-bonded complexes. Crystal structure is discussed by several authors, with data presented in the form of

- x-ray scattering data
- absorption spectra
- crystal spectra
- infrared spectra
- Mossbauer spectra
- vibrational spectra

165 pages with index Cloth bound (1971) $9.00

Postpaid in U.S. and Canada; plus 35 cents elsewhere.

Set of L. C. cards with library orders upon request.

Order from:
Special Issues Sales
American Chemical Society
1155 16th St., N. W.
Washington, D. C. 20036

New Mettler automatic titration system

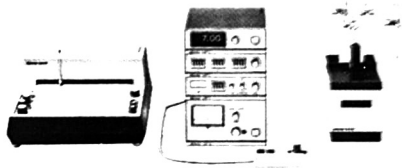

Mettler's new Automatic Titrator is setting new standards in equipment versatility . . . both for fixed end-point and recording titration in one system. Eight-unit instrument is completely modular with rapidly interchangeable burettes, all-electronic connection to modules, remote recording, provision for entry into data processing systems, and many more. Read about it in our new catalog. Contact Mettler Instrument Corporation, Box 3000, Princeton, New Jersey 08540. 609/448-3000.

Mettler

CIRCLE 123 ON READER SERVICE CARD

USE
ANALYTICAL CHEMISTRY'S
NEW FOLD-OUT READER SERVICE REPLY CARDS

YOUR REQUEST FOR FREE DATA IS COMPUTER PROCESSED FOR FAST ACTION

Measure mass and force changes in high vacuum and other controlled environments with the new Cahn R-100 ELECTROBALANCE

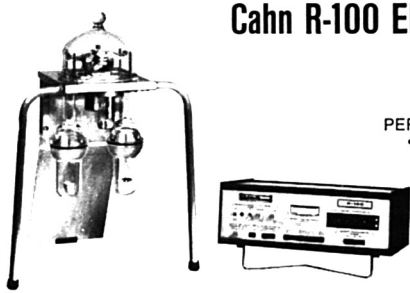

APPLICATIONS
- Thermogravimetric Analysis
- Adsorption
- Magnetic Susceptibility

PERFORMANCE AND FEATURES
- Symmetrical design improves performance in flowing gases
- 0.5 microgram sensitivity
- 100 gram capacity
- Gold-plating resists corrosive atmospheres
- Automatic Range Expander
- Percent of Sample Weight Control

Write or call today for new brochure.

Cahn Instruments Division / Ventron Corporation
7500 Jefferson Street, Paramount, California 90723 / (213) 634-7840

CIRCLE 39 ON READER SERVICE CARD

Analytical Chemistry **SEPTEMBER 1971** Valid through NOVEMBER 30, 1971

NEW PRODUCTS, CHEMICALS, LITERATURE: 401 402 403 404 405 406 407 408 409 410 411 412 413 414 415 416 417 418 419 420 421 422 423 424 425 426 427 428 429 430 431 432 433 434 435 436 437 438 439 440 441 442 443 444 445 446 447 448 449 450 451 452 453 454 455 456 457 458 459 460 461 462 463 464 465 466 467 468 469 470 501 502 503 504 505 506 507 508 509 510 601 602 603 604 605 606 607 608 609 610 611 612 613 614 615 616 617 618 619 620 621 622 623 624 625 626 627 628 629 630 631 632 633 634 635 636 637 638 639 640

ADVERTISED PRODUCTS: 1 2 3 4 5 6 7 8 9 10 11 12 13 14 15 16 17 18 19 20 21 22 23 24 25 26 27 28 29 30 31 32 33 34 35 36 37 38 39 40 41 42 43 44 45 46 47 48 49 50 51 52 53 54 55 56 57 58 59 60 61 62 63 64 65 66 67 68 69 70 71 72 73 74 75 76 77 78 79 80 81 82 83 84 85 86 87 88 89 90 91 92 93 94 95 96 97 98 99 100 101 102 103 104 105 106 107 108 109 110 111 112 113 114 115 116 117 118 119 120 121 122 123 124 125 126 127 128 129 130 131 132 133 134 135 136 137 138 139 140 141 142 143 144 145 146 147 148 149 150 151 152 153 154 155 156 157 158 159 160 161 162 163 164 165 166 167 168 169 170 171 172 173 174 175 176 177 178 179 180 181 182 183 184 185 186 187 188 189 190 191 192 193 194 195 196 197 198 199 200 201 202 203 204 205 206 207 208 209 210 211 212 213 214 215 216 217 218 219 220 221 222 223 224 225

PRODUCT CAPSULES
(Write in key numbers): _____

Name_____ Position_____

Company_____

Street_____

City_____ State_____ Zip_____

FIRST CLASS
Permit No. 25682
Philadelphia, Pa.
19101

BUSINESS REPLY CARD

NO POSTAGE STAMP NECESSARY IF MAILED IN THE UNITED STATES

POSTAGE WILL BE PAID BY

ANALYTICAL CHEMISTRY
P. O. Box #8660

Philadelphia, Pennsylvania 19101

Analytical Chemistry **SEPTEMBER 1971** Valid through NOVEMBER 30, 1971

NEW PRODUCTS, CHEMICALS, LITERATURE: 401 402 403 404 405 406 407 408 409 410 411 412 413 414 415 416 417 418 419 420 421 422 423 424 425 426 427 428 429 430 431 432 433 434 435 436 437 438 439 440 441 442 443 444 445 446 447 448 449 450 451 452 453 454 455 456 457 458 459 460 461 462 463 464 465 466 467 468 469 470 501 502 503 504 505 506 507 508 509 510 601 602 603 604 605 606 607 608 609 610 611 612 613 614 615 616 617 618 619 620 621 622 623 624 625 626 627 628 629 630 631 632 633 634 635 636 637 638 639 640

ADVERTISED PRODUCTS: 1 2 3 4 5 6 7 8 9 10 11 12 13 14 15 16 17 18 19 20 21 22 23 24 25 26 27 28 29 30 31 32 33 34 35 36 37 38 39 40 41 42 43 44 45 46 47 48 49 50 51 52 53 54 55 56 57 58 59 60 61 62 63 64 65 66 67 68 69 70 71 72 73 74 75 76 77 78 79 80 81 82 83 84 85 86 87 88 89 90 91 92 93 94 95 96 97 98 99 100 101 102 103 104 105 106 107 108 109 110 111 112 113 114 115 116 117 118 119 120 121 122 123 124 125 126 127 128 129 130 131 132 133 134 135 136 137 138 139 140 141 142 143 144 145 146 147 148 149 150 151 152 153 154 155 156 157 158 159 160 161 162 163 164 165 166 167 168 169 170 171 172 173 174 175 176 177 178 179 180 181 182 183 184 185 186 187 188 189 190 191 192 193 194 195 196 197 198 199 200 201 202 203 204 205 206 207 208 209 210 211 212 213 214 215 216 217 218 219 220 221 222 223 224 225

PRODUCT CAPSULES
(Write in key numbers): _____

Name_____ Position_____

Company_____

Street_____

City_____ State_____

FIRST CLASS
Permit No. 25682
Philadelphia, Pa.
19101

BUSINESS REPLY CARD

NO POSTAGE STAMP NECESSARY IF MAILED IN THE UNITED STATES

POSTAGE WILL BE PAID BY

ANALYTICAL CHEMISTRY
P. O. Box #8660

Philadelphia, Pennsylvania 19101

Analytical Chemistry

SEPTEMBER 1971

Valid through
NOVEMBER 30, 1971

NEW PRODUCTS, CHEMICALS, LITERATURE: 401 402 403 404 405 406 407 408 409 410 411 412 413 414 415 416 417 418 419 420 421 422 423 424 425 426 427 428 429 430 431 432 433 434 435 436 437 438 439 440 441 442 443 444 445 446 447 448 449 450 451 452 453 454 455 456 457 458 459 460 461 462 463 464 465 466 467 468 469 470 501 502 503 504 505 506 507 508 509 510 601 602 603 604 605 606 607 608 609 610 611 612 613 614 615 616 617 618 619 620 621 622 623 624 625 626 627 628 629 630 631 632 633 634 635 636 637 638 639 640

ADVERTISED PRODUCTS: 1 2 3 4 5 6 7 8 9 10 11 12 13 14 15 16 17 18 19 20 21 22 23 24 25 26 27 28 29 30 31 32 33 34 35 36 37 38 39 40 41 42 43 44 45 46 47 48 49 50 51 52 53 54 55 56 57 58 59 60 61 62 63 64 65 66 67 68 69 70 71 72 73 74 75 76 77 78 79 80 81 82 83 84 85 86 87 88 89 90 91 92 93 94 95 96 97 98 99 100 101 102 103 104 105 106 107 108 109 110 111 112 113 114 115 116 117 118 119 120 121 122 123 124 125 126 127 128 129 130 131 132 133 134 135 136 137 138 139 140 141 142 143 144 145 146 147 148 149 150 151 152 153 154 155 156 157 158 159 160 161 162 163 164 165 166 167 168 169 170 171 172 173 174 175 176 177 178 179 180 181 182 183 184 185 186 187 188 189 190 191 192 193 194 195 196 197 198 199 200 201 202 203 204 205 206 207 208 209 210 211 212 213 214 215 216 217 218 219 220 221 222 223 224 225

PRODUCT CAPSULES
(Write in key numbers): _____ _____ _____ _____ _____ _____ _____ _____

Name_____ Position_____

Company_____

Street_____

City_____ State_____ Zip_____

FIRST CLASS
Permit No. 25682
Philadelphia, Pa.
19101

BUSINESS REPLY CARD

NO POSTAGE STAMP NECESSARY IF MAILED IN THE UNITED STATES

POSTAGE WILL BE PAID BY

ANALYTICAL CHEMISTRY
P. O. Box #8660

Philadelphia, Pennsylvania 19101

Potentiometric recorders: here's the picture.

Shown here, a portrait of all there is to know about potentiometric recorders. All from Sargent-Welch. And each deserves its own personality profile:

Model SRG: The basic recorder, distinguished by its advanced performance. Seven pre-calibrated spans. Three chart speeds. Guarded circuits and filtered inputs. Accuracy: ±0.25%. Reproducibility: ±0.1%. Full-scale pen response: Less than one second. Basic price: $1025.

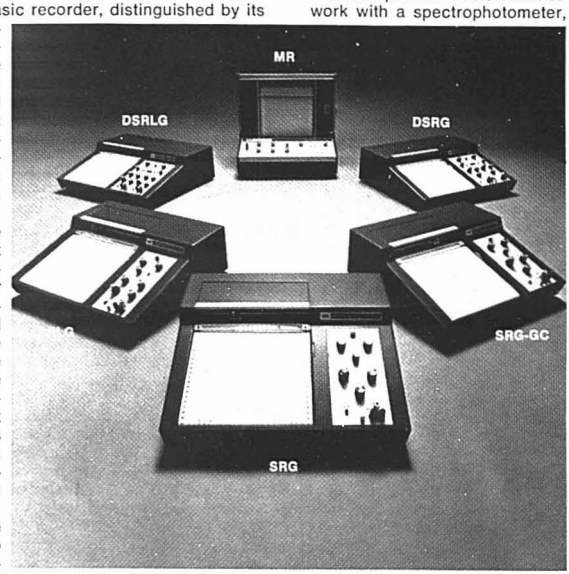

Model DSRG: The SRG times two. That is, a dual-pen recorder, with two linear channels, for recording two time-related variables, side by side or overlapping, on the same chart. Same matchless performance as the SRG, but only a few inches wider. Think of it as a space- and paper-saver. Basic price: $1800.

Model SRLG: The SRG taken one step further, with the addition of a logarithmic function. Eminently suited, therefore, for recording (say) the log of absorbance with a spectrophotometer. Precision, non-circular gears — which do the job much better than electrical approximations to the log function. Basic price: $1325.

Model DSRLG: Another logical move. Two SRLG's in one dual-pen recorder. Think of what that means if you work with a spectrophotometer, photometer, or densitometer — simultaneous recording of both transmittance *and* absorbance. Or linear/log recording of any two time-synchronized variables. Basic price: $2225.

Model SRG-GC: Something special, for use with a gas chromatograph. Fast response, high AC rejection, floating input, three chart speeds, and continuously variable wide-range spans. Optional integrator for precise measurement of areas under recorded curve. Basic price: $1025 (with integrator, $1820).

Model MR: The ultimate recorder? Perhaps. Few can match it for precision, speed, sensitivity, and versatility. Measures and records (vs. time) any variable that can be translated into voltage or current, *or* that can be time-related by synchronous drive. Twelve ranges, twelve speeds. Basic price: $2850.

As we said, a complete picture of a complete line.

Now read the book.

0-214

Still, in all fairness, one picture and these few words don't do justice to our complete line of recorders. So we've prepared a fully illustrated, 30-page catalog. It's yours, without obligation, for returning the coupon. Do it now.

I'd like a copy of your recorder catalog. I'm especially interested in:

- ☐ Model SRG Recorder
- ☐ Model DSRG Dual-Pen Recorder
- ☐ Model SRLG Linear-Log Recorder
- ☐ Model DSRLG Dual-Pen Linear-Log Recorder
- ☐ Model SRG-GC Recorder for Gas Chromatographs
- ☐ Model MR Multi-Range Recorder

Name _____ Title _____

Organization _____

Address _____

City _____ State _____ Zip _____

Telephone _____ AC

SARGENT-WELCH

Scientific instruments, apparatus, chemicals.
Sargent-Welch Scientific Company
7300 N. Linder Ave., Skokie, Illinois 60076

Chicago/Anaheim/Birmingham/Cincinnati
Cleveland/Dallas/Denver/Detroit
Springfield, N.J./Toronto/Montreal/Vancouver

CIRCLE 172 ON READER SERVICE CARD

LITERATURE OF CHEMICAL TECHNOLOGY

Advances in Chemistry Series No. 78

When you need information, knowing where to look is the hard part—right? Not any more. Forty articles in this volume tell you where—

—where the patents are
—where the abstracts and indexes are
—where the background information is
—where the new information is

More than 30 major fields in chemical technology are covered:

- *Chlor-alkali, electrochemistry, industrial gases, noble metals, ceramics, refractories, abrasives, cement, explosives, and rocketry*
- *Pharmaceutical and medicinal, synthetic dyes, photographic chemicals, cosmetics, soaps and detergents, waxes and polishes*
- *Resins and plastics, synthetic rubber, natural rubber, coatings, printing inks, cellulose, pulp and paper, wood naval stores, leather, gelatin, adhesives*
- *Coal, petroleum, carbon black, aerosols, pesticides, food.*

732 pages with index Cloth bound (1968) $17.50
Free set of L. C. cards with library orders upon request.
Other books in the Advances in Chemistry Series of related interest include:

No. 30 Searching the Chemical Literature. Surveys on the use of indexes and abstracts, on name, nomenclature, and language problems, on various types of literature sources, on government sources, on searching techniques, and on the facilities of four leading libraries. 326 pages.
Cloth (1961) $9.00

No. 20 Literature of the Combustion of Petroleum. Twenty-one papers about the chemistry and kinetics of combustion, petroleum products as the fuel for engines, and combustion studies in engines. 295 pages
Paper (1958) $8.00

No. 17 Training of Literature Chemists. Approaches to the training of literature chemists presented by a diversified group of authors from chemical industry, from a consulting laboratory, from a university, from a well known library school, from Chemical Abstracts. 44 pages.
Paper (1956) $5.00

No. 16 A Key to Pharmaceutical and Medicinal Chemistry Literature. Twenty-five illustrative articles range over the several disciplines in the physical and biological sciences which involve the interest of workers in pharmaceutical and medicinal chemistry. 254 pages.
Paper (1956) $7.50

No. 10 Literature Resources for Chemical Process Industries. Information sources on market research (13 papers), resins and plastics (7 papers), textile chemistry (6 papers), food industry (10 papers), petroleum (10 papers), literature searching and language problems (13 papers). 582 pages.
Paper (1954) $12.00

Postpaid in U.S. and Canada; plus 30 cents elsewhere

Order from: Special Issues Sales
American Chemical Society
1155 Sixteenth St., N.W.
Washington, D.C. 20036

NEW PRODUCTS

Ultrascan SM-3 has vacuum capability of 10^{-9}. This multipurpose analytical system incorporates advanced developments in high vacuum and electron optical technology to give the most complete microanalysis of a given specimen with a single instrument. When used with appropriate detectors, spectrometers, and auxiliary equipment, the system is capable of any of 10 different modes of operation. Magnification range is 10–100,000×; resolution capability extends below 100Å. The combination of an Auger analyzer provides a powerful tool for surface analysis. Other detection schemes are available for secondary emission, backscattered electrons, transmitted electrons, cathodoluminescence, charge collection current, specimen-absorbed current, voltage-induced current, deflection modulation, and X-ray analysis. The basic system consists of the electron-optical column with three-element gun, electromagnetic condenser lenses (2) and objective lens with associated electronics; specimen chamber, stage, and vacuum system; scanning generator and video display system; and detectors and signal processing modules array. $67,500–71,400. Ultrascan Co. 216-663-5006 **401**

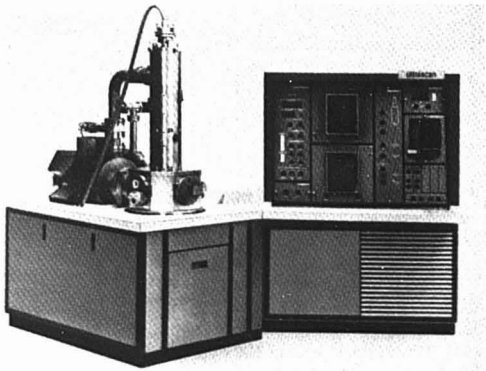

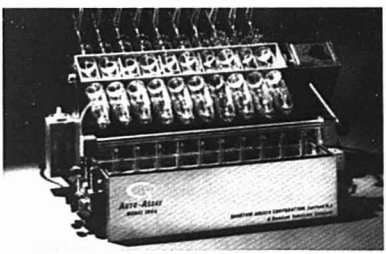

Auto-Assay 1000 is used in preparing extracts from cation paper for spotting on tlc plates in the detection of drugs in urine for methadone programs and in screening. The instrument permits simultaneous preparation of up to 10 discrete samples, including semiautomatic mixing and aliquoting of chloroform-like solvents from buffered solutions. Up to 80 tests per 8-hr day can be performed routinely. $3923. Quantum Assays Corp. 201-227-4882 **402**

Automatic enzyme analyzer can process up to 100 samples using kinetic methods. Test changeovers are easily and rapidly made. The system is complete and includes reagent package for the uv monitoring of CPK, LDH, GOT, and GPT activity. $7335. Gilford Instrument Laboratories. 216-774-1041 **403**

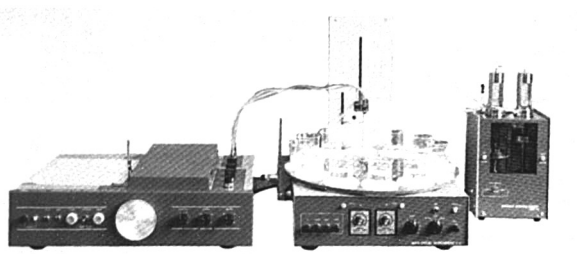

RAT-11 automatic recording titrator, Hiranuma, Japan (left) used with a cycling turntable permits up to 12 samples to be automatically titrated. At right is a double-action buret. The titrator features a unique equilibrium detecting system to provide intermittent delivery of titrant depending on the progress of the titration. Amount of titrant is decreased and the time interval between titrant additions is increased as the end point is approached. The unit can be preset to stop at any point between pH 1–13; time between titrant additions may be preset. The titrator is suitable for potentiometric, photometric, coulometric, and especially nonaqueous titrations. The basic titrator sells for $2600. Rainin Instrument Co. 201-947-4501 **404**

George real-time data acquisition and remote batch terminal has scientific applications and is capable of interactive data processing and local mode processing. George includes a minicomputer, selected peripherals, and a complete software package. $15,900 to $100,000. Applied Computer Systems, Inc. 512-926-1536 **405**

Unicam Weyfringe ADCP-1 digital printer provides simultaneous digital display and printout for Unicam spectrophotometers. The unit may be used in either a manual or automatic printout mode. It has two input ranges, 0 to ±2 V and 0 to ±200 mV. The former is used to obtain absorbance readout; the latter for concentration readout. Philips Electronic Instruments. 914-664-4500 **406**

Pocket-size pH meter has 0.01 pH accuracy and digital readout. The battery-operated unit can provide precise pH readings in the field for pollution studies, at bedside in medicine, or in a process control application. $595. Kruger & Eckels, Inc. 213-799-4200 **407**

Recorder amplifier BA-1 provides additional recorder amplifier gain and zero offset to control recorder amplitude and, if desired, expand a particular portion of the data record. BA-1 has voltage gain selections ranging from 1 to 100. $275. A thermocouple amplifier, BTA-2, produces a voltage proportional to sample temperature (100°C/1 V) from 0–1000°C. This voltage may be either recorded or observed. Range expansion and increased sensitivity over a narrow temperature band can be achieved. $265. Tetrahedron Assoc., Inc. 714-277-2820 **408**

Fracto-Scan linear dual beam ultraviolet photometer can monitor liquid effluent from flows. A deuterium lamp emits uniform energy through the region; this energy is directed through a 280 mμ wavelength filter. Optional interference filters are available for monitoring throughout the uv. The monitor is made up of an optical unit and a control unit. $1298. Buchler Instruments Div., Nuclear Chicago Corp. 201-945-1188 **409**

2095 HI-CAP high-performance table-model bath and circulator offers increased Btu capacity with a new proportional refrigeration system. The temperature is directly dialed from the control panel and eliminates thermoregulators, solenoids, and electrical contacts. Forma Scientific. 614-373-4763 **410**

Model 180 digital nanovoltmeter simplifies measurements by direct connection to the unknown potential. Resolution of up to five places can be obtained, with sensitivities as low as 10 nV per digit. Display rate is adjustable from $2^1/_2$–$^1/_6$ readings/sec; settling time to rated accuracy is less than 3 sec except on most sensitive range. Other features are remote programming, isolated input and output, and an optional BCD digital output (also isolated). $1695. Keithley Instruments, Inc. 216-248-0400 **411**

Environmental incubators for tissue culture studies and general purpose agitation come in four models. Model 2610, the basic incubator ($245), has five 18 × 13 in. shelves. Magnetic stirrer-incubator No. 7700 ($495) supplies agitation by 8 positions of magnetic stirring. Model 6620 ($395) has an oscillating platform that tilts through an angle variable from a few degrees up to about 25° and provides speed continuously variable from 0–50 oscillations/min. The fourth model, No. 6115 ($395) is a rotator-incubator with agitation supplied by a rotating shaker. The four models are supplied with thermometer and a 6-ft rubber-covered three-wire cord and plug. Eberbach Corp. 313-665-9977 **412**

IL Model 355 flameless sampler consists of a tantalum ribbon, controlled atmosphere atomization device for use with atomic absorption spectrophotometers, and a controlling module. The unit can be used with all commercially available AA instruments. Thousandfold improvement in sensitivities is typically experienced; for instance, 1 ng of Cd gives a signal of 0.5 absorbance. Sample size varies from a few to several hundred μl. $2390 includes all necessary supplies. Instrumentation Laboratory, Inc. 617-861-0710 **413**

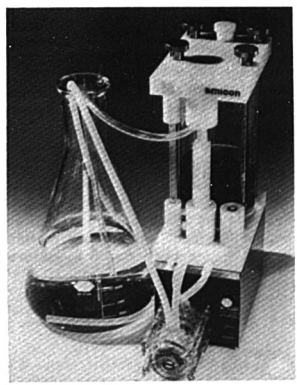

Hollow-fiber dialysis system comprises a reservoir, dual-head pump and a Diaflo membrane filter cartridge with 1.2 ft² surface area. The system can exchange 99% of most common salts from 2-liter volumes in 8 hr. Components in contact with liquid are made of inert plastics. Cartridges are easily replaced (but are useful for several hundred hours). $785; extra cartridges, $20 each. Amicon Corp. 617-861-9600 **414**

New Products

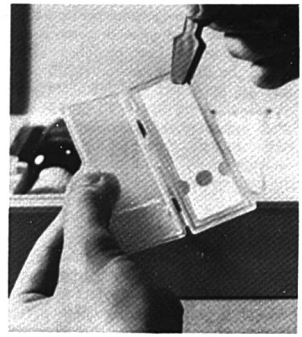

Chromat-O-Screen analysis kits provide trough, at lower left of plastic chamber to hold solvent gel. Chromatographic strip spotted with specimen for analysis is positioned at right. Trough containing solvent gel is folded over so base of strip will be in good contact with solvent gel. Six disposable kits using principles of thin-layer chromatography are available for detecting the presence of certain drugs, amino acids, sugars, and other compounds in biological fluids. Sets of kits that perform 60 screening tests for amphetamines, barbiturates, amino acids, alkaloids, sugars, or catecholamines measure 8 × 5¼ × 2⅛ in.; larger kits for performing 150 tests measure 9 × 6¾ × 3 in. Eastman Kodak Co. 716-325-2000 **415**

MP-1030 high-voltage supply provides regulated, current-limited power for MP-1021 photomultipliers and other uses. The supply will provide power up to 3 mA at −500 to −1000 V for 1 or 2 photomultipliers. Regulation is better than 0.01% for 10% change in line voltage. Models are available for 117 V, 60 Hz and 230 V, and 50 Hz. $255. McKee-Pedersen Instruments. 415-937-3630 **416**

Series 700C calculators start with a basic programmable calculator. A user can add core memory in increments of 4 K up to a maximum system of 524 K. Dual magnetic tape cassette units for data and program storage can also be added. Peripherals include an alpha-numeric typewriter printer, an *X-Y* plotter with alpha-numeric capabilities, an interface for on-line applications, paper tape editor, card reader, and software. The system is capable of serving multiple users, up to 16, with remote terminals accessing the calculator via voice-grade telephone lines. From $5200. Wang Laboratories, Inc. 617-851-7311 **417**

New Products

Model 10, Series 9800 calculator uses plug-in function blocks to expand its operational capabilities. The basic calculator with 51 registers and 500 program steps ($2975) can perform all basic arithmetic functions and can be programmed by simply pressing the keys in the desired sequence. Function blocks (read-only memories) plug in the top to give special capabilities. Accessories and peripheral products permit the user to expand memory, customize the keyboard, extend input/output capability, and provide solutions in words, numbers, drawings, or a combination of all three. Hewlett-Packard. 415-493-1501 **418**

Model 2104, compact potentiometer from Tettex (Zurich), measures up to 50 mV dc without drawing any current from the unknown voltage source. Voltages from 0 to 10.5 mV are read directly off an 11-in. slide wire scale, to which 4 steps of 10 mV each can be added. Accuracy is 0.5% of the particular range. The instrument has a built-in galvanometer and battery and is ideal for research applications. $230. Special Instruments & Machinery Co. 914-779-8981 **419**

Enviroline group of low-cost portable instruments for the study of fresh and seawater environments have been developed for instruction. Included are student manuals on theory, operating instructions, and experiments. The instruments include an underwater listening device ($98); underwater current meter ($40); Secchi disc for transparency ($98); turbidimeter ($135); temperature/salinity bridge ($149); temperature/conductivity meter ($149); water height gage ($40); and underwater camera package, less camera ($49). Beckman Instruments, Inc. 201-239-6200 **420**

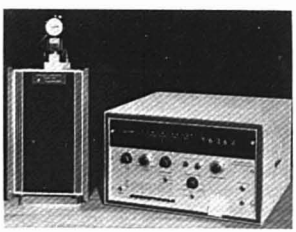

Digital dilatometer, Model Unitherm, determines linear thermal expansion of solids. Samples can be tested from −180–2500°C using different furnaces but with the same control and data acquisition system. $7800. Dynatech Corp. 617-868-8050 **421**

New Products

Bandpass optical filters with a bandwidth of only 0.05% in the infrared region are available. The center wavelength of the new units is located within 20% of the center wavelength; for example, a conventional 10-μ filter would be located within ± 0.1 μ; the new narrow band filter with a bandwidth of 0.05% would be located within 0.001 μ—an improvement of 100:1. Transmittance is 80% for filters in the 1–5 μ range and 70% for units in the 1–10 range. Filters are available for operation at any selected point from 1–25 μ. Heliotek Div., Textron, Inc. 213-365-4611 **422**

Hydrovoid compact controlled atmosphere system routinely provides atmospheres with dew points down to −40°F, even lower with the proper dry gas. Dust particles from 0.5 μ and up are filtered out. The basic chamber provides a work area 34 in. wide and 24 in. deep; either glove-type or iris-diaphragm entry ports can be provided; also electrical outlets, compressed air fittings, and microscope ports. Prices range from $300 to $800. Air Control, Inc. 215-561-4061 **423**

Model RB4-250 conductivity bridge is capable of measuring solution conductivities from 2.5–40,000 $\mu\Omega$/cm in four overlapping ranges when used with a cell of constant 1.00/cm. The range may be extended with other cells. This portable battery-operated instrument uses a 400 Hz ac Wheatstone bridge with a zero center meter as a null detector and has an accuracy of 2%. $280. Beckman Instruments, Inc. 714-871-4848 **424**

Integrating computer/printer to interface densitometers now in use offers the operator a choice of three output modes: percentages, grams percent, or raw integrals. The printer automates the quantitation of separated fractions and prints out the results in digital format; the operator may also manually enter fractions at any time during a scan; up to 30 fractions can be stored and computed. $3500. Transidyne General Corp. 313-663-9329 **425**

NFA-200 adiabatic distillation columns provide over 200 theoretical plate separations with only 0.7-ml holdup and less than 1-mm drop at atmospheric pressure. The console mounted still is offered with options for automatic reflux control, pot temperature control, and temperature deviation monitoring. Separation of species with boiling point differences of as little as 0.2°C can be made; distillation at pressures as low as 0.005 mm of Hg is possible. Electronic controls and an inert 36-in. Teflon and glass system permit distillation with long periods of unattended operation. $2900 to $3800. Nester/Faust. 302-737-6330 **426**

Laser microprobe system provides spectrochemical analysis with photographic recording and photoelectric detection for up to 12 elements. With the microscope the user selects an area of interest, sets the laser energy level and then a concentrated laser burst vaporizes a miniscule area of the sample for spectrographic analysis. There are 15 selectable energy levels for the neodymium glass laser which produce craters from 8 to 30 μ in diameter; repeatable shots can be made over 30 sec; laser output is reproducible to $\pm 5\%$; less than 10^{-6} gram of sample is used. The probe is suggested for use in elemental analysis of biological structures and perhaps in the mass screening of body fluids in health maintenance programs. The microprobe has digital display and is computer compatible. Complete system: $60,000. Fisher Scientific Co. 412-391-1330 **427**

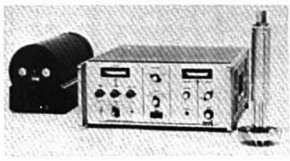

Model 100B precision gas analyzer for quantitative measurements in the lab, and in process control and monitoring, it scans a mass spectrum in a fraction of a second or continuously monitors an individual mass peak or total pressure. The instrument, a reproducible quadrupole mass analyzer, can be used directly in any high-vacuum system. Dual filaments in the ion source ensure continuity of operation. $7700. UTI. 408-739-3301 **428**

MAT 711 double-focusing mass spectrometer is of modified Mattauch-Herzog geometry (electrical recording only) using a spherical condenser. The instrument features maximum performance, and many accessories are available including digital mass display and mass marker, different inlet systems, combined electron impact/field ionization and desorption source, and gc coupling devices. The MAT 711 is made by Varian MAT GmbH in Bremen, Germany. $118,000. Varian MAT. 415-326-4000 **429**

Pol-E-Film system provides the materials and equipment for routine clinical electrophoresis of serum proteins, lipoproteins, hemoglobinopathies, and LDH-isoenzymes, with equal facility for immunoelectrophoresis. Major innovation is the use of prepared, very thin agarose films, which provide optimal porosity, more reproducible, sharper resolution, and clear separations of fractions. Also included in the system are a cell and power supply, microliter pipet, film slicer, oven/incubator, stain dishes, reagents, and stain sets. Pfizer Diagnostics. 212-573-2198 **430**

LP Series of power supplies includes the LP 400A available in six voltage and current ranges between 0–10 and 0–250 V dc. Current ranges are between 0–2 and 0–80 mA. The LP 500 Series comes in five models with voltages between 0–10 and 0–120 V dc and currents from 0–5 and 0–0.5 A. Regulation for both series is 0.01% + 1 mV line or load and ripple is 500 uv rms. The supplies are designed for both bench and rack. The 40-V, 1-A Model 400A costs $140; the 10-V, 5-A Model 500 costs $210. Lambda Electronics Corp. 516-694-4200 **431**

New Products

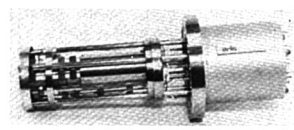

EEA Series high-resolution electron energy analyzer systems have applications including ESCA, Auger spectroscopy, photoelectron spectroscopy, and as Auger spectrometer attachments to scanning electron microscopes. Energy analysis range is from 0–3000 eV; resolution is better than 30 meV at 50 eV and better than 0.025% over the entire range. The systems operate on the modulated retarding potential difference principle and use all cylindrical optics. The company offers literature which explains in detail the principle of operation and illustrates the use of these systems. Price for a complete system with all electronics equipped with electron multiplier is $13,560. Advanced Research Instrument Systems, Inc. 512-926-6130 **432**

Testing kit for mercury, arsenic, and selenium fits any atomic absorption spectrophotometer. Mercury can be determined to 0.2 ppb and arsenic to 1.0 ppb. Arsenic is determined using arsine. The complete kit costs $250; mercury kit only, $200; arsenic and selenium kit only, $150. F & J Scientific. 203-268-3335 **433**

High-performance liquid chromatograph Model 830 combines the speed, resolution, and reproducibility of a research instrument with the operating simplicity of an instrument for repetitive, high-volume process and quality control work. All types of liquid chromatography, partition, absorption, ion exchange, and gel permeation, can be performed with quantitative results. The uv photometer detector has a sensitivity of 0.01 absorbance unit full scale; minimum level of detection is 2×10^{-4} absorbance unit (2× noise). Other detectors can be added as they become available. The instrument is available with an electronic integrator and is compatible with other electronic data reduction devices. The basic instrument ready to operate sells for $7700 plus recorder. E. I. du Pont de Nemours & Co. 302-774-2421 **434**

Twenty-kg capacity balances, sensitive to 1 gram, come in three basic models for lab, research, or pilot plant or production facility. Balances come in undamped ($149.50–199.50) and magnetically damped models ($175–225). Ohaus Scale Corp. 201-377-9000 **435**

Model KR-8 pH meter with an 8-in. mirrored scale has readability to 0.02 pH. The meter uses a taut band suspension meter movement. The unit is both line- and battery-operated and has a polarizing outlet for Karl Fischer and similar titrations and an automatic temperature-compensator probe. $335. Industrial and Mill Supply Co. 516-427-4354 **436**

Model 47 probe refractometer can be inserted into the sample to be measured. In the insertion probe a light beam is directed from a source located in a housing 6–8 in. away from the measuring tip. The beam refracts on a prism mounted in the measuring tip and is directed back to a photosensitive element. The instrument is sensitive to full-scale range of 0–5% dissolved solids in liquid streams or 0–5% concentration of one liquid in other liquids; other ranges can be obtained by adjustment. As many as eight sensing probes can be used with one electronic readout unit. $2850 with one probe; $995, individual probe. Anacon, Inc. 617-881-3000 **437**

Spring balance for rapid density measurements features a small, stainless steel bob, carefully sized for weight and volume displacement, which is suspended by a filament in the fluid to be measured. Balancing torque is read from a 6-in. diameter disc on which four scales are engraved. Hanging a 100-gram weight in place of the bob produces a reading of 1.0 sp gr or 8.32 lb/gal. $229.41. Fann Instrument Corp. 713-526-3031 **438**

Model 45A microsampling attachment fits any standard infrared instrument and can be used for transmission studies with ultramicro cells and KBr pellets as well as for micro ATR measurements. An efficient 4–1 reflecting beam condenser is included that can be easily shifted from transmission to reflecting mode. Ultramicro cells with a volume of $<0.5\ \mu l$ and KBr pellets of 1-, 2-, and 3-mm diameter can be analyzed. $495. Wilks Scientific Corp. 203-838-4537 **439**

N-CON Trebler samplers provide automatic sampling, proportional compositing, and preserving by refrigeration of all types of sanitary and industrial wastes. The sampler is mounted on a wall of the chamber to be sampled; its special sampling scoop operates in conjunction with a Parshall flume V-notch or rectangular weir to provide a cross-sectional sample of the entire flow. $795 and up. N-CON Systems Co. 914-834-6530 **440**

New Products

Radiometer PHM53 specific ion meter is a portable instrument equally applicable to all selective measurements of monovalent or divalent anions or cations. A meter provides a linear scale with a span from 0.00–1.00 for pX, pH, and mV readings plus logarithmic decade scale from 1.0–10.0 which may be calibrated as a_x in terms of molarity or molality, as well as ppm or partial pressure, as for P_{CO_2} measurements. Scales can be extended to cover any three consecutive spans of pH or decades of a_x within any range of practical importance for specific ion electrodes. $472, battery; $498, line. The London Co. 216-871-8900 **441**

Optical quality cells or cuvettes for spectrophotometers are of directly fused construction with no intermediate adhesives. Matched sets are offered in an unlimited number of cells in each set. Various grades of quartz cells for the uv, far uv, and the near-ir range are offered. Cells are also available in rectangular, cylindrical, and flow styles. Markson Science Supply. 714-755-6500 **442**

New analyzer-transmitters, two of which have new sensors, measure pH, ORP (oxygen reduction potential), DO (dissolved oxygen), and conductivity. They are designed for long low-maintenance operating life in outdoor and industrial-processing environments in water analysis. New sensors are those for conductivity and a pH "zero-flow" reference electrode. The line also includes pH/ORP actuation for Honeywell's new Electronic 111 multipoint recorder with large-scale integrated circuitry. A single sensor plus field-mounted transmitter costs from $900–1000; with Electronik 111 single pen recorder, $1400–1500. Honeywell Industrial Div. 215-643-1300 **443**

Model 112 recorder offers 1–100-V span; 12 chart speeds; $<\pm 0.5\%$ limit of error; disposable long-life pen; and 20 in./sec pen response. The recorder is designed for the sophisticated laboratory user as well as for OEM. $295–495 for single units; OEM discounts. Linear Instruments Corp. 714-546-6706 **444**

MP-1027-1 is an 8-range 10-in. strip chart recorder with the lowest range 1 mV full scale. Balancing time is 0.6 sec; error including dead zone is less than 0.25 full scale. The recorder is ideal for use with lab instruments including pH meters and spectrophotometers. $625. OEM units are also available. McKee-Pedersen Instruments. 415-937-3630 **445**

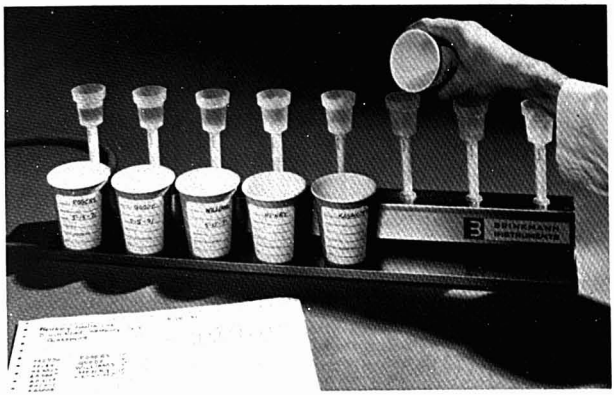

Drug-Skreen columns extract abused drugs from samples and allow positive identification of the following commonly abused drugs: heroin (as morphine), quinine, codeine, Doriden, methadone, barbiturates, amphetamines, phenothiazines, Dilantin, meprobamate, Valium, and Librium. The procedure is fast and simple; only 20 ml of urine are required to pass through the plastic Amberlite XAD-2 column. The detailed tlc procedure is available. Columns which are disposable or may be reused cost under $1.00. Brinkmann Instruments, Inc. 516-334-7500 **446**

CryoCool Model CC100F provides low temperatures and high cooling capacities needed for vapor traps and freezing baths subject to large loads. Each unit can handle a minimum of 100 watts at −70°C on a continuous basis. A dual-compressor cascaded refrigeration system is used allowing no load temperatures of −100°C to be obtained. $1110. Neslab Instruments, Inc. **447**

Thermometer that uses changes in electrical capacitance to measure temperature accurately down to 0.100°K offers some unique advantages over resistance change measurements. The capacitance thermometer (developed by Corning Glass Works) has an extremely small self-heating factor, is insensitive to strong magnetic fields, has a smooth capacitance-temperature relationship up to 70°K, and has large absolute sensitivity. $200–400. Lake Shore Cryotronics, Inc. 716-922-3411 **448**

Model 4400 programmed attenuator, part of the Valve-Minder system, provides an operationally simple, inexpensive method of preselecting as many as six different attenuation levels, and then automatically switching these levels at predetermined times during the course of the gas chromatograph's analysis. Model 4400 also enables unattended operation of the disc integrator, which requires that all peaks be on scale for proper performance. $245. Valve Minder, $295, $325. Carle Instruments, Inc. 714-879-9900 **449**

KCS-18 automatic Color-Eye is a computer-compatible automatic color-measuring device capable of providing tristimulus and spectrophotometric data for both fluorescent and nonfluorescent materials. Features include digital display of wavelength and reflectance or transmittance, dual photometric scales of 1–199.99% with 0.1% resolution and 0–19.999% with 0.001 resolution, and a wide choice of peripherals. $8500–10,000 depending on accessories. Kollmorgen Corp. 617-222-3880 **450**

CTC-25 Adapt-O-Cool refrigerated unit has a variety of different sized cooling coils. The units use pressurized Freon to permit quiet operation throughout a full range of bath temperatures from −25–100°C. The system exchanges 1850 Btu's/hr at ambient, 1100 Btu's/hr at 0°C, and 450 Btu's/hr at −20°C. $330. Bronwill Scientific, Inc. 716-254-4810 **451**

Series H photodetectors contain low-voltage vacuum photo diode pre-amp and are available in the standard EIA spectral responses of S-1 ($105), S-4 ($90), S-5 ($145), and S-20 ($185). When used with interference filters, these detectors result in high signal-to-noise ratios. Ditric Corp. 617-485-9311 **452**

NEW CHEMICALS

MethElute, a new reagent for quantitative methylation and detection of barbiturates, sedatives, xanthine bases, phenolic alkaloids, and diphenyl hydantoin in physiological samples by glc, is a 0.2 molar solution of trimethylanilinium hydroxide in methanol. The on-column reaction is instantaneous; troublesome secondary peaks are eliminated, giving a single quantitative response. A descriptive brochure gives details of its use. MethElute is packaged in 10 ml hypovials under nitrogen at $12.50 per vial. Pierce Chemical Co. 815-968-0747 **501**

1-Alkyl-3-*p*-tolyltriazenes have been shown to alkylate carboxylic acids under very mild conditions, rapidly, and in high yields. The crystalline triazenes as well as volumetric solutions of the methyl and ethyl esters, respectively, are available for use in such situations as synthesis, analysis, and biomedical research. Data and prices are available. Willow Brook Laboratories, Inc. 414-547-6378 **502**

Four narcotic detection kits provide on-the-spot testing of suspected material. The kits provide tests for marijuana (Kit 1891), cocaine, Demerol, and methadone (Kit 1892), opium, heroin, codeine, morphine, amphetamines, and mescaline (Kit 1893), and barbiturates (Kit 1894). Each test kit is supplied with instructions for use and individual ampules are labeled. Kits are less than $2.00 each. J. T. Baker Chemical Co. 201-859-2151 **503**

Reference standards for air and water pollution studies include a variety of particles and spheres packaged as liquid emulsions, dusts, and powders. Metals, oxides, minerals, spores, pollens, fly ash, and fluorescent materials are offered. The standards are packaged in small quantities and can be purchased for $5.00 to $20 per unit. They are described in a 6-page brochure, Bulletin 171. Duke Standards Co. 415-328-2400 **504**

Standards and reagents for clinical and research laboratories, FI/SOL products, are available in one-time ampules or color codes flip-top 125-ml and 250-ml inert polyethylene bottles. The FI/SOL line includes standards and reagents for use with all Fiske instruments (osmometers, cryoscopes, calcium titrators, chlor-o-counters, fat testers, and protein testers). Fiske Assoc., Inc. 617-278-2482 **505**

New Chemicals

Rotating graphite disc electrodes for use in spectrometric analysis of metals in oils are now available in a new grade designed for optimum sensitivity and repeatability. Grade U2-II has a narrower density range and lower resistivity than previous standard rotating disc graphite grades. Carbon purity is better than 99.9995%. Ultra Carbon Corp. 517-893-4575 **506**

Kits for the determination of serum cholesterol and urinary 17-ketosteroid are available. The kit for serum cholesterol contains all reagents and standards for 100+ determinations by a simplified colorimetric method. The other kit for the colorimetric determination of urinary 17-ketosteroid is also for 100+ determinations. Alpha Assoc. 215-945-0140 **507**

Stat-Pack for the enzymatic determination of triglycerides in blood serum is available as a clinical diagnostic set. The triglyceride test was developed by Dr. Giovanni Bucolo and is based on highly sophisticated biochemical reactions. Detailed instructions and prices are available from the company. Calbiochem. 714-453-7331 **508**

SRM 1571, Orchard Leaves ($68 for a 75-gram sample), is being issued on a provisional certificate by the NBS Office of Standard Reference Materials. The standard is intended for use in the calibration of apparatus and methods used in analyses of agricultural and other botanical materials for major, minor, and trace elements. SRM 1571 is certified for Ca, K, Fe, Na, Cu, and Ni. The content of the following elements is given for information only: Hg, Pb, N, Mg, P, As, Bi, B, Cr, Co, F, Mn, Se, U, and Zn.

Other new standards are SRM 984, rubidium chloride (RbCl weight % is 99.90 ± 0.02, absolute abundance ratio, $^{85}Rb/^{87}Rb$, is 2.593 ± 0.002, $43 per 1-gram sample) and SRM's 755 and 756, quartz and potassium nitrate for use in thermal analyses. Quartz (SRM 755) is furnished in 2-gram units, sized from 100–325 mesh; the potassium nitrate is supplied in 5-gram units of fine crystals. Each unit is priced at $35. Quartz has a phase transition at about 575°C and potassium nitrate at about 130°C. The transition temperatures given on the certificates are the means of the values obtained on several different thermal analysis instruments.

NBS also has available several new standards to help in defining pH scales. Information on all these standards is available from the National Bureau of Standards, U.S. Dept. of Commerce, Washington, D.C. 20234. 301-921-2691

MANUFACTURERS' LITERATURE

Lock-in Amplifiers. Twelve pages give a step-by-step approach to selecting a lock-in amplifier system. Basic units, preamplifiers, plug-in modules, special purpose systems, and a light chopping accessory are discussed. Ithaco, Inc. 607-272-7640 **601**

Water Pollution Analysis. Four new product application data sheets cover the measurement of organic and nutrient-type pollutants in water by spectrophotometric and gas chromatographic techniques. Instruments used include the IR-33 infrared, DB-GT and ACTA ultraviolet-visible spectrophotometers, and the GC-45 gas chromatograph. Beckman Instruments, Inc. 714-871-4848 **602**

Lab Apparatus. A 16-page brochure, "Problem Solvers for the Scientist," includes information on products for dispensing, shaking, rotating, stirring, printing and labeling, column eluting, and controlling liquid levels. Kraft Apparatus, Inc. 212-835-0086 **603**

Zonal Rotor. A 6-page brochure describes in detail IEC's CF-6 continuous flow zonal rotor which isolates, concentrates, and purifies large volumes of dilute particle suspensions with a sedimentation coefficient of 2000 and up. Damon Corp. 617-449-0800 **604**

Hollow Fiber Lab Processing. A literature kit describes the use of hollow fiber devices which make possible rapid and accurate processing of a wide variety of biochemical and biological solutions. Covered are purification, fractionation, concentration, osmosis, dialysis, ultrafiltration, permeation, and gas transfer. Dow Chemical. 517-636-0302 **605**

Nmr Shift Reagents. Four pages describe and illustrate the use of two new nmr shift reagents: Eu-Resolve II (Sievers' reagent) and Pra-Solve II (Rondeau's reagent). Illustrative spectra and a bibliography are included. Ventron, Alfa Products. 617-922-0768 **606**

Computer Catalog. A 158-page catalog details a wide range of computer and associated products and various applications. Computers from the smallest PDP-16 to the largest PDP-10 are covered. About 25% of the catalog describes computer uses. Digital Equipment Corp. 617-897-5111 **607**

Flowmeters. Specification 10A1460, a 6-page folder, describes low-flow rotameters (glass tube, variable area flowmeters) that provide visual indication of flow rate. Included are engineering data, capacity tables, ordering information, dimensions, and parts lists. Fischer & Porter Co. 215-675-6000 **608**

Chemical Kinetics. Application Note 2, 4 pages, "Elements of Chemical Kinetics" by J. E. Stewart, introduces some of the basic concepts of chemical kinetics. Included are equipment and calculations for chemical reactions and chemical relaxation kinetics. Durrum Instrument Corp. 415-321-6302 **609**

Medical Catalog. A special medical edition of the well-known Fisher catalog is called "70M" and contains 1168 pages of such items as equipment and instruments, chemicals, and culture media for medical and clinical uses. Fisher Scientific Co. 412-391-1330 **610**

pH Meters. "Accumet pH Meters," 12 pages, describes and illustrates Models 220 and 320 pH meters. Model 320 has accuracy of 0.05 pH (or 0.005 in expanded mode); Model 220, 0.5 pH. Fisher Scientific Co. 412-391-1330 **611**

Protein Reagents. A supplemental list, 17 pages, covers reagents for amino acid and protein analysis and synthesis. Included are Chromagram products and new reagents for acrylamide-gel electrophoresis. Eastman Kodak Co. 716-458-4080 **612**

Image Shearing Eyepiece. Four pages describe the Watson image shearing eyepiece which fits most standard microscopes. Applications include particle size analysis and fiber diameter measurements as well as bacteriological and biological specimen measurements. Hacker Instruments, Inc. 201-226-8450 **613**

Bioavailability Studies. A 4-page reprint from Drug and Cosmetic Industry describes the current status of bioavailability studies. Included is a summary of how the company can service in these studies. Harris Laboratories, Inc. 402-432-2811 **614**

Biochemicals. A 52-page catalog lists hundreds of research enzymes, diagnostic reagents, nucleotides, and specialty biochemicals. Also listed are analytical services of the company which provide complete amino acid analysis and ultracentrifugal analysis on a contract basis. Worthington Biochemical Corp. 201-462-3838 **615**

Effluent Surveillance. An 8-page article lists the major items to be considered and provided for to obtain information on the properties of liquid discharges. Sampling is given special attention. Nalco Chemical Co. 312-782-2035 **616**

AA Applications. "Technique and Applications of Atomic Absorption," describes the company's equipment and discusses the advantages and limitations of atomic absorption spectroscopy. Reprints of 120 articles on applications of AA to various fields are also cataloged and are available from the company. Perkin-Elmer Corp. 203-762-6973 **617**

Lab Drying. A 4-page bulletin describes a laboratory fluid bed dryer. The device directs a blast of air through material to be dried causing the particles to fluidize and rapidly give up moisture. Lots of 100–1000 grams can be dried in minutes. Pfaltz & Bauer, Inc. 212-898-2300 **618**

Selecting Gc Columns. A 16-page booklet by H. M. McNair discusses the difficulty of choosing the proper column for good gas chromatographic techniques. Factors affecting the selection are explained with tables, graphs, and formulas to assist the user. Gow-Mac Instrument Co. 201-377-3450 **619**

Ir Accessories. Catalog 1971 BE, 46 pages illustrates, describes, and prices the company's infrared accessories. The accessories can be used with all Perkin-Elmer and Beckman infrared spectrophotometers. Barnes Engineering Co. 203-348-5381 **620**

Scientific Instruments. An 8-page general catalog illustrates and describes Carlo Erba's instruments: automatic amino acid analyzers, automatic chemical analyzers, clinical analyzers, gas chromatographs, trace gas analyzers, automatic sample injectors, elemental analyzers, and others. Sanda, Inc. 215-839-0200 **621**

Ultrafiltration. A 58-page catalog, a system selection and applications guide, covers the laboratory and clinical uses of ultrafiltration for concentration, separation, and purification of colloids and macromolecules. Publication No. 403. Amicon Corp. 617-862-7050 **622**

Electronic Instrumentation. A 12-page brochure condenses information on the company's electronic counters, digital voltmeters, and multimeters, data amplifiers, and frequency synthesizer. Dana Laboratories, Inc. 714-833-1234 **623**

Chromatography. "Minimum Detectable Activity Using the Pye Unicam/Panax Radio Gas Chromatograph Assembly," 2 pages, and "A User's Guide to Liquid Column Chromatography," 3 pages, offer application advice to chromatographers. Philips Electronic Instruments. 914-664-4500 **624**

pH Systems. Kerneo's four basic pH systems designed for monitoring, recording, and controlling pH are illustrated and described in an 8-page catalog. Industrial and Mill Supply Co. 516-427-4354 **625**

Infrared Crystals. A 32-page guide for selecting suitable ir crystals discusses transmission range, reaction to various samples, refractive index, and reflection losses of crystals, and comparative costs. Chartered properties and spectra are included on 17 crystals. Barnes Engineering Co. 203-348-5381 **626**

Fluorescence Experiment. A 4-page experiment suitable for instrumental or physical chemistry courses determines the pK_a of β-naphthol in both ground and excited states. The procedure illustrates the principles of fluorescence. G. K. Turner Assoc. 415-324-0077 **627**

Amino Acid Analyzers. A 28-page booklet describes the company's complete line of amino acid analyzers. Detailed are major features, operating characteristics, and descriptions of component parts for each of four analyzers: two fully automatic, two semiautomatic. Beckman Instruments, Inc. 714-871-4848 **628**

Controlled Temperature Equipment. An 8-page short catalog illustrates and describes the company's complete line of controlled temperature and humidity equipment. Also introduced is a new line of table-top and portable rack-mounted cell production roller apparatus used in culture growth. Hotpack Corp. 215-333-1700 **629**

Scientific Instrumentation. A 6-page bulletin covers illumination and monochromatic systems and a complete series of photodetection equipment, analytical instrumentation, and other optoelectronic systems. Schoeffel Instrument Corp. 201-664-7263 **630**

Clinical Reagents. A 16-page descriptive listing of clinical diagnostic reagents includes special analytical systems, important basic reagents, improved new reagents, and special aids for the clinical lab. Pierce Chemical Co. 815-968-0747 **631**

Water Pollution. A 4-page bulletin describes sample handling equipment for monitoring/analyzing gas and liquid process streams. The Arcas Co. 713-529-5768 **632**

Magnetic Stirrer Hot Plates. A 4-page brochure describes the company's complete line of magnetic stirrer hot plates and accessories. Bulletin MS 171. Henry Thoemmer, Inc. 215-724-0800 **633**

Chemical Catalog. General chemical catalog of 72 pages includes amino acid and protein reagents, biochemicals and biochemical reagents, clinical reagents, lab accessories, organic fluorine and organosilicon compounds, and reagents and accessories for gc, ms, and nmr, and special vials and closures. Pierce Chemical Co. 815-968-0747 **634**

Chemicals. Catalog 5, 100 pages, includes a listing of the company's line of organometallics, ligands, homogeneous catalysts, heterogeneous catalysts and supports, and organophosphorus chemicals. Chemicals are available in research or development quantities. Strem Chemicals, Inc. 617-262-5800 **635**

Electrodes and Accessories. An 8-page brochure provides a guide to the company's complete line of electrodes and accessories for laboratory pH, redox, and selective ion measurements. Leeds & Northrup. 215-643-2000 **636**

Light Systems. A 16-page booklet on high intensity illumination systems describes the latest techniques and accessories for effectively distributing energy from a point and other light sources. Power supplies, arc lamps, and accessories for filtering light beams are covered. Schoeffel Instrument Corp. 201-664-7263 **637**

Ultracentrifuges Items. Catalog PL-174Q, 48 pages, lists nearly 1000 items, accessories, rotors, and tubes for use with the company's ultracentrifuges. Included are photographs, diagrams, basic specifications, and prices. Beckman Instruments, Inc. 714-871-4848 **638**

Diagnostic Reagents. An 80-page catalog, C204, describes diagnostic products of the Uni-Tech Div. of Baker. Over 2000 reagents for the clinical laboratory are listed. Also issued is a 5th edition supplement which contains additions, deletions, and price corrections. J. T. Baker Chemical Co. 201-859-2151

Company Periodicals

Requests for copies of the following publications should be sent directly to the address shown. Business or professional letterheads are requested.

Durrum Resin Report. No. 1, 8 pages, features an article on single-column analysis of amino acids. This is the first issue of a periodical devoted to problems in liquid chromatography. Durrum Chemical Corp., 3950 Fabian Way, Palo Alto, Calif. 94303

Fluorescence News. Vol. 6, No. 1, 8 pages, contains an article on the "Effects of Hydrogen Bonding upon Fluorescence of Organic Molecules," by E. L. Wehry. Also included is an article on ratio mode operation by R. L. Sellers and a bibliography of selected recent articles of interest to users of fluorescence instrumentation. American Instrument Co., 8030 Georgia Ave., Silver Spring, Md. 20910

Gas-Chrom Newsletter. Vol. 12, No. 4, 8 pages, includes information on the Desikator, new radiochemicals, liquid chromatography septums, preconditioned gc packing, and other accessories for gas chromatography. Applied Science Laboratories, Inc., P.O. Box 440, State College, Pa. 16801

Via. Vol. 5, No. 2, 12 pages, includes information on teaching chemistry at the University of Texas; a new line of electromagnets and power supplies; applications of ^{13}C Fourier transform nmr; and a new method for measuring metastable ion transitions. Varian, 611 Hansen Way, Palo Alto, Calif. 94303

EEL Bulletin. No. 14, 4 pages, is devoted to the company's new Model 244 fluorimeter and other instruments that were displayed at LABEX 71. Evans Electroselenium, Ltd., Church Lane, Braintree, Essex, England.

Environmental Reporter. The first edition of this magazine, 12 pages, provides important information on a wide range of instruments and methods for detecting and measuring pollutants in air, water, and other substances. Fisher Scientific Co., 711 Forbes Ave., Pittsburgh, Pa. 15219

MPI Applications Notes. Vol. 6, No. 2, 8 pages, discusses both constant current and constant potential coulometry. Six methods illustrate alternate methods of endpoint detection and readout. McKee-Pedersen Instruments, P.O. Box 322, Danville, Calif. 94526

PRODUCT CAPSULES

Short "refreshers" on last month's ads. Obtain free information on any of the products or services described by writing in the appropriate key numbers in the "Product Capsules" portion of the reply card preceding this section.

Adsorbents. 32-page book on TLC. **P 63**

Balances. Catalog on line of 17 analytical balances from macro to ultra micro. **P 115**

Balances, top loading. Catalog features 18 models with high load-to-precision ratio. **P 120**

Baths. 7-1/2 gallon capacity with temperature range −20° to 70° C ± 0.02° C. **P 61**

Bombs. Specs on oxygen bomb combustion apparatus to determine sulfur values. **P 140**

Books. Determination of organic structure by physical methods. **P 1**

Books. Infrared spectra of labelled compounds. **P 1**

Books. An introduction to gas-liquid chromatography. **P 1**

Books. Paper chromatography and electrophoresis. **P 1**

Books. Pulse and Fourier transform NMR. **P 1**

Books. Vol. 2 of spectroscopy in inorganic chemistry. **P 1**

Books. Statistical manual for chemists. **P 1**

Centrifuges. 2 table top and 2 floor units featuring universal heads and multi-tube carrier system. Catalog. **P 175**

Chemicals. New catalog lists over 80 products for liquid scintillation counting, together with more than 5,000 chemicals. **P 14**

Chemicals, reagent. Chelates to resolve NMR spectra. **P 145**

Chromatographs, gas. Info on low-cost, portable unit. **P 32**

Chromatographs, gas. New unit has 6 interchangeable state-of-the-art detectors which contribute to instrument performance. Bulletin. **P 75**

Chromatographs, gas. New units have complete analytical flexibility. Oven top opens pneumatically, makes for easy column removal. Bulletin. **P 135**

Chromatography. New price list features sections on gel electrophoresis, chromatographic columns, stable isotopes. **P 18**

Chromatography. Bulletin on TLC analysis of toxic drugs. **P 55**

Chromatography. Bulletin on chromatogram sheet and development apparatus for TLC. **P 55**

Chromatography. Bibliography on use of chromatography sheet in TLC. **P 55**

Chromatography. Bulletin on solvents and reagents for TLC. **P 55**

Computer interfaces. Series of modules to keep instrumented systems going continually with calculators, minicomputers, or time-shared system. **P 136**

(Continued on page 122 A)

Product Capsules

(Continued from page 121 A)

Cryogenic equipment. New unit uses cascaded refrigeration to reach −100° C under no load conditions. **P 121**

Digital readout. New linear/+log/−log device operating on 1 volt or 100 millivolt input from broad range of spectrophotometers. **P 167**

Electrodes, ion. Details on full line of ion-selective units. **P 142**

Electrometers. Detects currents on order of 10^{-17} ampere, charges as small as 5×10^{-16} coulomb, potentials down to 2×10^{-5} volt. **P 171**

Flow controllers. Maintain constant flow regardless of downstream pressure variations. Report. **P 117**

Integrators. GC unit with automatic baseline capacity. Brochure. **P 76**

Ion exchangers. Five different cartridges for water purity, in 2 sizes, meet need for varying levels of purity. Brochure. **P 89**

Labels. Permanent, pressure-sensitive microscope slide labels. Samples, brochure. **P 138**

Lamps. Literature on hollow-cathode units for 47 different elements. **P 72**

Liquid handling systems. Literature on line including micropipets, dispensers, motor-driven buret, dosimeters, peristaltic pumps. **P 15**

Mercury analyzer. Compact, self-contained, low-cost system. Bulletin. **P 33**

Microscopes. Catalog on line that includes all types. **P 170**

Microscopes, scanning electron. New self-maintaining column now permits routine 100 angstrom resolution. **P 91**

Modular systems. Flexible electrochemistry system accepts input from virtually any detector, has over 60 applications. Catalog. **P 118**

Moisture analyzers. Complete range of models for research and analysis. **P 45**

Nitrogen analyzers. Provides rapid results for an almost unlimited range of materials. Bulletin. **P 31**

pH meters. Data file provides info on wide line. **P 19**

pH meters. Lab-in-a-lid module carries accessories in this portable unit with 0.05 pH accuracy and 0.02 pH reproducibility. **P 100**

pH meters. Operates both as a full-range (0 to 14 pH) instrument and as an expanded-scale meter (span: 1.999 pH). **P 154**

Photometers. Ultraviolet unit for monitoring liquid effluent. Bulletin. **P 17**

Polarographs. Complete specs on new model strip-chart recording unit. **P 156**

Preamplifiers. AC or DC coupling, battery operated, noise figure of less than 0.3 dB. Data. **P 146**

(Continued on page 124 A)

Product Capsules

(Continued from page 122 A)

Pumps, metering. Deliver reproducible flow over wide dial selected ranges. Three models. Catalog. **P 90**

Pumps, peristaltic. 8-lb. portable unit features variable flow control from 100 ml to 2,500 ml per minute. **P 65**

Recorders. New 10″ strip chart unit records output from a spectrophotometer directly in per cent transmittance or absorbance units. Bulletin. **P 71**

Recorders, plug-in. Details on 5-inch and 10-inch units with 1 to 100 millivolt sensitivity. **P 73**

Recorders, transient. Record, observe and process signals and transfer data digitally to CRT display, computer analysis, strip chart recorder. **P 16**

Samplers, flameless. Simple-to-operate system for trace element determinations in atomic absorption spectroscopy. **P 88**

Sampling system. Unit increases capacity of chromatograph, eliminates variables of manual injection. **P 74**

Septums. Blue heat treated septums made of silicone rubber for use in gas chromatography. **P 2**

Signal averagers. Unit offers flexibility with range of plug-in modules. Brochure. **P 122**

Signal averagers. Computer based data aquisition and analysis system available with complete line of versatile magnetic tape systems. **P 124**

Signal averagers. Completely integrated unit includes a 5-inch CRT display, 3 memory address capabilities, 2 analysis routines. **P 125**

Solvents. 56-page reference book on spectrophysical propetries, specs, and typical uses. **P 119**

Spectrometers, mass. 60° sector, magnetically scanned unit features heated inlet, linear mass readout. **P 196**

Spectrometers, NMR. Unit has built-in integrator to perform quantitative analysis. **P 173**

Spectrophotometers, AA. Built-in features include signal integration, zero suppression, flame emission, readout. Data. **P 155**

Spectrophotometers, IR. New solid-state pneumatic detector has high sensitivity. **P 141**

Spectrophotometers, NMR. 4 systems with both multiscan averaging and pulse Fourier transform systems for studying ^{13}C. **P 172**

Spectrophotometers, UV/VIS. Double-beam, single-grating unit in the 190-800 nm range. Reads linear in absorbance and transmittance. Two models. **P 20**

Spectrophotometers, UV/VIS. Brochure on 7 models featuring digital readout and printout, precision synchronization or direct reading, automatic or manual operation. **P 137**

Spectroscopic accessories. New carbon rod atomizer fits any AA unit, produces detection limits 200 times better than orthodox flame. **P 176**

Supply house. Single source for lab equipment supplies, and scientific instruments. **P 151**

Supports, GC. Bulletin on 5 grades of polymer supports. **P 92**

Thermal analysis system. Modular, solid-state unit has push-button operation with digitally set temperature limits. **P 43**

Titrators. Handles wide range of materials. Sampling systems available for all types of materials. **P 44**

Titrators. Inexpensive Karl Fischer apparatus with 1 ppm to 100% water sensitivity, 1% accuracy, 0.5% reproducibility, 2-minute determinations. **P 99**

Titrators. Automatic Karl Fischer unit with digital readout. **P 139**

Transformers. Cord and plug type variable units designed for portable use or bench mounting. **P 152**

Tubes, NMR. Bulletin features complete line of tubes and accessories. **P 95**

Tubing. Flexible, plastic "Y" connectors available in 8 standard sizes from $^3/_{16}$″ to 1-$^1/_4$″ ID. **P 123**

Water testers. Portable unit provides for 23 different water quality tests. **P 70**

Laboratory Supply Center

(Continued from page 123 A)

INDEX TO ADVERTISERS IN THIS ISSUE

▼ ▼ ▼

Advertising Management for the American Chemical Society Publications

CENTURY COMMUNICATIONS CORP.

Edward P. Blanchard, President, Thomas N. J. Koerwer, Executive Vice President, 142 East Avenue, Norwalk, Connecticut 06851 (Area Code 203) 853-4488

ADVERTISING SALES MANAGER
Thomas N. J. Koerwer

SALES REPRESENTATIVES

Chicago 60601 . . . Eugene Eldridge, Century Communications Corp., 307 North Michigan Avenue, 312-641-0890.

Cleveland 44113 . . . Michael Hayes, Century Communications Corp., 75 Public Square, 216-523-1930.

Dallas 75207 . . . Parker Harris, Roy McDonald Asso., 714 Stemmons Tower West, 214-637-2444.

Denver 80203 . . . Robert H. Heidersbach, Roy McDonald Asso., Inc., 846 Lincoln Street, 303-825-3325.

Houston 77006 . . . Frank N. Vickrey, Richard Clothier, Roy McDonald Asso., Inc., 3130 Southwest Freeway, 713-529-6711.

Los Angeles 90045 . . . Clay S. Holden, The Connecticut Century Communications Corp., Airport Arcade Bldg., 8820 S. Sepulveda Blvd., Suite 215, 213-776-0552

Norwalk 06851 . . . Don Davis, Richard Feary, Century Communications Corp., 142 East Avenue, 203-853-4488.

Philadelphia 19034 . . . James A. Byrne, Century Communications Corp., 535 Pennsylvania Avenue, Fort Washington, Pa., 215-643-2586.

Great Britain and Western Europe . . . Brayton Nichols, The American Magazine Group, 27 Maddox Street, London, W.1, England, Telephone 499-0180.

Japan . . . Sumio Oka, International Media Representatives, Ltd., 1 Shiba-Kotohiracho, Minatoku, Tokyo.

PRODUCTION DEPARTMENT
Production Director
Joseph P. Stenza
Advertising Production Manager
Penelope Mallach

° *See ad in ACS Laboratory Guide*

°° *Companies so marked have advertisements in the foreign regional edition only*

FUTURE ARTICLES

Applications of Paramagnetic Shift Reagents in Proton Magnetic Resonance Spectrometry
D. L. Rabenstein

A Small Computer, Magnetic Tape Oriented, Rapid Search System Applied to Mass Spectrometry
L. E. Wangen, W. S. Woodward, and T. L. Isenhour

Spectrophotometric Determination of Xanthate and Total Sulfur in Viscose
M. Rahman

Specification of Gas Chromatographic Behavior Using Kovats Indices and Rohrschneider Constants
L. J. Lorenz and L. B. Rogers

Isolation and Analysis of Carbonyl Compounds as Oximes
J. W. Vogh

Computer Methods in Analytical Mass Spectrometry. Development of Programs for the Analysis of Low Resolution Mass Spectra
L. R. Crawford and J. D. Morrison

X-Ray Photoelectron Spectroscopy of Molybdenum Compounds. Use of ESCA in Quantitative Analysis
W. E. Swartz, Jr., and D. M. Hercules

Radiochemical Determination of Plutonium in Environmental and Biological Samples by Ion Exchange
N. A. Talvitie

Application of Forced-Flow Liquid Chromatography to the Determination of Iron
M. D. Seymour, J. P. Sickafoose, and J. S. Fritz

An X-Ray Fluorescence Ion Exchange Method for the Determination of Lanthanum, Cerium, and Praseodymium in Carbon Steels
A. T. Kashuba and C. R. Hines

Chemical Ionization Mass Spectrometry of Complex Molecules. Esters of Di- and Tricarboxylic Acids
H. M. Fales, G. W. A. Milne, and R. S. Nicholson

Behavior of Metal Particles Compared to Organo-Metallic Compounds Measured by Flame Atomic Absorption Spectrophotometry
J. H. Taylor, T. T. Bartels, and N. L. Crump

Atomic Fluorescence with Continuous Nebulization into a Platinum Furnace
M. S. Shull, T. H. Glenn, M. P. Bratzel, and J. D. Winefordner

An Investigation of the Fourier Transform Representation of Mass Spectra for Analysis by Computerized Learning Machine
P. C. Jurs

Mass Standards for Chemical Ionization Mass Spectrometry
I. Dzidic, D. M. Desiderio, M. S. Wilson, P. F. Crain, and J. A. McCloskey

Pulse Polarography of Halide Ions in Molten Nitrates
W. O'Deen and R. A. Osteryoung

Steric-Exclusion Chromatography at Pressures up to 3500 KG/CM²
B. A. Bidlingmeyer and L. B. Rogers

X-Ray Photoelectron Spectroscopic Investigation of the Group VI-A Elements
W. E. Swartz, Jr., K. J. Wynne, and D. M. Hercules

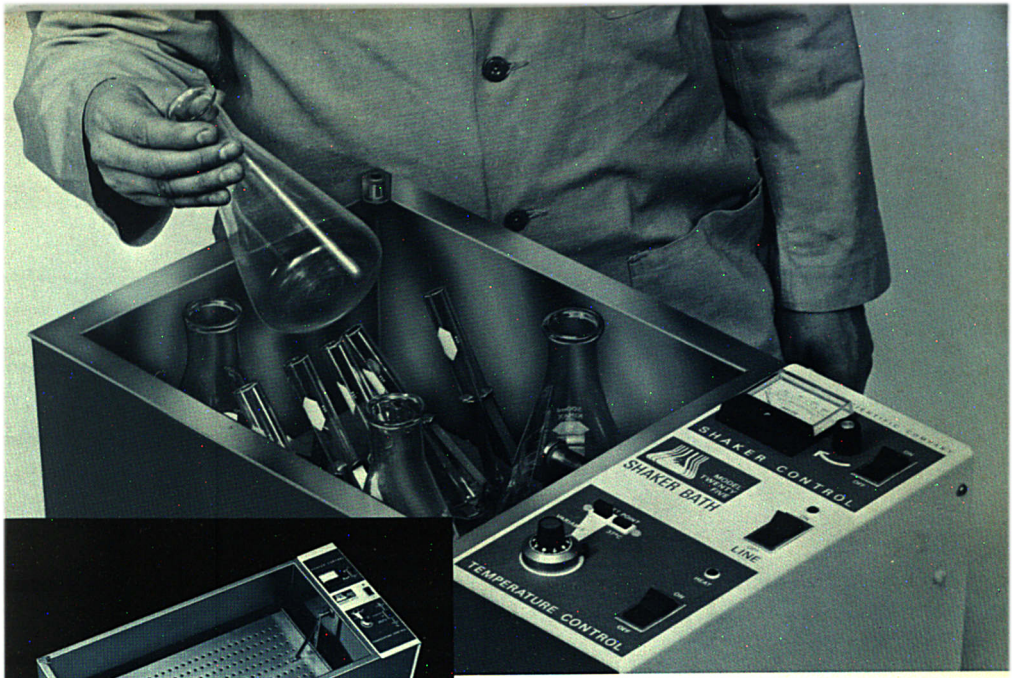

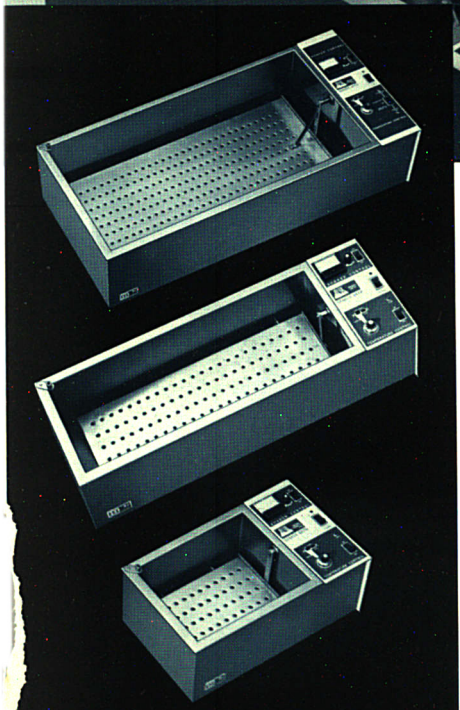

PRECISION SCIENTIFIC — SUBSIDIARY OF GCA CORPORATION

Here's a bath that's guaranteed to last you a long, long time

New Precision Shaker Baths

These are second generation models of a bath line that has been regarded as the industry standard for years. The new models incorporate the latest in solid state technology and, with available accessories, are suitable for virtually any microbiological, biochemical or physio-chemical studies.

Solid state temperature control provides a uniformity of 0.03°C, and the solid state shaker control has a built-in tachometer. You have push-button selection—fixed point or variable—of temperature control mode and precise push-button or dial-in temperature selection. Shaker speed may be set anywhere from 20 to 200 oscillations per minute.

Available in three sizes, all offering maximum flexibility in glassware combinations.

Gassing hoods and cooling coils available to increase versatility. Ask your Precision Scientific Dealer for complete information or write us. Precision Scientific Co., 3737 W. Cortland St., Chicago, Ill. 60647.

Guaranteed for five years or 50,000,000 oscillations!

CIRCLE 154 ON READER SERVICE CARD

For laboratories that don't need an 'expensive' top loader, yet can't use a 'cheap' one...

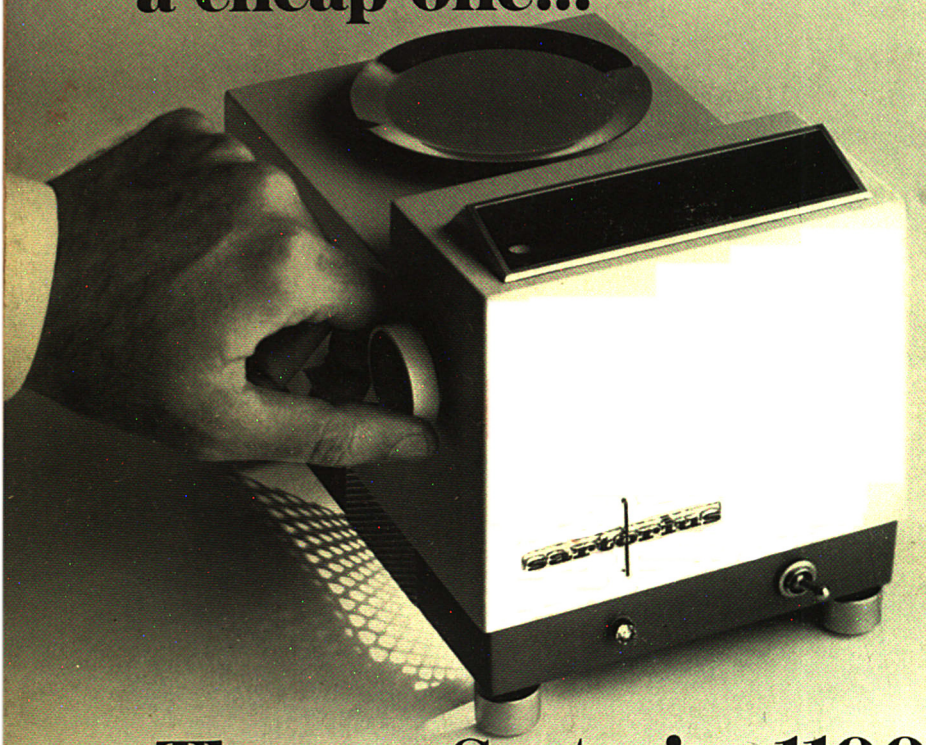

The new Sartorius 1100. Only $445.

Why pay for an expensive balance your lab may not really need? Why buy slower and cruder equipment that doesn't meet today's standards? Sartorius solves the dilemma with its new Series 1100 top-loaders – the first balances to bridge the gap between modern design and low price.

At only $445, the Series 1100 offers many features usually found only on more expensive, sophisticated weighing instruments. For example: all-digital readout; results in less than 3 seconds; wide-range mechanical taring; fast, easy operation with no weights to handle and not even any dialing of built-in weights. It's a torsion-type balance, and the optical scale covers the entire weighing range.

Available in three different capacity/accuracy ratios—1000g/0.1g, 200g/0.015g and 100g/0.01g—these new, reasonably priced balances are ideal for a variety of applications, from student use and research to quality control weighings.

If you're in the market for a new balance for weighing in the range from less than 100 grams up to 1500 grams, you really ought to find out more about the new Series 1100. We'll be happy to send you complete literature and our free 52-page catalog. Just write: Sartorius Division, Brinkmann Instruments, Cantiague Rd., Westbury, N.Y. 11590.

sartorius balances

CIRCLE 23 ON READER SERVICE CARD

– 2 AAU. 2515